UNIVERSITÉ LIBRE DE BRUXELLES | ULB

Faculté de Pharmacie

Ecole Doctorale en Sciences Pharmaceutiques

DEVELOPMENT AND EVALUATION OF CONTROLLED-RELEASE CISPLATIN DRY POWDERS FOR INHALATION AGAINST LUNG TUMOURS

Vincent LEVET

Pharmacien

Thèse présentée en vue de l'obtention du grade de Docteur en Sciences Biomédicales et Pharmaceutiques

Promoteur : Prof. Karim AMIGHI
Co-promoteur : Dr. Nathalie WAUTHOZ
Laboratoire de Pharmacie Galénique et de Biopharmacie, ULB

Composition du jury
Prof. Jean-Michel KAUFFMANN (Président, Faculté de Pharmacie, ULB)
Prof. François DUFRASNE (Secrétaire, Faculté de Pharmacie, ULB)
Prof. Jean-Paul SCULIER (Institut Jules Bordet, ULB)
Dr. Aurélie SCHOUBBEN (Università degli Studi di Perugia)
Dr. Francis VANDERBIST (S.M.B. Galéphar)

Année académique 2016-2017

Remerciements

Je souhaite tout d'abord exprimer ici mon infinie gratitude envers mon promoteur, le Professeur Karim Amighi. Je lui suis extrêmement reconnaissant pour cette chance qu'il m'a donnée en me permettant de réaliser ce travail dans son laboratoire, pour ses conseils judicieux et pour les nombreuses heures passées à la relecture des différents articles et de ce manuscrit. Je le remercie tout particulièrement pour les ressources que le laboratoire m'aura fournies durant ces 4 ans et 3 mois de thèse, et sans lesquelles il m'aurait été impossible de réaliser ce travail dans des conditions saines pour ma famille et moi-même. Je lui en serai éternellement reconnaissant.

Je remercie également tout particulièrement ma co-promotrice, le Docteur Nathalie Wauthoz, qui a lancé ce projet et défriché le concept de chimiothérapie inhalée à l'aide de poudres sèches pour inhalation pendant sa propre thèse. Grâce à son travail j'ai pu évoluer dans un laboratoire adapté à la manipulation d'anticancéreux et qui disposait déjà des techniques de production et de caractérisation adéquats. Je la remercie bien plus pour ses conseils et son jugement scientifique. Son expérience et sa connaissance approfondie de l'oncologie expérimentale dans le cadre de l'inhalation ont également été indispensables à la bonne réalisation de ce travail, du début à la fin.

Je remercie tout autant le Docteur Rémi Rosière ainsi que Julien Hecq avec qui nous avons partagé inlassablement nos points de vues sur les différentes manipulations, leurs concepts et leurs résultats. Je les remercie également pour leur aide indispensable dans la réalisation des expériences *in vitro* et *in vivo*, pour les nombreuses heures passées en culture cellulaire et à l'animalerie à réaliser des greffes tumorales et bien autant pour leur franche camaraderie.

Je me dois également de remercie ici le Professeur Ingrid Langer pour ses conseils dans la réalisation des tests ELISA sur le lavage broncho-alvéolaire, la réalisation des cytospins et colorations de cellules et pour m'avoir donné l'accès à son laboratoire de l'IRIBHM parfois dans des conditions d'organisation difficiles, me permettant ainsi d'être au plus près de la maternité de l'Hôpital Erasme…

Bien évidemment je salue et remercie mes « collègues » Romain et Audrey du bureau des « Frenchies ». Pour nos échanges scientifiques au quotidien bien évidemment mais aussi pour leur amitié, leur accent et la bonne humeur au quotidien. Je remercie ici aussi le Docteur

Gabrielle Pilcer avec qui j'ai pu partager les premiers mois de thèse également dans ce bureau, et avec qui j'ai pu énormément échanger au lancement du projet. Elle reste pour moi un exemple de probité et de rigueur scientifique. Merci également à Véronique de Bueger, pour sa sympathie, sa bonne humeur et son franc-parler.

Je souhaite également remercier le Docteur Gilles Berger, pour son aide dans la compréhension des particularités physico-chimiques du cisplatine au départ de ce travail et pour m'avoir mis en contact avec le Docteur Luca Fusaro que je remercie également tout particulièrement pour son aide et les nombreuses heures passées à la caractérisation précise du cisplatine par RMN du Platine 195.

Merci également à nos techniciens de laboratoire, Nancy Van Aelst, Maxime Paide et Ismaël Hennia, pour leur aide et leur travail au quotidien et pour leur sympathie bien sûr. Merci également à tous les membres présents du laboratoire et à ceux que j'ai croisé pendant ma thèse, j'espère n'en oublier aucun : Amélie, Federica, Majda, Mélanie, Christophe, Emeric, Jonathan, Jonathan, Philippe. Merci également à tous mes confères et amis du laboratoire de Chimie Pharmaceutique Organique avec qui nous partageons les murs du 6e BC à la Faculté : Caroline, Melissa, Florence, Cédric, Damien, Iyas et Pierre. Merci également à Marie et Dominique du laboratoire de Chimie analytique Instrumentale et Bioélectrochimie, chez qui j'ai passé de nombreuses semaines à doser le cisplatine.

D'un point de vue plus personnel, ces quatre années ont été la source d'énormément de joie et de bonheur. Pendant celles-ci, ma femme Raphaëlle et moi nous sommes mariés et avons eu deux bébés, Charles puis Victor. C'est donc du fond du cœur que je remercie mon épouse pour sa tendresse, son soutien indéfectible dans les moments de découragement et pour son courage face à mon mauvais caractère. Je la remercie de s'occuper si bien de nos deux garçons et pour avoir pris le relais si souvent pour que je puisse avancer dans mon doctorat, surtout ces derniers mois. Ce travail est donc un peu le sien aussi.

Je remercie également mes parents, grands-parents, beaux-parents, frères, sœur, famille et amis, pour leur présence, leur écoute et leur soutien. Merci en particulier à mes grands-parents Lucie et Darius, qui étaient tous deux chercheurs en chimie au Museum de Paris et à qui je dédie ce travail. Ce sont leurs valeurs, leur curiosité, leur franchise, leur passion pour la science et leur plaisir d'apprendre qu'ils m'auront transmis, qui m'a donné l'envie de poursuivre ces études.

Je leur dédie ce travail.

TABLE OF CONTENTS

ABBREVIATIONS

^{195}Pt-NMR	nuclear magnetic resonance of platinum 195
AUC	area under the curve
BALF	broncho-alveolar lavage fluid
Bw	body weight
CFC	chlorofluorocarbon
C_{max}	peak concentration
COPD	chronic obstructive pulmonary disease
CR	controlled release
CT	chemotherapy
CAT scan	computed-tomography scan
d_{ae}	aerodynamic diameter
DD	dry diluent
DNA	deoxyribonucleic acid
DMF	*N,N,*-dimethylformamide
DPB	dry powder blend
DPI	dry powder inhaler
DPPC	dipalmitoyl phosphatidylcholine
DSC	differential scanning calorimetry
DSPE-mPEG-2000	distearoyl phosphoethanolamine polyethylene glycol 2000
EE_D	emission efficiency in dose
EE_M	emission efficiency in mass
EGFR	epidermal growth factor receptor
EN	endotracheal nebulization
ETAAS	electrothermal atomic absorption spectrometry
FDA	food and drug administration
FPD	fine particle dose
FPF	fine particle fraction
FSI	Fast Screening Impactor
GMS	glyceryl monostearate
HFA	hydrofluoroalkanes
HPH	high-pressure homogenization
HPLC	high-performance liquid chromatography
HPMC	hydroxypropyl methylcellulose
HSH	high-speed homogenization
IASLC	international agency for the study on lung cancer
IP	intraperitoneal
IPA	isopropanol
IR	immediate release
IV	intravenous

$k_{el}{}^i$	initial elimination rate constant
$k_{el}{}^t$	terminal elimination rate constant
LDH	lactate dehydrogenase
LLOQ	lower limit of quantification
LOD	lower limit of detection
LPS	lipopolysaccharide
MCC	mucociliary clearance
MMAD	mass-median aerodynamic diameter
MPS	macrophage phagocytic system
MsLI	multistage liquid impactor
MTD	maximum tolerated dose
NSCLC	non-small cell lung cancer
PEG	polyethylene glycol
PET scan	positron emission tomography scan
PK	pharmacokinetic
PLA	polylactic acid
PLGA	poly(D,L-lactide-co-glycolide)
pMDI	pressurised metered dose inhaler
P90H	Phospholipon 90H
PSD	particle size distribution
SCLC	small cell lung cancer
SD	spray dried
SEM	scanning electron microscopy
SLM	solid-lipid microparticles
SLN	solid-lipid nanoparticles
$t_{1/2}$	half-life
$t_{1/2}{}^i$	initial half-life
$t_{1/2}{}^t$	terminal half-life
T_a	targeting advantage
T_e	targeting efficiency
t_{max}	time to reach C_{max}
TNM	tumour, node, metastasis
TPGS	tocopheryl polyethylene glycol succinate
TS	tristearin
TTF1	thyroid transcription factor-1
UD_D	uniformity of the delivered dose
UD_M	uniformity of the delivered mass

SUMMARY

Lung cancer is the deadliest cancer in the world, with a global 5-year survival rate of about 15%. Despite a notable impact of the latest improvements in prevention, screening, detection and staging, the efficacy of conventional treatments is not sufficient and has reached a therapeutic plateau. These conventional treatments involve a combination of surgery, radiotherapy and chemotherapy (CT). CT is used in almost all stages: in operable and inoperable stages to limit tumour cell invasion and in latest stages as a palliative treatment. Cisplatin is one of the most frequently used and most potent drugs available. It is administered by parenteral route at doses limited by its high and cumulative nephrotoxicity but also by other systemic toxicities (e.g. ototoxicity). Its administration therefore requires many precautions (long hydration procedure, surveillance of the renal function), which mobilize medical personnel. A major limitation of parental CT is the low concentration of drug that successfully reaches the tumour or the metastases. A potential additional modality could be aerosolized CT to localize lung cancer treatment. It has shown a relative local tolerance for cisplatin through preclinical and clinical studies in humans by means of nebulized solutions or liposomal formulations. As a local treatment, aerosolized CT has a clear pharmacokinetic (PK) advantage, as it can increase local exposure while decreasing systemic exposure. However, because CT drugs, such as cisplatin, are active at rather high doses (in the mg range), the duration of administration from nebulizers is very long as it depends on the drug solubility or on drug encapsulation into liposomes. They also pose a high risk of environmental contamination and require HEPA-filtrated hoods during the nebulization procedure.

Of all the inhalation devices available to deliver high drug doses, dry powder inhalers (DPIs) were chosen in this work. These were chosen to circumvent the above issues by providing higher deposited doses, in very short timeframes, using a patient-driven device that could help limit environmental exposure to only very low levels of drug. DPI in general also have the advantage of being applicable to both poorly-water-soluble and to water-soluble anticancer drugs. However, because direct deposition of high quantities of anticancer drugs to the lung parenchyma could pose a high risk of local irritation and pulmonary adverse effects, controlled release (CR) of cisplatin from deposited particles in the lung parenchyma was needed. However, in the lungs, foreign undissolved particles are rapidly eliminated by means of naturally occurring clearance mechanisms, in particular macrophage uptake in the alveoli. Therefore, formulation strategies able to limit the particles clearance are needed to assure high lung residence of these CR particles.

The formulation strategy of this work was to develop DPI formulation based on solid-lipid microparticles (SLM) able to (i) be deposited into the lung, (ii) control the release of cisplatin and (iii) escape macrophage uptake in order to remain in the lung long enough and at a

concentration able to optimize the therapeutic index (i.e. increase the potential therapeutic effect and decrease the potential side effects).

The primary objectives of the SLM-based DPI formulations were to (i) exhibit aerodynamic properties compatible with lung cancer patients abilities and cisplatin requirements (e.g. a high deposited fraction, high deagglomeration abilities under low airflow within a low-resistance DPI, deposition in the mg range), (ii) provide a CR matrix for cisplatin *in vitro*, (iii) be able to be retained into the lung long enough *in vivo*, (iv) using scalable production techniques and (v) using only potentially well-tolerated excipients.

Cisplatin was initially reduced to microcrystals under high-pressure homogenization (HPH) cycles up to 20 000 psi. This procedure permitted uncoated particles with mean diameters below 1.0 μm to be obtained. To assess the cisplatin release abilities of the DPI formulations on the deposited fraction only, a new dissolution test was adapted. This test used a classical paddle apparatus from the pharmacopoeia and a Fast Screening Impactor (FSI).

An excipient-free formulation, obtained from the spray dried suspension of cisplatin microcrystals (100% cisplatin) was initially produced. It was compared to a 95:5 cisplatin/tocopheryl polyethylene glycol succinate (TPGS) formulation, which exhibited a higher deposition ability (fine particle fraction (FPF) of 24.2 vs. 51.5% of the nominal dose, respectively). Both exhibited immediate release (IR), with 90% dissolved under 10 minutes.

Solid lipid microparticle (SLM)-based formulations were then produced using the cisplatin microcrystalline suspension and various lipid excipients. Those had previously been screened for their ability to be spray dried following their solubilisation in heated isopropanol. The addition of a triglyceride, tristearin (TS), as the main lipid component and if necessary a polyethylene glycol (PEG) excipient-comprising fraction with TPGS or distearoyl phosphoethanolamine polyethylene glycol 2000 (DSPE-mPEG-2000) as a surface modifier, provided spray dried particles with interesting characteristics. These formulations, comprised of at least 50% cisplatin, exhibited high CR abilities in simulated lung fluid at 37°C for more than 24 h (as low as 56% released after 24 h) and a low burst-effect (as low as 24% and 16% after 10 minutes with and without PEGylated excipients, respectively). They also showed high aerodynamic properties, with a high FPF ranging from 37.3 to 50.3% w/w of the nominal dose and a low median mass aerodynamic diameter (MMAD) between 2.0 and 2.4 μm. The process also offered high production yields (> 60%).

The best IR DPI formulation (evaluated on the FPF, i.e. cisplatin/TPGS 95:5) and the most promising CR formulations without (i.e. cisplatin/TS 50:50) and with PEGylated excipients (evaluated on CR abilities, i.e. cisplatin/TS/TPGS 50:49.5:0.5) were then administered to

CD-1 mice, concurrently to endotracheal nebulization (EN) of a cisplatin solution. This was done using specific endotracheal devices, the Penn-Century Inc. DP-4M© Dry Powder Insufflatorn and for the cisplatin solution, the Microsprayer™ IA-1C©. They were compared to intravenous (IV) injection during a PK study over 48 hours. The administration of DPI formulations required the development of a spray dried diluent (Mannitol:Leucine 10:1) and specific dilution method (3D mixing for 4 hours and double-sieving) to be able to deliver precise and repeatable quantities of powder into the lungs of mice at 1.25 mg/kg dose.

A PK study was carried out of the lungs, blood, kidneys, liver, mediastinum and spleen of the mice. The study used a developed and validated electrothermal atomic absorption spectrometry (ETAAS) method. Results showed that endotracheal administration of DPI formulations permitted the exposure of the lungs to cisplatin, expressed as the area under the curve (AUC) to be greatly increased while decreasing the systemic exposure. More precisely, the only formulation that exhibited prolonged lung retention was the one comprising PEGylated excipient (cisplatin/TS/TPGS 50:49.5:0.5), which was observed for ~7 hours. This lung retention was associated with smoother concentration $vs.$ time profiles in blood (higher t_{max} and lower C_{max}), which also confirmed its CR abilities in $vivo$ as dissolved cisplatin is a highly permeable drug. The overall exposure, established by the AUC, helped calculate the target efficiency (T_e: the ratio of AUC in the lungs to the sum of AUC in non-target organs) and the target advantage (T_a: ratio of AUC in the lungs by the tested route to the AUC in the lungs by the IV route). For instance, the T_a of the aforementioned formulation (cisplatin/TS/TPGS 50:49.5:0.5) was of 10.9, as compared to 1 for IV, 3.3 for EN, 2.6 for the IR DPI formulation (cisplatin/TPGS 95:5) and 3.7 for the non-PEGylated CR DPI formulation (cisplatin/TS 50:50). In the meantime, the T_e for the same formulations were 1.6, 0.09, 1.1, 0.4 and 0.9, respectively, showing again the great efficiency of the inhaled route $vs.$ the IV route in targeting the lungs. More importantly, it showed the added efficiency of the CR DPI formulation with lung retention abilities, provided by the addition of PEGylated excipients.

In the last part of the work, maximum tolerated doses (MTD) of formulations were established. These showed that the best candidate, selected based on the PK results (CR DPI with lung retention abilities composed of cisplatin/TS/TPGS 50:49.5:0.5) had better overall tolerance than IR approaches (DPI formulation at cisplatin/TPGS 95:5 and EN of a cisplatin solution). More precisely, it was possible to double the administered dosage for the CR formulation (1.0 mg/kg) $vs.$ the IR DPI and EN (both at 0.5 mg/kg) under a repeated administration scheme (3 times a week for 2 weeks).

Moreover, an assessment of the lung tolerance of this best candidate was realized and compared to the IR DPI, EN and the IV route. It was done through analysis of the broncho-alveolar lavage fluid (BALF) 24 hours following a single administration at the pre-determined MTD. IL-1β, IL-6 and TNF-α cytokines were not increased following the administrations. No evidence of tissue damage or cytotoxicity could be observed through quantification of the protein content and of lactate dehydrogenase (LDH) activity. The only observations were a decrease in total cells and an increase in polynuclear neutrophils (PN) cells in the BALF, which was not observed by IV or following the administration of the vehicle of the CR formulation alone (i.e. PEGylated SLM and dry diluent). This increase was not directly linked to the formulation but rather to cisplatin, as it was observed in each cisplatin inhalation experiments, and not with the vehicle of the CR formulation, which was comparable to the non-treated mice.

In parallel, we realized a survival study following the administration of the best DPI formulation candidate (cisplatin/TS/TPGS 50:49.5:0.5) *vs.* the IR DPI candidate (cisplatin/TPGS 95:5), both at their respective MTD under the aforementioned repeated dosing scheme. Cisplatin was administered to mice bearing a grafted orthotopic M109-HiFR lung tumour model, previously developed in the laboratory. The DPI formulations were evaluated against IV administration at each dose (0.5 and 1.0 mg/kg, respectively). This study first confirmed the lower toxicity of the CR approach, as the IR DPI formulation caused a much higher number of deaths during treatment of the grafted mice. The CR formulation administered at 1.0 mg/kg showed a higher survival than the negative control but a tumour response comparable to IV administered at half this dose (0.5 mg/kg). This unexpected outcome with regard to the PK results is explained by the fact that the tumour model is highly metastatic. Mice treated with inhaled formulations died due to distant tumour involvement, while those treated systemically died due to pulmonary tumour involvement. This led us to believe that this kind of treatment may have greater potential in combination, adjuvant to the parenteral route.

This work helped establish the proof-of-concept of a cisplatin CR DPI formulation with an up-scalable process. The SLM approach confirmed that encapsulation of drugs exhibiting low solubility, such as cisplatin, was possible using highly hydrophobic excipients and that surface modification was mandatory to provide notable lung retention *in vivo*. The SLM approach showed good signs of tolerance during the exploratory study but still needs to be confirmed under a chronic scheme using other determinants such as histopathological analyses of the lung tissue. Moreover, comparison of the nephrotoxicity of formulations

against that of the IV route should be conducted with appropriate and sensitive methods. Finally, the survival study of the CR DPI formulation showed mitigated results, partly because of the orthotopic model characteristics. This could be proof that inhaled CT has a role to play combined with classical systemic CT. This needs to be assessed in a further study.

RESUME

Le cancer du poumon est le cancer ayant le taux de mortalité le plus élevé au monde, avec un taux de survie global à 5 ans d'environ 15%. Malgré un impact notable des dernières améliorations en matière de prévention, de dépistage, et de classification du cancer du poumon, l'efficacité des traitements classiques n'est toujours pas suffisante et semble avoir atteint un plateau thérapeutique.

Ces traitements classiques comprennent de la chirurgie, de la radiothérapie et de la chimiothérapie, le plus souvent en combinaison. La chimiothérapie est utilisée à presque tous les stades: dans les stades opérables et inopérables afin de limiter l'invasion par les cellules tumorales jusqu'aux derniers stades en tant que traitement palliatif.

Le cisplatine est l'un des médicaments anticancéreux les plus fréquemment utilisés et les plus puissants actuellement disponibles. Il est administré par voie parentérale à des doses qui sont limitées par sa néphrotoxicité élevée et cumulative mais également par d'autres toxicités systémiques (par exemple, de l'ototoxicité). Son administration nécessite donc de nombreuses précautions (longue procédure d'hydratation, surveillance de la fonction rénale), ce qui mobilise fortement le personnel médical.

Une limitation importante de la chimiothérapie parentérale est la faible concentration d'actif qui atteint avec succès la tumeur ou les métastases. Une autre voie d'accès potentielle pourrait être la chimiothérapie inhalée pour traiter le cancer du poumon. Cette approche a montré une relativement bonne tolérance locale pour le cisplatine à travers différentes études précliniques et cliniques chez l'homme au moyen de solutions ou de formulations liposomales nébulisées. En tant que traitement via la voie pulmonaire, la chimiothérapie inhalée présente un avantage pharmacocinétique évident, car elle permet d'augmenter l'exposition locale tout en diminuant l'exposition systémique.

Cependant, du fait que les médicaments chimiothérapeutiques, tels que le cisplatine, soient actifs à des doses relativement élevées (dans la gamme du mg), la durée d'administration à partir des nébuliseurs s'avère en pratique très longue car elle dépend principalement de la solubilité de l'actif ou de son encapsulation dans les liposomes. Les nébuliseurs présentent également un risque élevé de contamination de l'environnement et nécessitent de lourds appareillages (hottes filtrantes en particulier) pendant la procédure d'administration.

Parmi tous les dispositifs d'inhalation existants, capables de délivrer des doses élevées de médicaments, les inhalateurs de poudre sèche (DPI) semblent être de bons candidats. Ceux-ci ont été choisis dans ce travail afin de contourner les problèmes énumérés ci-dessus, en

fournissant des doses pulmonaires plus élevées, dans des délais très courts. De plus, ces dispositifs sont activés par le flux inspiratoire du patient, ce qui pourrait aider à limiter l'exposition environnementale à des niveaux très faibles. Les inhalateurs à poudre sèche présentent également l'avantage d'être utilisables à la fois avec des médicaments solubles et des médicaments peu solubles dans l'eau.

Malgré tout, étant donné que la déposition directe de quantités élevées de médicaments chimiothérapeutiques dans le parenchyme pulmonaire pourrait présenter un risque élevé d'irritation et d'effets indésirables locaux, une libération contrôlée du cisplatine à partir de particules déposées dans le parenchyme pulmonaire s'avère nécessaire.

Cependant, dans les poumons, ces particules non dissoutes d'origine étrangère sont rapidement éliminées par les mécanismes d'élimination, en particulier par la clairance par les macrophages au niveau des alvéoles. Par conséquent, des stratégies de formulation capables de limiter la clairance des particules sont nécessaires pour assurer une résidence pulmonaire élevée de ces particules à libération contrôlée.

La stratégie de formulation de ce travail a donc consisté à développer une formulation pour inhalateur à poudre sèche à base de microparticules lipidiques solides capable de (i) être déposées dans le poumon, (ii) de contrôler la libération du cisplatine et (iii) de rester dans le poumon suffisamment longtemps dans le but d'optimiser l'indice thérapeutique (c'est-à-dire augmenter le potentiel thérapeutique du cisplatine et diminuer ses potentiels effets secondaires).

Les objectifs principaux des formulations basées sur les microparticules lipidiques solides étaient (i) de présenter des hautes charges en cisplatine au sein des microparticules lipidiques tout en présentant des propriétés aérodynamiques compatibles avec la capacité pulmonaire des patients atteints de cancer du poumon (par exemple, une fraction déposée élevée et une capacité élevée à la désagglomération sous faible débit d'air dans un inhalateur de faible résistance), (ii) de fournir une matrice capable de libérer le cisplatine de manière contrôlée *in vitro*, (iii) d'être capable de rester dans le poumon suffisamment longtemps *in vivo*, tout cela (iv) en utilisant des techniques de production ayant une bonne capacité d'augmentation d'échelle et (v) de n'utiliser que des excipients potentiellement bien tolérés au niveau du poumon.

Le cisplatine a été initialement réduit sous forme microcristalline à l'aide de cycles d'homogénéisation à haute pression jusqu'à 20 000 psi. Cette procédure a permis d'obtenir

des particules non enrobées ayant un diamètre moyen inférieur à 1.0 μm. Afin d'évaluer les capacités de libération du cisplatine des formulations à partir de la fraction capable théoriquement de se déposer dans les poumons, un nouveau test de dissolution a été adapté à partir d'un appareil à palettes classique de la pharmacopée et d'un impacteur à cascade « Fast Screening Impactor ».

Une formulation sans excipient, obtenue à partir de la suspension de cisplatine, soumise à la technique de séchage par l'atomisation (100% de cisplatine) a été produite comme point de départ. Celle-ci a ensuite été comparée à une formulation de cisplatine/tocophéryl polyéthylène glycol succinate (TPGS) (95:5), qui présentait une capacité de déposition pulmonaire *in vitro* (fraction de particules fines (FPF) de 24.2% pour la première et de 51.5% pour la deuxième, exprimée par rapport à la dose nominale). Toutes deux ont démontré des capacités de libération immédiate, avec 90% du cisplatin dissous en moins de 10 minutes.

D'autres formulations, cette fois élaborées sous la forme de microparticules lipidiques solides ont ensuite été produites à partir de la suspension microcristalline de cisplatine et de divers excipients lipidiques. Ces microparticules avaient préalablement été testées pour leur aptitude à être séchées par atomisation après solubilisation des excipients dans de l'isopropanol chaud. L'ajout d'un triglycéride, la tristéarine (TS), comme excipient lipidique principal et également d'une fraction comprenant un excipient contenant du polyéthylène glycol (PEG), à l'aide de TPGS ou de distéaroyl phosphoéthanolamine polyéthylène glycol 2000 (DSPE-mPEG-2000) a montré des résultats intéressants.

Ces formulations, ayant une teneur en cisplatine d'au moins 50%, ont présenté des aptitudes élevées pour la libération contrôlée dans le fluide pulmonaire simulé *in vitro* à 37 °C, et ce, pendant plus de 24 h (jusqu'à 56% libérées après 24 h) ainsi qu'un faible « burst-effect » (de seulement 24% et 16% après 10 minutes avec et sans excipients PEGylés, respectivement). Elles ont également montré des propriétés aérodynamiques élevées, avec une FPF élevée allant de 37.3 à 50.3% m/m par rapport à la dose nominale et un diamètre aérodynamique compris entre 2.0 et 2.4 μm. Le meilleur candidat à libération immédiate (évaluée sur base de la FPF, soit la formulation cisplatine/TPGS 95:5 m/m) et les formulations à libération contrôlée les plus prometteuses n'incluant pas d'excipients PEGylés (cisplatine/TS 50:50 m/m) et incluant des excipients PEGylés (évalués sur les capacités de libération contrôlée, c'est-à-dire la formulation cisplatin/TS/TPGS 50:49.5:0.5 m/m/m) ont ensuite été administrées à des souris CD-1, en comparaison d'une nébulisation endotrachéale d'une solution de cisplatine. Ceci a été fait à l'aide de dispositifs endotrachéaux dédiés aux poudres

pour le DP-4M© « Dry Powder Insufflator » et aux solutions pour le Microsprayer™ IA-1C© de Penn-Century. Ces formulations ont été comparées à l'injection intraveineuse (IV) au cours d'une étude pharmacocinétique étendue sur 48 heures.

L'administration de formulations de poudres sèches pour inhalation a nécessité le développement préalable d'un diluant par atomisation (Mannitol:Leucine 10:1 m/m) ainsi que d'une méthode de dilution des poudres (mélange tridimensionnel pendant 4 heures et suivi d'un double-tamisage) afin de pouvoir délivrer des quantités précises et répétables de poudre dans les poumons de souris à la dose d'1.25 mg/kg. Le suivi des paramètres pharmacocinétiques a ainsi pu être réalisé au niveau des poumons, du sang, des reins, du foie, du médiastin et de la rate des souris. Ceci a été fait à l'aide d'une méthode de spectrométrie d'absorption atomique électrothermique, qui a été préalablement développée et validée. Les résultats obtenus ont montré que l'administration endotrachéale de formulations de poudres sèches permettait d'augmenter fortement l'exposition des poumons par le cisplatine, exprimée en aire sous la courbe (AUC) tout en diminuant l'exposition systémique. Plus précisément, la seule formulation présentant une rétention pulmonaire prolongée était celle qui comprenait un excipient PEGylé (cisplatine/TS/TPGS 50:49.5:0.5 m/m/m), ce qui a été observé pendant environ 7 heures. Cette rétention pulmonaire a été associée à des profils de concentration en fonction du temps plus réguliers dans le sang (t_{max} supérieur et C_{max} inférieur), ce qui a également confirmé ses capacités de libération contrôlée *in vivo* car la perméabilité de l'épithélium pulmonaire pour le cisplatine dissous s'est avérée très élevée. L'exposition globale établie à partir de l'AUC a permis de calculer l'efficacité de ciblage (T_e: rapport de l'AUC mesurée dans les poumons et de la somme des AUC mesurées dans les organes non cibles) et l'avantage du ciblage (T_a: rapport de l'AUC mesuré dans les poumons suite à l'administration pulmonaire et de l'AUC mesurée dans les poumons suite à l'administration par la voie IV). Par exemple, le T_a de la formulation décrite ci-dessus (cisplatine/TS/TPGS 50:49.5:0.5 m/m/m) était de 10.9, comparativement à 1 pour l'IV, 3.3 pour la nébulisation endotrachéale, 2.6 pour la formulation de poudre sèche à libération immédiate (cisplatine/TPGS 95:5 w/w) et 3.7 pour la formulation de poudre sèche à libération contrôlée ne comprenant pas d'excipient PEGylé (cisplatine/TS 50:50). Dans le même temps, le T_e mesuré pour les mêmes formulations était de 1.6, 0.09, 1.1, 0.4 et 0.9, respectivement, démontrant également le rendement élevé de la voie inhalée par rapport à la voie IV dans sa capacité à cibler les poumons. Plus important encore, ceci a démontré le grand avantage des capacités de rétention pulmonaire de la formulation à libération contrôlée comprenant un excipient PEGylé.

Dans la dernière partie de ce travail, les doses maximales tolérées (DMT) des formulations ont été déterminées. Le meilleur candidat, choisi en fonction des résultats de pharmacocinétique (formulation à libération contrôlée ayant des capacités de rétention pulmonaire composé de cisplatine/TS/TPGS 50:49.5:0.5 m/m/m), avait une meilleure tolérance globale que les deux approches à libération immédiate testées (formulation de poudre sèche cisplatine/TPGS 95:5 et la nébulisation endotrachéale d'une solution de cisplatine). Plus précisément, il s'est avéré possible de doubler le dosage administré pour la formulation à libération contrôlée (1.0 mg/kg) par rapport à la poudre sèche à libération immédiate et à la nébulisation endotrachéale (toutes les deux à 0.5 mg/kg) suivant un schéma d'administration chronique (3 fois par semaine pendant 2 semaines). De plus, une évaluation de la tolérance pulmonaire de cette formulation à libération prolongée a été réalisée et comparée à la poudre sèche à libération immédiate, à la nébulisation endotrachéale et à la voie IV. Elle a été réalisée par analyse du liquide provenant du lavage broncho-alvéolaire, 24 heures après une administration unique à la dose maximale tolérée préalablement déterminée pour chaque formulation. Aucune augmentation des cytokines IL-1β, IL-6 et TNF-α n'a pu être détectée à la suite des administrations. Aucunes preuves de lésion tissulaire ou de cytotoxicité n'ont pu être observées au travers du dosage de la teneur en protéines totale et de l'activité de la lactate déshydrogénase. Les seules observations qui ont pu être faites ont été une diminution des cellules totales et une augmentation des polynucléaires neutrophiles dans le lavage broncho-alvéolaire, ce qui n'a pas été observé suite à l'administration IV ou après l'administration du véhicule de la formulation à libération contrôlée seul (c'est-à-dire les microparticules lipidiques solides PEGylées et le diluant). Cette augmentation ne semble pas liée aux microparticules lipidiques solides ou au diluent mais probablement à l'exposition pulmonaire au cisplatine, car cette augmentation a été observée pour chaque groupe inhalé contenant du cisplatine.

Le cisplatine a ensuite été administré à des souris qui ont été greffées de manière orthotopique par une lignée murine de carcinome pulmonaire M109-HiFR, modèle préclinique préalablement développé au sein de notre laboratoire. Les formulations de poudres sèches ont été évaluées par rapport à l'administration IV à chaque dose testée (0.5 et 1.0 mg/kg, respectivement). Cette étude a d'abord confirmé la toxicité plus faible de l'approche à libération contrôlée, car la formulation à libération immédiate a causé un nombre beaucoup plus élevé de décès pendant le traitement des souris greffées. La formulation à libération contrôlée administrée à 1.0 mg/kg, a montré une survie plus élevée que le contrôle négatif, mais une réponse comparable à la dose IV administrée à la moitié de la dose (0.5 mg/kg). Ce résultat inattendu par rapport aux résultats de l'étude

pharmacocinétique s'explique probablement par le fait que le modèle de tumeur utilisé est hautement métastatique. Les souris traitées avec des formulations inhalées sont mortes en raison de tumeurs secondaires distantes par rapport à la tumeur primaire implantée au niveau du poumon, alors que celles traitées par la voie systémique sont mortes en raison d'un envahissement tumoral pulmonaire. Cela nous amène à penser que ce type de traitement inhalé pourrait avoir un plus grand potentiel en combinaison à la voie parentérale.

Ce travail a ainsi permis d'établir la preuve du concept de formulation à base de poudre sèche de cisplatine à libération contrôlée, en utilisant un processus de fabrication capable de subir une mise à l'échelle industrielle. L'utilisation de microparticules lipidiques solides a confirmé que l'encapsulation d'actifs présentant une certaine hydrophilie, comme le cisplatine, était possible en utilisant des excipients hautement hydrophobes et qu'une modification de leur surface était cependant obligatoire pour obtenir une rétention pulmonaire intéressante *in vivo*. Les microparticules lipidiques solides ont montré de bons signes de tolérance au cours de l'étude exploratoire, mais celle-ci doit encore être confirmée avec une administration chronique des poudres. Ceci doit être fait en suivant des paramètres supplémentaires, tels que des analyses histologiques du tissu pulmonaire. De plus, la comparaison de la néphrotoxicité des formulations avec celle mesurée par la voie IV doit être effectuée avec des méthodes appropriées et sensibles. Enfin, l'étude de survie de la formulation à libération prolongée a montré des résultats mitigés, en partie à cause des caractéristiques du modèle orthotopique de tumeur pulmonaire. Cependant, il semblerait que la chimiothérapie inhalée à un rôle important à jouer en combinaison avec la chimiothérapie systémique classique. Ceci doit être évalué dans une étude future.

INTRODUCTION
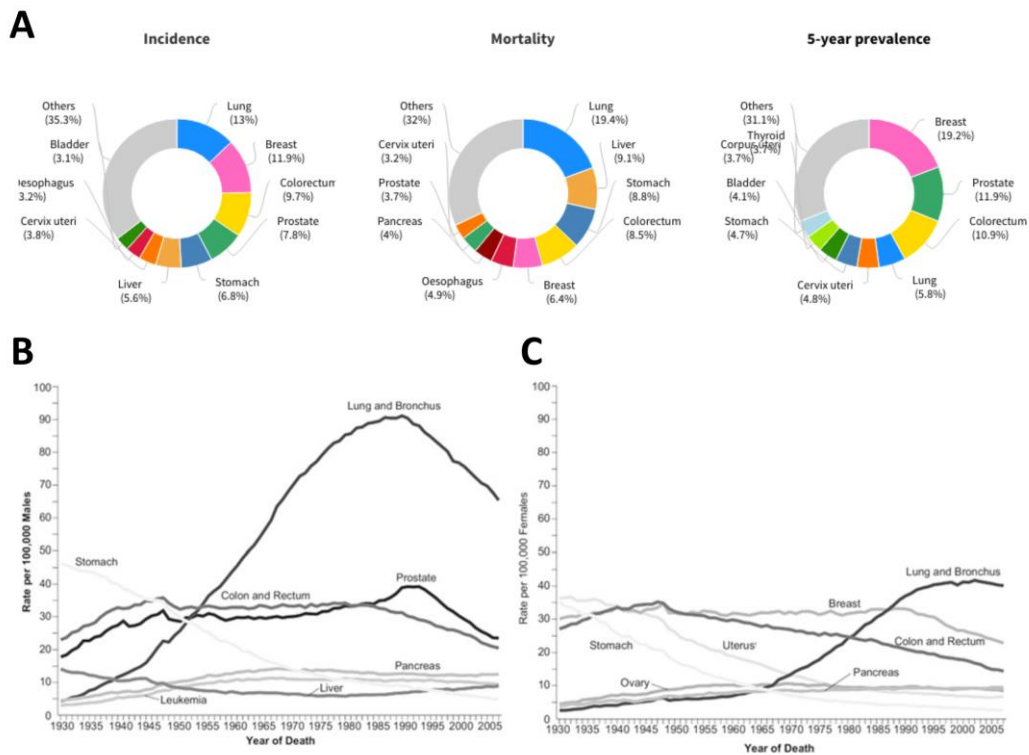
Figure 1.A. Incidence, mortality and 5-year prevalence of major primary cancers in both sexes worldwide in 2012. Annual age-adjusted cancer death rates in the US among men. **B.** and women **C.** for major cancers (age-adjusted to the 2000 US standard population), from Siegel et al. (2011) and from Ferlay et al. (2015)
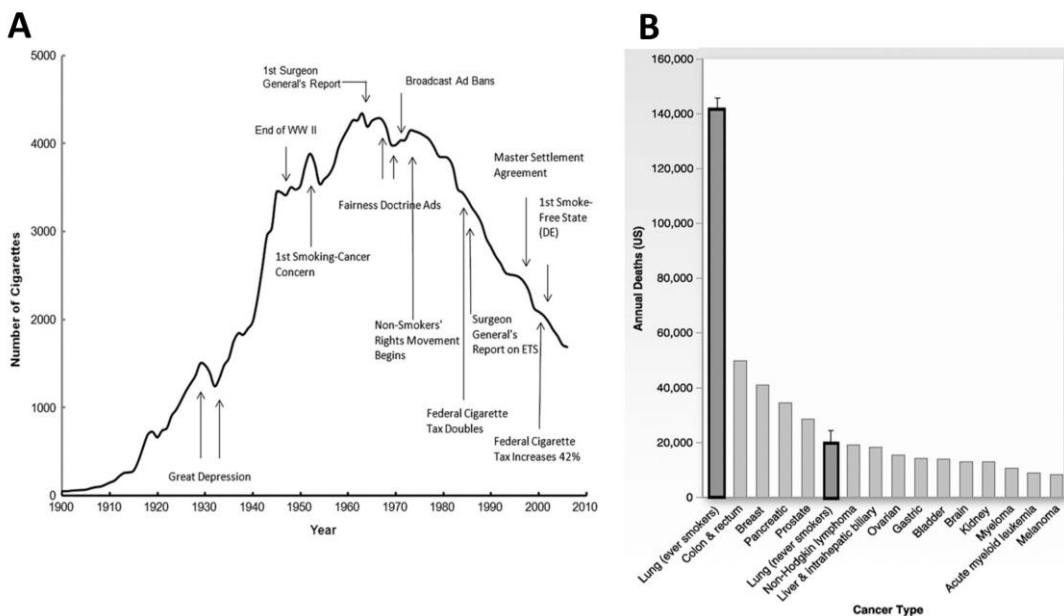
Figure 2.A. Per capita cigarette consumption in the United States, 1900–2006, with historical highlights from Warner and Mendez (2010) **B.** Common causes of death by cancer in the US with focus on never-smokers from Rudin et al. (2009) and Dela Cruz et al. (2011).

1. Lung cancer

1.1. Epidemiology, historical background and risk factors

Lung cancer is the commonest cause of death from cancer **(Figure 1.A)** in the world. The latest statistics, collected in 2012 (Ferlay et al., 2015), show that lung cancers altogether cause the death of 1.6 million people worldwide on a yearly basis and that each year, more than 1.8 million new cases are detected in both men and women **(Figure 1.A)**. The global lung cancer incidence trend reflects the mortality trend **(Figure 1.B, 1.C)** as most lung cancer patients die from the illness in a relatively short timeframe after detection. In Europe in 2012, it is estimated that of 3.4 million detected cancer cases, 409 900 were lung cancers (11.9%) and that of 1.7 million deaths from cancer, 353 500 were from lung cancer (20.1%) (Ferlay et al., 2013). In Belgium in 2012, the estimates are that of 65 345 detected cancers, 7 794 were lung cancers (11.9%) and that of 29 815 deaths from cancer, 7 179 were from lung cancers (24.1%) (Ferlay et al., 2013). The 5-year prevalence (5.8%, **Figure 1.A)** and the global 5-year survival rates are also very low for lung cancer (~15% in developed countries and reaching even lower levels in developing countries), especially when put in contrast with the other most frequent cancers (colon: 66%; skin-melanoma: 93%; breast: 90%; prostate: 100%). This survival rate is, however, widely variable among patients as it is contingent on the age, type and stage of lung cancer at the time of diagnosis (Dela Cruz et al., 2011).

The 1964 Surgeon General's "Smoking and Health" report (United States. Surgeon General's Advisory Committee on Smoking and Health., 1964) was the first official document to link smoking and poor health, including lung cancer and heart diseases **(Figure 2.A)**. The vast majority of lung cancers are now undoubtedly attributed to cigarette smoking, with 86% of cancers linked to active and passive smoking caused by the carcinogens contained in cigarette smoke (e.g. nitrosamines, cyanides, benzene) (Alberg et al., 2007, Secretan et al., 2009). Other risk factors include a history of lung disease (e.g. tuberculosis, chronic obstructive pulmonary disease (COPD)), a family history of lung cancer and exposure to other inhaled carcinogens such as asbestos (3-4%), diesel particles or radon gas. Yet, although smoking remains the major cause of cancer death in the US, lung cancer-related deaths from other causes (in never-smokers) are also frequent **(Figure 2.B)**.
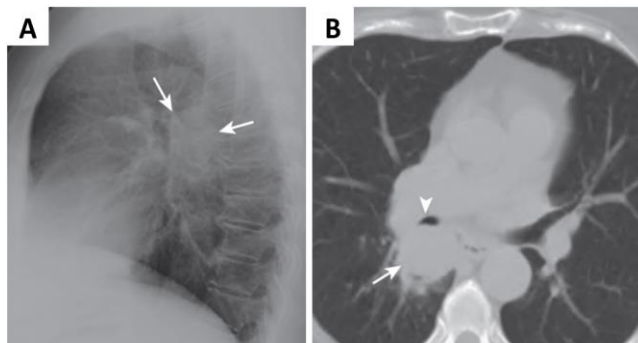
Figure 3.A. Lateral chest radiograph showing an abnormality (mass) in the hilar region, confirmed by **B.**, an axial chest CAT scan, and later determined as being a bronchogenic carcinoma, from Gotway et al. (2016).

Nevertheless, the incidence and mortality trends of lung cancer mainly follow the cigarette consumption pattern **(Figure 2.A)**, and the main lung cancer trend began in the 1960s and peaked in the 1980s-1990s for men in developed countries **(Figure 1.B)**. A comparable trend was observed later for women **(Figure 1.C)**, with a 10-20 year lag due to the increased social acceptance of women smoking. The current sex ratio (M:F) of lung cancer incidence is around 2.7 (Travis et al., 2015a).

Lung cancer prevalence has significantly decreased in developed countries in the last few decades and is slowly decreasing in less developed ones thanks to prevention through aggressive anti-tobacco campaigns **(Figure 2.A)**, screening for high-risk patients (see 1.2.2.) and earlier and more precise diagnosis (see 1.2.3. Diagnosis). Despite the development of new targeted therapies, suitable for very small subsets of patients, and the subsequent adapted classifications (see 1.2.4. Staging), treatment efficacy now seems to have reached a therapeutic plateau (Gridelli et al., 2003).

1.2. Symptoms, screening, diagnosis and staging

1.2.1. Symptoms

The primary symptoms in patients with detected lung cancer or metastatic cancer to the lungs comprise most often evolutive shortness of breath, cough, chest pain, weight loss, rust-coloured sputum, hoarseness of voice or recurrent pneumonia. About 5-20% of lung cancers are asymptomatic at detection, which is done through screening (see 1.2.2. Screening). Some patients present worse symptoms linked to distant metastases, and a disseminated disease sometimes involving distant organs such as the central nervous system, with neurologic symptoms, or the gut and the bones. Paraneoplastic symptoms are also observed with neuroendocrine tumours due to their inherent secretion activity (e.g. antidiuretic hormone, adrenocorticotropic hormone) (Travis et al., 2015a).

1.2.2. Screening

Screening consists of testing for lung cancer when there are no symptoms of the disease. For lung cancer, screening is usually done through medical imaging, classically using computed assisted tomography scans (CAT scans) **(Figure 3)**. Yearly screening is now indicated for the subset of patients with a history of heavy smoking, established as 30 pack-years or more, (a pack-year is equivalent to 1 pack of cigarettes per day for 1 year), who are currently smoking or have quit within the last 15 years and are aged between 55 and 80 years old. The indications for a yearly screening can also include patients above 50 years old who have smoked 20 packs-years and have one additional risk factor, such as those listed above
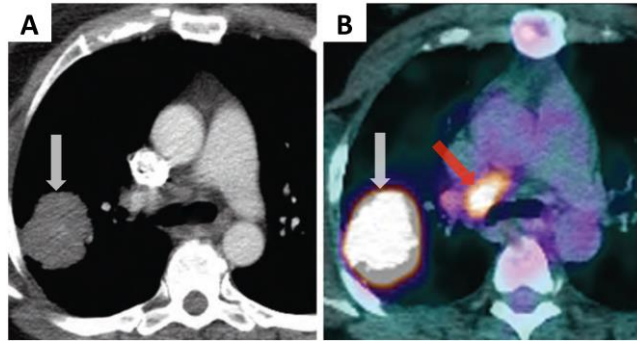
Figure 4. Patient with non-small cell lung cancer (NSCLC), with a large mass in the right lobe (white arrow), **A.** observed by CAT scan and **B.** by PET scan, exhibiting the right lung neoplasm and involvement of a paratracheal lymph node (red arrow), from Gotway et al. (2016).
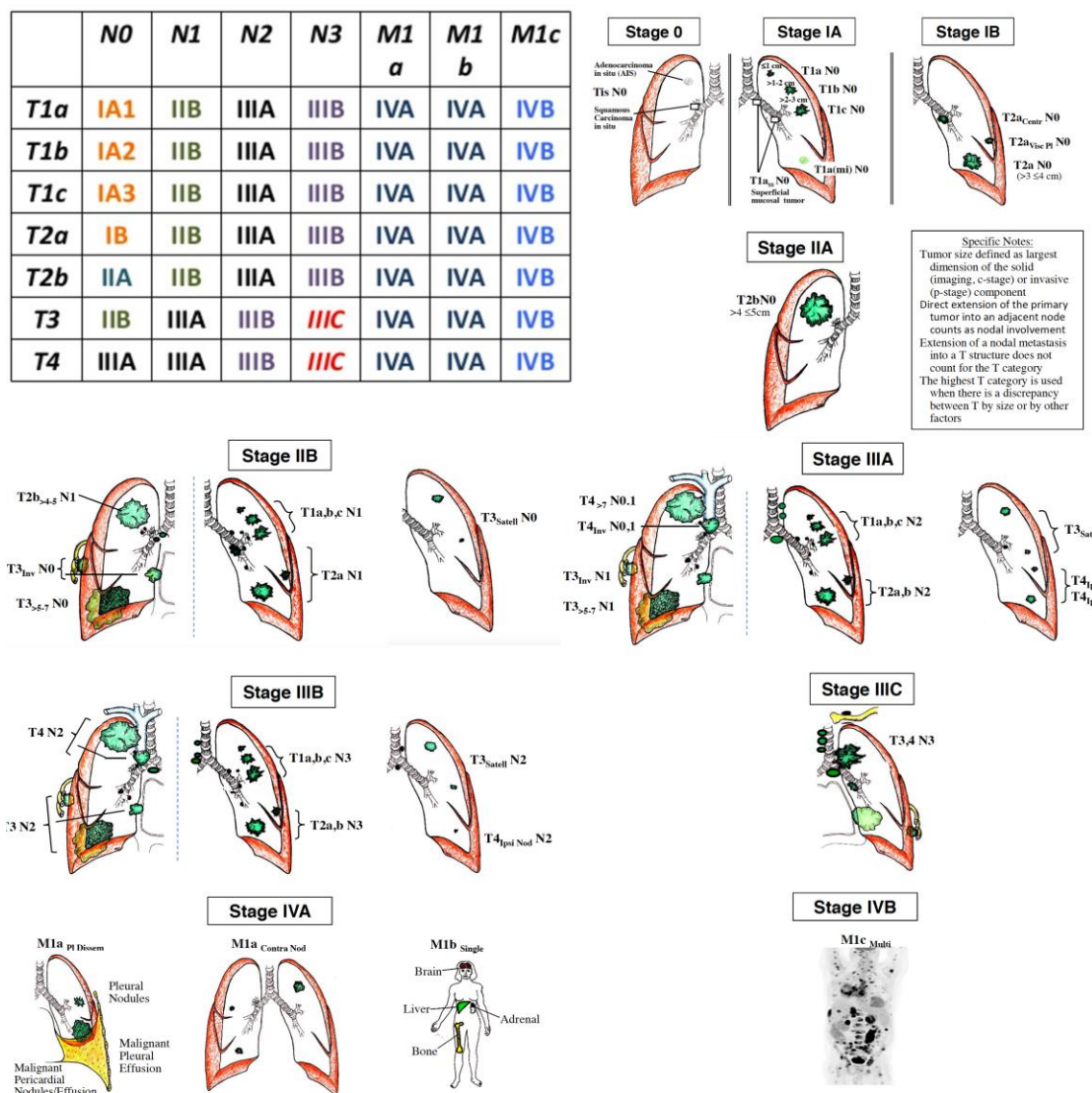
Figure 5. Stage groups for NSCLC according to the 8th TNM classification (upper left table), and graphic illustrations of the different T, N and M descriptors for stages 0 to IV NSCLC, from Detterbeck et al. (2017).

(e.g. history of lung disease, family history of lung cancer and exposure to other inhaled carcinogens) (NCCN, 2015). Screening of these high-risk patients is of tremendous importance to increase overall survival, as cancer is easier to cure when detected at the early stages. Some studies showed up to 80-85% of detected cancers at early stages using this systematic screening approach, despite a very high number of false positives (Henschke et al., 2001, The International Early Lung Cancer Action Program Investigators, 2006). For instance, this approach led to a 10-year survival rate of 88% for patients diagnosed at early stages (The International Early Lung Cancer Action Program Investigators, 2006). The clinical question, if screening for lung cancer is positive, is then to determine the type of lung tumour, and the stage of the disease as they are the major determinants of prognosis and treatment modalities (NCCN, 2014b, NCCN, 2015, Detterbeck et al., 2017).

1.2.3. Diagnosis

Diagnosis of lung cancer is based on imaging using chest radiographs, CAT scans and, if necessary positron emission tomography scans (PET scans) and biopsies **(Figure 3, Figure 4)**. CAT scans help assessing the extent of the tumour and the involvement of the lung periphery (mediastinum, chest walls, vascular structures) as well as the mediastinal lymph nodes (Gotway et al., 2016). PET scans, using radiolabelled fluorodeoxyglucose ^{18}F-FDG, exhibit the activity of the malignant cells through their increased glucose consumption **(Figure 4.B)** (Vansteenkiste et al., 2016). Biopsies of the tumorous tissue are done using fibre-optic bronchoscopy in order to obtain a tissue sample and establish the histologic features of the tumour. Bronchoscopy, thoracoscopy, mediastinoscopy and other biopsy procedures such as fine-needle aspiration are not very invasive and show high sensitivity and specificity for most cancers (Küpeli et al., 2016).

1.2.4. Staging

A universally shared cancer staging system has been a prominent topic among clinicians since the first tumour, node, metastasis (TNM) classification by P. Denoix in the 1950s at the Gustave-Roussy Institute (Denoix, 1946). A shared system is now used by physicians to classify all cancers. The International Association for the Study of Lung Cancer (IASLC) edits the TNM classification for lung cancer every seven years, based on the latest studies, by and for clinicians worldwide. TNM is typically based on the anatomical evaluation of the tumour and its expansion and is the basis for the prognosis and selection of therapy **(Figure 5)**. The 8th and latest major edition of the TNM (January 2017) is based on clinical observations among thousands of cancer patients (Detterbeck et al., 2017). Each letter of the TNM is associated with an alphanumerical number from 0 to 4, describing the size or the

Table 1. Stage and 5-year survival rate in NSCLC, adapted from (Detterbeck et al., 2017).

Stage (clinical)	5-year survival rate (%)
Ia1	92
1a2	83
1a3	77
Ib	68
IIa	60
IIb	53
IIIa	36
IIIb	26
IIIc	13
IVa	10
IVb	0
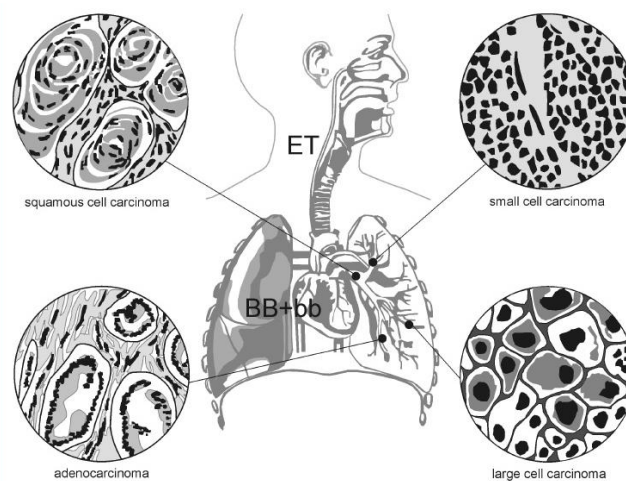
Figure 6. Principal sites of tumour formation for the main lung cancer types, from Sturm (2011).
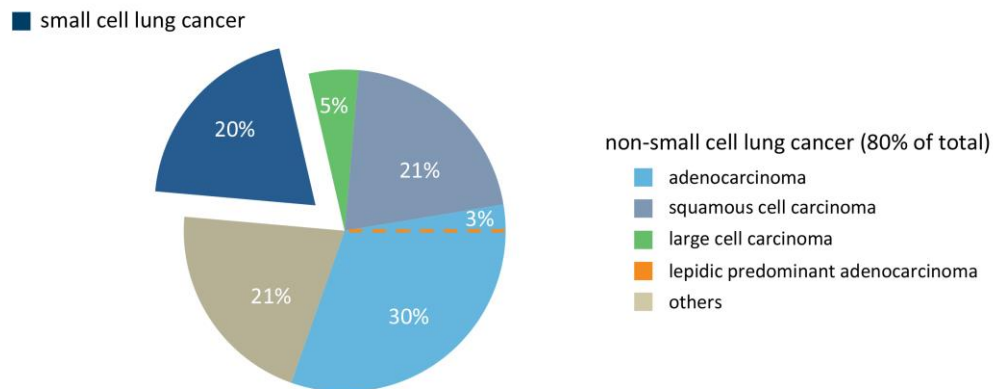
Figure 7. Lung cancers epidemiological distribution classified based on their histological features, adapted from Morgensztern et al. (2010).

extent of each parameter. The T (tumour) parameter is established from the dimensions of the primary tumour and its expansion to contiguous structures, for instance the mediastinum or the chest wall. The N (node) staging represents the extent of spread to regional lymph nodes. The M staging defines the presence of metastases apart from regional lymph nodes (solitary or multiple). Global stages of lung cancer are then classified from 0 to IV, based on each T, N and M involvement (Mountain and Dresler, 1997, Detterbeck et al., 2009, Rami-Porta et al., 2009, Detterbeck et al., 2017). Early stages show the best outcome, with a 5-year survival rate above 38% up to stage IIa, and later stages show the worst outcome, with a 5-year survival rate often below 5% at stages IIIb up to IVb **(Table 1)**

1.3. Primary lung cancer

Lung cancers are classified as primary and secondary tumours that either originate directly from the lung or from loco-regional and distant metastases from the lung or others organs, respectively. Primary lung tumours can originate in the peripheral lung (deep lung parenchyma) or more centrally in the upper conducting airways (large bronchi) and can be classified based on their histological features **(Figure 6).**

Among primary tumours, lung cancers have been historically divided into small cell lung cancer (SCLC) and non-small cell lung cancer (NSCLC). SCLC is the least common (~15%) and most aggressive type and includes small cell carcinoma and the combined subtype (displaying primarily heterogenic small and at least 10% non-small cells). NSCLC is much more frequent (~85%) and includes different subtypes such as adenocarcinoma, squamous cell carcinoma, large cell carcinoma and others **(Figure 7)** (Travis et al., 2015b). This classification is the basis for the clinical evaluation and treatment approach of lung cancer and is being constantly reevaluated. With the influence of immunohistochemistry staining and genetic evaluation of biopsies and resected specimens, and the development of new targeted therapies, classification is evolving toward a more specific evaluation of the patient's neoplasm (e.g. cell types and proportion in the tumour, genetic properties). The 2015 World Health Organization (WHO) histological classification of lung tumours **(Figure 8)** focuses on these aspects in order to push for the development of more personalized treatment strategies (Travis et al., 2015b).

1.3.1. Non-small cell lung cancer (NSCLC)

NSCLC represents the vast majority of lung cancers (~87% in the US in 2008 (Morgensztern et al., 2010)) and is characterized by two major types: non-squamous carcinoma and squamous carcinoma (Travis et al., 2015b). While other cancer types show a decreasing

Malignant epithelial tumours

Squamous cell carcinoma	8070/3
Papillary	8052/3
Clear cell	8084/3
Small cell	8073/3
Basaloid	8083/3
Small cell carcinoma	8041/3
Combined small cell carcinoma	8045/3
Adenocarcinoma	8140/3
Adenocarcinoma, mixed subtype	8255/3
Acinar adenocarcinoma	8550/3
Papillary adenocarcinoma	8260/3
Bronchioloalveolar carcinoma	8250/3
Nonmucinous	8252/3
Mucinous	8253/3
Mixed nonmucinous and mucinous or indeterminate	8254/3
Solid adenocarcinoma with mucin production	8230/3
Fetal adenocarcinoma	8333/3
Mucinous ("colloid") carcinoma	8480/3
Mucinous cystadenocarcinoma	8470/3
Signet ring adenocarcinoma	8490/3
Clear cell adenocarcinoma	8310/3
Large cell carcinoma	8012/3
Large cell neuroendocrine carcinoma	8013/3
Combined large cell neuroendocrine carcinoma	8013/3
Basaloid carcinoma	8123/3
Lymphoepithelioma-like carcinoma	8082/3
Clear cell carcinoma	8310/3
Large cell carcinoma with rhabdoid phenotype	8014/3
Adenosquamous carcinoma	8560/3
Sarcomatoid carcinoma	8033/3
Pleomorphic carcinoma	8022/3
Spindle cell carcinoma	8032/3
Giant cell carcinoma	8031/3
Carcinosarcoma	8980/3
Pulmonary blastoma	8972/3
Carcinoid tumour	8240/3
Typical carcinoid	8240/3
Atypical carcinoid	8249/3
Salivary gland tumours	
Mucoepidermoid carcinoma	8430/3
Adenoid cystic carcinoma	8200/3
Epithelial-myoepithelial carcinoma	8562/3
Preinvasive lesions	
Squamous carcinoma *in situ*	8070/2
Atypical adenomatous hyperplasia	
Diffuse idiopathic pulmonary neuroendocrine cell hyperplasia	

Mesenchymal tumours

Epithelioid haemangioendothelioma	9133/1
Angiosarcoma	9120/3
Pleuropulmonary blastoma	8973/3
Chondroma	9220/0
Congenial peribronchial myofibroblastic tumour	8827/1
Diffuse pulmonary lymphangiomatosis	
Inflammatory myofibroblastic tumour	8825/1
Lymphangioleiomyomatosis	9174/1
Synovial sarcoma	9040/3
Monophasic	9041/3
Biphasic	9043/3
Pulmonary artery sarcoma	8800/3
Pulmonary vein sarcoma	8800/3

Benign epithelial tumours

Papillomas	
Squamous cell papilloma	8052/0
Exophytic	8052/0
Inverted	8053/0
Glandular papilloma	8260/0
Mixed squamous cell and glandular papilloma	8560/0
Adenomas	
Alveolar adenoma	8251/0
Papillary adenoma	8260/0
Adenomas of the salivary gland type	
Mucous gland adenoma	8140/0
Pleomorphic adenoma	8940/0
Others	
Mucinous cystadenoma	8470/0

Lymphoproliferative tumours

Marginal zone B-cell lymphoma of the MALT type	9699/3
Diffuse large B-cell lymphoma	9680/3
Lymphomatoid granulomatosis	9766/1
Langerhans cell histiocytosis	9751/1

Miscellaneous tumours

Harmatoma	
Sclerosing hemangioma	8832/0
Clear cell tumour	8005/0
Germ cell tumours	
Teratoma, mature	9080/0
Immature	9080/3
Other germ cell tumours	
Intrapulmonary thymoma	8580/1
Melanoma	8720/3

Metastatic tumours

Figure 8. World Health Organization (WHO) histological classification of tumours of the lungs, from Travis et al. (2015a).

incidence globally, adenocarcinomas (a non-squamous carcinoma), which originate deeper in the lower airways (i.e. terminal bronchioles and alveoli), shows a stabilized trend (Morgensztern et al., 2010). This has been linked to broader use of low-tar filter cigarettes, which are responsible for less irritation and are inhaled deeper, exposing more profound structures such as the bronchioalveolar epithelium to carcinogens (Morgensztern et al., 2010). Survival rates of NSCLC vary depending on the stage **(Table 1)** and cancer type, as well as recent genetic prognostic factors, which are described below. In the following section, only malignant lung tumours, based on histological considerations will be discussed.

1.3.1.1. NSCLC sub-types

1.3.1.1.1. Adenocarcinoma

Adenocarcinoma is the most common type of NSCLC, both in non-smokers and heavy smokers. It represents approximately 37.5% of NSCLC (Morgensztern et al., 2010). Its growth is slower than other types of lung cancer but can metastasize at earlier stages. It is primarily located in the peripheral lung, where it often presents mixed histologic patterns. These heterogeneous carcinomas, reported unilaterally as "mixed adenocarcinomas" until recently (80% of resected adenocarcinomas), are now reported by clinicians with a quantitative evaluation of each type of observed cell, with the predominant pattern defining the name of the pathology. A thorough histologic determination of the sampled tumour, obtained after resection if operable or on a small biopsied sample is necessary for an adequate prognosis evaluation (Travis et al., 2015a).

The most frequent histological subtypes are lepidic (showing neoplastic cells along the alveolar lining), acinar (showing glandular formation), papillary (with fibrovascular structures and tumour cells replacing the alveolar lining), micropapillary (showing ill-defined clusters and no fibrovascular structures), solid (showing solid sheets of tumour) and others (Travis et al., 2015b). The lepidic subtype, recently reclassified as adenocarcinoma *in situ* (AIS) by the IASLC can be either minimally invasive or invasive. Its presentation can be either non-mucinous (mostly in smokers) showing the best chance for cure or mucinous (in non-smokers, women and Asian people) and associated with a poor prognosis. This sub-type originates from Clara cells and type II pneumocytes and has the particularity of being of aerogenous spread and is therefore often scattered throughout the lung (pneumonic multifocal or diffuse presentation). The cause of death associated with this cancer sub-type is therefore often caused by bilateral pulmonary involvement as opposed to the other lung cancer sub-types (for which death is most often caused by distant tumour spread). Moreover it shows particularly low responses with conventional chemotherapy (see 1.3.1.2.3.)
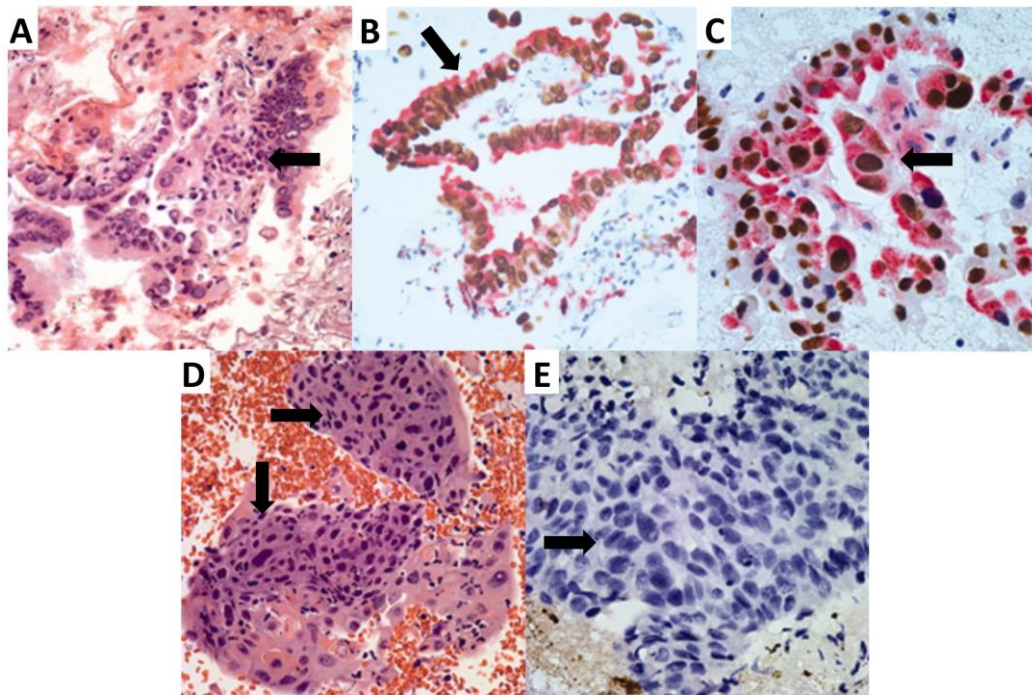
Figure 9. Histologic features of malignant lung adenocarcinomas: **A.** under a classical haematoxylin and eosin stain (× 40) and **B.** under immunohistochemistry with a combined double stain TTF-1/Napsin A (× 40) and **C.** (× 60), compared to **D.** a malignant squamous cell carcinoma under a haematoxylin and eosin stain (× 40) and a negative staining for TTF-1/Napsin A (× 60), from Fatima et al. (2011).
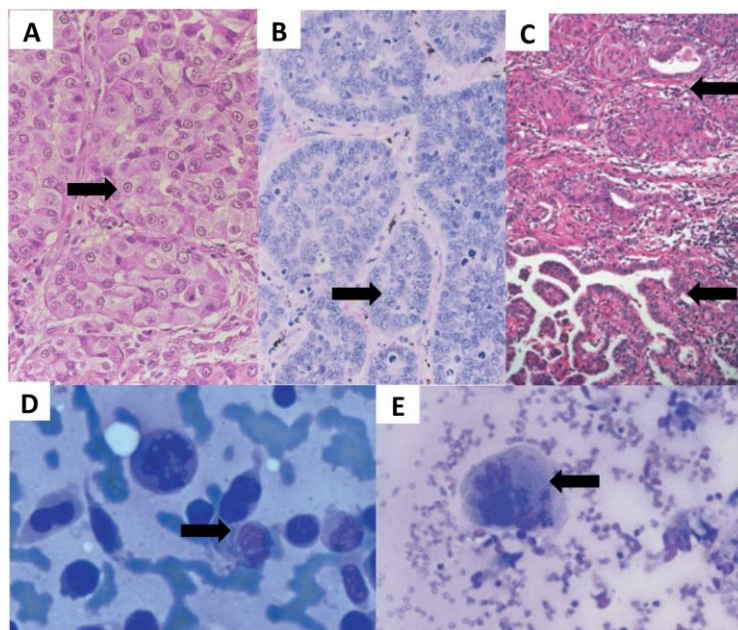
Figure 10. Histologic features of **A.** large cell carcinoma and **B.** large cell neuroendocrine carcinoma, showing endocrine features (palisading and a central rosette), **C.** adenosquamous carcinoma with squamous cells (top) and papillary adenocarcinoma cells (bottom), and **D.** sarcomatoid carcinomas with a pleomorphic carcinoma and **E.** giant cell carcinoma exhibiting a very big solitary central cell, from Travis et al. (2015a).

(Cadranel et al., 2010, Tang et al., 2014, Travis et al., 2015a, Weingertner and Chenard, 2015). All the other subsets of adenocarcinoma are considered invasive and have a poor prognosis (Goldstraw et al., 2011, Travis et al., 2011).

Microscopically, adenocarcinoma cells, which generally originate from mucus cells (and occasionally from non-ciliated bronchioalveolar cells), can be differentiated with classical haematoxylin-eosin staining as these are generally mucin positive. Immunohistochemistry of adenocarcinoma is becoming more and more standard. For instance using a combined double staining for the thyroid transcription factor-1 (TTF-1) for the nucleus and Napsin A for the cytoplasm are very helpful markers to ensure differentiation of adenocarcinoma fromsquamous cell carcinoma, with a reported predictive value of 89% **(Figure 9)** (Fatima et al., 2011).

1.3.1.1.2.Squamous cell carcinoma

Squamous cell carcinomas are seen in 21% of all cancers and 27% of NSCLC (Morgensztern et al., 2010). Of these cancers, 90% are seen in smokers. They are often located in the central region of the lung as they often arise from the bronchial epithelium and frequently show keratinization and/or intercellular junctions.

Microscopically, cells are isolated, with irregular shape, hyper chromatic nuclei and abundant cytoplasm **(Figure 10.C)**. Some differentiated cells exhibit keratinization **(Figure 9.D, E)** (Travis et al., 2015a). Some squamous cell carcinomas derive from these main descriptors, including the papillary, clear cell, small cell and basaloid subsets.

Squamous cell carcinoma is locally aggressive, involving contiguous structures and metastases are mostly loco-regional.

The prognosis for this subtype of NSCLC is better than adenocarcinoma at each stage, for instance with a 5-year survival rate of 80% *vs.* 70% for the latter at the same resected stage I (Travis et al., 2015a).

1.3.1.1.3.Large cell carcinoma

Large cell carcinoma has been reported in up of 9% of all lung cancers (Travis et al., 2015a). At the time of diagnosis, 34% of patients exhibit localised disease (stages I, II), 28% of patients exhibit locally advanced disease (stages IIIA, IIIB) and 38% exhibit metastatic disease (stage IV) (Travis et al., 2015a). They are mostly seen in smokers. They represent a lung cancer subtype with no specific histological features (such as squamous, neuroendocrine or glandular differentiation) as compared to squamous cell carcinoma, adenocarcinoma or SCLC. They are generally situated in peripheral regions of the lung, except for the basaloid subtype.

Large cell neuroendocrine carcinoma was first described in 1991 and was integrated into the 1999 World Health Organization classification. These represent up to 3% of lung cancers and are also mostly seen in smokers. They differ from large cell carcinoma by their neuroendocrine features and exhibit a worse prognosis. They are often detected at later, metastasized stages.

Microscopically, large cell carcinomas present large, atypical polygonal cells, with vesicular nuclei and average sized cytoplasm **(Figure 10.A)**. Biopsies are often inconclusive and full resection of the tumour is often needed for a complete diagnosis (Pelosi et al., 2015).

As with adenocarcinoma, their classification is being revised as modern immunohistochemistry staining (TTF-1 expression in 50% of neuro-endocrine tumours) and genetic characterization are developed (Pelosi et al., 2015).

Large cell neuroendocrine carcinomas are large cells with evidence of differentiation. They also have more specific structures than large cell carcinomas, showing their endocrine features such as rosettes and palisading patterns **(Figure 10.B)** (Travis et al., 2015a). Some subtypes are described, including the basaloid carcinoma, clear-cell carcinoma, lymphoepithelioma-like carcinoma and rhabdoid phenotypes (Travis et al., 2015a).

Other forms of malignant lung tumours can also be observed. Among them, are adenosquamous carcinoma **(Figure 10.C)**, a mixed tumour type exhibiting squamous cell carcinoma and adenocarcinoma, with at least 10% of each sub-type. This type is observed in 0.4-4.0% of primary lung cancers. It is commonly located in the peripheral lung and is very close to the clinical presentation of adenocarcinoma. Its origin is believed to be a pluripotent bronchial cell, explaining the mixed cellular presentation. This type of cancer mostly involves smokers. It metastasizes quickly and has a poor prognosis, with a 5-year survival rate of 21%, which is worse than adenocarcinoma or squamous cell carcinoma. Resectable tumours have a better 5-year survival rate than non-resectable tumours (62.5% *vs.* 35%) (Travis et al., 2015a).

Sarcomatoid carcinoma, which is another NSCLC subtype, is very uncommon (0.3-1.3% of lung cancer patients) and is a very aggressive form of lung cancers with a 5-year survival rate of 20% (Travis et al., 2015a). It includes five histologic subtypes, defined according to the cell morphology. These include pleomorphic **(Figure 10.D)**, spindle cell and giant cell carcinomas **(Figure 10.E)**, carcinosarcoma and pulmonary blastoma. This cancer is also highly correlated to cigarette smoking and to a lesser extent to asbestos. They can be located in the central or the peripheral lung, with a tendency to be located in the upper lobes

Table 2. CT recommendations in the US, following the National Comprehensive Cancer Network 2015 guidelines for NSCLC, from NCCN (2015).

Non-Small Cell Lung Cancer (NSCLC)	
Chemotherapy Regimens For Neoadjuvant and Adjuvant Therapy	
REGIMEN	**DOSING**
Cisplatin + vinorelbine	**Days 1 and 8:** Cisplatin 50mg/m² IV <u>plus</u> **Days 1, 8, 15 and 22:** Vinorelbine 25mg/m² IV. Repeat cycle every 4 weeks for 4 cycles. 　**OR** **Day 1:** Cisplatin 100mg/m² IV <u>plus</u> **Days 1, 8, 15 and 22:** Vinorelbine 30mg/m² IV. Repeat cycle every 4 weeks for 4 cycles. 　**OR** **Day 1:** Cisplatin 75–80mg/m² <u>plus</u> **Days 1 + 8:** Vinorelbine 25–30mg/m². Repeat every 3 weeks for 4 cycles.
Cisplatin + etoposide	**Day 1:** Cisplatin 100mg/m² IV <u>plus</u> **Days 1–3:** Etoposide 100mg/m² IV. Repeat cycle every 4 weeks for 4 cycles.
Cisplatin + vinblastine	**Days 1, 22, 43, 64:** Cisplatin 80mg/m² IV. **Days 1, 8, 15, 22, 29, and then every 2 weeks after day 43:** Vinblastine 4 mg/m². Repeat every 3 weeks for 4 cycles.
Cisplatin + gemcitabine	**Day 1:** Cisplatin 75mg/m² IV <u>plus</u> **Days 1 and 8:** Gemcitabine 1,250mg/m² IV. Repeat cycle every 3 weeks.
Cisplatin + docetaxel	**Day 1:** Docetaxel 75mg/m² IV + cisplatin 75mg/m² IV. Repeat every 3 weeks for 4 cycles.
Cisplatin + pemetrexed	**Day 1:** Cisplatin 75mg/m² IV + pemetrexed 500mg/m² IV. Repeat every 3 weeks for 4 cycles.
For patients with comorbidities or patients not able to tolerate cisplatin	
Paclitaxel + carboplatin	**Day 1:** Paclitaxel 200mg/m² IV + carboplatin AUC=6 IV. Repeat cycle every 3 weeks for 4 cycles.
Concurrent Chemotherapy/Radiotherapy (RT)	
Cisplatin + etoposide (preferred regimen)	**Days 1, 8, 29 and 36:** Cisplatin 50mg/m² IV <u>plus</u> **Days 1–5 and 29–33:** Etoposide 50mg/m² IV <u>plus</u> Concurrent thoracic radiotherapy 1.8Gy/day for 5 days/week (total dose, 61Gy).
Cisplatin + vinblastine (preferred regimen)	**Days 1 and 29:** Cisplatin 100mg/m² IV <u>plus</u> **Days 1, 8, 15, 22 and 29:** Vinblastine 5mg/m² IV with concurrent thoracic radiotherapy (total dose, 60Gy).
Carboplatin + pemetrexed (nonsquamous)	**Day 1:** Carboplatin AUC 5 IV <u>plus</u> **Day 1:** Pemetrexed 500 mg/m² IV with concurrent thoracic radiotherapy. Repeat every 3 weeks for 4 cycles.
Cisplatin + pemetrexed (nonsquamous)	**Day 1:** Cisplatin 75 mg/m² IV. **Day 1:** Pemetrexed 500 mg/m² IV with concurrent thoracic radiotherapy. Repeat every 3 weeks for 3 cycles.
Sequential Chemotherapy/ Radiotherapy (RT)	
REGIMEN	**DOSING**
Cisplatin + vinblastine	**Days 1 and 29:** Cisplatin 100mg/m² IV. **Days 1, 8, 15, 22 and 29:** Vinblastine 5mg/m² IV; <u>followed by</u> thoracic radiotherapy with 60Gy in 30 fractions beginning on Day 50.
Paclitaxel + carboplatin	**Day 1:** Paclitaxel 200mg/m² IV over 3 hours + carboplatin AUC=6 IV over 1 hour. Repeat every 3 weeks for 2 cycles; <u>followed by</u> thoracic radiotherapy 63Gy beginning on Day 42.
Concurrent Chemotherapy/ Radiotherapy (RT) Followed by Chemotherapy	
Paclitaxel + carboplatin	**Day 1 (weekly):** Paclitaxel 45–50mg/m² IV and carboplatin AUC=2 IV. Concurrent thoracic radiotherapy; <u>followed by</u> two additional cycles of paclitaxel 200mg/m² IV and carboplatin AUC=6 IV.
Cisplatin + etoposide	**Days 1, 8, 29, and 36:** Cisplatin 50mg/m² IV. **Days 1–5, 29–33:** Etoposide 50mg/m² IV with concurrent thoracic radiotherapy; <u>followed by</u> two additional cycles of cisplatin 50mg/m² IV and etoposide 50mg/m² IV.

(Figure 6). They metastasize to the same sites as NSCLC but also to rarer sites such as the oesophagus, rectum or kidneys (Travis et al., 2015a).

Finally, very rare forms of tumours, such as lymphoproliferative tumours, harmatoma, sclerosing hemangioma, clear cell tumours, germ cells tumours including teratomas, intrapulmonary thymoma and melanoma can also be observed (Travis et al., 2015a).

1.3.1.2. Treatment

NSCLC treatment generally depends on the stage of the illness and involves surgery, radiotherapy and CT, which are often combined.

1.3.1.2.1. Surgery

Surgery aims at removing the tumorous tissue and can consist of a partial lobectomy, a full lobectomy or even pneumonectomy, depending on the cancer stage (tumour extent and nodal involvement) and health status of the patient. Generally, lobectomy is always preferred over pneumonectomy. It aims at removing the primary tumour and loco-regional lymph nodes. It is therefore mostly used at early stages (I, IIa, IIb), without (N0) or with very little nodal involvement (N1), when tumours are resectable and patients are in a condition to undergo surgery (approximately 20-25% of patients) (Datta and Lahiri, 2003). It is therefore limited to NSCLC that are detected early. The 5-year survival rates for these operable stages are the highest of all but still remain poor, ranging between 60% and 80% and 30% and 50% for stages I and II, respectively. Nevertheless, surgery remains the best chance for cure (Howington et al., 2013, Sculier, 2014). Surgery at later stages (IIIA) is controversial, and mainly dependent on nodal involvement (Sculier, 2014). It is usually excluded above N1. At the latest stages, IIIB and above, lung cancer is considered inoperable (NCCN, 2015).

1.3.1.2.2. Radiotherapy

RT aims at suppressing isolated and non-resectable tumours or local metastases using high-energy X-rays. It is widely used against NSCLC (Paesmans, 2014). The ability of RT to eradicate a tumour is mostly dependent on its size. It is generally used in loco-regional lung cancers that exhibit mild nodal involvement or when surgery is contraindicated or feared to be incomplete. It can show curative results even for inoperable patients at early stages and at localized stage III diseases. However it is generally used as a neoadjuvant treatment to surgery to shrink the tumour prior to removal, as a post-operative adjuvant treatment to limit tumour resurgence in the resection margins or concomitantly to CT (radiochemotherapy) in stages IIb, IIIa and IIIb that show nodal involvement (N2, N3). It is then given before or after surgery. It can also be used as "salvage" therapy to limit the risks of metastases and

Table 2. (continued).

First-Line Systemic Therapy for Advanced Disease	
REGIMEN	**DOSING**
Bevacizumab carboplatin + paclitaxel	**Day 1:** Paclitaxel 200mg/m² IV **Day 1:** Carboplatin AUC=6 IV. Repeat every 3 weeks for 6 cycles. **Day 1:** Bevacizumab 15mg/kg IV every 3 weeks until disease progression.
Cetuximab + cisplatin + vinorelbine	**Day 1:** Cetuximab 400mg/m² IV + cisplatin 80mg/m² IV, **plus** **Days 1 and 8:** Vinorelbine 25mg/m² IV, **plus** **Day 8:** Cetuximab 250mg/m² IV once weekly. Repeat every 3 weeks for 6 cycles.
Erlotinib	**Day 1:** Erlotinib 150mg PO once daily; following 4 cycles of platinum-based chemotherapy.
Cisplatin + paclitaxel	**Day 1:** Paclitaxel 135mg/m² IV over 24 hours **Day 2:** Cisplatin 75mg/m² IV. Repeat cycle every 3 weeks.
Cisplatin + gemcitabine	**Day 1:** Cisplatin 100mg/m² IV **Days 1, 8 and 15:** Gemcitabine 1,000mg/m² IV. Repeat cycle every 4 weeks.
Cisplatin + docetaxel	**Day 1:** Cisplatin 75mg/m² IV + docetaxel 75mg/m² IV. Repeat cycle every 3 weeks.
Cisplatin + vinorelbine	**Day 1:** Cisplatin 100mg/m² IV **Days 1, 8, 15 and 22:** Vinorelbine 25mg/m² IV over 10 minutes. Repeat cycle every 4 weeks.
Carboplatin + paclitaxel	**Day 1:** Carboplatin AUC=5–6 IV **Day 1:** Paclitaxel 225mg/m² IV over 3 hours. Repeat cycle every 3 weeks.
Pemetrexed + cisplatin	**Day 1:** Pemetrexed 500mg/m² IV + cisplatin 75mg/m² IV. Repeat cycle every 3 weeks.
Crizotinib	Crizotinib 250mg PO twice daily.
Second-Line Systemic Therapy for Advanced Disease	
REGIMEN	**DOSING**
Docetaxel	**Day 1:** Docetaxel 75mg/m² IV. Repeat cycle every 3 weeks.
Pemetrexed	**Day 1:** Pemetrexed 500mg/m² IV. Repeat cycle every 3 weeks.
Erlotinib	**Day 1:** Erlotinib 150mg PO once daily.
Third-Line Systemic Therapy for Advanced Disease	
Erlotinib	**Day 1:** Erlotinib 150mg PO once daily.

recurrence and even as a palliative treatment for patients with incurable lung cancer, in order to limit tumour growth and symptoms (Paesmans, 2014). The treatment regimen for curative RT consists of a 60-70 Gy dose, divided into 2 Gy individual doses over 6 to 7 weeks (Bradley et al., 2005, Paesmans, 2014). Treatment can be shorter with higher individual doses for patients with poor prognosis (NCCN, 2015).

1.3.1.2.3.Chemotherapy (CT)

CT in NSCLC is generally given in combination with surgery or RT. A two-drug regimen including platinum doublet CT is standard and is superior to single-drug and three-drug regimens. Non-platinum agents used against NSCLC are vinorelbine or taxanes (Berghmans, 2014) **(Table 2).** Between carboplatin and cisplatin, the latter is generally recommended as it gives a higher response-rate and survival (Berghmans, 2014). At the earliest stages of NSCLC and as an adjuvant therapy to surgery, cisplatin-etoposide is the first line of combined CT against primary NSCLC tumours. It is given in repeated cycles (between 20-25 mg/m² per week and up to 300 mg/m² in total), while the other anticancer agent, often less toxic, is given repeatedly, generally once a week over 3-4 weeks (Sculier, 2014). At later NSCLC stages, when CT is used concurrently to RT, cisplatin-etoposide and cisplatin-vinblastine are the preferred combinations (Berghmans, 2014). With the classical treatment with etoposide, cisplatin is generally given once a week over 3-4 weeks **(Table 2)**. Doses of cisplatin above 60 mg/m² per week have not been proved superior to 100 mg/m² doses and may even be the cause of higher side-effects (Berghmans, 2014)

Second-line CT usually shows reported responses inferior to 10%. It generally involves other anticancer agents, depending on the patient history of tumour response, with docetaxel or pemetrexed (for patients with large cell carcinoma or adenocarcinoma), erlotinib (for patients who bear the epidermal growth factor receptor (EGFR) mutation) or continuation of the platinum doublet CT with bevacizumab (for patients who have already received erlotinib or crizotinib) **(Table 2)** (Berghmans, 2014).

The role of adjuvant CT after completely resected stage I, II or III NSCLC is not yet final. In theory, adjuvant CT can help limit the presence of undetected micrometastasis in non-resected lymph nodes and therefore prevent recurrences. A large study showed that CT significantly improved the 5-year survival rate of a cisplatin-based CT group *vs.* the untreated one (45% *vs.* 40%) (Arriagada et al., 2004, Le Chevalier et al., 2005, Arriagada et al., 2010). In another study comparing a vinorelbine-cisplatin regimen after surgery, the 5-year survival
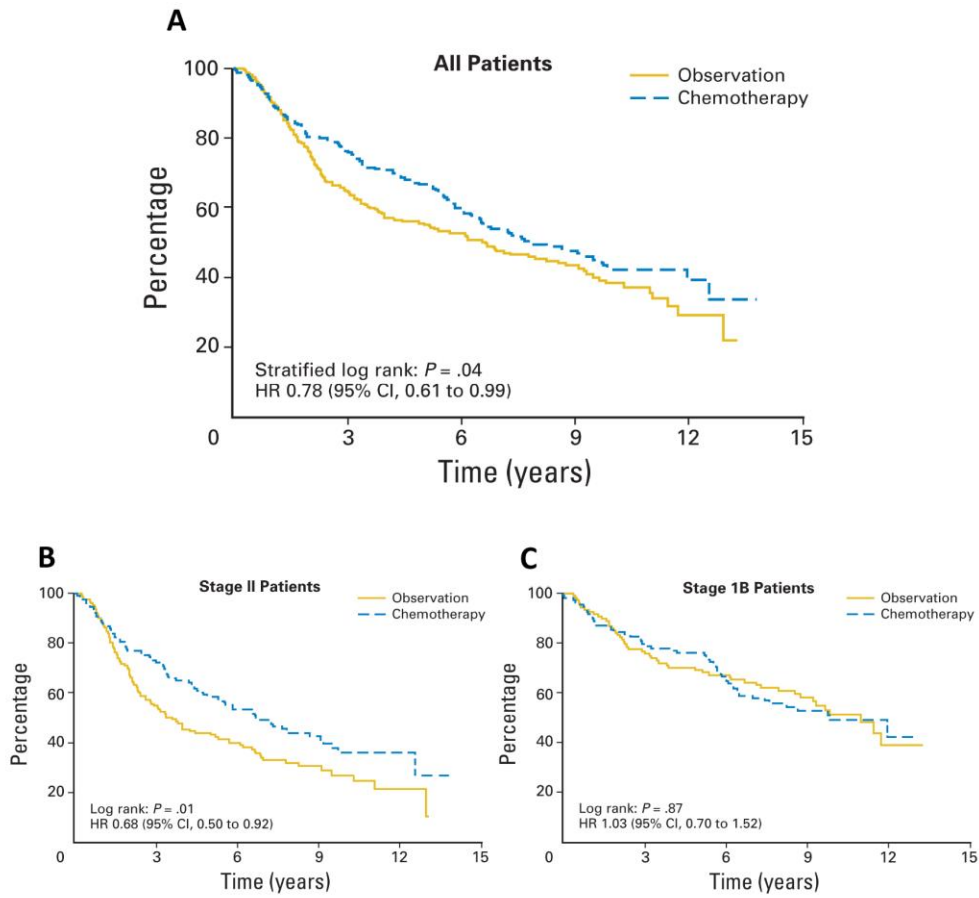
Figure 11. Survival graphs following adjuvant CT (without RT) with cisplatin after surgical resection of the primary tumour in the long run, for **A.** all, **B.** stage II and **C.** stage 1B (T2N0) patients, from Butts et al. (2010).
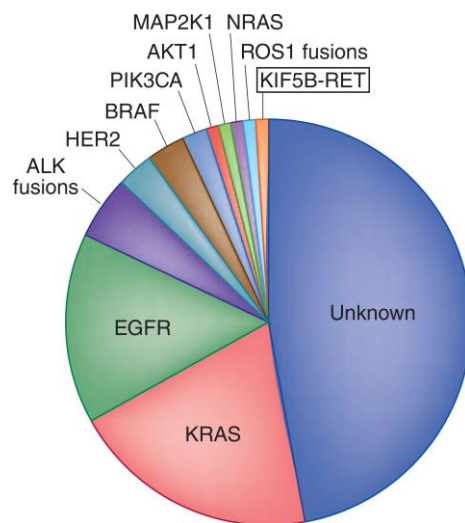
Figure 12. Distribution of genetic abnormalities in lung adenocarcinomas, from Pao and Hutchinson (2012).

rate was also increased, at 69% *vs.* 54% for the surgery alone group (Winton et al., 2005). A meta-analysis of all the adjuvant CT clinical trials done up to 2015, which included patients who had undergone surgery followed by CT (with or without radiotherapy) showed a globally similar response (Burdett et al., 2015). Overall, the CT group had a higher 5-year survival rate (64%) than the surgery alone one (60%). The same trend was observed for operated patients who received concurrent RT and CT (33%) compared to the concurrent RT alone group (29%). However, these results must be interpreted with caution because the few long-term follow-up results available show that the advantage of CT may decrease after some time. In the first study described above, more patients died after 7.5 years of follow-up in the CT group than in the surgery alone one (Arriagada et al., 2010). In the second study, this was observed only for stage IB patients (N0). For all others (including stage II), adjuvant CT was still superior after more than 12 years **(Figure 11)**. This observation seemed confined to patients with nodal involvement, who benefited the most from the postoperative CT (Butts et al., 2010).

1.3.1.3. New therapies

A few biomarkers have been identified for NSCLC. They are focused on detecting "driver oncogenes", which can help determine the best course of treatment to apply to small subsets of patients (Pao et al., 2012). For instance, a genetic mutation, relative to the EGFR has been reported to be largely represented in Asian non-smoking subsets of patients (up to 50%) but rarely in adenocarcinomas from patients of Caucasian origin (10%). This mutation in particular is representative of a better response to the tyrosine kinase inhibitors gefitinib, erlotinib or afatinib, leading to a great improvement in clinical response and prognosis (Pao et al., 2012).

This approach is now considered as a first-line treatment therapy (since 2013) as it permits a reduction in mortality and fewer side effects than standard CT. However the EGFR sensitizing variations must be documented early (Rosell et al., 2012, Yang et al., 2013).

Patients with a detected oncogene have low chance of exhibiting another mutation (Pao et al., 2012), which means that they will show poor response to other targeted therapies, such as the anaplastic lymphoma receptor tyrosine kinase inhibitors (ALK). This gene rearrangement, which concerns 2-7% of patients with NSCLC, is another predictive marker of lung carcinomas that are generally resistant to EGFR tyrosine kinase inhibitors but are sensitive to crizotinib (approved in 2011) (O'Bryant et al., 2013).
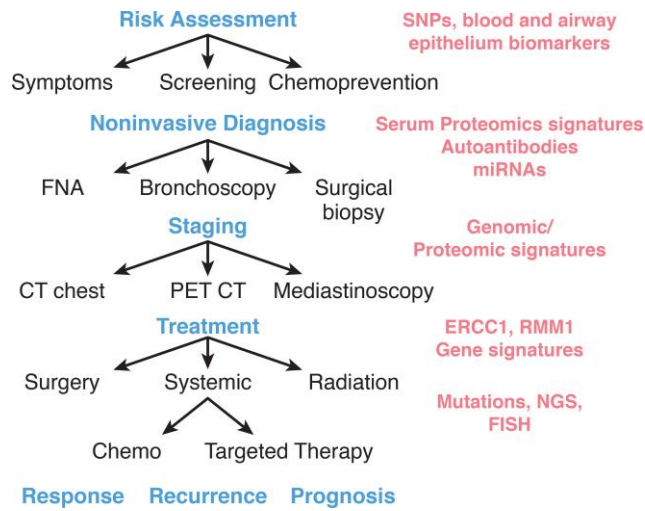
Figure 13. Management of lung cancer care future applications, from Massion et al. (2016).
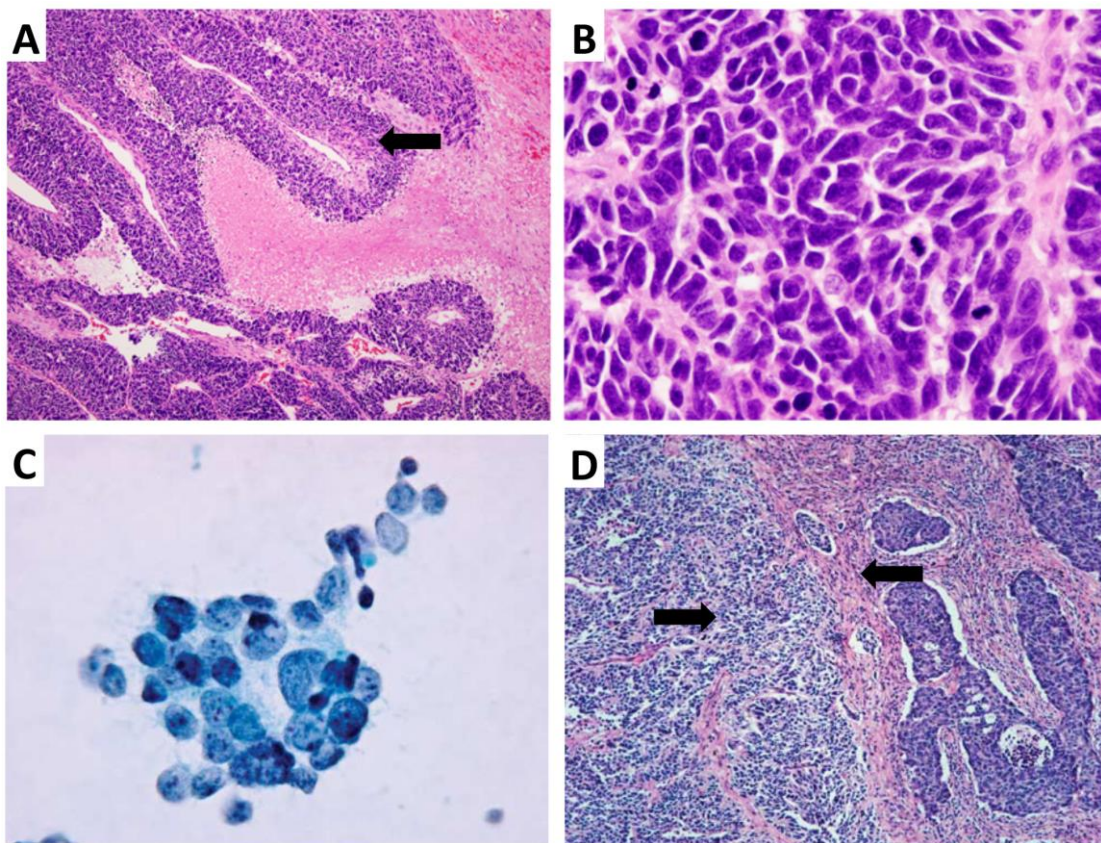
Figure 14. Histologic features of SCLC: **A.** diffuse sheets of small cells carcinoma; **B.** tumoural tissue exhibiting typical small cells with limited cytoplasm, finely granular nuclear chromatin, frequent mitoses and nearly absent nucleoli; **C.** cluster of small cells showing the same typical parameters; **D.** combined subtype of SCLC, exhibiting small cell (left) carcinoma and large cell carcinoma (right) showing more cytoplasm in non-small cells, adapted from Travis (2012).

V-Ki-ras2 Kirsten rat sarcoma viral oncogene homolog (KRAS) mutations are a much more common genetic variation (present in ~25% of North American people), often associated with smoking (while the EGFR and ALK variations are observed mostly in never-smokers). There is no particular target therapy for these patients yet, but they are generally insensitive. to EGFR tyrosine kinase inhibitors. This mutation is therefore useful for identifying patients who will not respond to EGFR tyrosine kinase inhibitors (Roberts and Stinchcombe, 2013). Conventional CT therefore remains of importance as is it believed that half of NSCLC show no relevant driver oncogene. Moreover, this new approach is costly and only shows results in the small subsets of patients who bear these sensitizing genetic variations. The most frequent mutations are reported in **Figure 12**, and the future management approach of lung cancer, from screening to therapy (including targeted therapy), is presented in **Figure 13**.

1.3.2. Small-cell lung cancer (SCLC)

1.3.2.1. Description

SCLC represents 10-20% of lungs cancers (Howlader et al., 2015). It is considered a very aggressive form of cancer and spreads quicker than NSCLC (Travis et al., 2015a). It is characterized by rapid mitoses, high growth and early metastases. It is diagnosed mostly at advanced stages, with only 5% of patients bearing only one solitary pulmonary nodule and as much as 70% of patients with metastatic disease. Almost all patients with SCLC are heavy smokers (Travis et al., 2015a). While SCLC responds very well to initial therapy (RT and CT), most patients die of the recurrent disease. Diagnosis mostly relies on cytology with the analysis of tumour cells from sputum, biopsy or a fine-needle aspiration sample. It is generally encountered in the central region of the lung (Travis et al., 2015a).

Microscopically **(Figure 14.A, B, C)**, SCLC, which is also called "oat cell carcinoma", is represented by small cells, with reduced cytoplasm, ill-defined cell borders, finely granular nuclear chromatin, and absent or discreet nucleoli (Travis, 2012). The cells are round to fusiform and nuclear moulding (conformity of adjacent cell nuclei) is frequent. A very high ratio of cells are mitotic (80 mitoses per 2-mm²) (Travis, 2012). Sometimes, small and non-small cells are present, categorizing the cancer in the combined subtype **(Figure 14.D).**

SCLC is commonly classified as limited-stage and extensive-stage diseases. The TNM classification can also be used regarding SCLC (NCCN, 2014b). Limited-stage disease comprises stages I to III (T1 or T2, any N, no metastasis) from TNM. Extensive-stage disease is generally stage IV (any T, any N, M1a or M1b) in order to include tumours that have metastasized, or any lower stage including T3 or T4, in order to include very large

Table 3. Anatomic stages of SCLC using the TNM classification system and the subsequent 5-year survival rate prognosis, adapted from NCCN (2014b).

	5-year survival rate	Anatomic stage		
Stage 0		T$_{\text{in situ}}$	N0	M0
Stage IA	40%	T1	N0	M0
Stage IB	40%	T2a	N0	M0
Stage IIA	40%	T2b	N0	M0
		T1	N1	M0
		T2a	N1	M0
Stage IIB	20%	T2b	N1	M0
		T3	N0	M0
Stage IIIA	15%	T1-2	N2	M0
		T3	N1-2	M0
		T4	N0-1	M0
Stage IIIB	10%	T1-2	N3	M0
		T3	N3	M0
		T4	N2-3	M0
Stage IV	1%	Any T	Any N	M1a
		Any T	Any N	M1b

Table 4. CT recommendations in the US, following the National Comprehensive Cancer Network 2014 guidelines for SCLC, adapted from NCCN (2014b).

Small Cell Lung Cancer (SCLC)	
Chemotherapy as Primary or Adjuvant Therapy	
Limited Stage (maximum of 4–6 cycles)	
Cisplatin + etoposide	**Day 1:** Cisplatin 60mg/m^2 IV **plus** **Days 1–3:** Etoposide 120mg/m^2 IV. Repeat cycle every 3 weeks for at least 4 cycles. **OR** **Day 1:** Cisplatin 80mg/m^2 IV **plus** **Days 1–3:** Etoposide 100mg/m^2 IV. Repeat every 4 weeks for 4–6 cycles.
Carboplatin + etoposide	**Day 1:** Carboplatin AUC=5–6 IV **plus** **Days 1–3:** Etoposide 100mg/m^2 IV. Repeat every 3 weeks for 4–6 cycles.
Extensive Stage (maximum of 4–6 cycles)	
Cisplatin + etoposide	**Day 1:** Cisplatin 75–80mg/m^2 IV **Days 1–3:** Etoposide 80–100mg/m^2 IV. Repeat every 3 weeks for 4–6 cycles.
Cisplatin + irinotecan	**Day 1:** Cisplatin 60mg/m^2 IV **Days 1, 8 and 15:** Irinotecan 60mg/m^2 IV. Repeat cycle every 4 weeks for 4 cycles. **OR** **Day 1 and 8:** Cisplatin 30mg/m^2 IV **Day 1 and 8:** Irinotecan 65mg/m^2 IV. Repeat every 3 weeks for 4–6 cycles.
Carboplatin + irinotecan	**Day 1:** Carboplatin AUC=5 IV **plus** **Days 1, 8 and 15:** Irinotecan 50mg/m^2 IV. Repeat cycle every 4 weeks for 4–6 cycles.
Carboplatin + etoposide	**Day 1:** Carboplatin AUC=5–6 IV. **Days 1–3:** Etoposide 100mg/m^2 IV. Repeat every 4 weeks for 4–6 cycles.

tumours (> 7 cm) that have a poor prognosis **(Table 3)** (Ignatius Ou and Zell, 2009). Survival rates for all patients with SCLC are poor **(Table 3)** and can be evaluated based on the stage of the illness. For limited-stage and extensive-stage diseases, median survival rates range between 14 and 20 month (2-year and 5-year survival rates of 40% and 27%) and 9 and 11 months (2-year and 5-year survival rates of 5% and 2.8%), respectively (NCCN, 2014b, Howlader et al., 2015). Detection of SCLC is often done through full examination, complete history, imaging with a CT scan of the chest with intravenous contrast and possibly lactate dehydrogenase (LDH) quantitation (Kalemkerian and Gadgeel, 2013). PET scans are also very useful in staging SCLC as the disease is highly metabolic.

1.3.2.2. Treatment

Unlike NSCLC patients, all those with SCLC disease, even limited-stage, are to be treated with primary or adjuvant CT (Holbrechts and Roelandts, 2014). RT is indicated mostly for patients with limited-stage disease and with a minimum of 45 Gy dose in total (Holbrechts et al., 2014). Surgery is indicated only for early-diagnosed patients with a small individualized and resectable tumour and no nodal involvement (T1 or T2 and N0), but this only concerns about 5% of patients (Ignatius Ou et al., 2009, Kalemkerian et al., 2013, Holbrechts et al., 2014). Adjuvant CT is recommended for patients who have undergone surgical resection and radiochemotherapy, which is recommended for patients with limited-stage disease. CT alone is only recommended for patients with extensive-stage disease, and it only aims at a palliation of the symptoms. In some cases (e.g. if there are brain metastases with neurological impairment), radiochemotherapy is sometimes given to these low prognosis patients but only as a palliative treatment, with RT applied to the brain to combat the metastases (Holbrechts et al., 2014).

Single agent and combination CT are both active against SCLC, but the latter is the preferred approach. The most common regimen includes etoposide, a topoisomerase inhibitor associated with cisplatin **(Table 4)**. This is the reference treatment for both limited- and extensive-stage disease (Grigoriu and Meert, 2014, Holbrechts et al., 2014). It shows an equivalent efficacy in patients with SCLC (Rossi et al., 2012). With the etoposide-platinum treatment in combination with RT in limited-stage disease, response rates are of 70-90%. In extensive-stage disease this response rate drops to 60-70% with CT alone (Simon et al., 2004). Despite these very high response rates, a large number of patients experience relapse, with a disease that was already resistant or that has become resistant to first-line therapy. These patients show a very low median survival rate of 4-5 months. They are therefore

Table 4. (continued).

Subsequent Chemotherapy	
Relapse <2–3 months, PS 0–2	
Paclitaxel	**Day 1:** Paclitaxel 175mg/m² IV over 3 hours **plus** **Day 1:** Cisplatin 80mg/m² IV. Repeat every 3 weeks for at least 2 cycles. **OR** **Day 1:** Paclitaxel 80mg/m² IV over 1 hour. Repeat every week for 6 weeks, followed by a 2-week break.
Docetaxel	**Day 1:** Docetaxel 100mg/m² IV over 1 hour. Repeat every 21 days.
Topotecan	**Days 1–5:** Topotecan 1.5mg/m² IV once daily over 30 minutes. Repeat every 3 weeks. **OR** **Days 1–5:** Topotecan 2.3mg/m² PO once daily. Repeat every 3 weeks.
Irinotecan	**Day 1:** Irinotecan 100mg/m² IV over 90 minutes. Repeat every week.
Temozolomide	**Day 1–21:** Temozolomide 75mg/m² PO for a 4-week cycle.
Gemcitabine	**Days 1, 8, and 15:** Gemcitabine 1,000mg/m² IV for a 4-week cycle.
Ifosfamide	**Day 1:** Ifosfamide/mesna 5,000mg/m² IV. Repeat every 3 weeks.
Relapse > 2–3 months up to 6 months	
Topotecan	**Days 1–5:** Topotecan 1.5mg/m² IV once daily over 30 minutes. Repeat every 3 weeks. **OR** **Days 1–5:** Topotecan 2.3mg/m² PO once daily. Repeat every 3 weeks.
Paclitaxel	**Day 1:** Paclitaxel 175mg/m² IV over 3 hours **plus** **Day 1:** Cisplatin 80mg/m² Repeat every 3 weeks for at least ² cycles. **OR** **Day 1:** Paclitaxel 80mg/m² IV over 1 hour. Repeat every week for 6 weeks, followed by a 2-week break.
Docetaxel	**Day 1:** Docetaxel 100 mg/m² IV over 1 hour. Repeat every 21 days.
Irinotecan	**Day 1:** Irinotecan 100mg/m² IV over 90 minutes. Repeat every week.
Gemcitabine	**Days 1, 8, and 15:** Gemcitabine 1,000mg/m² IV for a 4-week cycle.
Vinorelbine	**Day 1:** Vinorelbine 25–30mg/m² IV. Repeat every week
Etoposide (PO)	**Day 1–21:** Etoposide 50mg/m² PO.
Temozolomide 75 mg/m²/day × 21 days	**Day 1–21:** Temozolomide 75mg/m² PO for a 4-week cycle.
Cyclophosphamide/doxorubicin/ vincristine (CAV)	**Day 1:** Cyclophosphamide 1,000 mg/m² IV **plus** **Day 1:** Doxorubicin 45mg/m² IV **plus** **Day 1:** Vincristine 2mg IV. Repeat every 21 days.
Relapse> 6 months	
• Original regimen	

treated with paliative second-line treatment CT, for instance topotecan or irinotecan (well-tolerated in Asian patients only).

1.4. Secondary tumours to the lungs

Secondary tumours to the lungs are metastasis from other cancers than lung cancer and originate from cancer cells that either come from contiguous organs (e.g. thyroid, oesophagus, thymus, chest wall) or that derive in the bloodstream or the lymphatic system and then spread to the lung and carry the phenotype of the original cells. The lung is one of the most common sites of metastasis of solid tumours from other organs.

The most common metastatic lung cancers originate from breast, colorectal, head and neck, kidney and uterus cancers in adult populations and Wilms' tumour and sarcomas of the bone (osteosarcoma) and of soft tissues in paediatric populations (Seo et al., 2001, Dishop and Kuruvilla, 2008). They are seen in as much as 20-54% of adults with extrathoracic primary tumours (Crow et al., 1981, Arenberg and Pickens, 2016). In the paediatric population, they account for the largest share of all tumours found in the lung (83.3%), whereas primary lung tumours are uncommon in this population subset and show different histological features than for adults (Dishop et al., 2008).

Because the cells are mostly carried by the general venous circulation to the arterial pulmonary circulation, secondary tumours are often found in the lower and more vascularized part of the lung. The fact that the lung receives the entire bloodstream is one of the reasons metastases are often found in the lungs. Recently detected molecular mechanisms show that the targeting of cancer cells to metastatic sites is promoted by chemokine expression on the surface of cancer cells. For instance, the C-X-C chemokine receptor type 4 (CXCR4) and C-C chemokine receptor type 7 (CCR7), highly expressed in primary breast tumours have specific ligands C-X-C ligand 17 and C-C ligand 21, which are expressed in lung cells (Arenberg et al., 2016).

The entry of these cancer cells into lung sites is also promoted by a lung-specific increase of the vascular permeability, through the angiopoietin-like 4 (ANGPTL4) gene (Padua et al., 2008). The implantation of these cells, through the emission of specific growth factors such as the vascular endothelial cell growth factor (VEGF), may also be promoted by the primary tumour. Finally, the adherence of cancer cells to the vasculature of lung metastatic sites is

Table 5. 5-year survival rates of secondary cancer to the lungs, based on the original cancer type, from Arenberg et al. (2016).

Primary tumour	5-year survival rate (%)
Testis	50-80
Osteosarcoma	25-50
Breast	25-50
Colorectal	13-40
Soft tissue sarcoma	20-35
Melanoma	5-33
Head and neck	30
Renal	15-20

also promoted by the original tumour through the emission of specific proteins, such as metadherin (Brown and Ruoslahti, 2004). The symptoms associated with these cancers depend on the implantation of the secondary tumour (e.g. cough, haemoptysis, shortness of breath, chest pain). They are either synchronous (detected at the same time of the primary tumour) or metasynchronous (detected after the primary tumour, through a periodical surveillance screening for instance). The same techniques as primary lung tumours (e.g. X-ray, CAT scans, PET scan bronchoscopy, sputum cytology, fine-needle aspiration cytology) are used for detection of these secondary tumours (Arenberg et al., 2016).

Management of this type of cancer is too specific to elaborate thoroughly here but generally involves resection of the tumour, RT and CT and depends on the tumour extent and on the patient's ability to undergo surgery. Hormonal therapy can also be used for hormone-dependent tumours for instance originating from the breast. Nevertheless, treatment rarely aims at curing the patient but rather focuses on limiting cancer growth and patient discomfort. This is because secondary tumours are often discovered late, at advanced stages and therefore tend to have a very bad prognosis **(Table 5)** (Travis et al., 2015a, Arenberg et al., 2016).
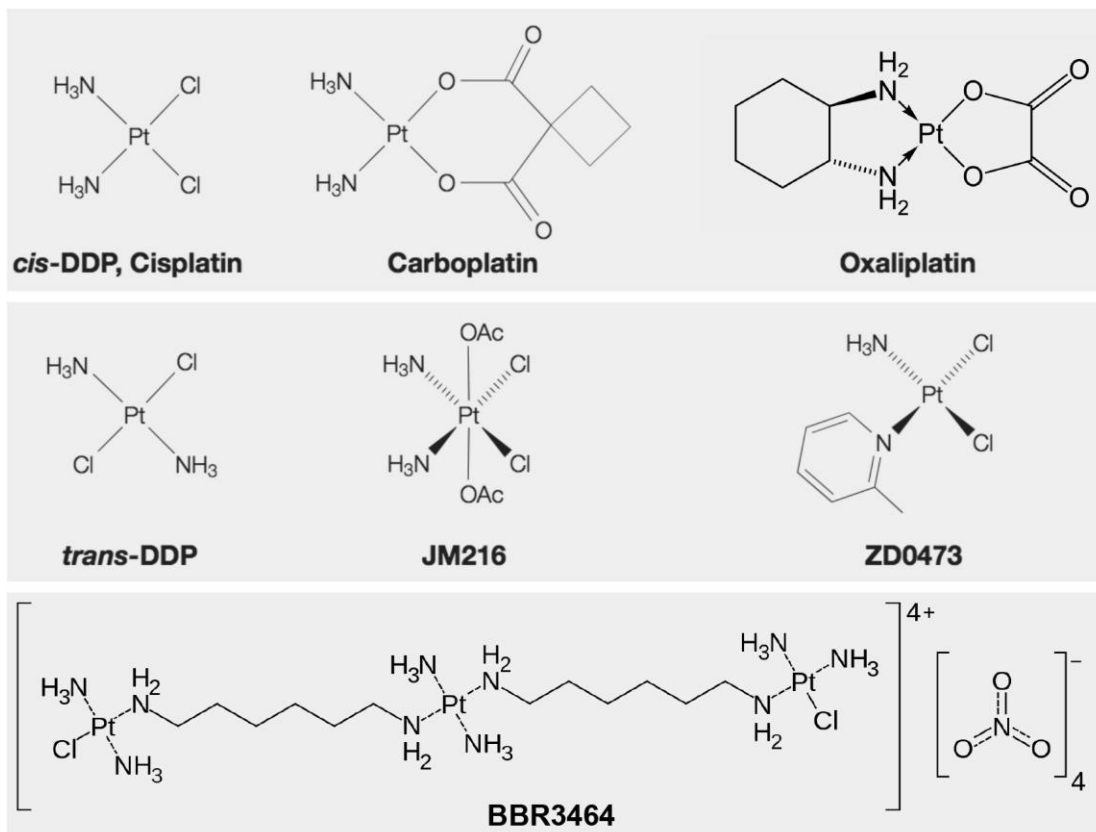
Figure 15. Cisplatin and other platinum-based anticancer drugs.

2. Cisplatin

2.1. Discovery and current use

Cisplatin **(Figure 15)** was first synthetized in the mid 19th century by the Italian chemist Michaele Peyrone, and was then known as "Peyrone's salt" (Peyrone, 1844). Its molecular configuration was used in the theory of coordination, which earned the chemist Alfred Werner a Nobel Prize in 1913 (Alderden et al., 2006). It was Barnett Rosenberg, an American biophysicist, who serendipitously discovered its antiproliferative properties during the 1960s, while working on *E. coli* cell division under electric fields produced using platinum electrodes (Rosenberg et al., 1965). With this discovery, he pursued his research and was able to confirm the antiproliferative activity of cisplatin on various types of cancer cells (Rosenberg et al., 1969, Harder and Rosenberg, 1970, Shimizu and Rosenberg, 1973). Cisplatin was ultimately subjected to preclinical studies in animals (Schaeppi et al., 1973) and fast-tracked to its first clinical trial in humans in 1972 (Lippman et al., 1973). Cisplatin was at the time the first and only platinum-comprising drug and showed spectacular clinical results on testicular cancer (Einhorn and Donohue, 1977). At the time, the cure rate for this cancer was less than 10%, and was improved to more than 90% thanks to cisplatin in combination.

With its increasing use in patients bearing multiple types of cancers, better understanding of its toxicities (see 2.6.1. Side-effects) and of the procedures to circumvent them were then developed (route of administration, doses, cycle length and periods, peri-hydration) (Cvitkovic et al., 1977, Hayes et al., 1977). New, less toxic platinum complexes with diverse physicochemical properties were also developed and are already approved and in clinical use. Some of these are carboplatin, (food and drug administration (FDA)-approved in 1989), oxaliplatin, (FDA-approved in 2002), nedaplatin (approved in 1995 in Japan), lobaplatin (approved in 2012 in China), while others are still under development or in clinical trials (e.g. satraplatin: JM216, picoplatin: ZD0473 or triplatin tetranitrate: BBR3464, **Figure 15**). For instance, nedaplatin recently showed a significant increase in median survival and fewer toxicities than cisplatin in combination with docetaxel against advanced squamous cell lung carcinoma in a phase III study. This success illustrates well the potential of these new platinum derivatives, as a way to circumvent adverse effects and combat cancer resistance (Shukuya et al., 2015).

Over the years, platinum derivatives regimens were adapted for a very wide spectrum of cancers, including breast, head and neck, ovarian, cervical, prostate, bladder, testicular,
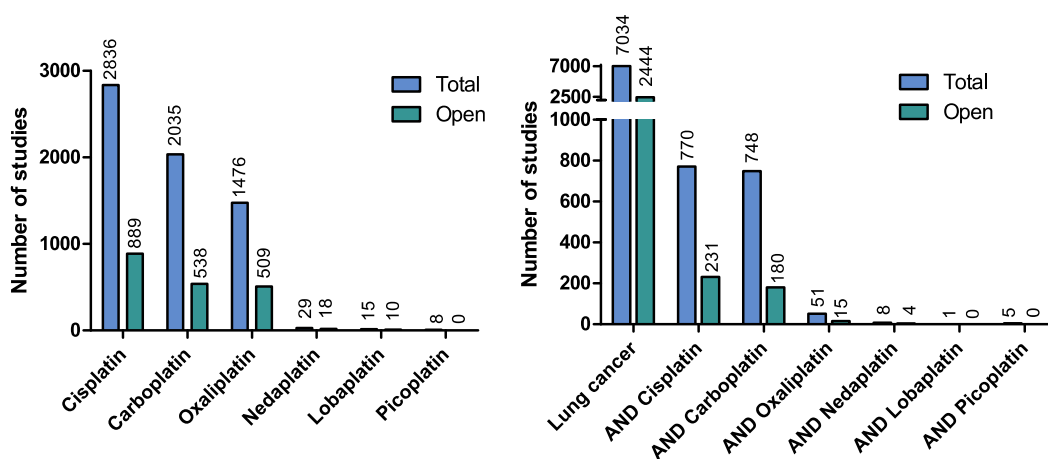
Figure 16. Distribution of platinum-based antineoplastic agents in total and open clinical trials, data from Clinicaltrials.gov as of November 2016.

Table 6. Overview of the chemical properties of cisplatin.

Molecular formula	$Pt(NH_3)_2Cl_2$
Molecular weight	300.01 g/mole
Appearance	Yellow to orange powder
Solubility in water at 37°C	1-2.5 g/L (unstable)
Solubility in NaCl 0.9% and pH 4 at 20°C	1 g/L (stable)
Solubility in DMF	12-16 g/L (stable)
Solubility in dimethylacetamide	18 g/L
Solubility in dimethylsulofxyde	35 g/L (rapidly forms a sulphur adduct)
Insoluble in	Alcohols, ketones, ethyl acetate
Density	3.74 g/cm³
log P	-2.19
Melting point	270°C (decomposition)

lymphoma, osteosarcoma and, of course, lung cancer, often in association with other antineoplastic agents presenting different mechanisms of action (Florea and Busselberg, 2011). Yet cisplatin remains the main platinum-based chemotherapeutic agent in clinical use against NSCLC and SCLC. To date, Clinicaltrials.gov shows that there is still great interest in cisplatin and that it is still the main platinum anticancer agent. More precisely, cisplatin is involved in 9.4% of all open trials against lung cancer, which is more than all other platinum derivatives combined **(Figure 16).**

2.2. Structure and chemical properties

Cisplatin or *cis*-diamminedichloroplatinum (II) is named after its chemical structure, comprising two amino ligand groups and two chlorido leaving groups, bound together through a central platinum atom **(Figure 15)**. Its diastereoisomer, *trans*-diamminedichloroplatinum (II) or transplatin **(Figure 15)** has little to no activity. This is because it is quickly deactivated due to its kinetic instability and because the interaction with deoxyribonucleic acid (DNA) is regioselective. Platinum complexes always exhibit two leaving groups (chlorido ligands for cisplatin), which are almost always in *cis* position for the active moiety to be able to bind with DNA through nucleophile substitution (Jamieson and Lippard, 1999, Coluccia and Natile, 2007).

2.3. Solubility and chemical reactivity

Cisplatin has low solubility in water (2.5 g/L, slightly soluble), and even less solubility in saline at pH 4 (1.0 g/L) **(Table 6)**. Cisplatin is soluble in some organic solvents **(Table 6)**, for instance dimethylsulfoxyde (~35 g/L), but strongly reacts by binding with its central sulphur atom, producing an inactive compound (Hall et al., 2014). It is also sparingly soluble in some class II solvents such as *N-N,*-dimethylformamide (DMF, ~16 g/L) and dimethylacetamide (USP30, 2007). During our work, we showed that cisplatin is stable in DMF, using ^{195}Pt nuclear magnetic resonance (^{195}Pt NMR) (British Columbia Cancer Agency, 2013).

In water, cisplatin is subjected to hydrolysis and loses its chlorido ligands to hydroxyl bonds. This particularly happens at low chloride concentrations as in the intracellular compartment. This produces the monocharged cation monoaquacisplatin $[Pt(NH_3)_2Cl(OH_2)]^+$ and the bivalent cation diaquacisplatin $[Pt(NH_3)_2(OH_2)_2]^{2+}$ **(Figure 17)** (Jamieson et al., 1999). These compounds are the activated moieties of cisplatin, with DNA binding abilities more than 1 000-fold higher than the original uncharged cisplatin (Wang and Lippard, 2005). Monoaqua
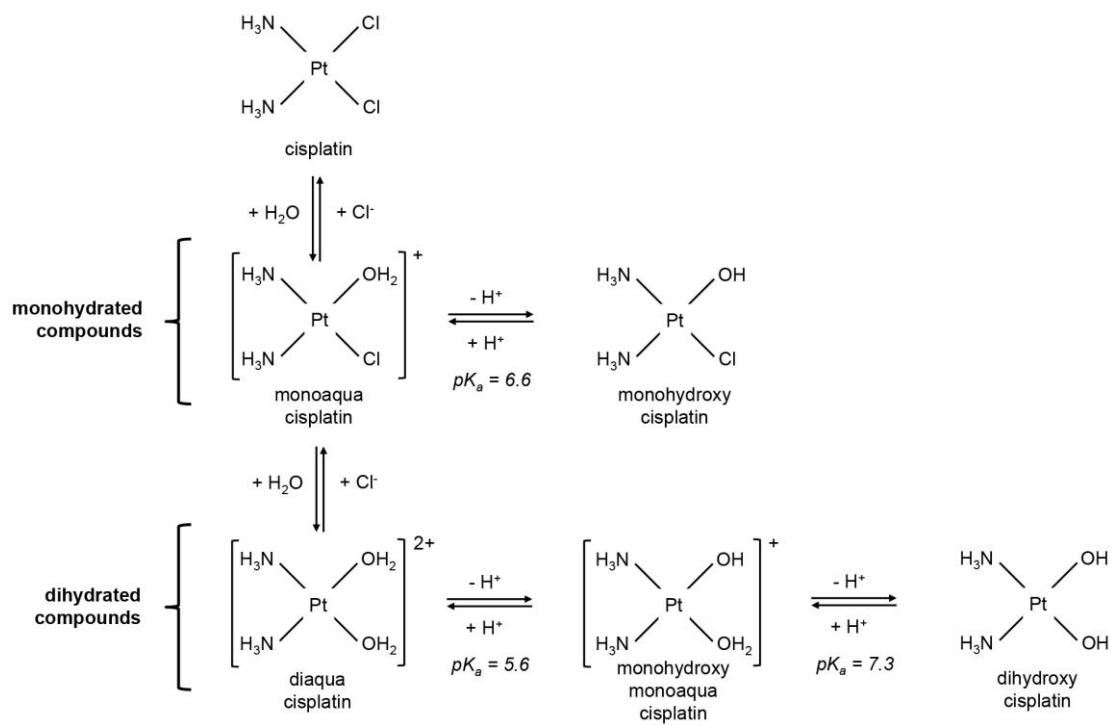
Figure 17. Cisplatin hydrolysis pathway in water.

and diaquacisplatin can also lose all their positive charges by proton loss and ultimately form monohydroxy and dihydroxycisplatin at pH above 5.6, which are less active products than cisplatin **(Figure 17)**.

In commercial forms (Platinol® and generics), cisplatin is usually stored at pH ~4, in 0.9% NaCl solutions, near saturation (~1 g/L), protected from light and at room temperature to avoid precipitation (Karbownik et al., 2012).

2.4. Cisplatin quantification methods

2.4.1. Generalities

Because of its inherent reactivity with the cellular components of the tissues where it is distributed, cisplatin and its large variety of metabolites are often found together in biological samples, which represents a challenge for their analysis. Various methods have been proposed for the quantification of intact cisplatin in aqueous medium, where it is often present with its aquated species, and of cisplatin and its adducts in tissues. These methods can be divided based on their selectivity for cisplatin or for the whole platinum fraction. Selective methods capable of identifying cisplatin alone are generally preceded by a separating step (i.e. high-performance liquid chromatography, HPLC) and followed by a detection step (in the UV-vis range for instance). HPLC-UV for cisplatin is, for instance, very ineffective, first because of the low molar absorptivity of cisplatin but also because of the high structural similarity between cisplatin aquated species, which are therefore very difficult to separate (Bosch et al., 2008). The separation of cisplatin and some of its aquated products was proven feasible using an ion-pairing reagent (i.e. sodium dodecyl sulphate) but the method was not fully able to provide an absolute quantification of the compounds (El-Khateeb et al., 1999). Consequently, HPLC-UV is often coupled with a prior or post-derivatization of cisplatin using, for instance, sodium diethyldithiocarbamate. This increases the sensitivity of the method but lacks the required selectivity, in particular for the aquated species (Augey et al., 1995).

While a few mass-spectrometry methods coupled with HPLC have been described, inductively coupled plasma-mass spectrometry (HPLC-ICP-MS) seems to remain the best approach for cisplatin quantification and speciation in tissue samples. With proper sample preparation and separation of the different platinum adducts in the chromatographic column, this method is probably the most sensitive and the most discriminant technique available today, with detection limits below the ng/L, in the part per trillion range (Hann et al., 2005). However, this technique is expensive and not broadly available.

(A common approach regarding determination of the cisplatin concentration is to use non-selective methods, such as ICP-MS or electrothermal atomic absorption spectrometry ETAAS). These methods are able to quantify the whole platinum fraction and therefore intact cisplatin and its adducts (see 2.4.2. Electrothermal atomic absorption spectrometry). Finally, thanks to the high natural abundance of the [195]Pt atom, an interesting method able to characterize each platinum complex independently (including cisplatin and each of its degradation product) is [195]Pt NMR. The chemical shifts of platinum species in solution are specific to platinum-bound atoms and are well described in the literature (Berners-Price et al., 2006). The method is even able to distinguish conformational isomers and *cis* or *trans* geometric isomers. Combined with a quantitative approach, this particular aspect of [195]Pt NMR is of tremendous interest to assess the purity of cisplatin during a pharmaceutical process that could potentially transform cisplatin into inactive transplatin or any other reactive species (O'Neil et al., 2013).

2.4.2. Electrothermal atomic absorption spectrometry (ETAAS)

The ETAAS method is based on the principle that a population of atoms at the fundamental state E_0 can absorb the energy from photons following the Planck equation.

As is observed with UV-visible spectrophotometry, the decreased intensity in the incident beam of photons going through a cloud of atoms in their fundamental state can be linked to the number of atoms that the beam is going through. This can further be linked to the concentration of the analyte in a solution, using a known volume of sample and a calibration curve. In atomic absorption spectrometry, the analyte must first be brought to its fundamental state to be able to absorb the photons from the incident beam. This is done by vaporizing the sample using large amounts of thermic energy in an atomizer (i.e. a flame with an air/acetylene mix or an electrothermal graphite furnace). Moreover, the atoms in their fundamental state only have the ability to absorb the photons of specific wavelengths, corresponding to the spectral line of each atom. The wavelengths of these spectral lines are defined by the energy levels between the ground state and excited state of the valence electrons of each type of atom. This means that, using a source of photons emitting only the emission lines (i.e. a hollow cathode lamp), the specificity of the method can then be achieved using a wavelength specific to the atom that is to be quantified in the sample.

The apparatus in ETAAS is composed of (i) a primary source, the hollow cathode lamp, which is made of the atom to analyse, (ii) the atomizer, which is comprised of two graphite electrodes applying a current to a graphite furnace, acting as a resistance and therefore heated based on Ohm's law, (iii) a monochromator, selecting a discrete wavelength from the ray

spectrum of the analyte and (iv) a detector and a photomultiplier, transforming the absorbance into a readable electronic signal. The major advantage of this method is that it can quantify atoms in complex matrices without requiring prior separation of samples, which can be solutions, suspensions or slurries (viscous homogenates). The most complex matrices that can be analysed are for instance digested blood, tissue digestates or soil extracts. The thermal programmes that can be progressively applied with ETAAS can help degrade the matrix *in situ* prior to the atomization of the samples. However, the method is destructive of the sample, which is atomized at temperatures well above 2500°C. Moreover, many interferences in signal can be observed, which are caused by non-specific absorption. They can be caused for instance by smoke, contaminants, light from the heated furnace or overlapping wavelength from other atoms in the sample. These interferences can be limited using signal correction systems, such as a deuterium lamp or a magnetic field applying the Zeeman effect, which is based on a distortion of the electronic orbitals, causing the splitting of the spectral absorption line. When the magnetic field is stopped, the signal is due to both the analyte and the background. When the magnetic field is on, the spectral line is distorted in the sample and the spectral line is only absorbed by the background. This is done sequentially during all the atomization and the signals are subtracted to consider the analyte only.

Cisplatin quantification using ETAAS of platinum has been widely used since the 1970s (LeRoy et al., 1977, Hopfer et al., 1989, Milacic et al., 1997, Zalba et al., 2010). It offers high sensitivity compatible with physiological levels and high versatility regarding the matrix preparation procedures. It is a non-selective method and quantifies the totality of the platinum fraction. Many studies have shown that the use of a standard addition method was unnecessary and that direct quantification using a calibration curve was appropriate (Hopfer et al., 1989, Milacic et al., 1997). For a sample to be analyzed using ETAAS, it must first be thoroughly digested to limit matrice effects and non-specific light absorption during heating. This degradation is further completed using a predetermined thermal programme. This programme, comprised a succession of ramps and hold times, applies increasing temperatures to the graphite furnace and the injected sample. The first period aims at drying the sample to avoid sputtering and loss of analyte, and directly depends on the solvent and volume (e.g. 2 s per µL for water-based samples). The next sequence is pyrolysis, and aims at removing the matrix components in biological samples. It is often realized between 800 and 1,200°C for durations that need to be optimized. Then, the temperature of the graphite tube is very quickly raised to reach the atomization temperature, which depends

1,2-intrastrand   1,3-intrastrand   interstrand
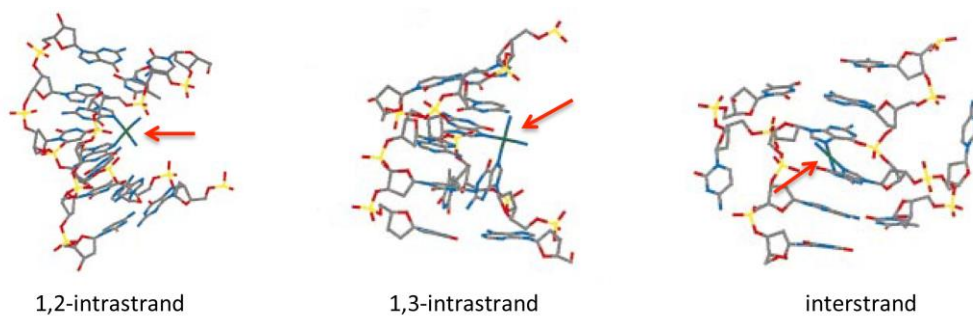
Figure 18. Cisplatin adducts with DNA: the red arrow emphasizes the central platinum atom position. Adapted from Jamieson et al. (1999).

on the type of element to be analyzed. For platinum, the reported atomization temperatures vary between 2,400 and 2,700°C (LeRoy et al., 1977, Milacic et al., 1997, Zalba et al., 2010).

2.5. Cell penetration, mechanism of action and cisplatin resistance

2.5.1. Cisplatin uptake and efflux

Cisplatin uptake is not saturable, not dependent on pH and its concentration seems to be the major limiting factor for its accumulation inside the cells (Ivy and Kaplan, 2013). Yet, recent works have shown that while passive diffusion is the main occurring mechanism (Eljack et al., 2014), some active transport may also be responsible for cisplatin entry into the cell. This transport is done through the high-affinity copper transporter hCTR1 (Ishida et al., 2002, Ivy et al., 2013) or the organic cation transporters OCT-2 in renal cells, which is responsible for the induced nephrotoxicity (Yonezawa and Inui, 2011).

Regarding efflux of cisplatin out of the cell, the ATP-binding cassette exporter protein ABCC2 (Borst et al., 2000) and other copper-related transporters, ATP7A and ATP7B (for copper-transporting P-type adenosine triphosphate), are major components of cisplatin resistance through efflux (Tadini-Buoninsegni et al., 2014).

2.5.2. Formation of nuclear DNA adducts

After its entry inside the cell, cisplatin preferentially forms the positively charged mono and diaquacisplatin (see 2.3. Solubility and chemical reactivity) because of a much lower chloride concentration in the cytoplasm (3 mM) than in the extracellular fluids (104-114 mM) (Jamieson et al., 1999, Wang et al., 2005, Jain, 2015). It can then produce intra- and interstrand crosslinks with DNA in the nucleus, which is the main target of the drug.

The most frequent bonds formed during "platination" of DNA are those with the N^7 position of purines bases, preferentially guanine, to form mainly 1,2-d(GpG), but also 1,2-d(ApG), 1,3-intrastrand and interstrand crosslinks in the original position of the chlorido ligands in the original cisplatin molecule **(Figure 18)** (Baik et al., 2003). The intrastrand 1,2-crosslinks bend DNA in such a way that the then-exposed parts of the helix can be recognized by many proteins, such as the high-mobility group (HMG) box proteins, mismatch-repair proteins (MMR), histones (H1) and transcription factors (Jamieson et al., 1999). This mechanism is fundamental to cisplatin activity as it prevents DNA replication and transcription, thus stopping the cell cycle and repair of the DNA and ultimately provoking cell death. After "platination" of DNA, the cell-cycle is stopped at G_2 (the last
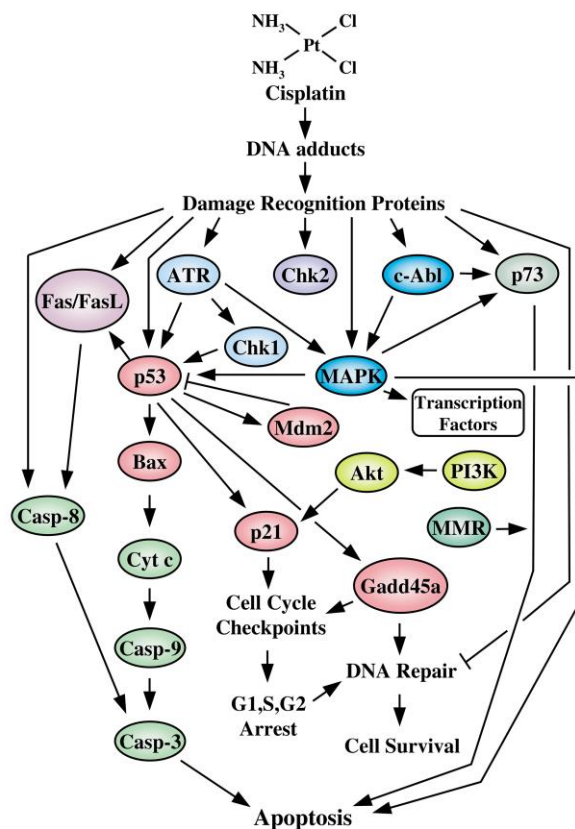
Figure 19. Overview of some of the major cellular mechanisms involved in cisplatin activity, from Siddik (2003).
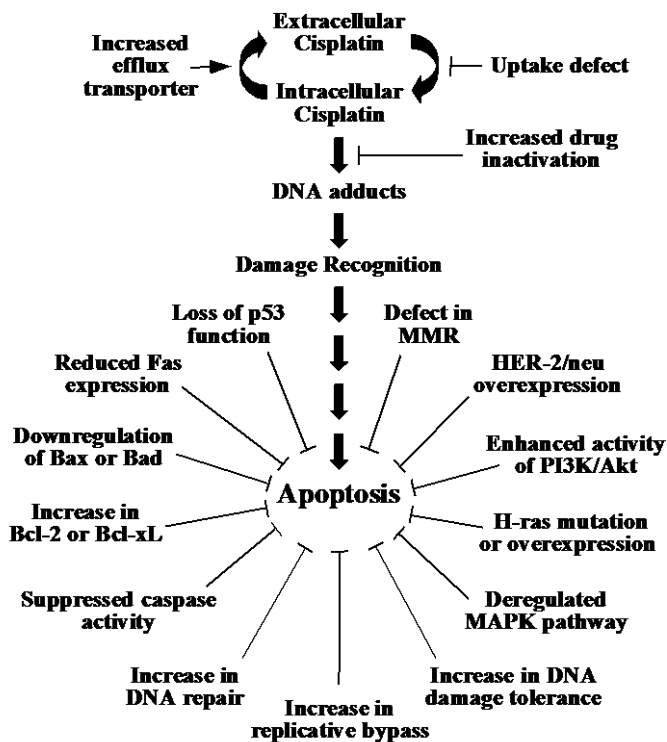
Figure 20. Inhibition mechanisms of the apoptotic signal in cisplatin-resistant tumour cells, from Siddik (2003).

step before mitosis). This is reversible (24-48 h) at low doses of cisplatin but irreversible (> 96 h) at high doses, ultimately causing cell death (Sorenson and Eastman, 1988).

2.5.3. Other cellular targets

Mitochondrial DNA has also been described as a less important target of cisplatin in the cell, but was still proved a sufficient factor to provoke cell death alone (Yang et al., 2006). Cisplatin also has affinity for RNA, proteins, membrane phospholipids and microfilaments of the cytoskeleton, but to a much lower extent (Akaboshi et al., 1992, Van de Water et al., 1994, Speelmans et al., 1996). For instance, some studies showed that after incubation of cisplatin at the IC50 of HeLa cancer cells, there were between 9 and 22 platinum atoms per DNA molecule in the cell. This ratio was much lower for proteins, for which 1 out of 3×10^4 to 3×10^5 proteins contained a single platinum atom and for RNA for which between 1 out of 10 and 1 out of 1 000 molecules contained a single platinum atom (Akaboshi et al., 1992). Altogether, cisplatin induces oxidative stress, which leads to apoptosis in the cell through the mitogen-activated protein kinase (MAPK), signaling cascade **(Figure 19)** (Siddik, 2003).

2.5.4. Cisplatin resistance

Cisplatin resistance is frequently encountered in patients, sometimes immediately or after a few cycles of treatment (Giaccone, 2000). *In vitro*, this resistance has been linked to (i) decreased accumulation of cisplatin inside the cells, through efflux increase and decreased uptake across the cell membrane (Eljack et al., 2014) (ii) increased mobilization of DNA repair mechanisms through higher damage recognition and mobilization of the nucleotide excision repair pathway and (iii) increased levels of drug inactivation through metallothioneins and of glutathione-*S*-transferase activity (Jansen et al., 2002, Siddik, 2003). As cisplatin also exhibits a very high affinity for sulphur groups, such as those that can be found on the cysteine amino-acid of glutathione or in metallothioneins, this is one of the major factors responsible for its deactivation in the cell (Jansen et al., 2002). An extensive presentation of the mechanisms involved is shown in **Figure 20.**

2.6. Challenges in cisplatin administration

2.6.1. Side-effects

Cisplatin (including its metabolites) is known to exhibit many toxicities that limit the administrable dose and sometimes require treatment interruption. Among them, the most serious and most frequent is cumulative and irreversible nephrotoxicity (~20-30% of patients). Ototoxicity, which is also cumulative, is less serious but is very frequently observed (~30% of patients). It is also fetotoxic and a mutagen (however some work show that it can be administered safely in pregnant women (Koren et al., 2013)). Cisplatin is also recognized as a potent carcinogenic compound (Sanderson, 1996). However, it is much less haematotoxic and myelosuppressive than other frequently used chemotherapeutic agents (e.g. paclitaxel, etoposide). At doses higher or more frequent than those now recommended **(Table 2, Table 4)**, neuropathy with irreversible symptoms can be observed in patients (e.g. paraesthesia, loss of reflexes, loss of proprioceptive and vibratory sensation, loss of motor function) (British Columbia Cancer Agency, 2013).

2.6.1.1. Nephrotoxicity

2.6.1.1.1. Pharmacology

Kidney excretion is the principal route of elimination for cisplatin, as up to 50% of the administered cisplatin is excreted in urine 24 hours after its administration. Kidneys are also known to concentrate cisplatin in greater amounts than other organs, and cisplatin found in the tubular region can be up to 5 times the serum concentration (Yao et al., 2007). The accumulation of free cisplatin (unbound to plasma proteins) is realized by peritubular uptake in the proximal and distal nephrons, particularly in the S3 and the S1 segments of the proximal tubule and in the distal collecting tubule. Cisplatin uptake through renal cell membrane is done by non-saturable active transport (Burger et al., 2010), primarily by the organic cation transporter 2 (OCT-2) transporter, the main isoform present in kidneys, and by passive diffusion (Ciarimboli et al., 2005, Yao et al., 2007). For instance, the uptake of platinum analogues such as carboplatin are not mediated by organic cation transporters and are in consequence much less nephrotoxic (Ciarimboli et al., 2005).

The molecular mechanisms causing the toxicity of cisplatin in these cells are caused by an end-product of metabolism, a reactive thiol-bearing nephrotoxin, obtained after conjugation of cisplatin with glutathione or cysteine and metabolization by the γ-glutamyl transpeptidase (GGT) or the cysteine-S-conjugate ß-lyase. Inhibition of these enzymes, pre-administration

of glutathione or inhibition of organic cation transporters with a transport competitor such as cimetidine, are promising approaches to limiting cisplatin nephrotoxicity (Townsend, 2003, Ciarimboli et al., 2005). The relationship between plasmatic C_{max} of free cisplatin and its metabolites (ultrafilterable) and nephrotoxicity has been reported. Precisely, Nagai et al. (1996) showed that the plasmatic C_{max} was related to the maximum blood urea nitrogen, serum creatinine and minimal serum creatinine clearance.

2.6.1.1.2.Prevalence and symptoms

Cisplatin nephrotoxicity is cumulative and time and dose-dependent. It can be observed in 28-36% of patients treated with a single 50 mg/m² dose. It is often reversible but large and repeated doses increase the risk of chronic kidney disease, which is why kidney impairment must be assessed by a proper follow-up (see 2.6.1.1.3.). Patients with history of kidney disease and older patients are at a higher risk of nephrotoxicity with cisplatin (Yao et al., 2007, Miller et al., 2010). Acute kidney injury is the most common and most serious observed nephrotoxicity and occurs in 20-30% of patients (Miller et al., 2010), generally after 2-6 days (Tsang et al., 2009). Polyuria is frequently observed a few hours after cisplatin administration. It is linked to early electrolyte disturbances, in particular increased sodium excretion caused by a decreased sodium reabsorption in the proximal tubule and decreased sodium and water reabsorption in the distal tubule (Yao et al., 2007). Excretion disturbances are frequently encountered, in particular regarding electrolytes, with frequent hypernatremia, hypokalemia, hypomagnesaemia (in 40-100% of patients) and hypocalcemia (Yao et al., 2007), as well as increased azotemia and hyperuricemia (Tsang et al., 2009). A reduction of the glomerular filtration rate from 78% and of the creatinine clearance rate by increased serum creatinine and decreased urinary creatinine (Yao et al., 2007) can be observed from 2-3 days after treatment (Santoso et al., 2003). Early markers of kidney injury are used or under development in clinical care. Examples are N-acetyl-ß-D-glucosaminidase (NAG), ß$_2$-microglobulin (BMG$_u$) or alanine aminopeptidase (AAP), to assess for tubular damage (Nagai et al., 1996, Yao et al., 2007), and more recently, neutrophil gelatinase-associated lipocalin (NGAL) or urinary IL-18, among others, which could permit early detection of kidney failure and proper care management for these patients (Alge and Arthur, 2015). Recovery of the kidney function is normally observed after 2-4 weeks of treatment but chronic renal failure is sometimes observed, particularly after repeated courses of treatment, and can last up to 2 years (Tsang et al., 2009).

2.6.1.1.3. Nephroprotection

Before cisplatin administration, the kidney function of patients must be evaluated or re-evaluated after previous cisplatin cycles. It is done through measurement of creatinine

clearance, serum creatinine, blood urea nitrogen, that are increased when kidneys are impaired and major electrolytes (magnesium, sodium, potassium, calcium) that show major disturbances in the case of kidney injury. Cisplatin can only be re-administered again after normalization of the renal function.

To avoid kidney impairment, cisplatin regimens include well-spaced cycles of administration, usually every 3-4 weeks, as shown above (**Table 2** for NSCLC and **Table 4** for SCLC). Large-scale peri-hydration is standard procedure with cisplatin (volume varies from 1 to 4 L) by IV infusion for up to 8-12 hours before administration and follows precise guidelines, which depends on the patient's prior kidney function and on the cisplatin administered doses (NHS, 2012). Additional nephroprotective agents (e.g. mannitol, furosemide) are given concomitantly to cisplatin to increase diuresis, over 6-8 hours (Santoso et al., 2003). Patients are also advised to have high oral water intake for at least 24 hours after therapy to maintain diuresis (NHS, 2012). Nephrotoxic drugs (e.g. aminosides, amphotericin B) must be avoided (Tsang et al., 2009).

2.6.1.2. Ototoxicity

Ototoxicity is observed in ~30% of patients after a single 50 mg/m² dose. Its main manifestations are tinnitus, observed in up to 36% of patients and loss of acuity for high frequencies (from 4 000 to 8 000 Hz), observed in ~25% of patients. Hearing losses in medium frequencies can also be observed with the highest doses, usually above 100 mg/m² (Rybak et al., 2009). These hearing losses are bilateral, irreversible and can ultimately cause complete deafness. They are worse and more frequently observed in pediatric populations. They are frequency-related and dose-related and usually occur after the second-dose. They are worsened with concurrent or previous cranial RT, above 48 Gy in total radiation dose. It seems that ototoxicity is linked to high plasmatic C_{max} as IV bolus showed a higher otic impairment than IV infusion (Rademaker-Lakhai et al., 2006) and hearing losses are very likely caused by a high cisplatin concentration in cells inside the inner ear (e.g. outer hair cells, vestibular system, cochlea: organ of Corti, stria vascularis) (Tsang et al., 2009). This high concentration leads to the generation of reactive oxygen species (ROS), while the antioxidant system is depleted by interaction with cisplatin, leading to higher oxidative stress inside the cells of the cochlear tissue (Rybak et al., 2009).

Potential otoprotectors (e.g. N-acetylcysteine, sodium thiosulfate, methionine, lactated Ringer's solution) with anti-oxidative properties have been administered by the general route

but have two major limitations. First, they must be able to cross the blood-brain barrier and second, as strong nucleophiles, they may alter cisplatin anti-tumoural activity. Local administration of some of these otoprotectors, using transtympanic perfusion has shown tremendous results *in vivo* but is not at all patient-friendly (Choe et al., 2004, Rybak et al., 2009).

Therefore, to date, there are no particular auditory protection measures that can be taken regarding ototoxicity, unlike with renal preventive care. Audiometric tests are therefore a mandatory part of every pre-treatment evaluation (Rybak et al., 2009).

2.6.1.3. Haematotoxicity

Haematotoxicity is observed in 25-30% of patients but is usually reversible. Nadirs (the lowest measured point) for platelets and leucocytes are observed between days 18-23, and normalization occurs after day 39. The effect is dose-dependent and higher at doses superior to 50 mg/m². Anaemia can also be observed at the same frequency and may be caused by a decrease in erythropoietin linked to renal damage or direct damage to erythroid stem cells. Myelosuppression is relatively rare with cisplatin and lower than with other antineoplastic drugs such as paclitaxel or irinotecan (British Columbia Cancer Agency, 2013).

2.6.1.4. Gastrointestinal toxicity

Acute nausea and emesis (from 4 to 24 hours) are very frequently observed in patients (more than 90% occurrence) and are sometime so intense that treatment has to be adjourned (Jordan et al., 2007). Delayed nausea and emesis can be observed up to 2 weeks (from 60 to 90% occurrence) after large doses and tend to increase the potential for kidney injury due to lasting dehydration and electrolyte loss (Yao et al., 2007, Tsang et al., 2009).

Treatment with potent antiemetic drugs such as 5-HT$_3$-receptor or neurokinin-1-receptor antagonists (e.g. ondansetron, aprepitant) may be given concurrently to peri-hydration (Jordan et al., 2007). Diarrhoea is possible but uncommon (Tsang et al., 2009).

2.6.1.5. Others

Neurotoxicity with headaches, dizziness, hallucinations, delirium, encephalopathy, seizures, paresthesia and numbness are sometimes encountered and are linked to axonal damage. Hepatotoxicity is also experienced as cisplatin tend to concentrate in the liver but to a lesser extent than in kidneys and the inner ear, causing for instance elevated transaminases (Tsang et al., 2009). Retinopathy and visual loss have been reported but only with high doses and remain uncommon (Omoti and Omoti, 2006).
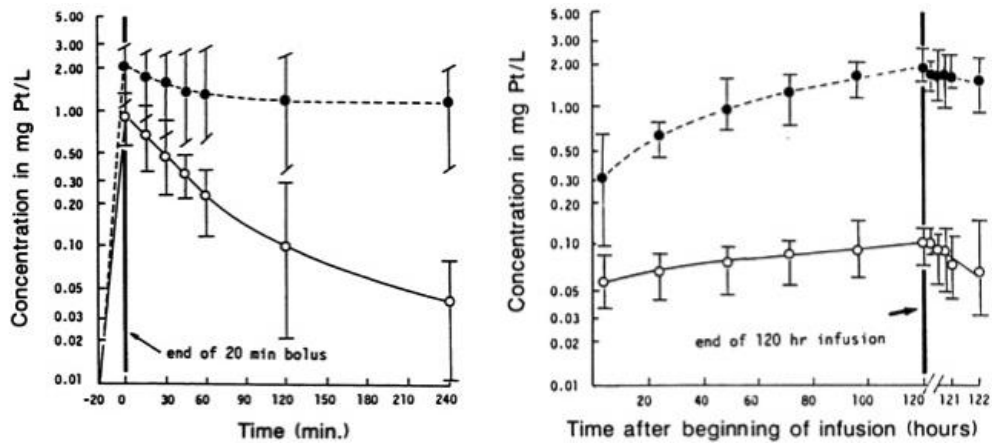
Figure 21. Semi-logarithmic free (O) and bound (●) plasmatic platinum comparative pharmacokinetics between cisplatin intermittent bolus (left) and continuous infusion at 30 mg/m²/day over 5 days (right), from Forastiere et al. (1988).

No specific pulmonary toxicity has been reported for cisplatin, except for one case of hyperpnoea followed by acute respiratory failure after drug overdose. This uncommon event was linked to administration of 3 times the planned dose at 450 mg or ~300 mg/m² IV over 3 days, which permitted its passage into the central nervous system and impaired the respiratory centre (Fassoulaki and Pavlou, 1989, Camus et al., 2016).

2.6.2. Routes of administration

2.6.2.1. Parenteral

In the early days of cisplatin administration, the outcomes of IV infusion were evaluated against repeated IV boluses. Slow IV infusion, lasting from 2 to 4 h, which is now standard (Nagai et al., 1996, NCCN, 2014b, NCCN, 2015), helps limit acute adverse effects through a diminution of plasmatic peaks of free cisplatin **(Figure 21)**. It also increases the exposure, measured as the plasmatic AUC. Together these effects increase the therapeutic index (Forastiere et al., 1988).

Intra-arterial administration of cisplatin has also been assessed against various cancers (e.g. head and neck, bladder, osteosarcoma). It has the theoretical ability to concentrate cisplatin near the site of injection and lower the adverse effects, but showed poor results (Bielack et al., 1989, Rasch et al., 2010, Jiang et al., 2014).

After the standard IV infusion C_{max} is achieved within the first hour and then decreases following a biphasic decay. In humans, the reported initial half-life ($t_{1/2^i}$) varies between 20 and 60 minutes, and represents distribution to afferent organs. The terminal half-life ($t_{1/2^t}$) is much longer and varies from 24 to 72 hours, representing progressive elimination of the 90% protein-bound platinum (Tsang et al., 2009).

2.6.2.2. Local (non-pulmonary)

Cisplatin has also been administered using non-parental routes of administration, seeking local action in target organs and reduction of exposure in non-target organs and of adverse effects. In particular, local action was investigated through intraperitoneal injection against ovarian cancer, which was not safe and increased the adverse effects (van Rijswijk et al., 1997), and by the intracavitary route against unresectable solid tumours in the abdominal cavity (Katzenstein et al., 2010) and against mesothelioma after pneumonectomy (Tilleman et al., 2009), both of which showed mixed results and nephrotoxicity. Cisplatin, which usually does not pass the blood brain barrier, was also assessed against glioblastoma multiforme

using local deposition followed by irradiation with a polymer depot-form implanted in the brain, which increased survival and decreased the toxicities (Sheleg et al., 2002). Finally, cisplatin intratumoural injection was assessed against mediastinal and hilar recurrences of lung cancer, with which patients are usually only candidates for palliative treatment and supportive care. This treatment exhibited high response rates (69%) and relatively low toxicities (Mehta et al., 2015).

2.6.2.3. Pulmonary

Cisplatin administered by the pulmonary route was assessed in three clinical trials in the last decade, all through jet nebulization of liposomal cisplatin. These are further described later on.
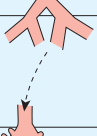
Figure 22. A. Subdivisions of the conducting and respiratory airways from Chesnutt and Prendergast (2014), and **B.** the human airway bronchial tree obtained from a 3D-CAT scan from Wu et al. (2014).

3. Inhaled therapies

3.1. Structure of the lung

The pulmonary tract is conventionally divided between the upper and the lower respiratory systems. The upper respiratory system comprises the oropharynx, the nasopharynx, the pharynx and the larynx. The lower respiratory system comprises the trachea, the bronchi and the lungs, divided in three and two lobes for the right and left lung, respectively. A model was described by Weibel in 1963 (Weibel, 1963, Albertine, 2016), where bronchi are made of a complex succession of dichotomous divisions from the tracheobronchial tree starting at the end of the trachea (generation 0) to the alveolar sacs in the deep lung (generation 23). From generation 0 to 15-16, the tracheobronchial tree is gradually divided into two primary bronchi, divided into smaller secondary bronchi, one for each lobe. These bronchi are then divided into segmental bronchi, which after a few generation become bronchioles to terminal bronchioles in what is called the conducting zone. This zone does not participate in any gas exchanges. After generation 16-17, the airway is considered a respiratory zone, involving structures providing gas exchanges, including the respiratory bronchioles, which divide into alveolar ducts and ultimately, alveolar sacs, the terminal end of the respiratory tree **(Figure 22.A, B)** (Albertine, 2016).

As the generation and number of individual structure increases, the diameter and length decreases from the centimetre to the millimetre range. In the meantime, the total surface at the last generations increases up to 140 m^2 for the total respiratory zone (Weibel, 1963, Albertine, 2016).

Regarding the conducting airways, the primary bronchi and the trachea are supported by cartilaginous rings, which progressively become thinner and finally disappear at the bronchiole division when its diameter reaches ~1 mm. The airway lumen is lined with columnar ciliated pseudostratified epithelial cells placed on top of basal cells and a few scattered mucus cells in the healthy lung. The latter can also be found more deeply in the bronchial epithelium (Evans and Koo, 2009). Mucus cells are found in the nose, trachea and bronchi. Their role is to secrete mucus, a viscous fluid comprised of glycoproteins and proteoglycans, which is secreted and spread on the lumen side of the bronchial epithelium (Mason and Dobbs, 2016). The roles of the mucus are: (i) to prevent adhesion and accumulation of foreign exogenous particles (e.g. microbes, pollution particles) in the airways; this is done as part of the mucociliary escalator with the added action of the
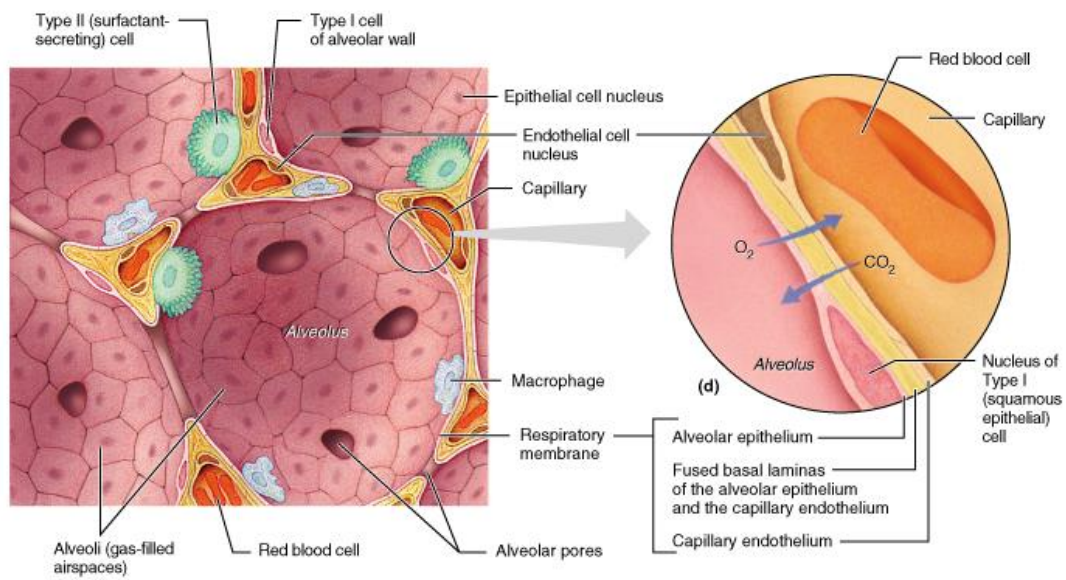
Figure 23. Representation and functions of the alveolar structure, from Martini et al. (2001).

uniformly distributed cilia on the lumen of the airways; (ii) to protect airways from microbial invasion though the antimicrobial activity of the mucus proteins; and finally, (iii) to prevent airway desiccation (Evans et al., 2009). Mucus overproduction is linked with many inflammatory lung diseases such as COPD and some lung cancers (Williams et al., 2006).

Cilia are uniformly distributed and beat towards the pharynx in a coordinated movement. They are part of the mucociliary escalator, an important protection mechanism, continuously moving the mucus from the lower part of the respiratory tract, up to the upper respiratory tract and the pharynx where the mucus is eliminated by coughing or swallowing.

Finally, Clara cells are found in the terminal bronchioles, among the ciliated cells. They are non-ciliated and secrete surfactant lipoproteins SP-A and SP-D, which have tensioactive properties and the principal role of avoiding luminal collapse during expiration (Mason et al., 2016).

At the end of the respiratory zone are alveoli **(Figure 23)**. These are polyhedral air-filled compartments, surrounded by a thin layer of connective tissue, the alveolar septum, which embeds a large number of blood capillaries. They are the main site of exchange of oxygen and carbon dioxide to and from the blood in the alveolar capillaries (Mason et al., 2016). There are three main cell types in the very thin alveolar membrane, called pneumocytes. Type I pneumocytes are squamous cells and are the structural cells of the alveolar membrane, representing 10% of the cell composition but about 95% of the surface area. Type II pneumocytes are also responsible for surfactant production and represent the remaining 5% surface area, despite being in the same numbers as type I pneumocytes (Mason et al., 2016). Finally, lung macrophages reside on the internal surface of the alveoli, and represent the remaining 80% of the cell composition. The alveolar membrane is also comprised of many pores (i.e. Kohn pores), responsible for interalveolar exchanges through the alveolar septum. The surfactant is a complex lipoprotein-based medium, composed of 90-95% w/w lipids and 5-10% w/w proteins. The lipid part of the pulmonary surfactant is composed of a very large proportion of saturated phospholipids: dipalmitoylphosphatidylcholine (DPPC) (~40% w/w); and unsaturated phospholipids: phosphatidylcholines (~35% w/w), phosphatidylglycerol (~10% w/w), phosphatidylinositol (~2% w/w), phosphatidylethanolamine (~3% w/w), lyso-*bis*-phosphatidic acid (~1.5% w/w), sphingomyelin (~2.5% w/w) and neutral lipids (3% w/w), mainly cholesterol (Possmayer et al., 2001). The protein part of the pulmonary surfactant comprises serum proteins and apoproteins. The role of pulmonary surfactant is to reduce surface tension in

A Inspiration Expiration

Baffle Venturi
Feeding tube Liquid
Air from compressor

B Air sucked through vent on inspiration Vent closed on expiration
PATIENT PATIENT
Feeding tube Liquid
Air from compressor Air from compressor

C Air
Therapeutic mist
Piezo electric crystal
High frequency source
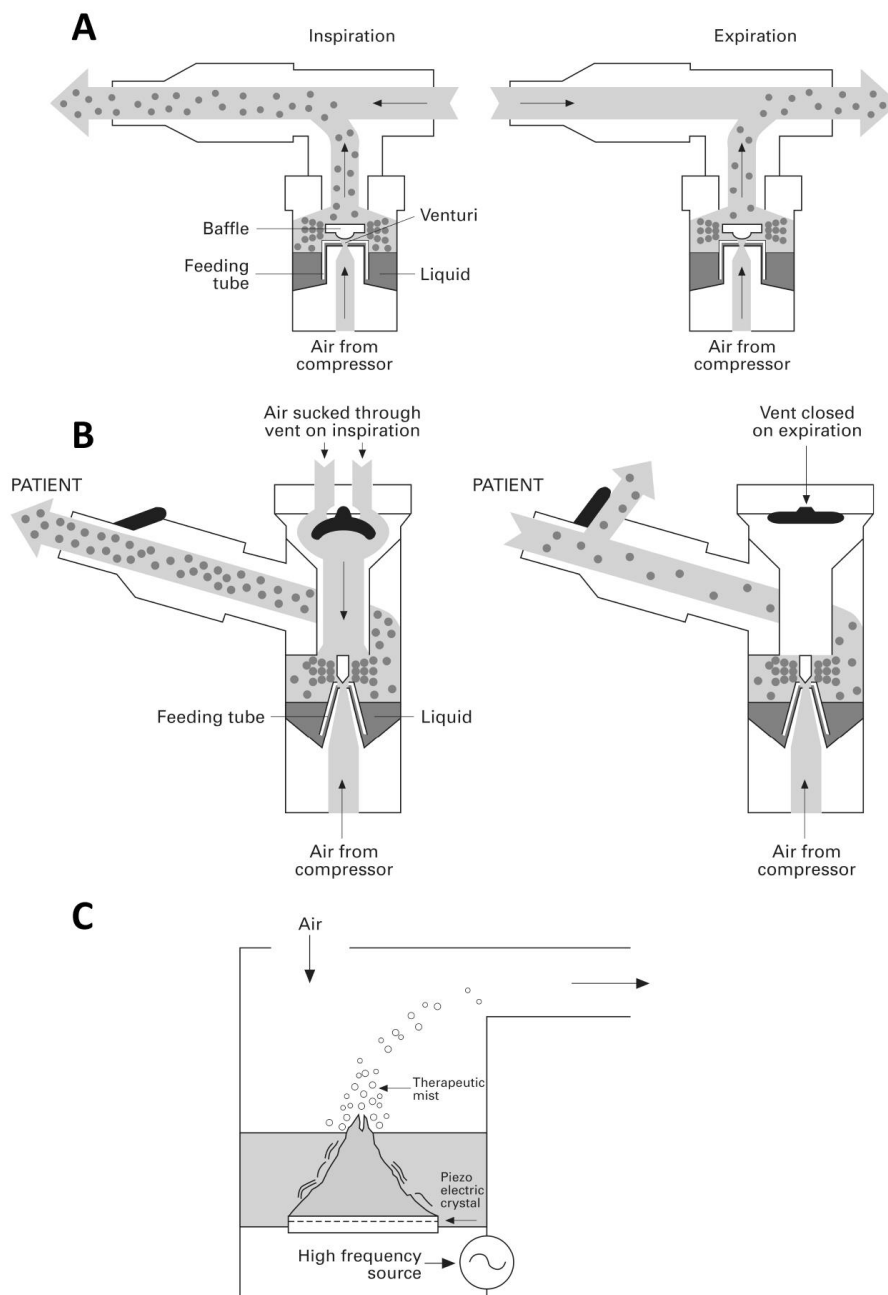
Figure 24. Schematization of **A.** a conventional jet nebulizer design, **B.** a breath-activated nebulizer design, **C.** an ultrasonic nebulizer design, from O'Callaghan and Barry (1997).

order to limit alveolar collapse during expiration and to facilitate lung inflation during inspiration. It also helps prevent fluid accumulation from the capillaries to the alveolar space by reducing surface tension. Finally, the pulmonary surfactant has an immune function attributed to the opsonisation abilities of apoproteins SP-A and SP-D, which can bind to pathogens and promote their phagocytosis by alveolar macrophages (Possmayer et al., 2001)

3.2. Advantages of the pulmonary administration route

Direct administration of drugs to the lungs has three main benefits. First, it can provide a rapid onset of action, which is particularly needed in the case of respiratory diseases with acute exacerbations such as asthma and COPD. The drugs for these diseases (e.g. ß2-mimetics, corticosteroids) aim at specific receptors located in the smooth muscle of an inflammation site. Second, it can provide high local drug concentration directly at the site of action and at the same time reduce concentration in the rest of the body, thus increasing the therapeutic ratio of drugs that exhibit systemic toxicity (e.g. antifungal, bronchodilators, corticosteroids). Finally, it provides an alternative administration route for drugs that have poor oral bioavailability, such as peptides (e.g. insulin, Afrezza®) (Patton and Byron, 2007, Loira-Pastoriza et al., 2014), and that require an invasive route of administration, such as vaccines (in development).

3.3. Inhalational delivery devices

Inhalation therapy is a very ancient administration route dating back to up to 4 600 years. Inhalation medicine started its modern era with the development of nebulizers, followed by the first pressurised metered dose inhaler (pMDI) by Riker (3M) in 1955, and with the approval of isoprenaline and adrenalin pMDIs in 1956 and of salbutamol in 1969. A the same time, DPIs were also developed, first as capsule-based inhalers and then as multi-unit dose inhalers, along with new inhalable drugs targeted against asthma or COPD, such as beclomethasone and budesonide (Sanders, 2007).

3.3.1. Nebulizers

Nebulizers produce aerosols of inhalable aqueous droplets. Jet nebulizers **(Figure 24. A)** are based on the Venturi effect, which states that there is a reduction in pressure of a fluid (airstream) and an increase in its velocity when is goes through a constricted section. In this type of device, an airstream comes into contact with the end of a solution (or suspension) feed tube and the applied fall in pressure results in liquid being sucked up and atomized into droplets by surface tension. While any resulting particles that are too large are impacted onto

successive baffles and onto the walls of the nebulizer, preventing them from being emitted, the smaller ones are let through to be inhaled, increasing the inhalable fraction of particles (Martin and Finlay, 2015). Improved designs have been developed over the years to increase lung deposition from jet nebulizers and decrease drug loss from re-exhalation. These designs include collection bag, breath-enhanced and breath-actuated nebulizers **(Figure 24. B)**, which deliver aerosol during inhalation only (Ari, 2014).

Ultrasonic nebulizers **(Figure 24. C)** use high-frequency vibrations as the droplet initiator. They are composed of a vibrating piezoelectric head (1-3 Mhz), submersed in the liquid to nebulize it. When activated, it creates an aerosol directly at the air-liquid interface or indirectly by extrusion of the liquid through a ceramic mesh (O'Callaghan et al., 1997, Martin et al., 2015). The so-called small-volume ultrasonic nebulizers are more likely to be used for drug delivery than large-volume ones, which are usually used to deliver hypertonic saline (Ari, 2014). Finally, vibrating mesh nebulizers produce aerosol through the vibration of a mesh or a membrane pierced with micron-sized pores, with a piezoelectric head acting as a micro-pump or by a transducer horn that induces vibrations to the perforated mesh (Ari, 2014).

In general, nebulizers have many disadvantages. First, they require a compressed air source (for jet nebulizers) and/or a fixed power source to create the aerosol (except for some recent vibrating mesh nebulizers which can be operated using small batteries). Administration using these devices can be quite long depending on the quantity to nebulize (e.g. 5 ml/15 min for a conventional jet nebulizer), require tedious post-administration cleaning and maintenance, which is not always easily done, and are much costlier than non-reusable units. Also, ultrasonic nebulizers are known to disrupt heat-sensitive materials and liposomes. Finally, one of the biggest issues regarding this kind of inhaler for highly toxic drugs is the lack of containment, associated with a large waste of medication in the environment during exhalations when the aerosol is generated but not delivered to the patient lung.

Nevertheless, these devices still present some advantages and are still widely used in home and hospital settings. This is because they do not require coordination between actuation and patient inhalation, unlike pMDIs, nor do they require active inhalation to generate the aerosol, unlike DPIs. These properties make them very useful for paediatric, elderly and unconscious patients or for those with impeded respiratory function (Ari, 2014, Martin et al., 2015). Nebulizers are also able to deliver high doses of medication (e.g. up to 300 mg for Tobi). Formulation of solutions for nebulizers is also quite simple but
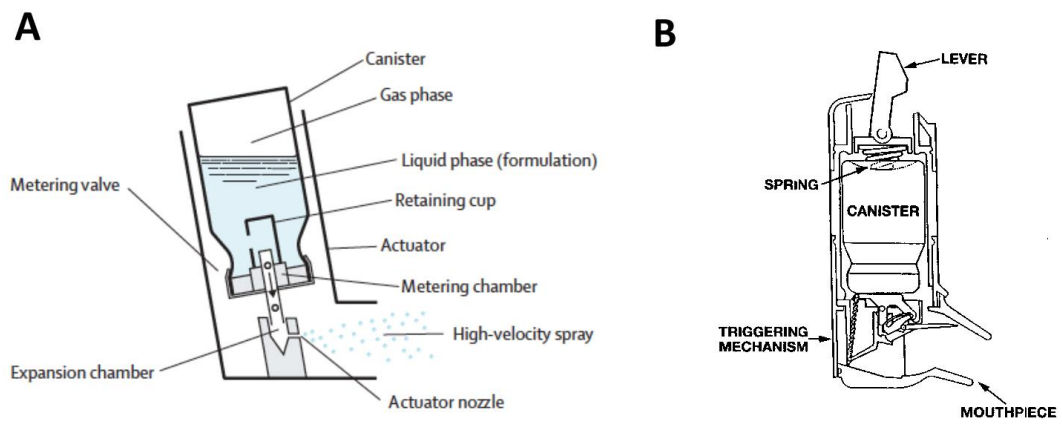
Figure 25. Representation of **A.** the classical pMDI mechanism, from Dolovich and Dhand (2011), and of **B.** a breath-actuated pMDI mechanism, from Newman et al. (1991).

is mostly applicable to water soluble drugs and depends on the dose to administer. For these reasons, it is the primary approach for development of new inhalation therapies in clinical settings (Pritchard, 2015).

3.3.2. Pressure metered-dose inhalers (pMDIs)

In this type of device, the drug is solubilized or dispersed into a propellant gas, pressurized into a liquid and set into a canister **(Figure 25)**. A metering valve, on top of the canister, sets the volume of liquid that is to be delivered (a few hundred µL). After actuation of the device, the propellant begins to boil as it expands and is expelled from the valve, forming drug-containing droplets. The aerodynamic properties of the formed aerosol depend on the formulation composition (e.g. vapour pressure of the propellant, drug particle size in the case of a suspension, drug concentration, viscosity) and valve parameters (Dolovich et al., 2011).

Formulations are often comprised of sorbitan esters, oleic acid and lecithins, which helps lubricate the valve mechanism and favours drug dispersion upon actuation of the device. Conservation agents such as antioxidants or chelating agents are added for stability purposes. Flavouring agents may also be added (Dolovich et al., 2011).

Propellants of pMDIs were historically chlorofluorocarbon (CFC)-based but these were discarded by the Montreal Protocol of 1987 (Ozone Secretariat, 1987) because of their negative impact on the ozone layer. They were replaced by the non-CFC-based propellants hydrofluoroalkanes (HFA), including heptafluoropropane (HFA-227) and tetrafluoroethane (HFA-134a) (Labiris and Dolovich, 2003). Ideally, new non-CFC-based pMDIs had to show equivalence to CFC-based pMDIs for the fastest approval. However, a profound re-design of formulations was also needed for some of them. This was because non-CFC propellants have poorer solvent abilities than CFCs, particularly regarding tensioactives, which greatly prejudices the aerosol and stability properties of the end products (Labiris et al., 2003, Dolovich et al., 2011). However, while HFA have a much lower impact on ozone depletion, they also participate in global warming as they are greenhouse gases, with a very high warming potency of up to 1 300-2 900 times that of CO_2 (Myrdal et al., 2014).

pMDIs have many advantages and are the most widely used inhalation devices worldwide (Pritchard, 2015). These multi-dose devices are cheap and portable and are able to provide a deposition in the lungs of 10-20% of the emitted dose (Labiris et al., 2003). They are, however, limited in terms of dose delivery. All commercial devices exhibit doses ranging in the µg, making them unable to deliver anticancer drugs, which are generally active at much
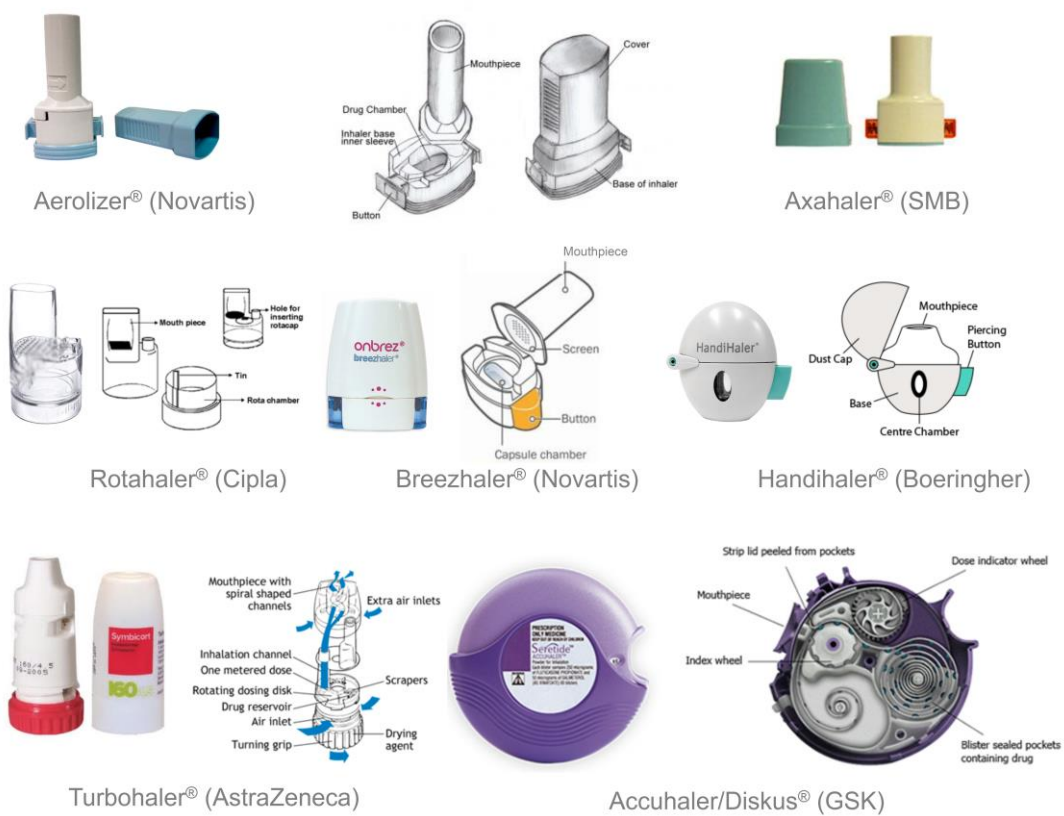
Figure 26. Some examples of DPIs: single-unit (two top rows), reservoir (bottom left) and multiple-unit (bottom right) designs.

higher doses. Moreover, the major issue with classical "press and breathe" pMDIs is probably that they require accurate coordination between inhalation and actuation of the puff to attain the appropriate lung deposition (Gross et al., 2003). As the device is pressurized, it creates a high velocity aerosol (> 30 m/s) that majorly impacts the upper airways and that is intensified if the flow rate created by the patient's inspiration is not timed properly (e.g. too rapid inhalation, too short breath-hold) (Labiris et al., 2003). Incorrect use of this type of pMDI is encountered in up to 91% of patients (Epstein et al., 1979). This can cause as low as 7% of the dose to be actually deposited in the lower airways. Spacers can be used to avoid this issue and facilitate delivery in patients with poor coordination (the elderly, children) but they are cumbersome and can lead to other issues such as static electricity (Dolovich et al., 2011). More expensive breath-activated devices have also been developed and have helped reach a 3-fold higher deposition than conventional press and breathe pMDIs (Newman et al., 1991). They are, however, unable to avoid the "cold-Freon® effect", which causes some patients to stop inhaling when the cold gas reaches the back of their throat (Labiris et al., 2003).

3.3.3. Dry powder inhalers (DPIs)

DPIs were developed as a consequence of the clinical difficulties encountered with bad coordination technique with pMDIs and by the re-design needed after the suppression of CFCs. In fact, DPIs are actuated by the patient inhalational effort and as consequence do not require propellant (Labiris et al., 2003). DPIs are small, portable devices that are either single-dose, in which the powder is set into a capsule (e.g. Axahaler®, Aerolizer®, Breezhaler©, Handihaler®), or multi-dose, in which the powder is set into multi-unit foil blisters (e.g. Diskus®) or as a bulk into a powder chamber (e.g. Turbohaler®) or into a cartridge (e.g. Novolizer®) **(Figure 26)**.

Major advantages of DPIs lie in the increased long-term stability of formulations in their dried form, and that they do not require extemporaneous reconstitution like some nebulized formulations or cold-chain storage like some pMDI formulations (e.g. Formoair®). These devices present high lung deposition abilities, ranging between 25 and 40% of the nominal dose and are able to deliver drugs regardless of the hydrophilic and hydrophobic properties of these (Hoppentocht et al., 2014). Moreover, the doses delivered by DPIs vary between the μg range up to a few mg (e.g. up to 28 mg for TOBI™ Podhaler™ and 40 mg for Bronchitol®) in a very short timeframe (~ 1 min).

Interparticulate forces in   Dispersion forces   Deposition forces in the
the powder formulation   generated by the DPI   respiratory tract
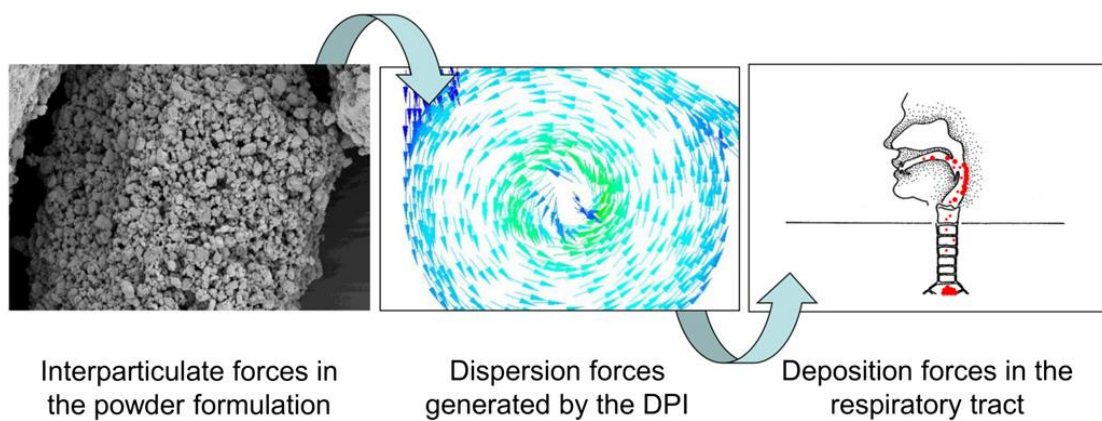
Figure 27. Desired balance between interparticulate forces in the formulation, dispersion forces generated by the inhaler and deposition profile in the respiratory tract, from Hoppentocht et al. (2014).

Nevertheless, DPIs also present some disadvantages. One is that because formulations are powder-based, they are quite sensitive to relative humidity. The breath-actuated approach could also have an impact on the deagglomeration abilities of the formulations under lower flow rates, as can be seen with impeded respiratory function of patients. This can be avoided using low-resistance devices and dry powder formulations with low dependency on the flow rate (Labiris et al., 2003).

3.3.3.1. Aerodynamic performance from a powder formulation through its attributed DPI

Formulation loaded in an inhalation device is characterized by the delivered dose, which is the quantity of drug particles able to be delivered by the inhalation device and therefore available for the patient on a per actuation basis. The efficacy of a formulation loaded in an inhalation device is defined as the fraction or the dose from the nominal dose (i.e. the loaded dose from the capsule, the reservoir or the blister) that presents a d_{ae} inferior or equal to 5 µm (i.e. fine particle fraction (FPF) or fine particle dose (FPD) and is so theoretically able to reach the deep lung following inhalation by the patient (Pilcer et al., 2012).

The d_{ae} is influenced by the particle geometrical diameter, shape and density, following **Equation 1**:

$$d_{ae} = d_{geo} \sqrt{\frac{\rho_{particle}}{\rho_0 \chi}}$$

Equation 1. Calculation of the aerodynamic diameter (d_{ae}).

Where d_{ae} is the aerodynamic diameter, d_{geo} the geometric diameter, $\rho_{particle}$ the density of the particle and ρ_0 the particle unit density (1 g/cm^3 sphere) and χ the dynamic shape factor (responsible for drag forces).

Most commercial formulations exhibit FPFs around 20% w/w of the nominal dose. The FPF is also sometimes expressed as a ratio of the emitted dose, without taking into account the fraction of particles that are impacted or remain in the device.

The FPF or FPD depends on three major types of forces: the interparticulate forces in the powder formulation, the dispersion forces generated through the DPI device by its design and the patient's inspiratory airflow and the deposition forces in the respiratory tract **(Figure 27)**.

3.3.3.2. Interparticulate forces in the powder formulation

Interparticulate forces are comprised of forces of physical interaction, primarily van der Waals forces, but also electrostatic, capillary and mechanical interlocking forces. These forces vary based on the particle size, shape, surface properties and hardness, and on relative humidity, for instance. Van der Waals attraction forces are preponderant in dry powders, especially when particles are very close (< 100 nm), and for micron-sized particles (below 10 µm). This type of interaction increases with smoother particles and reduces with those exhibiting uneven surfaces, as the latter increase the true inter-particle distance.

Electrostatic charges appear between donor and acceptor particles. The charging phenomenon usually appears following a charging contact due to very short collision and friction, either with other particles or with metal or glass during the production process (i.e. mixing, handling, filling), storage (e.g. stainless steel, polypropylene) and in the DPI during aerosolization. These forces can affect the powder flowability and the aerosolization process, which can in turn affect their dispersion and deposition abilities.

Capillary forces are caused by the appearance of a liquid meniscus around the contact area of two close particles and can even cause capillary condensation, which is due to vapour condensation between two very close hydrophilic particles. This can result in an attractive force, which is caused by the surface tension around the meniscus and by the negative pressure caused by the curved shape of the meniscus. This type of force depends widely on the relative humidity, but also on the physico-chemical properties of the drug and the presence of a carrier (e.g. lactose, mannitol), as well as the particle size, roughness, surface properties and shape (Pilcer et al., 2012).

Mechanical interlocking is a force of structural cohesion between particles, caused by irregularities at their surface, which can ultimately diminish dispersion of the formulation.

3.3.3.3. Dispersion forces generated by the DPI

The principal mechanisms responsible for powder deagglomeration within the DPI devices are particle interaction with shear flow and turbulence, particle-device impaction and particle-particle impaction. The deagglomeration force applied to the powder bed is directly dependent on the intensity of turbulence, itself dependent on DPI design (flow resistance, grids) and also on the inspiratory effort of the patient (peak flow rate and flow increase rate). Proper inhalation technique is also necessary to be able to reach the highest depositions

(e.g. exhalation before the inhalation through the DPI and breath-holding after inhalation) (Pilcer et al., 2012). High resistance devices generate high turbulence, and therefore tend to generate high dispersion of the powders and result in high FPFs. However, they need a high inspiratory effort, which is not always attainable in patients with impeded respiratory function, as in COPD for instance. Medium- and low-resistance devices should therefore be chosen for specific subsets of patients and specific diseases in order to maintain high deposition abilities. These devices offer high deposition abilities even under 60 L/min airflows. Moreover, in capsule-based devices, the capsule participates in the dispersion without increasing the device's resistance (Labiris et al., 2003). Another strategy to ensure high and reproducible deposition in all patients is to use power-assisted devices, which are under development but seem to be a much more expensive approach. These are therefore reserved for therapies with narrow therapeutic indexes. (Pilcer et al., 2012).

3.3.3.4. Deposition forces in the respiratory tract and the importance of aerodynamic diameter

There are five forces involved in particle deposition into the respiratory tract. These forces are (i) impaction forces, (ii) sedimentation forces, (iii) Brownian diffusion, (iv) interception forces and (v) electrostatic forces.

Impaction is linked to the inertia of particles, which end up colliding into the airways. This phenomenon majorly concerns particles of d_{ae} above 5 μm. It takes place principally in high-velocity airflows and following radical changes in direction of the airflow, therefore near bifurcations of the larger conducting airways (i.e. in the throat, the oropharynx and the primary bronchi). Sedimentation forces are linked to gravity. They are therefore preponderant when the airflow velocity is low (i.e. in smaller conducting airways) and mostly concern particles with a d_{ae} comprised between 0.5 and 5 μm, and generally increase with larger particle size. These sedimentation forces are therefore very dependent on the inhalation technique (e.g. deep inhalation, peak flow rate) and on the respiratory function of the patient. Brownian motion or diffusion involves particles below 1 μm in d_{ae}, and takes places in low velocity airflow, in the smaller airways and in alveoli. Interception forces involve the impaction of a portion of the particle onto the airway walls, while the centre of mass of the particle is still subjected to the airstream. Finally, electrostatic charges appear between particles during the generation of the aerosol. These charges rarely result in higher deposition onto the airways.
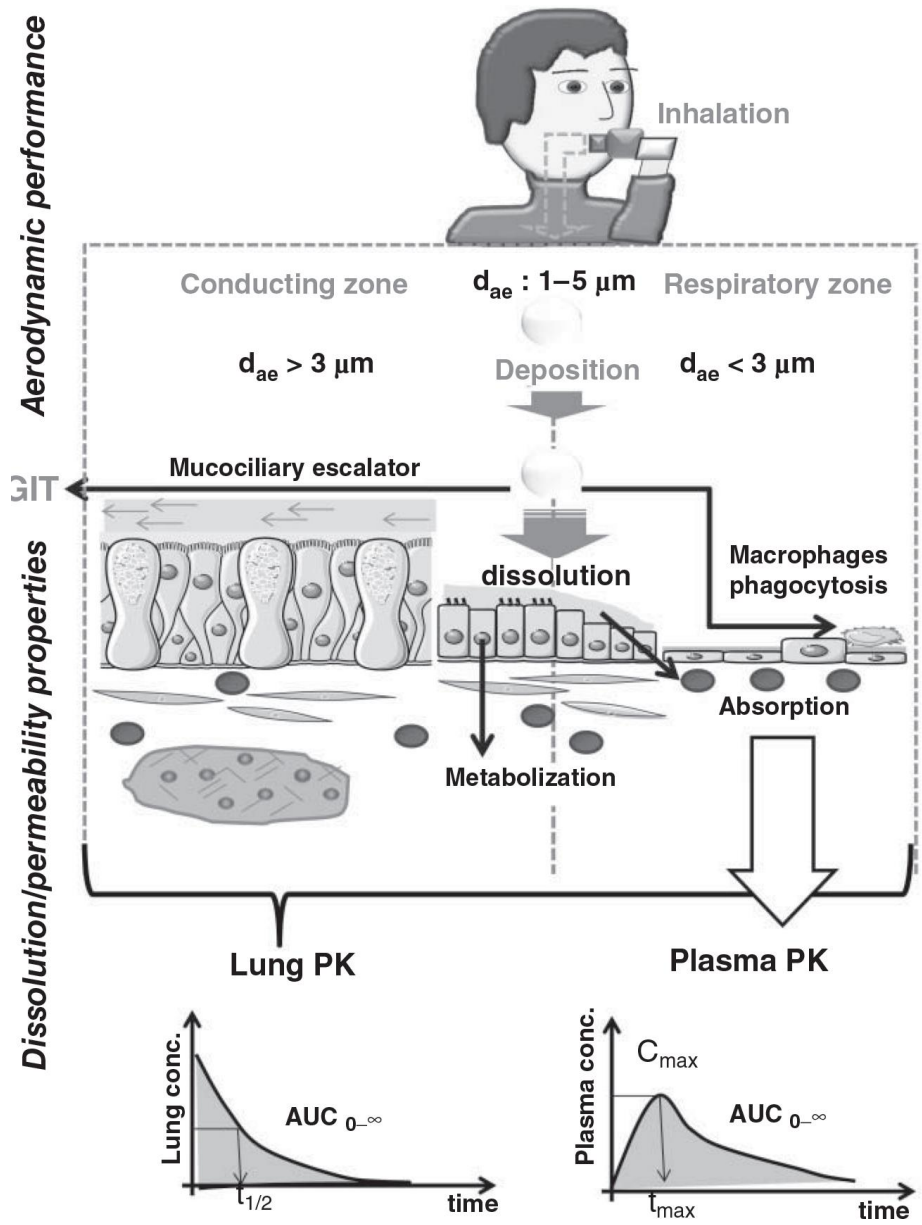
Figure 28. In vivo lung deposition, dissolution and fate of particles deposited in the conducting and in the respiratory zone of the lower respiratory airways, from Wauthoz and Amighi (2015a).

Particles that show the best ability to deposit in the lower lung (i.e. the generations after the bronchi up to the alveoli) are those presenting a d_{ae} of 1 to 5 µm, commonly defined as the inhalation range. Formulations and their associated DPI are engineered to obtain an aerosol in this range, based on the inhalation volume and airflow generated by a standardized healthy patient (i.e. 4 L at 60 L/min for 4 s, 4 kPa pressure drop across the inhaler device during the inhalation) (European Pharmacopoeia, 2014) within its defined DPI. This aspect must be considered during formulation design and testing, particularly with diseases that impede the respiratory function. Therefore, formulations that show low dependence on airflow are very much needed (Dolovich et al., 2011).

Moreover, particles with a d_{ae} in the lower fraction of the respirable range (i.e. 1 to 3 µm) will have the best chance of depositing in the respiratory zone (from respiratory bronchioles to the alveoli), while the upper fraction (i.e. 3 to 5 µm) will target the conducting zone after the bronchi (i.e. the bronchioles). Careful design of formulations could target lung diseases in specific regions of the lung (Hoppentocht et al., 2014).

3.4. Fate of deposited drug based particles into the lungs

Once deposited in the lungs, particles from the formulation come in contact with the mucosal layer lining the conducting zone and/or the lung surfactant lining the respiratory zone (~70 nm) depending on their d_{ae} **(Figure 28)**.

3.4.1. Drug particle dissolution and drug release from particles

The dissolution rate of particles in these respective fluids is defined by the Noyes-Whitney **Equation 2**.

$$\frac{dM}{dt} = \frac{A \times D \times (C_s - C_t)}{h}$$

Equation 2. Noyes-Whitney equation.

Where dM/dt is the dissolution rate, A the surface area of the drug in contact with lung fluids, D the diffusion coefficient in the respective fluid, C_s and C_t the drug saturation solubility and its concentration at a given time t, respectively, and h the fluid layer thickness around drug particles (Wauthoz et al., 2015a).

D is defined by the Stokes **Equation 3**, which describes the diffusion of dissolved drug in solution depending on the temperature, viscosity and drug molecule radius following Brownian motion, as follows:

$$D = \frac{RT}{N_A} \frac{1}{6\pi\eta r}$$

Equation 3. Stockes equation.

Where D is the diffusion coefficient in the fluid, R is the gas constant, T the absolute temperature, N_A the Avogadro number, η the the dynamic viscosity of the fluid and r the radius of drug molecules (Wauthoz et al., 2015a).

Together, these mean that particles show increased dissolution rates as their size reduces. Moreover, water-soluble particles will very likely be solubilized quickly. This is even truer with permeable drugs, which can cross epithelial barriers freely and be quickly eliminated from the lung by absorption (Patton et al., 2007, Wauthoz et al., 2015a).

In order to obtain a slower drug release confined to the lungs, inhalable carrier systems have to be designed with CR abilities (see 3.5. Controlled-release inhaled therapies).

Many mechanisms have been reported regarding CR from the different types of delivery systems that were developed for lung delivery. Generally, CR involves diffusion of the drug, following Brownian motion through a polymeric or hydrophobic system, or through a barrier (e.g. lipid bilayer, membrane).

In microspheres in which the drug is uniformly distributed in the CR particles, diffusion is mediated by the properties of the homogeneous matrix material or through pores. These designs produce a higher burst-effect. With time, the diffusion of the drug is impaired as the amount of drug near the surface decreases and the remaining drug is located closer to the centre of the particle, farther from the dissolution medium (Siegel and Rathbone, 2012). When considering solid drug particles incorporated into a homogeneous matrix, the mechanisms involved are first dissolution of the drug due to water diffusion into the matrix system and then drug diffusion through the outer shell of the CR matrix. The hydrophobicity of the matrix and presence of pores will therefore determine the dissolution, while the matrix layer thickness will affect the diffusion ability of the drug. Drug near the surface will provide a burst, and drug more deeply within the matrix structure will dissolve more slowly. In liposomes, the release rate will be influenced by an equilibrium between the localization of the drug (i.e. in the lipid bilayer if hydrophobic or in the aqueous compartment if hydrophilic) and the number and rigidity (transition temperature and ratio of composing lipids) of bilayers to cross, defining the diffusion abilities of the drug. Other parameters involved in CR from inhalable particles are, for instance, polymeric swelling and erosion of polymeric-matrix particles (Siegel et al., 2012).

3.4.2. Fate of dissolved or released drug

Once dissolved and released from its carrier in the lungs, drug can act on its local pharmacological target (e.g. corticosteroid receptors, infectious agent, smooth muscle, cancer cells). However, drug can also be absorbed into the bloodstream through the epithelial barrier of the lung, depending on its permeability. The rate of absorption generally depends on the hydrophobicity or hydrophilicity of the drug, its molecular size (influencing both the passive diffusion mechanisms) and the presence of passive or active transport mechanisms. For instance, small lipophilic drugs (size comprised between 100 and 1 000 Da) with a positive log P (partition coefficient between octanol and water) follow transcellular passive diffusion and exhibit a quicker absorption rate than small hydrophilic drugs with a negative log P, which follow paracellular passage by passive diffusion through aqueous pores in the tight junctions. Unlike active transport mechanisms, these absorptive mechanisms are non-saturable and account for the largest amount of drug passage.

Local metabolism of the dissolved or released drug is also possible within the lungs but to a much lesser extent than in the gut (Wauthoz et al., 2015a).

These absorptive processes are therefore responsible for the pharmacokinetic (PK) profiles that are observed systemically following deposition, distribution and absorption of the drug from the lung compartment to the blood **(Figure 28)**.

3.4.3. Fate of undissolved particles

3.4.3.1. Mucociliary clearance (MCC)

As described before, the composition of the lining fluid in the different regions of the airways varies significantly. In the upper conducting airways, it is a mucus viscous layer (10-15 Pa.s), with the thickness progressively decreasing from the trachea up to the terminal bronchioles (2-5 µm). In the respiratory zone, its composition (described in 3.1. Structure of the lung) changes to a less viscous pulmonary surfactant, with a thickness decreasing from 100 to 80 nm from the terminal respiratory bronchioles to the alveoli (Lai et al., 2009, Olsson et al., 2011).

In the upper regions of the lungs, the purpose of the mucus is to entrap foreign particles (e.g. dust, micro-organisms). These are then moved up by the mucociliary clearance (MCC) system (also called the mucociliary escalator) through the action of the ciliated cells, up to the throat where they can be either expectorated or swallowed. In healthy humans, the mucus moves at a high speed of up to 6 mm/min in the trachea (G0) but at a much lower speed in
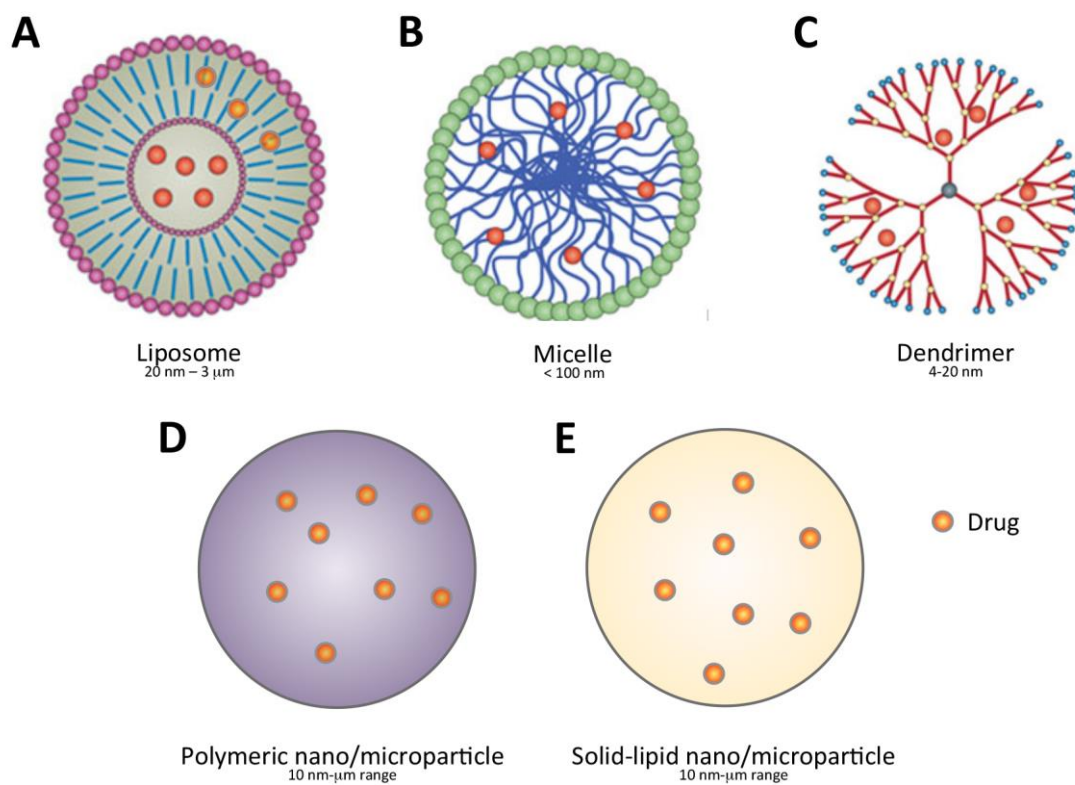
Figure 29. The different types of controlled-release particles developed for inhalation therapies, including **A.** liposomes, **B.** micelles, **C.** dendrimers, **D.** polymeric particles and **E.** solid-lipid particles, adapted from Orive et al. (2009).

terminal bronchioles (G15) (0.04 mm/min) (Fiegel et al., 2011, Olsson et al., 2011). This rate is lowered with lung diseases, age and smoking. Regarding inhalation therapies, this elimination process concerns larger particles (d_{ae} > 3 μm). These particles will therefore end up being either entrapped in the mucus and eliminated or will dissolve in it and be either eliminated with the mucus or diffused through the bronchial epithelium, where they can exert some pharmacological action (Olsson et al., 2011).

3.4.3.2. Macrophage phagocytosis system (MPS)

After generation 14-15 and closer to the alveoli, mucus and ciliated cells are less present in the bronchi. The MCC gives way to another preponderant mechanism, involving clearance of foreign particles by alveolar macrophages, the so-called macrophage phagocytosis system (MPS) (Loira-Pastoriza et al., 2014). This process particularly concerns undissolved particles. The macrophages, after incorporation of foreign particles following direct recognition by phagocytic receptors, or through specific and non-specific opsonisation (Aderem and Underhill, 1999), are either directed to upper airways where they are eliminated by the MCC, or eliminated by translocation to the lymphatic system or by enzymatic degradation.

Particles with diameters between 1.5 and 3 μm in geometrical size are the most prone to phagocytosis, which has been shown to take place in around 1 hour (Patel et al., 2015, Wauthoz et al., 2015a).

3.5. Controlled release inhaled therapies

Drug delivery by inhalation can be of great interest as localized therapy for respiratory diseases. However, the therapeutic advantage provided by local delivery to the lungs can be hindered by some particularities of this route of administration. First, rapid drug clearance from the lungs, due to rapid systemic absorption (for soluble and permeable drugs) or to local clearance mechanisms (for insoluble drugs or particles) can diminish the intended therapeutic effect. Second, in some applications, a drug load (peak concentration) higher than the therapeutic range could be potentially toxic. Therefore, CR of drugs using appropriate drug carrier systems **(Figure 29)**. compatible with (i) the lung parenchyma, (ii) the production methods able to provide particles in the inhalation range, (iii) the physico-chemical properties of the delivered drug and (iv) avoiding or limiting the lung clearance is greatly needed (Loira-Pastoriza et al., 2014, Aragao-Santiago et al., 2016).

These CR formulations must then be able to retain the drug within the lung in order to prolong its delivery to (i) ensure drug lung concentrations in the therapeutic range

Table 7. Formulation strategies for controlled release with their main class of excipients, lung tolerance, particle size range, controlled-release mechanism, production method up-scalability and latest stage of pharmaceutical development. For lung tolerance, + represents particles that have been safely administered to humans or during *in vivo* studies, +/- represents particles that have been partly tested *in vivo* or that use excipients that need further evaluation, - represents particles that have shown poor tolerance results *in vivo*.

	Excipients	Lung tolerance	Particle size	Controlled-release mechanism	Up-scalability	Latest stage of development
Liposomes	Lipids, phospholipids, aqueous phase	++	20-3 μm	Diffusion Translocation	+	Marketed (injectable) Phase III (inhalation)
Micelles	Lipid or Polymers, aqueous phase	-/+	< 100 nm	Diffusion	+/-	Phase II (injectable) Preclinical (inhalation)
Dendrimers	Polymers (PAMAM, PEHAM)	-/+	4-20 nm	Molecular disassembly	--	Phase I (injectable) Preclinical (inhalation)
Polymeric nanoparticles	Polymers (PLA, PLGA)	-	10-250 nm	Diffusion Erosion Swelling	+/-	Phase I (injectable) Preclinical (inhalation)
Polymeric microparticles	Polymers (PLA, PLGA)	-	250-a few μm	Diffusion Erosion Swelling	++	Phase I (injectable) Preclinical (inhalation)
Solid-lipid nanoparticles	Lipids, phospholipids	+	10-250 nm	Diffusion Erosion	+/-	Marketed (topical) Preclinical (all)
Solid-lipid microparticles	Lipids, phospholipids	+	250-a few μm	Diffusion Erosion	++	Marketed (topical) Preclinical (all)

over some hours with a lower peak concentration than that obtained with immediate-release forms, and (ii) decrease the duration of administration encountered with nebulizers or the frequence of administration encountered with conventional pMDIs and DPIs.

Many strategies have been developed to achieve CR in respiratory formulations **(Figure 29)**. Those include sub-micron sized particles (i.e. below 1 μm in diameter), such as polymeric and solid-lipid nanoparticles, micelles, liposomes and dendrimers. These strategies also include larger particles (i.e. above 1 μm in diameter), such as polymeric and SLM, the central subject matter of this work (Loira-Pastoriza et al., 2014, Aragao-Santiago et al., 2016). Each formulation strategy, with their main class of excipients, lung tolerance, particle size range, CR mechanisms, production method up-scalability and latest stage of pharmaceutical development, is summarized in **Table 7** and described below. Liposomes **(Figure 29.A)** have been thoroughly studied as CR drug-carriers in lung delivery in the last few decades. They are composed of one or more phospholipid bilayers arranged in a spherical vesicle, comprising a central aqueous compartment. They are classified as SUV (small unilamellar vesicles), with a diameter < 100 nm; LUVs (large unilamellar vesicles), with a diameter > 100 nm and MLV (multilamellar vesicles), which have multiple concentric bilayers. The carried drug can therefore be encapsulated either in the lipid part of the liposome (higher ratio in MLVs) if the drug is more lipophilic, in the aqueous part if it is more hydrophilic (higher ratio in LUVs) or at the interface if it is amphiphilic (Loira-Pastoriza et al., 2014). The stability of the drug inside the lipid bilayer will directly influence its ability to be retained inside the liposome and be progressively released (Wauthoz et al., 2015a). Liposomes for inhalation are composed of endogenous phospholipids, such as DPPC, a major component of the lung surfactant, and are therefore biocompatible and biodegradable. They can also contain cholesterol in order to stabilize and modulate the rigidity of the bilayer(s). Their surface can also be modified to present PEG chains on their outer shell, often obtained by using a fraction of PEGylated phospholipids or some specific ligands to target tumours. However, liposomes are rather difficult to stabilize and generally exhibit low drug loadings (< 4% w/w) and variable encapsulation efficiencies (from a few% to more than 90%), which are highly dependent on the physicochemical properties of the encapsulated drug (Loira-Pastoriza et al., 2014).

The most conventional production method for liposomes is the Bangham method (Bangham, 1978), consisting in the hydration of a thin lipid film. Other methods, such as reversed-phase evaporation, freeze drying of double emulsions, use of supercritical anti-solvents, reverse-phase evaporation and microfluidic methods, among others, have been

Table 8. Clinical status of inhaled liposomal formulations with controlled-release abilities, as of November 2016, updated from Loira-Pastoriza et al. (2014) using Clinicaltrials.gov data.

Name	Clinical phase	Indication	References (NCT: ClinicalTrials.gov identifier)
9-Nitro-20-S-camptothecin	I/II	Non-small cell lung cancer	Verschraegen et al. (2004)
Amikacine, Arikace®	III	Cystic fibrosis	NCT00558844 (2016), NCT00775138 (2016), NCT01315691 (2015)
Amikacine, Arikayce™	III	Mycobacterium lung infection	NCT01315678 (2015), NCT00777296 (2016), NCT01316276 (2016), NCT01315236 (2016)
Amphotericin B, Ambisome®	II/III	Prophylaxis of invasive pulmonary aspergillosis (e.g. lung and renal transplant, leukemia)	NCT00263315 (2006), NCT00235651 (2008), NCT01254708 (2011), NCT01615809 (2015)
Ciclosporine L-CsA	III	Bronchiolitis obliterans following lung transplant	NCT01334892 (2015)
		Against chronic rejection in lung transplant recipients	NCT01650545 (2015)
Ciprofloxacin, Pulmaquin®	III	Chronic lung infections with *Pseudomonas aeruginosa*	NCT02104245 (2015)
Cisplatin, Liposomal	I/II	Non-small cell lung cancer Osteosarcoma	Chou et al. (2013) Wittgen et al. (2007) NCT00102531 (2010) NCT01650090 (2016)
Doxorubicin	I/II	Lung cancers (primary and metastatic to the lungs)	Otterson et al. (2007), Otterson et al. (2010), NCT00082472 (2006), NCT00020124 (2012), NCT00004930 (2013)
Fentanyl, AeroLef®	II	Moderate/severe post-surgical acute pain	NCT00286065 (2007), NCT00791804 (2008)

developed over time (Huang et al., 2014). Scaling up is also not easy **(Table 7)**. Despite many promising results regarding their therapeutic advantages, only a few formulations, exclusively for parenteral administration, have reached commercialization (e.g. Myocet®, Doxil®, Ambisome®) (Loira-Pastoriza et al., 2014). Regarding CR inhaled therapies, liposomes are the only formulation strategies that have reached the clinical phase **(Table 8)**, including three formulations against lung cancer, which embed cisplatin, 9-Nitro-20-S-camptothecin or doxorubicin (Verschraegen et al., 2004, Chou et al., 2007, Otterson et al., 2007, Wittgen et al., 2007, Otterson et al., 2010, Chou et al., 2013). All of these clinical trials involve liposomal drugs that are administered using nebulizers. Liposomes can also be formulated into their solid state: lipospheres or proliposomes of adequate size to be delivered using DPIs after removal of bulk water through spray drying, spray congealing or freeze drying.

This aims at improving stability and delivery-related issues, for instance avoiding liposome disruption during nebulization (Willis et al., 2012).

The mechanisms inducing the CR of drugs embedded into liposomes are mostly drug diffusion through the phospholipid bilayer and translocation (flip-flop mechanism) for drugs with structural similarity with components of the lipid bilayer (Wauthoz et al., 2015a). This mechanism is slowed down further when the width or the rigidity of the bilayer increases. Rigidity of the bilayer is linked to the transition temperature of its components (i.e. higher rigidity if their glass transition temperature (T_g) is above the body temperature) and to the presence of cholesterol (Loira-Pastoriza et al., 2014).

3.5.1. Micelles

Micelles **(Figure 29.B)** are spherical colloidal particles formed of amphiphilic materials (e.g. phospholipids, block copolymers). They are the result of the formation of aggregates in aqueous solutions above the critical micelle concentration, where the most thermodynamically stable conformation leads the monomers of material to arrange themselves in such a way that hydrophilic heads are in contact with the aqueous solvent thus forming a shell, and the hydrophobic parts of the monomers are sequestered inside the particle by packing behaviour. Inverted micelles have an opposite conformation and are formed in non-polar solvents. Micelles present very small sizes (< 100 nm) and are generally used as a carrier of lipophilic drugs, solubilized or dispersed in the hydrophobic core with a loading efficiency ranging between 5 and 25% (Loira-Pastoriza et al., 2014). Materials include endogenous phospholipids, such as DPPC, but also hydrophobic polymers. The surface of these micelles can be modified using PEGylated excipients (Gill et al., 2011) or other specific

ligands presenting overexpressed receptors in tumours, such as the folate receptor (Rosiere et al., 2016), in order to promote their recognition and uptake at the site of action. They are also able to provide CR after lung deposition. For example, Gill et al. showed an increase in lung retention for more than 12 hours using PEG_{5000}-distearoylphosphatidylethanolamine micelles as paclitaxel carriers in Sprague-Dawley rats (Gill et al., 2011). Their tolerance in the pulmonary tract needs to be assessed on a case-by-case basis, particularly for polymeric-based micelles regarding their biodegradability (Nokhodchi and Martin, 2015).

3.5.2. Dendrimers

Dendrimers **(Figure 29.C)**, also called unimolecular micelles, form three-dimensional well-defined tree-like regularly branched structures with an apolar core and a polar shell. They are composed of four main regions: the initiator core, interior generations made of many repeated units, spaces or cavities able to entrap the loaded drug and terminal polar surface groups. Encapsulation within the dendrimer is done through electrostatic interactions or covalent binding. The outer shell of dendrimers exhibits a multifunctional surface that can be grafted with specific antigens or targeting agents using "click-chemistry". For instance, commercialized dendrimers such as polyamidoamine (PAMAM) can be purchased with a – NH2, –COOH or –OH surface, depending on the compound to encapsulate (Duncan and Izzo, 2005).

At higher generations, dendrimers have the ability to form very small nanoparticles (4-20 nm) that can easily avoid the MPS and provide a slow release. A few of them are on the market or in clinical trials, but not yet as inhaled therapies. They have been assessed as a carrier for inhalation of beclometasone dipropionate through different types of nebulizers. Polyamidoamine dendrimers have shown the ability to provide CR with low burst-effect, with only 35% of beclometasone released after 8h (Nasr et al., 2014). They also have been tested in inhalation on rodents. Results showed enhanced doxorubicin release in the lung parenchyma. They showed a high 60% burst-effect over 24h but 15% were still found 7 days after intratracheal administration to rats (Kaminskas et al., 2014).

As non-endogenous materials, their toxicity and immunogenicity is a key factor in favour of their broader use today, and they are highly dependent on the grafted moieties and surface properties of each end product. This means that toxicity is case-dependent and must be reassessed in full for each produced dendrimer (Duncan et al., 2005). For instance, while some of them have shown biocompatibility, others have induced cytotoxicity, complement activation or even hemolysis (Malik et al., 2000, Duncan et al., 2005). Un-grafted dendrimers

are also arduous to produce in large quantities as only a few of them can be produced on a kilogram scale.

3.5.3. Nano and microparticles

Nano-size particles are very interesting carriers for lung delivery because they add some functionalities to the drug such as CR but can also, for instance, increase cell, mucus or tumour penetration, overcome drug resistance or escape alveolar macrophage clearance thanks to their small size or surface properties. This can allow them to stay in the lung parenchyma for days to weeks after deposition, where they can act as CR delivery systems. These nanoparticles need to be included into larger micron-sized droplets or particles in order to be inhaled. Microparticles are larger but can be formulated to be readily inhaled without the need for a coarse carrier by particle engineering. Both are more stable during storage than liposomes (Jaspart et al., 2005).

3.5.3.1. Polymeric particles

Polymeric nanoparticles and microparticles **(Figure 29.D)** with CR properties are generally composed of poly(D,L-lactide-co-glycolide) (PLGA), polylactic acid (PLA), poly-ε-caprolactone (PCL), chitosan, alginate and gelatin (Mahapatro and Singh, 2011).

PLGA-based particles, for instance, were first believed to be a viable approach for inhalation as they are biodegradable and initially showed no lung toxicity. Drug diffusion from these particles involves many mechanisms over a short timeframe. These mechanisms are primarily polymer erosion but also drug diffusion through surface pores. These particles often present a very high burst-effect (up to 50% in a few hours), linked to unencapsulated drug at their surface or to higher particle porosity, which also increases the surface in contact with the dissolution medium. These can be controlled by careful formulation using osmotic agents (Lee et al., 2010), such as polyethyleneimine (PEI) (Gupta and Ahsan, 2011) and ß-cyclodextrin (Ungaro et al., 2009). However immunogenicity was ultimately observed after PLGA nanoparticle instillation in BALB/c mice lungs (Dailey et al., 2006). The same was observed with PLA microsphere in rabbit lungs, where histological damage and hypersensitivity reactions were observed (Armstrong et al., 1996). Some questions have now been raised regarding the chronic use of these polymers because of their potential accumulation in the lung parenchyma after repeated administrations. The processes of eliminating the remaining free polymer are always much longer than for drug delivery. Polymer degradation can last up to a year for some of them. Another limiting factor is their low drug-loading (~10%) and the fact that the hydrolytic erosion of PLGA or PLA induces acidic bursts in the particle core, which can damage sensitive drugs (e.g. proteins, antigens).

Table 9. The main lipid excipients used in solid lipid microparticle formulations, adapted from Jaspart et al. (2005)). Excipients used in formulations for inhalation are highlighted in bold and in italic. Regarding the potential lung tolerance, ++ stands for endogenous material that has been safely administered to humans by inhalation, + stands for material that has been tested *in vitro* or *in vivo* and showed no particular sign of low tolerance, +/- stands for material that has a high similarity with other + or ++ materials, - stands for material that either has not been tested or is not endogenous and therefore not expected to be well-tolerated.

Category	Description	Potential lung tolerance
Fatty alcohol	Cetyl alcohol	+
	Stearyl alcohol	
Fatty acid	*Stearic acid (C18 fatty acid)*	+
Fatty acid esters of glycerol	*Glyceryl monostearate (GMS)*	
	Glyceryl behenate	
	Glyceryl palmitostearate	
	Glyceryl ditristearate	+
	Glyceryl tripalmitate	
	Glyceryl tristearate	
Fatty acid esters of polyglycerol	Tetraglycerol pentastearate	+/-
	Tetraglycerol monostearate	
Hydrogenated fatty acid ester	Hydrogenated hardened castor oil	-
Polar wax	Complex mixture containing esters of acids and hydroxyacids	-
Others	Saturated polyglycolised glycerides	
	Beeswax	-
	Paraffin wax	
	Microcrystalline wax	
	Cholesterol	++
	Phospholipids	++*
	*Except for some non-endogenous and cationic phospholipids	

3.5.3.2. Solid lipid nanoparticles (SLN)

These have been investigated since the 1990s as a promising drug carrier system, able to provide sustained-release profiles. They are composed of a lipid core, solid at body temperature and preferably include physiologic excipients to improve their tolerability **(Figure 29.E)**. They have many other advantages, such as high stability, relatively easy up-scalability and low cost of raw materials. The major limitation of solid lipid nanoparticles lies in their poor ability to entrap hydrophilic drugs into their lipidic core (Jaspart et al., 2005). The major lipid excipients that can be used to produce SLN are the same as larger lipid microparticles and are listed in **Table 9**.

3.5.3.3. Solid lipid microparticles (SLM)

SLM, sometimes called lipid micropellets or lipospheres, have been widely described for pharmaceutical use as drug carrier systems with CR properties (Bodmeier et al., 1992a) since the 1980s. Like SLN, they are defined as solid fat core particles, based on biocompatible lipids stabilized with a layer of surfactant on their outer shell **(Figure 29.E)** (Jaspart et al., 2005). The major difference with SLN lies in their particle size, by definition above 1 000 nm. SLM have been used for a large variety of routes such as nasal (Dalpiaz et al., 2010, Üner and Karaman, 2013, Dalpiaz et al., 2014), oral (Eldem et al., 1991, Akiyama et al., 1993, Chime et al., 2013, Gugu et al., 2015), topical (Lauterbach and Mueller-Goymann, 2014, Rahimpour et al., 2016), parenteral (Masters and Domb, 1998, Dalpiaz et al., 2008) and inhalation delivery (Sanna et al., 2004, Jaspart et al., 2005, Pilcer et al., 2006, Sebti and Amighi, 2006a, Jaspart et al., 2007, Mezzena et al., 2009, Depreter and Amighi, 2010, Scalia et al., 2012, Scalia et al., 2013, Maretti et al., 2014).

3.5.3.3.1. Advantages

Such microparticles have the potential advantage of directly offering adequate aerodynamic properties for lung deposition without the need for embedment into larger inhalable carrier particles or aggregation into larger particles, as is the case with sub-micron particles. Each of these formulation strategies has their advantages and disadvantages regarding their production methods (e.g. encapsulation efficiency, drug-loading, up-scalability) or their behaviour once deposited *in vivo* (e.g. biocompatibility, elimination from the lungs through macrophage uptake). These are described below (Loira-Pastoriza et al., 2014).

3.5.3.3.2. SLM formulation

Excipients used to produce SLM are primarily lipids. Because of the production techniques and the administered routes, they preferably show a transition temperature higher than body temperature. They include fatty acids, fatty acid esters of glycerol (mono, di-, triglycerides) and cholesterol, for instance **(Table 9)**. Surfactants are added to enhance stability and particle wettability, add surface properties or act as emulsifiers during particle formation. Those include block copolymers (poloxamers), phospholipids, sorbitan esters and ethoxylates (Tween, Span) (Jaspart et al., 2005). For inhalation purposes, these excipients must be chosen with the highest biocompatibility possible (i.e. not interfere with the lung surfactant function or ciliated cell motility, and not create inflammation in the pulmonary parenchyma) while taking into account the production technique used.

Formulations of SLM with or without CR properties have been described that embed a large variety of lipophilic drugs, including anaesthetics (Masters et al., 1998), non-steroidal anti-inflammatory drugs (Chime et al., 2013), hormones (Eldem et al., 1991), calcium channel antagonists (Savolainen et al., 2002), anti-HIV drugs (Dalpiaz et al., 2014) and for inhalation: budesonide (Sebti et al., 2006a, Mezzena et al., 2009), quercetin (Scalia et al., 2013), rifampicin (Maretti et al., 2014) and salbutamol acetonide (Jaspart et al., 2007), for instance. SLM embedding hydrophilic drugs such as peptides (e.g. insulin, thymocartin) (Reithmeier et al., 2001, Depreter et al., 2010), a dopamine prodrug (Dalpiaz et al., 2010), tetracycline (Rahimpour et al., 2016) and, more specifically, SLM for inhalation embedding tobramycin (Pilcer et al., 2006) and insulin (Depreter et al., 2010) have also been described.

3.5.3.3.3. SLM production

Physical mixture of the drug with lipid excipients is generally not sufficient (Savolainen et al., 2002, Jaspart et al., 2007). The drug has to be either dispersed or dissolved into the lipid core of SLM to provide a CR. Different techniques have been described, involving particle formation through the emulsification of the lipid fraction or by direct particle formation using spray drying or spray congealing.

3.5.3.3.3.1. Emulsification

Emulsification techniques include the classical solvent evaporation method, in which lipids are dissolved under mild heating in an organic solvent and emulsified in an aqueous phase (O/W emulsion). The organic phase is then evaporated under ambient conditions under stirring. This technique has poor control over particle size and usually involves chlorinated solvents (e.g. chloroform, methylene chloride) that have low biocompatibility, particularly

1. Aqueous phase + emulsifying agent
2. Hot aqueous phase with emulsifying agent
3. Primary W/O emulsion

1. Solvent evaporation under ambient conditions
2/3. Cooling at room T or in an ice bath

Emulsification

Suspension of hardened microparticles

1. Lipids (and drug) dissolved in organic solvent
2. Drug dissolved in melted lipids
3. Aqueous phase

1. O/W emulsion
2. O/W emulsion
3. W/O/W emulsion

Figure 30. Schematic representation of SLM production using emulsions, with 1: solvent evaporation, 2: O/W melt dispersion and 3: W/O/W double emulsion, from Jaspart et al. (2005).

regarding the inhaled route. A derived method, based on S/O/W emulsion, designed for more hydrophilic drugs, was also described. It involves fine milling of the drug into the organic solvent, which is then emulsified in cold water following the classical solvent evaporation method (Reithmeier et al., 2001). As the particles are dispersed into an aqueous phase, they then have to be collected, which can be done by filtration, freeze drying or spray drying. This is also an issue regarding burst release from the SLM into the aqueous dispersion phase. Another method is to use multiple emulsions, such as the double emulsion technique W/O/W **(Figure 30)**. First, a classical W/O emulsion is produced. It is then dispersed into another aqueous phase and quickly cooled to help solidify the dispersed SLM (Bodmeier et al., 1992b, Reithmeier et al., 2001). The same remarks regarding burst release in the dispersing phase apply to this technique.

Particle size can be controlled in multiple ways, by the microchannel emulsification technique, the addition of ultrasound during the emulsification process (Kanda et al., 2010) or by the high-pressure hot homogenization (HPH) technique (Jaspart et al., 2005).

Overall, the emulsification techniques generally give better results with lipophilic drugs than with hydrophilic ones.

3.5.3.3.3.2. Cold homogenization technique

This method involves the dispersion or the solubilization of the drug into molten lipid, which is then quickly cooled, solidified and ground using a mortar and liquid nitrogen. The large particles obtained are then reduced as a dispersion using HPH, with careful control of the temperature to avoid early release of the drug (Demirel et al., 2001, Jaspart et al., 2005).

3.5.3.3.3.3. Spray-congealing / Spray-chilling

This method has been widely used to produce SLM and mainly involves hydrophobic drugs that are dissolved or dispersed into molten lipid. The molten lipid is then sprayed at high temperature and high pressure with a nozzle into a chilled container, using dry ice, cold air or liquid nitrogen, thus forming small solidified SLM. The obtained particles can then be vacuum dried. Control of the particle size is quite difficult and mainly depends on the temperature differential between the atomisation and the cold receptacle and on the air pressure in the nozzle (Eldem et al., 1991, Akiyama et al., 1993, Savolainen et al., 2002, Passerini et al., 2003).

.
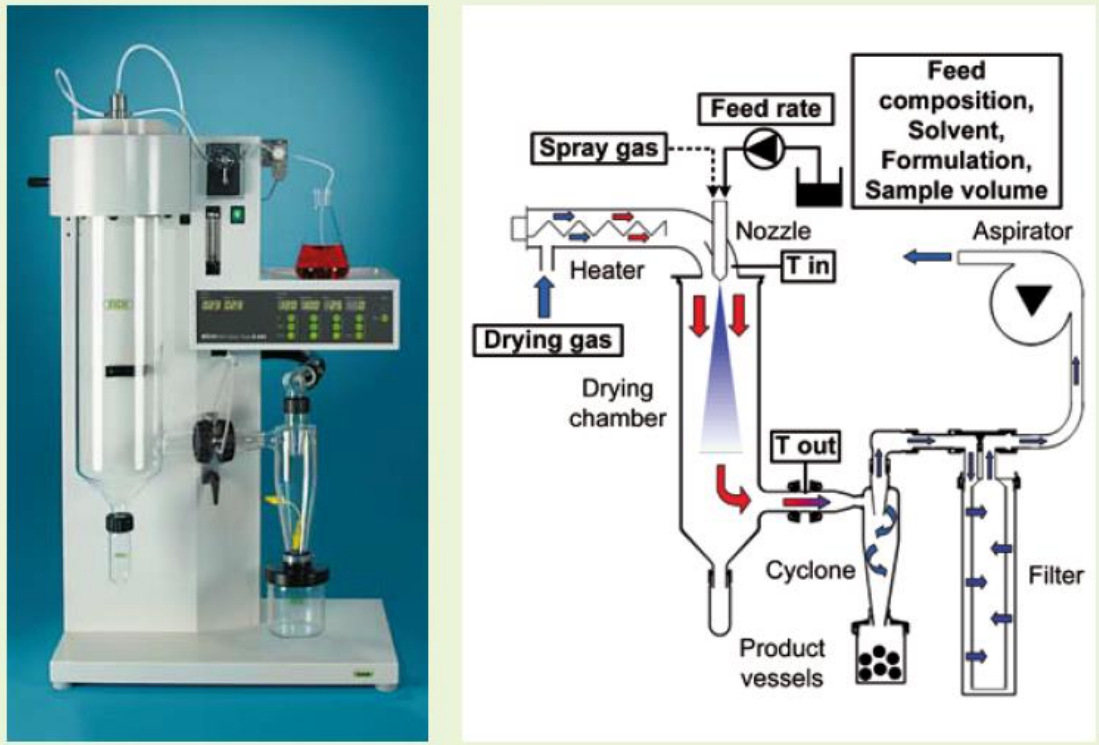
Figure 31. Schematization of the Mini Spray Dryer B290 (Büchi, Flawil, Switzerland). From buchi.com.

3.5.3.3.3.4. Spray drying

Spray drying is a short process that can transform a liquid (e.g. solution, suspension, emulsion) into a dried solid. The feed is first atomized into a spray with a nozzle, using compressed air, forming small droplets that are put in contact with a heated drying gas (air or N_2) causing the rapid evaporation of the dispersing phase **(Figure 31)**. The resulting powder is then collected into a cyclone through a centrifugal force that makes particles impact the walls of a glass vessel or a bag filter. Particle size is influenced by many parameters during spray drying (e.g. liquid feed rate, pressure in the nozzle, nozzle diameter, inlet and outlet drying air temperatures, solvent composition, transition/melting temperature of components), which together influence the particle size, shape, density and crystallinity. The twin-fluid method (liquid feed and compressed air) used with the co-current method (where the material is sprayed in the same direction as the heated air flow) generally produces particles below 10 μm. Particle shape is often but not always spherical. Depending on the material and on the spray drying parameters (drying rate, surface tension, viscosity of the dispersant), particles can exhibit pores, voids and intricate surfaces.

For SLM production, lipophilic drugs can be solubilized into a molten lipid then emulsified and spray dried into the atomization chamber to ensure the elimination of the external aqueous phase. Another way of producing SLM with this technique, used in this work and derived from Pilcer et al. (Pilcer et al., 2006) and Sebti and Amighi (Sebti et al., 2006a), is the solubilization of the lipid component into a spray dryable biocompatible solvent, preferentially a heated alcohol.

To generate CR formulations using the latter technique for hydrophobic drugs, the chosen lipids must be more soluble than the drugs in the dispersing alcoholic phase. If they are not, the drug will mostly end up on the outer shell of the lipid particles during spray drying, promoting low encapsulation efficiency, a high burst-effect and limited CR. For hydrophilic drugs, this technique can follow a previous particle size reduction process (e.g. HPH (Pilcer et al., 2006, Depreter et al., 2010)) to embed the submicron crystals, which act as a nucleation site.

The advantages of spray drying are its proven up-scalability and its ability to dry the produced droplets very quickly (a few hundred of milliseconds), thus protecting thermolabile drugs and materials with low glass transition temperatures, such as lipid excipients, and in a continuous manner. This fast drying generates narrow populations with
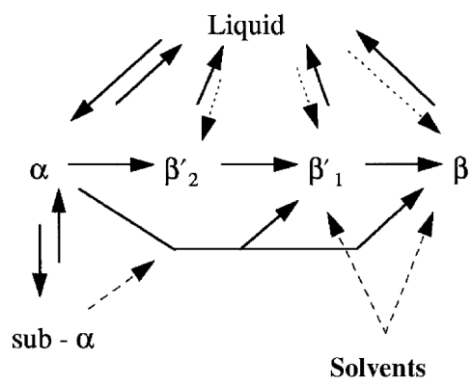
Figure 32. Polymorphic transitions in saturated monoacid triglycerides. Dotted lines show transitions happening only when applying specific thermal treatments. From Singh et al. (1999).

easily controllable parameters (Johnson, 1997). Moreover, the use of surfactants as emulsion stabilizers could be totally avoided. It also has a few disadvantages, as is uses hot inlet air to eliminate the dispersing phase and the minimal temperature to permit a fast drying of droplets is around the boiling point of the solvent. Most lipids have a transition temperature below 50°C, which, if attained in particles after drying of the dispersant, will cause sticking, particle agglomeration and inappropriate particle size, especially for inhalation purposes. Excipient (lipids and non-lipids) choice, based on transition Tg or melting point, and solvent choice, based on boiling point and residual limits, is therefore crucial. This can also be limited by lowering the outlet temperature using a modified apparatus such as the one described by Sebti and Amighi (Sebti et al., 2006a). The other main issue encountered with the spray drying of solution, is that the produced materials are often in an amorphous state, which tends to transform to more stable crystalline states. To avoid this, the best strategy is to directly spray dry material in suspension. For SLM including lipids and triglycerides in particular, the issue is that the crystalline forms also show polymorphism, with two or more forms. If the lipids are to be solubilized (permitting a shorter process than with emulsions), there is a great risk of observing a reorganization of the lipid core due to polymorphic changes, causing instability of the formulation, including drug expulsion or recrystallization. These risks need to be assessed together and will also influence the excipient choice **(Figure 32)** (Singh et al., 1999). This point is further discussed in Part I of the manuscript.

3.5.3.3.4. Controlled release (CR) and related characteristics

CR obtained with SLM formulations is mainly dependent on (i) the lipid matrix composition and its hydrophobicity and transition temperature, (ii) the drug log P and its potential interaction with the excipient, (iii) the matrix particle thickness and therefore the drug/lipid (drug loading) ratio, (iv) the presence of pores and (v) the polymorphic state of lipids.

It is expected that higher CR will be obtained with more hydrophobic lipids. Their log P is directly dependent on their number of carbon chains and the number of carbon atoms.

Increase of the relative concentration of other hydrophobic or hydrophilic drug, filler or surfactants will also influence the release rate from the particles. For instance, hydrophilic drug will generally show faster release than more lipophilic ones. Lower drug-loadings will also show slower release rates (Jaspart et al., 2007). Depending on their relative concentration and their position, in the SLM core or at the SLM surface, surfactants will also play a role in the wettability of particles and in pore creation through the lipid matrix, which will enhance drug-release.
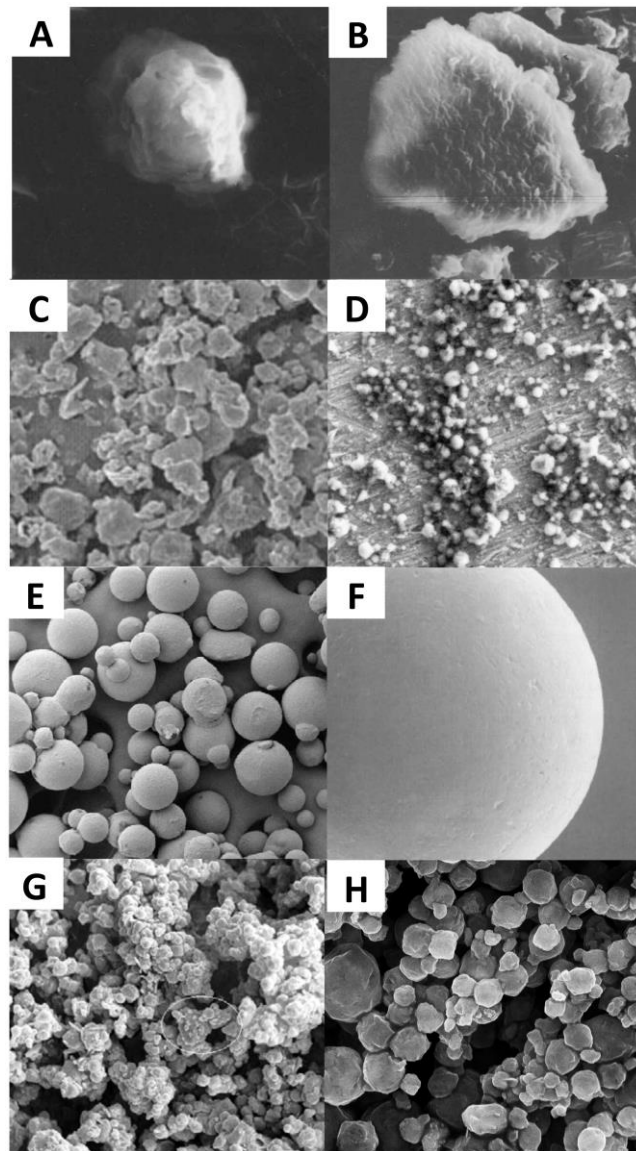
Figure 33. SEM micrograph overview of the different particle shapes that can be obtained with **A.** hot HPH from an O/W emulsion, from Demirel et al. (2001), **B.** cold HPH from a lipid suspension, from Demirel et al. (2001), **C.** ultrasonication of an emulsion, from Mezzena et al. (2009), **D.** high speed homogenizing of an emulsion, from Scalia et al. (2012), **E.** spray congealing combined with ultrasonication, from Passerini et al. (2003), **F.** direct spray congealing without size reduction, from Akiyama et al. (1993), **G.** spray drying of a lipid alcoholic solution, from Sebti et al. (2006a) and **H.** direct spray drying of a cholesterol/Phospholipon 90H (75:25) cisplatin comprising DPI formulation using a Büchi Mini Spray Dryer B290 (see Part I).

Particle size is an important parameter and larger particles are generally more prone to a slow release rate than smaller ones. This is linked to the higher surface area of smaller particles and by the higher distance through which drug in the central region of larger particles needs to diffuse.

Some polymorphic forms will be more stable and more prone to providing CR than unstable or metastable ones. This means that the production process for SLM formation has a major role in providing CR from SLM, in particular because of their influence on the final crystalline form, shape, size and density of SLM, as well as the solid state or dispersed state of the drug in the lipid core. For example, the cooling speed of particles, from solutions or from melts, has a major influence on the polymorphic state of the lipid matrix, particularly in triglyceride-comprising SLM. The faster the particles are cooled and dried, the more chances there are of obtaining poorly stable α forms or β' metastable forms of such triglycerides (Eldem et al., 1991).

3.5.3.3.5. Particle shape

Other physico-chemical properties can be determined, such as the particle shape (observable by scanning electron microscopy (SEM) and/or optical microscopy) or their density (measurable by melting a known mass of SLM in order to determine the corresponding volume) (Jaspart et al., 2005). SLM are generally spherical particles. However, all the techniques involving suspended materials and subsequent size reduction with HPH, ultrasound or high-shear mixing may give irregular particles with much coarser surfaces (Jaspart et al., 2007, Mezzena et al., 2009, Scalia et al., 2012) **(Figure 33)**.

3.5.3.3.6. Toxicity

One of the major advantages of SLM compared to polymeric particles or dendrimers is their inherent biocompatibility thanks to the use of well-tolerated physiological lipids, in particular regarding the inhalation route. To be well-tolerated, the excipients must be biodegradable, non-immunogenic and should not provoke inflammatory responses (Sanna et al., 2004).

However, evaluation of SLM toxicity following inhalation has not been very widely reported. It has been done *in vitro* and showed that TS-based SLM of quercetin did not have an impact on Calu-3 cell viability over 72 h, over the tested concentration range (from 0.15 nM to 200 μM) (Scalia et al., 2013). An *in vivo* study of glyceryl behenate based-SLM toxicity in male Sprague-Dawley rats lungs was also realized and showed no significant inflammatory response following a single administration (Sanna et al., 2004). In humans, a clinical trial realized by Sebti et al. (Sebti et al., 2006b) of the pharmacoscintigraphic and PK study of

budesonide SLM-based DPI (cholesterol/Phospholipon budesonide-based SLM) showed no particular event and good tolerance.

However, knowing that the excipients used in SLM formulation are physiological or well-tolerated is not sufficient to ensure their lung tolerance. It is therefore recommended to establish the local tolerance profile for each candidate excipient as well as *in vivo* tolerance studies of whole formulations (Pilcer and Amighi, 2010).

3.5.4. Overcoming particle clearance mechanisms

CR particles for inhalation are to be deposited in the lower respiratory zone. Therefore, they will exhibit d_{ae} between 1 and 5 µm and d_{geo} in the same order of magnitude. Elimination of inhalable particles by the MCC, restricted to the larger bronchioles and above, will by definition not impact the deposition abilities of the formulations. The MPS, however, is active in the alveoli and in the respiratory bronchioles and is very effective against particles exhibiting diameters comprised between 1 and 3 µm, such as potentially inhaled SLM (Loira-Pastoriza et al., 2014). To provide a CR, the deposited particles must reside in the lungs long enough to release the drug. A first approach is to engineer particles with diameters below 200 nm, such as SLN, micelles, liposomes or dendrimers (Loira-Pastoriza et al., 2014), to lower their uptake by the MPS. Another strategy is to deliver particles with mean diameters larger than 3-5 µm, but with adequate aerodynamic diameters to ensure high deposited fractions. This is possible with low-density particles, such as SLM (Loira-Pastoriza et al., 2014), or with large porous particles exhibiting a geometrical diameter above 5-6 µm but still able to deposit in the deep lung thanks to their low density (Edwards et al., 1997, Patel et al., 2012).

PEGylation is another very common strategy for prolonging particle residence in the body. This is also true for the pulmonary route, and particle surface modification using PEG chains has been demonstrated as effective against uptake by the alveolar macrophages (Loira-Pastoriza et al., 2014). PEG is a polyether comprised of the repeated $HO-(CH_2-CH_2-O)_n-H$ moiety, forming chains of varying length. A 1 kDa PEG molecule is formed by approximately 23 repeated units of 44 g/mol each. Its structure gives it both hydrophilic and hydrophobic properties, explaining its unique conformations when present at the surface of a particle. In water, PEG preferentially takes the gauche conformation, offering two hydrogen bond acceptors to interact with water. This particular conformation gives PEG its properties in aqueous mediums, with high flexibility and mobility of the PEG chains (Wattendorf and Merkle, 2008). This in particular is responsible for protein repellence,

avoiding the adsorption of opsonins at the particle surface and their further recognition by phagocytic cells. PEG, if present in sufficient quantity at the surface of particles, also has the ability to totally bypass recognition by the MPS as being foreign material. Patel et al. showed that PLGA particles presenting PEG chains at their surface were not recognized by alveolar macrophages. It permitted a 4.5-fold increase in the half-life of heparin-comprising particles administered intratracheally to rats (Patel et al., 2012).

Addition of PEG to the surface of microparticles can be done in different ways, for example through self-assembled micelles using PEG polymers (Rosiere et al., 2016), by addition of PEG derivatives during the microparticles formation, by covalent linking or by post-insertion (Wattendorf et al., 2008).

PEG usually shows low toxicity and low immunogenicity. PEG3350 was first administered to rats to ensure its safety for the pulmonary route and showed no particular toxicological implications up to 1000 mg/m² (Klonne et al., 1989). It has been used since then in numerous inhalation studies *in vitro*, using different chain lengths and various derivatives.

Another interesting parameter that can help limiting macrophage uptake is particle shape, as non-spherical particles have been reported as less prone to be captured by macrophages than spherical PLGA particles. Rigid particles are also more likely to be internalized by macrophages. Finally, particle charge may also be a key factor as neutral particles are less recognized than charged ones (Patel et al., 2015).

3.6. Inhaled chemotherapy (CT)

3.6.1. Advantages

Despite a few decades of research, delivery of anticancer drugs to the lungs is still at an exploratory stage. Nevertheless, it possesses the evident PK advantage of all inhaled therapies, as it permits increased exposure at the site of action and at the same time a large decrease in systemic exposure (Zarogoulidis et al., 2012a). This is particularly helpful for systemically toxic drugs, such as anticancer agents, and could very well increase their therapeutic ratio (Gagnadoux et al., 2008). The high systemic toxicity of anticancer drugs often limits the administrable dose and the frequency of successive administrations, opening the way to higher risks of resurgence. Moreover, the classical IV route is criticized for being nonspecific, non-selective and toxic. It also poorly concentrates the drug at the target site and only creates high local concentrations for short periods of time. It is believed that only 5-10% of an IV dose effectively end up in the lungs, let alone the tumour. Adequate inhaled CT to the lungs could also help reduce treatment interruption and cancer resurgence.

Inhaled cisplatin as an adjuvant treatment following surgery, or in parallel to conventional less toxic CT, could help limit cancer resurgence by increasing the drug concentration in the tumour microenvironment, through lymph nodes and the local bloodstream. This can be of major importance in lung cancer, for which lymph nodes and local bloodstream are major sources of cancer metastases. This could help limit loco-regional but also distant resurgences. As a neoadjuvant treatment, inhaled CT could also help reduce the tumour size prior to surgery.

3.6.2. Challenges

Despite a few clinical trials and some active developments, no pharmaceutical forms for inhaled CT have been marketed yet. This can be explained by rational fear of lung toxicity, formulation/device limitations and safety infrastructures and procedures.

3.6.2.1. Lung toxicity

The toxicities of anticancer drugs by the IV route are various but they are strongly linked to their excretion mechanisms (renal, hepatic) or to their myelosuppressive activity. Some of these drugs also lead to specific tissue toxicities (e.g. cardiotoxicity for doxorubicin). However, it is believed that 10-30% of the conventional chemotherapeutic drugs administered by IV induce lung toxicity (Charpidou et al., 2009). These drugs, used against NSCLC and SCLC include docetaxel, paclitaxel, pemetrexed, irinotecan and gemcitabine for
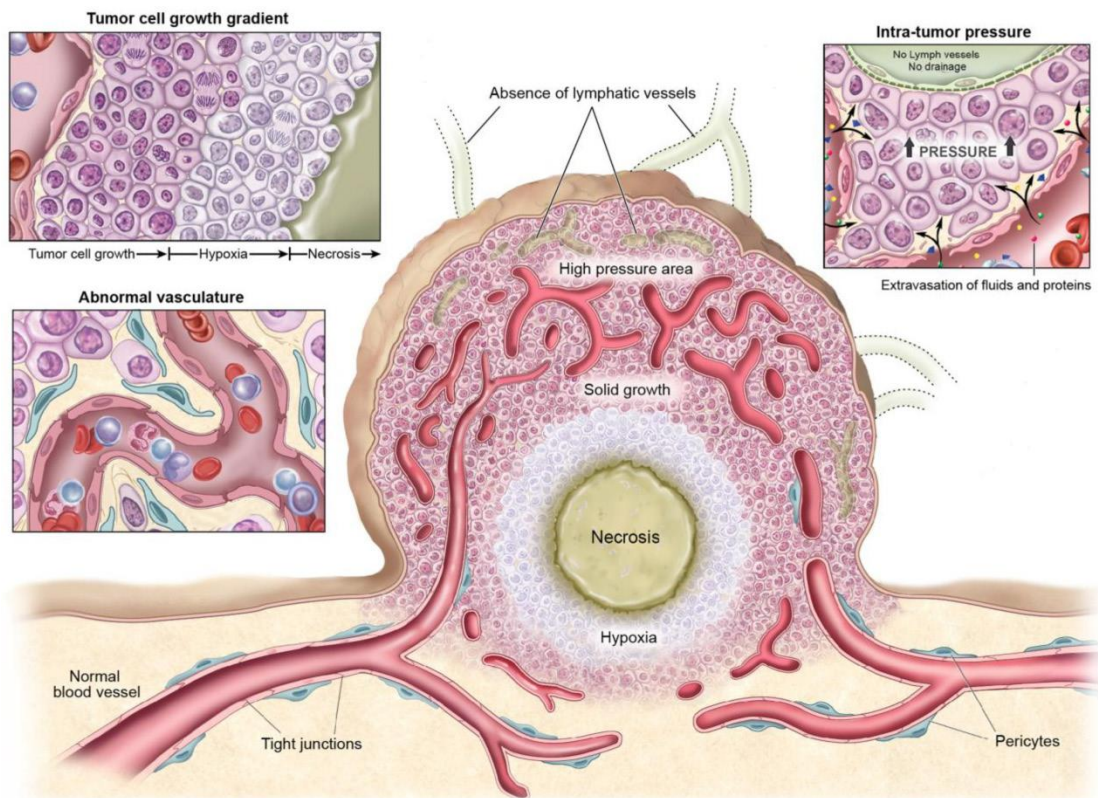
Figure 34. Characteristics of tumorous tissue, blood and lymph vessels involved in tumour penetration, from Kobayashi et al. (2013).

the most classical drugs, but also the most recent targeted therapies, including gefitinib, erlotinib and bevacizumab, for instance. The toxicities involved are various and include hypersensitivity reactions (increased lymphocytes and eosinophil counts), dyspnoea, altered diffusion capacity or forced expiratory volumes, lung fibrosis, interstitial pneumonitis and lung disease, or haemoptysis, for instance (Zarogoulidis et al., 2012a). There is therefore a rational fear of administering these drugs directly to the lung tissues. Local tolerance must therefore be thoroughly assessed for each of them.

The safety of inhaled platinum derivatives in particular has been studied in animals and in humans. In humans, the adverse effects observed were always mild and only included dose-dependent cough, fatigue, weight-loss and nausea for carboplatin (Zarogoulidis et al., 2012b). Only a single case reported fibrotic lesions, linked to too high concentrations of cisplatin locally in dogs (Selting et al., 2008). The systemic side effects were each time lower than for the IV groups (Darwiche et al., 2013). These early results are confirmed by the cisplatin clinical trials that were realized in the last decade and that are extensively discussed below (see 3.6.3. Current status of inhaled chemotherapy).

3.6.2.2. Formulations and device limitations

3.6.2.2.1. Drug penetration into the tumour

Solid tumours are composed of heterogeneous tissues, including tumorous cells, normal cells and extracellular matrix. The blood vessels in these tissues are often scarce, with variable blood flow. This poor vascularization makes the tumour difficult to reach for conventional CT by the parenteral route and can lead to lower drug delivery (Minchinton and Tannock, 2006) **(Figure 34)**. While delivery is generally closer to the tumour site with inhaled CT, this is still true and the drug may still have difficulties reaching the tumour from local blood vessels. With a neo-adjuvant approach, for instance in combination with IV, the tumour is also potentially exposed to the drug from its periphery rather than from the vessels only, offering an additional point of entry for the drug. This could help lower the tumour mass to a great extent. This ideal set-up needs to be balanced with the ability of particles to be deposited in patients bearing large tumours, particularly in the central region of the lung, which could disrupt and lower the airflow and in turn alter the deposition abilities of the DPI formulation.

Factors influencing distribution within tumours and around the deposition site depend on a few physico-chemical parameters of the drug, including its molecular weight, charge, shape and hydrophilicity or lipophilicity. Hydrophilic drugs penetrate the extracellular matrix easily and will diffuse around cells quickly. Diffusion will also be quicker for small molecules than for larger ones. Lipophilic drugs, on the other hand, will preferentially cross lipid bilayers and end-up in the tumorous cells more easily. Moreover, tumours often lack proper lymphatic vessels and are also hard to reach through this route (Minchinton et al., 2006).

Another key parameter regarding drug penetration is the time of contact between drug and the tumorous site. Higher lung retention times will generally improve drug penetration because they provide greater drug gradient and chances of tumour penetration (Saggar et al., 2013). Besides limitation of the acute toxicity, this is one of the major reasons to consider CR for inhaled CT.

3.6.2.2.2. Alteration of the respiratory tract

As discussed above, the modifications of the respiratory tract of cancer patients, due to an invasive solid tumour or following resective surgery, could very well alter the flow characteristics and the deposition pattern of the aerosol in patients. Another point to consider is the impeded respiratory function and ability to generate a sufficient airflow, which is very often encountered in lung cancer patients and is linked to tumour invasion.

3.6.2.2.3. Residence time

One of the main issues encountered with the IV route is the lack of chemotherapeutic drug concentration inside solid lung tumours. Despite the great PK advantage of the inhalation route in delivering the chemotherapeutic dose as close as possible to the tumorous mass, tumour penetration is not guaranteed, particularly when the dose reaching the site of action is quickly eliminated. This is particularly noticeable with inhaled therapies, as drug particles can be quickly eliminated by absorption or by MCC and/or the MPS, depending on their d_{ae} and their deposition site.

Table 10. Clinical status of inhalational chemotherapeutic drugs and their principal adverse effects and outcomes.

Drug	Author (Year)	Formulation	Inhalation device	Patients (n)	Clinical evaluation	Adverse effects	Principal outcomes
5-fluorouracil	Tatsumura et al. (1983)	Solution	Supersonic nebulizer	Unspecified (11)	Phase I/II Tumour response	Glottitis	Antitumour response in 4/6 alone and in 5/6 in combination with conventional CT
	Tatsumura et al. (1993)(Tatsumura et al., 1993)(Tatsumura et al., 1993)(Tatsumura et al., 1993)(Tatsumura et al., 1993)(Tatsumura et al., 1993)(Tatsumura et al., 1993)	Solution	Nebulizer	NSCLC (19)	Phase I/II Blood samples, tumour collection	Stomatitis	Antitumour response in 6/10 patients
9-nitro-camptothecin	Verschraegen et al. (2004)	Liposomes	Nebulizer	NSCLC and secondary cancers to the lungs (25)	Phase I/II Lung functional tests, blood samples, CT scan, urine analysis	Bronchitis, pharyingitis (dose-limiting), cough, nausea, vomiting (grade 2), fatigue (grade 2-3) (5) bronchial irritation (6), anemia (4), neutropenia (2), anorexia (1)	Systemic absorption of the study drug Partial remission in 2 patients with uterine cancer Stabilization in 3 patients with primary lung cancer
Carboplatin	Zarogoulidis et al. (2012)	Solution	Nebulizer	NSCLC (20)	Phase I/II Lung functional tests, blood samples, CT scan, survival	Cough Forced expiratory volume decrease	Increased median survival for the combination and inhaled CT

3.6.2.2.4. Tumour size

Tumour size may affect the distribution and deposition patterns of aerosolized formulations in the lungs. In the different clinical trials involving aerosolized CT, patients with tumour masses larger than 3-5 cm were excluded as this size can alter airflow characteristics and modify drug deposition patterns (Zarogoulidis et al., 2012a). Nevertheless, these large masses are often initially resected or shrunk using a radiochemotherapy approach when unresectable. Inhaled CT could then provide a support to combat cells that could have escaped these initial treatments, and micro-metastasis, which are poorly affected by initial treatments.

3.6.2.2.5. Delivery devices

Aerosolized CT has been administered in clinical trial solely using nebulizers (jet and ultrasonic nebulizers, **Table 10**). As described before, these devices are well suited for investigative studies as the formulations that are nebulized are easy to produce. They have a few disadvantages, particularly a low deposited fraction and a very high risk of environmental contamination. Therefore, administration involved drastic protection measures and the constant support of medical personnel, for many hours in some cases (Wittgen et al., 2007).

3.6.2.3. Protection measures

The safety of aerosolized therapy must consider the patient. However, limiting the exposure of the medical personnel involved should also be guaranteed, as well as limiting environmental contamination. To overcome this issue, closed and hermetic cabins, cytostatic hoods and negative pressure rooms equipped with charcoal and HEPA filters (High Efficiency Particulate Air) (able to filter a minimum of 99.97% of particles) have been used during clinical trials (Lemarie et al., 2011). It is accepted that breath-actuated devices would be the best mode of administration to limit these issues on a clinical basis (Darwiche et al., 2013). This highlights one big advantage for DPI over the other delivery systems available: they are patient activated, while jet nebulizers are initially not, needing to be modified to be breath-actuated, which increases the cost and the duration of administration. The latter are known to be particularly prone to drug exhalation and environmental contamination. Moreover, new low-cost single-use disposable devices have been developed, which is ideal for a CT setting (Friebel and Steckel, 2010, de Boer and Hagedoorn, 2015).

Table 10. (continued)

Drug	Author (Year)	Formulation	Inhalation device	Patients (n)	Clinical evaluation	Adverse effects	Principal outcomes
Cisplatin	Wittgen et al. (2007)	Liposomes	Jet nebulizer	NSCLC (18)	Phase I Lung functional tests	Nausea, vomiting, dyspnoea, fatigue hoarseness, grade 2 toxicities	Unable to reach the dose-limiting toxicities Stable disease (12/18) Progressive disease (4/18)
	Chou et al. (2007) and Chou et al. (2013)	Liposomes	Nebulizer	Osteosarcoma with pulmonary metastases	Phase Ib/IIa (and follow-up) Chest radiographs	Nausea, vomiting (grade 3) (1) Respiratory symptoms (13)	Progressive disease (8/19) Stable disease (7/10) Partial response (1/19) Complete response after metastatectomy (3/19)
Doxorubicin	Otterson et al. (2007)	Solution	Nebulizer	Metastatic tumour to the lungs (53) of which sarcoma (19), NSCLC (16)	Phase I/II CAT scan, antitumour activity lung functional tests, PK study	> 20% drop in forced vital capacity, wheezing, chest pain, grade 3 hypoxia (1), grade 4 dyspnoea (1), cough (grade 1-3) (28), hoarseness, haemoptysis, chest pain	Dose-limiting toxicity achieved Stable disease in Partial response (1) Stable disease (8)
	Otterson et al. (2010)	Solution	Nebulizer	Advanced NSCLC (24)	Phase I/II CAT scan, tumour evaluation, lung functional tests	> 20% drop in forced vital capacity, steroid use	Partial response (6) Complete response (1) Stable disease (13)
Gemcitabine	Lemarie et al. (2011)	Solution	Nebulizer	NSCLC (11)	Phase I Deposition (scintigraphy), lung functional tests, plasma, PK	Cough, dyspnoea, vomiting, severe bronchospasm	Dyspnea (8), Cough (7), Fatigue (4), Anorexia, Chest pain (2) Grade 3 bronchospasm (1)

3.6.3. Current status of inhaled chemotherapy (CT)

Much research has been and is being pursued on potential inhalation therapy with conventional chemotherapeutic drugs. These include, of course, cisplatin but a few formulations have been developed *in vitro* and tested *in vivo* (e.g. temozolomide (Wauthoz et al., 2010, Wauthoz et al., 2011), paclitaxel (El-Gendy and Berkland, 2009, Hureaux et al., 2009, Gill et al., 2011, Rosiere et al., 2016) and methotrexate (Shaik et al., 2002)). Some have reached the clinical stage **(Table 10)**, including 5-fluorouracil, 9-nitrocamptothecin, carboplatin, cisplatin, doxorubicin and gemcitabine. All of these clinical trials were realized using nebulized solutions or liposome suspensions, which is often the case for inhalational drug development as it helps limit the development cost. Of all these drugs, cisplatin has been one of the most studied drugs for inhalation in clinical trials during the last decade. The first clinical study by Wittgen et al., from 2007 (Wittgen et al., 2007), was directly focused against lung carcinoma (primary and secondary, metastatic to the lung) .

More precisely, of 18 patients, 1 patient had SCLC and 17 had NSCLC, of which 7 had adenocarcinoma, 5 had squamous cell carcinoma, 2 had broncho-alveolar carcinoma and 2 had large-cell undifferentiated carcinoma. All were unresponsive to classical treatment. In this phase I dose escalation study, the toxicities classically encountered with IV cisplatin were mild using the pulmonary route (nausea and emesis were observed in 64.7% and 47.1% of patients, respectively, and fatigue in 64.7%) or totally absent as no dose-limiting nephrotoxicity, haematotoxicity, ototoxicity or neurotoxicity could be observed in treated patients. The notable pulmonary events recorded were decreased forced expiratory volume, decreased diffusion lung capacity for carbon monoxide and dyspnoea in 76.5%, 70.6% and 64.7% of patients, respectively. Local irritation of the mucosa induced hoarseness in 47.1% of patients and irritative or productive cough in 11.8% and 17.7% of patients, respectively. A single patient exhibited considerable thickening of the bronchial wall and persistent dyspnoea consecutive to the study drug and had to be discontinued from the study. The main issues encountered in this study were linked to the administration method, jet nebulization, which showed low deposition efficiency in the deep lung (10-15%), and required very long administration time, which limited the administrable dose in a reasonable timeframe. To reach the maximal administered dose per cycle (60 mg/m²), one patient had to follow a total of 20 inhalation procedures for a total of 6.7 hours a day for 3 days over a week. Another patient, administered a lower dose (48 mg/m²), had to follow inhalation procedures for 8.0 hours a day for 4 days over a week. Despite these challenging conditions, the dose-limiting toxicity was never reached and no tumour response (which is never a phase I study

objective) other than stabilization (~70% of enrolled patients) was observed (Wittgen et al., 2007).

In another phase Ib/IIa clinical trial by Chou et al. from 2007 and its follow-up in 2013 (Chou et al., 2007, Chou et al., 2013), the same formulation of liposomal cisplatin was directed against osteosarcoma, a secondary tumour of the bone, which predominantly metastasizes in the lungs. Cisplatin was administered every 2 weeks at doses up to 36 mg/m^2. Of 19 treated patients, no hematotoxicity, nephrotoxicity or ototoxicity was observed. Nausea and vomiting were observed for 62% and 22% of patients, respectively. Respiratory symptoms were seen following the same pattern as the first study: cough was seen in 56% of patients, dyspnoea was seen in 25% of patients, but both were reversible and transitory. Other symptoms linked to the administration of the study drug, such as wheezing, mucosal inflammation and rhinorrhoea, were uncommon and very limited. Overall, this confirmed the safety of inhaled cisplatin, administered in this study following a gradual increase in exposure thanks to the jet nebulizer and long administration times. It was confirmed by the 24-hour systemic exposure, as measured by cisplatin concentration in serum, which was up to 35-fold lower than the values obtained after IV administration in another study (Kelsen et al., 1985). Regarding the efficacy assessment of inhaled cisplatin, it permitted platinum concentrations to be obtained that were up to 140-fold higher in the sputum than in the serum of a 36 mg/m^2 treated patient 24 hours after administration. It also permitted platinum concentrations to be obtained of up to 18.90 µg/g in resected tumorous tissue, as compared to the maximal 0.95 µg/g and the 0.2 µg/g obtained following intra-arterial and IV administration in another study (Bielack et al., 1989). Regarding survival, treatment was beneficial only to patients bearing small lesions and who could undergo concurrent surgical resection. Response was complete (disappearance of the tumour) in 2 patients (16%), partial response (decrease of size of the tumour) was obtained in 1 patient (5%) and disease was stable for 37% of patients. The remainder (42%) had quick progressive disease. After 1 year, about 80% of patients showed progression on follow-up. This efficacy assessment must be put in perspective with the very low survival rates generally observed for this aggressive and non-responsive secondary cancer at this stage, which normally shows recurrence within 6 months (Chou et al., 2013). Liposomal cisplatin against osteosarcoma has now been in an ongoing phase II clinical trial (efficacy study) since 2012 (Clinicaltrials.gov identification number NCT01650090).

SCIENTIFIC STRATEGY

Local delivery of anticancer drugs directly to the lungs seems to be a great opportunity to increase local exposure in and near the tumour site and decrease the high systemic toxicities encountered with the classical systemic routes.

Cisplatin is the cornerstone of anticancer CT since the 1970s. It is still widely used against NSCLC and SCLC, from early stage to the latest stages, despite the development of new targeted therapies, which only concern small subsets of patients. Cisplatin exhibits a strong anticancer activity. However, it is not at all selective of cancerous cells and as a small molecule enters freely into many tissues. Its main limitation is therefore the general toxicity it exerts by the systemic route, in particular dose-limiting acute and chronic renal impairment, for which countermeasures are taken involving heavy hydration and forced diuresis. Those increase the duration of treatment, the discomfort of patients and the mobilization of healthcare personnel and decrease the total administrable dose. Ototoxicity is seen in a large number of patients but no viable otoprotection measures exist to date. All these systemic toxicities have been linked to high plasmatic C_{max}.

Indications of inhaled CT as a new treatment modality is to act as a neoadjuvant treatment or as an adjuvant treatment. As a neoadjuvant treatment, it could help reduce tumour size and help the following surgical resection. As an adjuvant treatment, it could help lower metastatic involvement in places that are hardly reachable or in too low concentrations by conventional CT. Another potential target of inhaled CT can be found in less frequent cancer sub-types like mucinous lepidic adenocarcinomas, which are currently hard to cure due to their unusual presentation (e.g. less prone to surgery, aerogenous spread, low response to conventional CT). Development of inhaled cisplatin has been proved as a safe option against lung cancers (primary and secondary) through the nebulization of liposomal dispersions. However, this mode of administration, combined with the relatively low cisplatin encapsulation in liposomes has demonstrated a few disadvantages, even in a clinical setting. In particular, these are the long periods of time required to reach efficacious doses and increasing patient discomfort but they also include environmental contamination through nebulization, requiring appropriate safety infrastructures and procedures.

Delivery of cisplatin from a DPI formulation, using inexpensive and therefore disposable low-resistance single-unit DPI devices, seems to offer an attractive alternative, in order to increase the local dose in a short time of administration, lower the systemic dose and

therefore systemic toxicities and shorten treatment interruption periods, a major risk-factor for cancer resurgence. The choice of DPIs was made taking into account the high amount of powder to deliver to the lung, the ability to decrease the maintenance issue using disposable low-cost DPIs and reduce environmental exposure as compared to current nebulizers, and the ability of single-unit DPIs using capsules to be designed from low to high resistance DPIs following the indication. In this case, a low resistance device is preferred to assure an appropriate aerodynamic performance even at an airflow below 100 L/min but higher than 60 L/min as usually encountered even with patients with impaired lung function.

DPI formulations on the market are mostly low-dose therapies in the microgram range, which are obtained through milling and mixing of the drug with a carrier in large proportion. In the case of cisplatin, larger doses in the milligram range are needed. Furthermore, because cisplatin is relatively soluble in water and is a very small molecule, its direct delivery may create high C_{max} in the lungs directly available for pharmacological action and/or for absorption into the blood, which could increase the risk of lung and systemic toxicities. Therefore, there is a high need for formulations that can reside in the lung structures (bronchioles, alveoli, fluids) for a few hours following their deposition, ensuring slow delivery of cisplatin to maintain therapeutic concentrations and avoid toxic concentrations to the local tissues.

SLM offer an attractive option to generate this kind of formulation, as they are composed of biocompatible excipients and can be produced with appropriate particle size in the inhalation range and with appropriate surface properties in just a few steps with up-scalable techniques. Through their lipid matrix, they can protect and provide CR of the drug. They could be composed of biocompatible, biodegradable and usually well-tolerated excipients **(Table 9 in the introduction part)** (Sanna et al., 2004, Jaspart et al., 2005). However, two main issues may be encountered. First, classical emulsion techniques seem to be more suited for the encapsulation of lipophilic drug, which is not among cisplatin physicochemical properties (log P < 0). In particular, when these techniques involve hydrophilic drugs, those are always highly diluted in excipient, which decreases the dose of drug that can be delivered by inhalation. Second, because of their size, these particles are very likely to be confronted with macrophage clearance *in vivo*. To overcome this issue, they can be designed with stealth or drug-targeting abilities, using surface modification (Sanna et al., 2004).

The objectives of this research were therefore to develop a cisplatin DPI to overcome the limitations encountered with nebulizers during the cisplatin clinical studies in literature.

This approach could help deliver a high dose of powder in a few seconds within the lungs, with an objective of FPF superior to 30%.

Using a capsule-based low resistant device, this high dose of powder should be able to be delivered to patients bearing lung tumors.

The DPI formulations to be developed therefore aims at presenting

    (i)   a high-dose content of cisplatin to minimise the number of capsules

    (ii)   optimal aerodynamic performance leading to high lung deposition

    (iii)   CR properties to sustained the release of cisplatin to optimise its therapeutic potential and limit the risks of local toxicity

    (iv)   appropriate lung-retention properties to ensure prolonged local exposure.

These parameters were to be verified first *in vitro* and then confirmed *in vivo* through local and systemic pharmacokinetic studies. Based on the results of these studies, the best candidates were then to be assessed for their tolerance and efficacy using a preclinical model of lung tumor.

EXPERIMENTAL SECTION

Part I – Development of cisplatin DPI formulations

1. Introduction

Administration of cisplatin by the pulmonary route seems an interesting approach in the treatment of lung cancer. First by increasing the chemotherapeutic exposure of the tumour site, but also by lowering the toxicities of the general route. As a neoadjuvant or an adjuvant treatment, as detailed in the scientific strategy, this could help reduce the tumour(s) size and/or risk of resurgence by increasing the concentration in lung tissue and lymph nodes and potentially reduce the waiting periods between cisplatin administration.

Previous clinical studies showed that inhaled cisplatin was relatively well-tolerated in humans. However, the nebulizer devices used in these studies were not able to reach the dose-limiting toxicities and more importantly, led to very long administration times of up to 8 hours a day (Wittgen et al., 2007). This is why we have chosen to produce cisplatin DPI formulations. These could permit larger cisplatin doses to be administered in a few seconds, without the need for a large apparatus or the use of specific solubilization methods. However, this advantage could become a hindrance if the administered cisplatin was to cause high peak concentrations, resulting in local toxicity. Therefore, there was a need for a CR of cisplatin from the deposited particles.

The major criteria for the development of DPI formulations generated through a dry powder inhaler is to obtain dry powder aerosols with particles in the respirable range ($d_{ae} \leq 5$ μm) and a minimum of particles with $d_{ae} > 5$ μm, which will deposit in the oropharynx or the large bronchi. This parameter is characterized by the FPF as defined in the Introduction. In this case, the dry powder inhaler chosen for the formulation development was the Axahaler (SMB), an inexpensive low resistance N°3 capsule-based device designed by Plastiape (Osnago, Italy) and based on the design of the RS01 monodose DPI (Elkins et al., 2014a). It was chosen for its ability to deliver large doses of DPI formulation and to present a low resistance to airflow that could be more adequate for patients with impeded respiratory function (Elkins et al., 2014b). The loaded drug dose was therefore the drug dose packaged in the capsules, which were hydroxypropyl methylcellulose (HPMC) capsules (Qualicaps, Madrid, Spain) as they present more advantages in inhalation field than gelatine capsules (Wauthoz et al., 2016a, Wauthoz et al., 2016b).

Another important parameter for DPI formulation development is the FPD, also defined above. DPI devices have a maximum loadable powder mass of 30-40 mg (depending on the powder characteristics) which is set by the capsule size (generally size 3 capsules). Cisplatin activity is comprised within the milligram range and doses by the parental route are generally comprised from 30 up to 60 mg/m² for the most advanced stages of NSCLC and SCLC and even up to 100 mg/m² in some countries. A 10% lung distribution is a commonly accepted value for the parental route. To obtain the same dose in the lungs with a DPI, an FPD between 5.4 mg and 18 mg has to be deposited in patients with a body surface area of 1.8 m² (3-10 mg/m²) (Sacco et al., 2010). This array of dose has to be comprised within the inhaled capsules and be effectively deposited in the lungs. Overall, this means that with an FPF of 30% (average value for currently marketed DPIs), the excipient proportion had to be limited by design to a maximal 50% w/w in order to maintain the number of capsules at a reasonable value (maximum 5 by administration). This is consistent with the doses employed in the Sustained-release Liposomal Inhaled Therapy and Inhaled Lipid Cisplatin clinical trials knowing that nebulizers present a FPF around 10-20% and a maximal single dose of 80 mg/week (i.e. 40 mg/m²) was administered in the Wittgen et al. study against NSCLC and of 72 mg/week (i.e. 36 mg/m²) in the Chou et al. study against osteosarcoma, respectively (Chou et al., 2007, Chou et al., 2013).

In addition, the formulation strategy aims to provide CR properties to cisplatin and high lung residence of particles. Moreover, potentially well tolerated excipients and easily scalable techniques are preferred. Taking into account all these factors and limitations, solid lipid-based carrier systems such as SLN and SLM were chosen (**Table 7** and **Table 9**, in 3.5. Controlled release inhaled therapies of the Introduction).

2. Preliminary studies

SLN and SLM were the best candidates as cisplatin CR carrier-systems, with a great advantage for SLN of less than 250 nm for their MCC system escaping-abilities.

2.1. Safety procedures

The safety procedures that were used for cisplatin handling during formulation and characterization steps are described in the methods section of the Article 1 (see 3.3.2.1. Safety procedures).

2.2. Cisplatin characterization

Quantification of cisplatin in the final formulations was realized using ^{195}Pt NMR (see 3.3.2.10.2. Quantitative and qualitative analysis of cisplatin). In the meantime ETAAS (see 3.3.2.10.1. Platinum quantification) as described in Article 1 and the details of the validation method in Appendix 1) was used for quantification of the Pt content from cisplatin. The latter was realized for DPI formulations and throughout the intermediate steps of formulations, deposition and dissolution studies that required a high sensitivity.

2.3. Solid-lipid nanoparticles (SLN)

Size reduction techniques rely either on a "top-down" or on a "bottom-up" approach, with the former avoiding solubilization of the drug and the latter requiring its prior solubilization and its reprecipitation in an appropriate solvent. The only available stable solvent for cisplatin with greater solubility than water is DMF, which is a class II solvent (USP30, 2007) that would necessitate a thorough elimination during the formulation process.

2.3.1. Materials and Methods

2.3.1.1. Materials

Ethyl acetate and anhydrous DMF were purchased from Sigma-Aldrich (St-Louis, USA), ethanol was purchased from Merck-Millipore (Darmstadt, Germany), isopropanol (IPA) was the same as described in Article 1 (see 3.3.1. Materials). All solvents and non-solvents used were of analytical grade. Cisplatin, TPGS and cholesterol were those described in Article 1 (see 3.3.1. Materials). Stearic acid, myristic acid, palmitic acid, lauric acid, stearic acid, behenic acid, arachidic acid were purchased from Sigma-Aldrich (St-Louis, USA). Glyceryl monostearate (GMS), glycol stearate, PEG stearate, polypropylene glycol stearate were obtained from Gattefossé (Saint-Priest, France). Phospholipon 90H (P90H),

DPPC, 1,2-dilauroyl-*sn*-glycero-3-phosphocholine (DLPC), sodium oleate, hydrogenated phosphatidyl choline were obtained from Lipoid (Steinhausen, Germany).

2.3.1.2. Solid-lipid nanoparticles production

2.3.1.2.1. Uncoated nanocrystals

Cisplatin was first solubilized up to saturation into anhydrous DMF for a minimum of 48 hours under constant agitation at room temperature. This led to a cisplatin concentration in DMF of 12-16 mg/mL, as determined by ETAAS and confirmed by ^{195}Pt NMR, which showed no degradation over a 6 months period in solution.

Precipitation of cisplatin nanocrystals was then realized using the bottom-up approach under sonocrystallization in order to control the nucleation process. This was done using a Vibracell VCX 500 (Sonics, Newtown, USA) ultrasonic probe, under a 20 kHz frequency, fixed amplitude of 40% and fixed duration of 5 minutes. The probe was set 1-2 cm above the bottom of the beaker, which had previously been filled with 10-40 mL of an ice-cold non-solvent of cisplatin (i.e. IPA, EA, ethanol), set into an ice-bath. A 100 to 1000 μL volume of the cisplatin solution was then added continuously into the non-solvent using a 100 μL micropipette under ultrasonication for a maximum of 4 minutes. Surfactants (i.e. TPGS, P90H, DPPC, DLPC, sodium oleate, hydrogenated phosphatidyl choline, GMS) needed to help stabilize the nanosuspension were added into the DMF fraction or into the non-solvent fraction prior to the sonocrystallization step.

2.3.1.2.2. Solid-lipid nanoparticles (SLN)

The same procedure was applied for the production of SLN except that a lipid fraction was co-solubilized with cisplatin into DMF. The assayed non-solvents were IPA, ethyle acetate or a binary mix of water/IPA at 90:10 and 75:25 ratios. The lipids assayed were myristic acid, palmitic acid, lauric acid, stearic acid, GMS, glycol stearate, PEG stearate, behenic acid, arachidic acid and cholesterol, up to their pre-determined maximal concentration in the solvent admixture (i.e. between 20 and 40 mg/mL).

2.3.1.3. Nanoparticle characterization

2.3.1.3.1. Size-measurements

Aliquots of the nanocrystalline or the SLN suspensions were analysed for their particle size distribution (PSD) immediately using dynamic light scattering with a Zetasizer Nano ZS (Malvern Instruments, Worcestershire, UK). The 1 mL aliquots were set into a 12 mm PCS1115 glass cuvette (Malvern Instruments, Worcestershire, UK), which was set into the apparatus at 2°C or 25°C, with a refraction index of 1.69 and absorbance of 0.1 for cisplatin.

Viscosity of the non-solvents were set at 0.56 and 0.43 mPa.s for ethyle acetate and 4.56 and 2.13 mPA.s for IPA at 2 and 25°C, respectively and at 2.4 and 2.3 mPa.s for water/IPA at 90:10 and 75:25 ratios at 25°C, respectively. Measurements were generally carried-out after 120 s of stabilization and redone after 1, 3 and 19 hours to evaluate the stability of the nanosuspensions. This procedure helped establish the Z-average (nm) of the particles' populations (i.e. the intensity weighted mean hydrodynamic size of the entire population), as well as their polydispersity index, representative of the extent of the PSD.

2.3.1.3.2. Precipitation efficiency

Precipitation efficiency was established through the quantification of Pt by ETAAS, and calculated as the ratio of precipitated Pt (i.e. Pt quantified in the suspension) to the total Pt content (i.e. Pt quantified in the supernatant and in the suspension) following centrifugation of the suspensions at 17 000 g for 30 minutes.

2.3.2. Results

2.3.2.1. Uncoated nanocrystals

This bottom-up approach, first evaluated for uncoated nanocrystals of cisplatin gave the best results (e.g. smallest Z-average and peak diameter, smaller polydispersity index, best stability) using ethyle acetate as the precipitation medium (non-solvent) and saturated DMF as the cisplatin solvent. More precisely, the best conditions were with 5% w/w GMS, 2% w/w GMS and 2% w/w TPGS as surfactants, previously solubilized in the non-solvent. This gave Z-averages of 112.0 ± 5.6 nm, 115.8 ± 5.9 nm and 120 ± 13.7 nm at t_0, respectively. Stability after 19 h at 2°C exhibited Z-averages of 126.8 ± 2.6, 144.7 ± 30.0 and 309.6 ± 257.4, respectively. These were all obtained by injecting 200 μL of cisplatin-saturated DMF into 20.0 mL of EA. The polydispersity indexes were always below 0.250 for each of these conditions but increased with time. Increase in GMS or TPGS concentration, up to 10% w/w led to uncontrolled nucleation with higher particle size and less stable suspensions. Increase in cisplatin and in DMF volume also increased the particle size and decreased the stability of suspensions. All in all, thanks to its very low solubility in ethyle acetate (~2 μg/L), the precipitation of cisplatin was very effective and led to precipitation efficiencies above 92% for the best conditions cited above. Nevertheless, this technique was only able to produce very low quantities (i.e. maximum 2 mg at a time) of stable uncoated cisplatin nanocrystals.

2.3.2.2. Solid-lipid nanoparticles (SLN)

It was altogether impossible to co-precipitate cisplatin and lipids into stable SLN using this bottom-up approach because of the relatively high solubility of the assayed lipids in ethyle

acetate or IPA under ultrasonication. Water was therefore added to IPA and ethanol to form a ternary non-solvent mixture, able to precipitate both lipids and cisplatin but this was not sufficient to precipitate lipids rapidly and increased the solubility of cisplatin to a too great extent. This therefore led to unstable SLN suspensions. On a side note, the same technique was used to produce polymeric nanoparticles with a PEG hydrophobically-modified dextran (PEG-HMD), developed in our lab by Rosiere et al. (2016) but also led to unstable particles, with Z-averages comprised between 298 ± 55 and 446 ± 83 nm at t_0, quickly sedimenting or growing after 1 h.

2.3.3. Conclusion

This technique was inefficient, tedious and exhibited poor up-scalability. Because of the unique properties of cisplatin (general reactivity and low solubility in spray dryable solvents) the next strategy was to avoid its solubilization.

2.4. Solid-lipid microparticles (SLM)

Because to be inhalable, particles must lay in the low micrometre range (d_{ae} between 1-5 µm), which is related in part to their geometrical size. Bulk cisplatin exhibited large PSD **(Table 12)**, so the formulation process needed to begin with a size reduction step. It was necessary to choose a technique with high size reduction abilities in order to leave enough room for embedment of the obtained microcrystals into the lipid matrix system provided by SLM. This technique had to be efficient at lab scale and still easily up-scalable, with an easily decontaminable apparatus and easily implementable with the rest of the formulation process (i.e. spray drying). The top-down approach using combined HSH and HPH, consisted of reducing the large crystals by applying shear forces to the suspension. It was proven adequate for obtaining cisplatin microcrystals in the targeted lower micrometre range. HSH and HPH are well-established techniques, available at lab scale for the production of small batches of a few mL, and easily up-scalable to produce larger volumes. The process then involved spray drying of the resulting microcrystalline suspension with and without lipids, solubilized in the heated dispersant, to obtain the dry powders for inhalation.

The HPH works in a closed loop in which a defined number of cycles of increasing pressure are applied to the suspension. The parameters that are the most important for the size reduction process with HPH are (i) the number of cycles applied, (ii) the pressure applied, (iii) the concentration of the suspension, (iv) the temperature of the process and (v) the hardness of drug particles (Hecq, 2006).

2.4.1. Material and methods

2.4.1.1. Material

Cisplatin, TS, TPGS, DSPE-mPEG-2000, DPPC, isopropanol, DMF, Suprapur nitric acid, dichloromethane, DMF-d_7 were obtained as described in the material section of Article 1 (see 3.3.1. Materials). P90H was purchased from Lipoid (Steinhausen, Switzerland), GMS was obtained from Gattefossé, Saint-Priest, France) and cholesterol was purchased from Sigma-Aldrich (St. Louis, USA).

2.4.1.2. Cisplatin size reduction

The size reduction method with the HSH and the HPH steps is fully described in Article 1 (see 3.3.2.2 Cisplatin size reduction). Briefly here, cisplatin at 2.0 and 5.0% w/v in isopropanol with or without surfactant was submitted to HPH for 10 pre-milling cycles at 5 000 psi, 10 milling cycles at 10 000 psi and 20 or 60 milling cycles at 20 000 psi.

Table 11. Theoretical composition of the DPI preliminary formulations.

Formulation	Cisplatin-TPGS/Lipid ratio	GMS/DSPE-mPEG-2000	Cisplatin (%w/w$_{total}$)	TPGS (%w/w)	GMS (%w/w)	DSPE-mPEG-2000 (%w/w)
MC F1*	100:0		100.0%	0%	-	-
MC F2	100:0	-	95.0%	5.0%	-	-
MC F3	90:10	100:0	85.5%	4.5%	10.0%	0.0%
MC F4	75:25	100:0	71.3%	3.8%	25.0%	0.0%
MC F5	50:50	100:0	47.5%	2.5%	50.0%	0.0%
MC F6	25:75	100:0	23.8%	1.3%	75.0%	0.0%
MC F7	10:90	100:0	9.5%	0.5%	90.0%	0.0%
MC F8	90:10	90:10	85.5%	4.5%	9.0%	1.0%
MC F9	75:25	90:10	71.3%	3.8%	22.5%	2.5%
MC F10	50:50	90:10	47.5%	2.5%	45.0%	5.0%
MC F11	25:75	90:10	23.8%	1.3%	67.5%	7.5%
MC F12	10:90	90:10	9.5%	0.5%	81.0%	9.0%
MC F13	90:10	75:25	85.5%	4.5%	7.5%	2.5%
MC F14	75:25	75:25	71.3%	3.8%	18.8%	6.3%
MC F15	50:50	75:25	47.5%	2.5%	37.5%	12.5%
MC F16	25:75	75:25	23.8%	1.3%	56.3%	18.8%
MC F17	10:90	75:25	9.5%	0.5%	67.5%	22.5%

* indicates formulations embedding cisplatin reduced without TPGS during the HPH process

Formulation	Cisplatin-TPGS/ Lipid ratio	Cholesterol/ P90H	Cisplatin (%w/w)	TPGS (%w/w)	Cholesterol (%w/w)	P90H (%w/w)
MC F18	75:25	75:25	71.3%	3.8%	18.8%	6.3%
MC F19	50:50	75:25	47.5%	2.5%	37.5%	12.5%
MC F20	50:50	90:10	47.5%	2.5%	45.0%	5.0%

2.4.1.3. Preparation and characterization of cisplatin dry powder preliminary formulations

The preparation method for cisplatin DPI preliminary formulations is fully described in Article 1 (see 3.3.2.3. Preparation of cisplatin dry powder formulations), briefly, this was done through spray drying of the microcrystalline cisplatin suspension obtained following size reduction. This was done directly at 2.0% w/v or in addition with a solubilized lipid fraction. The composition of the spray dried suspensions and the resulting DPI preliminary formulations are reported in **Table 11**. Spray drying was realized using the same parameters as those used in Article 1 (see 3.3.2.3. Preparation of cisplatin dry powder formulations). Particle size, shape and surface morphology of DPI preliminary formulations were determined by laser diffraction in suspension and by scanning electron microscopy (SEM) as described in Article 1 (see 3.3.2.7.1. Individualized particles and 3.3.2.6. Particle size, shape and surface morphology).

2.4.1.4. Aerodynamic performance

Aerodynamic performance was determined either with a multistage liquid impactor (MsLI) as described in Article 1 (3.3.2.8. Aerodynamic performance) or with an abbreviated impactor, the FSI, as mentioned below. To do so, a mass of 20 mg of each DPI preliminary formulation, previously sieved through a 355 μm stainless steel mesh, was weighed in a size 3 HPMC capsule (Qualicaps, Madrid, Spain) and deposited onto a Fluoropore 9 cm PTFE membrane with 0.45 μm pore size bonded on a high-density polyethylene support (Merck Millipore, Darmstadt, Germany) using an Axahaler® DPI mounted on the inhalation port with its adapter (n = 3). A deposition flow rate of 100 ± 5 L/min measured using a DFM3 flow meter (Copley Scientific, Nottingham, UK) was obtained with one HCP5 air pumps (Copley Scientific, Nottingham, UK) connected to a TPK critical flow controller (Copley Scientific, Nottingham, UK). After impaction, cisplatin from the formulation, deposited onto the filter was solubilized with 100.0 mL of 0.5% w/v Poloxamer 407 in Milli-Q water/IPA (60:40 v/v) under ultrasonication for 30 minutes. The impacted mass was determined by quantification of the Pt content by ETAAS. This permitted to obtain the FPD, and the FPF below 5 μm, which was expressed as a percentage of the nominal dose.

2.4.1.5. Dissolution properties

The dissolution method developed during the preliminary formulation step is fully disclosed in Article 1 (see 3.3.2.9. Dissolution properties). Briefly, the method is based on the FSI deposition onto the fluoropore filter, then set-up into a paddle apparatus from the pharmacopoeia. During the method development described here, the aforementioned filter
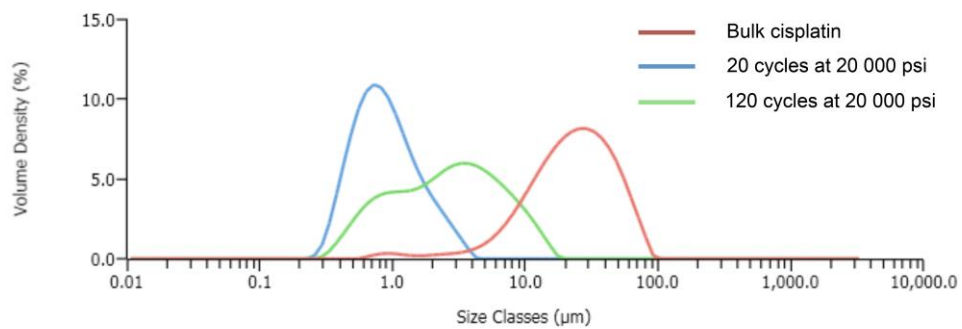
Figure 35. Particle size distribution after application of HPH cycles on suspensions of 5% w/w cisplatin in isopropanol without surfactant.
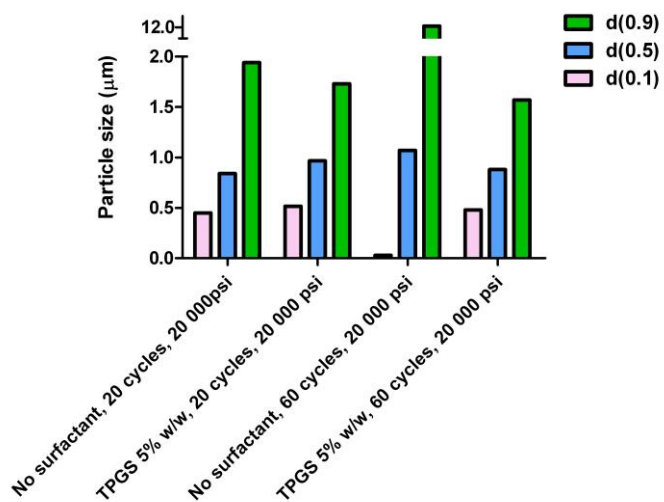
Figure 36. Particle size distribution of cisplatin microcrystals in suspension after 20 cycles and 60 cycles HPH at 20 000 psi, without surfactant and with TPGS at 5% w/w.

with the deposited powder was either facing up (set-up A and C) or facing down (set-up B). If facing up, was then either left uncovered (set-up A) or covered (set-up C) with an Isopore® 0.4 µm hydrophilic polycarbonate filter (Merck-Millipore, Germany) and fixed onto a watch glass-PTFE disk assembly (Copley, Nottingham, UK) with the clips and PTFE mesh screen provided.

2.4.2. Results and discussion

2.4.2.1. Size reduction

In our experimental process, we first reduced cisplatin particles in suspension at 2.0 and 5.0% w/v in IPA without surfactants. This gave a comparable d(0.5) of 2.15 ± 0.01 µm after 10 minutes of HSH and 10 cycles at 5000 psi, of 1.42 ± 0.0 µm after 10 cycles at 10 000 psi and of 0.89 ± 0.01 after 20 cycles at 20 000 psi. However, the suspension was unstable after 120 cycles at 20 000 psi, which created agglomerates, as seen with a d(0.5) of 2.65 ± 0.02 µm and a d(0.9) of 8.34 ± 0.02 µm **(Figure 35)**.

Stabilization of the suspension using surfactants is often needed to obtain smaller particles, as it helps reduce the interfacial tension between solid particles and the suspending liquid and avoids creating agglomerates as particles are broken down. We therefore assayed the addition of surfactants (5% w/w$_{cisplatin}$) that were known to be well tolerated in the lungs, based on a quick visual preselection of those most able to stabilize cisplatin in isopropanol (e.g. P90H, GMS, TPGS). TPGS was the only excipient that led to the production of cisplatin microcrystals of smaller PSD than the previous conditions without surfactant. PSD was established through the mass median diameter d(0.5), the d(0.9), for which 90% of particles lie under the expressed diameter, the volume mean diameter D[4,3] and the percentage of fine particles determined from the cumulative undersize curves (% of particles below 5 µm). This was observable after 60 cycles at 20 000 psi (0.88 ± 0.0 µm *vs.* 1.07 ± 0.03 µm in d(0.5) and 1.57 ± 0.0 *vs.* 12.2 ± 0.2 in d(0.9), with TPGS and without surfactant, respectively). Moreover, TPGS gave a comparable d(0.5), of 0.97 ± 0.0 µm *vs.* 0.84 ± 0.00 µm after 20 cycles at 20 000 psi, with and without TPGS, respectively but a narrower and more stable PSD, as seen with the lower d(0.9) of 1.73 ± 0.01 µm *vs.* 1.94 ± 0.05 µm with and without surfactant, respectively **(Figure 36)**.

Stability of cisplatin during the production process was assessed using the [195]Pt NMR technique. It showed that cisplatin structure was not affected by size reduction. The process yield was also assessed using ETAAS and showed that it was close to 100%, with a higher cisplatin concentration at the end of the process due to a loss of dispersant volume. This was
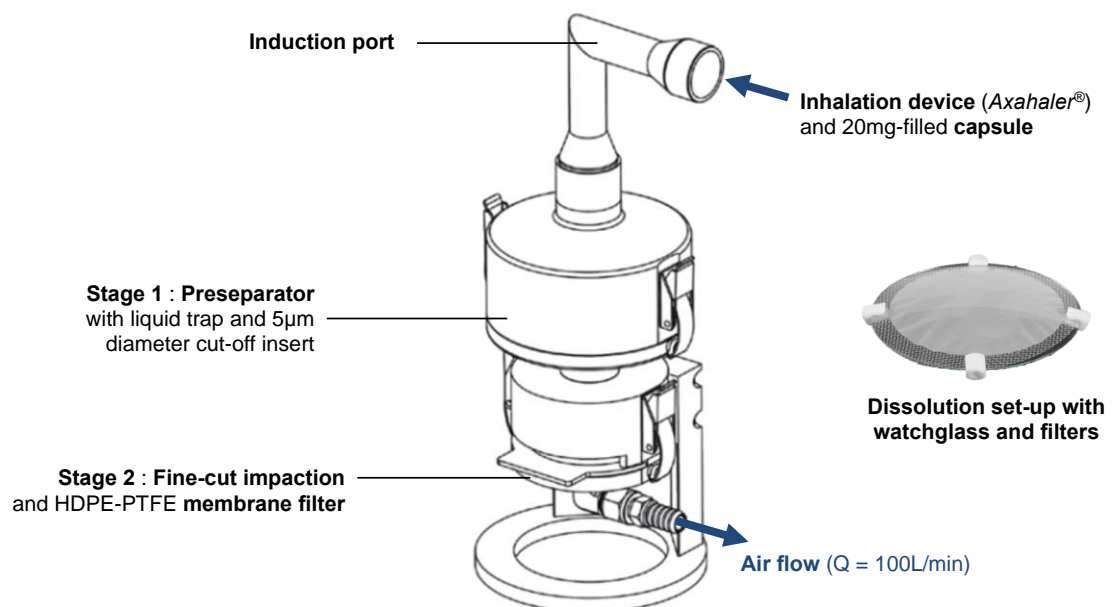
Figure 37. Schematic representation of the Fast Screening Impactor (FSI, Copley, UK) and of the watchglass-PTFE dissolution assembly.

attributed to solvent evaporation, linked to the high pressure applied, which caused an increase in the temperature in the tank and concentrated the cisplatin suspension. The first DPI formulations (i.e. F2 up to F24, **Table 11**) presented in this work were produced using 5% w/w TPGS after 60 cycles at 20 000 psi to ensure the narrowest PSD as possible. It however had the drawback of adding a high concentration of surfactant into the SLM formulations. The following formulations (i.e. F1*, F21* up to F24*, **Table 11** and F25 up to F27, **Table 15**) were produced using the primary size reduction method without TPGS, after 20 cycles at 20 000 psi.

2.4.2.2. Development of the FSI pre-separated particle dissolution test

As described earlier, there are no official pharmacopoeial dissolution tests for DPI formulations. Some dissolution tests are discussed in a few publications but they rarely take into account the whole respirable fraction (Jaspart et al., 2007, Son and McConville, 2009, Wauthoz et al., 2011) or involve modified impactors (Son et al., 2009) or modified dissolution apparatus such as diffusion cells (Davies and Feddah, 2003, Cook et al., 2005). The main issue encountered with this is that assessing the dissolution abilities of formulations based on the whole PSD of the powder (i.e. by dispersing bulk DPI formulation in a dissolution bath or a Franz cell) or only on a small powder fraction using a commercial dissolution cup for the next generation impactor (NGI) (i.e. by selecting only a small powder fraction using 1 over 6-7 stages with a $d_{ae} < 5$ μm) is not the closest representation of what happens *in vivo*. Other issues are that very fine powders are hard to fully disperse manually and may stick to the walls of the dissolution bath. Moreover, despite preventive filtration at each dosing time, inappropriately-dispersed powder particles that are floating can be an issue if they are collected. This is because they are still undissolved and their removal from the dissolution medium leads to inaccurate results.

May et al. had previously developed a similar test using an Andersen cascade impactor (ACI) with deposition of the powder onto a regenerated cellulose membrane, set either in a dissolution bath using the paddle method or in a Franz cell. They showed that the paddle method was superior as it better differentiated small differences between dissolution profiles for budesonide, fenoterol HBr and an undisclosed molecule, all showing different hydrophilic-hydrophobic properties (May et al., 2012).

In our work we used another abbreviated impactor, the FSI **(Figure 37)**, which has only one stage selecting d_{ae} below 5 μm, specifically aimed at the first stages of product development.
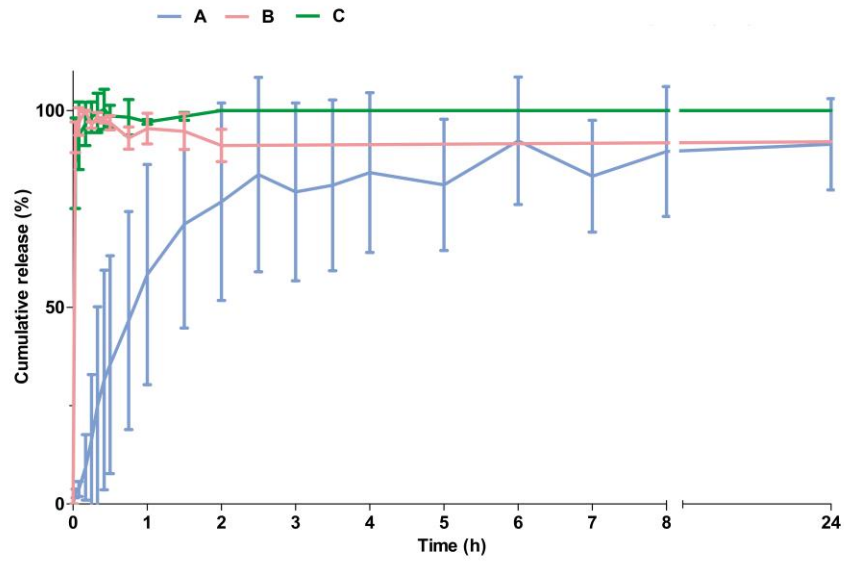
Figure 38. Dissolution profiles obtained with the different deposition and dissolution membrane set-ups (A: deposition filter facing up, B: deposition filter facing down, C: deposition filter facing up and an additional dissolution membrane) after deposition of approx. 4 mg of the same immediate-release DPI formulations using the Fast Screening Impactor. The deposition membrane was a hydrophobic 0.45 μm-pore size PTFE Fluopore® filter (Merck-Milipore, Darmstard, Germany) and the dissolution membrane was a 0.4 μm pore-size polycarbonate hydrophilic Isopore® filter (Merck-Milipore, Darmstadt, Germany).

Its design permits to quickly select inhalable particles, which are deposited onto a washable filter made of a high-density resistant polymer (HDPE-PTFE) to endure the demanding airflow conditions applied during deposition. This set-up was used as a deposition membrane for the dissolution studies. The 90 mm diameter watch glass and its PTFE grid **(Figure 37)** are made by Copley Scientific and are initially provided for the ACI.

Preliminary tests were therefore realized to determine the best membrane set-up for the dissolution studies with the FSI, using a deposition and a dissolution membrane **(Figure 38)**. These were done using the DPI formulation F2 (Cisplatin 95% w/w, TPGS 5% w/w, **Table 11**) with ~4 mg cisplatin deposited onto the FSI filter at a 100 L/min airflow for 2.4 s, n = 3.

As shown in **Figure 38**, the first set-up (A), which is the one described by May et al. (but with an hydrophilic polycarbonate deposition membrane, not applicable for deposition with the FSI), showed very high variability between each dissolution bath and did not permit to produce precise and repeatable measurements. These are essential regarding the limits permitted by the FDA related Guidance for Industry regarding the calculation of the difference and similarity ratios (f1, f2, see 3.3.2.9. Dissolution properties) using the model independent approach for bioequivalence studies (i.e. no more than 20% standard deviation from the mean of the earlier time points and maximum 10% afterwards) (Center for Drug Evaluation and Research, 1997). Moreover, set-up A led to entrapment of air bubbles between the filter and the watch glass, which led to a high undissolved fraction of the deposited powder. Set-ups B and C gave better and similar results. This showed that the original deposition filter was not to be used as the dissolution membrane, as it mediated the dissolution rate of particles, while the polycarbonate filter did not. Set-up C was chosen as it avoids the issue of floating particles described above.

2.4.2.3. Preliminary formulations

The first formulations were developed using 5% w/v cisplatin dispersed in isopropanol and 5% w/w$_{cisplatin}$ TPGS as described above. GMS and cholesterol were selected as a lipid matrix to control the drug release because of their high hydrophobicity (log P$_{o/w}$ of 6.6 and 7.1, respectively) and their ability to be spray dried from solutions, thanks to their high melting temperatures (58 and 150°C, respectively). Lipid-based SLM were then produced and assessed for their spray drying yield, drug-loading, particle size distribution, deposition patterns (FPF and FPD) using a multistage liquid impinger (MsLI, Copley Scientific,

Table 12 Particle size distributions (PSD) of DPI preliminary formulations, measured by laser diffraction in suspension, fine particle fraction (FPF) and fine particle dose (FPD) calculated for a 20 mg-filled capsule, as described in Article 1. FPF and FPD with a standard deviation are expressed as mean ± SD (n = 3). FPF and FPD from Bulk cisplatin to MC F20 are determined using the MsLI. FPF and FPD from MC F21 to MC F24* are determined using the FSI.

Formulation	d(0.1) (µm)	d(0.5) (µm)	d(0.9) (µm)	D[4;3] (µm)	% < 5 µm	FPF (% w/w)	FPD (mg)
Bulk cisplatin	4.67 ± 2.28	16.5 ± 3.6	36.6 ± 8.4	18.9 ± 4.3	10.2 ± 4.0	4.2 ± 2.1	0.6 ± 0.3
MC F1*	0.91 ± 0.02	1.59 ± 0.02	2.86 ± 0.06	1.75 ± 0.03	100.0 ± 0.0	24.2 ± 6.3	4.8 ± 1.3
MC F2	1.07 ± 0.02	2.13 ± 0.02	4.71 ± 0.05	2.55 ± 0.00	91.9 ± 0.4	51.5 ± 2.9	9.8 ± 0.6
MC F3	0.93 ± 0.01	1.89 ± 0.01	4.49 ± 0.07	2.35 ± 0.03	92.9 ± 0.5	18.9	3.3
MC F4	1.78 ± 0.0	3.47 ± 0.01	6.36 ± 0.00	3.80 ± 0.01	76.5 ± 0.2	12.4	1.7
MC F5	4.75 ± 0.01	7.91 ± 0.12	12.40 ± 0.31	8.27 ± 0.15	12.5 ± 0.1	0.5	0.1
MC F6	1.65 ± 0.0	4.19 ± 0.02	9.50 ± 0.29	4.95 ± 0.10	58.9 ± 0.6	1.7	0.1
MC F7	1.83 ± 0.02	6.33 ± 0.20	20.30 ± 2.74	8.92 ± 0.81	41.3 ± 1.2	1.6	0.0
MC F8	0.86 ± 0.01	1.86 ± 0.01	4.08 ± 0.06	2.20 ± 0.02	95.6 ± 0.4	21.6 ± 2.3	4.1 ± 0.4
MC F9	2.13 ± 0.10	4.76 ± 0.11	7.90 ± 0.36	4.91 ± 0.13	54.3 ± 2.0	9.8 ± 1.6	1.4 ± 0.1
MC F10	1.52 ± 0.01	3.11 ± 0.02	5.58 ± 0.03	3.35 ± 0.02	84.0 ± 0.4	6.6	0.6
MC F11	1.74 ± 0.00	4.31 ± 0.00	9.58 ± 0.06	5.05 ± 0.02	57.7 ± 0.1	3.5	0.2
MC F12	1.77 ± 0.01	4.50 ± 0.03	12.40 ± 0.48	5.90 ± 0.15	54.8 ± 0.4	2.8	0.0
MC F13	0.71 ± 0.01	1.68 ± 0.01	3.58 ± 0.03	1.95 ± 0.00	97.9 ± 0.2	39.0 ± 2.3	6.7 ± 0.7
MC F14	1.40 ± 0.01	3.17 ± 0.01	6.95 ± 0.03	3.72 ± 0.00	74.8 ± 0.1	22.4 ± 5.0	3.1 ± 0.8
MC F15	1.67 ± 0.01	4.24 ± 0.02	8.85 ± 0.23	4.80 ± 0.07	59.1 ± 0.4	17.3 ± 3.2	1.7 ± 0.3
MC F16	1.68 ± 0.00	5.87 ± 0.01	17.90 ± 0.20	8.00 ± 0.06	43.7 ± 0.1	5.4	0.2
MC F17	1.75 ± 0.00	5.92 ± 0.03	10.80 ± 0.09	6.13 ± 0.04	40.4 ± 0.2	12.6	0.2
MC F18	0.88 ± 0.00	2.14 ± 0.08	4.70 ± 0.22	2.49 ± 0.09	92.5 ± 1.7	38.0 ± 4.7	4.9 ± 0.8
MC F19	1.11 ± 0.01	2.79 ± 0.02	4.84 ± 0.03	2.90 ± 0.02	91.6 ± 0.3	34. 8 ± 1.0	3.2 ± 0.1
MC F20	1.02 ± 0.00	1.82 ± 0.00	3.39 ± 0.00	2.03 ± 0.00	99.4 ± 0.0	44.2 ± 5.8	3.5 ± 0.6
MC F21	1.89 ± 0.02	3.97 ± 0.04	6.58 ± 0.09	4.12 ± 0.04	69.7 ± 1.1	N.D.	N.D.
MC F22	1.60 ± 0.05	3.21 ± 0.04	5.38 ± 0.16	3.37 ± 0.05	85.5 ± 1.7	15.2 ± 1.9	1.5 ± 0.2
MC F23	1.34 ± 0.00	3.71 ± 0.01	7.07 ± 0.02	3.99 ± 0.01	69.8 ± 0.2	34.2 ± 13.1	5.1 ± 2.0
MC F24	1.67 ± 0.03	3.66 ± 0.07	6.01 ± 0.22	3.77 ± 0.08	76.9 ± 2.3	41.7 ± 3.0	4.2 ± 0.3
MC F21*	1.39 ± 0.01	2.95 ± 0.03	5.08 ± 0.12	3.11 ± 0.05	89.0 ± 1.4	N.D.	N.D.
MC F22*	1.69 ± 0.00	3.94 ± 0.01	7.36 ± 0.06	4.26 ± 0.02	66.3 ± 0.3	39.7 ± 4.5	4.0 ± 0.4
MC F23*	2.34 ± 0.05	3.25 ± 0.08	4.43 ± 0.11	3.32 ± 0.08	97.4 ± 1.3	9.6 ± 6.6	1.4 ± 1.0
MC F24*	1.50 ± 0.00	3.63 ± 0.01	6.41 ± 0.02	3.81 ± 0.01	73.8 ± 0.2	46.0 ± 1.0	4.6 ± 0.1

N.D. not determined, * Indicates formulations embedding cisplatin reduced without TPGS during the HPH process
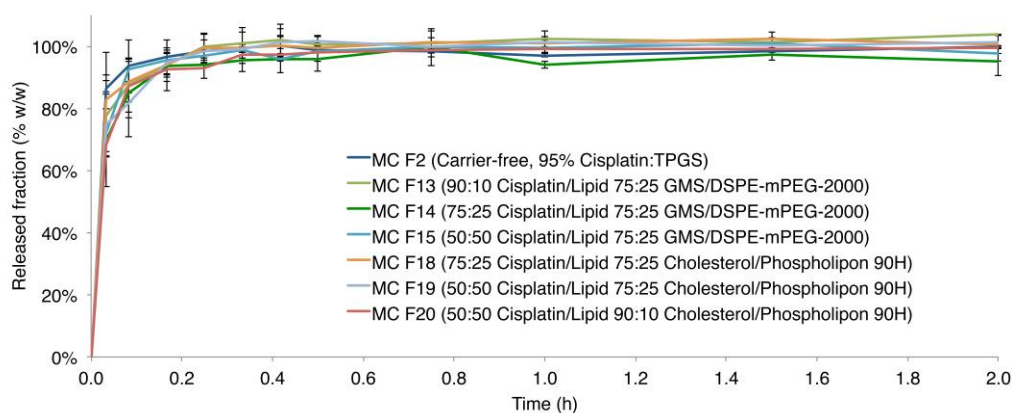
Figure 39. Dissolution profiles of DPI preliminary formulations selected based on their FPFs.

Nottingham, UK) and dissolution properties (only for formulations with an FPF > 20% w/w of the nominal dose), using the FSI dissolution methods described above.

2.4.2.3.1.Glyceryl monostearate (GMS)-based DPI formulations

DSPE-mPEG-2000 was chosen in order to provide PEGylation (i.e. presence of PEG moieties) at the particle surface and added to GMS as the main lipid component of the lipid matrix. This solubilized lipid fraction was added to a micronized suspension of cisplatin as described before (using TPGS at 5% w/w during the size reduction step). GMS/DSPE-mPEG-2000-based particles at different ratios (100:0, 90:10 and 75:25) and DPIs of different drug-loadings (from 90 to 10% in drug-loading) were produced (MC F1* to MC F17, **Table 11**).

With these formulations, we observed that cisplatin was not altered during the spray drying process (by ^{195}Pt NMR) and that no cisplatin was lost during the process considering the difference between the theoretical and the measured drug-loading (by ETAAS). We also observed that the PSD of the powders (measured by laser diffraction) increased with increasing lipid-ratios and that it led to lower FPF **(Table 12)**. Of all formulations, the best FPFs were obtained with the 75:25 GMS/DSPE-mPEG-2000 ratio (MC F13 up to MC F17). However, of all formulations, only one had an FPF above 30% w/w of the nominal dose (MC F13: 90:10 cisplatin/lipid with 75:25 GMS/DSPE-mPEG-2000 ratio) **(Table 12)**. Finally, the dissolution tests for these formulations showed that cisplatin was quickly released. Therefore these excipients were not studied further **(Figure 39)**. Moreover, the SEM images of these formulations showed that the increased PEG ratio increased in turn the presence of sheet structures. This was probably caused by higher sticking tendencies of the formulations, altogether explaining the lower observed FPFs **(Figure 40)**.

2.4.2.3.2.Cholesterol-based formulations

Another preliminary formulation strategy involved cholesterol/P90H-based SLM that had given interesting results in the encapsulation of insulin in another study from Depreter et al. (2010). The produced DPI formulations (50:50 cisplatin/lipid including 90:10 cholesterol/P90H, 50:50 cisplatin/lipid including 75:25 cholesterol/P90H, and 75:25 cisplatin/lipid including 75:25 cholesterol/P90H) showed much more interesting PSD **(Table 12)**, higher FPF (all above 35% w/w of the nominal dose **(Table 12)**, and better particle shape (well-defined, spherical particles) as observed by SEM **(Figure 40)**. However, these formulations were not able to provide a slower release of cisplatin either **(Figure 39)**.

Sheet structure frequency increases

Rough surface

MC F13
Cisplatin-TPGS/Lipid 90:10
GMS/DSPE-mPEG-2000 75:25
$d(0.5)_{Spraytec}$ = 3.64 μm
FPF = 39%

MC F14
Cisplatin-TPGS/Lipid 75:25
GMS/DSPE-mPEG-2000 75:25
$d(0.5)_{Spraytec}$ = 11.4μm
FPF = 22%

MC F15
Cisplatin-TPGS/Lipid 50:50
Geleol/DSPE-mPEG-2000 75:25
$d(0.5)_{Spraytec}$ = 10.98μm
FPF = 17%

MC F18
Cisplatin/Lipid 75:25
Cholesterol/P90H 75:25
$d(0.5)_{Spraytec}$ = 5.93 μm
FPF = 38%

MC F19
Cisplatin/Lipid 50:50
Cholesterol/P90H 75:25
$d(0.5)_{Spraytec}$ = 6.53 μm
FPF = 35%

MC F20
Cisplatin/Lipid 50:50
Cholesterol/P90H 90:10
$d(0.5)_{Spraytec}$ = 4.36 μm
FPF = 44%

Figure 40. SEM micrographs of selected DPI preliminary formulations based on their FPFs.

2.4.2.3.3. Cisplatin microcrystal-based DPI formulations (without lipid matrix)

During this preliminary study, we also produced cisplatin microcrystals directly from the HPH tank, using the size reduction methods with a surfactant (5% w/w TPGS) and without (100% size-reduced cisplatin, **Table 11**.). These results are integrated into and discussed in Article 1 as formulations F1 and F2. They showed the great advantage of adding TPGS to cisplatin microcrystals in order to obtain a better deposition pattern and higher FPFs **(Table 12)**. As explained further in Article 1, this was probably caused by the smoother particle surface from the added excipient in F2.

2.4.2.3.4. Conclusion

During this first attempt at producing DPI formulations, we showed that it was possible to obtain high FPFs and high FPDs, in particular using the cholesterol/P90H lipid mixtures as the lipid matrix, up to 50% w/w in the SLM (FPF comprised between 34.8 ± 3.7 and 44.2 ± 5.8% of the nominal dose and FPD comprised between 3.2 ± 0.1 and 4.9 ± 0.8 mg). The spray drying process gave average yields ranging between 44.8 and 57.8%, showing no excessive sticking. It was however impossible to obtain a CR of cisplatin from the produced SLM. Because these formulations included high amounts of excipients with tensioactive properties (TPGS, P90H, DSPE-mPEG-2000), we decided to assess the dissolution properties of SLM based on more lipophilic excipients.

2.4.2.4. Optimisation of solid-lipid microparticles

2.4.2.4.1. Optimisation of the lipid composition

The available lipid excipients showing potential tolerability in the lungs and exhibiting the highest log $P_{o/w}$ (by increasing the number of carbons and increasing the number of carbon chains) and high melting temperature to avoid to be softened during spray drying were first compared **(Table 13).** It is generally considered that particles inside the spray drying chamber are not subjected to temperatures higher than the outlet temperature. During spray drying of isopropanol lipid solutions, using the conditions described in Article 1, the outlet temperatures ranged between 38 and 42°C. As the softening of lipid can already begin 10°C below the reported melting temperature, the lipids were selected to take into account a margin.

Therefore, the selected lipid excipients for the following study were glyceryl behenate (Compritol© 888 ATO, Gatefossé, Saint-Priest, France), tripalmitin (Tokyo Chemical Industry, Tokyo, Japan) and TS (Tokyo Chemical Industry, Japan, **Figure 41**) described in **Table 13**.

Table 13. Lipid candidates for the optimisation of SLM.

Lipid	Log $P_{o/w}$	Melting temperature (°C)
Glyceryl monostearate (GMS)	6.60	58
Cholesterol	7.11	148
Arachidic acid (C20)	9.29	75
Compritol© 888 ATO (Glyceryl behenate C22)	**9.35**	**70**
Tripalmitin (C16)	**19.9**	**55**
Tristearin (C18)	**21.6**	**75**
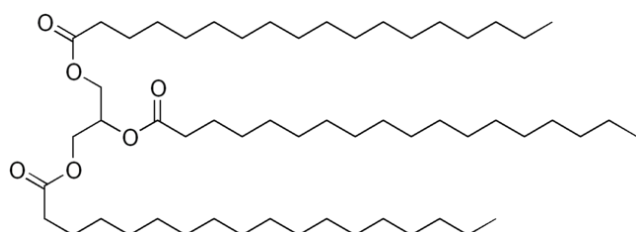
Figure 41. Structure of tristearin (TS)
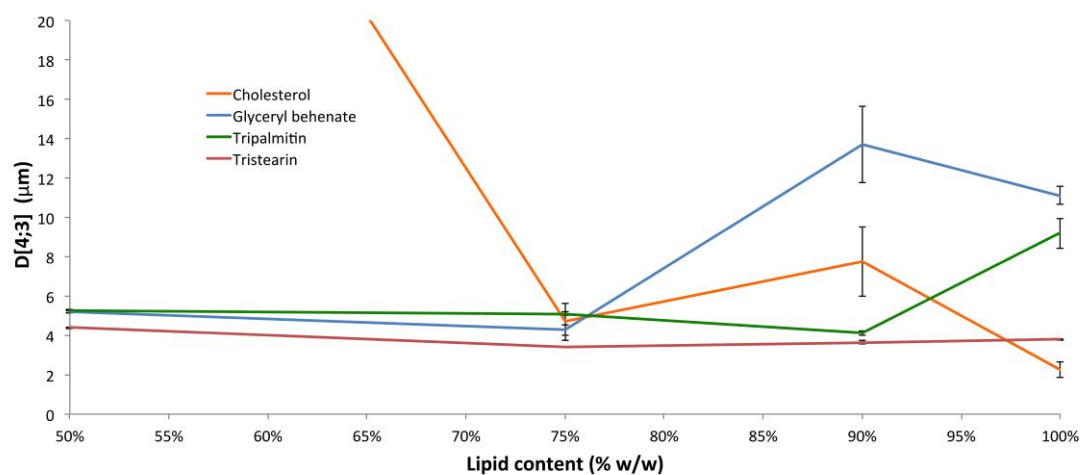
Figure 42. Evolution of the D[4;3] of the spray dried SLM in function of their lipid content (% w/w), using either cholesterol, glyceryl behenate, tripalmitin or TS, and P90H mixtures. Spray drying was realized using isopropanol solutions of lipids and P90H at 2% w/v in total solutes.

2.4.2.4.2.Cisplatin-free SLM

The preliminary formulations were spray dried in the presence of increasing ratios of P90H, which seemed to offer interesting properties (e.g. easily spray dried, low sticking tendencies, good aerosolization properties, high logP) in the preliminary study and in previous works (Pilcer et al., 2006, Depreter et al., 2010) as it did without cisplatin. This help to exhibit that TS was the best candidate as it offered the highest yields (above 63% w/w) and the smallest PSD, as seen in **Figure 42** with the D[4;3] (below 4.3 μm at each ratio), which was not influenced by the presence of P90H. This could be attributed in part to the higher melting point of TS when compared to the other lipid excipients, in particular tripalmitin.

2.4.2.4.3.Cisplatin SLM

Two TS/Phospholipon 90H ratios were compared (75:25 and 90:10, respectively). The cisplatin/lipid ratios in the SLM were 50:50 and 75:25 as they had the best chances of providing a slower release of cisplatin, while still maintaining high FPFs and sufficient FPDs to be delivered in humans and potentially obtain a therapeutic action. To assess the influence of TPGS on the dissolution of the SLM, the cisplatin microcrystals were also produced using the size reduction process without surfactant **(Figure 36)**. The produced formulations are described in **Table 14**.

These formulations confirmed the great ability of TS to be spray dried directly from IPA solutions as it produced cisplatin SLM with small and narrow PSD **(Table 12)**. In general, all formulations had a D[4;3] below 5 μm and at least 65% of particles below 5 μm. Smaller particles were obtained when TPGS was present. The FPF of these formulations were evaluated using the FSI, and were relatively high (with 4 out of 6 values above 30% w/w of the nominal dose). As observed previously, increasing the lipid proportion increased the PSD but it also increased the deposited fraction, probably due to a lower particle density, which directly affected the d_{geo} and in consequence, the d_{ae}. The dissolution profiles of these formulations **(Figure 43)** showed that the presence of TPGS and P90H were both detrimental as they prevented the CR of cisplatin from SLM. In particular, MC F22 and MC F22* (50:50 cisplatin/lipid, including 75:25 of TS/P90H and 5% w/w TPGS or no TPGS, respectively) exhibited a clear immediate-release profile. Finally, MC F24*, the only formulation that showed a slower release, included the lowest concentrations of P90H tested and no TPGS (50:50 cisplatin/lipid with 90:10 TS/P90H and no TPGS)

Table 14. Theoretical composition of the cisplatin DPI formulations produced during the preliminary study and comprising TS and P90H.

Formulation	Cisplatin drug-to-lipid ratio (% w/w)	Lipid ratio (TS/P90H)	TPGS content during size reduction
MC F21	75:25	75:25	
MC F22	50:50	75:25	5%
MC F23	75:25	90:10	w/w$_{cisplatin}$
MC F24	50:50	90:10	
MC F21*	75:25	75:25	
MC F22*	50:50	75:25	/
MC F23*	75:25	90:10	
MC F24*	50:50	90:10	

* Indicates formulations embedding cisplatin reduced without TPGS during the HPH process
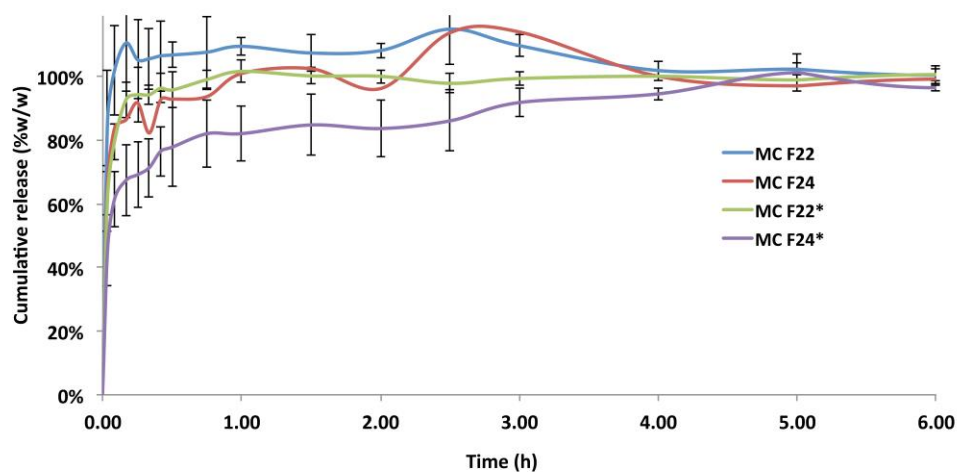
Figure 43. Cisplatin release from DPI preliminary formulations based on a 50:50 cisplatin/lipid ratio with a TS/P90H ratio of either 75:25 (MC F22 and MC F22*) or 90:10 (MC F24 and MC F24*), with (*) or without TPGS.

Table 15. Relative proportions of cisplatin/TS based SLM DPI formulations and their respective FPF and FPD (for a 20 mg powder-filled capsule), determined using the FSI (mean ± SD, n = 3).

	Cisplatin/TS ratio	FPF$_{FSI}$ (% w/w)	FPD$_{FSI}$ (mg)
MC F25	75:25	52 ± 12	7.8 ± 1.0
MC F26	50:50	52 ± 2	5.2 ± 0.1
MC F27	25:75	46 ± 10	2.3 ± 0.2

* These formulations embedded cisplatin reduced without TPGS during the HPH process
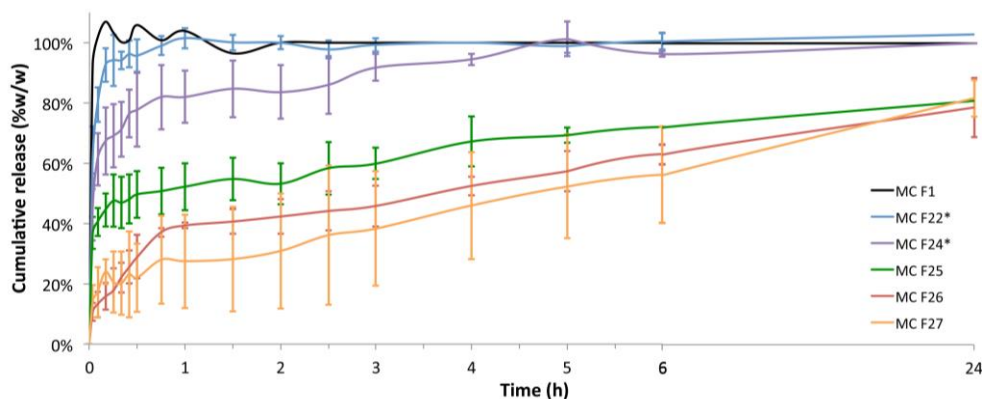
Figure 44. Dissolution profiles (n = 3) of cisplatin/TS based SLM DPI formulations with increasing lipid ratios (MC F25, F26, F27, respectively 75:25, 50:50 and 25:75), compared to MC F22* and MC F24*: 50:50 cisplatin/lipid based SLM DPI formulations using TS/P90H at 75:25, respectively and uncoated size-reduced cisplatin (MC F1, n = 1).
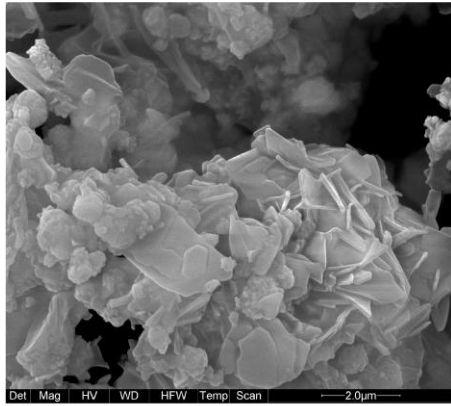
F22
(Cisplatin 50:50 Tristearin/P90H 75:25,
TPGS 5% w/w$_{cisplatin}$)
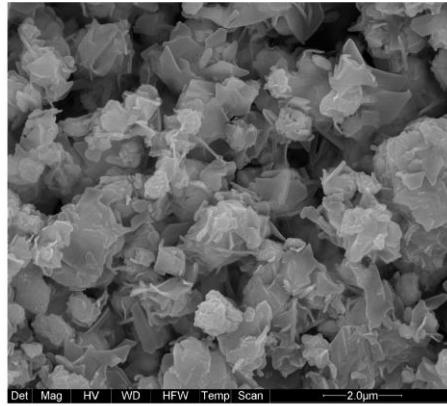
F22*
(Cisplatin 50:50 Tristearin/P90H 75:25,
no TPGS)
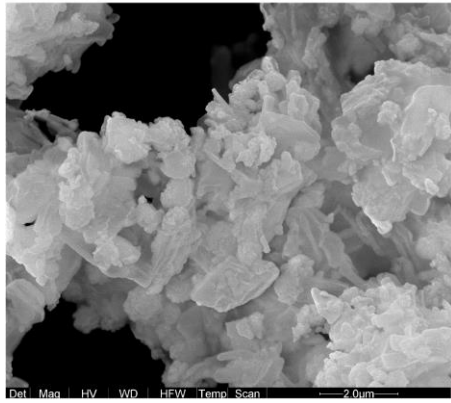
F24
(Cisplatin 50:50 Tristearin/P90H 90:10,
TPGS 5% w/w$_{cisplatin}$)
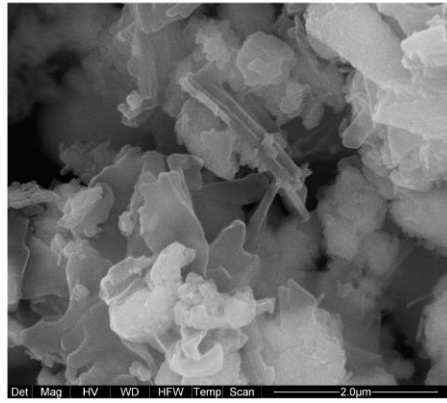
F24*
(Cisplatin 50:50 Tristearin/P90H 90:10,
no TPGS)

Figure 45. SEM micrographs of cisplatin DPI preliminary formulations based on 75:25 and 90:10 TS/P90H matrices, and a 50:50 cisplatin/lipid ratio.

This formulation exhibited a very high burst-release of more than 60% w/w after the first dosing time at 2 minutes and the remainder was slowly released over the next 5 hours. Because of these still poor dissolution results, the 75:25 cisplatin/lipid formulations were not assessed for their dissolution properties. SEM micrographs of these formulations showed that microparticles with rough surfaces and sheet structures were obtained **(Figure 45)**. The frequency of these sheet structures seemed to increase with higher P90H concentration and in the presence of TPGS.

2.4.2.4.4. Conclusion

This study confirmed that TS was a good candidate for production of SLM for inhalation with CR abilities. It showed PSD and deposition profiles compatible with inhalation when spray dried without cisplatin, which was confirmed when it was spray dried with cisplatin in suspension. The study helped determine that P90H and TPGS were both detrimental to the CR abilities of cisplatin from the SLM. From these results, we decided to assess the dissolution properties and the deposition abilities of SLM based on TS alone as the lipid fraction.

2.4.2.5. Formulations of cisplatin-based SLM with controlled-release properties

Following the previous study, cisplatin microcrystals were embedded into SLM produced using TS only as the lipid fraction. These microcrystals were produced using 20 HPH cycles at 20 000 psi without surfactant. The following spray drying steps were realized as described previously. The produced formulations were of decreasing cisplatin/lipid ratios (i.e. 75:25, 50:50 and 25:75) in order to establish the influence of the embedding **(Table 15)**.

The obtained formulations showed high deposition abilities established using the FSI, with FPF_{FSI} over 30% w/w and CR over more than 24 hours, with a clear influence of the lipid proportion on the burst-release of cisplatin for the first hours. As observed previously, with FPF in this order of magnitude, a lipid ratio over 50% w/w may give too low FPD values for a potential treatment in humans, as seen for MC F27, which exhibited just above 2 mg cisplatin for a 20 mg-filled capsule **(Table 15)**. These low deposited amounts could result in the need for a high number of capsules to reach efficacious doses. Overall, it showed a limited advantage over the 50:50 cisplatin/TS formulation MC F26. This latter formulation exhibited a very high FPF_{FSI} of 52 ± 2% and as a consequence an FPD_{FSI} of 5.2 ± 0.1 mg for a 20-mg capsule. This was also associated with a relatively low burst-effect of less than 40% after 1 hour.

2.4.2.6. Conclusion and perspectives

Avoiding P90H in the lipid fraction and TPGS during the size reduction process was determined as the most adequate choice to obtain an *in vitro* CR of cisplatin from TS-based DPI formulations.

Some of these formulations (MC F25 and MC F26) were further analysed, in particular, for their PSD in suspension and in the aerosol plume, for their deposition patterns using the MsLI and for their thermal properties for instance. All the results for these and their implications are described in Article 1, with the formulations F3 and F4, respectively **(Table 16)**.

The resulting approach regarding this formulation strategy was to re-introduce PEGylated excipients (i.e. TPGS, DSPE-mPEG-2000), in smaller fractions than previously, in order to avoid an excessive burst-effect and add potential stealth properties to the SLM. The resulting formulations are described in Article 1 as formulations F5 and F6, respectively **(Table 16)**.
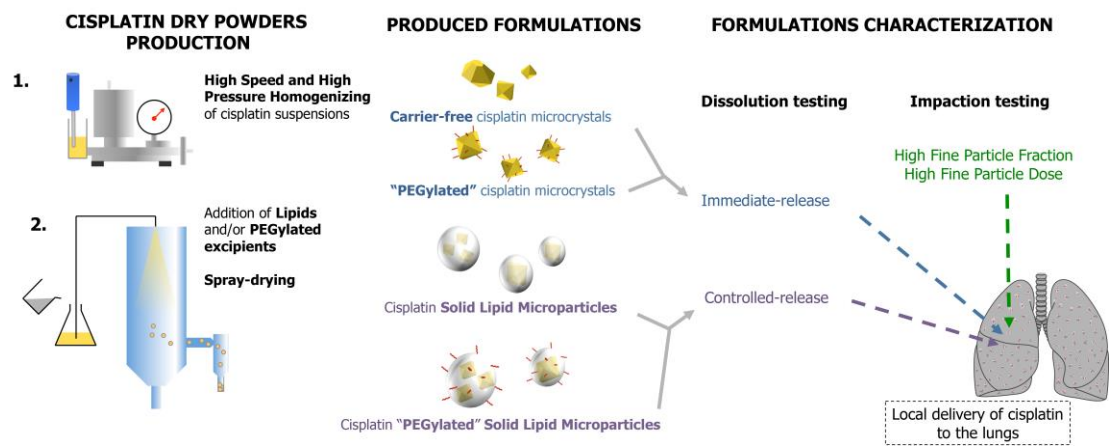
Figure 46. Graphical abstract of Article 1.

3. Article 1
"Development of controlled-release cisplatin dry powders for inhalation against lung cancers"

[a]Levet V., [a]Rosière R., [a]Merlos R., [b]Fusaro L., [c]Berger G., [a]Amighi K., [a]Wauthoz N.

[a]Laboratory of Pharmaceutics and Biopharmaceutics, CP207, Faculty of Pharmacy, Université libre de Bruxelles (ULB), Boulevard du Triomphe, Campus Plaine B-1050 Brussels, Belgium.

[b]Unité de Chimie des Nanomatériaux (CNANO), Université de Namur, 61 rue de Bruxelles, B-5000, Namur, Belgium.

[c]Laboratoire de Chimie Pharmaceutique Organique, CP205/5, Faculty of Pharmacy, Université libre de Bruxelles (ULB), Boulevard du Triomphe, Campus Plaine, B-1050 Brussels, Belgium.

3.1. Abstract

The present study focuses on the development of dry powders for inhalation as adjuvant chemotherapy in lung cancer treatment. Cisplatin was chosen as a potential candidate for a local treatment as it remains the main platinum component used in conventional chemotherapies, despite its high and cumulative systemic toxicities. Bulk cisplatin was reduced to submicron sizes using high-pressure homogenization, mixed with a solubilized lipid and/or PEGylated component and then spray dried to produce controlled-release dry powder formulations. The obtained formulations were characterized for their physicochemical properties (particle size and morphology), aerodynamic performance and release profiles. Cisplatin content and integrity were assessed by electrothermal atomic absorption spectrometry and ^{195}Pt nuclear magnetic resonance spectroscopy. DPI formulations with cisplatin contents ranging from 48.5 to 101.0% w/w exhibited high fine particle fractions ranging from 37.3% to 51.5% of the nominal dose. Formulations containing cisplatin microcrystals dispersed in solid lipid microparticles based on acceptable triglycerides for inhalation and PEGylated excipients showed a controlled-release for more than 24 hours and a limited burst effect. These new formulations could provide an interesting approach to increasing and prolonging drug exposure in the lung while minimizing systemic toxicities.

3.2. Introduction

Lung cancer remains the most common type of cancer worldwide, with an estimated yearly incidence of 1.8 million new cases and a yearly mortality rate of 1.6 million deaths for both genders, and is therefore the leading cause of cancer-related death (Ferlay et al., 2015). Non-small cell lung cancer (NSCLC) and small cell lung cancer (SCLC) account for approximately 85% and 15% of primary lung carcinoma, respectively (Johnson et al., 2008). Besides, secondary lung carcinomas caused by metastatic outgrowth from cancerous tissues are also frequently encountered (Kaifi et al., 2010). Because only 16% of lung cancers are detected at early loco-regional stages, the 5-year survival rates for lung cancer are among the lowest for all cancers, from 59% for localized NSCLC to 5% for distant NSCLC, and from 27% for localized SCLC to 3% for distant SCLC, as reported for the USA (Howlader et al., 2015). Cancer recurrence is also a prominent issue for survivors – regional recurrence is, for instance, encountered in up to 45% and 55% of stage I and II NSCLC, and up to 63% of limited-disease SCLC due to loco-regional lymph node involvement (Kelsey et al., 2009, Xu et al., 2014).

Lung cancer treatment generally involves surgery, RT and chemotherapy, which are often combined depending on the stage and progression of the illness. Adjuvant chemotherapy is administered after resective surgery at stage II or IIIA. It is associated with radiotherapy at later stages IIIB to IV in NSCLC and in all stages in SCLC (NCCN, 2014a, NCCN, 2015).

Guidelines for first-line regimens against lung cancer rely on platinum-doublet chemotherapy. This administers platinum derivatives – predominantly cisplatin – in combination with other antineoplastic agents, such as etoposide for SCLC or taxane derivatives, vinorelbine, vinblastine, gemcitabine or pemetrexed for NSCLC. The most recent targeted agents aimed against tyrosine kinase (tinibs) or specific growth factors (bevacizumab, cetuximab), in addition to being costly, show only a modest outcome improvement. Moreover, they are indicated only in small groups of advanced disease NSCLC patients facing therapeutic failure with conventional chemotherapy and bearing specific tumour mutations. All these chemotherapeutic agents, which are currently administered through intravenous (IV) infusion or occasionally by the oral route, are usually associated with numerous systemic and dose-limiting side effects (NCCN, 2014a, NCCN, 2015). Only a low pulmonary uptake is obtained after distribution from a systemic administration, with typically 5-10% of the administered that effectively reaches the lungs, let alone the tumour, which is a major determinant of treatment

failure (Minchinton et al., 2006). New adjuvant therapy regimens that are able to increase drug exposure in the target organ, the tumour and local lymph nodes, which is concomitant with an overall decrease in systemic toxicities, are therefore highly desirable. Such therapies include the local administration of well-known cytostatic drugs.

Cisplatin or *cis-dichlorodiammineplatinum(II)* was discovered in 1965 (Rosenberg et al., 1965) and subjected to its first clinical trial as early as 1972 (Lippman et al., 1973). It remains involved in first-line regimens against many cancers such as lung, head and neck, ovarian, cervical, osteosarcoma, lymphoma, bladder or testicular cancer (Jamieson et al., 1999, Boulikas and Vougiouka, 2003). The potent antitumour activity of this class of compounds mostly rely on their ability to be aquated in the low-chloride intracellular medium, having one or its two chloro ligands replaced by water molecules (Jamieson et al., 1999). The positively charged mono-aqua and di-aqua cisplatin complexes formed are then able to bind DNA in the cell nucleus and proteins in the cytoplasm, inducing apoptosis (Jamieson et al., 1999, Boulikas et al., 2003, Alderden et al., 2006). Despite its potent antitumour properties, clinical use of cisplatin is strongly hindered by its side effects. These are essentially dose-limiting nephrotoxicity, but also ototoxicity, myelosuppression, anemia, electrolyte disturbances and gastrointestinal reactions. Because cisplatin is preferentially excreted through urine (> 90%) and is accumulated in proximal and distal nephrons at up to 5 times the plasma concentration, it can cause severe tubular damage and acute and chronic renal insufficiency in up to 36% of patients (Yao et al., 2007). Cisplatin, currently administered through IV infusion at doses ranging from 30 to 100 mg/m² of body surface area, is therefore administered cautiously in cycles every 3 weeks in SCLC or at days 1, 8 and 21 or 28 in NSCLC to limit kidney and other sensitive organ exposure. It is always supplemented by high hydration regimens including significant volumes of saline, potassium, magnesium and nephroprotective mannitol before and after administration (British Columbia Cancer Agency, 2013, NCCN, 2014a, NCCN, 2015). Consequently, pulmonary administration of cisplatin could stand as an interesting approach as neoadjuvant and adjuvant chemotherapy for the treatment of lung tumours in both SCLC and NSCLC at later stages, but also specifically at early stages against lymph node involvement and cancer recurrence.

Aerosol therapy has been used since the early 20th century and has many advantages against respiratory diseases. It can avoid the first-pass metabolism, increasing treatment efficacy, while decreasing systemic exposure, systemic side effects and drug-drug interactions.

Pulmonary delivery of chemotherapy has been investigated since the 1960s (Shevchenko and Resnik, 1968), but its development has been limited by drug-induced pulmonary toxicity as reported for some antineoplastic agents, such as taxanes or gemcitabine, during or shortly after IV administration. These side effects were, however, not observed when these drugs were delivered by the pulmonary route (Gagnadoux et al., 2008, Dulohery et al., 2016). Aerosol chemotherapy can thus provide a higher therapeutic index for systemically toxic drugs by limiting total body exposure while increasing drug concentration at the tumour site and in loco-regional lymph nodes; keeping in mind that these advantages can be counterbalanced by potential direct local toxicity to the lungs linked to higher local exposure, which depends directly on the considered drug (Gagnadoux et al., 2008).

The ability of aerosol chemotherapy to deliver a systemically toxic drug slowly – allowing smoother concentration profiles and thus limiting peak concentration in sensitive organs – is therefore critical. This could allow an effective drug concentration to be maintained at the site of action between administrations while limiting systemic exposure and lowering the risk of acute pulmonary toxicity and the ensuing adverse effects. It can also greatly help decrease patient discomfort by lowering the strain of repeated administrations. The ability of long-lasting particles to remain in the lungs and diffuse drugs locally can be hindered by clearance systems, including the mucociliary escalator and phagocytosis by alveolar macrophages. PEGylation of particle surface has been shown to provide an effective "stealth" shield for microparticles by preventing phagocytosis by macrophages (Wattendorf et al., 2008). Inhalation of PEG has been demonstrated as safe (Klonne et al., 1989), and PEGylated excipients derived from vitamin E such as tocopheryl polyethylene glycol succinate (TPGS) or from endogenous phospholipids such as distearoyl phosphoethanolamine polyethylene glycol 2000 (DSPE-mPEG-2000) are of low potential pulmonary toxicity (Yan et al., 2007, Gill et al., 2011, Shah and Banerjee, 2011).

Herein we disclose the development of DPI formulations composed of cisplatin-based solid lipid microparticles (SLM) with good dispersion properties and a high theoretical lung deposition fraction, even under lower inspiratory flows. Controlled-release using lipid excipients and potential stealth properties using PEGylated excipients were sought to maintain drug concentration inside the lungs between administrations.

3.3. Materials and methods

3.3.1. Materials

Cisplatin was purchased from Shanghai Jinhe Bio-technology Co., Ltd. (Shanghai, PRC). Tristearin (TS) was purchased from Tokyo Chemical Company (Tokyo, Japan), alpha-tocopheryl polyethylene glycol 1000 succinate (TPGS) from Sigma-Aldrich (St. Louis, USA), distearoyl phosphoethanolamine polyethylene glycol 2000 (DSPE-mPEG-2000) and dipalmitoyl phosphatidylcholine (DPPC) from Lipoid (Steinhausen, Switzerland). Isopropanol (IPA), *N,N*-Dimethylformamide (DMF) and Suprapur® nitric acid were obtained from Merck Millipore (Darmstadt, Germany). Dichloromethane was obtained from VWR Chemicals (Leuven, Belgium). Deuterated DMF (DMF-d$_7$) was obtained from Sigma-Aldrich (St. Louis, USA). All chemicals and solvents were of analytical grade.

3.3.2. Methods

3.3.2.1. Safety procedures

In order to manipulate cisplatin safely and avoid personnel and environmental exposure, preventive procedures and equipment were used as described in (Wauthoz et al., 2011). Disposable equipment was used when possible, if not, it was rinsed thoroughly with *N,N*-Dimethylformamide (DMF) and copious amount of hot soapy water. All recovered rinsing solutions were disposed of as cytotoxic waste and incinerated. Cleanliness of sensitive apparatus was verified by swabbing and quantification of the residual platinum by electrothermal atomic absorption spectrometry (ETAAS).

3.3.2.2. Cisplatin size reduction

Cisplatin was reduced in concentrated suspension using a method derived from (Pilcer et al., 2009). Bulk cisplatin was dispersed in isopropanol (IPA, 5.0% w/v) using a round-bottomed glass tube, set in an ice-water bath and subjected to high-speed homogenization (HSH) using a X620 motor and a T10 dispersing shaft (Ingenieurbüro CAT M. Zipperer GmbH, Staufen, Germany) for 10 minutes at 24,000 rpm. The resulting suspension was then poured in the tank of a lab scale EmulsiFlex-C5 high-pressure homogenizer (Avestin Inc., Ottawa, Canada) equipped with a ceramic stem and seat. It was cycled through the apparatus using a closed loop approach. Cisplatin microcrystals were submitted to high-pressure homogenization (HPH) for 10 pre-milling cycles at 5,000 psi, 10 milling cycles at 10,000 psi and 20 milling cycles at 20,000 psi. The rotor of the high-speed homogenizer was operated in the high-pressure homogenizer tank at 8,000 rpm throughout the size reduction process to prevent particle sedimentation and clogging of the apparatus from larger aggregates. The temperature

Table 16. Composition of the spray dried suspensions and the resulting theoretical and actual compositions, along with the measured moisture content in DPI formulations produced. Cisplatin content was obtained using ETAAS (Pt content) and ^{195}Pt NMR

	Composition of the spray dried suspensions in isopropanol (% w/v)	Theoretical composition of the dry powder formulations (% w/w)	Actual cisplatin content by ETAAS (% w/w, mean ± SD, n = 9)	Actual cisplatin content by ^{195}Pt NMR (% w/w, n = 1)	Moisture content by thermogravimetric analysis (mean ± SD, n = 3)
F1	Cisplatin **2.0%**	Cisplatin **100%**	**101.0** ± 2.0%	**106.0**%	**0.10** ± 0.04%
F2	Cisplatin **1.9%** TPGS **0.1%**	Cisplatin **95%** TPGS **5%**	**95.6** ± 2.6%	**98.2**%	**0.08** ± 0.03%
F3	Cisplatin **1.5%** TS **0.5%**	Cisplatin **75%** TS **25%**	**77.7** ± 3.1%	**82.5**%	**0.08** ± 0.01%
F4	Cisplatin **1.0%** TS **1.0%**	Cisplatin **50%** TS **50%**	**48.5** ± 2.2%	**52.4**%	**0.11** ± 0.07%
F5	Cisplatin **1.00%** TS **0.99%** TPGS **0.01%**	Cisplatin **50%** TS **49.5%** TPGS **0.5%**	**48.9** ± 2.3%	**50.0**%	**0.10** ± 0.02%
F6	Cisplatin **1.000%** TS **0.995%** DSPE-mPEG-2000 **0.005%**	Cisplatin **50%** TS **49.75%** DSPE-mPEG-2000 **0.25%**	**49.9** ± 2.7%	**52.0**%	**0.11** ± 0.01%

of the suspension was maintained at 5-10°C using a heat exchanger connected to the homogenizing valve, with propylene-glycol/water (1:1 v/v) circulating at -15°C using an F32-MA cooling circulator (Julabo GmbH, Seelbach, Germany). Solvent evaporation was therefore kept to a minimum. Aliquots of 1 mL were removed from the suspension after each size reduction step in order to measure the particle size distribution (PSD) of cisplatin microcrystals by laser diffraction. Platinum concentration in the final microcrystal suspension was determined by ETAAS.

3.3.2.3. Preparation of cisplatin dry powder formulations

A suitable amount of excipient was solubilized in heated IPA (65°C) at 5.0% w/v and added to the previously size-reduced cisplatin microcrystalline suspension under heating and stirring. The final concentration of excipient was 2.0% w/v of solid content. The formulations were then spray dried using a B-290 Mini Spray Dryer (Büchi Labortechnik AG, Flawil, Switzerland). The composition of the spray dried suspensions and the resulting DPI formulations are reported in **Table 16**. The operating parameters were as follows: feed rate 3.0 g/min, inlet temperature 70°C, 0.7 mm nozzle, 1.5 mm nozzle-cap, compressed air at 800 L/min and drying air flow 35 m³/h. In these conditions, the outlet temperature during spray drying ranged from 38 to 42°C. The apparatus was equipped with a B-296 dehumidifier (Büchi Labortechnik AG, Flawil, Switzerland) to maintain the relative humidity at 50% HR during spray drying. Heating of the feed solution tubing with a blow dryer was necessary to prevent crystallization of tristearin (TS) during atomization. The spray drying yield was determined from the ratio (percentage) of the weighed recovered powder to the mass of solid content in the spray dried suspension. The DPI formulations produced were stored at ambient temperature in a desiccator until further analysis.

3.3.2.4. Residual solvents

The absence of residual solvents in the bulk cisplatin and the DPI formulations was verified using thermogravimetric analysis. This was done using a Q500 thermogravimetric analyzer (TA Instruments, New Castle, USA) and Universal Analysis 2000 software v5.5.20 (TA Instruments, New Castle, USA), assessing the ability of the spray drying conditions to (i) thoroughly evaporate IPA or (ii) eliminate water moisture from the powder. The experimental parameters were as follows: weight of sample 10 mg (n = 3), range 25-300°C, ramp 10°C/min. The weight losses between 25°C and 125°C were used to determine the total residual solvent content.

3.3.2.5. Thermal properties

The thermal properties of bulk cisplatin, excipients and DPI formulations were determined using differential scanning calorimetry (DSC). This was done using a Q2000 differential scanning calorimeter (TA Instruments, New Castle, USA) equipped with a RCS90 refrigerated cooling system (TA Instruments, New Castle, USA) and calibrated with indium. Analyses were performed with a heat/cool rate set at 10°C/min. A first heating scan was realized from -10 to 180°C, directly followed by a cooling scan from 180 to -10°C and a second heating scan from -10 to 180°C using 5 mg of powder in Tzero aluminum pans and Tzero hermetic lids (TA Instruments, New Castle, USA). Nitrogen was used as blanket gas and an empty pan as a reference. The DSC curves were plotted using Universal Analysis software.

3.3.2.6. Particle size, shape and surface morphology

The particle shape, size and surface morphology of DPI formulations and bulk cisplatin were determined using scanning electron microscopy (SEM). This was done using a Tecnai FEG ESEM Quanta 200 scanning electron microscope (FEI, Hilsboro, USA). Powders were spread on 12 mm double-sided sticky carbon pads (Agar Scientific, Stansted, UK) and directly coated with platinum using standard procedures. Images were processed using iTEM software (FEI, Hilsboro, USA).

3.3.2.7. Particle size distribution (PSD)

3.3.2.7.1. Individualized particles

The geometrical PSD of bulk cisplatin, and cisplatin microparticles from the size reduction process and from DPI formulations was measured as suspended and individualized particles. This was done using a Mastersizer® 3000 laser diffractometer (Malvern Instruments Ltd., Worcestershire, UK) connected to a Hydro MV dispenser equipped with a 40 W ultrasonic probe (Malvern Instruments Ltd., Worcestershire, UK). Measurements of bulk cisplatin and aliquots from the size reduction process and of high drug content DPI formulations (i.e. F1, F2) were realized in cisplatin-saturated IPA. DPI formulations with a drug content ≤ 75% (i.e. F3, F4, F5, F6) were previously dispersed, vortexed and measured in cisplatin-saturated 0.1% w/v Poloxamer 407 (BASF, Ludwigshafen, Germany) NaCl 0.9% aqueous solution. The agitation rate in the Hydro MV disperser was set to 2,900 or 1,800 rpm for IPA- or water-based measurements, respectively. The refractive index and absorption coefficient for dispersed material was set to 1.6 and 0.1 using a 100% intensity of the sonic probe for 10 s for IPA- or for 1 min for water-based measurements, respectively. The refractive index of dispersant media was set to 1.377 for IPA and to 1.33 for water. The liquid dispenser was

thermostated with tap water to avoid excessive temperature-rising due to the ultrasonication of dispersions. The PSD was expressed as the mass median diameter d(0.5), d(0.9) (for which 90% of particles lie under the expressed diameter), the volume mean diameter D[4,3] and the percentage of fine particles determined from the cumulative undersize curves (% of particles below 5 μm).

3.3.2.7.2. Particles dispersed under simulated breathing conditions

A second size-measurement technique, which accounts only for the emitted fraction of the DPI formulation, was used to measure the PSD of dry powders directly outside an actuated inhalation device under inspiratory airflow. This measurement was realized in triplicate using a Spraytec® laser diffractometer (Malvern Instruments Ltd., Worcestershire, UK) equipped with an inhaler and nebulizer accessory (Malvern Instruments Ltd., Worcestershire, UK). 10 mg of bulk cisplatin or DPI formulation, previously sieved through a 355 μm stainless steel mesh, were aerosolized from a size 3 hydroxypropyl methylcellulose (HPMC) capsule (Qualicaps, Madrid, Spain) inserted into an Axahaler® (SMB, Brussels, Belgium) connected onto an induction port (throat) to the Inhaler and Nebulizer Accessory. The assembly was then connected to a multistage liquid impinger (MsLI, Copley Scientific, Nottingham, UK) apparatus. This formed a closed system that allowed size measurements under different inspiratory airflows for durations enabling 4 L of air to be drawn through the inhaler and the MsLI (i.e. 100 L/min for 2.4 s, 60 L/min for 4.0 s and 40 L/min for 6.0 s). Measurements were expressed as the d(0.5) and cumulative undersize (% of particles below 5 μm) for the 100 L/min airflow and D[4,3] for each airflow. The agglomeration tendency of the DPI formulations was established by estimating an agglomeration index, which is the ratio of the D[4,3] values obtained from the aerosolized powder for each airflow to the average D[4,3] values obtained for the individualized particles **(Equation 4)**.

$$AI = {D[4,3]^{\text{aerosol plume}}}\Big/{D[4,3]^{\text{individualized particles}}}$$

Equation 4. Calculation of the agglomeration index.

This was done to simulate normal (i.e. 100 L/min) and impeded breathing conditions (i.e. 40 and 60 L/min).

3.3.2.8. Aerodynamic performance

The fine particle dose (FPD) and fine particle fraction (FPF) – which are the mass or the percentage related to the recovered dose of cisplatin-based particles with an aerodynamic

diameter (d_{ae}) below 5 µm – and the aerodynamic PSD, characterized by the mass median aerodynamic diameter (MMAD), were determined using an MsLI (Copley Scientific, Nottingham, UK) – Apparatus C – as described in the European Pharmacopoeia. A mass of 20 mg of each DPI formulation and bulk cisplatin, previously sieved through a 355 µm stainless steel mesh, was weighed in a size 3 HPMC capsule (Qualicaps, Madrid, Spain) and deposited in the MsLI using an Axahaler® DPI mounted on the inhalation port with its adapter (n = 3). A deposition flow rate of 100 ± 5 L/min measured using a DFM3 flow meter (Copley Scientific, Nottingham, UK) was obtained with two HCP5 air pumps (Copley Scientific, Nottingham, UK) connected in series to a TPK critical flow controller (Copley Scientific, Nottingham, UK). At this flow rate, cut-off diameters were 10.0, 5.3, 2.4, 1.3 and 0.4 µm between each stage of the MsLI. The micro-orifice collector (MOC) filter (i.e. stage 5) contained a Fluoropore 9 cm PTFE membrane with 0.45 µm pore size bonded on a high-density polyethylene support (Merck Millipore, Darmstadt, Germany). The critical flow controller was used to ensure a deposition time of 2.4 s at 100 L/min and a critical flow with a P3/P2 ratio < 0.5, as required by the European Pharmacopoeia.

After impaction, the four upper stages of the MsLI were given a first rinse using 20 mL of previously filled 0.5% w/v Poloxamer 407 in Milli-Q water/IPA (60:40 v/v) as the dilution phase, a second rinse using 25 mL of DMF and a third rinse using dilution phase, adjusted to 100.0 mL and ultrasonicated for 30 minutes. Drug deposition in the capsule, in the device, in the induction port and on the MOC filter were determined after solubilization with 100.0 mL of dilution phase and ultrasonication for 30 minutes. The impacted mass in each stage was determined by quantification of the Pt content by ETAAS. Results were then plotted in Copley Inhaler Testing Data Analysis Software® (Copley Scientific, Nottingham, UK) to obtain the FPD below 5 µm. This was done from interpolation of the recovered mass *vs.* the cut-off diameter of the corresponding stage. The FPF was expressed as a percentage of the nominal dose.

3.3.2.9. Dissolution properties

Dissolution properties of DPI formulations were established by applying a method derived from the paddle over disk method from USP39 using a modified dissolution apparatus type V for transdermal patches. The release profile of cisplatin was determined from the whole respirable fraction ($d_{ae} \leq 5$ µm) of the DPI formulation, selected using a Fast Screening Impactor (FSI, Copley Scientific, Nottingham, UK). An appropriate mass of each DPI formulation, equivalent to a deposited dose of 3 mg of cisplatin, was weighed into a size 3 HPMC capsule (Qualicaps, Madrid, Spain). This was then deposited using an Axahaler®
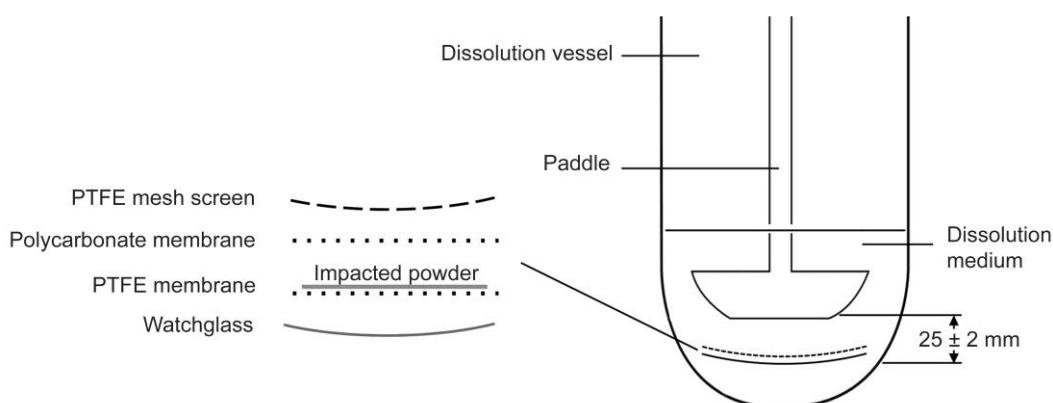
Figure 47. Schematic representation of the watch glass-PTFE disk assembly and its setup in the adapted US Pharmacopoieia 39 dissolution apparatus V used for DPI formulation dissolution profiling (400 mL mSLF, 37°C, 50 rpm) after impaction with an FSI (100 L/min, 2.4 s, n = 3).

Table 17. Composition of the mSLF dissolution medium, [originally in supplementary material].

The concentrated liposomes suspension was prepared by weighing 2.0 g of DPPC in a round bottom flask, dissolved with 200 mL of chloroform/methanol (1:1), and evaporated with a rotary evaporator at 60°C, 215 mBar and 100 rpm. The dry film was then rehydrated with 1.0 L of preheated Milli-Q water at 55°C and 120 rpm during 2 h and ultimately ultrasonicated at 55°C during 1 h. The suspension was then stored at 4°C until the dissolution test and re-prepared weekly.

Chemical	Concentration (w/v)
Magnesium chloride	0.0203%
Sodium chloride	0.6019%
Potassium chloride	0.0298%
Sodium hydrogen phosphate	0.0358%
Sodium sulfate	0.0071%
Calcium chloride	0.0368%
Sodium acetate	0.0953%
Sodium bicarbonate	0.2604%
Sodium citrate	0.0097%
Dipalmitoylphosphatidylcholine (DPPC) liposomes	0.02%

DPI device (SMB, Brussels, Belgium) onto a Fluoropore® hydrophobic PTFE membrane filter with 0.45 μm pore size (Merck Millipore, Darmstadt, Germany), with the FSI (2.4 s, 100 L/min) equipped with the corresponding preseparator insert. The Fluoropore filter, with the deposited powder facing up, was then covered with an Isopore® 0.4 μm hydrophilic polycarbonate filter (Merck-Millipore, Germany) and fixed onto a watch glass-PTFE disk assembly (Copley, Nottingham, UK) with the clips and PTFE mesh screen provided **(Figure 47)**. The disk assembly was then submerged in a dissolution vessel of an AT7 dissolution apparatus (Sotax AG, Aesch, Switzerland) with 400 mL of modified simulated lung fluid (mSLF) (Son et al., 2009) – a medium that mimics the lungs electrolytic and surfactant composition (**Table 17**). Dissolution testing was realized in accordance with sink conditions, at $37 \pm 0.2°C$, pH 7.35 ± 0.05. Paddles, set at 25 ± 2 mm between the blade and the center of the disk-assembly, were set at a rotating speed of 50 ± 4 rpm. Sampling volumes of 2.0 mL were filtered through 0.22 μm pore size cellulose acetate syringe filters (VWR, Leuven, Belgium) at pre-established times between 2 min and 24 h, and replaced with 2.0 mL of free pre-heated mSLF. At the end of the dissolution assay, the disk assembly was opened into the dissolution vessel and ultrasonicated for 30 minutes to establish the 100% cisplatin dissolution value. Dissolution tests were realized in triplicate for each DPI formulation.

The similarity of dissolution profiles was determined using the difference (f_1) and the similarity (f_2) factors, as recommended by the FDA's Guidelines for Industry and described by Costa and Sousa Lobo (2001). f_1 has to be smaller than 15 (close to 0) and f_2 has to be higher than 50 (close to 100) to confirm the similarity between two dissolution profiles. If they are not, the profiles can be considered different and non-similar.

3.3.2.10. Cisplatin and platinum quantification

Quantification of cisplatin in the final formulations was realized using ^{195}Pt NMR **(Table 16)** while ETAAS was used for quantification of cisplatin from the Pt content of DPIs and throughout the intermediate steps of formulations, deposition properties and dissolution studies that required a high sensitivity.

3.3.2.10.1. Platinum quantification

The platinum from cisplatin was quantified by ETAAS. This was done using a SpectrAA 300 atomic absorption spectrometer equipped with a GTA-96 graphite tube atomizer (Varian, Mulgrave, Australia), a Zeeman background corrector and an autosampler. Measurements were carried out in SP-12 pyrolytically coated partitioned graphite tubes (Spectrotech, Tubize, Belgium) with a platinum hollow cathode lamp (Photron Pty. Ltd., Narre Warren, Australia) operated at 7 mA, at a wavelength of 265.9 nm with a slit width set at 0.2 nm.

Table 18. Graphite furnace program used for platinum quantification.

Step n°	Step	Temperature (°C)	Ramp (s)	Gas flow (L/min)	Read command
1		85	5.0	3.0	-
2	**Drying**	95	40.0	3.0	-
3		150	10.0	3.0	-
4		800	5.0	3.0	-
5	**Charring**	800	1.0	3.0	-
6		800	2.0	0.0	-
7	**Atomization**	2700	1.0	0.0	Yes
8		2700	4.0	0.0	Yes
9	**Cleaning**	2700	1.0	3.0	-
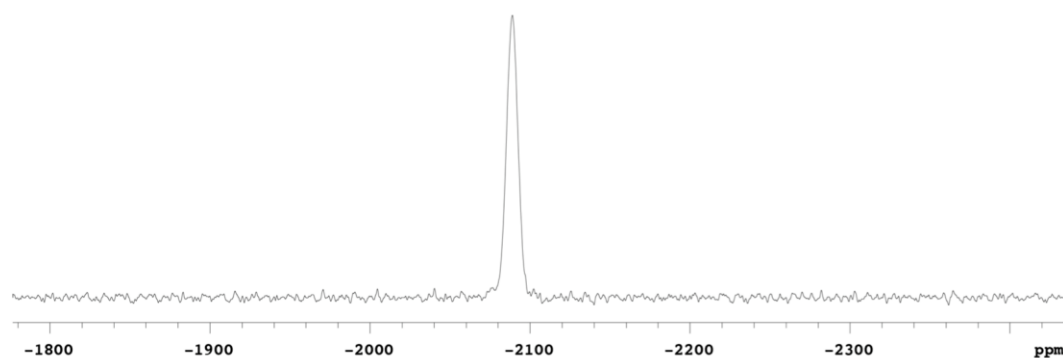
Figure 48. Typical 195Pt NMR spectrum obtained with a 9 mg/mL cisplatin standard in DMF-d7/DMF (1:9), [originally in supplementary material].

Argon of 99.999% purity (Air Liquide, Liège, Belgium) was used as purge gas at a 3.0 L/min flow rate. Samples of 20 µL were injected in the graphite tube following the graphite furnace temperature program **(Table 18)**.

Calibration was realized using the autosampler with a fresh matrix-matched standard (800 ng/mL) and automatically diluted (600, 400, 200 and 80 ng/mL) with blank matrix. The recalibration rate was set at 9 samples and consisted of a reslope using a blank and the 400 ng/mL standard measurement. Samples were diluted with 0.1% v/v Suprapur® nitric acid to fit the calibration curve. The analytical sensitivity of the method was 74 pg of platinum of characteristic mass. The linearity ($r^2 > 0.995$), accuracy ($\geq 95\%$) and precision (RSD $\leq 5.0\%$) of the method were high along the calibration curve. The limit of detection (LOD) and lower limit of quantification (LLOQ) of the method were 26.3 and 79.0 ng/mL, respectively, as determined by the standard deviation of the response and the slope. They showed a minimum accuracy of $\pm$ 5% at this range.

Cisplatin content in DPI formulations was determined through Pt content by ETAAS analysis. Powder samples with a mass of 10 mg were diluted in 10.0 mL of DMF, ultrasonicated for 1 hour and diluted 2,500-fold with 0.1% v/v Suprapur HNO_3 (n = 9).

3.3.2.10.2. Quantitative and qualitative analysis of cisplatin

Quantitative and qualitative analysis of cisplatin in DPI formulations was carried out by 195-Platinum nuclear magnetic resonance spectroscopy (^{195}Pt NMR). Natural abundance ^{195}Pt NMR spectra were recorded on a Varian VNMRS spectrometer equipped with temperature regulation, operating at 9.4 T (85.78 MHz) and 25°C, using a 5 mm automated triple broadband probe. The longitudinal relaxation time was measured using the inversion recovery pulse sequence on a saturated cisplatin solution in DMF-d_7/DMF 1:9 ($T_1 = 0.015 \pm 0.001$ s). Quantitative ^{195}Pt NMR spectra were recorded using the improved RIDE (ring down elimination) pulse sequence of Koźmiński et al., which improves the baseline of the NMR spectra of several nuclei (Fusaro et al., 2012, Le Gac et al., 2014, Ndoyom et al., 2015) using the following acquisition parameters: spectral width of about 662 ppm (56.8 kHz), relaxation delay 90 ms, acquisition time 10 ms, excitation pulse 90°, number of transients 1.2 $\times$ 10^4. The spectra were recorded lock on without sample spinning. The processing comprised exponential multiplication of the free induction decay (FID), with a line broadening factor of 100 Hz, zero filling, Fourier transform, zero-order phase correction, baseline correction and correction of the FID by backward linear prediction (typical spectrum in **Figure 48**). The ^{195}Pt chemical shift scale was calibrated at 25°C with respect to

an external reference sample of K_2PtCl_4 in D_2O (-1,624 ppm) (Peleg-Shulman et al., 2001). Quantitative NMR was performed using absolute integration of three external cisplatin standards of 6.0, 9.0 and 12.0 mg/mL, extemporaneously solubilized in DMF-d_7/DMF 1:9. Precision of the method was estimated by measuring the cisplatin integrated area of the 9.0 mg/mL standard (43 spectra, standard deviation = 3.9%).

DPI formulations were weighed in order to obtain a final theoretical concentration of 9.0 mg/mL cisplatin in DMF-d_7/DMF (1:9). In order to thoroughly eliminate lipids from the DPI formulation matrices, particles were washed with 1.0 mL of dichloromethane, centrifuged for 15 minutes at $10,000 \times g$ and the supernatant was ultimately eliminated. The procedure was repeated twice, the washed cisplatin microcrystals were then dried by air-flow overnight and then extemporaneously solubilized in 700 μL of DMF-d_7/DMF, of which 550 μL was transferred into an NMR 5 mm glass tube prior to the analysis.

3.4. Results and Discussion

3.4.1. Formulation processes

In addition to its high and fast reactivity, valuable as a cytostatic active pharmaceutical ingredient (API) but potentially critical to formulation processes, cisplatin is insoluble in alcohols and most non-toxic volatile solvents, and is only slightly soluble in water (< 1 g/L). Moreover, without a minimal 0.9% chloride concentration and a pH < 4 cisplatin quickly hydrolyses into very reactive aquated species (Karbownik et al., 2012). Production of DPI powders from water-based solutions was therefore unfeasible (high chloride concentration, low pH, low expected yield). Solutions of the few other organic solvents available were ruled out because of their toxicity (DMF), potential undesirable reactions (e.g. dimethyl sulfoxyde can displace the chlorido ligands) or high evaporation temperatures. Size reduction of cisplatin particles in suspension using HSH and a few cycles of HPH were therefore chosen as easily up-scalable effective methods. These promote the formation of well-controlled micron-sized inhalable particles. The selected non-solvent was IPA because it (i) prevents cisplatin solvation (C_{sat} < 0.005 mg/L), (ii) is easily spray dryable at low temperatures (boiling point = 82.5°C), (iii) is a non-toxic class III solvent (USP30, 2007) and (iv) is able to solubilize lipid and PEG fractions under heating at relatively high concentrations (above 1% w/v). TS was chosen as the main lipid component of SLM as it was a good candidate for successfully embedding cisplatin microcrystals. Indeed, TS is a triglyceride comprised of three units of stearic acid, exhibiting potential acceptable biocompatibility (Pilcer et al., 2010), very high hydrophobicity (logP = 21.59), good solubility in hot alcohols and a

Table 19. Particle size distribution of individualized particles of bulk cisplatin, cisplatin microcrystals after size reduction and DPI formulations. The PSD of individualized particles in IPA suspension (Bulk, After HPH, F1, F2) or water-based suspension (F3, F4, F5, F6) were measured using a Mastersizer® 3000 Hydro MV laser diffractometer (mean ± SD, n = 3). The PSD in the aerosol plume was measured using a Spraytec® laser diffractometer with an Axahaler® at 100 L/min for 2.4 s (mean ± SD, n = 3). The average agglomeration index of DPI formulations were calculated from the D[4,3] measurements obtained in liquid suspensions and at all airflows (i.e. 40, 60 and 100 L/min, mean ± SD, n = 9).

	PSD in suspension			PSD in the aerosol plume (100 L/min airflow)			Average agglomeration index (mean ± SD, n = 9)
	d(0.5) (µm)	D[4,3] (µm)	Undersize (% < 5 µm)	d(0.5) (µm)	D[4,3] (µm)	Undersize (% < 5 µm)	
Bulk cisplatin	16.5 ± 3.6	18.9 ± 4.3	10.2 ± 4.0	-	-	-	-
After HPH	0.89 ± 0.01	1.0 ± 0.0	97.9 ± 1.0	-	-	-	-
F1	1.6 ± 0.0	1.8 ± 0.0	100.0 ± 0.0	2.5 ± 0.1	6.3 ± 0.5	80.4 ± 0.9	3.9 ± 0.9
F2	2.1 ± 0.0	2.6 ± 0.0	91.9 ± 0.4	3.4 ± 0.6	6.8 ± 0.7	79.7 ± 5.8	2.3 ± 0.4
F3	3.5 ± 0.0	3.9 ± 0.0	70.0 ± 0.2	3.8 ± 0.2	6.4 ± 0.2	68.6 ± 2.7	1.7 ± 0.3
F4	3.8 ± 0.1	4.1 ± 0.1	70.1 ± 1.4	4.7 ± 0.0	10.0 ± 0.7	53.3 ± 0.3	2.2 ± 0.3
F5	4.2 ± 0.2	4.4 ± 0.12	63.4 ± 3.3	5.7 ± 0.7	9.9 ± 3.0	43.5 ± 6.6	1.9 ± 0.2
F6	3.1 ± 0.0	3.3 ± 0.0	87.0 ± 0.2	4.7 ± 0.0	7.1 ± 0.5	54.6 ± 0.4	2.2 ± 0.2

relatively high melting temperature (T_m = 74.4°C), with a propensity to be spray dried into small particles in the inhalation range. TPGS and DSPE-mPEG-2000 were chosen as they are polyethylene-glycol-comprising excipients with relatively low melting temperatures and PEG chains of 1 kDa and 2 kDa, respectively. They also bring stealth properties to the final inhaled particles and have a low potential intrinsic pulmonary toxicity (Yan et al., 2007, Gill et al., 2011, Shah et al., 2011). After spray drying, these PEG fractions would likely be located on the surface of particles (cisplatin microcrystals or SLM). For microcrystals, this is because of the very low solubility of cisplatin as compared to the high solubility of TPGS in heated IPA (F2) and because of the very low size of cisplatin microcrystals. Droplets of equal or larger size than cisplatin will therefore more likely coat cisplatin microcrystals with TPGS and end-up in the spray dryer cyclone. Smaller droplets composed of TPGS only would likely end-up in the spray dryer filter. For SLM, the PEGylated chains would preferentially end-up on the outer shell of SLM because TPGS and DSPE-mPEG-2000 have tensioactive properties and therefore tend to be located at the air-liquid interface during spray drying.

Moreover, because they show a higher solubility than TS in heated IPA they would also likely precipitate last during spray drying. The compositions of formulations before and after spray drying are presented in **Table 16**.

The PSD of cisplatin microcrystals was evaluated throughout the size reduction process in IPA suspensions **(Table 19)**. HPH allowed a global 19-fold size reduction of cisplatin with a final d(0.5) of 0.89 μm with 97.9% of the particles under 5 μm, compared to an initial d(0.5) of 16.5 μm with only 10.2% of particles under 5 μm for the bulk powder. Cisplatin concentration in the HPH tank, verified by ETAAS, increased from 5.0 to 5.3% w/v after size reduction due to some evaporation of IPA. The overall yield of the size reduction process was 90%, with losses probably caused by the 7 mL dead volume inside the homogenizer. The cisplatin concentration in suspension in the HPH tank was used to control pre-spray drying cisplatin levels by dilution to the desired levels **(Table 16).**

The spray drying yield ranged from 45 to 61% for all formulations, which is an acceptable value for a lab scale process.

3.4.2. Drug content

ETAAS is a powerful and versatile tool for transition metals quantification providing high sensitivity and high reliability. Unlike chromatographic methods, it has the advantages of fast sample preparation with *in situ* matrix treatment and does not need previous separation, yet it only specifically quantifies platinum that can originate from cisplatin or from any other Pt-derivatives in solution. Cisplatin, which exerts low molar absorptivity in the UV spectrum,
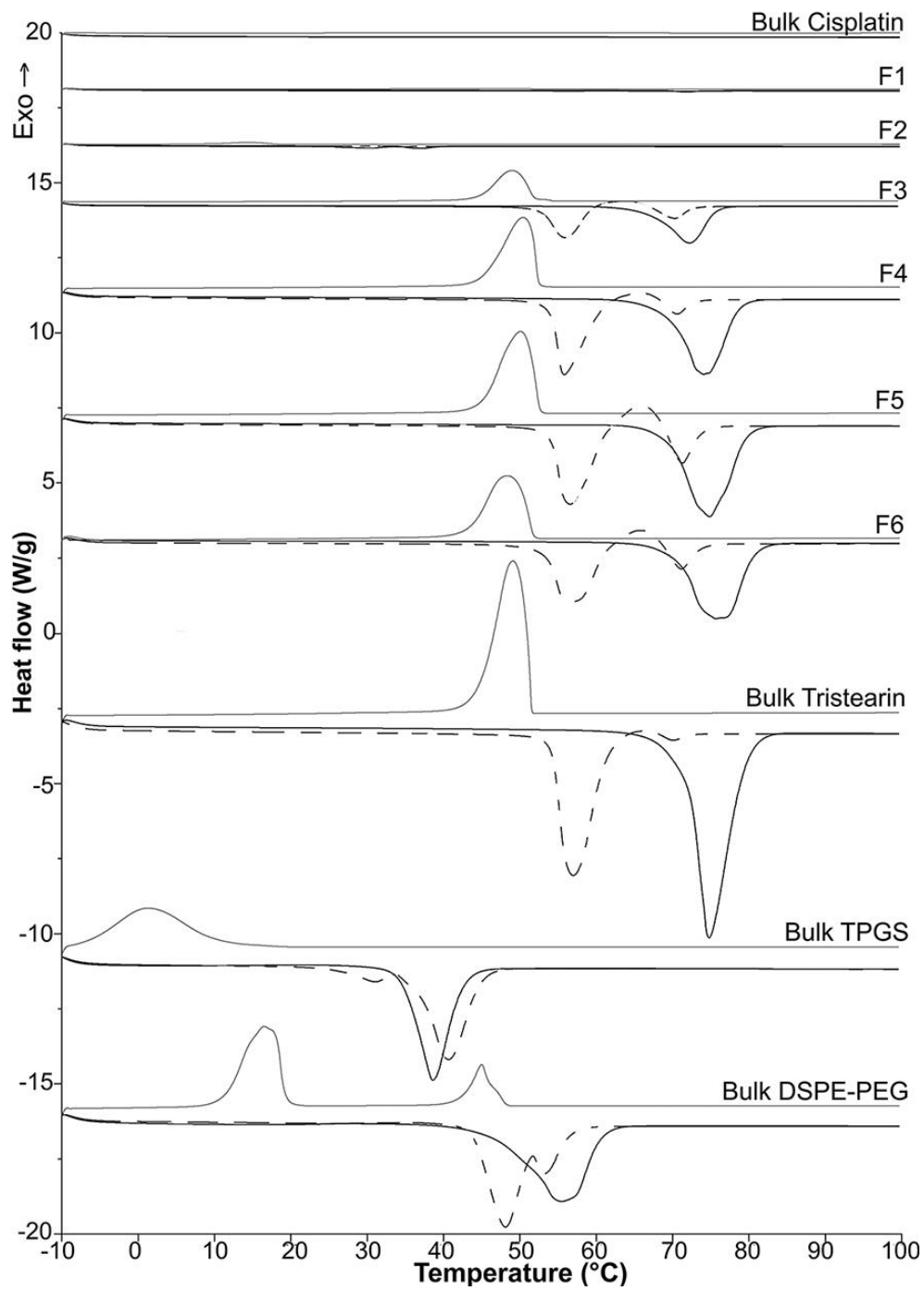
Figure 49. Thermal behavior of bulk cisplatin, bulk excipients, and the produced formulations in DSC analysis including three scans at 10°C/min.

requires a derivatization reaction prior to the analysis in order to be quantified by the most sensitive chromatographic methods (Bosch et al., 2008). These methods are therefore also unspecific as the derivatizing agent can react with many Pt-derivatives in solution, in particular undesirable cisplatin degradation products (transplatin, dimers, etc.), and therefore exhibits the same issues regarding specificity. The well characterized ^{195}Pt NMR chemical shifts of platinum species in solution (Berners-Price et al., 2006) are, however, specific to the first coordination sphere (i.e. platinum-bound atoms) and capable to distinguish between oxidation states, conformational isomers and can fully differentiate *cis* or *trans* geometric isomers.

Cisplatin quantification obtained from the integration of the ^{195}Pt NMR signal and from the whole Pt content with ETAAS were consistent with each other within the standard deviation **(Table 16)**.

The slightly higher drug content observed using ^{195}Pt NMR could be the result of a less precise quantification method and the lack of triplicate measurements, as were done for ETAAS. However, both methods exhibited drug contents consistent with the expected theoretical values for all DPI formulations, showing that cisplatin integrity was well preserved and that no excipient was lost during the size reduction processes and spray drying.

3.4.3. Residual solvent and thermal properties of formulations

Very low weight loss (< 0.2% w/w, from thermogravimetric analysis, **Table 16**), was observed for all DPI formulations between 25 and 125°C. These are related to residual solvent (IPA) and to the moisture content in formulations. IPA, as a low-toxicity class III solvent, is accepted up to 0.5% or 50 mg per day in pharmaceutical formulations (USP30, 2007). Spray drying proved here to be suitable for thorough elimination of the IPA used as a nonsolvent during size reduction. The elimination of unwanted moisture in dosage forms is usually a key issue in pharmaceutical development, and is highly desirable for the long-term stability and constancy of DPI physicochemical and aerodynamic properties. The formulations ultimately produced contained almost no moisture at all. Conversely, too low moisture contents in powders can

result in the appearance of electrostatic charges that are detrimental for good delivery from a capsule and adequate aerosolization of powders in DPI. However, this issue was not observed except during the handling of F1.

The thermal properties of bulk cisplatin, F1 and F2 DPI formulations as determined by DSC **(Figure 49)** showed no particular thermal events (i.e. no crystallization peak) for cisplatin before its melting, with degradation at 270°C (data not shown). This suggests that cisplatin was not originally in an amorphous state but in a crystalline state, as described in literature (Ting et al., 2010, Marques et al., 2013). That crystalline state is probably maintained during size reduction and after spray drying, an essential feature for the long-term stability of formulations.

Regarding the thermal properties of TS-comprising DPI formulations (F3-F6), the first heating scan shows an endotherm peak (scan a), representative of the melting of the ß form of TS (T_m = 74.9°C for bulk TS *vs.* 74.4°C for DPI formulations). The cooling scan (scan b) then shows the recrystallization of TS from the melt as the α form (49.1°C for bulk TS *vs.* 49.5°C for DPI formulations). During the last re-heating scan (scan c), the α form melts (endotherm at 56.9°C for bulk TS *vs.* 55.9°C for DPI formulations), then converts to the ß form upon heating (exotherm crystallization at 65.9°C for bulk *vs.* 65.2°C) and then melts again upon further heating (endotherm at 70.1°C *vs.* 70.8°C). The enthalpies of the different thermal transitions observed were directly dependent on the proportion of TS in DPI formulations. The differences in ß fusion temperature and enthalpy observed between scan a and scan c could be explained either by the formation of a ß' metastable form as described by Oh et al. (2002) or by the overlap of an exotherm and an endotherm peak (α to ß transition and ß fusion). This can happen over a wide range of temperature, as described by Singh et al. (1999) who analyzed this issue using modulated temperature DSC. TS was hereby exclusively observable as a ß form in TS-comprising formulations during scan a. This ß form could help promote the stability of the lipid matrix of SLM, as its melting point is much higher than that of the α form (T_m = 56.9°C). This would certainly prevent the ß to α transition at normal storage temperatures (below 40°C). Moreover, the presence of a stable polymorphic state of TS is essential to avoid drug expulsion and modification of the particle size or shape and the resulting properties (deposition, dissolution) due to a polymorphic transition, as is frequently observed with the α to ß transition of triglycerides (Xia et al., 2014). The presence of the ß form observed here is probably attributable to the approach of preparing TS by direct spray drying from a solution and not from a melt (Singh et al., 1999) and to the fact that spray drying involves cisplatin as a suspension in its alleged crystalline state. This approach allows high drug loadings and encapsulation of hydrophilic or hydrophobic drugs, as the API is not solubilized in the lipid layer. However, it offers less control of particle size. Other excipients, such as TPGS and DSPE-mPEG-2000 in PEGylated excipient-comprising formulations (F2, F5 and F6), were not discernable because
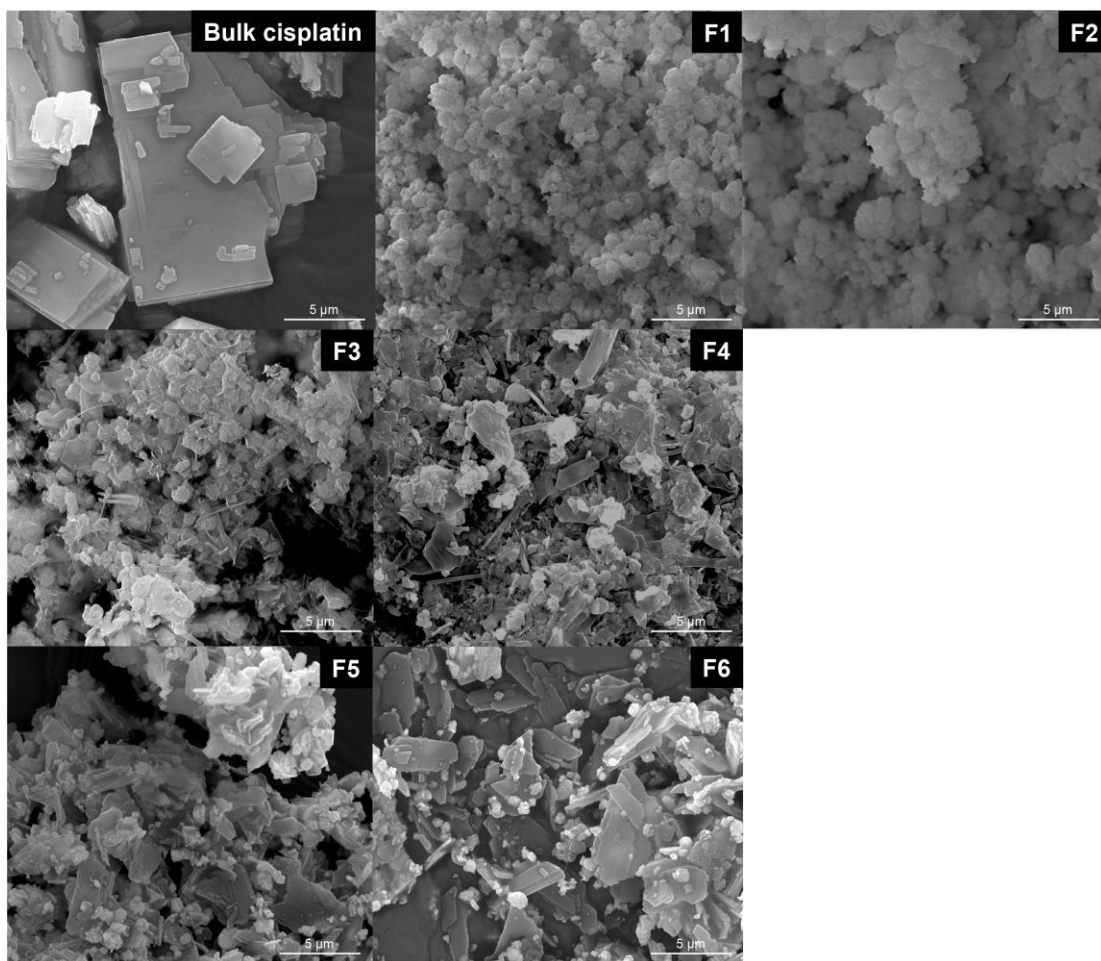
Figure 50. SEM micrographs of bulk cisplatin and of DPI formulations (magnification 12 000×).

of their low content in DPI. No particular observations regarding their influence could be made except for the fact they did not alter the polymorphic state of TS. Therefore, the thermal characteristics of produced DPI can be considered suitable for the long-term stability of formulations.

3.4.4. Particle shape and morphology

Shape and morphology evaluation by SEM **(Figure 50)** showed that particles produced without excipient (F1) were much smaller and spherical than in the bulk powder. This was due to the high pressure applied during the size reduction process. The addition of TPGS (F2) produced slightly bigger and more agglomerated particles than observed for F1. This was probably due to the sticking properties of TPGS caused by its lower melting point (T_m = 38°C). The addition of TS with or without PEGylated-excipients (F3-F6) produced particles with a more irregular shape than F1. Regarding TS-comprising formulations (F3-F6), the presence of TS produced unevenly shaped particles, with many small needle-shaped inclusions mixed together with larger angular particles. These particular structures can be explained by the fact that TS directly precipitates into a crystalline form during spray drying. The structures are typical of the ß form of TS described in literature (deMan et al., 1985, Oh et al., 2002). The increased ratio of TS between F3 and F4 increased the heterogeneity of the observed particle population. Larger angular particles and fewer needle-shaped particles were observed with the addition of PEGylated excipients to the lipid fraction (F5 and F6).

3.4.5. Geometric particle size distributions of DPI

The PSD of individualized particles in formulations were measured in IPA suspensions for formulations without lipid matrices (F1 and F2). The median particle size increased from 0.89 µm after HPH to a d(0.5) of 1.6 and 2.1 µm after spray drying, respectively **(Table 19)**. This was probably because of the formation of non-dispersible agglomerates during solvent evaporation. The PSD of lipid-comprising formulations was measured in water-based suspensions. These particles showed much higher overall sizes but were all comprised between 3.1 and 4.2 µm in d(0.5), with 63.4-87.0% of particles below 5 µm. The addition of the lipid fraction comprised of TS only to previously reduced cisplatin microcrystals (F3 and F4) caused an increase in the PSD of formulations, from 1.6 µm for excipient-free F1 to 3.5 and 3.8 µm for F3 and F4, respectively. This increase was directly related to the extent of the lipid ratio. Indeed, the lipid fraction that is crystallized during spray drying increases as well **(Table 16)**, which can promote sticking between particles. Regarding PEGylated excipient-comprising formulations, TPGS in F2 and F5 increased the geometrical PSD because of its lower melting point, which is close to the outlet temperatures observed during spray drying
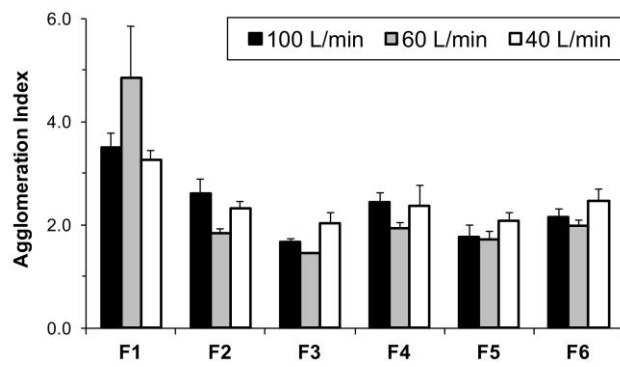
Figure 51. Agglomeration index (mean value ± SD, n = 3) of DPI formulations under decreasing airflows (100, 60 and 40 L/min for 2.4, 4.0 and 6.0 s, respectively).

(i.e. 38 – 42°C), which could have promoted particle sticking. However, the opposite effect was observed in F6 with DSPE-mPEG-2000, which has a higher melting point (T_m = 55°C). Its addition diminished the PSD with an even smaller distribution than the corresponding non-PEG-comprising formulation (F4). This peculiar characteristic could be explained by a better lipid organization inside the droplets and around cisplatin microcrystals due to the more amphipathic and surface-active characteristics of DSPE-mPEG-2000 and to its lower proportion in the formulation than in F5 (0.25% w/w in F6 *vs.* 0.5% w/w in F5).

Measurements of PSD obtained in the aerosol plume through an inhaler for human use at 100 L/min (i.e. normal dispersion conditions during an inhalation procedure) showed an overall increase in sizes for all formulations **(Table 19)**. The moderate increase in the d(0.5) more than doubled for the geometric D[4,3] parameter and the undersize decreased for all formulations. This is attributable to the lower ability of a powder bed to be deagglomerated by a normal air stream, causing a high fraction of particles to be measured in the form of undispersed aggregates compared to the drastic conditions used for the PSD measurements of individualized particles.

The deagglomeration ability of formulations was therefore evaluated by measuring the PSD of formulations under different flow rates. These rates were 40, 60 and 100 L/min to take into account the influence of suboptimal air flow that patients could generate in relation to the air flow recommended for the aerodynamic behavior analysis **(Table 19**, **Figure 51)**. The analysis of the agglomeration index, a ratio of D[4,3], taking into account the volumetric weighted mean diameter of particles **(Equation 4)**, helped to better visualize the overall ability of formulations to deagglomerate thoroughly under the lower flow rates that are usually achievable for patients with impeded respiratory function such as chronic obstructive pulmonary disease (COPD) or lung cancer. Excipient-free F1 exhibited low and variable dispersibility at different flow rates. For this formulation we visually observed a greater amount of powder in the capsule and the device at lower flow rates. This fraction was not measured by the Spraytec, as it is placed after the induction port where the inhaler is connected. It is therefore possible that agglomerates that were not completely aerosolized from the powder bed at 40 L/min were aerosolized and measured at 60 L/min and aerosolized and deagglomerated at 100 L/min.

Except for some large agglomerates, formulation F2, however, presented a high ability to be dispersed at all flow rates, as shown by its low average agglomeration index of 2.3 *vs.* 3.9 for F1. The PSD for F2 showed a low dependency on the flow rate at 60 L/min but seemed to
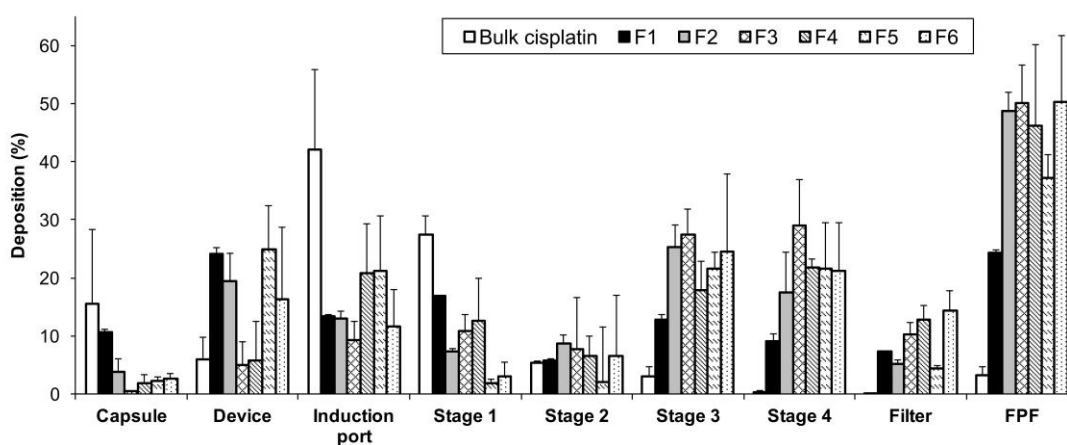
Figure 52. Deposition profiles and fine particle fraction (FPF) as the fraction of the nominal dose of the generated DPI formulations. Impaction was realized from a 20 mg powder mass in an HPMC n°3 capsule in an Axahaler® device, using an MsLI operated at 100 L/min for 2.4 s (mean ± SD, n = 3). Cut-off diameters for this flow-rate correspond to 10.0, 5.3, 2.4, and 1.3 μm for stages 1 to 4, respectively, the filter cut-off is 0.4 μm.

Table 20. Aerodynamic characteristic values for bulk cisplatin and for generated DPI formulations, measured from an Axahaler ® device, using an MsLI operated at 100 L/min for 2.4 s (mean ± SD, n = 3).

	FPF (%)	**FPD** (mg)	**MMAD** (μm)
Bulk cisplatin	4.2 ± 2.1	0.84 ± 0.42	6.6 ±1.4
F1	24.2 ± 6.3	4.89 ± 1.27	2.0 ± 0.2
F2	51.5 ± 2.9	9.84 ± 0.55	2.5 ± 0.3
F3	50.1 ± 5.1	7.79 ± 0.79	2.3 ± 0.2
F4	46.1 ± 6.8	4.47 ± 0.66	2.2 ± 0.3
F5	37.3 ± 2.0	3.65 ± 0.20	2.4 ± 0.2
F6	50.3 ± 5.8	5.02 ± 0.57	2.3 ± 0.7

have a higher dependency at 100 L/min and 40 L/min, with more undispersed aggregates in the 10 µm area for the latter. Compared to F1, formulations comprised of a lipid matrix (F3 to F6) showed lower average agglomeration indexes at all flow rates, ranging from 1.7 to 2.3 for F3 and F4, respectively, and from 1.9 to 2.2 for F5 and F6, respectively. All the lipid-containing formulations PSD showed little dependency on flow rates compared to F1. This was probably because lipids helped diminishing interparticle interactions such as mechanical interlocking by lowering surface roughness (Pilcer et al., 2010). All formulations, except F1, were better deagglomerated under a 60 L/min flow rate. The powder deagglomeration abilities rely on forces generated by airflow in the DPI device (mainly turbulence and particle-device impaction). Higher flow rates increase turbulence levels in the device and generally improves deagglomeration. However, this effect can be counterbalanced by particle impaction, which also increases with air flow. Coates et al. (2005) confirmed that deposition abilities of powders are increased with airflow but also showed that they reach a plateau after a critical flow rate. In particular, they showed that the critical flow rate of an Aerolizer® was 65 L/min, which relates well with the better results obtained at 60 L/min in our study as this device is very similar to the Axahaler. The only differences being a shorter mouthpiece and 1 pin on each side to puncture the capsule for the latter vs. 4 pins for the Aerolizer.

Moreover a balance has to be found between the time taken for powder to empty out the capsule through the punctured holes and the time taken to reach the full flow rate and the highest levels of turbulence in the device. At lower flow rates (below 45 L/min), the capsule takes a long time to empty and turbulence is not sufficient for total deagglomeration of powders. At the highest flow rates (above 70 L/min), capsule is emptied quickly and the powder is subjected to stronger turbulence but also to a higher air velocity through the mouthpiece, causing more device deposition and lower inhaler performance (Coates et al., 2005).

3.4.6. Aerodynamic behavior

The aerodynamic behavior **(Figure 52)** of cisplatin DPI formulations was characterized from the deposition at each stage of the MsLI and by determining FPF, FPD and MMAD values **(Table 20)**. The average recovery for all MsLI analyses was 89.8% and ranged from 77.2 to 106.4%.

Compared to bulk cisplatin, micronized F1 without excipient showed a greater overall increase in deposition in the deeper stages, mostly stage 3, stage 4 and the MOC filter, with an FPF of 24.2%. This formulation also exhibited higher drug retention in the capsule and

the device but a lower impacted fraction in the throat and in stage 1, which mimics deposition in the trachea. However, higher and more efficient lung deposition in the deeper stages was obtained for F2, comprising 5% w/w TPGS, than for F1, which had an FPF of 51.5% and less retention in the capsule and the device. Here, retention was 3.8% and 19.4% *vs.* 10.8% and 24.2% for F2 *vs.* F1. Moreover, a higher proportion was impacted in the lower stages, which mimic lung deposition, for F2 *vs.* F1, with 25.3% *vs.* 17.4% in stage 3 and 12.8% *vs.* 9.0% in stage 4. Because of the very high drug content of F2 (95% w/w) and its higher deposition abilities, the FPD almost doubled for F2 in comparison to F1. These differences could be explained by the presence of electrostatic forces, which are detrimental to the deposition abilities of formulations. They were clearly observable during handling of F1 only and not observed after the addition of TPGS in F2.

Regarding lipid-comprising formulations, lung depositions were high in the deeper stages (stages 3, 4 and in the MOC filter) for all lipid ratios and compositions, with FPF between 37.3% and 50.3%. TS-only comprising formulations (F3, F4) had similar deposition profiles at all stages, within the device and induction port but F3, which had a lower TS fraction provided a higher FPD. The increase in geometric PSD **(Table 19)** that is observed for TS-comprising formulations was, however, not detrimental to the very high deposition abilities of DPI formulations. This can be observed from the high FPF and low MMAD measured for F3 and F4. Indeed, TS helped maintain the d_{ae} to an adequate level for inhalation purposes. This was because of the inherent lower density of lipids (d_{TS} = 862 kg/m³) compared to cisplatin ($d_{cisplatin}$ = 3 700 kg/m³), which probably led to a decreased density of the cisplatin SLM.

PEGylated excipient-comprising formulations F5 and F6 exhibited higher interaction with the device than F3 and F4 (F3: 4.9% and F4: 5.7% *vs.* F5: 24.8% and F6: 16.3%). However, they also presented a lower impaction in stage 1 (representing the trachea, F3: 10.9%, F4: 12.6% *vs.* F5: 1.9% and F6: 3.0%), which is highly desirable for avoiding peripheral exposure and local toxicity in patients. A lower deposition was observed for formulation F5, which included TPGS, than for formulation F6, which included DSPE-mPEG-2000. This was particularly observable in the MOC filter (F5: 4.4% *vs.* F6: 14.3%), that represents very small particles (0.4 to 1.3 µm aerodynamic diameter). Higher FPF-variability was also found for F6 than for F5. Overall, the deposition results observed for F5 and F6 are mostly related to the geometrical PSD related to each formulation **(Table 19)**, which is expected considering shapes and densities of particles in F5 and F6 are very similar **(Figure 50)**. With comparable cisplatin content (50%) and a lower FPF for F5, the TPGS-comprising formulation seems of
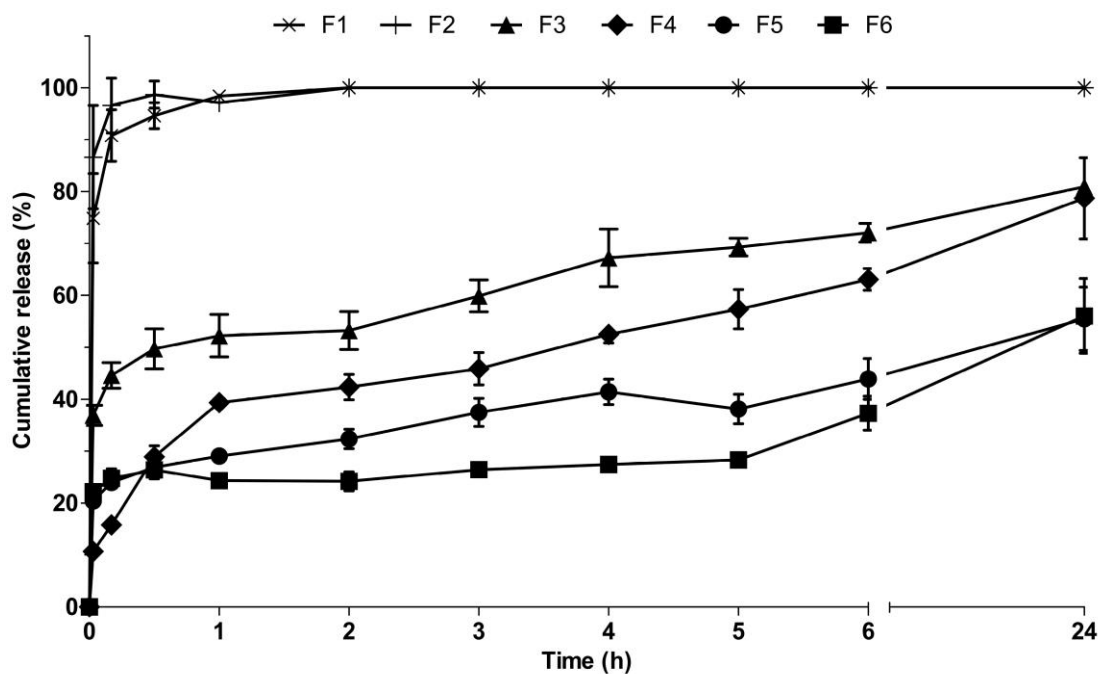
Figure 53. Release profiles of cisplatin from the respirable fraction of the DPI formulations generated (Mean ± SD, n = 3), determined from the impaction of an equivalent mass of 3 mg cisplatin on an FSI® filter using an Axahaler® device (100 L/min, 2.4 s) and placed in a dissolution vessel **(Figure 47)** as a PTFE/watch glass disk-assembly (400 mL mSLF, 37°C, 50 rpm).

less interest than the DSPE-mPEG-2000-comprising formulation F6, which logically exhibits a higher FPD. However, this formulation contains fewer PEGylated excipients and a longer PEG chains, which could temper its stealth abilities when compared to F5.

The calculated MMAD for all formulations were comprised between 2.0 and 2.5 µm in the 0.5-5.0 µm target sizes. However, this result has to be balanced by considering that the MMAD is calculated only from the emitted fraction of the dose using the Copley software, unlike the FPF and the FPD, which can be calculated from the nominal dose. This explains why F1, which shows the highest capsule and device retention, exhibits an interesting MMAD despite its poor deposition abilities in the deeper lung.

3.4.7. Dissolution properties

An official dissolution test for DPI formulations has yet to be implemented in pharmacopoeia but there is a strong interest in evaluating dissolution profiles from their inhalable fraction only and many approaches for this have been developed. Next generation impactor dissolution cups have been used but are imperfect as they only assess for a fraction of the powder, selected by the cutoff diameter array of a particular stage (Wauthoz et al., 2011). It was also demonstrated that an adapted dissolution technique involving a membrane from and an impaction device in a paddle apparatus was superior to flow- through and a Franz cell. The former had better reproducibility and less influence from the membrane load and the solubility of the active agents (May et al., 2012). The FSI, which is considered as an "abbreviated" impactor, is not supported by any official pharmacopoeia but can be considered as an efficient tool for DPI development. It can quickly segregate particles with a $d_{ae} < 5$ µm on a membrane filter for recovery.

The DPI formulations **(Figure 53)** showed fast dissolution of cisplatin, with more than 90% dissolved after 10 minutes with similar profiles for F1 and F2 ($f_1^{F1/F2} = 6$, $f_2^{F1/F2} = 56$). However, all lipid-comprising formulations showed a slowed release and varying burst effects. Dissolution profiles of formulations containing TS only were statistically different and not similar ($f_1^{F3/F4} = 35$, $f_2^{F3/F4} = 38$) and showed a lower burst effect, with 36.9% and 10.6% dissolved after 2 minutes for F3 and F4, respectively. The final measured concentration was, however, similar with 80.9% and 78.7% dissolved after 24 h. The large size of the lipid ratio was clearly responsible for the decreased dissolution rate at 50% w/w (F5) compared to 25% w/w (F4) TS content. This can be attributed to F5 thicker lipid coating and better covering of cisplatin microcrystals. This higher lipid ratio was also responsible for a lower burst effect through better encapsulation of cisplatin microcrystals.

The dissolution profiles of formulations comprised of 50% w/w lipid matrix without (F4) and with a PEGylated fraction (F5 and F6) were also different and not similar ($f_1^{F4/F5} = 23$, $f_2^{F4/F5} = 43$; $f_1^{F4/F6} = 41$, $f_2^{F4/F6} = 35$). PEGylated excipient-comprising formulations exhibited a higher burst effect than F4, with 20.4% and 22.2% (*vs.* 10.6%) dissolved after 2 minutes for F5 and F6, respectively. The overall dissolution rate of F5 and F6 was slowed down in both cases, showing the dissolution of 55.4% and 56.0% of the cisplatin content after 24 h. Both PEGylated excipient-comprising formulations were different but statistically similar ($f_1^{F5/F6} = 17$; $f_2^{F5/F6} = 56$). The addition of PEGylated excipients therefore exerted a higher burst effect but a lower overall dissolution rate. These can be explained by the surfactant effect of TPGS and DSPE-mPEG-2000, which may enhance the solubilization of unencapsulated cisplatin microcrystals on the SLM surface and, by promoting a better encapsulation of microcrystals during spray drying, slow down the dissolution after this initial burst.

3.5. Conclusion

This study demonstrates the effectiveness of a combined HSH, HPH and spray drying process to produce cisplatin microcrystals and further, DPI powders with a very high drug loading. These formulations composed of cisplatin microcrystals embedded into SLM showed high dispersion properties and *in vitro* lung deposition. They also exhibited controlled-release abilities over more than 24 h in lung fluid simulated media, with a limited and controllable burst effect. These particles, based on acceptable triglycerides for lung administration came with adequate crystalline properties for potential long-term storage and showed a low residual solvent and moisture content. The addition of PEGylated excipients to the lipid fraction of these dry powder formulations was proven to be feasible, potentially bringing stealth abilities against macrophages to the cisplatin SLM. Moreover, localized administration along with appropriate deposition in the deeper lung of controlled-release cisplatin at high doses can potentially promote better treatment efficiency. Cisplatin DPI, as an alternative to the dose-limiting systemic treatment of lung cancer, offer interesting perspectives as an adjuvant treatment in both SCLC and NSCLC at later stages or as a localized treatment specifically aimed against cancer recurrence. It could also be used in early stages as a neoadjuvant treatment to surgery by lowering lymph node involvement, preventing micrometastasis and offering lower patient discomfort than the current adjuvant chemotherapy.

In vivo pharmacokinetic studies are underway to confirm the controlled-release and stealth properties of the formulations developed, along with tolerance and efficacy studies.

3.6. Acknowledgements

4. Conclusion and perspectives regarding cisplatin dry powder formulations for inhalation

The preliminary formulation studies showed that it was possible to obtain SLM with a narrow PSD in the dry powder formulations with the combination of scalable technique such as HPH and spray drying using a solubilized fraction of potential well tolerated lipids. A new adapted method was developed to evaluate drug release/dissolution ability from the respirable fraction of the DPIs, based on the abbreviated impactor FSI.

Following this development, we showed that the first lipid excipients chosen (GMS, cholesterol) were unable to slow the release of cisplatin from the SLM. Moreover, the addition of tensioactive agents (Phospholipids and PEGylated excipients) in too large proportions was proven to be detrimental to the CR abilities of the DPI formulations.

Selection of TS, a highly hydrophobic and high melting point triglyceride was done after thorough preliminary formulation and optimisation studies without cisplatin, using the same spray drying conditions as those we would use next. TS had the best theoretical abilities to provide CR for the formulations, as it was the most hydrophobic excipient that was tested and was easily spray dryable in the defined lab conditions. Because of its high melting temperature, it was also possible to introduce a PEGylated fraction, in low amounts, in order to add potential stealth properties to the produced SLM without impeding the PSD of the produced particles, causing sticking during spray drying or experiencing unwanted thermal events.

Incorporation of cisplatin microcrystals proved to be feasible using this excipient and we obtained small and narrow PSD values with sizes compatible for inhalation. This was confirmed by the high FPFs measured (between 37% and 52% for all the formulations). We also observed CR profiles for more than 24 h for all the TS-based formulations. This CR was proportional to the added lipid fraction and was even higher for the PEGylated excipient-comprising formulations, probably because of the tensioactive effect of these excipients, which helped obtain a better organization of the lipid around the cisplatin microcrystals during spray drying.

Keeping in mind that the CR abilities of the formulations had to be balanced with their drug-loadings in order to provide FPDs compatible with human use and a therapeutic effect of cisplatin, we chose not to lower the drug-loadings by more than 50% w/w.

We therefore had three CR candidates, of which two had a PEGylated fraction and one immediate-release formulation. Because the determination of CR *in vitro* is far from recreating the conditions that are observed *in vivo*, in particular regarding the natural fate of deposed particles by macrophage uptake, we wanted to confirm the ability of these formulations to reside in mice lungs and exhibit their CR abilities. This was done through the following PK and body distribution study.
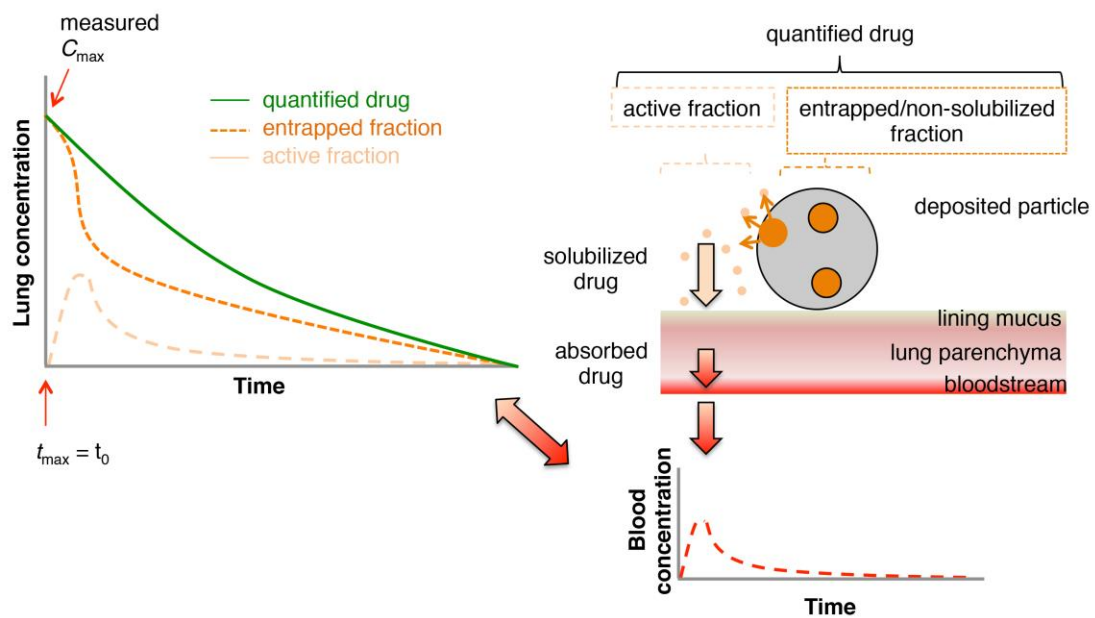
Figure 54. Schematization of the mechanisms involved regarding quantification of the "non-active" drug-entrapped and the solubilized active fraction of drug following particle deposition in the lung parenchyma and the subsequent distribution into the bloodstream.

Part II – Local and Systemic Pharmacokinetic assessment of DPI cisplatin formulations

1. Introduction

Pharmacokinetics, from ancient Greek *pharmakon* (drug) and *kineticos* (moving) aims at the determination of the fate of molecules throughout the body.

Unlike the IV route, where blood can be sampled directly from the administration compartment, direct quantification of the fate of a drug administered through a local route such as inhalation is not easy. This is because sample collection is always destructive as it involves killing the animal. *In vivo* PK studies assessing a local route of administration therefore require a large number of animals at each dosing time. It also must try to assess separately for the local and following systemic pharmacokinetic fate of the administered drug, in particular its distribution to other sensitive organs where it can exert unwanted toxic effects. While retention abilities of a formulation can be assessed by quantifying the remaining fraction of the drug in the target tissue, it is not as easy to assess its CR abilities. In lung homogenates, both the active solubilized drug and the unreleased fraction are quantified together. Therefore, the CR properties of those can only be extrapolated from the delayed distribution of the drug into the systemic compartment and compared to immediate-release formulations, and only for drug molecules that are permeable and cross the epithelial barrier by passive diffusion.

The peak concentration (C_{max}) in the lungs is obtained at t_{max} which corresponds to the administration time with immediate-release formulations by the inhalation route. However, it may not be the true reflection of the local activity of the drug **(Figure 54)**, which is obtained following dissolution of the drug in a variable timeframe, depending on its properties. The drug elimination half-time ($t_{1/2}$) takes into account all the elimination mechanisms of the lung parenchyma (i.e. MCC, MPS, absorption, metabolism). Absorption in the lungs influences the progressive passage of the drug to the systemic compartment, characterized by the serum C_{max}, t_{max}, $t_{1/2}$ and AUC. These are also influenced by the drug's simultaneous distribution into other distant organs or compartments (e.g. kidneys, liver, muscles) and the drug's metabolism and excretion properties (Wauthoz et al., 2015a).

Therefore, one other important parameter to consider is the ability of the inhaled formulation to be successfully retained in the lungs and exert its pharmacological action locally and not systemically. This can be assessed by calculating a targeting efficiency ratio that compares the AUC in the lungs to the AUC in the blood and in all the non-target organs. The targeting advantage of the inhaled route in concentrating the drug into the target organ can also be assessed using another ratio, taking into account the lung AUC using the inhaled route and comparing it to the standard IV route (Gill et al., 2011, Yapa et al., 2014). Finally, because cisplatin is highly concentrated in the kidneys' tubular region, which ultimately causes the dose-limiting nephrotoxicity, it is important to assess if cisplatin is still preferentially found in kidneys after inhalation. Toxicity of cisplatin has often been linked to the C_{max} in the serum and we can suppose that the same is experienced in the tissues and in the cells. Therefore, the systemic C_{max} is probably a key parameter in cisplatin nephrotoxicity and must also be assessed.

The administration of DPIs in rodents is an experimental procedure and can only be done using specific devices. In our laboratory, Duret et al. (Duret et al., 2012a) had already used and validated the delivery of itraconazole-based dry powders using the DP-4M® (Penn-Century Inc., Wyndmoor, USA) endotracheal device for mice, showing that it was able to deliver repeatable doses of drug deeply into mice lungs. However, dilution of the selected DPI formulations using a proper diluent had to be conducted to be able to deliver a specific dose into mice lungs. This further required the development of a mannitol/L-leucine spray dried diluent and the validation of the delivery of each of these blends, *in vitro* and *in vivo*, to ensure that the administered dose was repeatable between each animal.

We therefore conducted a PK study in which mice were sacrificed following a pre-determined timing after the administration of cisplatin dry powder blends (DPB) obtained from the DPI formulations that were selected following the prior study. These formulations were comprised of a 50:50 cisplatin/lipid ratio, including TS only or TS and a small fraction of TPGS or DSPE-mPEG-2000 to add potential stealth properties *in vivo*.

The mice's organs of interest (i.e. lungs, kidneys, liver, mediastinum and spleen) and total blood were collected and quantified for platinum using an ETAAS method, which was validated (see Appendix 1 for the validation details), following the procedures described earlier. This process aimed at assessing the retention abilities of the DPI into the lungs and confirming the controlled-release abilities of the formulations.
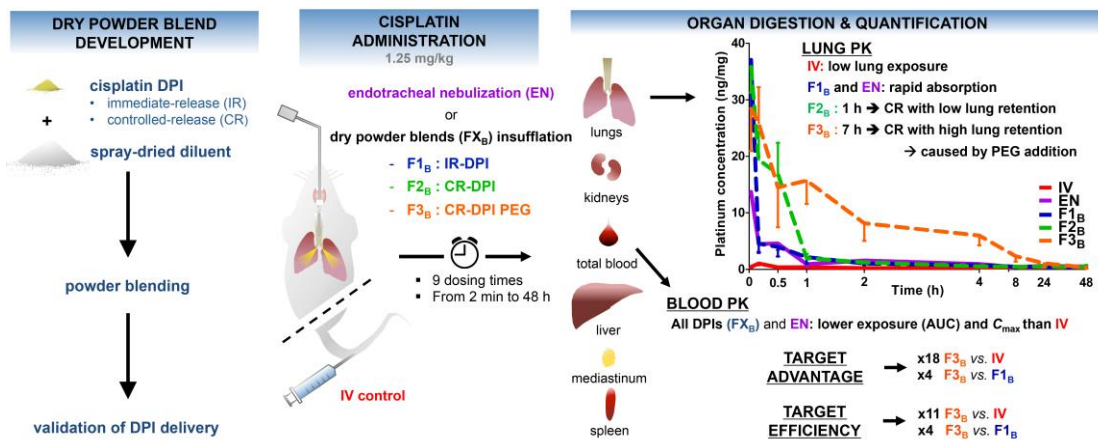
Figure 55. Graphical abstract of Article 2.

2. Article 2
"Platinum pharmacokinetics in mice following inhalation of cisplatin dry powders with different release and retention properties"

[a]Levet V., [a]Merlos R, [a]Rosière R., [a]Amighi K., [a]Wauthoz N.

[a] Laboratory of Pharmaceutics and Biopharmaceutics, Faculty of Pharmacy, Université libre de Bruxelles (ULB), Bd. du Triomphe CP 207, Campus de la Plaine, 1050 Brussels, Belgium.

2.1. Abstract

Pharmacokinetics of cisplatin administered by the pulmonary route were established in mice using dry powders inhaler (DPI) formulations showing immediate (F1) and controlled release (CR, solid lipid microparticles) *in vitro*, without (F2) or with PEGylated excipients (F3, F4). Formulation administration was realized using dry powder blends (correspondingly named thereafter F1$_B$ to F4$_B$) able to reproducibly deliver particles *in vivo* using a DP-4M Dry Powder Insufflator™. Their platinum pharmacokinetics were established over 48 hours in lungs, total blood and non-target organs *vs.* IV and endotracheal nebulization (EN). EN and F1$_B$ were rapidly distributed from the lungs ($t_{1/2}{}^i$ 2.6 and 5.0 min). F2$_B$ was eliminated in ~1 hour ($t_{1/2}{}^i$ 9.0 min). F3$_B$ lung retention was sustained for ~7 hours ($t_{1/2}{}^i$ 59.9 min), increasing lung AUC 11-, 4- and 3-fold *vs.* IV, F1$_B$ and F2$_B$. Total blood t_{max} were higher and AUC and C_{max} lower using the pulmonary route *vs.* IV. Kidney C_{max} was reduced 6-, 2- and 3-fold for F1$_B$, F2$_B$ and F3$_B$. AUC in kidneys were 2- to 3-fold lower for F1$_B$ and F2$_B$ *vs.* IV but comparable for IV *vs.* F3$_B$, probably because of kidney saturation. PEGylated solid lipid microparticles provided cisplatin particles with interesting lung retention and CR properties.

2.2. Introduction

Cisplatin is one of the most potent anticancer drugs. It is used against various cancers (e.g., lung, bladder, brain, cervical, testicular, ovarian, esophageal, gastric, head and neck, osteosarcoma). Its activity lies in its ability to bind with sulfurs, DNA and proteins, causing cell apoptosis (Jamieson et al., 1999). It is administered against small cell and non-small cell lung cancer (SCLC and NSCLC) as part of the "doublet chemotherapy" (e.g., one platinum derivative agent associated with a non-platinum derivative such as taxanes, gemcitabine or

pemetrexed for NSCLC). It is prescribed for delivery every 1 to 3 weeks by intravenous (IV) infusion at doses ranging from 30 to 100 mg/m² of body surface area (NCCN, 2014b, NCCN, 2015). Because of its particularly cumulative and irreversible renal toxicity, which is dose-limiting, nephroprotective action such as large water intakes with mannitol and electrolytes is crucial before and after administration (NHS, 2012). Consequently, administration of cisplatin often requires up to 6 to 8 hours and day care hospitalization, mobilizing healthcare personnel and increasing health costs and patient discomfort.

The pulmonary route has proven its usefulness in the treatment of various lung diseases (e.g., asthma, chronic obstructive pulmonary disease, pulmonary infections). Inhaled chemotherapy against lung cancer as a local treatment could be proposed as a novel modality for treating patients (Gagnadoux et al., 2008, Zhou et al., 2015). It could be administered as a (neo)adjuvant treatment to surgery or radiotherapy at all stages in SCLC and NSCLC. This would increase drug concentration at the site of action while limiting systemic exposure and the adverse effects frequently observed through parenteral administration, resulting in a higher therapeutic index (Gagnadoux et al., 2008, Zarogoulidis et al., 2012a). It could also increase drug concentration locally, in the tumour and its surroundings, particularly in loco-regional lymph nodes. This would help to prevent micrometastasis, the principal cause of cancer resurgence (Kelsey et al., 2009, Kaifi et al., 2010).

Regarding pulmonary drug delivery, dry powder inhalers (DPIs) provide many advantages over nebulizers. These include large inhalation doses of poorly water-soluble drugs in a short administration time, long-term storage stability of formulations and patient-activated inhaler devices that can easily be disposed of, helping to limit environmental and healthcare personnel contamination (Friebel et al., 2010, de Boer et al., 2015). Once inhaled and deposited in the lungs, drug particles are progressively solubilized in lung fluids at a speed rate depending on many parameters. The dissolved part will be available for pharmacological action locally but will also be distributed into the systemic compartment through the blood in the case of permeable drugs. The undissolved part will be subjected to non-absorptive mechanisms and will be progressively eliminated by mucociliary clearance (MCC) and the macrophage phagocytic system (MPS) (Gill et al., 2011). Moreover, too high doses of chemotherapy could lead to high peak concentrations of solubilized drug in the lungs and cause acute pulmonary toxicity, especially with immediate-release (IR) formulations. These issues could be avoided by careful dosage and progressive increase in drug concentration locally through controlled release (CR) delivery systems designed to promote lung retention and avoid clearance mechanisms, especially the MPS (Loira-Pastoriza et al., 2014). The CR of DPI formulations is a challenge in itself: in order to be inhaled, the aerodynamic diameter (d_{ae}) must lie in the low micrometre range (1-5 μm). This generally necessitates reducing the

Table 21. Theoretical and actual composition, aerodynamic properties - median-mass aerodynamic diameter (MMAD, mean ± SD, n = 3) and fine particle fraction (FPF, mean ± SD, n = 3) - and released fractions of the developed DPI formulations after 10 min, 6 hours and 24 hours (mean ± SD, n = 3).

		Theoretical composition (% w/w)	*Actual cisplatin content (% w/w)	*FPF (% w/w)	*MMAD (µm)	*Released fractions (%w/w)		
						10 min	6 h	24 h
F1	Cisplatin	95	95.6	52 ± 3	2.0 ± 0.2	97	100	100
	TPGS	5	± 2.6			± 5	± 0	± 0
F2	Cisplatin	50	48.5	46 ± 7	2.2 ± 0.3	16	63	79
	TS	50	± 2.2			± 4	± 3	± 10
F3	Cisplatin	50.0	48.9	37 ± 2	2.4 ± 0.2	24	44	55
	TS	49.5	± 2.3			± 3	± 9	± 11
	TPGS	0.5						
F4	Cisplatin	50.00	49.9	50 ± 6	2.3 ± 0.7	25	37	56
	TS	49.75	± 2.7			± 7	± 9	± 13
	DSPE-mPEG-2000	0.25						

*from Article 1.

geometric particle size and can in turn increase the burst effect and dissolution rates. More importantly, avoidance of recognition of particles and ensuing phagocytosis by the MPS through surface modification is an even greater challenge. Most DPI formulations developed up to now have been unsuccessful in controlling the pharmacokinetic (PK) profiles of drugs after lung deposition because of low lung retention (Gill et al., 2011, Loira-Pastoriza et al., 2014). Many strategies have also been developed to try to control drug release from inhaled particles, using delivery systems from the nanometer to the micrometre range. Strategies have used liposomes, solid nanoparticles, micelles and polymeric or lipidic biodegradable microspheres (Loira-Pastoriza et al., 2014). Moreover, PEGylation of the particle surface is a well-known and effective approach to limiting macrophage uptake (Patel et al., 2015) and most PEGylated excipients or particles are recognized as safe for inhalation (Klonne et al., 1989).

DPI formulations were developed in a previous study **(Article 1)** in the form of solid lipid microparticles (SLM) embedding cisplatin microcrystals into a biocompatible matrix. The matrix was composed of a highly hydrophobic triglyceride, tristearin (TS), alone or with PEGylated excipients such as alpha-tocopheryl polyethylene glycol 1000 succinate (TPGS) or distearoyl phosphoethanolamine polyethylene glycol 2000 (DSPE-mPEG-2000) to modify the particle surface properties. Interesting results were obtained *in vitro* **(Table 21)**. The particles exhibited dissolution properties, established on the inhalable fraction of particles only and in simulated lung fluid (Son et al., 2009), with a low burst-effect and CR over more than 24 hours. They also showed a high drug content ($\geq$ 50% w/w) and high fine particle fraction (FPF, expressed as the fraction of particles from the loaded dose with a d_{ae} < 5 μm) of up to 52%, which helped to deposit high doses in the lungs **(Article 1)**.

Confirmation of the CR abilities *in vivo* of the DPI formulations produced is essential. These abilities may vary greatly because particles deposited in the lungs are subjected to many other mechanisms than *in vitro*. For instance, the remaining undissolved particles will also be subjected to MCC and MPS, increasing their elimination rate from the lung.

Preclinical testing of respiratory drugs is often realized on rodents to assess PK, toxicity and efficacy. However, many precautions are required for their administration. First, when using high drug content DPI formulations initially developed for human use, a proper dilution must be realized to meet acceptable doses in rodents. Second, dose-dependent preclinical studies require administration methods and devices that are reliable to deposit said diluted formulations at accurate and reproducible doses in rodent lungs. The DP-4M Dry Powder Insufflator™ (Penn-Century, Inc., Wyndmoor PA, USA) used in this study is an endotracheal device. This necessitates prior anaesthesia of the mouse but has many

advantages over the other possible systems (e.g., intratracheal devices, nose-only and full-body aerosols). The DP-4M is able to deliver large, accurate doses of powder in mice lungs, helps to limit aerosol propagation and is easily decontaminable, which is of tremendous interest regarding environmental and personnel contamination when using cytostatic/cytotoxic agents. It was demonstrated to be a viable administration method for dose-dependent preclinical studies in a previous work from our lab (Duret et al., 2012a). Finally, thorough investigation of PK and ADME mechanisms, particularly after local administration at low doses and in small animals, require an adaptable and very sensitive quantification method. This method should be able to assess the fate of the drug and of its metabolites in various tissues and at very low quantification thresholds. This was done here by validated methods using electrothermal atomic absorption spectrometry (ETAAS) of platinum.

The aim of this study was therefore to develop a dry powder blend (DPB) for each of the cisplatin DPI formulations developed previously and to verify their reproducibility of delivery *in vitro* and *in vivo* using the DP-4M. This was done to ultimately establish the lung retention abilities of formulations and their relative systemic exposure in mice through a PK and distribution study in lung, blood and non-target tissues after a single dose administration. In the following sections, implications regarding the initial formulation compositions were detailed by citing formulations F1 to F4. All further implications regarding the DPBs obtained from these initial formulations (e.g. physico-chemical characterization, *in vitro* and *in vitro* emission abilities, pharmacokinetic results) were cited after their corresponding blend $F1_B$ to $F4_B$.

2.3. Materials and methods

2.3.1. Materials

Cisplatin was purchased from Shanghai Jinhe Bio-technology Co., Ltd. (Shanghai, PRC). TS was purchased from Tokyo Chemical Industry Co. Ltd. (Tokyo, Japan), TPGS from Sigma-Aldrich (St. Louis, USA), DSPE-mPEG-2000 from Lipoid (Ludwigshafen, Germany). Pearlitol® 25C mannitol was donated by Roquette Frères (Lestrem, France). L-leucine, Triton™ X-100 and Suprapur© nitric acid were purchased from Merck Millipore (Darmstadt, Germany). Ultrapure Milli-Q® water was obtained from a Purelab Ultra® purification system (Elga Veolia Water Technologies, Wasquehal, France) providing a resistivity higher than 18.2 $M\Omega.cm^{-1}$. Reference standard cisplatin was purchased from the U.S. Pharmacopeial Convention (USP) and used throughout the methods' validation. Xylazine (Proxylaz®) was obtained from Prodivet Pharmaceuticals (Eynatten, Belgium), ketamine (Nimatek®) was

obtained from Eurovet Animal Health (Ae Bladel, Netherlands), sodium pentobarbital (Nembutal®) was obtained from Ceva Santé Animale (Brussels, Belgium). All chemicals and solvents were of analytical grade.

2.3.2. Production of dry powders for inhalation

Cisplatin DPI formulations **(Table 21)** were initially developed and characterized as described before **(Article 1)**. Briefly, raw cisplatin microcrystals from bulk powder were first suspended in isopropanol and reduced in size by high-speed (10 min at 24 000 rpm) and high-pressure homogenization at 5 000 psi then 10 000 psi over 10 pre-milling cycles each, then at 20 000 psi over 20 milling cycles. A lipidic fraction, solubilized in heated isopropanol and containing PEGylated excipients such as TPGS, DSPE-mPEG-2000 and/or TS, was then added to the suspension and spray dried with a Mini-Spray Dryer B-290 (Büchi Labortechnik AG, Flawil, Switzerland) to obtain DPI formulations for human use. The *in vitro* results required to better understand the dry blend development and PK parameters are reported in **Table 21**.

2.3.3. Dry diluent

2.3.3.1. Production

Highly dispersive spray dried (SD) diluents with improved flow properties (compared to the commercially available ones) were developed. They were produced through the spray drying of a 1.0% w/v mannitol (SD mannitol) or 1.0% w/v mannitol and 0.1% w/v L-leucine (dry diluent, DD) solution in Milli-Q water. The solutions were stirred at ambient temperature until full dissolution and spray dried using a B-290 Mini Spray Dryer coupled with a B-296 dehumidifier (Büchi Labortechnik AG). The spray drying parameters were as follows: solution feed rate 3.0 g/min, inlet temperature 130°C, 0.7 mm spraying nozzle, 1.5 mm nozzle-cap, spraying air at 800 L/min and drying air flow 35 m³/h. The spray drying yield was determined from the ratio (percentage) of the weighed recovered powder to the mass of weighed material before solubilization. Powders were passed through a 355 μm stainless steel mesh sieve before characterization or blending.

2.3.3.2. Particle size distribution

Particle size distribution (PSD) of raw mannitol, SD mannitol and DD were measured in triplicate using laser diffraction with a Mastersizer® 3000 connected to an Aero S dry powder disperser (Malvern Instruments Ltd.). The parameters were as follows: 4 bar dispersing pressure and 50% vibration feed rate, refractive index: 1.52 for particles and 1.0 for air, absorption index: 0.1. The PSD was expressed as the volumetric mean diameter d(0.5) (the particle size under which 50% of the samples lies), d(0.9) (the particle size under which 90%

of the sample lies), the D[4,3] (the volume mean diameter) and the fine particle cumulative undersize fraction (% < 5 μm). The PSD was also measured from the plume emitted from a DP-4M delivery device, as described by Duret et al. (2012a). Briefly, the device was equipped with an AP-1® air pump (Penn-Century, Inc.) with an actuation volume of approximately 200 μL, reflecting the mouse lung tidal volume. Measurements were realized by laser diffraction using a Spraytec® equipped with an Inhaler and Nebulizer Accessory (Malvern Instruments Ltd.) and connected to an HEPA filter. The Spraytec was set using compressed air to avoid particles sticking onto the lenses. The DP-4M was loaded with approximately 2.0 mg of SD mannitol or DD (n = 5) – a powder mass within the expected range of the *in vivo* study – and actuated 5 times into the induction port under 30 L/min airflow. PSD was expressed as the d(0.5), d(0.9), D[4,3] and the fine particle cumulative undersize fraction (% < 5 μm). The PSD of raw mannitol was not measured using this technique as it was not deliverable through the DP-4M and instantaneously caused blockage in the tip of the device.

2.3.3.3. Flowability

The powder flowability of raw mannitol, SD mannitol and the DD was determined by calculating the Carr compressibility index (CI) or "Carr's Index", as described in the European Pharmacopoeia 8.0 section 2.9.16. A pre-weighed quantity of powder was placed in a graduated 10-mL cylinder. The apparent volume occupied by the powder was then noted before and after the application of 1 000 taps to the cylinder using a Stampfvolumeter STAV 2003 tap density tester (J. Engelsmann AG, Ludwigshafen, Germany). This helped determine bulk and tapped densities. The CI was then calculated as the ratio (percentage) of the difference between the bulk and tapped density to the tapped density of the powder.

2.3.3.4. Morphology

The morphology of raw mannitol, SD mannitol and the DD was determined by scanning electron microscopy (SEM) using a JSM-6100 microscope (Jeol, Tokyo, Japan), following platinum coating for 3 × 90 s under Argon at 10 mbar and 35 mA with a SCD 30 sputtercoater (Oerlikon Balzers, Schaumburg, USA). The acceleration during observation was 15 KeV.

2.3.3.5. Residual water content

The residual water content was determined from the weight losses between 25 and 125°C at 10°C/min for raw mannitol, SD mannitol and the DD by thermogravimetric analysis using a Q500 analyser (TA Instruments, New Castle, USA), as described elsewhere (Article 1).

2.3.3.6. Crystalline state

The crystalline states of raw mannitol, SD mannitol, the physical mixture (in the same proportions) and the DD were established by X-ray powder diffraction using a D5000 diffractometer (Siemens, Munich, Germany). It was equipped with a mounting for Bragg-Brentano reflection that was connected to a monochromator and DIFFRACplus EVA software (Bruker Belgium SA, Brussels, Belgium). Measurements were conducted at room temperature using Cu K radiation at 40 mA and 40 kV, with an angular 2θ increment of $0.02°$ from $2°$ to $70°$ at a counting speed of 1.2 seconds per step. The percentage of α- and β-mannitol was estimated using Topas V3 software (Coelho, Brisbane, Australia) by subtracting the total area of each polymorph from the total area of all polymorphs. The amorphous content (expressed in%) was estimated as 100% minus the estimated degree of crystallinity. The degree of crystallinity was calculated as the ratio (percentage) of the area under the diffractogram without integrating the deviation from the baseline into the total area under the diffractogram.

2.3.4. Dry powder blends (DPB)

2.3.4.1. Blending

The DD and the DPI formulations were added to each other in a 2 mL glass vial following a "sandwich" method. This method involved weighing half the mass of diluent, adding the total mass of formulation and ultimately the remaining mass of diluent to give a total target mass of 250 mg. The powders were then mixed using a Turbula 2C three-dimensional motion mixer (Bachofen AG, Uster, Switzerland) at a mixing speed of 46.2 rpm for 4 h. Finally, the mixed powders were sieved twice using a 355 μm stainless steel mesh to obtain DPBs. These blends were then set in glass vials and stored in a desiccator until characterization or administration to mice.

2.3.4.2. Drug content and uniformity of the drug content

Drug content and uniformity of the drug content were determined through platinum quantification using of 2.00 mg of DPB (n = 10). Uniformity was considered acceptable based on the "Uniformity of content of single-dose preparations" requirements of the European Pharmacopoeia 8th ed. section 2.9.6. (individual contents between 85 and 115% of the mean drug content, maximum one drug content in the 75-125% limits of the mean drug content).

2.3.4.3. Particle size distribution of DPB from the DP-4M

The PSD was measured from the plume emitted from the DP-4M using laser diffraction with the Spraytec apparatus, as described earlier (see 2.3.3.2. Particle size distribution) for each DPB (n = 5) and expressed as the d(0.5), D[4,3], d(0.9) and the fine particle cumulative undersize fraction (% < 5 μm).

2.3.4.4. Emission efficiency from the endotracheal devices

The emission efficiency from the endotracheal device was first characterized without cisplatin to determine the best diluent. The emission efficiency in mass (EE_M) and uniformity of the delivered mass (UD_M) were measured *in vitro* using SD mannitol or DD by filling the DP-4M with approximately 2.0 mg of powder. Raw mannitol was not evaluated as it was not delivered at all from the DP-4M, as described above. The DP-4M was weighed before and after 5 actuations with 200 μL of air. The EE_M was expressed as the average ratio (percentage) of emitted powder to the loaded powder and the UD_M as the percentage of difference from the mean (n = 10). This was then done for DPBs made with the best diluent, with a loaded mass of DPB ranging from 1.0 to 3.4 mg to evaluate powder emission over the wide range needed to adjust the dose for mouse body weight (bw). The emission efficiency in dose (EE_D) as the recovery of the delivered drug was also assessed to evaluate the risk of particle demixing for DPBs in the DP-4M. It was defined as the ratio (percentage) of the amount of drug within the delivered mass of powder to the theoretical emitted amount (calculated from the emitted mass). It was characterized in terms of mean, standard deviation and uniformity of the delivered dose (UD_D) after 5 actuations through the septum of a 10 mL-glass vial. The drug content in the vial was determined using ETAAS (n = 10, see 2.9.). The same procedure was applied with the endotracheal liquid administration device, the MicroSprayer© Aerosolizer - Model IA-1C for mouse equipped with an FMJ-250 high-pressure syringe (Penn Century Inc.). The EE_D was directly measured in a glass vial after emission of a fixed 50 μL volume of the most concentrated cisplatin solutions later administered to mice (see 2.3.7. Pharmacokinetic and biodistribution experiment).

2.3.5. Animals

CD1(ICR) female mice (Charles River, Saint-Germain-Nuelles, France and Janvier Labs, Le Genest-Saint-Isle, France) aged between 8 and 15 weeks and weighing from 20 to 33 g were housed 2-3 per cage in disposable plastic SUMC cages (Tecniplast S.p.A., Buguggiate, Italy), given water and dry food *ad libitum* and subjected to conventional housing conditions (12 h / 12 h night and day cycles, 22 ± 2°C, 55 ± 10% RH). All the experiments were realized in accordance with EU Directive 2010/63/EU for animal experiments and under

the approval and supervision of the CEBEA (Comité d'Ethique et du Bien-Etre Animal), animals ethics committee of the Federal Department of Health, Nutritional Safety and the Environment (Belgium) under approval number 569N.

2.3.6. Accurate and reproducible lung delivery of DPBs

DPBs were administered to 5 mice each (then included in the lung PK results) by weighing an appropriate powder load, taking into account their measured drug content, their average *in vitro* delivery efficiency, the mouse bw and the targeted dose of 1.25 mg/kg bw. Administration of DPBs was realized as described previously by Duret et al. (2012a). Briefly, mice were anesthetized with a xylazine (1.5 mg/kg)-ketamine (112.5 mg/kg) intraperitoneal injection, administered cisplatin by introducing the tip of the device into the trachea just above the carina and activating the loaded device 5 times, then euthanized using a lethal 12 mg intraperitoneal injection of sodium pentobarbital. The drug dose recovery in mice lungs was evaluated for the DPBs, after removal of the trachea and of the apparent bronchi to avoid quantifying drug that was not deposited in the lung lobes. It was calculated as the ratio of platinum in the lungs, removed as fast as possible after administration (~2 min), *vs.* the theoretically delivered platinum based on the DPB concentration and the powder mass emitted from the DP-4M (n = 5). The actual delivered dose of each DPB was calculated by weighing the DP-4M before and after administration and used to determine the *in vivo* delivery efficiency in mass ($EE_M^{in\ vivo}$), calculated as the ratio (percentage) of powder delivered after 5 actuations (n = 45, using all the PK study administrations).

2.3.7. Pharmacokinetic and biodistribution experiment

2.3.7.1. Cisplatin administration

Mice were divided into five groups of 45 mice and administered (i) cisplatin solutions *via* the intravenous route (IV) or *via* endotracheal nebulization (EN) or (ii) one of the DPBs *via* endotracheal dry powder insufflation. Mice were then euthanized immediately (~2 min, see 2.6.) and after 10 min, 30 min, 1 h, 2 h, 4 h, 8 h, 24 h and 48 h (n = 5 per time). Blood, lungs, kidneys, liver, spleen and mediastinum were removed. The organs were rinsed in saline and quantified for their platinum content with the ETAAS method to establish the PK data. For the first dosing time (2 min), only the lungs were harvested to better evaluate cisplatin C_{max} before distribution to the systemic compartment. For DPBs, administration was realized as described before (see 2.3.6. Accurate and reproducible lung delivery of DPBs). The measured platinum concentrations in the total blood and in mouse organs were standardized for the PK study to match a 1.25 mg/kg bw administration, using the mice bw, the actual delivered mass and the drug content of DPBs. Cisplatin for IV injection was prepared in

saline at 0.125 g/L and sterilized using 0.22 μm pore filtration, kept protected from light at room temperature and used within 24 hours. Mice were weighed before the administration to adjust the dose to 1.25 mg/kg bw ± 5% using an injection volume of 10 mL/kg bw. Cisplatin solutions for EN (endotracheal nebulization) were prepared by diluting 37.5 mg of cisplatin into a 50.0 mL flask with sterile saline for mice of 28.5 to 33.0 g bw. These solutions were subsequently diluted 1.15-fold for mice of 24.5 to 28.4 g bw and 1.36-fold for mice of 20 to 24.4 g bw to accommodate variations of bw in mice, considering that the administration volume for the MicroSprayer IA-1C was fixed (i.e. 50 μL).

2.3.7.2. Pharmacokinetic parameters

The PK properties of each administered formulation (IV, EN, F1$_B$, F2$_B$ and F3$_B$) in all harvested organs and in total blood were established and PK curves of cisplatin and its adducts were graphed as platinum *vs.* time curves. PK parameters included acute exposure as the maximum platinum concentration (C_{max}) and the time to reach C_{max} (t_{max}), as well as total exposure as the area under the concentration-time curve (AUC). These were estimated for each administered formulation and route using standard non-compartmental analysis. The initial and terminal elimination rate constants k_{el}^i and k_{el}^t were calculated from the log regression of platinum *vs.* time curves between the two first and the two last dosing times, respectively. The initial and terminal half-life $t_{1/2}^i$ and $t_{1/2}^t$ were calculated as $\ln(2)/k_{el}^i$ and $\ln(2)/k_{el}^t$, respectively. AUC$_{10min-48h}$ was calculated using the trapezoidal rule between the same 10 minutes to 48 hours range for all organs to be able to compare them with each other. Targeting efficiency (T_e, **Equation 5**) as described by Gill et al. (2011) and targeting advantage (T_a, **Equation 6**) as described by Yapa et al. (2014) were calculated for inhaled routes to compare them with each other or with IV, respectively.

$$T_e = \frac{AUC_{lungs}}{\sum AUC_{non-target\ organs}}$$

Equation 5. Calculation of the targeting efficiency (T_e).

$$T_a = \frac{AUC_{lungs}{}^{inhaled}}{AUC_{lungs}{}^{IV}}$$

Equation 6. Calculation of the targeting advantage (T_a).

Table 22. Electrothermal atomic absorption spectrometry furnace programs for aqueous solutions total blood and digested organs.

		Duration (s)			Temperature (°C)	
		Aqueous solutions	Total blood	Organs	Total blood	Total blood and organs
		A	B, B'	C	A	B, B', C
1	Drying	5.0	5.0	5.0	85	85
2		40.0	40.0	40.0	95	95
3		10.0	10.0	10.0	150	150
4	Charring	5.0	25.0	5.0	800	1200
5		1.0	10.0	10.0	800	1200
6	*Gas Stop*	2.0	2.0	2.0	800	1200
7		1.0	1.0	1.0	2700	2700
8	Atomization	4.0	4.0	4.0	2700	2700
9	*Gas On*	1.0	1.0	1.0	2700	2700
10			0.2	0.2		3000
11	Cleaning		2.0	2.0		3000

2.3.8. Statistical analyses

The statistical significance of the results was assessed after checking the homoscedasticity of variance using either the Fisher test (n = 2) or the Cochran C test (n > 2). Sets of data were then compared using either a Student's unpaired t-test (n = 2) or a one-way ANOVA and Bonferroni's post-hoc analysis if the Fisher test or C test were not significant, respectively, and a Kruskal-Wallis non-parametric test and Dunn's multiple comparison test (n > 2) if the C test was significant. Analyses were realized using the GraphPad Prism® (v5.01) software. Results were considered significant for $p < 0.05$, indicated (*) on graphical results, very significant for $p < 0.01$ (**) and extremely significant for $p < 0.001$ (***).

2.3.9. Cisplatin quantification using ETAAS

2.3.9.1. Equipment

A SpectrAA 300 (Varian, Mulgrave, Australia) atomic absorption spectrometer, equipped with a graphite tube atomizer GTA-96, Zeeman correction, a platinum hollow cathode lamp (Photron Pty. Ltd., Narre Warren, Australia) and pyrolytically coated SP-12 graphite furnaces (Spectrotech, Tubize, Belgium) was used throughout the experiments to quantify platinum from cisplatin. The hollow cathode lamp was operated at 7 mA and a wavelength of 265.9 nm, using a slit width set at 0.2 nm. Argon of 99.999% purity (Air Liquide, Liège, Belgium) was used at 3.0 L/min as a purge gas and stopped during atomization.

2.3.9.2. Aqueous solutions

Quantification of platinum in aqueous solutions (to determine the drug content of DPB and the EE_D for DPBs and EN) was realized using the validated method described in our previous study (Article 1). Samples were diluted to fit the calibration curve using 0.1% v/v Suprapur® HNO_3 and subjected to furnace program A, described in **Table 22**, using a single 20 µL injection. Calibration was carried out by the autosampler using a fresh matrix-matched 800 ng/mL standard, automatically diluted to 600, 400, 200 and 80 ng/mL with blank matrix.

2.3.9.3. Total blood and organ tissue

Blood was collected in heparin-lithium tubes (Sarstedt AG & Co, Nümbrecht, Germany) by intracardiac puncture after mice were euthanized. Aliquots of 50 µL total blood were removed and stored at -20°C until analysis. Removed organs were rinsed in saline, weighed and stored at -20°C in polypropylene screw-cap tubes (VWR, Leuven, Belgium). The blood was digested using 50 µL of suprapur HNO_3 and ultrasonicated at ~65°C for 2 h in a

Table 23. Digestion, dilution volumes and quantification range for digestates analyzed by electrothermal atomic absorption spectrometry.

Organ	Approximate mass (mg)	HNO$_3$ volume (µL)	Final volume (µL)	Quantification range (ng/mg or ng/µL for blood)
Lungs	200	250	600	0.16 – 1.60
Kidneys	300	400	1000	0.21 – 2.10
Spleen	100	200	500	0.33 – 3.30
Mediastinum	80	200	500	0.53 – 5.30
Liver	1000	2000	5000	0.13 – 1.30
Total blood	-	50	200	0.066 – 2.10

Branson 2510 ultrasonic bath (Carouge, Switzerland). A volume of 100 µL of 1.0% v/v Triton X-100 solution was added as a chemical modifier and permeabilization agent and the samples were ultrasonicated again at ~65°C for 2 h. The organs were subjected to wet acid digestion using HNO_3 and ultrasonication at ~50°C for 3 h. The volume was then adjusted using Milli-Q water **(Table 23)**. Blank matrix and matrix-matched standards for total blood and organs were obtained from untreated animals using digested blood and organs and spiked to the correct concentration. Samples were quantified for their platinum content by ETAAS using a specific furnace program **(Table 22).** For blood, samples were quantified using furnace program B (20 µL injection) or B' (quadruple 20 µL injection). Furnace program B' consisted of applying the first steps of furnace program B from drying to charring (1 to 5) to each added 20 µL injection before following the remaining atomizing and cleaning steps once (6 to 11). This program helped increase platinum up to quantifiable levels while limiting non-specific absorption caused by matrix accumulation in the graphite furnace. For organs, samples were quantified for their platinum content using program C (20 µL of injection), using a shorter charring at 1200°C than with program B to slow furnace degradation. Results were expressed as platinum concentration per µL of blood or as platinum concentration per mg of organ tissue. The methods were developed following the Bioanalytical Methods Validation Guidance for Industry from the Food and Drug Administration (FDA, 2013). Repeatability for all methods was established (RSD% ≤ 7%). Accuracy was verified to be within 15% of the nominal value along the calibration curves using spiked blank matrix, except at the lower limit of quantification (LLOQ), where it was within 20% of the nominal value. In organ digestates, the range of linearity (r^2 ≥ 0.995) was 80-800 µg/L of cisplatin and the limit of detection (LOD) and LLOQ were 26 and 78 µg/L cisplatin. The total blood quantification methods B and B' were linear (r^2 ≥ 0.998 and 0.995, respectively) from 80 to 800 µg/L cisplatin and 25 to 250 µg/L cisplatin in digestate. Samples below the LLOQ using method B were analyzed again using method B'. The LOD and LLOQ were 8 and 25 ng/µL cisplatin in digestates. For values below the LOD, and between the LOD and the LLOQ, results were scored as half the LOD and as the mean of the LOD and LLOQ, respectively. The quantification range in organs and total blood for the method is presented in **Table 23**.

Table 24. Physicochemical properties of raw mannitol, SD mannitol and spray dried mannitol/L-Leucine (10:1) dry diluent (DD) in terms of bulk, tapped densities (mean ± SD, n = 3) and flowability (Carr's Index, mean ± SD, n = 3), of residual water content (mean ± SD, n =3, estimated amorphous content (n = 1) and particle size distribution measured with a Mastersizer 3000 (mean ± SD, n = 3).

	Bulk density (g.cm⁻³)	Tapped density (g.cm⁻³)	Carr's Index	Residual water content (% w/w)	Estimated amorphous content (%)	Particle size distribution			
						d(0.5) (µm)	D[4,3] (µm)	d(0.9) (µm)	% < 5 µm
Raw mannitol	0.42 ± 0.02	0.71 ± 0.01	41 ± 4	0.039 ± 0.004	12	19 ± 1	28 ± 2	57 ± 2	17 ± 1
SD mannitol	0.31 ± 0.02	0.51 ± 0.05	38 ± 1	0.340 ± 0.002	18	1.1 ± 0.1	1.3 ± 0.1	2.4 ± 0.1	100 ± 1
DD	0.38 ± 0.01	0.55 ± 0.01	31 ± 1	0.350 ± 0.010	34	1.2 ± 0.1	1.6 ± 0.2	2.8 ± 0.1	99 ± 1
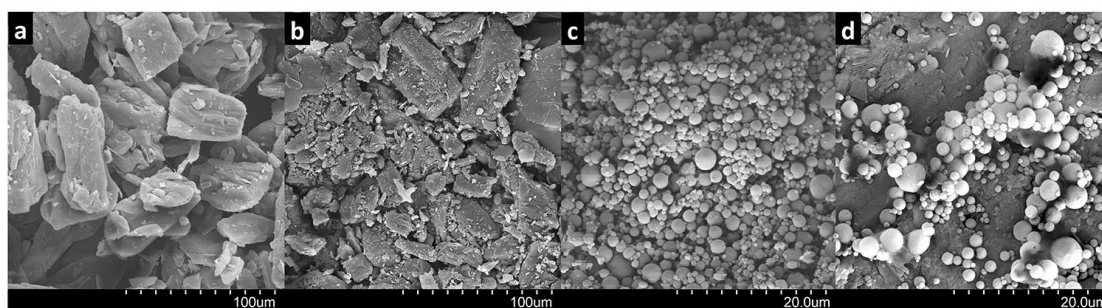
Figure 56. SEM micrographs of (a) raw mannitol, (b) physical mixture (mannitol and L-Leucine 10:1 m/m), (c) SD mannitol and (d) dry diluent (SD mannitol and L-Leucine 10:1 w/w), magnifications between ×500 and ×2200.

2.4. Results and discussion

2.4.1. Dry diluent characterization

The DP-4M used for dry powder administration to mice is able to deliver powder masses ranging from 0.5 to 4 mg. Duret et al. (2012a) showed that the ideal filling mass was between 2 and 4 mg to obtain an adequate volume of powder to be aerosolized from the sample chamber. This was visible through the drug dose recovery in the mice lungs, which was maximal (between 54 to 85% w/w) using these filling masses and led to delivered powder masses ranging between 1.0 and 2.5 mg in mice. We previously established the maximum tolerated dose of inhaled cisplatin using aerosolized solutions with the IA-1C. A 1.25 mg/kg single-dose was determined as safe for administrations in CD-1 mice (data not shown). This dose is equivalent in mice of 22-35 g bw to 27.5-43.8 μg total dose of cisplatin. These very small masses are impossible to weigh properly in the DP-4M delivery device considering the high drug content of the developed formulations (50-95% w/w, **Table 21**).

After unsuccessful tryouts with raw, microfine or SD lactose carriers (data not shown), we chose to develop diluents composed of mannitol, an excipient approved for inhalation by the FDA, as the main carrier component. The diluents were composed either of mannitol alone (SD mannitol) or of mannitol and L-leucine (10:1 w/w, DD). The mannitol and mannitol/L-leucine solutions, which were clear aqueous solutions, were spray dried into white micronized powders. During this process, the outlet temperatures ranged from 48 to 54°C and the yields were ~70% w/w.

The flowability of powders can be defined by the CI. It is considered "excellent to passable" for CI < 25, "poor" for CI between 26 and 31, "very poor" for CI between 32 and 37 and "very, very poor" for CI > 38 (Shah et al., 2008). In our study, CI was determined as "very, very poor" for raw mannitol and was not improved after spray drying for SD mannitol **(Table 24)**. However, the addition of L-leucine clearly increased the powder flowability (CI classified as "poor") by increasing the bulk density of the DD **(Table 24)**. This difference could not be explained by the morphology of particles, which were spherical for both SD mannitol and the DD, as seen by SEM **(Figure 56)**. Nor could it be explained by the slightly increased PSD for DD particles *vs.* SD mannitol particles, respectively d(0.5) of 1.2 ± 0.1 μm *vs.* 1.1 ± 0.1 μm, D[4,3] of 1.6 ± 0.1 μm vs. 1.3 ± 0.1 μm and d(0.9) of 2.4 ± 0.1 *vs.* 2.8 ± 0.1 μm **(Table 24)**. Moreover, the residual water content, as determined by thermogravimetric analysis **(Table 24)** was similar for SD diluents and higher than for raw mannitol but still
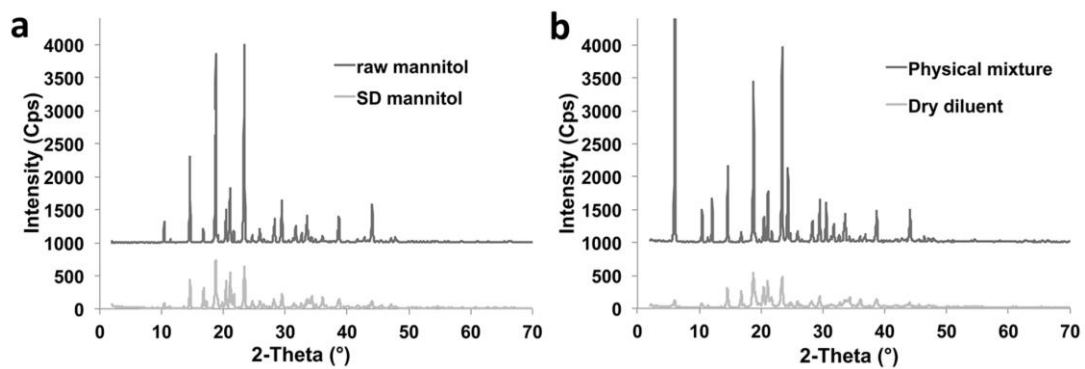
Figure 57. X-ray diffractograms of (a) raw mannitol and SD mannitol, and (b) physical mixture (mannitol and L-Leucine 10:1 w/w) and dry diluent (SD mannitol and L-Leucine 10:1 w/w) (b).

very low (below 1% w/w). These measurements furthermore confirm that an inlet temperature of 130°C is sufficient for a thorough spray drying process. A last hypothesis was that the flowability could be explained by the different particle chemical composition, particularly of their surface. This difference could have caused the increase in the bulk density of the DD **(Table 24)**. In DD, L-leucine is spray dried with mannitol in solution. It is known that L-leucine presents an amphiphilic nature and low water solubility, which leads L-leucine to be located at the interface of spray dried droplets and therefore at the surface of DD particles. Moreover, L-leucine seems to precipitate on the surface in a lamellar-like self-assembly, which may have modified the surface properties of particles and could explain the increase in their dispersibility (Sou et al., 2011).

In terms of particle physical state, the X-ray powder diffraction pattern of the DD showed the specific diffraction rays of raw mannitol in the β-polymorphic state (at 10.6°; 14.7°) and raw L-leucine (at 6.0°; 12.1°; 24.3°; 30.5°) but to a much lower extent than the physical mixture **(Figure 57)**. These patterns are similar to the patterns reported by Sou et al. (2013). The lower diffraction peak intensities observed for the SD components compared to the raw components could be explained partly by their reduced size but also by their increased amorphous content. Indeed, mannitol spray dried using the same concentration and the same procedure as the DD contained more estimated amorphous content than raw mannitol **(Table 24)**. Moreover, as reported before, L-leucine seemed to be in a "liquid-crystalline" state when spray dried and seemed to stabilize other spray dried components such as mannitol (Sou et al., 2013). This effect was observed with the high estimated amorphous content of DD of 34%, in comparison to 10% for the physical mixture. However, the estimated crystalline content of L-leucine in the DD was 1.8%, compared to the theoretical 9.1%. This content seemed to show that L-leucine was largely in a non-complete three-dimensional crystalline state, as suggested by Sou et al. (2013). Raw mannitol was exclusively in the most thermodynamically stable β-polymorphic state, with specific diffraction peaks at 10.56° and 14.71° (Hulse et al., 2009), whereas a low proportion (15.5%) of meta-stable α-polymorph was observed for the mannitol spray dried from aqueous solution at the specific diffraction peaks of 9.57° and 13.79° (Hulse et al., 2009). Indeed, the solvent in which mannitol has been dissolved influences the resulting polymorphic change obtained after spray drying. An aqueous solution of mannitol induces mostly the β-polymorph (Hulse et al., 2009) when spray dried whereas an isopropanolic solution induces mostly metastable α- and δ-polymorphs (Duret et al., 2012b). The DD also showed a low proportion of α-mannitol but in a higher proportion (23%), which could be explained by a stabilizing effect of L-leucine. This kind of stabilization had been observed before with proteins, such as with

Table 25. Dry powder inhaler (DPI) formulations used and dry diluent (DD) dilution factor, drug-content (mean $\pm$ SD, n = 10), particle size distribution of spray dried (SD) mannitol, DD and of DPBs at the tip of a DP-4M endotracheal delivery device (mean $\pm$ SD, n = 5) and *in vitro* emission efficiency in mass (EE_M ; mean $\pm$ SD, n = 15), and in dose (EE_D ; mean $\pm$ SD, n = 10). Statistical comparison between the EE_M of the SD mannitol and of the DD were realized using a Student's two-tailed unpaired *t*-test, *** $p < 0.001$. Statistical differences between the EE_M of F1$_B$ to F4$_B$ were non-significant (one-way ANOVA, Bonferroni's post-test. Statistical differences between the EE_D of F1$_B$ to F3$_B$ were non-significant (one-way ANOVA, Bonferroni's post-test).

Diluent or blend	DPI formulation and dilution factor	Drug-content (% w/w)	Particle size distribution from the DP-4M				DP-4M *in vitro* emission	
			d(0.5) (µm)	D[4,3] (µm)	d(0.9) (mm)	Undersize (% < 5 µm)	EE_M (% w/w)	EE_D (% D/D)
SD mannitol	-	-	2.8 ± 0.6	4.5 ± 2.3	9.7 ± 6.6	79 ± 12	46.7 ± 9.0	-
DD	-	-	2.1 ± 0.2	2.7 ± 0.1	5.4 + 0.7	89 ± 2	95.8 ± 5.4***	-
F1$_B$	F1, 1:50	2.37 ± 0.21	2.9 ± 0.7	3.7 ± 0.9	6.3 ± 1.8	83 ± 9	96.3 ± 7.6	96.6 ± 4.5
F2$_B$	F2, 1:25	1.67 ± 0.16	3.8 ± 0.8	5.9 ± 2.4	12.4 ± 6.8	69 ± 14	85.8 ± 17.4	98.0 ± 16.2
F3$_B$	F3, 1:25	1.64 ± 0.12	3.6 ± 0.5	6.0 ± 1.6	12.0 ± 5.3	69 ± 10	87.6 ± 16.5	104.8 ± 19.3
F4$_B$	F4, 1:25	1.60 ± 0.21	3.4 ± 0.5	4.7 ± 0.9	9.2 ± 2.4	74 ± 9	77.6 ± 19.3	198.3 ± 78.5

lysozyme on the crystallization of SD mannitol (Lee et al., 2011). However, to our knowledge it had not been reported before for L-leucine. We then evaluated the ability of the diluents to be properly emitted from the DP-4M delivery device. This device, composed of a valve and sample chamber and prolonged by a delivery tube (Duret et al., 2012a) can be connected to an air pump that provides small air volumes to displace and aerosolize the loaded powder. The objective was first to obtain maximum and repeatable aerosol delivery of the loaded diluents *in vitro*. Because they contain no active compounds, the only assessable parameter regarding the completeness and repeatability of the emission from the DP-4M was to evaluate that they emptied correctly when applying the volumes of air that we planned to apply *in vivo* (e.g., the tidal volume of mouse, ~200 µL). This was done with raw mannitol, SD mannitol and the DD and evaluated through their EE_M and UD_M before they could be chosen as potential diluents for powder blends. Raw mannitol immediately blocked the delivery tube of the device and was not emitted at all from the DP-4M. It was therefore discarded. For SD mannitol, the EE_M was significantly smaller ($p < 0.001$, two-tailed unpaired t-test) and more variable than for the DD (46.7 ± 9.0% *vs.* 95.8 ± 5.4%, respectively). Besides, the UD_M of SD mannitol showed 5 out of 10 values outside the 75-125% deviation from the mean delivered fraction, while the DD exhibited none out of 10.

Another important parameter is the PSD and the agglomerated state of the powder that is emitted from the device. This needs to be in a certain range for the powder to be properly impacted and deposited in lungs *in vivo* (see 2.4.2. Dry powder blends characterization). We first characterized the produced diluents from their PSD, obtained using the Mastersizer (**Table 24**). This technique accounts for individualized particles because of its highly dispersive applied conditions (dispersing pressure 4 bar), which can almost entirely scatter the agglomerates.

The PSD measured for raw mannitol *vs.* SD mannitol and the DD showed a 16- to 15-fold reduction in d(0.5), respectively, an 18- to 15-fold reduction in D[4;3], respectively and above 99% of particles below 5 µm for both spray dried diluents, compared to only 18% for raw mannitol. This confirms the well-known ability of spray drying to produce small, narrow particle populations from solutions, under adequate conditions. This also shows that the DD exhibited slightly larger individualized PSD than SD mannitol, because of the added L-leucine.

We then measured the PSD of the SD mannitol and the DD in the plume from the DP-4M using the Spraytec under actual deagglomeration conditions, which were less drastic than with the dry powder disperser of the Mastersizer **(Table 25)**. It was therefore possible to

assess the PSD outside the delivery device and the agglomeration tendency in comparison with the first PSD measurements.

Overall, the DD showed a smaller PSD than SD mannitol outside the delivery device, with a d(0.5) of 2.1 ± 0.2 μm and 2.8 ± 0.6 μm, a D[4,3] of 2.7 ± 0.1 μm and 4.5 ± 2.3 μm, a d(0.9) of 5.4 ± 0.7 and 9.7 ± 6.6, and 5 μm undersize of 89 ± 2% and 79 ± 12%, respectively. More importantly, the increase between the two PSD measurements (Mastersizer *vs.* Spraytec) was 1.5- to 2.1-fold greater for the d(0.5), D[4,3] and d(0.9) of SD mannitol than for the DD.

Overall, due to the addition of 10% w/w L-leucine, which modified the particle surface properties, the DD seemed to be better suited for delivery with the DP-4M. It provided better flowability, less agglomeration and a smaller PSD in the plume emitted from the delivery device. Together, these characteristics helped to obtain higher and more repeatable emission efficiency. The DD was thereafter blended with cisplatin DPI formulations and the resulting blends were characterized following an identical approach *in vitro*.

2.4.2. Dry powder blends characterization

The adequate dilution factors for DPBs were determined using the measured drug content of the DPI formulations **(Table 21)** and for a target cisplatin concentration in DPB of approximately 2% w/w to deliver 1.25 mg/kg of cisplatin in an emitted DPB volume of 1.25 mg for a mouse weighing 20 g. A blending process involving three-dimensional mixing for 4 hours was proven necessary to obtain proper powder blending and an acceptable uniformity of drug content. In fact, shorter mixing times created higher variability in results; the uniformity of the drug content criteria defined by the European Pharmacopoeia was never met for these batches (4 to 5 out of 10 values outside 85-115% of the mean after 2 hours of mixing). That can be explained in part by the very small particle size of the DD, which was in the same range as the original DPI formulation particles, and the low shearing forces generally developed in three-dimensional blenders. Indeed, smaller particles provide an increased particle surface and thus are more cohesive and present limited flowability. This means that more energy has to be put into the DPB to be able to disperse the DPI formulation particles fully during the blending process. The measured drug contents were close to the expected 2.0% w/w value, despite some deviation from the theoretical values (1.60 to 2.37% w/w, **Table 25)**. These could be caused by the very small size of the powder batches used for the mixing procedure, the poor flowability of the DD and by unmixed particles stuck to the walls of the glass vial as it was filled to around 60% of its volume during blending.

DPBs were also characterized by their PSD in the plume emitted from the DP-4M device using a Spraytec, which was set into a cytostatic hood and carefully decontaminated afterwards. We observed that the addition of DPI formulation particles increased the PSD of the final blend **(Table 25)** (d(0.5) from 2.1 ± 0.2 μm for the DD to 2.9 ± 0.7 μm for the highest diluted F1$_B$ (1:50)). This increase in PSD was observed even further for the less diluted blends F2$_B$, F3$_B$ and F4$_B$ (1:25), which were all comprised between 3.4 ± 0.5 and 3.8 ± 0.8 μm in d(0.5). The same trend was observed for the D[4,3], the d(0.9) and the 5 μm undersize parameters **(Table 25)**. It shows that the PSD in the plume is closer to the original DD values with higher dilutions, which is generally expected. It is important to note that the PSD values of the initial DPI formulations, measured with another technique (in suspension) but still as individualized particles, exhibited values in the same sequence as that observed here (Article 1). In essence, F1 exhibited smaller and narrower PSD (d(0.5) of 2.1 ± 0.0 μm, D[4,3] of 2.6 ± 0.0 μm, 5 μm undersize of 92 ± 0.2%) than for the TS-comprising formulations F2 to F4 (d(0.5) between 3.1 ± 0.0 and 4.2 ± 0.0 μm, D[4,3] between 3.3 ± 0.0 and 4.4 ± 0.1 μm and 5 μm undersize between 87 ± 0.2 and 63 ± 3.3%). This shows that the dilution factor may not be the only parameter to influence the PSD of the DPBs; blending of small DD particles around bigger DPI formulation particles that contained TS probably led to more particle agglomeration. This was much less observed with F1$_B$, for which the initial particles F1 were much closer to those of the DD and contained no TS, leading to a lower aggregation tendency. In humans, the geometrical diameter of particles defines in part the d$_{ae}$, which then defines the particle's behavior in the lower airways and the fraction that can be deposited in the alveoli (1-3 μm), the upper lung (3-5 μm), impacted in the throat (> 5 μm) or exhaled because of Brownian motion (< 0.5 μm) (Pilcer et al., 2012). In our study, the fraction deposited in mice lungs depends much less on particle or droplet size because the device tip is directly inserted in the bronchial tree just above the carina of the trachea. Unlike humans, the inspiratory flow is set using either a high-pressure syringe for IA-1C or an air pump for DP-4M to disperse the solution or the powder from the sample chamber of the endotracheal devices. Yet measurement of PSD emitted from the delivery device still provides important information for repeatability and deposition purposes. In previous studies from our lab, we demonstrated the ability to deposit fluorescent 1 μm-microparticles deep in the mouse lung (Duret et al., 2012a). In other studies, the PSD of aqueous droplets generated by IA-1C was characterized by a d(0.1), d(0.5) and d(0.9) of 10 ± 2 μm, 24 ± 4 μm and 44 ± 5 μm (Wauthoz et al., 2010) and the PSD of powder generated with a DP-4M was characterized by a d(0.5), D[4,3] and d(0.9) of 4.9 ± 0.7 μm, 10 ± 3 μm and 23 ± 3 μm (Duret et al., 2012a). Because EN is composed of an aqueous solution of cisplatin, the IA-1C

will generate a PSD equivalent to previously published results. For DPBs, it is noteworthy that the aerosol PSDs were below or equal to those observed previously by Duret et al. (2012a) as confirmed in **Table 25**, which leads us to believe that they also possess the ability to be deposited deep in mouse lung.

The DP-4M's ability to deliver the DPBs was also evaluated by the emission efficiency in mass (EE_M) and uniformity of delivery (UD_M) and by the emission efficiency in dose (EE_D) and uniformity of the delivered dose (UD_D). It showed the highest value of EE_M for F1$_B$ at 96.3% of the loaded mass and lower values of EE_M for F2$_B$ to F4$_B$ ranging between 77.6 to 87.3% of the loaded mass and with a higher variability (as seen with the coefficient of variation of the EE_M) for F2$_B$, F3$_B$ and F4$_B$ than for F1$_B$ **(Table 25)**. This increased variability seems to be linked to the higher PSD for F2$_B$ to F4$_B$ described above, which was linked to the lower dilution of the DPI formulation into the DD, to the presence of TS in these formulations and to larger DPI particles initially than for the F1 formulation. At the same time, F4$_B$ showed the lowest EE_M of all blends and very poor uniformity, with 5 out of 10 values outside the defined bracket. Together, these results show that powder dispersibility, exhibited by a low PSD from the plume, may be the main criterion for the thorough emission of a loaded powder from the DP-4M when using a powder blend.

The ability to predict the mass of loaded DPB that will effectively be emitted is of tremendous interest as it can then help set the dose of drug to administer, based on the animal bw. However, this information alone is not sufficient as (i) the delivery efficiency is known to be diminished *in vivo* (Duret et al., 2012a) due to the less predictable insufflation conditions of powders in the damper environment of mice trachea and (ii) the DPB could suffer from demixing caused by interactions within the device (e.g. high pressure of actuations, electrostatic forces, cohesion forces). Therefore, the EE_D of each DPB had to be further established. This was done through the quantification of cisplatin in the emitted powder (the actual emitted dose) and its comparison with the theoretical emitted dose (established from the emitted mass of DPB and its drug content). The quantified EE_D were acceptable for F1$_B$, F2$_B$ and F3$_B$, with average values comprised between 97 and 105% **(Table 25)**. The differences in EE_D between these three DPB were non-significant ($p >$ 0.05, one-way ANOVA, Bonferroni's post-test) as they were close to 100%, with higher variability for F2$_B$ and F3$_B$ than for F1$_B$. However severe demixing was observed for F4$_B$, with high inconsistencies in the mean EE_D, which was close to twice the expected dose (198 ± 78%), and all individual doses above 100% of the expected value.

Table 26. Platinum lung and total blood (in brackets) pharmacokinetics parameters after a single administration at 1.25 mg/kg by the IV route or the inhaled route through endotracheal nebulization or insufflation of $F1_B$, $F2_B$ and $F3_B$. The emission efficiency in mass ($EE_M^{in\ vivo}$) and the emitted dose were calculated for all the time-points (mean $\pm$ SD, n = 45). Drug dose recovery in the lungs is the ratio of the recovered cisplatin in the lungs at the first dosing time (2 minutes) to the expected cisplatin, calculated from the emitted mass and the drug-content of the DPBs (mean $\pm$ SD, n = 5). Initial and terminal elimination constants (k_{el}^i and k_{el}^t) and half-lives ($t_{1/2}^i$ and $t_{1/2}^t$) were measured between the two first decreasing time points and the two last time points, respectively. The targeting advantage T_a is the ratio of the platinum AUC in the lungs from an inhaled route to the AUC from the IV route. The targeting efficiency T_e is the ratio of the platinum AUC in the lungs to the sum of AUC in non-target organs, for a specific route. Statistical comparisons were performed in comparison with $F1_B$ for $EE_M^{in\ vivo}$ (one-way ANOVA, Bonferroni's post-test), in comparison with the IV control for the emitted dose (one-way ANOVA, Bonferroni's post-test) and C_{max} in lungs (Kruskal-Wallis test, Dunn's post-test) and in comparison with EN for the drug dose recovery in lungs (one-way ANOVA, Bonferroni's post-test) * $p < 0.05$, ** $p < 0.01$, *** $p < 0.001$.

	IV	EN	$F1_B$	$F2_B$	$F3_B$
$EE_M^{in\ vivo}$ (% w/w)	-	-	69 $\pm$ 34	64 $\pm$ 27	78 $\pm$ 29
Emitted dose (mg/kg bw)	1.25 $\pm$ 0.06	1.25 $\pm$ 0.12	1.13 $\pm$ 0.41	1.09 $\pm$ 0.47	1.34 $\pm$ 0.52
Drug dose recovery in lungs (% w/w)	-	21 $\pm$ 9	35 $\pm$ 22	33 $\pm$ 8	30 $\pm$ 16
C_{max} (ng/mg)	1.04 $\pm$ 0.3	13.7 $\pm$ 0.5	37.1 $\pm$ 10.8*	35.8 $\pm$ 4.6**	28.4 $\pm$ 7.5*
k_{el}^i (min^{-1})	0.05 (0.05)	0.14	0.26	0.077	0.012
$t_{1/2}^i$ (min)	13.1 (15.3)	5.0	2.6	9.0	59.9
k_{el}^t (h^{-1})	0.012 (0.015)	0.0086	0.0071	0.0095	0.047
$t_{1/2}^t$ (h)	56.8 (45.6)	80.9	97.0	72.7	14.8
$AUC_{10min-48h}$ (ng.min.mg^{-1} and ng.min.μL^{-1})	558 (370)	1869 (60)	1462 (102)	2079 (256)	6072 (282)
T_e	0.09	1.1	0.4	0.9	1.6
T_a	1	3.3	2.6	3.7	10.9

The uniformity of the delivered dose (UD_D) is an important requirement for the quality assessment of inhaled products, DPIs in particular (USP39, 2016). Its requires that a minimum of 9 out of 10 assays are within a [75-125%] bracket of the mean dose, maximum 1 out of 10 are within a [65-135%] bracket and that none are outside these limits. Because DPIs are fixed-dosage forms, the UD_D is usually calculated directly using the deviation from the mean target dose. In our study, we assessed the UD_D on the percentage of the mean recovered dose (expressed as EE_D) because we wanted to be able to adjust the cisplatin dose to mice of different bw.

The calculated UD_D for each assay were all within the [75-125%] bracket defined by the US Pharmacopoeia for F1$_B$, while 1 out of 10 was in the [65-135%] bracket for F2$_B$ and F3$_B$, which is in accordance with US Pharmacopoeia requirements. In contrast, UD_D for F4$_B$ showed 6 out of 10 values outside the [75-125%] bracket, of which 3 were outside the [65-135%] bracket. Inconsistencies had already been observed with the UD_M of this blend, which also exhibited the lowest EE_M and the highest variability for the uniformity of the drug content. Together, these characteristics led to unreliable delivery for F4$_B$, probably caused by an interaction between the DSPE-mPEG-2000 at the particle surface of F4 and DD particles. Regarding EN, the EE_D was also measured and showed a high recovery (96.1 ± 6.5%), with the UD_D well within the required limits of the US Pharmacopoeia (all values within the [75-125%] bracket). Based on these results, F1$_B$ (from F1, an IR carrier-free DPI formulation), F2$_B$ and F3$_B$ (from F2 and F3, CR lipid-based DPI formulations, the latter of which included 0.5% w/w TPGS) and EN of cisplatin solutions were administered to mice to assess their PK parameters. F4$_B$ was discarded.

2.4.3. Pharmacokinetic results

Cisplatin was administered to mice using IV, EN and endotracheal insufflation of the dry powder blends F1$_B$, F2$_B$ and F3$_B$. The target dose was 1.25 mg/kg bw. The $EE_M^{in\ vivo}$ **(Table 26)** were established from all the emitted masses (n = 45 per DPB) for the PK study and showed overall lower efficiency and much higher variability (between 64 ± 27 and 77 ± 29% w/w) for all DPBs compared to the *in vitro* results **(Table 25)**. This was probably caused by powder accumulation in the tip of the DP-4M, linked to the damper environment in mouse trachea associated with the high hydrophilicity of the mannitol-based DD, as described previously (Duret et al., 2012a). The average calculated emitted doses for F1$_B$, F2$_B$ and F3$_B$ are shown in **Table 26**. All were around the 1.25 mg/kg target (from 1.09 ± 0.47 to 1.34 ± 0.52 mg/kg) despite the difficulty in weighing the low amounts of DPB (~2.0 mg), the large range of mice bw (20 - 33 g) and the high encountered variability in $EE_M^{in\ vivo}$. The target
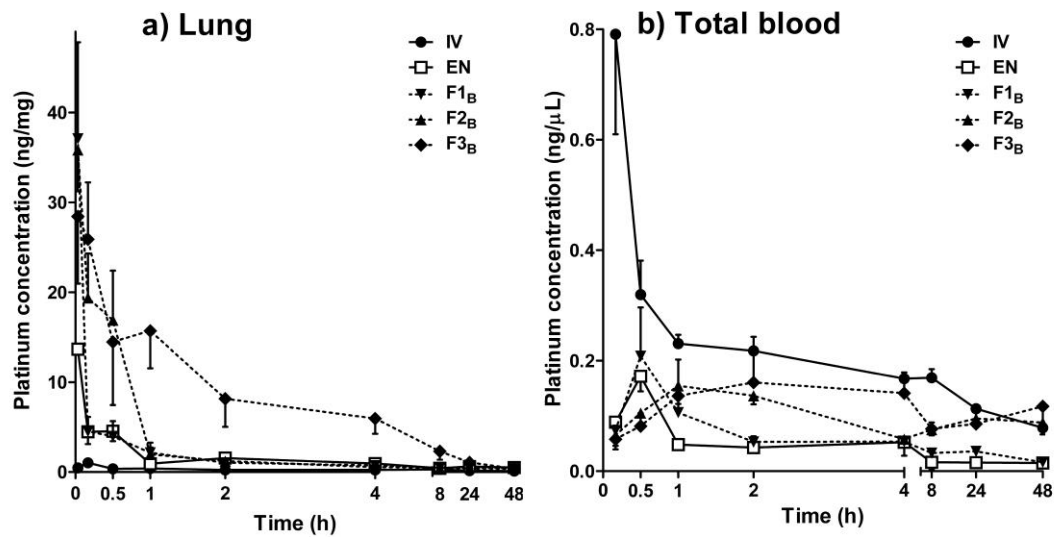
Figure 58. PK curves of platinum in the lungs (**a**) and in total blood (**b**) for all administered formulations and routes (mean ± SEM, n = 5 per time). First measurement times in the lungs and in total blood were 2 min and 10 min, respectively.

dose was much easier to adjust with IV ($\pm$ 5% error, using the 10 μL graduations on the syringe) and with EN ($\pm$ 10% error, using a fixed 50 μL volume and three matching solutions adapted to the mice bw). However a statistical difference was observed when comparing the emitted doses of DPBs between $F2_B$ and $F3_B$ ($p < 0.05$, one-way ANOVA, Bonferroni's post-test, **Table 26**). Nevertheless, this is not detrimental to the following pharmacokinetic results as we applied a correcting factor to the measured platinum concentration, taking into account the emitted dose for each individual result.

Drug dose recovery of the emitted dose in the lungs was assessed at the first dosing time (2 min), for which platinum was quantified in the lungs only in the PK study. It was calculated as the mass of platinum (calculated from the concentration in the digestate) recovered in the lungs compared to the theoretical mass of platinum that was emitted from the DP-4M (based on the emitted mass and the drug content of the DPB) or from the IA-1C for EN (based on the emitted volume and the EN solution concentration). It showed that the drug dose recovered in mouse lung ranged between 35 $\pm$ 22%, 33 $\pm$ 8% and 30 $\pm$ 16% of the theoretical dose for $F1_B$, $F2_B$ and $F3_B$, and was slightly lower for EN, for which 21 $\pm$ 9% was recovered **(Table 26)**. The differences between these values were non-significant (one-way ANOVA with Bonferroni's post-test). These values and their associated coefficients of variation, consistent with previous observations (Duret et al., 2012a, Duret et al., 2014), show a rather high unrecovered proportion of the emitted drug. This could be attributed to re-exhaled powder, deposition in upper airways that were not harvested for platinum quantification (bronchi, trachea) and, as was observed hereafter, to cisplatin being absorbed and distributed very quickly, despite a very narrow timing between administration and lung removal.

The PK curves of platinum lung concentration *vs.* time **(Figure 58.a)** obtained over the dosing period showed the highest platinum concentration in lung tissue right after administration (at the first dosing time of ~2 min) for all inhaled experiments when compared to IV. More precisely, the increase was particularly visible for $F1_B$, $F2_B$ and $F3_B$ as they generated lung C_{max} 36-, 34- and 27-fold higher than IV, respectively **(Figure 58.a**, **Table 26**, $p < 0.01$, Kruskal-Wallis test with Dunn's post-test) and no significant differences were observed for EN and DPBs between each other ($p > 0.05$, Kruskal-Wallis test with Dunn's post-test). Moreover, $F1_B$ and EN, which are both IR dosage forms with soluble or quickly soluble drug, show comparable PK profiles over time, as expected, but not at the very first dosing times (between ~2 and 10 min). The lower lung C_{max} observed with EN (13.7-fold higher than for IV and 2.7-fold lower than for $F1_B$) is very probably linked to a

high fraction of the deposited solution already being distributed in the systemic compartment before the first dosing time. This shows that the cisplatin microcrystals in F1$_B$ need a few more minutes to be absorbed than a cisplatin solution to be solubilized before they can be absorbed at a comparable (and very fast) rate to that of the EN solution. Indeed, the measured initial lung half-life $t_{1/2}{}^i$ and blood profiles show that cisplatin is absorbed very quickly with these two formulations **(Table 26)**. The longer lung $t_{1/2}{}^i$ (5.0 min *vs.* 2.6 min) observed with EN as compared to F1$_B$ is probably attributable to the partially missed decrease that took place before the first dosing time and to practical experimental difficulties at the first dosing times (e.g. anaesthesia, endotracheal administration, short time slot for lung harvest).

It is worth mentioning that the digestion procedure followed by platinum quantification by ETAAS is able to quantify all platinum-based products, dissolved or not. Therefore high platinum concentrations measured over time with formulations that remained in the lungs longer (F2$_B$ and F3$_B$) can be evidence of dissolved active cisplatin, inactive platinum adducts and cisplatin still entrapped in SLM present in lung fluids. This phenomenon is particularly observable through the PK lung profile of F3$_B$, which exhibited a slower decay than F2$_B$ and can therefore only be interpreted as higher lung retention. Again, this is particularly visible through the lung $t_{1/2}{}^i$ of F2$_B$ and F3$_B$ (9.0 *vs.* 59.9 min; **Table 26**). SLM from F2$_B$ seemed not to be maintained in the lungs after 1 hour, whereas F3$_B$ exhibited high lung retention over 24 hours. This is also visible through the high lung terminal half-life ($t_{1/2}{}^t$ = 72.7 h, measured between 24 and 48 h) of F2$_B$, which was the same order of magnitude as the IR formulation F1$_B$ ($t_{1/2}{}^t$ = 97.0 h) and EN ($t_{1/2}{}^t$ 80.9 h). The slow decrease in platinum long after the majority of inhaled particles are eliminated is probably linked to platinum adducts bound to cell-material in tissues. Platinum can in fact be found up to 6 months in tissues after cisplatin administration (Stewart et al., 1982). In comparison, F3$_B$ had a much lower value ($t_{1/2}{}^t$ = 14.8 h) as cisplatin was still decreasing, probably because some SLM were still present during these measured time-points **(Table 26)**.

Regarding the total exposure of lungs, F3$_B$ had the highest value, with a 10-fold higher lung AUC$_{10min-48h}$ than IV **(Table 26)**. It also exhibited a 3- to 4-fold higher lung AUC than EN, F1$_B$ and F2$_B$. This also confirms the prolonged lung retention abilities of F3$_B$ over the other formulations, and particularly over F2$_B$. The original formulations, blended into F2$_B$ and F3$_B$ had *in vitro* release profiles exhibiting CR over more than 24 hours, and even more so for the latter thanks to better encapsulation provided by the tensioactive effects of TPGS (Article 1). The CR seemed to be preserved in the lungs *in vivo* as suggested by the total blood profile (lower C_{max} and higher t_{max} for F2$_B$ and even further for F3$_B$, see below) but depended

strongly on the ability of particles to stay in the lungs. The non-PEGylated-excipient-comprising formulation F2$_B$ was eliminated from the lungs quicker than F3$_B$, despite showing CR abilities for around 24 hours *in vitro*, but lasted only 1 hour *in vivo*.

After deposition in the lungs, cisplatin after its release from SLM can be subjected to absorptive processes through the lung epithelium. SLM can also be subjected to non-absorptive processes, notably the MCC and MPS. MCC is known to be a slow process (between 2 and 24 h) in human lungs (1 mm/min, *vs.* 20 mm/min in the trachea) (Wauthoz et al., 2015a) and even longer in mice (up to 35 days) (Snipes et al., 1983). MPS is, however, much faster. Maximum alveolar macrophage mobilization has been described to be around 1 hour after incubation for ~1.5 μm particles in humans and around 4.1 hours in mice, using aluminosilicate particles with aerodynamic diameters from 0.7 to 2.8 μm (Snipes et al., 1983). MPS is, however, known to be controllable by surface modification through PEGylation (Wattendorf et al., 2008). Indeed, charging and hydrophobicity of the particle surface are known to enhance phagocytosis. Addition of PEG, which is highly hydrophilic, is therefore an appropriate strategy to try to limit macrophage recognition and phagocytosis. Moreover, they are generally well-tolerated and show little to no toxicity or immunogenicity, even in the lungs (Klonne et al., 1989). TPGS carries a 1000 Da PEG chain and is classified as a generally recognized as safe, or "GRAS", excipient by the FDA.

To limit MPS, TPGS was added to the formulation that was blended into F3$_B$. This also explains the great increase in lung retention when compared to F2$_B$. It also shows that *in vitro* dissolution tests cannot be easily extrapolated to *in vivo* conditions as the deposition surface is much larger in the alveolar epithelium (100 m^2 *vs.* a few cm^2), the volume and exact composition of the lung surfactant are not easily imitated and particle residency and MCC or MPS cannot be reproduced (Wauthoz et al., 2015a). However, these tests remain very useful as they give indications of the release abilities of formulations, helping to compare them with each other.

Regarding the PK curves of platinum total blood concentration *vs.* time **(Figure 58.b)**, we observed lower concentrations for all inhaled profiles compared to IV and that all were very different to IV, which exhibited a 4-fold higher blood C_{max} (at the first dosing time, as expected). This was observed throughout the observed period (10 min to 48 h), except the last dosing time of F3$_B$, which showed a higher concentration than for IV. Cisplatin is well-known to exhibit a biphasic decay when administered by IV bolus. In humans, the initial clearance exhibits a blood $t_{1/2}{}^i$ of 25.5 to 49.0 min. This is followed by slow elimination, with a blood $t_{1/2}{}^t$ of up to 3 days (DeConti et al., 1973). In mice, these values are shorter, with a

a) Lungs — b) Total blood — c) Kidneys

t_{max}	10 min	2 min#	2 min#	2 min#	2 min#
t_{max}	10 min#	30 min	30 min	1 h	2 h
t_{max}	10 min#	30 min	60 min	10 min#	30 min
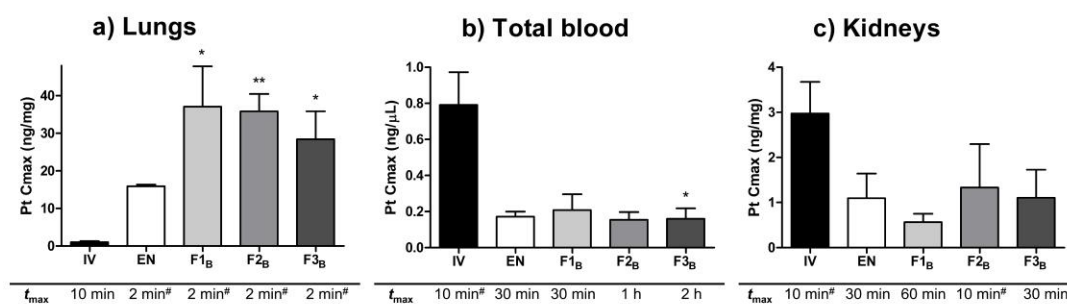
#first measured time point

Figure 59. C_{max} and t_{max} of platinum in the lungs (**a**), blood (**b**) and kidneys (**c**) for all administered formulations and routes (mean ± SEM, n = 5 per time), statistical comparisons were performed in comparison with the IV control, * $p < 0.05$, ** $p < 0.01$ (Kruskal-Wallis test with Dunn's post-test for lungs and total blood, one-way ANOVA with Bonferroni's post-test for kidneys).
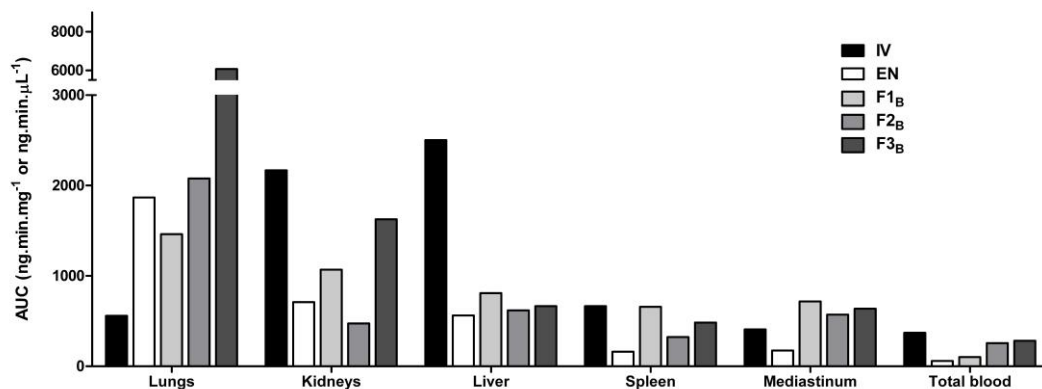
Figure 60. $AUC_{10min-48h}$ of all PK curves of platinum in harvested organs for all administered formulations and routes (mean, n = 5 per time, 8 times).

reported first elimination exhibiting a blood $t_{1/2}^i$ of 7.4 min and a blood terminal elimination $t_{1/2}^t$ of approximately 2 days (van Hennik et al., 1987). These IV values were in the same order of magnitude in our study (**Table 26**, values between brackets), but not with the inhaled formulations. The latter was predictable considering that the inhaled assays follow a more complex multi-compartmental PK model and need to be solubilized and absorbed before they are distributed in the blood. Indeed, once dissolved or release from its formulation in the lungs, the drug is available to either bind to its designed target or be absorbed through the lung epithelium, either by passive diffusion or by saturable active transport (Wauthoz et al., 2015a). Cisplatin is slightly soluble in saline (1 g/L) and slightly hydrophilic (logP -2.21). However, our results show that cisplatin can be readily absorbed through the lung epithelium with IR formulations or EN. This is probably attributable in part to the very small size of this molecule, which can diffuse through tight junction pores and through the very large and very thin permeable lung membrane.

IR formulation $F1_B$ and EN showed lower concentrations in total blood over time than their CR counterparts $F2_B$ and $F3_B$ **(Figure 58.b),** but comparable blood C_{max} **(Figure 59.b)**. Meanwhile, $F2_B$ showed its highest total blood concentration after 1 hour **(Figure 59.b)**, compatible with the shifted and accelerated decrease observed with its lung PK profile. Finally, $F3_B$ had a blood t_{max} of 2 hours **(Figure 59.b)**, but with high and close values all over the measured period, which led to the highest measured blood $AUC_{10min-48h}$ of all inhaled experiments **(Figure 60)**. This profile confirms that the lung retention of $F3_B$ in lungs is probably combined with the formulation's CR.

In the literature, analysis of cisplatin is frequently done through platinum quantification with ETAAS (which is a non-specific method) on plasma to assess the total active platinum species only. This process is easier because the matrix is less complex than total blood and requires little to no digestion. In blood, more than 90% of cisplatin is considered inactive and bound to proteins after a few hours. This is however impossible to assess in organs, where the quantified platinum reflects both active and inactive species. To compare all platinum species distribution in tissues with that in blood, we chose to analyze platinum in total blood without protein separation. However, this led to comparable blood C_{max} measurements for all inhaled experiments **(Figure 59.b)**, which is compatible with the progressive accumulation of platinum species (reacted or not) in this compartment and their slow elimination **(Figure 58.b)**. In addition, cisplatin does not seem to trigger saturable transport mechanisms in the lungs (it is absorbed quickly and freely). For these reasons the blood t_{max} is a better indicator of the cisplatin release from the formulations in the lungs than

lung C_{max} in this case. The dissolution rate of deposited permeable drug is often assessed from the plasma PK only. Indeed, direct lung PK requires whole organ harvesting, which does not discriminate between dissolved and undissolved drug particles (Wauthoz et al., 2015a). In terms of lung elimination of deposited drug particles, lung $t_{1/2}$ and AUC are the best parameters for determining this as they take into account all clearance mechanisms (Wauthoz and Amighi, 2015). This is shown with $F2_B$, where an active elimination process has been assessed.

Regarding renal exposure for platinum derivatives, a dose-effect relationship is well-known (Yao et al., 2007) and localized administration could theoretically help lower the dose-limiting toxicities in kidneys by lowering the unwanted exposure. Kidney C_{max} were higher for the IV route (2.97 ± 1.58 ng/mg) than for all inhaled experiments (from 0.57 ± 0.41 to 1.33 ± 2.16 ng/mg) but the differences were non-significant due to the high encountered variability **(Figure 59.c)**. Additionally, we observed a kidney $AUC_{10min-48h}$ for $F3_B$ that was higher than for all the other inhaled experiments and in the same range as the kidney $AUC_{10min-48h}$ for IV **(Figure 60)**.

Platinum concentrations in kidneys are generally higher than in blood after IV administration, which suggests an active accumulation of drug in renal cells (Yao et al., 2007). It was verified in our study, where we found an average 4-fold increase in kidney concentrations compared to that in blood, independent of the route of administration. Renal clearance of cisplatin is known to be a non-linear and saturable process (Reece et al., 1985). In kidneys, cisplatin undergoes glomerular filtration and tubular secretion and reabsorption (Yao et al., 2007). Cisplatin reabsorption is known to be saturated immediately after IV bolus administration, when blood concentration is the highest (Reece et al., 1985, Forastiere et al., 1988). With IR inhaled formulations (i.e. EN and $F1_B$), platinum blood concentrations followed similar PK profiles **(Figure 58.b),** which could provoke early saturation of reabsorption, lowering renal clearance and *in fine* kidney exposure. Slowly-decreasing platinum concentrations in kidneys and therefore in the blood could be another indication of tubular reabsorption saturation. This is also visible through the shorter kidney t_{max} compared to that of blood (**Figure 59.b.c**, $F3_B$). Indeed, cisplatin and its reactive species are mostly eliminated from the body through renal excretion. CR combined with lung retention could lead to kidneys being exposed for longer periods to circulating unbound platinum species, leading here to higher platinum exposure. Still, the presence of platinum in the kidneys after administration does not necessarily imply renal toxicity. Forastiere et al. (1988) showed no higher kidney toxicity when administering the same dose of cisplatin in patients over 5 days by continuous infusion than by intermittent bolus (which in our case could be compared to

CR versus IR) despite a 2-fold increase in unbound platinum in the plasma. This is in accordance with other observations, showing that cisplatin plasma C_{max} seems to have more importance than the AUC as a predictive parameter of its nephrotoxicity (Nagai et al., 1996) or its ototoxicity (Rademaker-Lakhai et al., 2006). Finally, increased platinum exposure in kidneys may not be an issue as it could be administered at much lower doses by inhalation and yet still provide increased lung exposure overall. Regarding the PK of other organs (i.e. liver, spleen, mediastinum), exposure was lower in the liver after inhalation than from IV, with a 2.5-fold reduction in exposure overall **(Figure 60)**. There were also very few differences in exposure between inhaled formulations. Exposure in the spleen showed some variability, with a lower $AUC_{10min-48h}$ for EN than for all other experiments. In the mediastinum, the same kind of observation was made, but mostly for DPBs, which is particularly interesting as it could help promote higher concentrations in the periphery of the lungs and help combat micrometastasis. However, measurements were often close to the LOD or the LLOQ of the quantification methods in these low-weight samples.

To measure the interest of the inhaled route using CR DPI formulations, we used two ratios of AUC, T_e the targeting efficiency and T_a the targeting advantage. The T_e is the ratio of the AUC in the lungs to the sum of the AUC in all the others non-target organs (Gill et al., 2011). It represents the efficiency of a formulation in reaching the targeted organ while avoiding unwanted exposure in distant ones. The T_e was 18-fold higher than for IV (0.09) with F3$_B$ (1.6), due to the lung retention and CR abilities of the formulation, while it ranged between 2- and 4-fold higher than for IV with the other inhaled administrations **(Table 26)**. This again shows the validity of a cisplatin CR DPI concept, which, to our knowledge, we are the first to report *in vivo*. For comparison, in their work using paclitaxel, a much more lipophilic cytostatic drug than cisplatin, embedded in PEG-lipid micelles, Gill et al. (2011) exhibited a T_e for IV in the same range as our results (0.05) but that was much higher (132-fold) for their long-lasting formulations (6.57) than that which we observed for F3$_B$. This lower targeting efficiency in our study is caused by the higher platinum concentrations found in the kidneys for F3$_B$. Again, this may not reflect cisplatin concentration only but rather active and inactive platinum species that are filtered by the kidneys. The benefits of CR through the lung parenchyma will therefore only be assessed through a systemic toxicity evaluation.

We also measured the T_a, as the ratio of the AUC in the lungs for an inhaled route to the AUC in the lungs with the IV route. It represents the advantage of lung exposure to cisplatin versus that achieved by IV administration, and does not consider the other organs

(Yapa et al., 2014). It is therefore closer to a prospective efficacy assessment than T_e, which is more focused on the potential systemic toxicity. The T_a was 11-fold higher for F3$_B$ than for IV (10.9 *vs.* 1) due to the localized delivery and prolonged lung retention of the formulation **(Table 26)**. The T_a ranged between 2.6 and 3.7 for the other inhaled DPBs. In their study, Yapa et al. (2014) focused their work against cystic fibrosis using nebulized colistimethate sodium, which is a much larger molecule than cisplatin. It therefore has the natural ability to remain in the lungs for much longer periods even without a complex carrier. These properties explain the much higher T_a (387) that they measured in sputum, compared to what we observed with cisplatin in lung digestates.

2.5. Conclusion

Inhaled delivery of cisplatin using DPI is an interesting approach. It helps increase cisplatin exposure in the lungs while potentially decreasing toxicities through lower exposure of non-target organs. Cisplatin, because of its low molecular size is readily absorbed through the lung epithelium. The CR of DPI previously achieved *in vitro* were confirmed *in vivo* but for a shorter extent relative to *in vitro* profile and only through PEGylated-excipient-comprising formulations that permitted the absorption of platinum to be sustained for up to 48 hours, due to their prolonged lung retention properties. In contrast, the non-PEGylated-excipient comprising formulations showed a rapid lung clearance independently to its controlled release, certainly due to a rapid uptake from alveolar macrophages. Therefore, if active elimination was not overcome for an easy soluble and permeable drug-based formulation such as cisplatin, formulation with controlled release properties will not bring higher lung retention.

Because of platinum species' particular renal clearance mechanisms, the CR of DPI and their prolonged retention in the lung caused an increase in kidney exposure when compared to IR DPI but to a level comparable to IV. However, it was associated with a 10.6-fold increase in lung exposure. Acute exposure was also greatly reduced using this approach by reducing the C_{max} in non-target organs and probably the active cisplatin in the lungs. Local and systemic toxicity, along with the DPIs' efficacy on lung tumour models in mice using this approach are now being assessed in vivo.

2.6. Acknowledgments

3. Conclusion and perspectives regarding platinum pharmacokinetics in mice

This study confirmed that the presence of PEGylated excipients in the composition of the SLM is mandatory for their prolonged residence in the lung following their deposition. This longer residence time helps obtain a controlled delivery of cisplatin embedded into the SLM for ~7 h in the lung parenchyma, which results in decreased C_{max} and increased t_{max} in the systemic compartment (total blood) and in distant organs. The PK profile in blood is partly the reflect of the dissolved cisplatin able to be absorbed. Therefore a lower C_{max} in the blood could be the reflect of a slower release of cisplatin in the lungs. This was not observed for SLM without PEGylated excipients, which were more rapidly eliminated from the lungs in ~1 h, making them unable to provide a CR of cisplatin after deposition. The IR formulation and the inhaled solution, used as comparators showed that solubilized cisplatin was by nature highly permeable in lung tissues. This was observed through a very short $t_{1/2}$ of a few minutes in the lungs. This quick passage from the lungs to the systemic compartment was also observable through a shorter t_{max} in the systemic compartment (total blood). This shows the importance of CR for drugs exhibiting high lung permeability, as it could cause a systemic action rather than the desired local one. Moreover, the prolonged exposure to drugs near the tumour site is a known factor in increased tumour penetration. Finally, too high solubilized drug concentrations could provoke higher local toxicity in the lungs (Minchinton et al., 2006, Saggar et al., 2013). The PK advantage of inhalation route was also confirmed through the calculation of the targeting advantage and targeting efficiency. However, when comparing these values to those of other drugs such as paclitaxel (Gill et al., 2011), cisplatin exhibited a lower targeting advantage to the lungs, very probably because of its higher solubility and its very high permeability. Moreover, while the platinum AUC in the lungs clearly increased with inhaled formulations, in particular with the CR and lung lasting formulation (cisplatin/TS/TPGS 50:49.5:0.5), the controlled-release of cisplatin from the lungs was also responsible for an increase in platinum kidney exposure. After these PK evaluations, the most interesting formulations have been evaluated in terms of their efficacy on a preclinical model and in terms of local and systemic tolerance.

Part III – Tolerance and efficacy assessment of DPI formulations

1. Introduction

The best formulation candidates were determined by the formulation study and the PK study, as described earlier in this work. One immediate release (95:5 cisplatin/TPGS) formulation and one controlled release (50:49.5:0.5 cisplatin/TS/TPGS) formulation showing prolonged lung retention properties were selected. The end goals of the remaining part of the work were to evaluate (i) the toxicity of these formulations in mice lungs and (ii) their efficacy against the Madison 109 (M109-HiFR) lung tumour model on mice. This model had been previously developed in the laboratory (Rosière, 2016) to assess the efficacy of temozolomide and paclitaxel folated nanoparticles. To do so, the activity of cisplatin on the M109-HiFR cell line before and after grafting needed to be assessed beforehand. This preliminary study included an *in vitro* cell-viability assessment using a colorimetric MTT assay. It was followed by an *in vivo* survival assessment of grafted mice following the administration of cisplatin solutions (EN and IV).

Following these preliminary studies, systemic toxicity of the best two selected DPI formulations was assessed by their tolerance. It was established by determination of the maximum tolerated doses (MTD) following their administration 3 times a week for 2 weeks, and compared to that of EN and IV. This chronic administration scheme, which would then be set as the basis of the following efficacy evaluation, was as close as possible to what would be envisioned in a clinical setting (once or twice-a-day administration). The frequency of repeated endotracheal administrations *in vivo* is in practice limited by the concomitant general anaesthesia of the mice. After anaesthesia, full recovery can take a few hours, during which the animals do not eat or drink. If the administrations are done too frequently, this recovery phase and the stress induced by the endotracheal procedure is enough to impact the bw of mice when compared to a negative control. As bw is the major end point of the MTD studies in mice, 48 h was previously determined as the minimum interval between two administration procedures (Wauthoz et al., 2010). Moreover, because the developed efficacy model showed the first deaths in control mice ~20 days following the graft, a maximum of 2 weeks was determined for the treatment arm, starting after a 5 days post-graft recovery period where tumour involvement is observed. Therefore, the chronic administration scheme was fixed at 3 times a week for 2 weeks.
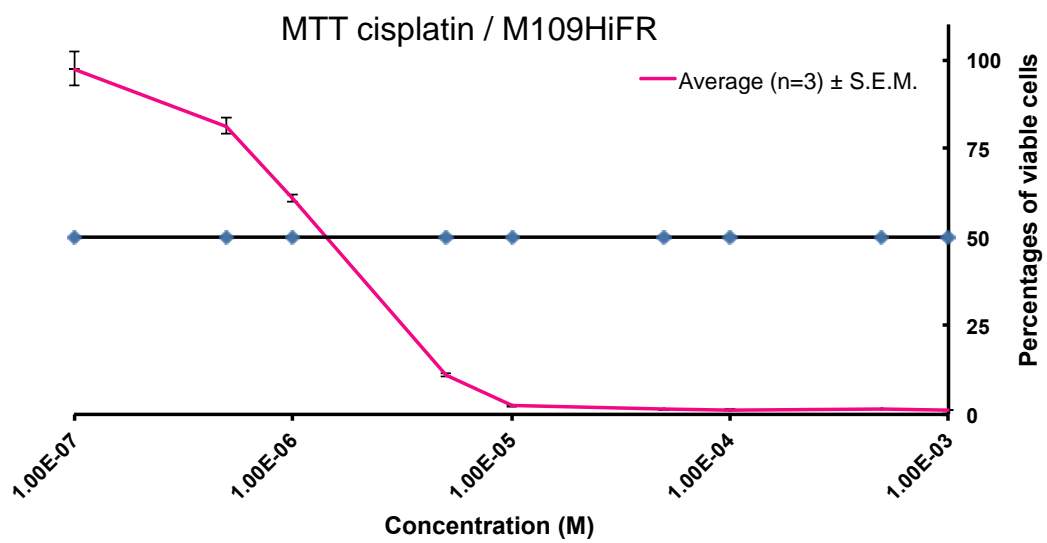
Figure 61. Colorimetric MTT assay of M109-HiFR cells incubated with cisplatin solutions between 10^{-3} and 10^{-7} M.

Acute local toxicity was then assessed by analyzing the BALF 24 h following the endotracheal administration of DPI formulations, EN and IV as described before, at their respective chronic MTDs. Total and cell-differential counts were realized, as well as the quantification in the BALF supernatant of pro-inflammatory markers (cytokines TNF-α, IL-6, IL-1β), and tissue-damage markers (total protein content, cytotoxicity). All the tolerance and efficacy experiments were realized on the same strain of BALB/c mice, as difference in sensibility have been observed previously between different mouse strains.

Following this tolerance study, a pre-clinical assessment of the antitumour efficacy of the two selected formulations at their respective MTD was realized against their corresponding IV dose, following the chronic administration scheme, using the M109-HiFR orthotopic lung tumour model.

2. Preliminary evaluations

2.1. Anti-proliferative assay (MTT)

2.1.1. Method

The anti-proliferative activity of cisplatin on the M109-HiFR cell-line was determined by means of a colorimetric MTT assay. Briefly, cells were allowed to grow in a 96-well plate for 24 h at 37°C in an incubator. The culture medium (see 3.2.5.1 M109-HiFR cell culture and grafting) was replaced by fresh medium containing cisplatin at concentrations ranging from 1 mM to 0.1 μM for 2 h (1000, 500, 100, 50, 10, 5, 1, 0.5 and 0.1 μM) and with a cisplatin-free medium-based control. The medium was then refreshed and cells were left to grow for 72 h. The amount of insoluble purple formazan crystals obtained from the mitochondrial reduction of the yellow MTT dye (3-(4,5-dimethylthiazol-2-yl)-2,5-diphenyltetrazolium bromide) is proportional to the activity of remaining living cells. Formazan concentration was determined by spectrophotometry using a Biorad 680XR spectrometer (Biorad, Nazareth, Belgium) at 570 nm. The half maximal inhibitory concentration (IC50) is the concentration of cisplatin that is able to inhibit 50% of cell growth, compared to the untreated control. This experiment was realized three times in sextuplate.

2.1.2. Results and discussion

It showed that the M109-HiFR cell viability was already hindered by cisplatin concentrations as low as ~10^{-7} M, equivalent to ~30 μg/L, **(Figure 61)** and that the IC50 was equal to 1.85 ± 0.32 μM. This confirmed the *in vitro* activity of cisplatin against the M109-HiFR tumour cell-line, which was therefore grafted into mice to assess cisplatin activity *in vivo*.
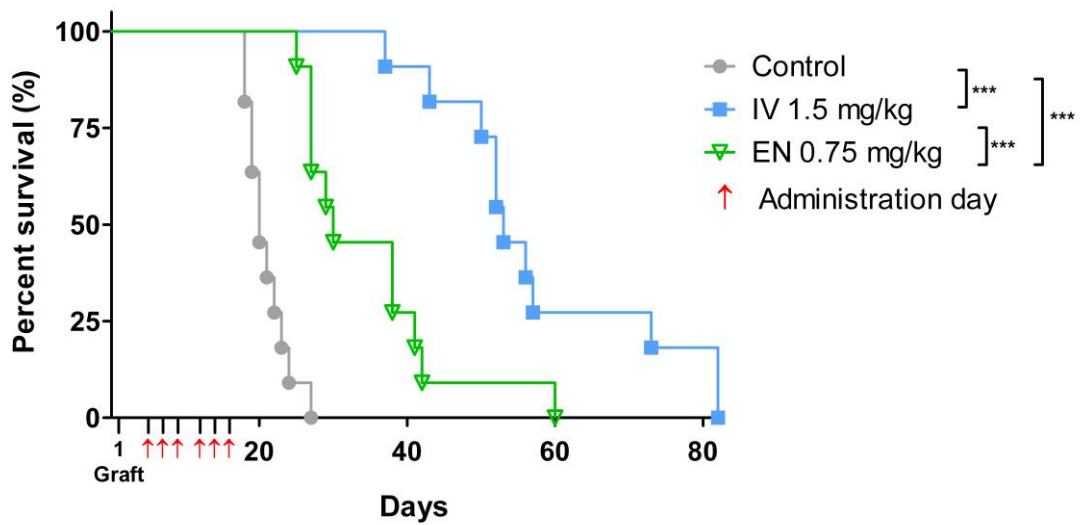
Figure 62. Kaplan-Meier survival curve of M109-HiFR grafted mice following tri-weekly treatment with cisplatin for 2 weeks, by IV at 1.5 mg/kg (n = 11) by EN at 0.75 mg/kg (n = 11) and without any treatment (control group).
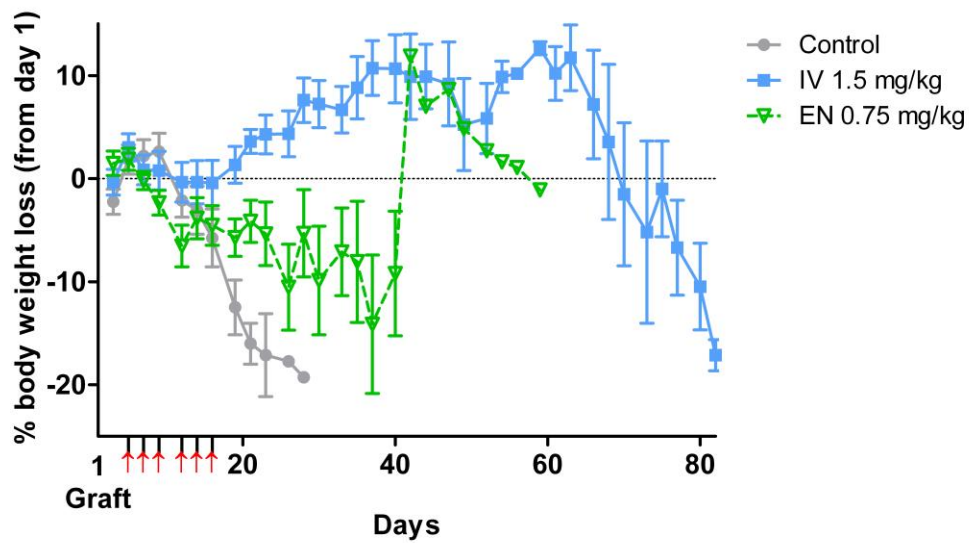
Figure 63. Body weight loss following cisplatin administration in M109-HiFR grafted mice. After day 40, only 1 mouse remains in the EN 0.75 mg/kg group.

2.2. Exploratory survival study

The aim of this exploratory study was to confirm the sensitivity of the M109-HiFR orthotopic model to cisplatin *in vivo* and evaluate the different time-scale for response using cisplatin at regular doses.

2.2.1. Method

The M109-HiFR cells were cultured and grafted into 6-week-old BALB/c mice (Charles River, L'Asbresle, France), following the procedures (i.e. number of cells, surgery) further described in Article 3 (see 3.2.5.1 M109-HiFR cell culture and grafting). Cisplatin was administered to mice following the chronic administration scheme that was used later (3 times a week, 2 consecutive weeks). This scheme consisted in the administration of cisplatin solutions (NaCl 0.9%) at a grossly pre-determined chronic MTD of 1.5 mg/kg by IV and 0.75 mg/kg by EN *vs.* a control group of untreated grafted mice (n = 11 for each group). Mice were grafted on day 1 and cisplatin was administered on days 5, 7, 9, 12, 14 and 16. Mouse survival was verified each day in the morning. Mice exhibiting bw losses higher than 20% w/w from their initial bw on the day of the graft or 15% w/w from the previous weighing, or any of the pre-determined humane surrogate endpoints (e.g. respiratory distress, paralysis, prostration for more than a day) were euthanized and counted on the next day.

2.2.2. Results and discussion

We observed that all control mice died between day 18 and day 27, with a median survival (MS) of 20 days and that death was preceded by a steep bw loss **(Figure 62**, **Figure 63)**. The group treated with IV cisplatin at the highest dose of 1.5 mg/kg had a significantly higher survival ($p < 0.001$ *vs.* control, log-rank test), with a MS of 53 days. The EN group at 0.75 mg/kg showed a lower survival, with a MS of 30 days, which was significantly different from the control and from IV at 1.5 mg/kg ($p < 0.001$, log-rank test). Bw losses, attributable to tumour invasion a few days before mouse death, were also seen in the EN group and to a higher extent in the IV group **(Figure 63)**.

This lower survival for the EN arm could be explained by the lower administered dose of cisplatin than for IV. However, this does not account for the PK advantage we had determined for EN. During the PK study, EN at 1.25 mg/kg had shown a T_a of 3.3 **(Table 26)**. One possibility is that cisplatin in solution crosses the lung epithelium too quickly to exhibit a local action. One other possibility is that the model is too aggressive and metastasizes too quickly, which makes IV treatment more efficacious (see Article 3). Finally,

during treatment with EN in particular, high bw loss was observed, especially during the two-week administration period. These losses came dangerously close to the critical bw end points of total bw loss **(Figure 63)** and were in the beginning higher than the negative control, which was not the case for IV. The MTD of EN had been pre-evaluated on healthy untreated mice (data not shown). This dose had shown little influence on the bw of healthy mice but was determined using wider margins than those finally described in Article 3 (see 3.2.3. Maximum tolerated dose of repeated administrations). We had initially defined the maximum level of bw loss for mice at a 10% w/w threshold to establish the tolerance of cisplatin by EN. This led to the determination of a maximal dose of 0.75 mg/kg by EN under the repeated dosing scheme. IV cisplatin (1.5 mg/kg) had a lower influence than EN on the bw losses of grafted mice. This influence on bw loss was however higher in tumour grafted mice than that previously observed in healthy mice. This may be attributable to the repeated administrations of cisplatin in mice, which are weakened by lung tumour involvement. These results called for a thorough evaluation of the MTD to determine the safest administration dose, in particular for the evaluation of formulations. However, it is technically difficult to establish the MTD on grafted mice (e.g. synchronized cell culture, grafting procedure and multiple dose preparation). Therefore, for the following MTD study, a narrower margin was defined for the determination of the MTD in healthy mice (i.e. 5% w/w mean bw loss), which finally led to a lower MTD value for EN (see Article 3 below).

3. Article 3
"In vivo local and systemic toxicity and antitumour efficacy of cisplatin solid lipid microparticles with controlled-release properties against lung cancers"

[a]Levet V., [a]Rosière R., [b]Langer I., [a]Amighi K., [a]Wauthoz N.

Submission pending

[a] Laboratory of Pharmaceutics and Biopharmaceutics, Faculty of Pharmacy, Université libre de Bruxelles (ULB), Bd. du Triomphe CP 207, Campus de la Plaine, 1050 Brussels, Belgium. [b]Institut de Recherche Interdisciplinaire en Biologie Humaine et Moléculaire (IRIBHM), Université libre de Bruxelles (ULB), Route de Lennik, 808, Campus Erasme, 1070 Brussels, Belgium.

3.1. Introduction

Since the early 1970s, inhaled chemotherapy (CT) has been proposed as a potential treatment of lung malignancies, including primary cancers (i.e. non-small cell lung cancer and small cell lung cancer) but also secondary cancers metastatic to the lungs such as osteosarcoma. It has reached the clinic (Gagnadoux et al., 2008) but not yet the market. The local administration of conventional chemotherapeutic drugs provides an evident pharmacokinetic advantage. It is theoretically able to increase the therapeutic index of fairly toxic drugs, which are typically administered systemically, by increasing drug exposure near the tumour site, and at the same time decrease the systemic exposure (Gagnadoux et al., 2008, Zarogoulidis et al., 2012a). However, lung tolerance following the local administration of these drugs must be assessed, as many chemotherapeutic agents are prone to causing pulmonary toxicity by the systemic route (e.g. paclitaxel, docetaxel, irinotecan, bleomycin). Some are even known to cause lung injury by inhalation (e.g. bleomycin-induced pneumonitis), which could have dramatic consequences in lung cancer patients (Sleijfer, 2001, Gagnadoux et al., 2008, Camus et al., 2016).

To date, a few of the conventional CT drugs have reached early-phase clinical trials for locally treating lung cancers, all as solutions or liposomal dispersions administered using a nebulizer device. These are, respectively, 5-fluorouracil (Tatsumura et al., 1983, Tatsumura et al., 1993), 9-nitro-camptothecin (Verschraegen et al., 2004), doxorubicin (Otterson et al., 2007, Otterson et al., 2010), gemcitabine (Lemarie et al., 2011), carboplatin

(Zarogoulidis et al., 2012b) and cisplatin (Chou et al., 2007, Wittgen et al., 2007, Chou et al., 2013).

All these drugs exhibit different physico-chemical properties, which can influence their ability to stay within the lung epithelium and avoid reaching the systemic compartment. Small molecules can usually readily cross thin epitheliums and reach the underlying bloodstream, making them adequate candidates for systemic action through the pulmonary route. However, this property is undesired in the case of inhaled CT, as the drug is quickly eliminated from the lungs, which is prejudicial in terms of pulmonary exposure. Indeed, solid tumour penetration has been linked in part to the duration of drug residence near the tumour site (Minchinton et al., 2006).

Cisplatin in particular is one of the most potent drugs available to clinicians against various types of primary and secondary lung cancers as the centrepiece of the platinum doublet CT (NCCN, 2014b, NCCN, 2015). It is a slightly hydrophilic (log P -2.19) small molecule ($PtCl_2(NH_3)_2$, Mr 300.05 g.mol^{-1}). We have demonstrated in a previous pharmacokinetic (PK) study in mice that it readily crossed the lung epithelium and was quickly distributed in the systemic compartment following its administration as a nebulized solution or with an immediate-release (IR) dry powder inhaler (DPI) formulation (Article 2). The administration of cisplatin to human patients was first realized in the last decade, by means of nebulized liposomes against different subsets of non-small cell lung cancer (i.e. adenocarcinoma, squamous cell carcinoma, bronchoalveolar carcinoma, large cell undifferentiated carcinoma) during a phase I dose-escalating study (Wittgen et al., 2007). It was later administered against a secondary lung cancer in teenaged patients (i.e. osteosarcoma) in a phase Ib/IIa study (Chou et al., 2007, Chou et al., 2013). The observed adverse effects during these two trials were mild after administration of cisplatin up to 40 and 36 mg/m². They included non-pulmonary and mostly gastro-intestinal grade II reactions like nausea, vomiting, dyspnea, fatigue and hoarseness in the first study (Wittgen et al., 2007) and non-pulmonary grade II reactions such as nausea and vomiting in the second study (Chou et al., 2013). Cisplatin therefore seems to be generally well-tolerated by the pulmonary route.

Cisplatin is generally active at relatively high doses by the systemic route (i.e. in the hundreds of mg) against lung cancers (NCCN, 2014b, NCCN, 2015). Moreover, and in particular during the first clinical study by Wittgen et al. (2007) and despite up to 8 hours administration sessions, liposomal nebulizer formulations were never able to reach the

toxicity limiting the dose. This flaw could prevent clinicians from increasing the dose to efficacious levels in a reasonable administration timeframe. This limitation was attributable to the relatively low solubility of cisplatin in aqueous NaCl 0.9% solution (i.e. ~1 mg/mL) and the well-known low deposition abilities of the aerosols generated by nebulizer devices.

To circumvent this issue, formulations delivered by dry powder inhalers were developed previously (Article 1). They involved the formulation of tristearin (TS)-based solid lipid microparticles (SLM) embedding cisplatin microcrystals. These SLM are able to provide a high drug loading, a high deposited fraction and a slower release of cisplatin in lung fluids. This slower release, essential to limit quick passage of cisplatin to the systemic compartment, was proven feasible *in vivo* thanks to the addition of alpha-tocopheryl polyethylene glycol 1000 succinate (TPGS), providing PEG chains potentially able to hinder surface recognition and therefore alveolar macrophage clearance mechanisms in the lung (Article 2).

This caused a decrease in the systemic exposure and in the total blood C_{max} and an increase in the total blood t_{max} compared to the IV route and to IR inhaled formulations. A lower concentration of cisplatin solubilized in lungs fluids could influence the local tolerance of formulations but could also influence their efficacy.

Very few excipients are approved for inhalation. The addition of new excipients must always be fully evaluated in animal models, particularly regarding their safety and in terms of inflammation and overall tolerance, prior to human investigations (Pilcer et al., 2010).

The aim of this work was therefore to evaluate the safety of cisplatin DPI formulations with controlled release (CR) and prolonged lung retention properties in terms of maximal tolerated dose (MTD) and local tolerance in order to compare their antitumour efficacy in terms of survival on a preclinical model of lung tumour.

3.2. Materials and methods

3.2.1. Materials

Cisplatin was purchased from Shanghai Jinhe Bio-technology Co., Ltd. (Shanghai, PRC). TS was purchased from Tokyo Chemical Industry Co. Ltd. (Tokyo, Japan) and TPGS from Sigma-Aldrich (St. Louis, USA), Pearlitol® 25C mannitol was donated by Roquette Frères (Lestrem, France). L-leucine was purchased from Merck Millipore (Darmstadt, Germany). Ultrapure Milli-Q® water was obtained from a Purelab Ultra® purification system (Elga Veolia Water Technologies, Wasquehal, France) providing a resistivity higher than

Formulation	Composition (% w/w)	Released fraction		$t_{1/2}^{i}$lungs (min)	C_{max} lung (ng/mg)	C_{max} blood (ng/μL)	t_{max} (min)	*Ta*
		10 min	24 h					
F1	95:5 Cisplatin/TPGS	97 ± 5	100 ± 0	2.6	#37 ± 24	0.21 ± 0.20	30[blood]	2.6
F2	50:49.5:0.5 Cisplatin/TS/TPGS	24 ± 3	55 ± 11	59.9	#28 ± 17	0.16 ± 0.13	120[blood]	10.9
EN	100% w/v cisplatin in 0.9% NaCl	ND	ND	5.0	#16 ± 1	0.17 ± 0.06	30[blood]	3.3
IV	100% w/v cisplatin in 0.9% NaCl	ND	ND	15.3	1.0 ± 0.3	#0.8 ± 0.4	10[lung]	1

From Article 1 and Article 2, ND not determined. #C_{max} at first time-point.

18.2 MΩ.cm^{-1}. Roswell Park Memorial Institute medium (RPMI) 1640 (folate-free), fetal bovine serum (FBS), phosphate buffer saline (PBS) and gentamycin, penicillin-streptomycin and trypsin-EDTA solutions were purchased from Life Technologies (Merelbeke, Belgium). Matrigel was purchased from Corning (Lasne, Belgium). Xylazine (Proxylaz®) was obtained from Prodivet Pharmaceuticals (Eynatten, Belgium), ketamine (Nimatek®) was obtained from Eurovet Animal Health (Ae Bladel, Netherlands), sodium pentobarbital (Nembutal®) was obtained from Ceva Santé Animale (Brussels, Belgium). All chemicals and solvents were of analytical grade.

3.2.2. Dry powder inhaler formulation production, characterization and administration

Cisplatin dry powder inhaler (DPI) formulations were produced and characterized as described previously (Article 1). Briefly, bulk cisplatin powder was first suspended in isopropanol and subjected to an 18-fold size reduction into microcrystals in the low micrometre range. This was done by high-speed-homogenization (10 min at 24 000 rpm) followed by high-pressure homogenization at 5 000 psi (10 pre-milling cycles), 10 000 psi (10 pre-milling cycles) and 20 000 psi (20 milling cycles). TS and/or PEGylated excipient TPGS were solubilized in isopropanol, added to the cisplatin microsuspension and spray dried to produce DPI formulations based on SLM embedding cisplatin. These formulations exhibited high drug loading ($\geq$ 50% w/w cisplatin), high deposition abilities (fine particle fraction $\geq$ 37%) and CR in simulated lung fluid for more than 24 h.

The most promising DPI formulations were selected from the performed pharmacokinetic study *in vivo* (Article 2). The same general administration and cisplatin preparation procedures were used in the present study. Briefly, the DPI formulations were first blended to adjust the administered dose to the body weight (bw) of mice, using a highly dispersive spray dried mannitol/L-leucine (10:1) diluent with improved flow properties. The diluent was then mixed with the DPI formulation in a sandwich mix method and 3D-mixed with a Turbula 2C motion mixer (Bachofen AG, Uster, Switzerland) for 4 h to reach ~2% w/w cisplatin. The same procedures were applied in order to produce a cisplatin-free DPI powder of the vehicle of the F2 formulation (F2$_V$: TS/TPGS 99:1). F2$_V$ was then mixed with the mannitol/L-leucine (10:1) diluent, following the same blending procedures and at a theoretical ~1% w/w concentration, in order to match the excipient doses of F2.

The composition of the selected DPIs for this study and their main in *vitro* release and *in vivo* pharmacokinetic properties are reported in **Table 27**.

The administration of the resulting dry powder blends and of a cisplatin solution by endotracheal nebulization (EN) to the lungs were realized using a DP-4M® dry powder insufflator (Penn-Century Inc., Wyndmoor PA, USA) and a Microsprayer IA-1C® connected to a FMJ-250 high-pressure syringe (Penn-Century Inc.), respectively. Administration was realized under anaesthesia using an intra-peritoneal injection of a xylazine/ketamine (1.5:112.5 mg/kg) mix (Proxylaz®, Prodivet Pharmaceuticals, Eynatten, Belgium - Nimatek®, Eurovet Animal Health, Ae Bladel, Netherlands). The DP-4M device was loaded with ~2.0 mg of powder blend, its tip was introduced into the mouse trachea and the AP-1® air pump (Penn-century, Inc.), set at 200 µl (tidal volume of a mouse) was activated 5 times. EN was realized using a fixed 50 µL administration volume using solutions of cisplatin with different concentrations adapted to the bw of mice. Cisplatin was also administered by the IV route using sterile solution and a 10 µL/g volume of injection.

3.2.3. Maximum tolerated dose of repeated administrations

The cisplatin-based DPI formulations and cisplatin-based EN and IV solutions described in **Table 27** were administered to 6-week-old BALB/cAnNRj (Janvier Labs, France) healthy mice (i.e. non-tumour-bearing mice). Administration was realized following the procedures described previously (see 3.2.2. Dry powder inhaler formulation production, characterization and administration), under a repeated administration scheme of 3 days/week for 2 weeks (n = 3, day 0, 2, 4 7, 9 and 11). The cisplatin doses were escalated from 0.5 mg/kg up to the MTD, defined as the last dose for which mean body weight (bw) loss did not exceed 5% w/w during the 40 days of follow-up after first dosing. For F1 and EN, the assayed doses were 0.5 and 1.0 mg/kg. For F2, the assayed doses were 0.5, 1.0 and 1.5 mg/kg. For IV, the assayed doses were 0.5, 1.0, 1.5 and 3.0 mg/kg. The powder blends of F1 and F2, diluted to 1.84 and 1.64% w/w, respectively, were from the same batch as the previous PK study (Article 2). The powder amounts weighed into the device were adjusted to the current bw of mice, taking into account the powders' respective cisplatin concentration and *in vivo* emission efficiency, established during the previous PK study (i.e. 69 ± 34% w/w and 78 ± 29% w/w, respectively). For EN, two cisplatin solutions were prepared at 0.15 and 0.30 g/L in sterile saline. For IV, four solutions were prepared at 0.050, 0.10, 0.15 and 0.30 g/L in saline and sterilized using a 0.22 µm-pore size Acrodisc® syringe filter (Pall Corporation, Port Washington, NY, USA). All solutions were kept protected from light and used within 24 h. Mouse bw was recorded 3 times a week, on Mondays, Wednesdays and Fridays. The bw progression of non-treated control mice of the same age was also recorded (n = 3).

3.2.4. Acute local toxicity

Acute local toxicity was assessed 24 h following a single administration by analysis of the bronchoalveolar lavage fluid (BALF) from 6-week-old BALB/cAnNRj healthy mice (Janvier Labs). For this, mice were administered cisplatin to the lungs as dry powder blends (F1 and F2, n = 7) or EN (n = 5), at the MTD determined previously, following the procedures described previously (see 3.2.3. Maximum tolerated dose of repeated administrations). Cisplatin was also administered by the IV route at doses matching the MTD of F1 and F2, respectively (n = 5). A negative and a positive control, involving untreated mice (n = 4-5) and ~1 μg of lipopolysaccharide (LPS) from *E. coli*-treated mice (n = 5) were included for each assay.

In order to establish whether the observed effects were due to cisplatin or to the excipients in F2, the local effect of F2$_V$ on the BALF was established after its endotracheal administration using the same procedures as described previously, at the same dose as F2 at its MTD, considering a theoretical concentration of 1.0% w/w in the dry diluent.

At 8 h (for the LPS group) and 24 h (for all the other groups) post-administration, mice were euthanized using an intra-peritoneal injection of 12 mg sodium pentobarbital (Nembutal®, Ceva Santé Animale, Brussels, Belgium) and BALF were collected as described by Rosiere et al. (2016). Briefly, immediately following euthanasia, mice were exsanguinated by retro-orbital puncture to avoid BALF contamination. The neck region of mice was then opened and a 20-gauge Surflo catheter cannula (Terumo, Leuven, Belgium) was inserted into the trachea and held in place with a silk. Lungs were flushed 3 times with 0.7 mL PBS at 4°C and the collected BALF was kept on ice until total cell count. The total cell count was performed using a Z2™ Coulter Counter (Beckman Coulter, Brea, CA, USA) and then centrifuged for 5 minutes at 160g and 4°C. The cell pellet was then re-suspended in 200 μL cold PBS and set on cytospin slides to establish the differential cell count following cell staining with May Grünwald (Merck, Darmstadt, Germany) and Giemsa (Merck, Germany). In each slide the relative proportions of alveolar macrophages, polymorphonuclear neutrophils (PN), lymphocytes or eosinophils were determined based on observation of 200 cells by optical microscopy. The supernatant was collected and stored at -80°C. The cytokine content in the BALF supernatant was then determined using a mouse-specific enzyme linked immunosorbent assay (ELISA) for IL-1β, IL-6 and TNF-α (DuoSet, RnD Systems, Abingdon, UK), using the procedures defined by the manufacturer. The protein content in the BALF was determined using a Pierce bicinchoninic acid (BCA) Protein Assay Kit (Thermo Fisher Scientific, Zellik, Belgium). The lactate dehydrogenase (LDH) activity in

the BALF was evaluated using a Cayman Chemical LDH Cytotoxicity Assay Kit (Ann Arbor, MI, USA) following adapted procedures from the manufacturer. Briefly, 100 µL of each BALF thawed supernatant were pipetted in duplicate in a 96-well assay plate set on ice and LDH was quantified using 100 µL of LDH reaction solution containing LDH diaphorase. Absorbance was read at 490 nm using a Biorad 680XR spectrometer (Biorad, Nazareth, Belgium) and results were expressed as the relative LDH activity by comparison to the LDH positive control provided in the kit. Local toxicity assays were realized sequentially, as presented in the results section, with new positive and negative controls each time.

3.2.5. Efficacy evaluation on an orthotopic M109-HiFR tumour model

3.2.5.1. M109-HiFR cell culture and grafting

The M109-HiFR mouse lung carcinoma was cultured as described by Rosiere et al. (2016). Briefly, cells were cultured in folate-free Roswell Park Memorial Institute (RPMI) medium (Life Technologies, Merelbeke, Belgium), with 10% v/v FBS (Life Technologies) supplementation, 1% v/v penicillin-streptomycin (Life Technologies) and 0.02% v/v gentamycin (Life Technologies), in an incubator under standard cell culture conditions (37°C, 5% CO_2).

Intrapulmonary implantation of tumour cells from the M109-HiFR sub-line was performed on day 1 as described before (Wauthoz et al., 2015b, Rosiere et al., 2016) on 6-week-old BALB/cAnNrJ female mice (Janvier Labs). Briefly, under general anaesthesia, the skin of the right intercostal region of mice was incised and muscles underneath were discarded to obtain a clear view of the costal region. Mice were then injected between the third and fourth costal bone, into the right lung with 20 µL of a 50:50 v/v mix of RPMI and Matrigel® (Corning, Lasne, Belgium) containing 1.4×10^6 dispersed M109-HiFR cells. The muscle and skin incisions were sutured using an Ethicon Inc. 3-0 silk (Johnson & Johnson, Somerville, NJ, USA).

3.2.5.2. Treatment

Dry powder blends of F1 and F2 were administered to mice (n = 15) on day 5 post-tumour graft, following randomization, using the procedures described previously (see 3.2.2. Dry powder inhaler formulation production, characterization and administration) and under the repeated administration scheme described previously (see 3.2.3. Maximum tolerated dose of repeated administrations) at their respective chronic MTD. These were compared to a negative control of untreated grafted mice (n = 11) and to IV cisplatin at the MTD of F1 and

F2, respectively (n = 11). A larger number of mice were used in the endotracheal arms because of the impact of repeated anaesthesia on the death of grafted mice.

3.2.5.3. Follow-up

Survival was verified each day in the morning (typically at 9 AM). Mouse bw was recorded 3 times a week on Mondays, Wednesdays and Fridays. Mice that showed a bw loss higher than 15% w/w between two weighings or higher than 20% w/w from their bw at the first dosing were immediately euthanized by intra-peritoneal injection of 12 mg sodium pentobarbital (Nembutal®, Ceva Santé Animale, Brussels, Belgium). Mice that showed respiratory distress and prostration with no improvement the next day were then euthanized. For the survival study, all euthanized mice were counted on the next day. Dead and euthanized mice were necropsied and photographs of the lungs and of the empty thoracic cage were taken to evaluate tumour spreading.

3.2.6. Housing conditions and ethics committee approval

For all animal experiments, BALB/cAnNrJ female mice (Janvier Labs, Le Genest-Saint-Isle, France) aged 5-6 weeks were housed 2-3 per cage in filter-top disposable plastic cages (Tecniplast, Buguggiate, Italy). They were subjected to a conventional diet (food and water *ad libitum*) and conventional housing conditions (22 ± 2°C, 55 ± 10% humidity, 12 h night/day cycles.

Experimentation was realized under EU Directive 2010/63/EU for animal experiments and the control of the ULB animal ethics committee (Comité d'Ethique et du Bien-Etre Animal) under approval number 585N.

3.2.7. Statistical analyses

Statistical comparison of three or more sets of data was realized after verifying the homoscedasticity of variance using the Cochran C test. Groups of data were afterwards compared using a Kruskal-Wallis non-parametric test and a Dunn's post-hoc analysis if the C test was significant and a one-way ANOVA and Bonferroni's post-test if the C test was not significant. Survival analyses were realized by plotting a Kaplan-Meier curve and analyzed following a log-rank test. Each analysis and curve plotting was realized using GraphPad Prism® 5.01 software. The significance of results was classified between non-significant for $p \geq 0.05$, significant for $p < 0.05$, very significant for $p < 0.01$ and extremely significant for $p < 0.001$ (scored *ns*, *, ** and *** in tables and graphical results, respectively).
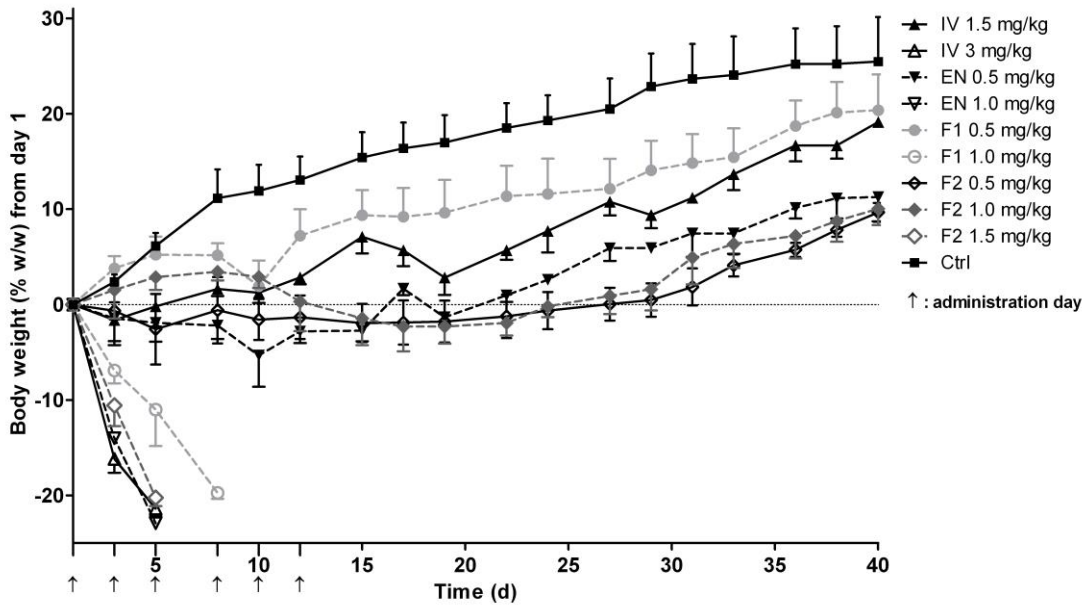
Figure 64. Body weight profiles following cisplatin administration by the IV route, the EN route and with the F1 and F2 formulations at different doses, *vs.* an untreated control (mean ± SEM, n = 3).
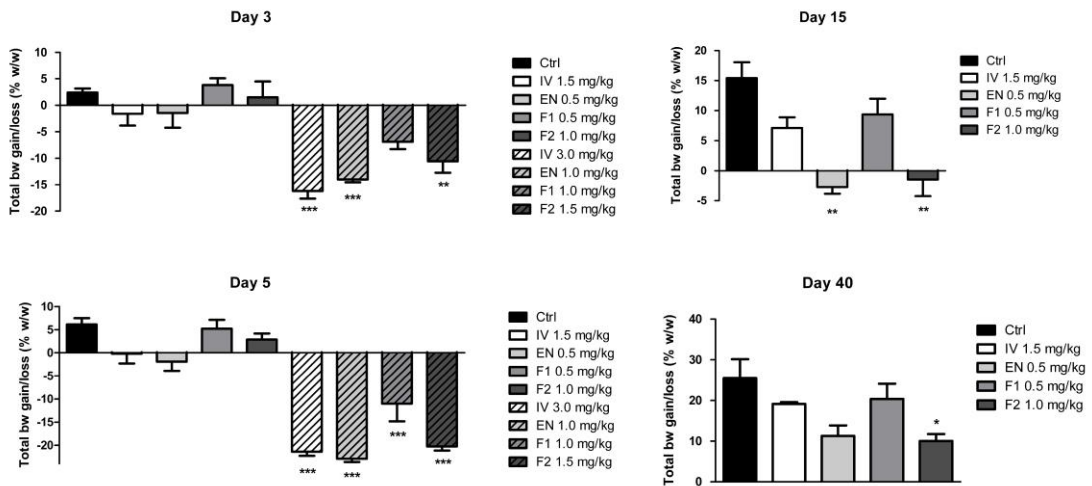
Figure 65. Body weight gain and loss at remarkable time points of the MTD study (mean ± SEM, n = 3). Statistical comparison is done *vs.* an untreated healthy control (Ctrl).

3.3. Results and discussion

3.3.1. Systemic tolerance following chronic administrations

As shown in **Figure 64**, repeated administration of cisplatin under the 3 times a week for 2 weeks scheme was altogether better tolerated by the IV route than it was after each inhaled formulation. More precisely, cisplatin was already well-tolerated by IV at 0.625 and 1.25 mg/kg (individual bw loss < 5% w/w from the beginning of the administration scheme) and up to a 1.5 mg/kg dose following the repeated administration scheme. A higher dose of 3.0 mg/kg was also administered but ended in a very steep total bw loss of 16.2 ± 2.5% w/w only 2 days after the first administration (day 3, **Figure 64**) and of 21.4 ± 1.5% w/w 2 days after the second administration (day 5, **Figure 65**). The 3.0 mg/kg IV group was therefore discontinued. These bw losses were significantly higher than in healthy control mice ($p < 0.001$, one-way ANOVA, Bonferroni's post-test). This remains in accordance with the tolerated IV doses reported for mice, taking into account the various sex, mouse strain and dosing schemes used in other publications. For instance, Siddik et al. (Siddik et al., 1988) reported a 4.0 mg/kg MTD after a single IV dose of cisplatin in female and male BALB/c mice of bw ranging from 20 to 25 g. Staffhorst et al. (Staffhorst et al., 2008) reported an identical 4.0 mg/kg MTD in athymic nude mice after administration of cisplatin once a week for 2 weeks. These values correspond to our observations, as we did not let mice recover for more than 2 days after the first dose. At the lower 1.5 mg/kg dose, total bw loss did not exceed 5% w/w mean bw loss after the first dose (day 3, **Figure 65**), and mice had already recovered more than their initial bw at the end of the two weeks of administration (day 15, **Figure 65**, non-significant difference from the healthy control, $p \geq 0.05$, one-way ANOVA, Bonferroni's post-test).

With aerosolized cisplatin administered as a solution by EN, cisplatin was not well tolerated above 0.5 mg/kg using the repeated scheme. For instance, the upper increment at 1.0 mg/kg resulted in a mean total bw loss of 14.0 ± 0.9% w/w 2 days after the initial administration (day 3, $p < 0.001$ *vs.* Ctrl, one-way ANOVA, Bonferroni's post-test). This steep bw loss was not observed as intensely as during our previous pharmacokinetic study on CD-1 mice with the 48-h group, which were administered a single higher 1.25 mg/kg dose of cisplatin (Article 2). This could be attributed to the different mouse strain and to the older age and therefore slightly higher initial bw of the CD1 mice. At 2 days after the second dosing by EN at 1.0 mg/kg the total bw loss amounted to 22.9 ± 1.2% w/w (day 5, $p < 0.001$ *vs.* Ctrl, one-way ANOVA, Bonferroni's post-test, **Figure 65**), which required withdrawal of this group.

At the same time, the 0.5 mg/kg administration of cisplatin by EN resulted in a low 1.4 ± 4.8% w/w bw loss at day 3 and a 1.9 ± 3.4% w/w bw loss at day 5 respectively, which were not significantly different from the healthy control ($p \geq 0.05$, one-way ANOVA, Bonferroni's post-test, **Figure 65**). The bw loss amounted to 2.8 ± 1.9% w/w 3 days after the last administration (day 15), which was significantly lower than the healthy control ($p >$ 0.01, one-way ANOVA, Bonferroni's post-test), and mice started gaining weight thereafter.

A slightly higher tolerance was observed with the DPI IR formulation F1, composed of 95% w/w cisplatin and 5% w/w TPGS. This higher tolerance did not permit to the cisplatin dose to be increased to the upper 1.0 mg/kg incremental dose. While the bw loss 2 days after the first dosing (day 3, **Figure 65**) amounted to a lower value than EN (6.9 ± 2.3% *vs.* 14.0 ± 0.9% w/w), showing better tolerance, it continued decreasing after dosing repetition to 11.0 ± 6.2% w/w 2 days after the second dosing (day 5, **Figure 65**) and to 19.7 ± 1.1% w/w, 3 days after the third, which required discontinuation of this group. The bw loss of F1 at 1.0 mg/kg was not significantly different from the control at day 3, but was significantly different at day 5 ($p < 0.001$, one-way ANOVA, Bonferroni's post-test).
The better tolerance of the DPI IR formulation than EN was confirmed by the administration at 0.5 mg/kg, which ended-up in bw gain between each administration, for instance of 3.8 ± 2.2% w/w and 9.4 ± 4.4% w/w, 2 days after the first and 3 days after last administration, (day 3 and day 15, **Figure 65**). These values were significantly different from its administration at a higher 1.0 mg/kg dose ($p < 0.05$, and $p < 0.001$ one-way ANOVA, Bonferroni's post-test, respectively). At day 15 for instance, the measured bw loss of EN was significantly different from the healthy control ($p < 0.01$, one-way ANOVA, Bonferroni's post-test, **Figure 65**), but was not significant for F1 at the same dose ($p \geq 0.05$, one-way ANOVA, Bonferroni's post-test, **Figure 65**), showing again its better tolerance than for an aerosolized solution. This better tolerance could be explained by a higher latency between administration and availability of cisplatin for pharmaceutical action, solubilized in lung tissues. Indeed, cisplatin microcrystals might take a few minutes to entirely solubilize in lung fluids after deposition.

Finally, the CR inhaled formulation with prolonged lung retention properties (F2, **Table 27**) comprised of cisplatin, TS and TPGS (50:49.5:0.5% w/w/w) showed higher tolerance than both the IR inhaled formulations as it permitted the cisplatin dose in the lungs to be doubled, up to 1.0 mg/kg. At this dose, the bw 2 days after the first dosing (day 3, **Figure 65**) increased to 1.5% ± 5.1% w/w and was then relatively stable over the whole 2-week administration **(Figure 64)**, with a bw loss of 1.5 ± 4.8% w/w 2 days after the last

administration (day 15, **Figure 65**). Nevertheless, F2 at 1.0 mg/kg still had a significantly higher impact on the bw of mice at this time-point (**Figure 65**, $p < 0.01$, one-way ANOVA, Bonferroni's post-test) when compared to the healthy control. However, the bw loss remained within the defined limits and it was not significantly different that with IV at 1.5 mg/kg or from F1 and EN at 0.5 mg/kg ($p \geq 0.05$, one-way ANOVA, Bonferroni's post-test).

Overall, the higher MTD of F2 than for EN or F1 is probably attributable to the PK profile of the CR formulation, particularly in the lungs, where previous data **(Table 27)** exhibited a much higher lung $t_{1/2}$ of nearly an hour (*vs.* a few minutes for F1 and EN, respectively). Cisplatin is known to exert its systemic toxicity through high peak concentration, in renal cells (Nagai et al., 1996) and in inner ear cells (Rademaker-Lakhai et al., 2006). This may also be the case here, as a large fraction of cisplatin in F2 is not readily released from the deposited SLM and may therefore end-up at a lower concentration in cells of the lung parenchyma. At the same time, a higher dose of 1.5 mg/kg was not as well-tolerated ($10.6 \pm 3.8\%$ and $20.2 \pm 1.6\%$ w/w bw loss, at days 3 and 5, respectively). This weight loss was significantly different from the control ($p < 0.01$ and $p < 0.001$, respectively, one-way ANOVA, Bonferroni's post-test, **Figure 65**) and from F2 at the MTD of 1.0 mg/kg ($p < 0.05$ and $p < 0.001$, one-way ANOVA, Bonferroni's post-test). At this dose, the burst-effect of F2 probably created peak concentrations that were too high, which resulted in toxicity comparable to EN or F1 at lower doses. Another possibility is that non-solubilized lipid particles could induce local toxicities.

In a preliminary work in our lab, the repeated administration procedure alone at a higher frequency than that was done here (e.g. once a day) was already not tolerated. In order to maximize CT exposure for the evaluation of the antitumour efficacy and mimic as much as possible a clinical setting (e.g. once or twice a day) with a cisplatin DPI, the closest repetition that was possible with a mouse model was every 2 days (Wauthoz et al., 2010). The fact that mice were able to gain weight (i.e. EN at 0.5 mg/kg, F1 at 0.5 mg/kg) or show very little bw loss (F2 at 1.0 mg/kg) confirms that the administration procedure (i.e. anaesthesia and endotracheal insufflation) does not have a meaningful impact on the bw of healthy mice at this frequency.

After the two-week administration period, mice in all groups restarted gaining bw again and ended up with a total bw gain at the last day of follow-up (day 40). However, while mice in EN and F1 groups at 0.5 mg/kg and in IV at 1.5 mg/kg had a final bw gain that was not

significantly different from the control group (~20% w/w, $p \geq 0.05$, one-way ANOVA, Bonferroni's post-test, **Figure 65**), this was not the case for F2 at 1.0 mg/kg ($p < 0.01$, one-way ANOVA, Bonferroni's post-test, **Figure 65**). This lower recovery trend was observed starting 3 days after the third administration (day 8, **Figure 64**). However, the bw loss never exceeded 2.3% w/w at any time. The same profile was observed for F2 at 0.5 mg/kg (data not shown).

The MTD value was determined in order to establish the maximal dose that is administrable to mice, linked to bw loss, which is representative of the global toxicity of formulations through their specific route. As is shown in Article 2, the inhaled route is able to concentrate the cisplatin dose between 2.6 and 10.9-fold in the lungs when compared to the IV route **(Table 27)**. Therefore, the MTD in the lungs seems very high for the CR formulation F2 in comparison to the slightly higher dose that is tolerated with IV (1.5-fold higher for F2 and 3-fold higher for EN and F1). While administration by the IV route is more probably limited by cisplatin nephrotoxicity, administration by the inhaled route is more likely linked to local lung toxicity.

Nevertheless, a CR approach in the lung parenchyma permitted the MTD of the IR formulations to be doubled (DPI IR and EN). The higher MTD obtained for F2 confirms the blood PK data, which permitted exposure of the lung parenchyma to released cisplatin to be smoothened. Nevertheless, during the previous PK study, we had determined the target advantage (T_a) of this formulation, which showed that F2 increased the exposure in the lungs 11-fold when compared to IV **(Table 27)**. This means that F2 could be administered at 1/11th of the IV dose to reach the same levels of exposure in the lungs. Therefore, the slight reduction in dose required to limit the local toxicity of F2 might not be detrimental to its efficacy. Moreover, reducing the dose but increasing the frequency of administration is a more practical approach to what is envisioned in human patients. This is however impossible to carry out in rodents with the endotracheal procedures, because of the impact of anaesthesia.

3.3.2. Acute pulmonary tolerance of inhaled cisplatin formulations

Following the determination of the MTD, the local acute effects of cisplatin were evaluated on the BALF for each formulation at their MTD and at the corresponding dose for IV.

As described before, the SLM formulation approach that was selected to obtain a CR of cisplatin implies the use of lipids and PEGylated excipients. Very scarce *in vivo* toxicity data exists on this matter but SLM are usually well-tolerated because of their inherent biocompatibility, thanks to the lipids and surfactants used in their composition
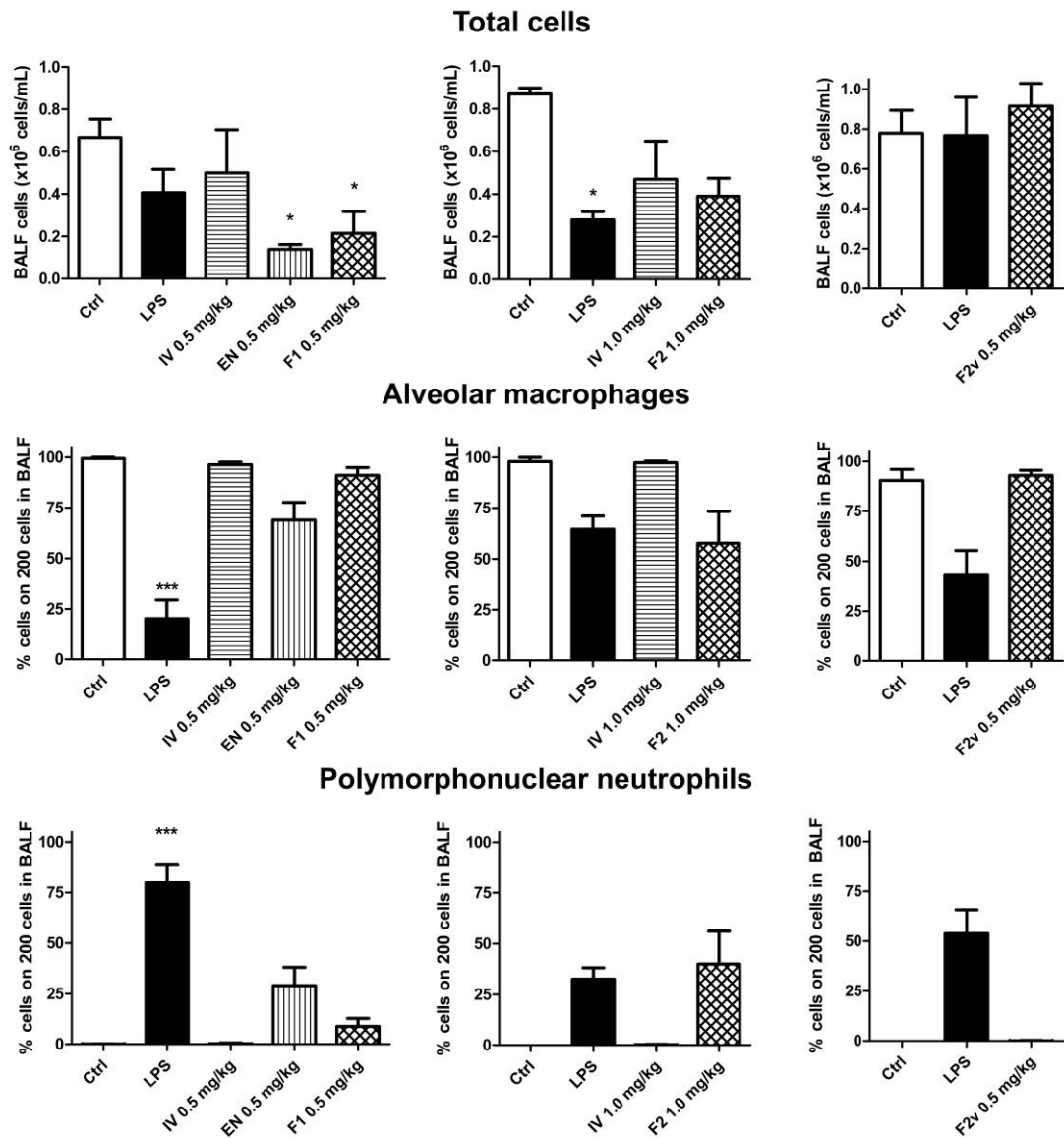
Figure 66. Total and differential cell count (mean ± SEM, n = 2-6) between alveolar macrophages and polymorphonuclear neutrophils in the BALF, 24 h post-administration (8 h post-administration for the LPS group). Statistical comparisons, determined by a one-way ANOVA or a Kruskal-Wallis test (with Bonferroni's or Dunn's post-tests, respectively) are established *vs.* the Ctrl group and are non-significant ($p \geq 0.05$) unless otherwise specified by * $p < 0.05$, ** $p < 0.01$ and *** $p < 0.001$.

(Sanna et al., 2004). Nevertheless, each excipient and drug used in pharmaceutical development needs to be fully physiologically compatible, especially considering the pulmonary route. This can be assessed by a BALF collection and analysis, to ensure that no immunogenic or inflammatory reactions are encountered following the administration of these particles. There is a higher risk of these reactions because of the particles' lung retention properties. To assess this particular effect alone, particles without cisplatin as the vehicle of F2 (F2$_V$) were also produced using excipients only and administered under the same conditions, and at the same dose as in F2.

The total cell count and cell differential cell count, as well as quantification of pro-inflammatory cytokines (IL-1β, IL-6, TNF-α) were performed to detect any acute pro-inflammatory effect of the formulations on the lung parenchyma.

Each inhaled cisplatin formulation decreased the number of total cells in the BALF **(Figure 66)**, which is logical considering the cytotoxic mode of action of cisplatin. The total cell-count decrease was significant for F1 (at its 0.5 mg/kg MTD) *vs.* the healthy control ($p < 0.05$, Kruskal-Wallis test with Dunn's multiple comparison post-test). This effect seemed higher for EN at it 0.5 mg/kg MTD than for F1. However, the difference between them was non-significant ($p \geq 0.05$, Kruskal-Wallis test with Dunn's multiple comparison post-test).

A lower non-significant cell count than for the control was also observed for F2 at its 1.0 mg/kg MTD, and was comparable to IV at the same dose ($p \geq 0.05$, Kruskal-Wallis test with Dunn's multiple comparison post-test), keeping in mind that F2 has been shown to increase the lung exposure more than 10-fold when compared to IV (T_a, **Table 26**). This is also in total accordance with the lower bw losses described earlier. It is probably linked to the lower C_{max} encountered in lung fluids and in the lungs' parenchyma cells, which generates a lower local toxicity and a better tolerance. The slow release of cisplatin from SLM generated lower peak exposure of the cells in the BALF, which led to a higher tolerance. This effect was probably caused by the cytotoxic cisplatin as unloaded F2$_V$ particles created a non-significant total cell-count similar to the control ($p \geq 0.05$, Kruskal-Wallis test with Dunn's multiple comparison post-test) **(Figure 66)**.

Regarding the differential cell-count in the BALF **(Figure 66)**, in the healthy controls, the vast majority of cells are usually AM cells. PN cells are only recruited in the case of local inflammation. As expected IV did not create any difference from the healthy control, as a lower dose reached the lung. For inhaled cisplatin treatments, a larger proportion of PN (and therefore a lower proportion of AM) were encountered. Indeed, following EN at 0.5 mg/kg

Table 28. Pro-inflammatory cytokine IL-1β, IL-6, TNF-α concentrations (mean ± SD, n = 4-7) in the BALF, 24 h post-administration (8 h post-administration for the LPS group). Statistical comparisons are *vs.* the negative control (Ctrl) and were realized using a Kruskal-Wallis test. The statistical significance is expressed as *** for $p < 0.001$, ** for $p < 0.01$ and * for $p < 0.05$.

	Ctrl	LPS	IV 0.5 mg/kg	EN 0.5 mg/kg	F1 0.5 mg/kg
IL-1β (pg/mL)	89 ± 42	151 ± 48***	91 ± 31	93 ± 19	70 ± 11
IL-6 (pg/mL)	< 15.6	392 ± 156	< 15.6	< 15.6	< 15.6
TNF-α (pg/mL)	< 31.3	961 ± 261	< 31.3	< 31.3	< 31.3

	Ctrl	LPS	IV 1.0 mg/kg	F2 1.0 mg/kg
IL-1β (pg/mL)	50 ± 16	399 ± 115**	45 ± 19	52 ± 20
IL-6 (pg/mL)	55 ± 36	221 ± 75*	51 ± 16	92 ± 41
TNF-α (pg/mL)	< 31.3	388 ± 145	< 31.3	< 31.3

	Ctrl	LPS	F2v 0.5 mg/kg
IL-1β (pg/mL)	< 15.6	91 ± 35	< 15.6
IL-6 (pg/mL)	< 15.6	36 ± 50	< 15.6
TNF-α (pg/mL)	< 31.3	116 ± 91	< 31.3
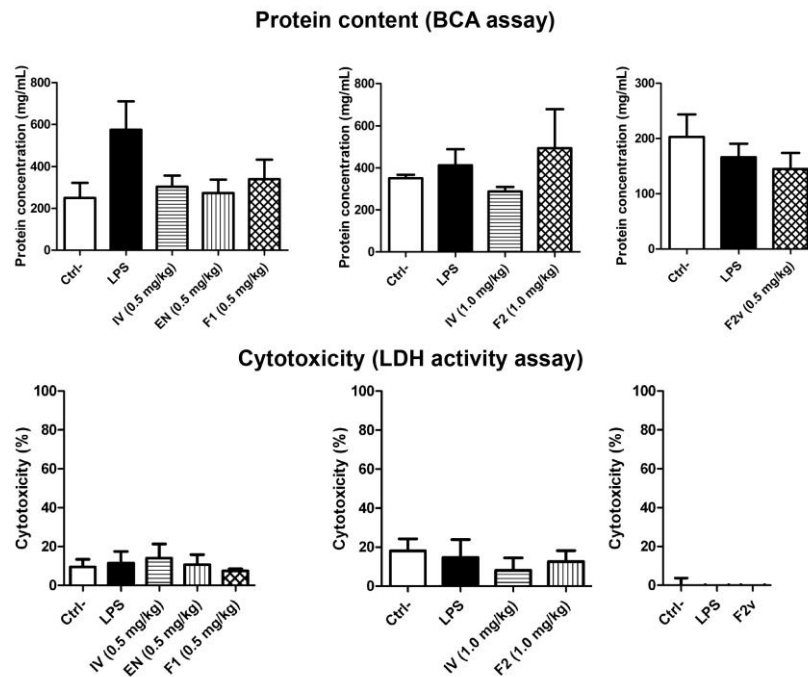
Figure 67. Protein content and LDH activity in the BALF (mean ± SEM, n = 5-7), 24 h post-administration (8 h post-administration for the LPS group). Statistical comparisons, determined by a one-way ANOVA or a Kruskal-Wallis test (with Bonferroni's or Dunn's post-tests, respectively) were established *vs.* the Ctrl group and were non-significant ($p \geq 0.05$).

where cisplatin solution is directly delivered to the lung, a higher PN proportion was observed in comparison to the administration of the IR-DPI F1 at the same dose (29 ± 18% *vs.* 9 ± 11%). This seems to confirm that the IR DPI formulation was able to offer a better tolerance than a fully solubilized solution nebulized in the lungs in terms of local toxicity and more specifically in terms of local inflammation. For the administration of the CR-DPI F2 at 1.0 mg/kg, a slightly higher fraction of PN was encountered (40 ± 38%) **(Figure 66)**. This was not directly attributable to the lung retention effect of the SLM excipients on the lung parenchyma as no PN were observed with F2$_V$. This may therefore have been caused by the sustained released of cisplatin and therefore sustained exposure on the lung parenchyma inducing the recruitment of PN. The pro-inflammatory activity evaluated through the quantification of IL-1ß, IL-6 and TNF-α showed no significant elevation higher than baseline for either of these markers for IV, EN, F1 and F2 at the assayed doses **(Table 28)**. The LPS positive control was however always significantly different from the negative control ($p < 0.05$, Kruskal-Wallis test with Dunn's multiple comparison post-test). The measured values for each formulation were often lower than the limit of quantification specified by the manufacturer (i.e. 15.6 pg/mL for IL-1β and IL-6 and 31.3 pg/mL for TNF-α). In either case, the only elevation that could be observed was for IL-6 following the administration of F2 at 1.0 mg/kg (92 ± 41 pg/mL), but to a non-significant extent (55 ± 36 pg/mL for the negative control, $p \geq 0.05$, Kruskal-Wallis test with Dunn's multiple comparison post-test).

Cytotoxicity was assessed by the quantification of the protein content and by the LDH activity **(Figure 67)**. Protein content in the BALF was not increased significantly from the negative control for any of the IV assays or EN. This is in accordance with previous data from our laboratory (Rosiere et al., 2016). For the DPI formulations, the same trend was observed for F1 and a non-significant increase from baseline was observed for F2 at 1.0 mg/kg but with a very high variability between mice. This slight increase was not confirmed by the administration of the unloaded particles in F2$_V$. This suggests that if present, this increase could only be attributed to the sustained exposure of the lungs to cisplatin. Regarding the LDH activity **(Figure 67)**, no statistical difference or notable increase from the baseline could be observed between the negative control, the LPS group, and all the others administered cisplatin assays (IV, EN, F1 and F2). The same was observed for F2$_V$, which also showed good tolerance regarding this parameter. LPS may not be a proper positive control for this assay as it has very low influence on the LDH activity (Rosiere et al., 2016). All in all, the local administration of F1 and F2 at their respective MTD

after a single dosing seemed to be relatively well-tolerated in healthy mice. The only notable effects were the diminution of the total cell-count in the BALF and a recruitment of PN. These effects were definitely caused by cisplatin and not by the formulation as they were also observed by EN and were not observed after the administration of F2v.

Regarding the potential elimination mechanisms of tristearin and TPGS in the lungs following particle deposition, the fact that unloaded vehicle particles do not create either inflammation of cytoxicity is very encouraging. The ability of the excipient material to either be taken up by macrophages after some time or to dissolve in lung fluids (less likely with very hydrophobic material) is in fact needed to limit inflammatory reactions. Following internalization into the cytoplasm of macrophages, particles can be digested by incorporation into lysosomes. There, tristearin for instance, can be broken down by enzymes like the lysosomal acid lipase into free fatty acids and glycerol (Yan et al., 2006). Regarding PEG moeities, increased internalization into lysosomes followed by cellular vacuolation has been observed with chains of high molecular weight (above 30 kDa), showing lower elimination rates, and creating safety concerns regarding their tolerance, regardless of the route of administration. This has however not been observed with low molecular weight PEG chains (of less than 3350 Da) (Baumann et al., 2014). Because the low molecular weight PEG excipients, like TPGS for instance are amphiphilic, they could therefore very well be solubilized and absorbed by lung tissues at some point following the deposition of particles into lung fluids. They would then end-up in the systemic circulation, where they would be eliminated mostly by urinary excretion (Baumann et al., 2014).

While AM cells are normally the sole residents of the alveolar space and represent the vast majority of cells found in the BALF of healthy subjects (80-100%), the recruitment of PN cells from the peripheral circulation is generally a sign of lung irritation. It is observed in animals and in humans following contact with known irritants such as LPS or cigarette smoke. Because PN release neutrophil elastase and defensins, they are potentially toxic to other cells and are therefore known to be potential precursors to lung injury (Bhavsar et al., 2008). PN are known to be a significant source of various pro-inflammatory and immunoregulatory cytokines. Those are mainly described for mice and humans and vary depending on the species, on the site and mechanism of inflammation as they involve interactions between multiple signaling pathways (Tecchio et al., 2014). The fact that we were not able to observe concomitant elevations of pro-inflammatory cytokines IL-6, TNF-α or IL-1β (which are the most frequently observed cytokines in acute lung injury and were observed for the LPS group) could therefore be explained by the complexity of the pathways
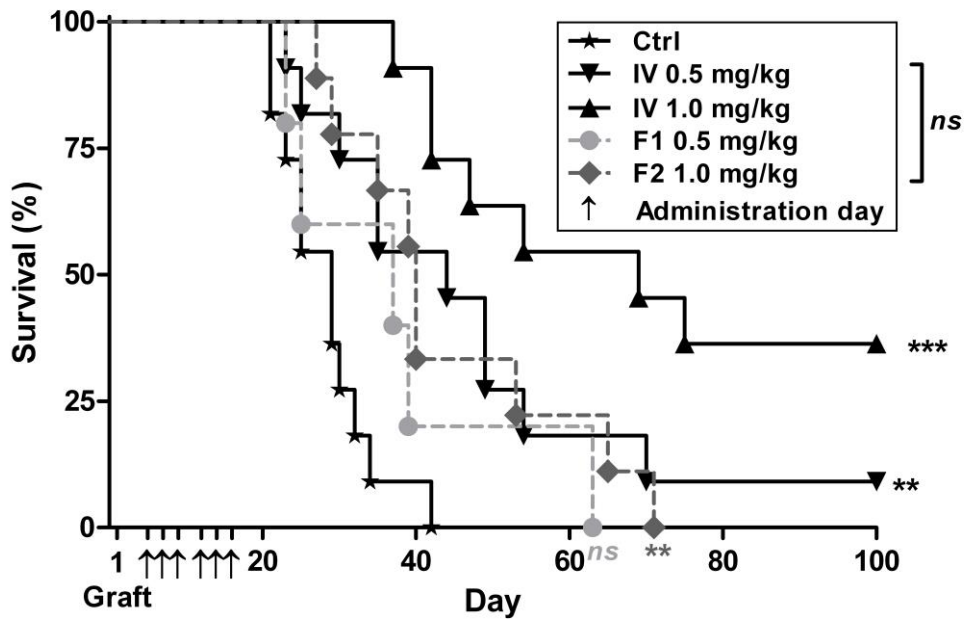
Figure 68. Kaplan-Meier survival curves of M109 HiFR tumour-bearing BALB/cAnNrJ mice left untreated (Ctrl, n = 11) or following cisplatin administration with DPI formulations showing immediate release *in vitro* and low lung retention *in vivo* (F1, n = 5) or controlled-release *in vitro* and prolonged lung retention *in vivo* (F2, n = 10), at their respective MTD, as well as solutions by the IV route, administered at matching doses (n = 11). Statistical comparisons, determined by a log-rank (Mantel-Cox) test were established *vs.* the Ctrl group and are expressed as non-significant (*ns* $p \geq 0.05$), significant (* $p < 0.05$), very significant (** $p < 0.01$) and extremely significant (*** $p < 0.001$).

involving a very high number of other cytokines (IFNγ and IL-2 for instance) that could have been emitted following the exposition of lungs to cisplatin. For instance in humans, IL-8 is the most frequent chemokine responsible for neutrophil infiltration. In rodents, the most relevant chemokine is the keratinocyte-derived chemokine (CXCL1) and the macrophage inflammatory protein-2 (CXCL2) which were unfortunately not quantified here (Grommes and Soehnlein, 2011).

3.3.3. Anticancer activity on the orthotopic lung cancer model

Following the graft of mice with M109-HiFR cells, cisplatin was administered using the DPI formulations at their pre-determined MTD for the chronic scheme (i.e. F1 at 0.5 mg/kg and F2 at 1.0 mg/kg). These were compared to IV at the corresponding doses of 0.5 mg/kg and 1.0 mg/kg. During the administration of F1 to grafted mice, a high number of mice died immediately following the administration (8/15) and 1 mouse died due to the anaesthesia (i.e. death occurred between 30 minutes and 1 hour following the administration). The same phenomenon was observed for F2, but to a lesser extent (4/15) and 1 mouse also died due to the anaesthesia. In each case, the recorded mice died of pulmonary distress in the seconds following device actuation. No particular pattern regarding the mouse death in relation to the administration day or to the evolution of the bw of mice could be discerned. This was also not observed during the previous MTD study, which was realized on smaller samples, although on mice of comparable bw (between 16 and 20 g). The probable cause of this is the prior grafting of the mice, which could have been weakened by the prior surgery and tumour involvement, whereas the MTD was determined on healthy animals. Nevertheless, because the objective of the study was to determine survival based on the influence of the grafted tumour alone, these mice were removed from the subsequent survival analysis, which started on the day of the last administration (day 16).

Control mice exhibited a median survival (MS) of 29 days and none survived more than 42 days following the graft as shown on the Kaplan-Meier survival curve **(Figure 68)**. Remaining mice (5/15) in the F1 group at 0.5 mg/kg showed a higher MS of 37 days, with the last dead mouse at day 63. The survival in this group was however not significantly different from the untreated control ($p \geq 0.05$, Log-rank test). In the F2 group at 1.0 mg/kg (10/15 mice remaining at the end of administrations), the MS was slightly higher at 40 days, and the last mouse survived until day 71. The survival in this group was significantly different from the untreated control ($p < 0.01$, Log-rank test). In the meantime, IV at 0.5 mg/kg showed a comparable survival to that of the F2 group, with an MS of 44 days and a single (1/11: 9%) long-survivor mouse after 100 days. Finally, IV at 1.0 mg/kg showed the highest survival with a much higher MS of 69 days and four (4/11: 36%) long-survivor mice after
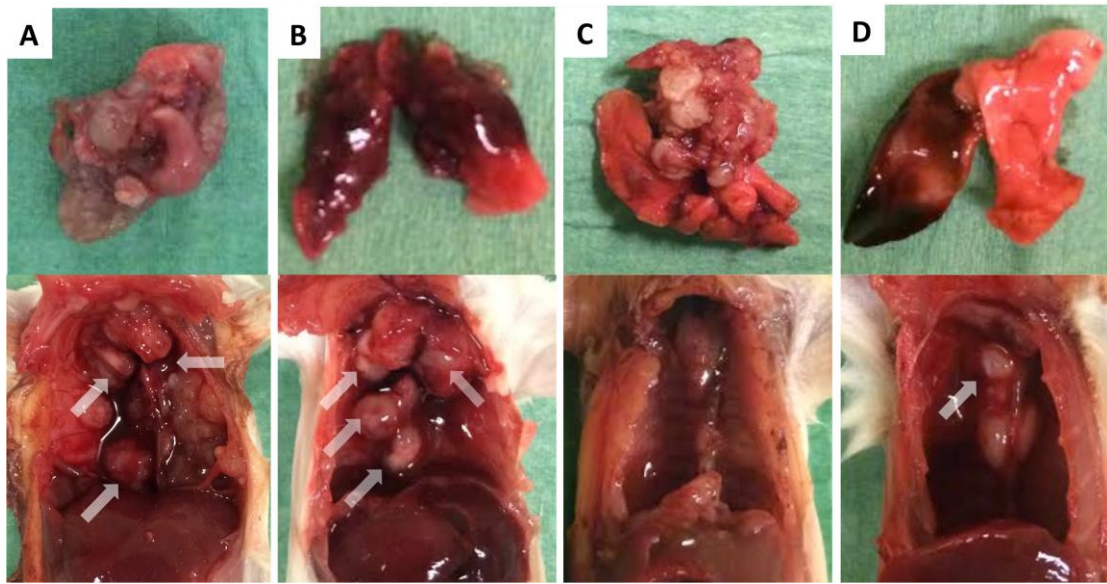
Figure 69. Pictures of grafted mice lungs (top) and thoracic cages (bottom) for **A**. an untreated control mouse (death: day 23), **B.** an F2-treated mouse at 1.0 mg/kg (death: day 40) and IV-treated mice **C.** at 0.5 mg/kg (death: day 40) and **D.** at 1.0 mg/kg (death: day 47). Arrows show lung nodules in the thoracic cage.

100 days. Both IV groups showed significantly higher survival rates than the untreated control ($p < 0.01$ and $p < 0.001$ for 0.5 and 1.0 mg/kg, respectively).

The first observation from these results is that treatment with F1 at its 0.5 mg/kg DMT does not seem to offer a significantly higher efficacy than the untreated control. Moreover, it might even show a lower tolerance than F2 at double the dose on a fragilized lung of tumour-bearing mice. Secondly, doubling the dose with F2 helped to obtain a significantly higher survival than the untreated control. This higher survival was not significantly different from IV at 0.5 mg/kg ($p \geq 0.05$, log-rank test), but was significantly lower than IV at the same dose ($p < 0.01$, log-rank test). In untreated mice necropsy, the tumour spread was generally limited to the lungs. Its invasive growth, with a large number of lung tumour nodules **(Figure 69)** was established as the probable cause of death as mice also showed signs of respiratory distress before dying or being euthanized. However, in the F2 group, while lungs of necropsied mice appeared without visible lung nodules, the surrounding thoracic cage and surrounds of the spine were invaded **(Figure 69)**. This caused more general symptoms, in particular high bw loss or paralysis that required euthanasia of mice. Conversely, in IV mice groups, the opposite phenomenon was observed, and mice that died at a later time still showed pulmonary nodules and very few to none in the outer lung thoracic region **(Figure 69)**. Our previous PK evaluation had confirmed that cisplatin was found in much greater quantities in the lung parenchyma following the administration of inhaled formulations than following IV administration. For F2, this PK advantage was established as a targeting advantage of 10.9 (ratio between the lung exposure by the inhaled route to the lung exposure by the IV route), determined after a single 1.25 mg/kg dose.

This much higher exposure was not sufficient to obtain a higher efficacy than IV with the inhaled CR formulation F2 at the same dose. This modest result can probably be explained by the very high metastatic behaviour of the grafted tumour model, for which a systemic treatment seems to be more effective. This however shows the potential setting of this kind of localized treatment. These would probably show a higher efficacy at a higher frequency (once or twice a day) and lower doses to reduce the potential local toxicities on fragilized lung-bearing tumours. This localized treatment could help to reduce tumour size before a surgery, to combat local micrometastasis after a surgery and/or a radiotherapy and could be combined with intravenous less toxic CT (lower doses during shorter timeframes, combination with other chemotherapeutic drug), the latter limiting tumour cell invasion.

3.4. Conclusion

Cisplatin exhibits some inflammatory reaction in the lung parenchyma following its local administration, in particular regarding its impact on the total cell count, attributable to its inherent cytotoxicity, and on the recruitment of PN cells. Nevertheless, it seems to be rather well-tolerated by inhalation (e.g. low bw loss under a chronic scheme, no elevation of the protein-content and of the LDH activity in the BALF) particularly considering the much higher cisplatin dose in the lungs following inhalation than for IV. As with other cisplatin-related toxicities, its systemic and local tolerance seems to be linked to the C_{max} near or inside the cells. This was confirmed by the superiority of a formulation comprising SLM embedding cisplatin microcrystals able to provide lung retention and the CR of cisplatin. This DPI formulation had a lower impact on bw loss during the initial MTD determination and permitted the inhaled dose of cisplatin to be doubled. This higher administrable dose is of tremendous importance, as patients in clinical settings are usually treated near or at the MTD. This double dose helped obtain a significant survival during an efficacy assessment against a lung-tumour model, which was not the case with the lower dosage using the IR formulation. However, despite the promising PK results obtained previously, superiority of the CR formulation alone was not observed *vs.* IV. This was probably because of the involvement of the metastases in the cause of death. Moreover, because of the repeated anaesthesia procedures needed to administer DPI formulations to mice, administration of lower but more frequent doses is not possible in mice. Further evaluation of the local tolerance of inhaled formulations should still be studied at lower administered doses. It should be associated with a supplementary evaluation of their chronic administration, through lung histology, quantification of other maybe more relevant cytokines, and measurement of respiratory parameters particularly regarding that comprising SLM (F2).

Concerning the efficacy of the DPI formulations, further studies using a combination approach (IV and inhalation) evaluating for instance the tumour size in addition to another survival study should be realized. This could for instance help to properly evaluate the local action of cisplatin on the primary tumour.

GENERAL CONCLUSION AND PERSPECTIVES

Lung cancer treatment through inhaled CT seems to be a promising approach and a valid additional modality to conventional parenteral CT. It seems to provide a valuable pharmacokinetic advantage (i.e. higher lung exposure, lower systemic exposure). A few clinical trials in the last decades have shown the feasibility and safety of the cisplatin administration, all through the nebulization of liposomal dispersions. However, none have reached the market so far, in part, but not only because of technical limitations. As opposed to the long routine experienced with systemic administration (i.e. peri-hydration, slow infusion) that is necessary to limit the nephrotoxicity, administration of inhaled cisplatin should be achievable quickly, with a low environmental exposure of cisplatin to provide interest compared to the existing CT modalities. However, nebulizers used in clinical trials were altogether unable to circumvent these particular issues. They were notably unable to reach efficacious doses under reasonable timeframes and required expensive apparatus and impractical adapted facilities, which are not cost-effective.

DPI technology could potentially avoid these issues thanks to a greater ability for higher dose delivery (even for hydrophobic and low-soluble drugs) and easier limitation of environmental exposure (thanks to their breath-actuated approach and low-cost single-use devices). Low-resistance devices could be particularly adapted to patients with impeded respiratory function already exist. While delivery of higher doses in a shorter timeframe seems practical, it also poses a higher risk of lung toxicity due to higher peak concentrations of solubilized drug locally. To limit this phenomenon, CR particles have to be designed within the general specifications of a DPI formulation (e.g. particle diameter, aerosolization properties, lung tolerance of excipients, stability) but also with regard to the natural clearance mechanisms occurring in the lungs.

This work therefore consisted of proposing a valid approach to circumventing the aforementioned issues, using DPI technology with a CR approach. This offers high lung retention and compatibility with lung tissues.

In the first part of the work, we designed SLM formulations of cisplatin, a widely-used CT drug exhibiting poor water solubility and high systemic toxicity. During preliminary studies we particularly observed that hydrophobicity of the lipid matrix and the concentrations of surfactant excipients and/or PEGylated excipients were key parameters in providing CR of cisplatin from SLM. We also showed that lipid excipients, selected based on their melting point, were able to be spray dried without modification of the spray dryer and still offer low particle size, low sticking and high yields. The SLM were therefore produced using a

previously reduced suspension of cisplatin and TS, a highly hydrophobic but potentially well-tolerated triglyceride as the main component of the lipid matrix. Surface modification of the SLM was realized using TPGS or DSPE-mPEG-2000, two well-known and potentially well-tolerated PEGylated excipients. Using efficient and up-scalable techniques (HPH, spray drying), we were able to generate DPI formulations with interesting aerodynamic properties (narrow geometric and aerodynamic diameters, high *in vitro* deposition, high deagglomeration abilities), high drug loadings and CR for more than 24 hours in conditions simulating lung deposition *in vitro*. These formulations could therefore pose as a convenient solution to the limitations observed with the nebulization of liposomal cisplatin. In the Wittgen *et al.* study, patients had to endure treatment for up to 6.7 and 8.0 hours a day for 3 and 4 days over a week in order to reach a total emitted dose of 60 mg/m² and 48 mg/m², respectively. With only 10 to 15% of the dose deposited in the lower lung, this corresponded to a mere 9.8 to 18 mg of cisplatin over a week of treatment. The best DPI formulations obtained here showed a high deep lung deposition (between 37 and 52% FPF), and low oropharyngeal deposition (< 15%), which is interesting as no therapeutic effect is needed in this zone and as a way to limit adverse effects. With an FPD of nearly 10 mg for a 20 mg-filled capsule, the best IR DPI formulation that was produced here reach doses comparable to those obtained through nebulization by inhaling only 1 or 2 capsules. While slightly lower, the same can be said from the FPD of the best candidate CR DPI formulation that was produced. In comparison to the maximum exposure that was reached in the nebulized cisplatin study, the same dose could be delivered in only 5 capsules with the CR DPI, thanks to its FPD of 3.6 mg. This could be easily done over the course of 4 days or less in order to reach higher doses, and would need one or two minutes per capsule, also helping to limit the mobilization of medical personnel. Moreover, the MMAD of 2.3 μm obtained for the best CR DPI formulation will preferably deposit in the peripheral lung, thus easily reaches the site of action for most cancer types. Moreover, thanks to their particular design and their patient-driven approach, cisplatin DPI confirm their very low environmental impact. A large proportion of the dose is in fact deposited into the patient's lungs and another major portion is deposited onto the device, which can easily be disposed of. This patient-driven approach, which could initially pose as an issue regarding patients with impeded respiratory function should also not be such a problem with the developed formulations. This is because they were specifically developed with a low-resistance device and showed low aggregation tendencies, even at very low inspiratory flow rates.

In the second part of the work, we verified that the CR abilities were still observed *in vivo* in CD-1 mice. This required the validation of administration of DPI using endotracheal devices and the development of a validated ETAAS quantification method for platinum in organ

digestates and total blood. Following the administration of the DPI formulations, we observed that surface modification using PEGylated excipients (using TPGS in this case) was mandatory to prolong retention of SLM in the lungs, which was observed for up to 7 hours. This prolonged retention was necessary to observe the systemic consequences of CR in the lungs (higher lung exposure, lower blood C_{max}, lower non-target organs C_{max} and higher non-target organs t_{max}). Overall, PEGylation seemed sufficient to limit non-absorptive clearance mechanisms and also probably uptake by alveolar macrophages. Cisplatin absorbed through the blood into the systemic compartment is reflecting in part the solubilized fraction in lung fluids. This solubilized fraction could promote pharmacologic action but also be metabolized or absorbed. With CR formulations, exposure is therefore sustained in the lungs but it may also be the case, to a lower extent, in the systemic compartment. This may have caused the observed increase in kidney exposure, as compared to IR and EN formulations, as it permitted the accumulation of cisplatin or of its metabolites. Ideally, the drug concentrations obtained from controlled-release formulations should remain within therapeutic and non-toxic intervals.

In the last part of the work, we therefore focused on assessing the local and systemic tolerance of the best SLM candidate formulation. C_{max} had previously been reported as the most critical variable regarding cisplatin toxicity in kidneys and in the inner ear. Following this last study, we were able to draw the same assumptions regarding lung toxicity. The CR formulation was in fact administrable at double the dose of an IR DPI formulation (and of EN of a cisplatin solution) under a chronic administration scheme in BALB/c mice. This confirmed the need for a CR approach for these kinds of CT drugs with narrow therapeutic indexes. Through a local assessment of DPI formulations, we also observed promising results regarding the tolerance of the excipients in the BALF from BALB/c mice. No signs of cytokine liberation or tissue damage were observed following unloaded SLM or cisplatin administration. However, we observed that cisplatin was responsible for cytotoxicity through a lower cell-count in the BALF. This is almost certainly linked to the drug's mode of action and of PN recruitment, which may be a sign of local irritation.

Finally, the preclinical evaluation of the best candidate formulation using the M109-HiFR orthotopic mouse lung cancer model that was readily available in our laboratory showed very interesting results. These confirmed a higher overall tolerance with the CR formulation than with an IR one. The efficacy of the CR DPI formulation was, however, comparable to that of half the dose of cisplatin administered as an IV solution, despite the high PK advantage we had determined previously. This result was explained by the highly metastatic rate of the

grafted cells, which caused mice treated in the inhalation groups to die quicker from the secondary metastases than mice in the IV groups, which died from primary tumour involvement in the lung. This very interesting result will help define the future antitumour evaluations (i.e. tumour size, local metastatic involvement) and the scope of inhaled therapy, particularly regarding highly metastatic cancers such as lung cancers.

All these very interesting observations now require confirmation through the evaluation of antitumour efficacy using a combined approach with systemic administration, using for instance aerosolized CT as a new modality. This could be realized though a survival rate analysis under the same lung tumour model as described in this work. Another way of determining the local efficacy of the inhaled approach could be through the evaluation of cancer growth (i.e. measurement of the primary tumour), at different times following the administration of the formulations. This could be done through direct measurement at a determined time or continuously using mouse PET or MRI scans.

Regarding the evaluation of the tolerance of formulations, the potentiality of acute lung injury should be ruled out at lower doses through a dose-response study. Other inflammatory markers should be used, as well as the evaluation of the respiratory function through unrestrained plethysmography for instance. The effect on the lungs should also be assessed under a more chronic use. This is because, regardless of their compositions, the repeated administration of long-lasting particles in the lung raises questions regarding accumulated local toxicity in the long run. This could for instance be assessed by histopathological evaluation of lung tissue, looking for evidence of tissue damage or scar tissue. However, because of the required prior anaesthesia, repeated administration to mice using the endotracheal devices described in this work is neither practical nor representative, and greatly limits the frequency of administrations. It however has the advantage of being relatively cheap, portable, easily decontaminated and is able to deliver a precise dose into the lungs of the animals, which is a great advantage for dose-response studies. Development of new administration models is very much needed for DPI evaluation in general. This is possible in rodents using less invasive approaches such as inhalation towers. However, those are expensive, not as precise as endotracheal devices and pose a high risk of environmental exposure with CT drugs. This could also be possible in larger animals such as sheep, which have the advantage of greater tracheobronchial similarity with humans and do not require prior anaesthesia. Indeed, mice lungs have fewer generations than humans, a thinner respiratory epithelium and a relatively larger airway lumen, which also exhibit the necessity of using larger animal models for further confirmation studies.

Finally, the diminished C_{max} in kidneys but comparable AUC following administration of the CR formulation against IV suggests the need for a thorough evaluation of its nephrotoxicity with a more direct approach than the PK one. It is generally done in humans through measurement of the serum creatinine quantification, evaluation of the glomerular filtration rate or of blood urea nitrogen. However, this technique is not sensitive enough in mice or only under very high nephrotoxic stress, and cisplatin doses are higher than those tested in this work and experimented through the local route. Development of a new and more sensitive technique, able to early detect AKI in mice (through the quantification of neutrophil gelatinase-associated lipocalin in mouse serum for instance) was undertaken near the end of this work. This will be pursued in order to be able to link the PK results to tangible systemic effects.

Nevertheless, the proofs-of-concept formulations described here and their administered doses should still be refined and optimized. The optimisation of the formulations could be done following two main goals. First, the CR abilities and prolonged residence in the lungs are very much needed. Screening of varying ratios or of other spray dryable excipients (lipid fraction and PEGylated fraction) could therefore help modulate these properties and *in fine* the lung and systemic exposure. This must be done keeping in mind the manufacturability of the dry powders. Secondly, targeting specific regions of the tracheobronchial tree is possible with DPI. It could further limit the exposure of aerosolized CT to confined regions of interest inside the lung. This particular aspect could be initially assessed *in vitro* through the measurement of the MMAD but should be confirmed *in vivo*, ideally in clinical patients through a pharmacoscintigraphic evaluation of the lung deposition patterns. This could onlt be done after a thorough evaluation of the chronic toxicity of formulations, as described above, and after refining the scope of inhaled CT with cisplatin.

REFERENCES

Aderem A. and Underhill D. M. **Mechanisms of phagocytosis in macrophages**. *Annu Rev Immunol* 17: 593-623 (1999).

Akaboshi M., Kawai K., Maki H., Akuta K., Ujeno Y. and Miyahara T. **The number of platinum atoms binding to DNA, RNA and protein molecules of HeLa cells treated with cisplatin at its mean lethal concentration**. *Jpn J Cancer Res* 83(5): 522-526 (1992).

Akiyama Y., Yoshioka M., Horibe H., Hirai S., Kitamori N. and Toguchi H. **Novel oral controlled-release microspheres using polyglycerol esters of fatty acids**. *J Control Release* 26(1): 1-10 (1993).

Alberg A. J., Ford J. G., Samet J. M. and American College of Chest P. **Epidemiology of lung cancer: ACCP evidence-based clinical practice guidelines (2nd edition)**. *Chest* 132(3 Suppl): 29S-55S (2007).

Albertine K. H. **1 - Anatomy of the Lungs** in *Murray and Nadel's Textbook of Respiratory Medicine (Sixth Edition)*. Mason R. J., Ernst J. D., King T. E. et al. Philadelphia, W.B. Saunders: 3-21.e25 (2016).

Alderden R. A., Hall M. D. and Hambley T. W. **The Discovery and Development of Cisplatin**. *J Chem Ed* 83(5): 728 (2006).

Alge J. L. and Arthur J. M. **Biomarkers of AKI: a review of mechanistic relevance and potential therapeutic implications**. *Clin J Am Soc Nephrol* 10(1): 147-155 (2015).

Aragao-Santiago L., Bohr A., Delaval M., Dalla-Bona A. C., Gessler T., Seeger W. and Beck-Broichsitter M. **Innovative formulations for controlled drug delivery to the lungs and the technical and toxicological challenges to overcome**. *Curr Pharm Des* 22(9): 1147-1160 (2016).

Arenberg D. A. and Pickens A. **55 - Metastatic Malignant Tumors A2 - Broaddus, V. Courtney** in *Murray and Nadel's Textbook of Respiratory Medicine (Sixth Edition)*. Mason R. J., Ernst J. D., King T. E. et al. Philadelphia, W.B. Saunders: 981-990.e985 (2016).

Ari A. **Jet, Ultrasonic, and Mesh Nebulizers: An Evaluation of Nebulizers for Better Clinical Outcomes**. *Eurasian J Pulmonol* 16(1): 1-7 (2014).

Armstrong D. J., Elliott P. N., Ford J. L., Gadsdon D., McCarthy G. P., Rostron C. and Worsley M. D. **Poly-(D,L-lactic acid) microspheres incorporating histological dyes for intra-pulmonary histopathological investigations**. *J Pharm Pharmacol* 48(3): 258-262 (1996).

Arriagada R., Bergman B., Dunant A., Le Chevalier T., Pignon J. P., Vansteenkiste J. and International Adjuvant Lung Cancer Trial Collaborative G. **Cisplatin-based adjuvant chemotherapy in patients with completely resected non-small-cell lung cancer**. *N Engl J Med* 350(4): 351-360 (2004).

Arriagada R., Dunant A., Pignon J. P., Bergman B., Chabowski M., Grunenwald D., Kozlowski M., Le Pechoux C., Pirker R., Pinel M. I., Tarayre M. and Le Chevalier T. **Long-term results of the international adjuvant lung cancer trial evaluating adjuvant Cisplatin-based chemotherapy in resected lung cancer**. *J Clin Oncol* 28(1): 35-42 (2010).

Augey V., Cociglio M., Galtier M., Yearoo R., Pinsani V. and Bressolle F. **High-performance liquid chromatographic determination of cis-dichlorodiammineplatinum(II) in plasma ultrafiltrate**. *J Pharm Biomed Anal* 13(9): 1173-1178 (1995).

Baik M. H., Friesner R. A. and Lippard S. J. **Theoretical study of cisplatin binding to purine bases: why does cisplatin prefer guanine over adenine?** *J Am Chem Soc* 125(46): 14082-14092 (2003).

Bangham A. D. **Properties and uses of lipid vesicles: an overview**. *Ann N.Y. Acad Sci* 308(1): 2-7 (1978).

Baumann A., Tuerck D., Prabhu S., Dickmann L. and Sims J. **Pharmacokinetics, metabolism and distribution of PEGs and PEGylated proteins: quo vadis?** *Drug Discov Today* 19(10): 1623-1631 (2014).

Berghmans T. **Traitement des cancers bronchiques non à petites cellules : maladies avancées (métastatiques). Recommandations de pratique clinique de l'*European Cancer Working Party**. *Rev Med Brux* 35: 145-159 (2014).

Berners-Price S. J., Ronconi L. and Sadler P. J. **Insights into the mechanism of action of platinum anticancer drugs from multinuclear NMR spectroscopy**. *Prog Nucl Magn Reson Spectrosc* 49(1): 65-98 (2006).

Bhavsar T., Liu X. J., Patel H., Stephani R. and Cantor J. O. **Preferential recruitment of neutrophils by endothelin-1 in acute lung inflammation induced by lipopolysaccharide or cigarette smoke**. *Int J Chron Obstruct Pulmon Dis* 3(3): 477-481 (2008).

Bielack S. S., Erttmann R., Looft G., Purfurst C., Delling G., Winkler K. and Landbeck G. **Platinum disposition after intraarterial and intravenous infusion of cisplatin for osteosarcoma. Cooperative Osteosarcoma Study Group COSS**. *Cancer Chemother Pharmacol* 24(6): 376-380 (1989).

Bodmeier R., Wang J. and Bhagwatwar H. **Process and formulation variables in the preparation of wax microparticles by a melt dispersion technique. I. Oil-in-water technique for water-insoluble drugs**. *Journal of Microencapsulation* 9(1): 89-98 (1992a).

Bodmeier R., Wang J. and Bhagwatwar H. **Process and formulation variables in the preparation of wax microparticles by a melt dispersion technique. II. W/O/W multiple emulsion technique for water-soluble drugs**. *Journal of Microencapsulation* 9(1): 99-107 (1992b).

Borst P., Evers R., Kool M. and Wijnholds J. **A family of drug transporters: the multidrug resistance-associated proteins**. *J Natl Cancer Inst* 92(16): 1295-1302 (2000).

Bosch M. E., Sanchez A. J., Rojas F. S. and Ojeda C. B. **Analytical methodologies for the determination of cisplatin**. *J Pharm Biomed Anal* 47(3): 451-459 (2008).

Boulikas T. and Vougiouka M. **Cisplatin and platinum drugs at the molecular level. (Review)**. *Oncol Rep* 10(6): 1663-1682 (2003).

Bradley J., Graham M. V., Winter K., Purdy J. A., Komaki R., Roa W. H., Ryu J. K., Bosch W. and Emami B. **Toxicity and outcome results of RTOG 9311: a phase I-II dose-escalation study using three-dimensional conformal radiotherapy in patients with inoperable non-small-cell lung carcinoma**. *Int J Radiat Oncol Biol Phys* 61(2): 318-328 (2005).

British Columbia Cancer Agency. **Cisplatin Monograph** in *Cancer Drug Manual* (2013).

Brown D. M. and Ruoslahti E. **Metadherin, a cell surface protein in breast tumors that mediates lung metastasis**. *Cancer Cell* 5(4): 365-374 (2004).

Burdett S., Pignon J. P., Tierney J., Tribodet H., Stewart L., Le Pechoux C., Auperin A., Le Chevalier T., Stephens R. J., Arriagada R., Higgins J. P., Johnson D. H., Van Meerbeeck J., Parmar M. K., Souhami R. L., Bergman B., Douillard J. Y., Dunant A., Endo C., Girling D., Kato H., Keller S. M., Kimura H., Knuuttila A., Kodama K., Komaki R., Kris M. G., Lad T., Mineo T., Piantadosi S., Rosell R., Scagliotti G., Seymour L. K., Shepherd F. A., Sylvester R., Tada H., Tanaka F., Torri V., Waller D., Liang Y. and Non-Small Cell Lung Cancer Collaborative G. **Adjuvant chemotherapy for resected early-stage non-small cell lung cancer**. *Cochrane Database Syst Rev*(3): CD011430 (2015).

Burger H., Zoumaro-Djayoon A., Boersma A. W., Helleman J., Berns E. M., Mathijssen R. H., Loos W. J. and Wiemer E. A. **Differential transport of platinum compounds by the human organic cation transporter hOCT2 (hSLC22A2)**. *Br J Pharmacol* 159(4): 898-908 (2010).

Butts C. A., Ding K., Seymour L., Twumasi-Ankrah P., Graham B., Gandara D., Johnson D. H., Kesler K. A., Green M., Vincent M., Cormier Y., Goss G., Findlay B., Johnston M., Tsao M. S. and Shepherd F. A. **Randomized phase III trial of vinorelbine plus cisplatin compared with observation in completely resected stage IB and II non-small-cell lung cancer: updated survival analysis of JBR-10**. *J Clin Oncol* 28(1): 29-34 (2010).

Cadranel J., Lavolé A., Gounant V., Antoine M. and Wislez M. **Carcinome bronchiolo-alvéolaire (CBA) : particularités et prise en charge thérapeutique**. *Rev Mal Respir Actual* 2: 298-305 (2010).

Camus P., Foucher P., Bonniaud P., Camus C., Guerriaud M., Jacquet L., Favrolt N., Baudouin N., Fanton A. and Rabec C. (2016). **"Pneumotox v 2.0."** Retrieved 18/11/16, from http://www.pneumotox.com/drug/view/401/cisplatin/.

Center for Drug Evaluation and Research. **Guidance for Industry Dissolution Testing of Immediate Release Solid Oral Dosage Forms**. **BP 1**. Food and Drug Administration. Rockville, USA (1997).

Charpidou A. G., Gkiozos I., Tsimpoukis S., Apostolaki D., Dilana K. D., Karapanagiotou E. M. and Syrigos K. N. **Therapy-induced toxicity of the lungs: an overview**. *Anticancer Res* 29(2): 631-639 (2009).

Chesnutt M. S. and Prendergast T. J. **Pulmonary Disease** in *Pathophysiology of Disease*. Mc Graw Hill Education (2014).

Chime S. A., Attama A. A., Builders P. F. and Onunkwo G. C. **Sustained-release diclofenac potassium-loaded solid lipid microparticle based on solidified reverse micellar solution: in vitro and in vivo evaluation**. *J Microencapsul* 30(4): 335-345 (2013).

Choe W. T., Chinosornvatana N. and Chang K. W. **Prevention of cisplatin ototoxicity using transtympanic N-acetylcysteine and lactate**. *Otol Neurotol* 25(6): 910-915 (2004).

Chou A. J., Bell M. D., Mackinson C., Gupta R., Meyers P. A. and Gorlick R. **Phase Ib/IIa study of sustained release lipid inhalation targeting cisplatin by inhalation in the treatment of patients with relapsed/progressive osteosarcoma metastatic to the lung**. *J Clin Oncol* 25(90180): 9525-9525 (2007).

Chou A. J., Gupta R., Bell M. D., Riewe K. O., Meyers P. A. and Gorlick R. **Inhaled lipid cisplatin (ILC) in the treatment of patients with relapsed/progressive osteosarcoma metastatic to the lung**. *Pediatr Blood Cancer* 60(4): 580-586 (2013).

Ciarimboli G., Ludwig T., Lang D., Pavenstädt H., Koepsell H., Piechota H.-J., Haier J., Jaehde U., Zisowsky J. and Schlatter E. **Cisplatin Nephrotoxicity Is Critically Mediated via the**

Human Organic Cation Transporter 2. *The American Journal of Pathology* 167(6): 1477-1484 (2005).

Coates M. S., Chan H. K., Fletcher D. F. and Raper J. A. **Influence of air flow on the performance of a dry powder inhaler using computational and experimental analyses**. *Pharm Res* 22(9): 1445-1453 (2005).

Coluccia M. and Natile G. **Trans-platinum complexes in cancer therapy**. *Anticancer Agents Med Chem* 7(1): 111-123 (2007).

Cook R. O., Pannu R. K. and Kellaway I. W. **Novel sustained release microspheres for pulmonary drug delivery**. *J Control Release* 104(1): 79-90 (2005).

Costa P. and Sousa Lobo J. M. **Modeling and comparison of dissolution profiles**. *Eur J Pharm Sci* 13(2): 123-133 (2001).

Crow J., Slavin G. and Kreel L. **Pulmonary metastasis: a pathologic and radiologic study**. *Cancer* 47(11): 2595-2602 (1981).

Cvitkovic E., Spaulding J., Bethune V., Martin J. and Whitmore W. F. **Improvement of cis-dichlorodiammineplatinum (NSC 119875): therapeutic index in an animal model**. *Cancer* 39(4): 1357-1361 (1977).

Dailey L. A., Jekel N., Fink L., Gessler T., Schmehl T., Wittmar M., Kissel T. and Seeger W. **Investigation of the proinflammatory potential of biodegradable nanoparticle drug delivery systems in the lung**. *Toxicol Appl Pharmacol* 215(1): 100-108 (2006).

Dalpiaz A., Cacciari B., Mezzena M., Strada M. and Scalia S. **Solid lipid microparticles for the stability enhancement of a dopamine prodrug**. *J Pharm Sci* 99(11): 4730-4737 (2010).

Dalpiaz A., Ferraro L., Perrone D., Leo E., Iannuccelli V., Pavan B., Paganetto G., Beggiato S. and Scalia S. **Brain uptake of a Zidovudine prodrug after nasal administration of solid lipid microparticles**. *Mol Pharm* 11(5): 1550-1561 (2014).

Dalpiaz A., Mezzena M., Scatturin A. and Scalia S. **Solid lipid microparticles for the stability enhancement of the polar drug N6-cyclopentyladenosine**. *Int J Pharm* 355(1-2): 81-86 (2008).

Darwiche K., Zarogoulidis P., Karamanos N. K., Domvri K., Chatzaki E., Constantinidis T. C., Kakolyris S. and Zarogoulidis K. **Efficacy versus safety concerns for aerosol chemotherapy in non-small-cell lung cancer: a future dilemma for micro-oncology**. *Future Oncol* 9(4): 505-525 (2013).

Datta D. and Lahiri B. **Preoperative evaluation of patients undergoing lung resection surgery**. *Chest* 123(6): 2096-2103 (2003).

Davies N. M. and Feddah M. R. **A novel method for assessing dissolution of aerosol inhaler products**. *Int J Pharm* 255(1-2): 175-187 (2003).

de Boer A. H. and Hagedoorn P. **The role of disposable inhalers in pulmonary drug delivery**. *Expert Opin Drug Deliv* 12(1): 143-157 (2015).

DeConti R. C., Toftness B. R., Lange R. C. and Creasey W. A. **Clinical and pharmacological studies with cis-diamminedichloroplatinum (II)**. *Cancer Res* 33(6): 1310-1315 (1973).

Dela Cruz C. S., Tanoue L. T. and Matthay R. A. **Lung cancer: epidemiology, etiology, and prevention**. *Clin Chest Med* 32(4): 605-644 (2011).

deMan J. M., Mostafa A. N. and Smith A. K. **Thermal Analysis Microscopy for the Study of Phase Changes in Fats**. *Food Structure* 4(2): 233-239 (1985).

Demirel M., Yazan Y., Müller R. H. and Bozan F. K. B. **Formulation and in vitro-in vivo evaluation of piribedil solid lipid micro- and nanoparticles**. *Journal of Microencapsulation* 18(3): 359-371 (2001).

Denoix P. **Enquête permanente dans les centres anticancéreux**. *Bull Inst Natl Hyg* 1: 12-17 (1946).

Depreter F. and Amighi K. **Formulation and in vitro evaluation of highly dispersive insulin dry powder formulations for lung administration**. *Eur J Pharm Biopharm* 76(3): 454-463 (2010).

Detterbeck F. C., Boffa D. J., Kim A. W. and Tanoue L. T. **The Eighth Edition Lung Cancer Stage Classification**. *Chest* 151(1): 193-203 (2017).

Detterbeck F. C., Boffa D. J. and Tanoue L. T. **The new lung cancer staging system**. *Chest* 136(1): 260-271 (2009).

Dishop M. K. and Kuruvilla S. **Primary and metastatic lung tumors in the pediatric population: a review and 25-year experience at a large children's hospital**. *Arch Pathol Lab Med* 132(7): 1079-1103 (2008).

Dolovich M. B. and Dhand R. **Aerosol drug delivery: developments in device design and clinical use**. *Lancet* 377(9770): 1032-1045 (2011).

Dulohery M. M., Maldonado F. and Limper A. H. **71 - Drug-Induced Pulmonary Disease** in *Murray and Nadel's Textbook of Respiratory Medicine (Sixth Edition)*. Philadelphia, W.B. Saunders**: 1275-1294.e1217 (2016).

Duncan R. and Izzo L. **Dendrimer biocompatibility and toxicity**. *Adv Drug Deliv Rev* 57(15): 2215-2237 (2005).

Duret C., Merlos R., Wauthoz N., Sebti T., Vanderbist F. and Amighi K. **Pharmacokinetic evaluation in mice of amorphous itraconazole-based dry powder formulations for inhalation with high bioavailability and extended lung retention**. *Eur J Pharm Biopharm* 86(1): 46-54 (2014).

Duret C., Wauthoz N., Merlos R., Goole J., Maris C., Roland I., Sebti T., Vanderbist F. and Amighi K. **In vitro and in vivo evaluation of a dry powder endotracheal insufflator device for use in dose-dependent preclinical studies in mice**. *Eur J Pharm Biopharm* 81(3): 627-634 (2012a).

Duret C., Wauthoz N., Sebti T., Vanderbist F. and Amighi K. **New respirable and fast dissolving itraconazole dry powder composition for the treatment of invasive pulmonary aspergillosis**. *Pharm Res* 29(10): 2845-2859 (2012b).

Edwards D. A., Hanes J., Caponetti G., Hrkach J., Ben-Jebria A., Eskew M. L., Mintzes J., Deaver D., Lotan N. and Langer R. **Large porous particles for pulmonary drug delivery**. *Science* 276(5320): 1868-1871 (1997).

Einhorn L. H. and Donohue J. **Cis-diamminedichloroplatinum, vinblastine, and bleomycin combination chemotherapy in disseminated testicular cancer**. *Ann Intern Med* 87(3): 293-298 (1977).

El-Gendy N. and Berkland C. **Combination chemotherapeutic dry powder aerosols via controlled nanoparticle agglomeration**. *Pharm Res* 26(7): 1752-1763 (2009).

El-Khateeb M., Appleton T. G., Charles B. G. and Gahan L. R. **Development of HPLC conditions for valid determination of hydrolysis products of cisplatin**. *J Pharm Sci* 88(3): 319-326 (1999).

Eldem T., Speiser P. and Hincal A. **Optimization of spray-dried and -congealed lipid micropellets and characterization of their surface morphology by scanning electron microscopy**. *Pharm Res* 8(1): 47-54 (1991).

Eljack N. D., Ma H. Y., Drucker J., Shen C., Hambley T. W., New E. J., Friedrich T. and Clarke R. J. **Mechanisms of cell uptake and toxicity of the anticancer drug cisplatin**. *Metallomics* 6(11): 2126-2133 (2014).

Elkins M. R., Anderson S. D., Perry C. P., Daviskas E. and Charlton B. **Inspiratory Flows and Volumes in Subjects with Non-CF Bronchiectasis Using a New Dry Powder Inhaler Device**. *Open Respir Med J* 8: 8-13 (2014a).

Elkins M. R., Robinson P., Anderson S. D., Perry C. P., Daviskas E. and Charlton B. **Inspiratory flows and volumes in subjects with cystic fibrosis using a new dry powder inhaler device**. *Open Respir Med J* 8: 1-7 (2014b).

Epstein S. W., Manning C. P., Ashley M. J. and Corey P. N. **Survey of the clinical use of pressurized aerosol inhalers**. *Can Med Assoc J* 120(7): 813-816 (1979).

European Pharmacopoeia. **2.9.18. Preparations for inhalation: Aerodynamic assessment of fine particles** (2014).

Evans C. M. and Koo J. S. **Airway mucus: the good, the bad, the sticky**. *Pharmacol Ther* 121(3): 332-348 (2009).

Fassoulaki A. and Pavlou H. **Overdosage intoxication with cisplatin--a cause of acute respiratory failure**. *J R Soc Med* 82(11): 689 (1989).

Fatima N., Cohen C., Lawson D. and Siddiqui M. T. **TTF-1 and Napsin A double stain**. *Cancer Cytopathol* 119(2): 127-133 (2011).

FDA. **Guidance for Industry, Bioanalytical Method Validation**. Food and Drug Administration (2013).

Ferlay J., Soerjomataram I., Dikshit R., Eser S., Mathers C., Rebelo M., Parkin D. M., Forman D. and Bray F. **Cancer incidence and mortality worldwide: sources, methods and major patterns in GLOBOCAN 2012**. *Int J Cancer* 136(5): E359-386 (2015).

Ferlay J., Steliarova-Foucher E., Lortet-Tieulent J., Rosso S., Coebergh J. W., Comber H., Forman D. and Bray F. **Cancer incidence and mortality patterns in Europe: estimates for 40 countries in 2012**. *Eur J Cancer* 49(6): 1374-1403 (2013).

Fiegel J., Brenza T. and Hamed R. **Controlled Transport for Pulmonary Drug Delivery** in *Controlled Pulmonary Drug Delivery*. Smyth H. D. C. and Hickey A. J. New York, NY, Springer**:** 143-163 (2011).

Florea A. M. and Busselberg D. **Cisplatin as an anti-tumor drug: cellular mechanisms of activity, drug resistance and induced side effects**. *Cancers (Basel)* 3(1): 1351-1371 (2011).

Forastiere A. A., Belliveau J. F., Goren M. P., Vogel W. C., Posner M. R. and O'Leary G. P., Jr. **Pharmacokinetic and toxicity evaluation of five-day continuous infusion versus intermittent bolus cis-diamminedichloroplatinum(II) in head and neck cancer patients**. *Cancer Res* 48(13): 3869-3874 (1988).

Friebel C. and Steckel H. **Single-use disposable dry powder inhalers for pulmonary drug delivery**. *Expert Opin Drug Deliv* 7(12): 1359-1372 (2010).

Fusaro L., Mameli G., Mocci F., Luhmer M. and Cerioni G. **Dynamic NMR of low-sensitivity fast-relaxing nuclei: 17O NMR and DFT study of acetoxysilanes**. *Magn. Reson. Chem.* 50(2): 152-158 (2012).

Gagnadoux F., Hureaux J., Vecellio L., Urban T., Le Pape A., Valo I., Montharu J., Leblond V., Boisdron-Celle M., Lerondel S., Majoral C., Diot P., Racineux J. L. and Lemarie E. **Aerosolized chemotherapy**. *J Aerosol Med Pulm Drug Deliv* 21(1): 61-70 (2008).

Giaccone G. **Clinical perspectives on platinum resistance**. *Drugs* 59 Suppl 4: 9-17; discussion 37-18 (2000).

Gill K. K., Nazzal S. and Kaddoumi A. **Paclitaxel loaded PEG(5000)-DSPE micelles as pulmonary delivery platform: formulation characterization, tissue distribution, plasma pharmacokinetics, and toxicological evaluation**. *Eur J Pharm Biopharm* 79(2): 276-284 (2011).

Goldstraw P., Ball D., Jett J. R., Le Chevalier T., Lim E., Nicholson A. G. and Shepherd F. A. **Non-small-cell lung cancer**. *Lancet* 378(9804): 1727-1740 (2011).

Gotway M. B., Panse P. M., Gruden J. F. and Elicker B. M. **18 - Thoracic Radiology: Noninvasive Diagnostic Imaging** in *Murray and Nadel's Textbook of Respiratory Medicine (Sixth Edition)*. Philadelphia, W.B. Saunders**:** 299-331.e228 (2016).

Gridelli C., Rossi A. and Maione P. **Treatment of non-small-cell lung cancer: state of the art and development of new biologic agents**. *Oncogene* 22(42): 6629-6638 (2003).

Grigoriu B. and Meert A. P. **Traitement des cancers bronchiques à petites cellules : maladies étendues. Recommandations de pratique clinique de l'*European Cancer Working Party***. *Rev Med Brux* 35: 164-168 (2014).

Grommes J. and Soehnlein O. **Contribution of neutrophils to acute lung injury**. *Mol Med* 17(3-4): 293-307 (2011).

Gross G., Cohen R. M. and Guy H. **Efficacy response of inhaled HFA-albuterol delivered via the breath-actuated Autohaler inhalation device is comparable to dose in patients with asthma**. *J Asthma* 40(5): 487-495 (2003).

Gugu T. H., Chime S. A. and Attama A. A. **Solid lipid microparticles: An approach for improving oral bioavailability of aspirin**. *Asian J Pharm Sci* 10(5): 425-432 (2015).

Gupta V. and Ahsan F. **Influence of PEI as a core modifying agent on PLGA microspheres of PGE(1), a pulmonary selective vasodilator**. *Int J Pharm* 413(1-2): 51-62 (2011).

Hall M. D., Telma K. A., Chang K. E., Lee T. D., Madigan J. P., Lloyd J. R., Goldlust I. S., Hoeschele J. D. and Gottesman M. M. **Say no to DMSO: dimethylsulfoxide inactivates cisplatin, carboplatin, and other platinum complexes**. *Cancer Res* 74(14): 3913-3922 (2014).

Hann S., Stefanka Z., Lenz K. and Stingeder G. **Novel separation method for highly sensitive speciation of cancerostatic platinum compounds by HPLC-ICP-MS**. *Anal Bioanal Chem* 381(2): 405-412 (2005).

Harder H. C. and Rosenberg B. **Inhibitory effects of anti-tumor platinum compounds on DNA, RNA and protein syntheses in mammalian cells in virtro**. *Int J Cancer* 6(2): 207-216 (1970).

Hayes D. M., Cvitkovic E., Golbey R. B., Scheiner E., Helson L. and Krakoff I. H. **High dose cis-platinum diammine dichloride: amelioration of renal toxicity by mannitol diuresis**. *Cancer* 39(4): 1372-1381 (1977).

Hecq J. **Development, characterization and evaluation of crystalline nanoparticles for enhancing the solubility, the dissolution rate and the oral bioavailability of poorly water-soluble drugs (Doctoral thesis)**. Doctoral Thesis, Université libre de Bruxelles (ULB) (2006).

Henschke C. I., Naidich D. P., Yankelevitz D. F., McGuinness G., McCauley D. I., Smith J. P., Libby D., Pasmantier M., Vazquez M., Koizumi J., Flieder D., Altorki N. and Miettinen O. S. **Early Lung Cancer Action Project**. *Cancer* 92(1): 153-159 (2001).

Holbrechts S. and Roelandts M. **Traitement du cancer bronchique à petites cellules : maladies limitées. Recommandations de pratique clinique de l'***European Cancer Working Party***. *Rev Med Brux* 35: 160-163 (2014).

Hopfer S. M., Ziebka L., Sunderman F. W., Jr., Sporn J. R. and Greenberg B. R. **Direct analysis of platinum in plasma and urine by electrothermal atomic absorption spectrophotometry**. *Ann Clin Lab Sci* 19(6): 389-396 (1989).

Hoppentocht M., Hagedoorn P., Frijlink H. W. and de Boer A. H. **Technological and practical challenges of dry powder inhalers and formulations**. *Adv Drug Deliv Rev* 75: 18-31 (2014).

Howington J. A., Blum M. G., Chang A. C., Balekian A. A. and Murthy S. C. **Treatment of Stage I and II Non-small Cell Lung Cancer: Diagnosis and Management of Lung Cancer, 3rd ed: American College of Chest Physicians Evidence-Based Clinical Practice Guidelines**. *Chest* 143(5, Supplement): e278S-e313S (2013).

Howlader N., Noone A., Krapcho M., Garshell J., Miller D., Altekruse S., Kosary C., Yu M., Ruhl J., Tatalovich Z., Mariotto A., Lewis D., Chen H., Feuer E. and Cronin K. **SEER Cancer Statistics Review, 1975-2012**, National Cancer Institute. Bethesda, MD. (2015).

Huang Z., Li X., Zhang T., Song Y., She Z., Li J. and Deng Y. **Progress involving new techniques for liposome preparation**. *Asian J Pharm Sci* 9(4): 176-182 (2014).

Hulse W. L., Forbes R. T., Bonner M. C. and Getrost M. **The characterization and comparison of spray-dried mannitol samples**. *Drug Dev Ind Pharm* 35(6): 712-718 (2009).

Hureaux J., Lagarce F., Gagnadoux F., Vecellio L., Clavreul A., Roger E., Kempf M., Racineux J. L., Diot P., Benoit J. P. and Urban T. **Lipid nanocapsules: ready-to-use nanovectors for the aerosol delivery of paclitaxel**. *Eur J Pharm Biopharm* 73(2): 239-246 (2009).

ICH Expert Working Group. **Validation of Analytical Procedures: Text and Methodology Q2(R1), ICH Harmonised Tripartite Guideline** (2005).

Ignatius Ou S. H. and Zell J. A. **The applicability of the proposed IASLC staging revisions to small cell lung cancer (SCLC) with comparison to the current UICC 6th TNM Edition**. *J Thorac Oncol* 4(3): 300-310 (2009).

Ishida S., Lee J., Thiele D. J. and Herskowitz I. **Uptake of the anticancer drug cisplatin mediated by the copper transporter Ctr1 in yeast and mammals**. *Proc Natl Acad Sci U S A* 99(22): 14298-14302 (2002).

Ivy K. D. and Kaplan J. H. **A re-evaluation of the role of hCTR1, the human high-affinity copper transporter, in platinum-drug entry into human cells**. *Mol Pharmacol* 83(6): 1237-1246 (2013).

Jain A. **Body fluid composition**. *Pediatr Rev* 36(4): 141-150; quiz 151-142 (2015).

Jamieson E. R. and Lippard S. J. **Structure, Recognition, and Processing of Cisplatin-DNA Adducts**. *Chem Rev* 99(9): 2467-2498 (1999).

Jansen B. A., Brouwer J. and Reedijk J. **Glutathione induces cellular resistance against cationic dinuclear platinum anticancer drugs**. *J Inorg Biochem* 89(3-4): 197-202 (2002).

Jaspart S., Bertholet P., Piel G., Dogne J. M., Delattre L. and Evrard B. **Solid lipid microparticles as a sustained release system for pulmonary drug delivery**. *Eur J Pharm Biopharm* 65(1): 47-56 (2007).

Jaspart S., Piel G., Delattre L. and Evrard B. **Solid lipid microparticles: formulation, preparation, characterisation, drug release and applications**. *Expert Opin Drug Deliv* 2(1): 75-87 (2005).

Jiang L., Zhang Z., Dong P., Li Y., Yao K., Liu Z., Han H., Qin Z., Yao M. and Zhou F. **Efficacy of radical cystectomy plus adjuvant intraarterial chemotherapy with gemcitabine and cisplatin on locally advanced bladder cancer**. *Chin Med J (Engl)* 127(7): 1249-1254 (2014).

Johnson D. H., Blot W. J., Carbone D. P., Gonzalez A., Hallahan D., Massion P. P., Putnam J. B. and Sandler A. B. **Cancer of the Lung: Non-Small Cell Lung Cancer and Small Cell Lung Cancer** in *Abeloff's clinical oncology*. Philadelphia, Churchill Livingstone/Elsevier: 1307-1366 (2008).

Johnson K. A. **Preparation of peptide and protein powders for inhalation**. *Adv Drug Deliv Rev* 26(1): 3-15 (1997).

Jordan K., Sippel C. and Schmoll H. J. **Guidelines for antiemetic treatment of chemotherapy-induced nausea and vomiting: past, present, and future recommendations**. *Oncologist* 12(9): 1143-1150 (2007).

Kaifi J. T., Gusani N. J., Deshaies I., Kimchi E. T., Reed M. F., Mahraj R. P. and Staveley-O'Carroll K. F. **Indications and approach to surgical resection of lung metastases**. *J Surg Oncol* 102(2): 187-195 (2010).

Kalemkerian G. P. and Gadgeel S. M. **Modern staging of small cell lung cancer**. *J Natl Compr Canc Netw* 11(1): 99-104 (2013).

Kaminskas L. M., McLeod V. M., Ryan G. M., Kelly B. D., Haynes J. M., Williamson M., Thienthong N., Owen D. J. and Porter C. J. **Pulmonary administration of a doxorubicin-conjugated dendrimer enhances drug exposure to lung metastases and improves cancer therapy**. *J Control Release* 183: 18-26 (2014).

Kanda T., Harada T., Tominaga Y. and Suzumori K. **Emulsion generation using microchannel plates and 2.25 MHz ultrasonic vibrators**. 2010 IEEE International Ultrasonics Symposium (2010).

Karbownik A., Szalek E., Urjasz H., Gleboka A., Mierzwa E. and Grzeskowiak E. **The physical and chemical stability of cisplatin (Teva) in concentrate and diluted in sodium chloride 0.9%**. *Contemporary oncology* 16(5): 435-439 (2012).

Katzenstein H. M., Petricca S., Ricketts R., Wasilewski-Masker K., Powell C., Rapkin L., George B., Woods W. G. and Olson T. A. **Intracavitary cisplatin therapy for pediatric malignancies**. *Pediatr Blood Cancer* 55(3): 452-456 (2010).

Kelsen D. P., Alcock N. and Young C. W. **Cisplatin nephrotoxicity. Correlation with plasma platinum concentrations**. *Am J Clin Oncol* 8(1): 77-80 (1985).

Kelsey C. R., Marks L. B., Hollis D., Hubbs J. L., Ready N. E., D'Amico T. A. and Boyd J. A. **Local recurrence after surgery for early stage lung cancer: an 11-year experience with 975 patients**. *Cancer* 115(22): 5218-5227 (2009).

Klonne D. R., Dodd D. E., Losco P. E., Troup C. M. and Tyler T. R. **Two-week aerosol inhalation study on polyethylene glycol (PEG) 3350 in F-344 rats**. *Drug Chem Toxicol* 12(1): 39-48 (1989).

Kobayashi H., Watanabe R. and Choyke P. L. **Improving conventional enhanced permeability and retention (EPR) effects; what is the appropriate target?** *Theranostics* 4(1): 81-89 (2013).

Koren G., Carey N., Gagnon R., Maxwell C., Nulman I. and Senikas V. **Cancer Chemotherapy and Pregnancy**. **SOGC Clinical Practice Guideline** (2013).

Koźmiński W. and Jackowski K. **Application of adiabatic inversion pulses for elimination of baseline distortions in Fourier transform NMR. A natural abundance 17O NMR spectrum for gaseous acetone**. *Magn. Reson. Chem.* 38(6): 459-462 (2000).

Küpeli E., Feller-Kopman D. and Mehta A. C. **22 - Diagnostic Bronchoscopy** in *Murray and Nadel's Textbook of Respiratory Medicine (Sixth Edition)*. Mason R. J., Ernst J. D., King T. E. et al. Philadelphia, W.B. Saunders**:** 372-382.e375 (2016).

Labiris N. R. and Dolovich M. B. **Pulmonary drug delivery. Part II: the role of inhalant delivery devices and drug formulations in therapeutic effectiveness of aerosolized medications**. *Br J Clin Pharmacol* 56(6): 600-612 (2003).

Lai S. K., Wang Y. Y., Wirtz D. and Hanes J. **Micro- and macrorheology of mucus**. *Adv Drug Deliv Rev* 61(2): 86-100 (2009).

Lauterbach A. and Mueller-Goymann C. C. **Development, formulation, and characterization of an adapalene-loaded solid lipid microparticle dispersion for follicular penetration**. *Int J Pharm* 466(1-2): 122-132 (2014).

Le Chevalier T., Arriagada R., Pignon J. P. and Scagliotti G. V. **Should adjuvant chemotherapy become standard treatment in all patients with resected non-small-cell lung cancer?** *Lancet Oncol* 6(3): 182-184 (2005).

Le Gac S., Fusaro L., Roisnel T. and Boitrel B. **Heterobimetallic Porphyrin Complexes Displaying Triple Dynamics: Coupled Metal Motions Controlled by Constitutional Evolution**. *J. Am. Chem. Soc.* 136(18): 6698-6715 (2014).

Lee J., Oh Y. J., Lee S. K. and Lee K. Y. **Facile control of porous structures of polymer microspheres using an osmotic agent for pulmonary delivery**. *J Control Release* 146(1): 61-67 (2010).

Lee Y. Y., Wu J. X., Yang M., Young P. M., van den Berg F. and Rantanen J. **Particle size dependence of polymorphism in spray-dried mannitol**. *Eur J Pharm Sci* 44(1-2): 41-48 (2011).

Lemarie E., Vecellio L., Hureaux J., Prunier C., Valat C., Grimbert D., Boidron-Celle M., Giraudeau B., le Pape A., Pichon E., Diot P., el Houfia A. and Gagnadoux F. **Aerosolized gemcitabine in patients with carcinoma of the lung: feasibility and safety study**. *J Aerosol Med Pulm Drug Deliv* 24(6): 261-270 (2011).

LeRoy A. F., Wehling M. L., Sponseller H. L., Friauf W. S., Solomon R. E., Dedrick R. L., Litterst C. L., Gram T. E., Guarino A. M. and Becker D. A. **Analysis of platinum in biological materials by flameless atomic absorption spectrophotometry**. *Biochem Med* 18(2): 184-191 (1977).

Lippman A. J., Helson C., Helson L. and Krakoff I. H. **Clinical trials of cis-diamminedichloroplatinum (NSC-119875)**. *Cancer Chemother Rep* 57(2): 191-200 (1973).

Loira-Pastoriza C., Todoroff J. and Vanbever R. **Delivery strategies for sustained drug release in the lungs**. *Adv Drug Deliv Rev* 75: 81-91 (2014).

Mahapatro A. and Singh D. K. **Biodegradable nanoparticles are excellent vehicle for site directed in-vivo delivery of drugs and vaccines**. *J Nanobiotechnology* 9: 55 (2011).

Malik N., Wiwattanapatapee R., Klopsch R., Lorenz K., Frey H., Weener J. W., Meijer E. W., Paulus W. and Duncan R. **Dendrimers:: Relationship between structure and biocompatibility in vitro, and preliminary studies on the biodistribution of 125I-labelled polyamidoamine dendrimers in vivo**. *J Control Release* 65(1–2): 133-148 (2000).

Maretti E., Rossi T., Bondi M., Croce M. A., Hanuskova M., Leo E., Sacchetti F. and Iannuccelli V. **Inhaled Solid Lipid Microparticles to target alveolar macrophages for tuberculosis**. *Int J Pharm* 462(1–2): 74-82 (2014).

Marques M. P., Valero R., Parker S. F., Tomkinson J. and Batista de Carvalho L. A. **Polymorphism in cisplatin anticancer drug**. *J Phys Chem B* 117(21): 6421-6429 (2013).

Martin A. R. and Finlay W. H. **Nebulizers for drug delivery to the lungs**. *Expert Opin Drug Deliv* 12(6): 889-900 (2015).

Martini M., Ober W. C., Garrison C. W., Welch K. and Hutchings R. T. **Fundamentals of Anatomy & Physiology**, Prentice Hall College Div. (2001).

Mason R. J. and Dobbs L. G. **8 - Alveolar Epithelium and Pulmonary Surfactant** in *Murray and Nadel's Textbook of Respiratory Medicine (Sixth Edition)*. Philadelphia, W.B. Saunders: 134-149.e135 (2016).

Massion P. P., Sequist L. V. and Pao W. **51 - Biology of Lung Cancer** in *Murray and Nadel's Textbook of Respiratory Medicine (Sixth Edition)*. Mason R. J., Ernst J. D., King T. E. et al. Philadelphia, W.B. Saunders: 912-926.e916 (2016).

Masters D. B. and Domb A. J. **Liposphere local anesthetic timed-release for perineural site application**. *Pharm Res* 15(7): 1038-1045 (1998).

May S., Jensen B., Wolkenhauer M., Schneider M. and Lehr C. M. **Dissolution techniques for in vitro testing of dry powders for inhalation**. *Pharm Res* 29(8): 2157-2166 (2012).

Mehta H. J., Begnaud A., Penley A. M., Wynne J., Malhotra P., Fernandez-Bussy S., Cope J. M., Shuster J. J. and Jantz M. A. **Treatment of isolated mediastinal and hilar recurrence of lung cancer with bronchoscopic endobronchial ultrasound guided intratumoral injection of chemotherapy with cisplatin**. *Lung Cancer* 90(3): 542-547 (2015).

Mezzena M., Scalia S., Young P. M. and Traini D. **Solid lipid budesonide microparticles for controlled release inhalation therapy**. *AAPS Journal* 11(4): 771-778 (2009).

Milacic R., Cemazar M. and Sersa G. **Determination of platinum in tumour tissues after cisplatin therapy by electrothermal atomic absorption spectrometry**. *J Pharm Biomed Anal* 16(2): 343-348 (1997).

Miller R. P., Tadagavadi R. K., Ramesh G. and Reeves W. B. **Mechanisms of Cisplatin nephrotoxicity**. *Toxins (Basel)* 2(11): 2490-2518 (2010).

Minchinton A. I. and Tannock I. F. **Drug penetration in solid tumours**. *Nat Rev Cancer* 6(8): 583-592 (2006).

Morgensztern D., Ng S. H., Gao F. and Govindan R. **Trends in stage distribution for patients with non-small cell lung cancer: a National Cancer Database survey**. *J Thorac Oncol* 5(1): 29-33 (2010).

Mountain C. F. and Dresler C. M. **Regional lymph node classification for lung cancer staging**. *Chest* 111(6): 1718-1723 (1997).

Myrdal P. B., Sheth P. and Stein S. W. **Advances in metered dose inhaler technology: formulation development**. *AAPS PharmSciTech* 15(2): 434-455 (2014).

Nagai N., Kinoshita M., Ogata H., Tsujino D., Wada Y., Someya K., Ohno T., Masuhara K., Tanaka Y., Kato K., Nagai H., Yokoyama A. and Kurita Y. **Relationship between pharmacokinetics of unchanged cisplatin and nephrotoxicity after intravenous infusions of cisplatin to cancer patients**. *Cancer Chemother Pharmacol* 39(1): 131-137 (1996).

Nasr M., Najlah M., D'Emanuele A. and Elhissi A. **PAMAM dendrimers as aerosol drug nanocarriers for pulmonary delivery via nebulization**. *Int J Pharm* 461(1-2): 242-250 (2014).

NCCN. (2014a). "**National Comprehensive Cancer Network , Clinical Practice Guidelines in Oncology, Small Cell Lung Cancer. v2.2014.**" Retrieved 25/01/2016, from https://www.nccn.org/professionals/physician_gls/pdf/sclc.pdf.

NCCN. (2014b). "**National Comprehensive Cancer Network, Clinical Practice Guidelines in Oncology Small Cell Lung Cancer. v2.2014.**" Retrieved 25/01/2016, from https://www.tri-kobe.org/nccn/guideline/lung/english/small.pdf.

NCCN. (2015). "**National Comprehensive Cancer Network, Clinical Practice Guidelines in Oncology Non-Small Cell Lung Cancer. v 7.2015.**" Retrieved 25/11/2016, from http://www.nccn.org/professionals/physician_gls/pdf/nscl.pdf.

Ndoyom V., Fusaro L., Dorcet V., Boitrel B. and Le Gac S. **Sunlight-Driven Formation and Dissociation of a Dynamic Mixed-Valence Thallium(III)/Thallium(I) Porphyrin Complex**. *Angew. Chem. Int. Ed. Engl.* 54(12): 3806-3811 (2015).

Newman S. P., Weisz A. W., Talaee N. and Clarke S. W. **Improvement of drug delivery with a breath actuated pressurised aerosol for patients with poor inhaler technique**. *Thorax* 46(10): 712-716 (1991).

NHS. **National Health Services Guidelines for intravenous hydration for chemotherapy regimes in adults**. Network S. C., Cancer Chemotherapy Group (2012).

Nokhodchi A. and Martin G. P. **Pulmonary drug delivery : advances and challenges**. Chichester, United Kingdom ; Hoboken, NJ, John Wiley and Sons (2015).

O'Bryant C. L., Wenger S. D., Kim M. and Thompson L. A. **Crizotinib: a new treatment option for ALK-positive non-small cell lung cancer**. *Ann Pharmacother* 47(2): 189-197 (2013).

O'Callaghan C. and Barry P. W. **The science of nebulised drug delivery**. *Thorax* 52 Suppl 2: S31-44 (1997).

O'Neil M. J., Heckelman P. E., Dobbelaar P. H., Roman K. J., Kenny C. M., Karaffa L. S. and Royal Society of Chemistry (Great Britain). **The Merck index : an encyclopedia of chemicals, drugs, and biologicals**. Cambridge, UK, Royal Society of Chemistry (2013).

Oh J. H., McCurdy A. R., Clark S. and Swanson B. G. **Characterization and Thermal Stability of Polymorphic Forms of Synthesized Tristearin**. *J Food Sci* 67(8): 2911-2917 (2002).

Olsson B., Bondesson E., Borgström L., Edsbäcker S., Eirefelt S., Ekelund K., Gustavsson L. and Hegelund-Myrbäck T. **Pulmonary Drug Metabolism, Clearance, and Absorption** in *Controlled Pulmonary Drug Delivery*. Smyth H. D. C. and Hickey A. J. New York, NY, Springer New York**:** 21-50 (2011).

Omoti A. E. and Omoti C. E. **Ocular toxicity of systemic anticancer chemotherapy**. *Pharm Pract (Granada)* 4(2): 55-59 (2006).

Orive G., Anitua E., Pedraz J. L. and Emerich D. F. **Biomaterials for promoting brain protection, repair and regeneration**. *Nat Rev Neurosci* 10(9): 682-692 (2009).

Otterson G. A., Villalona-Calero M. A., Hicks W., Pan X., Ellerton J. A., Gettinger S. N. and Murren J. R. **Phase I/II study of inhaled doxorubicin combined with platinum-based therapy for advanced non-small cell lung cancer**. *Clin Cancer Res* 16(8): 2466-2473 (2010).

Otterson G. A., Villalona-Calero M. A., Sharma S., Kris M. G., Imondi A., Gerber M., White D. A., Ratain M. J., Schiller J. H., Sandler A., Kraut M., Mani S. and Murren J. R. **Phase I study of inhaled Doxorubicin for patients with metastatic tumors to the lungs**. *Clin Cancer Res* 13(4): 1246-1252 (2007).

Ozone Secretariat. **The Montreal Protocol on Substances that Deplete the Ozone Layer**. United Nations Environment Programme (UNEP) (1987).

Padua D., Zhang X. H., Wang Q., Nadal C., Gerald W. L., Gomis R. R. and Massague J. **TGFbeta primes breast tumors for lung metastasis seeding through angiopoietin-like 4**. *Cell* 133(1): 66-77 (2008).

Paesmans M. **Traitement des cancers bronchiques non à petites cellules locorégionaux. Recommandations de pratique clinique de l'*European Cancer Working Party***. *Rev Med Brux* 45: 140-144 (2014).

Pao W. and Hutchinson K. E. **Chipping away at the lung cancer genome**. *Nat Med* 18(3): 349-351 (2012).

Passerini N., Perissutti B., Albertini B., Voinovich D., Moneghini M. and Rodriguez L. **Controlled release of verapamil hydrochloride from waxy microparticles prepared by spray congealing**. *J Control Release* 88(2): 263-275 (2003).

Patel B., Gupta N. and Ahsan F. **Particle engineering to enhance or lessen particle uptake by alveolar macrophages and to influence the therapeutic outcome**. *Eur J Pharm Biopharm* 89: 163-174 (2015).

Patel B., Gupta V. and Ahsan F. **PEG-PLGA based large porous particles for pulmonary delivery of a highly soluble drug, low molecular weight heparin**. *J Control Release* 162(2): 310-320 (2012).

Patton J. S. and Byron P. R. **Inhaling medicines: delivering drugs to the body through the lungs**. *Nat Rev Drug Discov* 6(1): 67-74 (2007).

Peleg-Shulman T., Gibson D., Cohen R., Abra R. and Barenholz Y. **Characterization of sterically stabilized cisplatin liposomes by nuclear magnetic resonance**. *Biochim Biophys Acta* 1510(1-2): 278-291 (2001).

Pelosi G., Barbareschi M., Cavazza A., Graziano P., Rossi G. and Papotti M. **Large cell carcinoma of the lung: A tumor in search of an author. A clinically oriented critical reappraisal**. *Lung Cancer* 87(3): 226-231 (2015).

Peyrone M. **Ueber die Einwirkung des Ammoniaks auf Platinchlorür**. *Justus Liebigs Annalen der Chemie* 51(1): 1-29 (1844).

Pilcer G. and Amighi K. **Formulation strategy and use of excipients in pulmonary drug delivery**. *Int J Pharm* 392(1-2): 1-19 (2010).

Pilcer G., Sebti T. and Amighi K. **Formulation and characterization of lipid-coated tobramycin particles for dry powder inhalation**. *Pharm Res* 23(5): 931-940 (2006).

Pilcer G., Vanderbist F. and Amighi K. **Preparation and characterization of spray-dried tobramycin powders containing nanoparticles for pulmonary delivery**. *Int J Pharm* 365(1-2): 162-169 (2009).

Pilcer G., Wauthoz N. and Amighi K. **Lactose characteristics and the generation of the aerosol**. *Adv Drug Deliv Rev* 64(3): 233-256 (2012).

Possmayer F., Nag K., Rodriguez K., Qanbar R. and Schurch S. **Surface activity in vitro: role of surfactant proteins**. *Comp Biochem Physiol A Mol Integr Physiol* 129(1): 209-220 (2001).

Pritchard J. N. **Industry guidance for the selection of a delivery system for the development of novel respiratory products**. *Expert Opin Drug Deliv* 12(11): 1755-1765 (2015).

Rademaker-Lakhai J. M., Crul M., Zuur L., Baas P., Beijnen J. H., Simis Y. J. W., Zandwijk N. v. and Schellens J. H. M. **Relationship Between Cisplatin Administration and the Development of Ototoxicity**. *J Clin Oncol* 24(6): 918-924 (2006).

Rahimpour Y., Javadzadeh Y. and Hamishehkar H. **Solid lipid microparticles for enhanced dermal delivery of tetracycline HCl**. *Colloids Surf B Biointerfaces* 145: 14-20 (2016).

Rami-Porta R., Crowley J. J. and Goldstraw P. **The revised TNM staging system for lung cancer**. *Ann Thorac Cardiovasc Surg* 15(1): 4-9 (2009).

Rasch C. R., Hauptmann M., Schornagel J., Wijers O., Buter J., Gregor T., Wiggenraad R., de Boer J. P., Ackerstaff A. H., Kroger R., Hoebers F. J., Balm A. J. and Hilgers F. J. **Intra-arterial versus intravenous chemoradiation for advanced head and neck cancer: Results of a randomized phase 3 trial**. *Cancer* 116(9): 2159-2165 (2010).

Reece P. A., Stafford I., Russell J. and Gill P. G. **Nonlinear renal clearance of ultrafilterable platinum in patients treated with cis-dichlorodiammineplatinum (II)**. *Cancer Chemother Pharmacol* 15(3): 295-299 (1985).

Reithmeier H., Herrmann J. and Göpferich A. **Lipid microparticles as a parenteral controlled release device for peptides**. *J Control Release* 73(2–3): 339-350 (2001).

Roberts P. J. and Stinchcombe T. E. **KRAS mutation: should we test for it, and does it matter?** *J Clin Oncol* 31(8): 1112-1121 (2013).

Rosell R., Carcereny E., Gervais R., Vergnenegre A., Massuti B., Felip E., Palmero R., Garcia-Gomez R., Pallares C., Sanchez J. M., Porta R., Cobo M., Garrido P., Longo F., Moran T., Insa A., De Marinis F., Corre R., Bover I., Illiano A., Dansin E., de Castro J., Milella M., Reguart N., Altavilla G., Jimenez U., Provencio M., Moreno M. A., Terrasa J., Muñoz-Langa J., Valdivia J., Isla D., Domine M., Molinier O., Mazieres J., Baize N., Garcia-Campelo R., Robinet G., Rodriguez-Abreu D., Lopez-Vivanco G., Gebbia V., Ferrera-Delgado L., Bombaron P., Bernabe R., Bearz A., Artal A., Cortesi E., Rolfo C., Sanchez-Ronco M., Drozdowskyj A., Queralt C., de Aguirre I., Ramirez J. L., Sanchez J. J., Molina M. A., Taron M. and Paz-Ares L. **Erlotinib versus standard chemotherapy as first-line treatment for European patients with advanced EGFR mutation-positive non-small-cell lung cancer (EURTAC): a multicentre, open-label, randomised phase 3 trial**. *The Lancet Oncology* 13(3): 239-246 (2012).

Rosenberg B., Vancamp L. and Krigas T. **Inhibition of Cell Division in Escherichia Coli by Electrolysis Products from a Platinum Electrode**. *Nature* 205: 698-699 (1965).

Rosenberg B., VanCamp L., Trosko J. E. and Mansour V. H. **Platinum compounds: a new class of potent antitumour agents**. *Nature* 222(5191): 385-386 (1969).

Rosière R. **Development of dry powder formulations for inhalation based on nanomedicine for targeted lung cancer therapy**. Doctoral Thesis, Université libre de Bruxelles (ULB) (2016).

Rosiere R., Van Woensel M., Mathieu V., Langer I., Mathivet T., Vermeersch M., Amighi K. and Wauthoz N. **Development and evaluation of well-tolerated and tumor-penetrating polymeric micelle-based dry powders for inhaled anti-cancer chemotherapy**. *Int J Pharm* 501(1-2): 148-159 (2016).

Rossi A., Di Maio M., Chiodini P., Rudd R. M., Okamoto H., Skarlos D. V., Fruh M., Qian W., Tamura T., Samantas E., Shibata T., Perrone F., Gallo C., Gridelli C., Martelli O. and Lee S. M. **Carboplatin- or cisplatin-based chemotherapy in first-line treatment of small-cell lung cancer: the COCIS meta-analysis of individual patient data**. *J Clin Oncol* 30(14): 1692-1698 (2012).

Rudin C. M., Avila-Tang E. and Samet J. M. **Lung cancer in never smokers: a call to action**. *Clin Cancer Res* 15(18): 5622-5625 (2009).

Rybak L. P., Mukherjea D., Jajoo S. and Ramkumar V. **Cisplatin ototoxicity and protection: clinical and experimental studies**. *Tohoku J Exp Med* 219(3): 177-186 (2009).

Sacco J. J., Botten J., Macbeth F., Bagust A. and Clark P. **The average body surface area of adult cancer patients in the UK: a multicentre retrospective study**. *PLoS One* 5(1): e8933 (2010).

Saggar J. K., Yu M., Tan Q. and Tannock I. F. **The tumor microenvironment and strategies to improve drug distribution**. *Front Oncol* 3: 154 (2013).

Sanders M. **Inhalation therapy: an historical review**. *Prim Care Respir J* 16(2): 71-81 (2007).

Sanna V., Kirschvink N., Gustin P., Gavini E., Roland I., Delattre L. and Evrard B. **Preparation and in vivo toxicity study of solid lipid microparticles as carrier for pulmonary administration**. *AAPS PharmSciTech* 5(2): 17-23 (2004).

Santoso J. T., Lucci J. A., 3rd, Coleman R. L., Schafer I. and Hannigan E. V. **Saline, mannitol, and furosemide hydration in acute cisplatin nephrotoxicity: a randomized trial**. *Cancer Chemother Pharmacol* 52(1): 13-18 (2003).

Savolainen M., Khoo C., Glad H., Dahlqvist C. and Juppo A. M. **Evaluation of controlled-release polar lipid microparticles**. *Int J Pharm* 244(1–2): 151-161 (2002).

Scalia S., Haghi M., Losi V., Trotta V., Young P. M. and Traini D. **Quercetin solid lipid microparticles: a flavonoid for inhalation lung delivery**. *Eur J Pharm Sci* 49(2): 278-285 (2013).

Scalia S., Salama R., Young P. and Traini D. **Preparation and in vitro evaluation of salbutamol-loaded lipid microparticles for sustained release pulmonary therapy**. *J Microencapsul* 29(3): 225-233 (2012).

Schaeppi U., Heyman I. A., Fleischman R. W., Rosenkrantz H., Ilievski V., Phelan R., Cooney D. A. and Davis R. D. **cis-Dichlorodiammineplatinum(II) (NSC-119875): Preclinical Toxicologic Evaluation of Intravenous Injection in Dogs, Monkey and Mice**. *Toxicology And Applied Pharmacology* 25: 230-241 (1973).

Sculier J.-P. **Traitement des cancers bronchiques non à petites cellules de petit stade. Recommandations de pratique clinique de l'*European Cancer Working Party***. *Rev Med Brux* 35: 134-139 (2014).

Sebti T. and Amighi K. **Preparation and in vitro evaluation of lipidic carriers and fillers for inhalation**. *Eur J Pharm Biopharm* 63(1): 51-58 (2006a).

Sebti T., Pilcer G., Van Gansbeke B., Goldman S., Michils A., Vanderbist F. and Amighi K. **Pharmacoscintigraphic evaluation of lipid dry powder budesonide formulations for inhalation**. *Eur J Pharm Biopharm* 64(1): 26-32 (2006b).

Secretan B., Straif K., Baan R., Grosse Y., El Ghissassi F., Bouvard V., Benbrahim-Tallaa L., Guha N., Freeman C., Galichet L., Cogliano V. and W. H. O. International Agency for Research on Cancer Monograph Working Group. **A review of human carcinogens--Part E: tobacco, areca nut, alcohol, coal smoke, and salted fish**. *Lancet Oncol* 10(11): 1033-1034 (2009).

Selting K., Waldrep J. C., Reinero C., Branson K., Gustafson D., Kim D. Y., Henry C., Owen N., Madsen R. and Dhand R. **Feasibility and safety of targeted cisplatin delivery to a select lung lobe in dogs via the AeroProbe intracorporeal nebulization catheter**. *J Aerosol Med Pulm Drug Deliv* 21(3): 255-268 (2008).

Seo J. B., Im J. G., Goo J. M., Chung M. J. and Kim M. Y. **Atypical pulmonary metastases: spectrum of radiologic findings**. *Radiographics* 21(2): 403-417 (2001).

Shah A. R. and Banerjee R. **Effect of D-alpha-tocopheryl polyethylene glycol 1000 succinate (TPGS) on surfactant monolayers**. *Colloids Surf B Biointerfaces* 85(2): 116-124 (2011).

Shah R. B., Tawakkul M. A. and Khan M. A. **Comparative evaluation of flow for pharmaceutical powders and granules**. *AAPS PharmSciTech* 9(1): 250-258 (2008).

Shaik M. S., Haynes A., McSween J., Ikediobi O., Kanikkannan N. and Singh M. **Inhalation Delivery of Anticancer Agents via HFA-Based Metered Dose Inhaler Using Methotrexate as a Model Drug**. *J Aer Med* 15(3): 261-270 (2002).

Sheleg S. V., Korotkevich E. A., Zhavrid E. A., Muravskaya G. V., Smeyanovich A. F., Shanko Y. G., Yurkshtovich T. L., Bychkovsky P. B. and Belyaev S. A. **Local chemotherapy with cisplatin-depot for glioblastoma multiforme**. *J Neurooncol* 60(1): 53-59 (2002).

Shevchenko I. T. and Resnik G. E. **Inhalation of chemical substances and oxygen in radiotherapy of bronchial cancer**. *Neoplasma* 15(4): 419-426 (1968).

Shimizu M. and Rosenberg B. **A similar action to UV-irradiation and a preferential inhibition of DNA synthesis in E. coli by antitumor platinum compounds**. *J Antibiot (Tokyo)* 26(4): 243-245 (1973).

Shukuya T., Yamanaka T., Seto T., Daga H., Goto K., Saka H., Sugawara S., Takahashi T., Yokota S., Kaneda H., Kawaguchi T., Nagase S., Oguri T., Iwamoto Y., Nishimura T., Hattori Y., Nakagawa K., Nakanishi Y., Yamamoto N. and West Japan Oncology G. **Nedaplatin plus docetaxel versus cisplatin plus docetaxel for advanced or relapsed squamous cell carcinoma of the lung (WJOG5208L): a randomised, open-label, phase 3 trial**. *Lancet Oncol* 16(16): 1630-1638 (2015).

Siddik Z. H. **Cisplatin: mode of cytotoxic action and molecular basis of resistance**. *Oncogene* 22(47): 7265-7279 (2003).

Siddik Z. H., Jones M., Boxall F. E. and Harrap K. R. **Comparative distribution and excretion of carboplatin and cisplatin in mice**. *Cancer Chemother Pharmacol* 21(1): 19-24 (1988).

Siegel R., Ward E., Brawley O. and Jemal A. **Cancer statistics, 2011: the impact of eliminating socioeconomic and racial disparities on premature cancer deaths**. *CA Cancer J Clin* 61(4): 212-236 (2011).

Siegel R. A. and Rathbone M. J. **Overview of Controlled Release Mechanisms** in *Fundamentals and Applications of Controlled Release Drug Delivery*. Siepmann J., Siegel R. and Rathbone M. J., Springer**:** 19-43 (2012).

Simon M., Argiris A. and Murren J. R. **Progress in the therapy of small cell lung cancer**. *Crit Rev Oncol Hematol* 49(2): 119-133 (2004).

Singh S. K., Jalali A. F. and Aldén M. **Modulated temperature differential scanning calorimetry for examination of tristearin polymorphism: I. Effect of operational parameters**. *J Am Oil Chem Soc* 76(4): 499-505 (1999).

Sleijfer S. **Bleomycin-induced pneumonitis**. *Chest* 120(2): 617-624 (2001).

Snipes M. B., Boecker B. B. and McClellan R. O. **Retention of monodisperse or polydisperse aluminosilicate particles inhaled by dogs, rats, and mice**. *Toxicol Appl Pharmacol* 69(3): 345-362 (1983).

Son Y. J. and McConville J. T. **Development of a standardized dissolution test method for inhaled pharmaceutical formulations**. *Int J Pharm* 382(1-2): 15-22 (2009).

Sorenson C. M. and Eastman A. **Mechanism of cis-diamminedichloroplatinum(II)-induced cytotoxicity: role of G2 arrest and DNA double-strand breaks**. *Cancer Res* 48(16): 4484-4488 (1988).

Sou T., Kaminskas L. M., Nguyen T. H., Carlberg R., McIntosh M. P. and Morton D. A. **The effect of amino acid excipients on morphology and solid-state properties of multi-component spray-dried formulations for pulmonary delivery of biomacromolecules**. *Eur J Pharm Biopharm* 83(2): 234-243 (2013).

Sou T., Orlando L., McIntosh M. P., Kaminskas L. M. and Morton D. A. **Investigating the interactions of amino acid components on a mannitol-based spray-dried powder formulation for pulmonary delivery: A design of experiment approach**. *Int J Pharm* 421(2): 220-229 (2011).

Speelmans G., Sips W. H., Grisel R. J., Staffhorst R. W., Fichtinger-Schepman A. M., Reedijk J. and de Kruijff B. **The interaction of the anti-cancer drug cisplatin with phospholipids is specific for negatively charged phospholipids and takes place at low chloride ion concentration**. *Biochim Biophys Acta* 1283(1): 60-66 (1996).

Staffhorst R. W., van der Born K., Erkelens C. A., Hamelers I. H., Peters G. J., Boven E. and de Kroon A. I. **Antitumor activity and biodistribution of cisplatin nanocapsules in nude mice bearing human ovarian carcinoma xenografts**. *Anticancer Drugs* 19(7): 721-727 (2008).

Stewart D. J., Benjamin R. S., Luna M., Feun L., Caprioli R., Seifert W. and Loo T. L. **Human tissue distribution of platinum after cis-diamminedichloroplatinum**. *Cancer Chemother Pharmacol* 10(1): 51-54 (1982).

Sturm R. **Radioactivity and lung cancer-mathematical models of radionuclide deposition in the human lungs**. *J Thorac Dis* 3(4): 231-243 (2011).

Tadini-Buoninsegni F., Bartolommei G., Moncelli M. R., Inesi G., Galliani A., Sinisi M., Losacco M., Natile G. and Arnesano F. **Translocation of platinum anticancer drugs by human copper ATPases ATP7A and ATP7B**. *Angew Chem Int Ed Engl* 53(5): 1297-1301 (2014).

Tang E. R., Schreiner A. M. and Pua B. B. **Advances in lung adenocarcinoma classification: a summary of the new international multidisciplinary classification system (IASLC/ATS/ERS)**. *J Thorac Dis* 6(Suppl 5): S489-501 (2014).

Tatsumura T., Koyama S., Tsujimoto M., Kitagawa M. and Kagamimori S. **Further study of nebulisation chemotherapy, a new chemotherapeutic method in the treatment of lung carcinomas: fundamental and clinical**. *British Journal of Cancer* 68(6): 1146-1149 (1993).

Tatsumura T., Yamamoto K., Murakami A., Tsuda M. and Sugiyama S. **[New chemotherapeutic method for the treatment of tracheal and bronchial cancers--nebulization chemotherapy]**. *Gan No Rinsho* 29(7): 765-770 (1983).

Tecchio C., Micheletti A. and Cassatella M. A. **Neutrophil-derived cytokines: facts beyond expression**. *Front Immunol* 5: 508 (2014).

The International Early Lung Cancer Action Program Investigators. **Survival of Patients with Stage I Lung Cancer Detected on CT Screening**. *N Engl J Med* 355(17): 1763-1771 (2006).

Tilleman T. R., Richards W. G., Zellos L., Johnson B. E., Jaklitsch M. T., Mueller J., Yeap B. Y., Mujoomdar A. A., Ducko C. T., Bueno R. and Sugarbaker D. J. **Extrapleural pneumonectomy followed by intracavitary intraoperative hyperthermic cisplatin with pharmacologic cytoprotection for treatment of malignant pleural mesothelioma: a phase II prospective study**. *J Thorac Cardiovasc Surg* 138(2): 405-411 (2009).

Ting V. P., Schmidtmann M., Wilson C. C. and Weller M. T. **Cisplatin: Polymorphism and Structural Insights into an Important Chemotherapeutic Drug**. *Angew Chem* 122(49): 9598-9601 (2010).

Townsend D. M. **Metabolism of Cisplatin to a Nephrotoxin in Proximal Tubule Cells**. *J Am Soc Nephrol* 14(1): 1-10 (2003).

Travis W. D. **Update on small cell carcinoma and its differentiation from squamous cell carcinoma and other non-small cell carcinomas**. *Mod Pathol* 25 Suppl 1: S18-30 (2012).

Travis W. D., Brambilla E., Müller-Hermelink H. K. and Harris C. **Tumours of the Lung, Pleura, Thymus and Heart**. Geneva, World Health Organization (2015a).

Travis W. D., Brambilla E., Nicholson A. G., Yatabe Y., Austin J. H. M., Beasley M. B., Chirieac L. R., Dacic S., Duhig E., Flieder D. B., Geisinger K., Hirsch F. R., Ishikawa Y., Kerr K. M., Noguchi M., Pelosi G., Powell C. A., Tsao M. S. and Wistuba I. **The 2015 World Health Organization Classification of Lung Tumors**. *Journal of Thoracic Oncology* 10(9): 1243-1260 (2015b).

Travis W. D., Brambilla E., Noguchi M., Nicholson A. G., Geisinger K. R., Yatabe Y., Beer D. G., Powell C. A., Riely G. J., Van Schil P. E., Garg K., Austin J. H. M., Asamura H., Rusch V. W., Hirsch F. R., Scagliotti G., Mitsudomi T., Huber R. M., Ishikawa Y., Jett J., Sanchez-Cespedes M., Sculier J.-P., Takahashi T., Tsuboi M., Vansteenkiste J., Wistuba I., Yang P.-C., Aberle D., Brambilla C., Flieder D., Franklin W., Gazdar A., Gould M., Hasleton P., Henderson D., Johnson B., Johnson D., Kerr K., Kuriyama K., Lee J. S., Miller V. A., Petersen I., Roggli V., Rosell R., Saijo N., Thunnissen E., Tsao M. and Yankelewitz D. **International Association for the Study of Lung Cancer/American Thoracic Society/European Respiratory Society International Multidisciplinary Classification of Lung Adenocarcinoma**. *J Thorac Oncol* 6(2): 244-285 (2011).

Tsang R. Y., Al-Fayea T. and Au H. J. **Cisplatin overdose: toxicities and management**. *Drug Saf* 32(12): 1109-1122 (2009).

Üner M. and Karaman E. F. **Preliminary Studies on Solid Lipid Microparticles of Loratadine for the Treatment of Allergic Reactions via the Nasal Route**. *Trop J Pharm Res* 12(3) (2013).

Ungaro F., d'Emmanuele di Villa Bianca R., Giovino C., Miro A., Sorrentino R., Quaglia F. and La Rotonda M. I. **Insulin-loaded PLGA/cyclodextrin large porous particles with improved aerosolization properties: in vivo deposition and hypoglycaemic activity after delivery to rat lungs**. *J Control Release* 135(1): 25-34 (2009).

United States. Surgeon General's Advisory Committee on Smoking and Health. **Smoking and health; report of the advisory committee to the Surgeon General of the Public Health Service**. Washington, U.S. Dept. of Health, Education, and Welfare, Public Health Service; for sale by the Superintendent of Documents, U.S. Govt. Print. Off. (1964).

USP30. **<467> Residual Solvents**, United States Pharmacopoeia 30 (2007).

USP39. **<601> Inhalation and Nasal Drug Products - Aerosols, Sprays, and Powders**, United States Pharmacopoeia 39 (2016).

Van de Water B., Jaspers J. J., Maasdam D. H., Mulder G. J. and Nagelkerke J. F. **In vivo and in vitro detachment of proximal tubular cells and F-actin damage: consequences for renal function**. *Am J Physiol* 267(5 Pt 2): F888-899 (1994).

van Hennik M. B., van der Vijgh W. J., Klein I., Elferink F., Vermorken J. B., Winograd B. and Pinedo H. M. **Comparative pharmacokinetics of cisplatin and three analogues in mice and humans**. *Cancer Res* 47(23): 6297-6301 (1987).

van Rijswijk R. E., Hoekman K., Burger C. W., Verheijen R. H. and Vermorken J. B. **Experience with intraperitoneal cisplatin and etoposide and i.v. sodium thiosulphate protection in ovarian cancer patients with either pathologically complete response or minimal residual disease**. *Ann Oncol* 8(12): 1235-1241 (1997).

Vansteenkiste J. F., Deroose C. and Dooms C. **21 - Positron Emission Tomography** in *Murray and Nadel's Textbook of Respiratory Medicine (Sixth Edition)*. Mason R. J., Ernst J. D., King T. E. et al. Philadelphia, W.B. Saunders**:** 360-371.e364 (2016).

Verschraegen C. F., Gilbert B. E., Loyer E., Huaringa A., Walsh G., Newman R. A. and Knight V. **Clinical Evaluation of the Delivery and Safety of Aerosolized Liposomal 9-Nitro-20(S)-Camptothecin in Patients with Advanced Pulmonary Malignancies**. *Clinc Canc Res* 10(7): 2319-2326 (2004).

Wang D. and Lippard S. J. **Cellular processing of platinum anticancer drugs**. *Nat Rev Drug Discov* 4(4): 307-320 (2005).

Warner K. E. and Mendez D. **Tobacco control policy in developed countries: yesterday, today, and tomorrow**. *Nicotine Tob Res* 12(9): 876-887 (2010).

Wattendorf U. and Merkle H. P. **PEGylation as a tool for the biomedical engineering of surface modified microparticles**. *J Pharm Sci* 97(11): 4655-4669 (2008).

Wauthoz N. and Amighi K. **Formulation Strategies for Pulmonary Delivery of Poorly Soluble Drugs** in *Pulmonary Drug Delivery Advances and Challenges*. Nokhodchi A. and Martin G. P., Wiley (2015a).

Wauthoz N., Bastiat G., Moysan E., Cieslak A., Kondo K., Zandecki M., Moal V., Rousselet M. C., Hureaux J. and Benoit J. P. **Safe lipid nanocapsule-based gel technology to target lymph nodes and combat mediastinal metastases from an orthotopic non-small-cell lung cancer model in SCID-CB17 mice**. *Nanomedicine* (2015b).

Wauthoz N., Deleuze P., Hecq J., Roland I., Saussez S., Adanja I., Debeir O., Decaestecker C., Mathieu V., Kiss R. and Amighi K. **In vivo assessment of temozolomide local delivery for lung cancer inhalation therapy**. *Eur J Pharm Sci* 39(5): 402-411 (2010).

Wauthoz N., Deleuze P., Saumet A., Duret C., Kiss R. and Amighi K. **Temozolomide-based dry powder formulations for lung tumor-related inhalation treatment**. *Pharm Res* 28(4): 762-775 (2011).

Wauthoz N., Hennia I., Ecenarro S. and Amighi K. **Impact of different capsules for dry powder inhalers on the aerodynamic performances of formoterol-based binary and ternary blends (Poster)**. Drug Delivery to the Lungs 27, Edinburgh, UK (2016a).

Wauthoz N., Hennia I., Ecenarro S. and Amighi K. **Influence of flow rate and usage in drastic conditions on the aerodynamic performance of a formoterol dry powder formulation using different kinds of capsules for inhalation (Poster)**. AAPS Conference, Denver, USA (2016b).

Weibel E. R. **Geometry and Dimensions of Airways of Conductive and Transitory Zones** in *Morphometry of the Human Lung*. Weibel E. R. Berlin, Heidelberg, Springer Berlin Heidelberg: 110-135 (1963).

Weingertner N. and Chenard M. P. **Démembrement des adénocarcinomes bronchopulmonaires : le point de vue du pathologiste**. *Revue des Maladies Respiratoires Actualités* 7(4): 290-305 (2015).

Williams O. W., Sharafkhaneh A., Kim V., Dickey B. F. and Evans C. M. **Airway mucus: From production to secretion**. *Am J Respir Cell Mol Biol* 34(5): 527-536 (2006).

Willis L., Hayes D., Jr. and Mansour H. M. **Therapeutic liposomal dry powder inhalation aerosols for targeted lung delivery**. *Lung* 190(3): 251-262 (2012).

Winton T., Livingston R., Johnson D., Rigas J., Johnston M., Butts C., Cormier Y., Goss G., Inculet R., Vallieres E., Fry W., Bethune D., Ayoub J., Ding K., Seymour L., Graham B., Tsao M.-S., Gandara D., Kesler K., Demmy T. and Shepherd F. **Vinorelbine plus Cisplatin vs. Observation in Resected Non–Small-Cell Lung Cancer**. *N Engl J Med* 352(25): 2589-2597 (2005).

Wittgen B. P., Kunst P. W., van der Born K., van Wijk A. W., Perkins W., Pilkiewicz F. G., Perez-Soler R., Nicholson S., Peters G. J. and Postmus P. E. **Phase I study of aerosolized SLIT cisplatin in the treatment of patients with carcinoma of the lung**. *Clin Cancer Res* 13(8): 2414-2421 (2007).

Wu D., Tawhai M. H., Hoffman E. A. and Lin C. L. **A numerical study of heat and water vapor transfer in MDCT-based human airway models**. *Ann Biomed Eng* 42(10): 2117-2131 (2014).

Xia D., Cui F., Gan Y., Mu H. and Yang M. **Design of lipid matrix particles for fenofibrate: effect of polymorphism of glycerol monostearate on drug incorporation and release**. *J. Pharm. Sci.* 103(2): 697-705 (2014).

Xu Y. J., Zheng H., Gao W., Jiang G. N., Xie H. K., Chen C. and Fei K. **Is neoadjuvant chemotherapy mandatory for limited-disease small-cell lung cancer?** *Interact. Cardiovasc. Thorac. Surg.* 19(6): 887-893 (2014).

Yan A., Von Dem Bussche A., Kane A. B. and Hurt R. H. **Tocopheryl Polyethylene Glycol Succinate as a Safe, Antioxidant Surfactant for Processing Carbon Nanotubes and Fullerenes**. *Carbon N Y* 45(13): 2463-2470 (2007).

Yan C., Lian X., Li Y., Dai Y., White A., Qin Y., Li H., Hume D. A. and Du H. **Macrophage-specific expression of human lysosomal acid lipase corrects inflammation and pathogenic phenotypes in lal-/- mice**. *Am J Pathol* 169(3): 916-926 (2006).

Yang J. C., Hirsh V., Schuler M., Yamamoto N., O'Byrne K. J., Mok T. S., Zazulina V., Shahidi M., Lungershausen J., Massey D., Palmer M. and Sequist L. V. **Symptom control and quality of life in LUX-Lung 3: a phase III study of afatinib or cisplatin/pemetrexed in patients with advanced lung adenocarcinoma with EGFR mutations**. *J Clin Oncol* 31(27): 3342-3350 (2013).

Yang Z., Schumaker L. M., Egorin M. J., Zuhowski E. G., Guo Z. and Cullen K. J. **Cisplatin preferentially binds mitochondrial DNA and voltage-dependent anion channel protein in the mitochondrial membrane of head and neck squamous cell carcinoma: possible role in apoptosis**. *Clin Cancer Res* 12(19): 5817-5825 (2006).

Yao X., Panichpisal K., Kurtzman N. and Nugent K. **Cisplatin nephrotoxicity: a review**. *Am J Med Sci* 334(2): 115-124 (2007).

Yapa W. S., Li J., Patel K., Wilson J. W., Dooley M. J., George J., Clark D., Poole S., Williams E., Porter C. J., Nation R. L. and McIntosh M. P. **Pulmonary and systemic pharmacokinetics of inhaled and intravenous colistin methanesulfonate in cystic fibrosis patients: targeting advantage of inhalational administration**. *Antimicrob Agents Chemother* 58(5): 2570-2579 (2014).

Yonezawa A. and Inui K. **Organic cation transporter OCT/SLC22A and H(+)/organic cation antiporter MATE/SLC47A are key molecules for nephrotoxicity of platinum agents**. *Biochem Pharmacol* 81(5): 563-568 (2011).

Zalba S., Navarro-Blasco I., Moreno D. and Garrido M. J. **Application of non-aggressive sample preparation and electrothermal atomic absorption spectrometry to quantify platinum in biological matrices after cisplatin nanoparticle administration**. *Microchem J* 96(2): 415-421 (2010).

Zarogoulidis P., Chatzaki E., Porpodis K., Domvri K., Hohenforst-Schmidt W., Goldberg E. P., Karamanos N. and Zarogoulidis K. **Inhaled chemotherapy in lung cancer: future concept of nanomedicine**. *Int J Nano* 7: 1551-1572 (2012a).

Zarogoulidis P., Eleftheriadou E., Sapardanis I., Zarogoulidou V., Lithoxopoulou H., Kontakiotis T., Karamanos N., Zachariadis G., Mabroudi M., Zisimopoulos A. and Zarogoulidis K. **Feasibility and effectiveness of inhaled carboplatin in NSCLC patients**. *Invest New Drugs* 30(4): 1628-1640 (2012b).

Zhou Q. T., Leung S. S., Tang P., Parumasivam T., Loh Z. H. and Chan H. K. **Inhaled formulations and pulmonary drug delivery systems for respiratory infections**. *Adv Drug Deliv Rev* 85: 83-99 (2015).

APPENDIX

1. Validation of the ETAAS methods

1.1. Context

For this work, a "light-matrix" method was first developed. It aimed at the quantification of cisplatin in aqueous solutions during the development of formulations. Then, the furnace parameters and the digestion procedures were adapted for "heavy-matrix" methods, to obtain the lowest background noise as possible for blanks and the highest signal as possible for the spiked organ digestates, while maintaining linearity and accuracy.

The optical parameters (e.g. wavelength, slit width, hollow cathode lamp amperage) of the method were those recommended by the respective manufacturers and are described in the following Article 1 and Article 2 in the Manuscript.

The furnace parameters used for the first light-matrix method were sequentially determined using a trial and error approach from published methods. The most recent reports of cisplatin quantification using ETAAS in the literature, for instance from Zalba et al. (Zalba et al., 2010) used a lower atomization temperature (2400°C), a much quicker sample degradation program and lower gas flow (250 mL/min) than what is recommended by Varian, the manufacturer of the SpectrAA 300 atomic spectrometer we used in this study. These parameters were initially assayed but led to poor absorbance results and quick furnace wear. To accommodate with the requirements of the spectrometer, we used another method for the furnace program, based on the older Milacic et al. work (Milacic et al., 1997). In this publication, aimed at quantifying cisplatin in digested tumor samples, the furnace program used was as follow: an initial drying step of 60 s between 60 and 150°C, followed by a pyrolysis ramp and hold between 150 and 1200°C for 10 and 20 s, respectively, and a final atomization at 2700°C. However, they also used a more recent apparatus, which permitted a low argon gas flow of 200 mL/min. The reported atomization temperature, which is slightly lower than the temperature recommended by Varian (i.e. 2750°C) was adequate in our case. We finally used the program described in Article 1 for the quantification of cisplatin in light-matrices. It involved a very quick pyrolysis ramp to 800°C for 5.0 s, held for 3.0 s before atomization at 2700°C (see Article 1 and Article 2). This, altogether with the avoidance a triplicate injection, which was not useful to obtain adequate validation results helped limit the wear of graphite furnaces.

The following "heavy-matrices" methods were then developed in parallel with digestion procedures, using organs from untreated animals and spiked with known concentrations of cisplatin. The same approach was used to obtain low matrix-effects, and resulted in the development of three different furnace programs (Part II, 2.3.9., **Table 22** and **Table 23**). The first (program C) is optimized for organ digestates. It involves a pyrolysis ramp to 1200°C for 5.0 s and a 12.0 s hold, followed by atomization at 2700°C and a cleaning step at 3000°C. The second program (program B) for blood samples involves the same pyrolysis temperature but a longer 25.0 s pyrolysis ramp, which limits foaming of the digested blood into the graphite furnace during heating. The last program (program B') was needed because of the lower limit of quantification (LLOQ) of the initial total blood method, due to its 4-fold dilution. It involved a multiple-injection technique, including the drying to pyrolysis steps between each of the 4 injections (20 μL). With limited increase of the background noise, it permitted a 3-fold decrease of the LLOQ for the lowest platinum-containing samples.

1.2. Validation parameters

Validation of the light-matrix method was performed following the ICH Q2 (R1), Validation of Analytical Procedures: Text and Methodology (ICH Expert Working Group, 2005). Validation of the heavy-matrices methods was realized following the FDA Guidance for Industry, Bioanalytical method validation requirements (FDA, 2013). In particular, the following validation characteristics were evaluated: Specificity, Linearity, Range, Accuracy, Precision (Repeatability and Intermediate precision), Limit of Detection (LOD) and LLOQ.

1.2.1. Specificity

The developed methods aimed at quantifying platinum from cisplatin and its potential adducts after *in vivo* administration. The specificity of ETAAS for platinum already lays in its principles (i.e. platinum hollow cathode lamp with a specific emission spectrum, specific absorption spectrum during atomization, only one specific spectral wavelength analyzed, narrow slit width) but still needs to be considered as part of the validation procedure. In ETAAS, analytes in the sample are not separated prior to the measurement of the absorbance, which increases the risk of measuring impurities. However, non-specific absorption can be avoided using Zeeman correction. In all cases, the methods were able to give absorbance of blank measurements around 0 ± 10 mA.

1.2.2. Linearity

Linearity is defined as the ability of the method to obtain results directly proportional to the concentration of analyte in the sample. In the case of ETAAS, linearity of the absorbance *vs.* concentration curve can be affected by a few parameters and in particular the setting of the graphite furnace and of the optical portion. Even over narrow concentration ranges, this can lead to non-linear absorbance responses and a quadratic fit (2 order polynomial) is often more accurate than a linear one.

To limit this issue, during routine use, the Varian proprietary software takes into account the non-linear behavior of the calibration curve and directly correlates the concentration of the samples from the measured absorbance using a polynomial fit between each standard. The linearity of the absorbance read for samples of known concentration was still verified with the best setting. Yet, the concentrations calculated by the Varian software were used for all the following validation and sample analyses, as it provided a better accuracy overall.

The slope (b) and the intercept (a), the correlation (r) coefficient and determination (r^2) were calculated using Excel. Each were statistically tested using the Student *t*-test to check if the slope, correlation coefficient and intercept were significantly different from 0. The validity of the regression slope and the existence of a significant slope were assessed. It involved verifying the homoscedasticity of variances using a Cochran C test. It was done by analyzing 3 different stock solutions and their subsequent dilutions over the course of 3 days. The concentration of the stock cisplatin standard was always 200 mg/L, prepared by weighing 20.0 mg in 100.0 mL of NaCl 0.9% w/v. The subsequent dilution (800 µg/L) for the light-matrix method was realized in HNO_3 0.1% v/v. For organ digestates, each were spiked using 10% of the final volume with an 8.00 mg/L stock solution in HNO_3 0.1% v/v. For blood digestates, it was done using 50 µL of a 3.20 mg/L solution in HNO_3 69% v/v prepared extemporaneously, as a replacement of the digestion medium.

Each time, the subsequent dilutions were realized by the autosampler, with the following set-up: standard 1 (20 µL of standard, 0 µL of blank), standard 2 (15 µL of standard, 5 µL of blank), standard 3 (10 µL of standard, 10 µL of blank), standard 4 (5 µL of standard, 15 µL of blank), and standard 5 (18 µL of standard, 2 µL of blank).

1.2.3. Range

The range was derived from the linearity data. It was over 800 to 80 µg/L for all methods, except the multiple-inject method for total blood (B'), which had a 25 to 250 µg/L range. Because we aimed at the lowest sensitivity that the method could provide, the lowest

standard (standard 5) was first set using an approximate determination of the LLOQ. The method is then limited by the maximum dilution ability of the autosampler (10-fold). This determined the highest standard of the range for the method.

1.2.4. Accuracy

Accuracy was verified over the range of linearity for each matrix. It was done by comparing the results obtained with the ETAAS methods with the concentrations of prepared and spiked samples at 10%, 25%, 50%, 75% and 100% of the range, in order to calculate a recovery range. Homoscedasticity of results was then verified using the Cochran C test. Validity of the means was then evaluated by comparing the inter-group and intra-group errors. Finally, a Fisher test was used to establish the origin of the observed differences between the groups (experimental errors or errors due to the method). The mean recovery and the confidence interval (95%) were then calculated.

1.2.5. Precision

Precision is the closeness of agreement between a series of measurement obtained from repeated sampling of a single homogeneous sample. It can be considered as the repeatability, the intermediate precision and reproducibility. Precision was expressed as the relative standard deviation of the series of measurements. We established the intra-day repeatability as the repeated quantification of the same sample (n = 4). This was then done again on day 2 and day 3 to establish the inter-day repeatability. This was done over the whole range of the method using 5 different samples at 10%, 25%, 50%, 75% and 100% of the range.

A 2-factor analysis of variance was then established to determine if there was a notable difference between days. The total repeatability error was determined as the variance of all measurements. The relative standard deviations (RSD%) were determined at each level, each day and for the whole method.

1.2.6. Limit of detection (LOD) and lower limit of quantification (LLOQ)

The LOD is the smallest concentration that can be attributed to the analyte but not quantified with enough certainty. The LLOQ is the smallest concentration of the analyte that can be quantified with certainty. They were determined from the standard deviation of the blank (σ) and the slope (b) of 6 independent calibration curves, using the following equation

$$LLOQ = \frac{10\sigma}{b} = 3 \times LOD$$

1.3. Results

The ETAAS method was validated for aqueous dilutions (light matrix), for each organ and in total blood. The abbreviated results are presented below for each matrix.

1.3.1. Light matrix

The method exhibited linearity over the range from 80 to 800 µg/L, with an r^2 of 0.996. The LLOQ and LOD of the method were 79.0 and 26.3 µg/L, respectively. Accuracy was verified over the range with a mean recovery of 99.0 ± 3.2 %. Intra-day and inter-day precision was verified with an average recovery of 101.0 % and a repeatability error of 0.2 %.

1.3.2. Kidneys

The method exhibited linearity over the range from 80 to 800 µg/L, with an r^2 of 0.997. The LLOQ and LOD of the method were 63.6 and 21.2 µg/L, respectively. Accuracy was verified over the range with a mean recovery of 99.0 ± 9.6%. Intra-day and inter-day precision was verified with an average recovery of 100.7 % and a repeatability error of 1.2 %.

1.3.3. Lungs

The method exhibited linearity over the range from 80 to 800 µg/L, with an r^2 of 0.997. The LLOQ and LOD of the method were 51.6 and 17.2 µg/L, respectively. Accuracy was verified over the range with a mean recovery of 101.2 ± 9.0 %. Intra-day and inter-day precision was verified with an average recovery of 98.9 % and a repeatability error of 1.05 %.

1.3.4. Liver

The method exhibited linearity over the range from 80 to 800 µg/L, with an r^2 of 0.996. The LLOQ and LOD of the method were 68.0 and 22.3 µg/L, respectively. Accuracy was verified over the range with a mean recovery of 99.0 ± 9.6 %. Intra-day and inter-day precision was verified with an average recovery of 100.4 % and a repeatability error of 7.4 %.

1.3.5. Spleen

The method exhibited linearity over the range from 80 to 800 µg/L, with an r^2 of 0.996. The LLOQ and LOD of the method were 109.1 and 36.4 µg/L, respectively. Accuracy was verified over the range with a mean recovery of 101.2 ± 6.7 %. Intra-day and inter-day precision was verified with an average recovery of 100.7 % and a repeatability error of 1.0 %.

1.3.6. Mediastinum

The method exhibited linearity over the range from 80 to 800 µg/L, with an r^2 of 0.997. The LLOQ and LOD of the method were 96.5 and 32.2 µg/L, respectively. Accuracy was verified over the range with a mean recovery of 101.6 ± 8.4 %. Intra-day and inter-day precision was verified with an average recovery of 101.0 % and a repeatability error of 1.2 %.

1.3.7. Total blood

1.3.7.1. ETAAS method A

The method exhibited linearity over the range from 80 to 800 µg/L, with an r^2 of 0.998. The LLOQ and LOD of the method were 81.3 and 27.1 µg/L, respectively. Accuracy was verified over the range with a mean recovery of 96.6 ± 8.8 %. Intra-day and inter-day precision was verified with an average recovery of 100.0 % and a repeatability error of 1.6 %.

1.3.7.2. ETAAS method B (multiple injection programme)

The method exhibited linearity over the range from 25 to 250 µg/L, with an r^2 of 0.996. The LLOQ and LOD of the method were 81.3 and 27.1 µg/L, respectively. Accuracy was verified over the range with a mean recovery of 102.4 ± 12.3 %. Intra-day and inter-day precision was verified with an average recovery of 102.6 % and a repeatability error of 1.2 %.

1.4. Conclusion

The ETAAS method, with the adapted furnace programmes presented in Part I (Article 1) and Part II (Article 2) were validated for each matrix and showed adequate linearity over the tested ranges. The different absorbances read at each levels changed between each type of matrix, probably due to the varying concentration of digested proteins from organs in the solution. This led to varying LLOQ and LOD for each type of organ. The high matrix-effect also increased the variability of the recovery but the parameter stayed into the previously defined limits. As a consequence, this matrix-effect was not detrimental to the accurate and precise quantification of platinum from cisplatin.

1.5. Raw data

Light-matrix Linearity

Assay 1

		St weight
		20

N	x (mg/L)	y (mA)	x^2	y^2	xy
B	0.00	1	0.0	1.0	0.0
St 1	0.80	280	0.6	78400.0	224.0
St 2	0.60	220	0.4	48400.0	132.0
St 3	0.40	155	0.2	24025.0	62.0
St 4	0.20	80	0.0	6400.0	16.0
St 5	0.08	30	0.0	900.0	2.4

Sum	6	2.1	766.0	1.2	158126.0	436.4
Average		0.3	127.7	0.2		

Sxx	0.5		Slope b	352.033	r		0.998446355
Syy	60333.3		Intercept a	5.628571	r^2		0.996895125
Sxy	170.9						
S^2xy	46.8318681			S^2r	46.83187		
SE b	9.82314786			S^2a	27.20709		
				S^2b	96.49423		

One-sided test on the slope

F	352.033				
dof num.		4	F(0,05;1;4)	7.71	*significant*
dof denom.		4			
					→ Existence of a slope

One-sided test on r

t	35.837				
ddl		4	t(0,05;4)	2.776	*significant*
		→ Existence of a correlation between x and y			

Two-sided comparison between intercept and 0

t	1.0791				
ddl		4	t(0,05;4)	2.776	*non-significant*
			→ Intercept different from 0		

Assay 2

		St weight
		19.8

N	x (mg/L)	y (mA)	x^2	y^2	xy
B	0.00	-2	0.0	4.0	0.0
St 1	0.79	270	0.6	72900.0	213.8
St 2	0.59	219	0.4	47961.0	130.1
St 3	0.40	144	0.2	20736.0	57.0
St 4	0.20	79	0.0	6241.0	15.6
St 5	0.08	28	0.0	784.0	2.2

Sum	6	2.1	738.0	1.2	148626.0	418.8
Average		0.3	123.0	0.2		

Sxx	0.5		Slope b	347.9853	r		0.997831074
Syy	57852.0		Intercept a	3.571429	r^2		0.995666851
Sxy	165.5						
S^2xy	62.6703297			S^2r	62.67033		
SE b	11.4782515			S^2a	36.40848		
				S^2b	131.7503		

One-sided test on the slope

F	347.985				
dof num.		4	F(0,05;1;4)	7.71	*significant*
dof denom.		4			
					→ Existence of a slope

One-sided test on r

t	30.317				
ddl		4	t(0,05;4)	2.776	*significant*
		→ Existence of a correlation between x and y			

Two-sided comparison between intercept and 0

t	0.5919				
ddl		4	t(0,05;4)	2.776	*non-significant*
			→ Intercept different from 0		

					St weight
					20.1

N	x (mg/L)	y (mA)	x^2	y^2	xy
B	0.00	0	0.0	0.0	0.0
St 1	0.80	267	0.6	71289.0	214.7
St 2	0.60	215	0.4	46225.0	129.6
St 3	0.40	150	0.2	22500.0	60.3
St 4	0.20	80	0.0	6400.0	16.1
St 5	0.08	36	0.0	1296.0	2.9

Sum	6	2.1	748.0	1.2	147710.0	423.6
Average		0.3	124.7	0.2		

Sxx	0.5	Slope b	332.4859	r	0.9975237
Syy	54459.3	Intercept a	8.828571	r^2	0.995053533
Sxy	163.0				
S^2xy	67.3453297		S^2r	67.34533	
SE b	11.7210797		S^2a	39.12443	
			S^2b	137.3837	

One-sided test on the slope

F	332.486			
dof num.	4	F(0,05;1;4)	7.71	significant
dof denom.	4			
			→ Existence of a slope	

One-sided test on r

t	28.366			
ddl	4	t(0,05;4)	2.776	significant
		→ Existence of a correlation between x and y		

Two-sided comparison between intercept and 0

t	1.4115			
ddl	4	t(0,05;4)	2.776	non-significant
		→ Intercept different from 0		

Symbols

N	Number of observations		r	Correlation coefficient
k	Number of groups		r^2	Coefficient of determination
Sxx	Standard-deviation of x		S^2r	Variance of the correlation coefficient
Syy	Standard-deviation of y		S^2a	Variance of the intercept
Sxy	Covariance of x and y		S^2b	Variance of the slope
S^2xy	Regression variance, Residual variance		F	Fisher F test
SE b	Error on the slope		t	Student t test
a	Intercept of the regression line		dof	Degrees of freedom
b	Slope of the regression line			x = Cisplatin concentration (mg/L)
				y = Measured absorbance (mA)

Comparison between the slopes

J1/J2			
t	0.26791651	non-significant	
t (0,05;8)	2.306		
J1/J3			
t	1.2781637	non-significant	
t (0,05;8)	2.306		
J2/J3			
t	0.94478145	non-significant	
t (0,05;8)	2.306		

The three slopes are not significantly different

Comparison between the intercepts

J1/J2			
t	0.257919	non-significant	
t (0,05;8)	2.306		
J1/J3			
t	0.392907	non-significant	
t (0,05;8)	2.306		
J2/J3			
t	0.604897	non-significant	
t (0,05;8)	2.306		

The three intercepts are not significantly different

Light-matrix — Accuracy

Real concentration of sampled assays				100	75	50	25	10
	Weight assay 1	20.5	mg	0.82	0.615	0.41	0.205	0.082
	Weight assay 2	20.1	mg	0.804	0.603	0.402	0.201	0.0804
	Weight assay 3	19.7	mg	0.788	0.591	0.394	0.197	0.0788

	x measured	x real (ppb)	Recovery (%)	Variances	Y	yi-Y/	(yi-Y/)^2	yi-Y//	(yi-Y//)^2
Assay 1-100	801	820	97.68%		99.10%	-1.42%	0.0002	-1.32%	0.0002
Assay 2-100	799	804	99.38%		99.10%	0.27%	0.0000	0.38%	0.0000
Assay 3-100	790	788	100.25%	0.0002	99.10%	1.15%	0.0001	1.26%	0.0002
Assay 1-75	585	615	95.12%		98.33%	-3.21%	0.0010	-3.88%	0.0015
Assay 2-75	591	603	98.01%		98.33%	-0.32%	0.0000	-0.99%	0.0001
Assay 3-75	602	591	101.86%	0.0011	98.33%	3.53%	0.0012	2.86%	0.0008
Assay 1-50	424	410	103.41%		99.30%	4.11%	0.0017	4.42%	0.0020
Assay 2-50	386	402	96.02%		99.30%	-3.28%	0.0011	-2.98%	0.0009
Assay 3-50	388	394	98.48%	0.0014	99.30%	-0.83%	0.0001	-0.52%	0.0000
Assay 1-25	195	205	95.12%		97.56%	-2.44%	0.0006	-3.88%	0.0015
Assay 2-25	191	201	95.02%		97.56%	-2.54%	0.0006	-3.97%	0.0016
Assay 3-25	202	197	102.54%	0.0019	97.56%	4.98%	0.0025	3.54%	0.0013
Assay 1-10	86	82	104.88%		100.69%	4.19%	0.0018	5.88%	0.0035
Assay 2-10	81	80.4	100.75%		100.69%	0.06%	0.0000	1.75%	0.0003
Assay 3-10	76	78.8	96.45%	0.0018	100.69%	-4.24%	0.0018	-2.55%	0.0007
		AVG (%)	99.00%						
N	15	SUM (%)	1484.98%	0.0064	14.8498	0.00%	0.0127	0.00%	0.0144
k	5	STDEV (%)	3.20%						

Cochran C test between groups (Homoscedasticity)

C	0.2917
C (0.05;5;2)	0.6838

C < C (0.05;5;2)
Homoscedasticity of variances between groups is met

Validity of means

Variation	dof	Sum of square	Variance (%^{2})	St-dev (%)	CV (%)	F	
Total variation	15	0.0144				F	0.32
Intra-group variation	10	0.0127	0.0013	0.0357	0.0360	F	0.32
Inter-group variation	4	0.0016	0.0004	0.0203	0.0205	p	0.86
						F (0,05;4;10)	3.48

F < F (0.05;4;10)
Variation of observations between groups are due to experimental errors

Estimation of the mean recovery

Mean recovery (%)	99.00%		
Stdev (%)	3.20%		
N	15		
t (0,05;14)	2.1448		
t*S/√(N) (%)	0.01774695		
CI 95 (%)	97.22%	to	100.77%

Light-matrix

Precision

Concentration (mg/L)	Results SpectrAA			Recovery (%)			(Recovery - Average)			RSD%			
	Day 1	Day 2	Day 3	Day 1	Day 2	Day 3	Day 1	Day 2	Day 3	Day 1	Day 2	Day 3	Average
0.80	0.798	0.801	0.805	99.75%	100.13%	100.63%	-0.29%	-1.14%	-0.96%	1.34%	0.79%	1.30%	1.14%
	0.812	0.789	0.815	101.50%	98.63%	101.88%	1.46%	-2.64%	0.29%				
	0.786	0.788	0.791	98.25%	98.50%	98.88%	-1.79%	-2.76%	-2.71%				
	0.797	0.797	0.811	99.63%	99.63%	101.38%	-0.41%	-1.64%	-0.21%				
0.60	0.604	0.598	0.605	100.67%	99.67%	100.83%	0.63%	-1.60%	-0.75%	1.25%	1.54%	1.69%	1.49%
	0.593	0.592	0.607	98.83%	98.67%	101.17%	-1.20%	-2.60%	-0.42%				
	0.586	0.612	0.585	97.67%	102.00%	97.50%	-2.37%	0.74%	-4.08%				
	0.595	0.593	0.595	99.17%	98.83%	99.17%	-0.87%	-2.43%	-2.42%				
0.40	0.39	0.424	0.417	97.50%	106.00%	104.25%	-2.54%	4.74%	2.67%	3.89%	3.24%	3.19%	3.44%
	0.397	0.405	0.397	99.25%	101.25%	99.25%	-0.79%	-0.01%	-2.33%				
	0.42	0.41	0.429	105.00%	102.50%	107.25%	4.96%	1.24%	5.67%				
	0.385	0.392	0.414	96.25%	98.00%	103.50%	-3.79%	-3.26%	1.92%				
0.20	0.206	0.21	0.2	103.00%	105.00%	100.00%	2.96%	3.74%	-1.58%	0.93%	1.53%	2.69%	1.72%
	0.208	0.203	0.199	104.00%	101.50%	99.50%	3.96%	0.24%	-2.08%				
	0.204	0.206	0.209	102.00%	103.00%	104.50%	1.96%	1.74%	2.92%				
	0.204	0.209	0.209	102.00%	104.50%	104.50%	1.96%	3.24%	2.92%				
0.08	0.08	0.077	0.083	100.00%	96.25%	103.75%	-0.04%	-5.01%	2.17%	3.77%	4.07%	3.25%	3.69%
	0.08	0.082	0.078	100.00%	102.50%	97.50%	-0.04%	1.24%	-4.08%				
	0.075	0.082	0.081	93.75%	102.50%	101.25%	-6.29%	1.24%	-0.33%				
	0.082	0.085	0.084	102.50%	106.25%	105.00%	2.46%	4.99%	3.42%				
	Average (%)			100.04%	101.26%	101.58%	0.00%	0.00%	0.00%			RSD% ≤	2.30%
	Standard Deviation (%)			2.69%	2.81%	2.69%	2.69%	2.81%	2.69%				

Variance of repetitions (%²)	0.07%^2	0.08%^2	0.07%^2
St-dev (%)	2.69%	2.81%	2.69%
Variance of repetability (%²)		0.22%^2	
Average recovery (%)		100.96%	
Average - Average of averages^2 (%^2)	0.01%^2	0.00%^2	0.00%^2

Homogeneity of variances inside groups
Cochran C test inter-days
$\quad$ C 0.35
C (0.05,2,19 0.7164

C < C (0.05,;Homoscedasticity conditions are met

Repetability error	
Average (%)	100.96%
Repetability error (%)	0.22%

Light-matrix — LOD/LLOQ

Assay 4

		St weight
		20

N	x (mg/L)	y (mA)
B	0.00	5
St 1	0.80	270
St 2	0.60	215
St 3	0.40	145
St 4	0.20	83
St 5	0.08	34

Slope b	333.022
Intercept a	9.885714
R^2	0.99733

Assay 5

		St weight
		20.2

N	x (mg/L)	y (mA)
B	0.00	4
St 1	0.81	290
St 2	0.61	220
St 3	0.40	155
St 4	0.20	80
St 5	0.08	30

Slope b	355.674
Intercept a	5.3
R^2	0.998881

Assay 6

		St weight
		19.7

N	x (mg/L)	y (mA)
B	0.00	4
St 1	0.79	295
St 2	0.59	225
St 3	0.39	155
St 4	0.20	80
St 5	0.08	30

Slope b	372.0924
Intercept a	4.442857
R^2	0.999348

Slope b		
	Assay 1	352.033
	Assay 2	347.9853
	Assay 3	332.4859
	Assay 4	333.022
	Assay 5	355.674
	Assay 6	372.0924
	Average slope	348.8821

Blank		
	Assay 1	1
	Assay 2	-2
	Assay 3	0
	Assay 4	5
	Assay 5	4
	Assay 6	4
	St-dev	2.75681

LLOQ (mg/L)	0.07901838
LOD (mg/L)	0.02633946

Kidneys Linearity

	St weight
	20.3

N	x (mg/L)	y (mA)	x^2	y^2	xy
B	0.00	3	0.0	9.0	0.0
St 1	0.81	230	0.7	52900.0	186.8
St 2	0.61	182	0.4	33124.0	110.8
St 3	0.41	122	0.2	14884.0	49.5
St 4	0.20	73	0.0	5329.0	14.8
St 5	0.08	33	0.0	1089.0	2.7

Sum	6	2.1	643.0	1.2	107335.0	364.6
Average		0.4	107.2	0.2		

Sxx	0.5	Slope b	276.7553	r	0.99830833
Syy	38426.8	Intercept a	9.785714	r^2	0.996619521
Sxy	138.4				
S^2xy	32.4752747		S^2r	32.47527	
SE b	8.05916996		S^2a	18.86659	
			S^2b	64.95022	

One-sided test on the slope
F	276.755				
dof num.		4	F(0,05;1;4) 7.71		significant
dof denom.		4			
			→ Existence of a slope		

One-sided test on r
t	34.340				
ddl		4	t(0,05;4) 2.776		significant
		→ Existence of a correlation between x and y			

Two-sided comparison between intercept and 0
t	2.2529				
ddl		4	t(0,05;4) 2.776		non-significant
		→ Intercept different from 0			

	St weight
	19.6

N	x (mg/L)	y (mA)	x^2	y^2	xy
B	0.00	2	0.0	4.0	0.0
St 1	0.78	220	0.6	48400.0	172.5
St 2	0.59	175	0.3	30625.0	102.9
St 3	0.39	115	0.2	13225.0	45.1
St 4	0.20	68	0.0	4624.0	13.3
St 5	0.08	27	0.0	729.0	2.1

Sum	6	2.0	607.0	1.2	97607.0	335.9
Average		0.3	101.2	0.2		

Sxx	0.5	Slope b	278.2294	r	0.998393868
Syy	36198.8	Intercept a	6.642857	r^2	0.996790316
Sxy	129.7				
S^2xy	29.0467033		S^2r	29.0467	
SE b	7.89409391		S^2a	16.87475	
			S^2b	62.31672	

One-sided test on the slope
F	278.229				
dof num.		4	F(0,05;1;4) 7.71		significant
dof denom.		4			
			→ Existence of a slope		

One-sided test on r
t	35.245				
ddl		4	t(0,05;4) 2.776		significant
		→ Existence of a correlation between x and y			

Two-sided comparison between intercept and 0
t	1.6171				
ddl		4	t(0,05;4) 2.776		non-significant
		→ Intercept different from 0			

<u>Assay 3</u>

	St weight
	19.9

	N	x (mg/L)	y (mA)	x^2	y^2	xy
B		0.00	-2	0.0	4.0	0.0
St 1		0.80	210	0.6	44100.0	167.2
St 2		0.60	160	0.4	25600.0	95.5
St 3		0.40	115	0.2	13225.0	45.8
St 4		0.20	62	0.0	3844.0	12.3
St 5		0.08	25	0.0	625.0	2.0

Sum	6	2.1	570.0	1.2	87398.0	322.8
Average		0.3	95.0	0.2		
Sxx	0.5		<u>Slope b</u>	262.5766	<u>r</u>	0.998197391
Syy	33248.0		<u>Intercept a</u>	4.428571	<u>r^2</u>	0.996398032
Sxy	126.2					
S^2xy	29.9395604			S^2r	29.93956	
SE b	7.89368095			S^2a	17.39346	
				S^2b	62.3102	

<u>One-sided test on the slope</u>
F	262.577				
dof num.	4	F(0,05;1;4)	7.71	*significant*	
dof denom.	4				

→ Existence of a slope

<u>One-sided test on r</u>
t	33.264			
ddl	4	t(0,05;4)	2.776	*significant*

→ Existence of a correlation between x and y

<u>Two-sided comparison between intercept and 0</u>
t	1.0619			
ddl	4	t(0,05;4)	2.776	*non-significant*

→ Intercept different from 0

<u>Symbols</u>

N	Number of observations		r	Correlation coefficient
k	Number of groups		r^2	Coefficient of determination
Sxx	Standard-deviation of x		S^2r	Variance of the correlation coefficient
Syy	Standard-deviation of y		S^2a	Variance of the intercept
Sxy	Covariance of x and y		S^2b	Variance of the slope
S^2xy	Regression variance, Residual variance		F	Fisher F test
SE b	Error on the slope		t	Student t test
a	Intercept of the regression line		dof	Degrees of freedom
b	Slope of the regression line			x = Cisplatin concentration (mg/L)
				y = Measured absorbance (mA)

Comparison between the slopes		
J1/J2		
t	0.13067322	*non-significant*
t (0,05;8)	2.306	
J1/J3		
t	1.25686333	*non-significant*
t (0,05;8)	2.306	
J2/J3		
t	1.40212337	*non-significant*
t (0,05;8)	2.306	
The three slopes are not significantly different		

Comparison between the intercepts		
J1/J2		
t	0.525702	*non-significant*
t (0,05;8)	2.306	
J1/J3		
t	0.88965	*non-significant*
t (0,05;8)	2.306	
J2/J3		
t	0.378258	*non-significant*
t (0,05;8)	2.306	
The three intercepts are not significantly different		

Kidneys Accuracy

Real concentration of sampled assays				100	75	50	25	10
	Weight assay 1	20.2	mg	0.808	0.606	0.404	0.202	0.0808
	Weight assay 2	20	mg	0.8	0.6	0.4	0.2	0.08
	Weight assay 3	20.1	mg	0.804	0.603	0.402	0.201	0.0804

	x measured	x real (ppb)	Recovery (%)	Variances	Y	yi-Y/	(yi-Y/)^2	yi-Y//	(yi-Y//)^2
Assay 1-100	851	808	105.32%		102.03%	3.29%	0.0011	6.28%	0.0039
Assay 2-100	844	800	105.50%		102.03%	3.47%	0.0012	6.46%	0.0042
Assay 3-100	766	804	95.27%	0.0034	102.03%	-6.76%	0.0046	-3.76%	0.0014
Assay 1-75	630	606	103.96%		103.74%	0.22%	0.0000	4.92%	0.0024
Assay 2-75	569	600	94.83%		103.74%	-8.91%	0.0079	-4.21%	0.0018
Assay 3-75	678	603	112.44%	0.0078	103.74%	8.69%	0.0076	13.40%	0.0180
Assay 1-50	404	404	100.00%		100.27%	-0.27%	0.0000	0.96%	0.0001
Assay 2-50	443	400	110.75%		100.27%	10.48%	0.0110	11.71%	0.0137
Assay 3-50	362	402	90.05%	0.0107	100.27%	-10.22%	0.0104	-8.99%	0.0081
Assay 1-25	207	202	102.48%		100.84%	1.64%	0.0003	3.44%	0.0012
Assay 2-25	216	200	108.00%		100.84%	7.16%	0.0051	8.96%	0.0080
Assay 3-25	185	201	92.04%	0.0066	100.84%	-8.80%	0.0077	-7.00%	0.0049
Assay 1-10	65	80.8	80.45%		88.31%	-7.87%	0.0062	-18.59%	0.0346
Assay 2-10	66	80	82.50%		88.31%	-5.81%	0.0034	-16.54%	0.0274
Assay 3-10	82	80.4	101.99%	0.0141	88.31%	13.68%	0.0187	2.95%	0.0009
		AVG (%)	99.04%						
N	15	SUM (%)	1485.58%	0.0426	14.8558	0.00%	0.0852	0.00%	0.1305
k	5	STDEV (%)	9.65%						

Cochran C test between groups (Homoscedasticity)

C	0.3318
C (0.05;5;2)	0.6838

C < C (0.05;5;2)
Homoscedasticity of variances between groups is met

Validity of means

Variation	dof	Sum of square	Variance (%^{2})	St-dev (%)	CV (%)	F	
Total variation	15	0.1305					
Intra-group variation	10	0.0852	0.0085	0.0923	0.0932	F	1.33
Inter-group variation	4	0.0453	0.0113	0.1064	0.1074	p	0.32
						F (0,05;4;10)	3.48

F < F (0.05;4;10)
Variation of observations between groups are due to experimental errors

Estimation of the mean recovery

Mean recovery (%)	99.04%		
Stdev (%)	9.65%		
N	15		
t (0,05;14)	2.1448		
t*S/√(N) (%)	0.05346185		
CI 95 (%)	93.69%	to	104.38%

Kidneys Precision

Concentration (mg/L)	Results SpectrAA			Recovery (%)			(Recovery - Average)			RSD%			
	Day 1	Day 2	Day 3	Day 1	Day 2	Day 3	Day 1	Day 2	Day 3	Day 1	Day 2	Day 3	Average
0.80	0.823	0.837	0.782	102.88%	104.63%	97.75%	1.36%	6.06%	-4.30%				
	0.831	0.791	0.813	103.88%	98.88%	101.63%	2.36%	0.31%	-0.43%				
	0.823	0.757	0.809	102.88%	94.63%	101.13%	1.36%	-3.94%	-0.92%				
	0.764	0.794	0.758	95.50%	99.25%	94.75%	-6.01%	0.69%	-7.30%	3.83%	4.13%	3.25%	3.74%
0.60	0.602	0.646	0.554	100.33%	107.67%	92.33%	-1.18%	9.11%	-9.72%				
	0.566	0.603	0.569	94.33%	100.50%	94.83%	-7.18%	1.94%	-7.22%				
	0.589	0.572	0.604	98.17%	95.33%	100.67%	-3.35%	-3.23%	-1.38%				
	0.593	0.617	0.598	98.83%	102.83%	99.67%	-2.68%	4.27%	-2.38%	2.61%	5.05%	4.08%	3.91%
0.40	0.383	0.387	0.442	95.75%	96.75%	110.50%	-5.76%	-1.81%	8.45%				
	0.438	0.396	0.411	109.50%	99.00%	102.75%	7.99%	0.44%	0.70%				
	0.441	0.398	0.392	110.25%	99.50%	98.00%	8.74%	0.94%	-4.05%				
	0.445	0.429	0.38	111.25%	107.25%	95.00%	9.74%	8.69%	-7.05%	6.87%	4.55%	6.65%	6.02%
0.20	0.207	0.198	0.214	103.50%	99.00%	107.00%	1.99%	0.44%	4.95%				
	0.213	0.2	0.207	106.50%	100.00%	103.50%	4.99%	1.44%	1.45%				
	0.2	0.22	0.213	100.00%	110.00%	106.50%	-1.51%	11.44%	4.45%				
	0.216	0.217	0.215	108.00%	108.50%	107.50%	6.49%	9.94%	5.45%	3.38%	5.44%	1.69%	3.51%
0.08	0.076	0.073	0.086	95.00%	91.25%	107.50%	-6.51%	-7.31%	5.45%				
	0.071	0.068	0.083	88.75%	85.00%	103.75%	-12.76%	-13.56%	1.70%				
	0.082	0.069	0.081	102.50%	86.25%	101.25%	0.99%	-12.31%	-0.80%				
	0.082	0.068	0.092	102.50%	85.00%	115.00%	0.99%	-13.56%	12.95%	6.84%	3.43%	5.61%	5.29%
			Average (%)	101.51%	98.56%	102.05%	0.00%	0.00%	0.00%			RSD% ≤	4.49%
			Standard Deviation (%)	5.92%	7.44%	5.81%	5.92%	7.44%	5.81%				

Variance of repetitions (%^2)	0.35%^2	0.55%^2	0.34%^2
St-dev (%)	5.92%	7.44%	5.81%
Variance of repeatability (%^2)	1.24%^2	
Average recovery (%)	100.71%	
Average – Average of averages^2 (%^2)	0.01%^2	0.05%^2	0.02%^2

Homogeneity of variances inside groups
Cochran C test inter-days
C 0.45
C (0.05,2,19 0.7164

C < C (0,05,:Homoscedasticity conditions are met

Repetability error	
Average (%)	100.71%
Reproducibility error (%)	1.23%

Kidneys LOD/LLOQ

Assay 4		St weight
		20
N	x (mg/L)	y (mA)
B	0.00	1
St 1	0.80	221
St 2	0.60	171
St 3	0.40	121
St 4	0.20	71
St 5	0.08	31

Slope b	269.78022
Intercept a	9.14285714
R^2	0.99548774

Assay 5		St weight
		20.2
N	x (mg/L)	y (mA)
B	0.00	2
St 1	0.81	215
St 2	0.61	161
St 3	0.40	122
St 4	0.20	61
St 5	0.08	29

Slope b	259.87379
Intercept a	7.34285714
R^2	0.99571662

Assay 6		St weight
		19.7
N	x (mg/L)	y (mA)
B	0.00	1
St 1	0.79	219
St 2	0.59	176
St 3	0.39	119
St 4	0.20	66
St 5	0.08	30

Slope b	276.510292
Intercept a	7.41428571
R^2	0.99634358

Slope b		
	Assay 1	276.755264
	Assay 2	278.229424
	Assay 3	262.576619
	Assay 4	269.78022
	Assay 5	259.87379
	Assay 6	276.510292
	Average slope	270.620935

Blank		
	Assay 1	3
	Assay 2	2
	Assay 3	-2
	Assay 4	1
	Assay 5	2
	Assay 6	1
	St-dev	1.72240142

LLOQ (mg/L digestate)	0.063646274
LOD (mg/L digestate)	0.021215425

Lungs — Linearity

	St weight
	20.3

N	x (mg/L)	y (mA)	x^2	y^2	xy
B	0.00	1	0.0	1.0	0.0
St 1	0.81	217	0.7	47089.0	176.2
St 2	0.61	170	0.4	28900.0	103.5
St 3	0.41	123	0.2	15129.0	49.9
St 4	0.20	67	0.0	4489.0	13.6
St 5	0.08	28	0.0	784.0	2.3

Sum	6	2.1	606.0	1.2	96392.0	345.5
Average		0.4	101.0	0.2		

Sxx	0.5	Slope b	264.6295	r		0.997560726
Syy	35186.0	Intercept a	7.885714	r^2		0.995127401
Sxy	132.3					
S^2xy	42.8618132		S^2r	42.86181		
SE b	9.25868198		S^2a	24.90067		
			S^2b	85.72319		

One-sided test on the slope

F	264.629				
dof num.		4	F(0,05;1;4) 7.71		*significant*
dof denom.		4			
					→ Existence of a slope

One-sided test on r

t	28.582			
ddl		4	t(0,05;4) 2.776	*significant*
			→ Existence of a correlation between x and y	

Two-sided comparison between intercept and 0

t	1.5803			
ddl		4	t(0,05;4) 2.776	*non-significant*
			→ Intercept different from 0	

	St weight
	19.6

N	x (mg/L)	y (mA)	x^2	y^2	xy
B	0.00	2	0.0	4.0	0.0
St 1	0.78	202	0.6	40804.0	158.4
St 2	0.59	160	0.3	25600.0	94.1
St 3	0.39	110	0.2	12100.0	43.1
St 4	0.20	65	0.0	4225.0	12.7
St 5	0.08	25	0.0	625.0	2.0

Sum	6	2.0	564.0	1.2	83358.0	310.3
Average		0.3	94.0	0.2		

Sxx	0.5	Slope b	254.5694	r		0.99776956
Syy	30342.0	Intercept a	7.514286	r^2		0.995544094
Sxy	118.7					
S^2xy	33.8002747		S^2r	33.80027		
SE b	8.51557502		S^2a	19.63635		
			S^2b	72.51502		

One-sided test on the slope

F	254.569				
dof num.		4	F(0,05;1;4) 7.71		*significant*
dof denom.		4			
					→ Existence of a slope

One-sided test on r

t	29.895			
ddl		4	t(0,05;4) 2.776	*significant*
			→ Existence of a correlation between x and y	

Two-sided comparison between intercept and 0

t	1.6957			
ddl		4	t(0,05;4) 2.776	*non-significant*
			→ Intercept different from 0	

		St weight
		19.9

N	x (mg/L)	y (mA)	x^2	y^2	xy
B	0.00	3	0.0	9.0	0.0
St 1	0.80	224	0.6	50176.0	178.3
St 2	0.60	174	0.4	30276.0	103.9
St 3	0.40	126	0.2	15876.0	50.1
St 4	0.20	67	0.0	4489.0	13.3
St 5	0.08	31	0.0	961.0	2.5

Sum	6	2.1	625.0	1.2	101787.0	348.1
Average		0.3	104.2	0.2		
Sxx	0.5		Slope b	275.8573	r	0.998380751
Syy	36682.8		Intercept a	9.014286	r^2	0.996764124
Sxy	132.5					
S^2xy	29.6752747			S^2r	29.67527	
SE b	7.85876375			S^2a	17.23992	
				S^2b	61.76017	

One-sided test on the slope

F	275.857			
dof num.	4	F(0,05;1;4)	7.71	*significant*
dof denom.	4			
			→ Existence of a slope	

One-sided test on r

t	35.102			
ddl	4	t(0,05;4)	2.776	*significant*
		→ Existence of a correlation between x and y		

Two-sided comparison between intercept and 0

t	2.1710			
ddl	4	t(0,05;4)	2.776	*non-significant*
		→ Intercept different from 0		

Symbols		r	Correlation coefficient
N	Number of observations	r^2	Coefficient of determination
k	Number of groups	S^2r	Variance of the correlation coefficient
Sxx	Standard-deviation of x	S^2a	Variance of the intercept
Syy	Standard-deviation of y	S^2b	Variance of the slope
Sxy	Covariance of x and y	F	Fisher F test
S^2xy	Regression variance, Residual variance	t	Student t test
SE b	Error on the slope	dof	Degrees of freedom
a	Intercept of the regression line		x = Cisplatin concentration (mg/L)
b	Slope of the regression line		y = Measured absorbance (mA)

Comparison between the slopes

J1/J2			
t	0.79973189	*non-significant*	
t (0,05;8)	2.306		

J1/J3			
t	0.92453863	*non-significant*	
t (0,05;8)	2.306		

J2/J3			
t	1.83710892	*non-significant*	
t (0,05;8)	2.306		

The three slopes are not significantly different

Comparison between the intercepts

J1/J2			
t	0.055656	*non-significant*	
t (0,05;8)	2.306		

J1/J3			
t	0.173852	*non-significant*	
t (0,05;8)	2.306		

J2/J3			
t	0.247012	*non-significant*	
t (0,05;8)	2.306		

The three intercepts are not significantly different

Lungs — Accuracy

Real concentration of sampled assays			100	75	50	25	10
Weight assay 1	20.2	mg	0.808	0.606	0.404	0.202	0.0808
Weight assay 2	20	mg	0.8	0.6	0.4	0.2	0.08
Weight assay 3	20.1	mg	0.804	0.603	0.402	0.201	0.0804

	x measured	x real (ppb)	Recovery (%)	Variances	Y	yi-Y/	(yi-Y/)^2	yi-Y//	(yi-Y//)^2
Assay 1-100	830	808	102.72%		99.41%	3.31%	0.0011	1.52%	0.0002
Assay 2-100	765	800	95.63%		99.41%	-3.78%	0.0014	-5.58%	0.0031
Assay 3-100	803	804	99.88%	0.0013	99.41%	0.47%	0.0000	-1.33%	0.0002
Assay 1-75	555	606	91.58%		101.74%	-10.15%	0.0103	-9.62%	0.0093
Assay 2-75	630	600	105.00%		101.74%	3.26%	0.0011	3.79%	0.0014
Assay 3-75	655	603	108.62%	0.0081	101.74%	6.89%	0.0047	7.42%	0.0055
Assay 1-50	451	404	111.63%		102.14%	9.49%	0.0090	10.43%	0.0109
Assay 2-50	405	400	101.25%		102.14%	-0.89%	0.0001	0.04%	0.0000
Assay 3-50	376	402	93.53%	0.0083	102.14%	-8.61%	0.0074	-7.67%	0.0059
Assay 1-25	215	202	106.44%		104.48%	1.95%	0.0004	5.23%	0.0027
Assay 2-25	220	200	110.00%		104.48%	5.52%	0.0030	8.79%	0.0077
Assay 3-25	195	201	97.01%	0.0045	104.48%	-7.47%	0.0056	-4.19%	0.0018
Assay 1-10	70	80.8	86.63%		98.26%	-11.63%	0.0135	-14.57%	0.0212
Assay 2-10	71	80	88.75%		98.26%	-9.51%	0.0090	-12.46%	0.0155
Assay 3-10	96	80.4	119.40%	0.0336	98.26%	21.14%	0.0447	18.20%	0.0331
		AVG (%)	101.21%						
N	15	SUM (%)	1518.08%	0.0557	15.1808	0.00%	0.1114	0.00%	0.1186
k	5	STDEV (%)	9.20%						

Cochran C test between groups (Homoscedasticity)

C	0.6036	C < C (0.05;5;2)
C (0.05;5;2)	0.6838	Homoscedasticity of variances between groups is met

Validity of means

Variation	dof	Sum of squares	Variance (%^{2})	St-dev (%)	CV (%)	F	
Total variation	15	0.1186				F	0.16
Intra-group variation	10	0.1114	0.0111	0.1056	0.1043	F	0.16
Inter-group variation	4	0.0071	0.0018	0.0422	0.0417	p	0.95
						F (0,05;4;10)	3.48

F < F (0.05;4;10)
Variation of observations between groups are due to experimental errors

Estimation of the mean recovery

Mean recovery (%)	101.21%		
Stdev (%)	9.20%		
N	15		
t (0,05;14)	2.1448		
t*S/√(N) (%)	0.05096454		
CI 95 (%)	96.11%	to	106.30%

Lungs

Precision

Concentration (mg/L)	Results SpectrAA			Recovery (%)			(Recovery - Average)			RSD%			
	Day 1	Day 2	Day 3	Day 1	Day 2	Day 3	Day 1	Day 2	Day 3	Day 1	Day 2	Day 3	Average
0.80	0.799	0.819	0.843	99.88%	102.38%	105.38%	2.45%	1.20%	7.37%				
	0.781	0.813	0.797	97.63%	101.63%	99.63%	0.20%	0.45%	1.62%				
	0.766	0.849	0.758	95.75%	106.13%	94.75%	-1.68%	4.95%	-3.26%				
	0.793	0.807	0.823	99.13%	100.88%	102.88%	1.70%	-0.30%	4.87%	1.86%	2.27%	4.56%	2.89%
0.60	0.57	0.609	0.559	95.00%	101.50%	93.17%	-2.43%	0.33%	-4.84%				
	0.565	0.642	0.57	94.17%	107.00%	95.00%	-3.26%	5.83%	-3.01%				
	0.56	0.55	0.629	93.33%	91.67%	104.83%	-4.09%	-9.50%	6.83%				
	0.598	0.567	0.624	99.67%	94.50%	104.00%	2.24%	-6.67%	5.99%	2.97%	7.02%	6.07%	5.35%
0.40	0.392	0.442	0.428	98.00%	110.50%	107.00%	0.57%	9.33%	8.99%				
	0.396	0.443	0.374	99.00%	110.75%	93.50%	1.57%	9.58%	-4.51%				
	0.375	0.41	0.399	93.75%	102.50%	99.75%	-3.68%	1.33%	1.74%				
	0.36	0.415	0.411	90.00%	103.75%	102.75%	-7.43%	2.58%	4.74%	4.35%	4.08%	5.63%	4.69%
0.20	0.2	0.2	0.209	100.00%	100.00%	104.50%	2.57%	-1.17%	6.49%				
	0.201	0.2	0.203	100.50%	100.00%	101.50%	3.07%	-1.17%	3.49%				
	0.179	0.189	0.193	89.50%	94.50%	96.50%	-7.93%	-6.67%	-1.51%				
	0.179	0.214	0.18	89.50%	107.00%	90.00%	-7.93%	5.83%	-8.01%	6.55%	5.10%	6.46%	6.04%
0.08	0.084	0.071	0.069	105.00%	88.75%	86.25%	7.57%	-12.42%	-11.76%				
	0.077	0.076	0.07	96.25%	95.00%	87.50%	-1.18%	-6.17%	-10.51%				
	0.08	0.081	0.08	100.00%	101.25%	100.00%	2.57%	0.08%	1.99%				
	0.09	0.083	0.073	112.50%	103.75%	91.25%	15.07%	2.58%	-6.76%	6.79%	6.92%	6.80%	6.84%
Average (%)				97.43%	101.17%	98.01%	0.00%	0.00%	0.00%			RSD% ≤	5.16%
Standard Deviation (%)				5.41%	5.91%	6.29%	5.41%	5.91%	6.29%				

Variance of repetitions (%²)	0.29%^2	0.35%^2	0.40%^2
St-dev (%)	5.41%	5.91%	6.29%
Variance of repetability (%²)		1.04%^2	
Average recovery (%)		98.87%	
Average - Average of averages^2 (%^2)	0.02%^2	0.05%^2	0.01%^2

Homogeneity of variances inside groups
Cochran C test inter-days
C 0.38
C (0.05,2,19 0.7164

C < C (0.05,;Homoscedasticity conditions are met

Repetability error	
Average (%)	98.87%
Reproducibility error (%)	1.05%

Lungs — LOD/LLOQ

Assay 4

		St weight
		20

N	x (mg/L)	y (mA)
B	0.00	1
St 1	0.80	202
St 2	0.60	165
St 3	0.40	112
St 4	0.20	64
St 5	0.08	25

Slope b	253.324176
Intercept a	7.01428571
R^2	0.99395336

Assay 5

		St weight
		20.2

N	x (mg/L)	y (mA)
B	0.00	-1
St 1	0.81	214
St 2	0.61	163
St 3	0.40	120
St 4	0.20	60
St 5	0.08	27

Slope b	263.273855
Intercept a	4.98571429
R^2	0.99620572

Assay 6

		St weight
		19.7

N	x (mg/L)	y (mA)
B	0.00	2
St 1	0.79	225
St 2	0.59	166
St 3	0.39	112
St 4	0.20	65
St 5	0.08	28

Slope b	276.817092
Intercept a	5.14285714
R^2	0.99848669

Slope b		
	Assay 1	264.629459
	Assay 2	254.56941
	Assay 3	275.857309
	Assay 4	253.324176
	Assay 5	263.273855
	Assay 6	276.817092
	Average slope	264.745217

Blank		
	Assay 1	1
	Assay 2	2
	Assay 3	3
	Assay 4	1
	Assay 5	-1
	Assay 6	2
	St-dev	1.3662601

LLOQ (mg/L digestate)	0.051606602
LOD (mg/L digestate)	0.017202201

Liver — Linearity

Assay 1

	St weight
	20.3

N	x (mg/L)	y (mA)	x^2	y^2	xy
B	0.00	2	0.0	4.0	0.0
St 1	0.81	260	0.7	67600.0	211.1
St 2	0.61	195	0.4	38025.0	118.8
St 3	0.41	130	0.2	16900.0	52.8
St 4	0.20	80	0.0	6400.0	16.2
St 5	0.08	33	0.0	1089.0	2.7

	N	x	y	x^2	y^2	xy
Sum	6	2.1	700.0	1.2	130018.0	401.6
Average		0.4	116.7	0.2		

Sxx	0.5	Slope b	310.5343	r 0.998599726
Syy	48351.3	Intercept a	7.4	r^2 0.997201414
Sxy	155.3			
S^2xy	33.8288462	S^2r	33.82885	
SE b	8.22540877	S^2a	19.65295	
		S^2b	67.65735	

One-sided test on the slope

F	310.534		
dof num.	4	F(0,05;1;4) 7.71	*significant*
dof denom.	4		
			→ Existence of a slope

One-sided test on r

t	37.753		
ddl	4	t(0,05;4) 2.776	*significant*
		→ Existence of a correlation between x and y	

Two-sided comparison between intercept and 0

t	1.6692		
ddl	4	t(0,05;4) 2.776	*non-significant*
		→ Intercept different from 0	

Assay 2

	St weight
	19.6

N	x (mg/L)	y (mA)	x^2	y^2	xy
B	0.00	2	0.0	4.0	0.0
St 1	0.78	275	0.6	75625.0	215.6
St 2	0.59	201	0.3	40401.0	118.2
St 3	0.39	134	0.2	17956.0	52.5
St 4	0.20	83	0.0	6889.0	16.3
St 5	0.08	35	0.0	1225.0	2.7

	N	x	y	x^2	y^2	xy
Sum	6	2.0	730.0	1.2	142100.0	405.3
Average		0.3	121.7	0.2		

Sxx	0.5	Slope b	337.5196	r 0.998273334
Syy	53283.3	Intercept a	7	r^2 0.99654965
Sxy	157.3			
S^2xy	45.9615385	S^2r	45.96154	
SE b	9.93004331	S^2a	26.70147	
		S^2b	98.60576	

One-sided test on the slope

F	337.520		
dof num.	4	F(0,05;1;4) 7.71	*significant*
dof denom.	4		
			→ Existence of a slope

One-sided test on r

t	33.990		
ddl	4	t(0,05;4) 2.776	*significant*
		→ Existence of a correlation between x and y	

Two-sided comparison between intercept and 0

t	1.3547		
ddl	4	t(0,05;4) 2.776	*non-significant*
		→ Intercept different from 0	

Assay 3

	St weight
	19.9

N	x (mg/L)	y (mA)	x^2	y^2	xy
B	0.00	-2	0.0	4.0	0.0
St 1	0.80	257	0.6	66049.0	204.6
St 2	0.60	201	0.4	40401.0	120.0
St 3	0.40	133	0.2	17689.0	52.9
St 4	0.20	80	0.0	6400.0	15.9
St 5	0.08	30	0.0	900.0	2.4

Sum	6	2.1	699.0	1.2	131443.0	395.8
Average		0.3	116.5	0.2		

Sxx	0.5		Slope b	321.967	r	0.997994656
Syy	50009.5		Intercept a	5.442857	r^2	0.995993333
Sxy	154.7					
S^2xy	50.0928571			S^2r	50.09286	
SE b	10.2104471			S^2a	29.10156	
				S^2b	104.2532	

One-sided test on the slope

F	321.967			
dof num.		4	F(0,05;1;4) 7.71	*significant*
dof denom.		4		
			→ Existence of a slope	

One-sided test on r

t	31.533			
ddl		4	t(0,05;4) 2.776	*significant*
		→ Existence of a correlation between x and y		

Two-sided comparison between intercept and 0

t	1.0089			
ddl		4	t(0,05;4) 2.776	*non-significant*
		→ Intercept different from 0		

Symbols		r	Correlation coefficient
N	Number of observations	r^2	Coefficient of determination
k	Number of groups	S^2r	Variance of the correlation coefficient
Sxx	Standard-deviation of x	S^2a	Variance of the intercept
Syy	Standard-deviation of y	S^2b	Variance of the slope
Sxy	Covariance of x and y	F	Fisher F test
S^2xy	Regression variance, Residual variance	t	Student t test
SE b	Error on the slope	dof	Degrees of freedom
a	Intercept of the regression line		x = Cisplatin concentration (mg/L)
b	Slope of the regression line		y = Measured absorbance (mA)

Comparison between the slopes

J1/J2		
t	2.09280991	*non-significant*
t (0,05;8)	2.306	

J1/J3		
t	0.87196071	*non-significant*
t (0,05;8)	2.306	

J2/J3		
t	1.09196104	*non-significant*
t (0,05;8)	2.306	

The three slopes are not significantly different

Comparison between the intercepts

J1/J2		
t	0.058751	*non-significant*
t (0,05;8)	2.306	

J1/J3		
t	0.280295	*non-significant*
t (0,05;8)	2.306	

J2/J3		
t	0.208449	*non-significant*
t (0,05;8)	2.306	

The three intercepts are not significantly different

Liver — Accuracy

Real concentration of sampled assays				100	75	50	25	10
	Weight assay 1	20.2	mg	0.808	0.606	0.404	0.202	0.0808
	Weight assay 2	20	mg	0.8	0.6	0.4	0.2	0.08
	Weight assay 3	20.1	mg	0.804	0.603	0.402	0.201	0.0804

	x measured	x real (ppb)	Recovery (%)	Variances	Y	yi-Y/	(yi-Y/)²	yi-Y//	(yi-Y//)²
Assay 1-100	836	808	103.47%		103.82%	-0.35%	0.0000	3.10%	0.0010
Assay 2-100	842	800	105.25%		103.82%	1.43%	0.0002	4.88%	0.0024
Assay 3-100	826	804	102.74%	0.0002	103.82%	-1.08%	0.0001	2.37%	0.0006
Assay 1-75	611	606	100.83%		98.23%	2.60%	0.0007	0.46%	0.0000
Assay 2-75	586	600	97.67%		98.23%	-0.56%	0.0000	-2.70%	0.0007
Assay 3-75	580	603	96.19%	0.0006	98.23%	-2.04%	0.0004	-4.18%	0.0017
Assay 1-50	445	404	110.15%		104.97%	5.18%	0.0027	9.78%	0.0096
Assay 2-50	431	400	107.75%		104.97%	2.78%	0.0008	7.38%	0.0055
Assay 3-50	390	402	97.01%	0.0049	104.97%	-7.96%	0.0063	-3.35%	0.0011
Assay 1-25	211	202	104.46%		103.64%	0.81%	0.0001	4.09%	0.0017
Assay 2-25	203	200	101.50%		103.64%	-2.14%	0.0005	1.13%	0.0001
Assay 3-25	211	201	104.98%	0.0004	103.64%	1.33%	0.0002	4.61%	0.0021
Assay 1-10	84	80.8	103.96%		91.18%	12.79%	0.0163	3.59%	0.0013
Assay 2-10	66	80	82.50%		91.18%	-8.68%	0.0075	-17.87%	0.0319
Assay 3-10	70	80.4	87.06%	0.0128	91.18%	-4.11%	0.0017	-13.30%	0.0177
		AVG (%)	100.37%						
N	15	SUM (%)	1505.50%	0.0188	15.0550	0.00%	0.0375	0.00%	0.0774
k	5	STDEV (%)	7.43%						

Cochran C test between groups (Homoscedasticity)

C	0.6816
C (0.05;5;2)	0.6838

C < C (0.05;5;2)
Homoscedasticity of variances between groups is met

Validity of means

Variation	dof	Sum of squares	Variance (%²)	St-dev (%)	CV (%)	F	
Total variation	15	0.0774					
Intra-group variation	10	0.0375	0.0038	0.0612	0.0610	F	2.66
Inter-group variation	4	0.0399	0.0100	0.0998	0.0995	p	0.10
						F (0,05;4;10)	3.48

F < F (0.05;4;10)
Variation of observations between groups are due to experimental errors

Estimation of the mean recovery

Mean recovery (%)	100.37%		
Stdev (%)	7.43%		
N	15		
t (0,05;14)	2.1448		
t*S/√(N) (%)	0.04117082		
CI 95 (%)	96.25%	to	104.48%

Liver — Precision

Concentration (mg/L)	Results SpectrAA Day 1	Day 2	Day 3	Recovery (%) Day 1	Day 2	Day 3	(Recovery - Average) Day 1	Day 2	Day 3	RSD% Day 1	Day 2	Day 3	Average
0.80	0.776	0.839	0.765	97.00%	104.88%	95.63%	-3.00%	10.24%	-7.48%				
	0.759	0.84	0.793	94.88%	105.00%	99.13%	-5.13%	10.37%	-3.98%				
	0.82	0.838	0.82	102.50%	104.75%	102.50%	2.50%	10.12%	-0.60%				
	0.815	0.776	0.755	101.88%	97.00%	94.38%	1.87%	2.37%	-8.73%	3.76%	3.83%	3.74%	3.77%
0.60	0.598	0.588	0.613	99.67%	98.00%	102.17%	-0.34%	3.37%	-0.94%				
	0.578	0.572	0.598	96.33%	95.33%	99.67%	-3.67%	0.70%	-3.44%				
	0.63	0.599	0.578	105.00%	99.83%	96.33%	5.00%	5.20%	-6.77%				
	0.65	0.611	0.582	108.33%	101.83%	97.00%	8.33%	7.20%	-6.10%	5.24%	2.80%	2.70%	3.58%
0.40	0.4	0.377	0.444	100.00%	94.25%	111.00%	0.00%	-0.38%	7.90%				
	0.395	0.365	0.445	98.75%	91.25%	111.25%	-1.25%	-3.38%	8.15%				
	0.387	0.378	0.432	96.75%	94.50%	108.00%	-3.25%	-0.13%	4.90%				
	0.412	0.397	0.388	103.00%	99.25%	97.00%	3.00%	4.62%	-6.10%	2.63%	3.49%	6.28%	4.13%
0.20	0.206	0.184	0.218	103.00%	92.00%	109.00%	3.00%	-2.63%	5.90%				
	0.218	0.179	0.207	109.00%	89.50%	103.50%	9.00%	-5.13%	0.40%				
	0.21	0.19	0.201	105.00%	95.00%	100.50%	5.00%	0.37%	-2.60%				
	0.193	0.208	0.21	96.50%	104.00%	105.00%	-3.50%	9.37%	1.90%	5.05%	6.65%	3.38%	5.03%
0.08	0.071	0.061	0.091	88.75%	76.25%	113.75%	-11.25%	-18.38%	10.65%				
	0.077	0.066	0.09	96.25%	82.50%	112.50%	-3.75%	-12.13%	9.40%				
	0.075	0.064	0.084	93.75%	80.00%	105.00%	-6.25%	-14.63%	1.90%				
	0.083	0.07	0.079	103.75%	87.50%	98.75%	3.75%	-7.13%	-4.35%	6.54%	5.79%	6.51%	6.28%
Average (%)				100.00%	94.63%	103.10%	0.00%	0.00%	0.00%			RSD% ≤	4.56%
Standard Deviation (%)				5.10%	8.32%	6.09%	5.10%	8.32%	6.09%				

Variance of repetitions (%²)	0.26%^2	0.69%^2	0.37%^2
St-dev (%)	5.10%	8.32%	6.09%
Variance of repetability (%²)	1.32%^2		
Average recovery (%)	99.25%		
Average - Average of averages^2 (%^2)	0.01%^2	0.21%^2	0.15%^2

Homogeneity of variances inside groups
Cochran C test inter-days
C 0.52
C (0.05,2,19 0.7164

C < C (0.05,;Homoscedasticity conditions are met

Repetability error	
Average (%)	99.25%
Reproducibility error (%)	1.33%

Liver LOD/LLOQ

Assay 4		St weight 20			
N	x (mg/L)	y (mA)			
B	0.00	0	Slope b	306.538462
St 1	0.80	245	Intercept a	5.4
St 2	0.60	195	R^2	0.9963605
St 3	0.40	127		
St 4	0.20	75		
St 5	0.08	28		

Assay 5		St weight 20.2			
N	x (mg/L)	y (mA)			
B	0.00	-2	Slope b	329.18072
St 1	0.81	265	Intercept a	3.24285714
St 2	0.61	205	R^2	0.99795874
St 3	0.40	138		
St 4	0.20	77		
St 5	0.08	28		

Assay 6		St weight 19.7			
N	x (mg/L)	y (mA)			
B	0.00	-3	Slope b	306.548781
St 1	0.79	244	Intercept a	3.15714286
St 2	0.59	184	R^2	0.9969138
St 3	0.39	121		
St 4	0.20	73		
St 5	0.08	28		

Slope b		
	Assay 1	310.534293
	Assay 2	337.519623
	Assay 3	321.966978
	Assay 4	306.538462
	Assay 5	329.18072
	Assay 6	306.548781
	Average slope	318.71481

Blank		
	Assay 1	2
	Assay 2	2
	Assay 3	-2
	Assay 4	0
	Assay 5	-2
	Assay 6	-3
	St-dev	2.16794834

LLOQ (mg/L digestate)	0.068021575
LOD (mg/L digestate)	0.022673858

Spleen Linearity

Assay 1

					St weight
					20.3

N	x (mg/L)	y (mA)	x^2	y^2	xy
B	0.00	0	0.0	0.0	0.0
St 1	0.81	205	0.7	42025.0	166.5
St 2	0.61	161	0.4	25921.0	98.0
St 3	0.41	110	0.2	12100.0	44.7
St 4	0.20	60	0.0	3600.0	12.2
St 5	0.08	28	0.0	784.0	2.3

Sum	6	2.1	564.0	1.2	84430.0	323.6
Average		0.4	94.0	0.2		

Sxx	0.5		Slope b	250.3383	r	0.998738602
Syy	31414.0		Intercept a	5.914286	r^2	0.997478796
Sxy	125.2					
S^2xy	19.8002747			S^2r	19.80027	
SE b	6.2928808			S^2a	11.50302	
				S^2b	39.60035	

One-sided test on the slope

F	250.338				
dof num.		4	F(0,05;1;4)	7.71	*significant*
dof denom.		4			

→ Existence of a slope

One-sided test on r

t	39.781				
ddl		4	t(0,05;4)	2.776	*significant*

→ Existence of a correlation between x and y

Two-sided comparison between intercept and 0

t	1.7438				
ddl		4	t(0,05;4)	2.776	*non-significant*

→ Intercept different from 0

Assay 2

					St weight
					19.6

N	x (mg/L)	y (mA)	x^2	y^2	xy
B	0.00	2	0.0	4.0	0.0
St 1	0.78	210	0.6	44100.0	164.6
St 2	0.59	165	0.3	27225.0	97.0
St 3	0.39	115	0.2	13225.0	45.1
St 4	0.20	55	0.0	3025.0	10.8
St 5	0.08	22	0.0	484.0	1.7

Sum	6	2.0	569.0	1.2	88063.0	319.2
Average		0.3	94.8	0.2		

Sxx	0.5		Slope b	270.1839	r	0.998873214
Syy	34102.8		Intercept a	3.042857	r^2	0.997747698
Sxy	125.9					
S^2xy	19.2024725			S^2r	19.20247	
SE b	6.41848367			S^2a	11.15572	
				S^2b	41.19693	

One-sided test on the slope

F	270.184				
dof num.		4	F(0,05;1;4)	7.71	*significant*
dof denom.		4			

→ Existence of a slope

One-sided test on r

t	42.095				
ddl		4	t(0,05;4)	2.776	*significant*

→ Existence of a correlation between x and y

Two-sided comparison between intercept and 0

t	0.9110				
ddl		4	t(0,05;4)	2.776	*non-significant*

→ Intercept different from 0

					St weight
					19.9

N	x (mg/L)	y (mA)	x^2	y^2	xy
B	0.00	-3	0.0	9.0	0.0
St 1	0.80	205	0.6	42025.0	163.2
St 2	0.60	155	0.4	24025.0	92.5
St 3	0.40	108	0.2	11664.0	43.0
St 4	0.20	64	0.0	4096.0	12.7
St 5	0.08	25	0.0	625.0	2.0

Sum	6	2.1	554.0	1.2	82444.0	313.4
Average		0.3	92.3	0.2		

Sxx	0.5		Slope b	254.5972	r	0.997664833
Syy	31291.3		Intercept a	4.514286	r^2	0.99533512
Sxy	122.3					
S^2xy	36.4925824			S^2r	36.49258	
SE b	8.71483478			S^2a	21.20045	
				S^2b	75.94835	

One-sided test on the slope

F	254.597				
dof num.		4	F(0,05;1;4)	7.71	*significant*
dof denom.		4			
				→ Existence of a slope	

One-sided test on r

t	29.214				
ddl		4	t(0,05;4)	2.776	*significant*
			→ Existence of a correlation between x and y		

Two-sided comparison between intercept and 0

t	0.9804				
ddl		4	t(0,05;4)	2.776	*non-significant*
			→ Intercept different from 0		

Symbols

N	Number of observations		r	Correlation coefficient
k	Number of groups		r^2	Coefficient of determination
Sxx	Standard-deviation of x		S^2r	Variance of the correlation coefficient
Syy	Standard-deviation of y		S^2a	Variance of the intercept
Sxy	Covariance of x and y		S^2b	Variance of the slope
S^2xy	Regression variance, Residual variance		F	Fisher F test
SE b	Error on the slope		t	Student t test
a	Intercept of the regression line		dof	Degrees of freedom
b	Slope of the regression line			x = Cisplatin concentration (mg/L)
				y = Measured absorbance (mA)

Comparison between the slopes

J1/J2		
t	2.2078274	*non-significant*
t (0,05;8)	2.306	
J1/J3		
t	0.3961939	*non-significant*
t (0,05;8)	2.306	
J2/J3		
t	1.44010046	*non-significant*
t (0,05;8)	2.306	

The three slopes are not significantly different

Comparison between the intercepts

J1/J2		
t	0.603226	*non-significant*
t (0,05;8)	2.306	
J1/J3		
t	0.244811	*non-significant*
t (0,05;8)	2.306	
J2/J3		
t	0.258679	*non-significant*
t (0,05;8)	2.306	

The three intercepts are not significantly different

Spleen Accuracy

Real concentration of sampled assays			100	75	50	25	10
	Weight assay 1	20.2 mg	0.808	0.606	0.404	0.202	0.0808
	Weight assay 2	20 mg	0.8	0.6	0.4	0.2	0.08
	Weight assay 3	20.1 mg	0.804	0.603	0.402	0.201	0.0804

	x measured	x real (ppb)	Recovery (%)	Variances	Y	yi-Y/	(yi-Y/)^2	yi-Y//	(yi-Y//)^2
Assay 1-100	792	808	98.02%		98.21%	-0.19%	0.0000	-3.23%	0.0010
Assay 2-100	766	800	95.75%		98.21%	-2.46%	0.0006	-5.50%	0.0030
Assay 3-100	811	804	100.87%	0.0007	98.21%	2.66%	0.0007	-0.37%	0.0000
Assay 1-75	582	606	96.04%		96.08%	-0.04%	0.0000	-5.21%	0.0027
Assay 2-75	581	600	96.83%		96.08%	0.76%	0.0001	-4.41%	0.0019
Assay 3-75	575	603	95.36%	0.0001	96.08%	-0.72%	0.0001	-5.89%	0.0035
Assay 1-50	445	404	110.15%		104.31%	5.84%	0.0034	8.90%	0.0079
Assay 2-50	428	400	107.00%		104.31%	2.69%	0.0007	5.75%	0.0033
Assay 3-50	385	402	95.77%	0.0057	104.31%	-8.54%	0.0073	-5.47%	0.0030
Assay 1-25	202	202	100.00%		102.33%	-2.33%	0.0005	-1.25%	0.0002
Assay 2-25	213	200	106.50%		102.33%	4.17%	0.0017	5.25%	0.0028
Assay 3-25	202	201	100.50%	0.0013	102.33%	-1.83%	0.0003	-0.75%	0.0001
Assay 1-10	93	80.8	115.10%		105.30%	9.80%	0.0096	13.85%	0.0192
Assay 2-10	87	80	108.75%		105.30%	3.45%	0.0012	7.50%	0.0056
Assay 3-10	74	80.4	92.04%	0.0142	105.30%	-13.26%	0.0176	-9.21%	0.0085
		AVG (%)	101.25%						
N	15	SUM (%)	1518.68%	0.0219	15.1868	0.00%	0.0438	0.00%	0.0627
k	5	STDEV (%)	6.69%						

Cochran C test between groups (Homoscedasticity)

C	0.6472
C (0.05;5;2)	0.6838

C < C (0.05;5;2)
Homoscedasticity of variances between groups is met

Validity of means

Variation	dof	Sum of squares	Variance (%^{2})	St-dev (%)	CV (%)	F	
Total variation	15	0.0627					
Intra-group variation	10	0.0438	0.0044	0.0662	0.0654	F	1.08
Inter-group variation	4	0.0189	0.0047	0.0687	0.0678	p	0.42
						F (0,05;4;10)	3.48

F < F (0.05;4;10)
Variation of observations between groups are due to experimental errors

Estimation of the mean recovery

Mean recovery (%)	101.25%		
Stdev (%)	6.69%		
N	15		
t (0,05;14)	2.1448		
t*S/√(N) (%)	0.03706176		
CI 95 (%)	97.54%	to	104.95%

Concentration (mg/L)	Results SpectrAA			Recovery (%)			(Recovery - Average)			RSD%			
	Day 1	Day 2	Day 3	Day 1	Day 2	Day 3	Day 1	Day 2	Day 3	Day 1	Day 2	Day 3	Average
0.80	0.85	0.827	0.806	106.25%	103.38%	100.75%	5.70%	1.90%	0.61%	4.32%	4.07%	3.56%	3.98%
	0.774	0.84	0.773	96.75%	105.00%	96.63%	-3.80%	3.53%	-3.52%				
	0.782	0.776	0.79	97.75%	97.00%	98.75%	-2.80%	-4.47%	-1.39%				
	0.791	0.779	0.84	98.88%	97.38%	105.00%	-1.68%	-4.10%	4.86%				
0.60	0.594	0.598	0.62	99.00%	99.67%	103.33%	-1.55%	-1.80%	3.19%	3.61%	3.87%	4.31%	3.93%
	0.625	0.646	0.595	104.17%	107.67%	99.17%	3.61%	6.20%	-0.98%				
	0.604	0.649	0.558	100.67%	108.17%	93.00%	0.11%	6.70%	-7.14%				
	0.644	0.646	0.594	107.33%	107.67%	99.00%	6.78%	6.20%	-1.14%				
0.40	0.39	0.369	0.422	97.50%	92.25%	105.50%	-3.05%	-9.22%	5.36%	4.85%	6.84%	4.68%	5.46%
	0.418	0.429	0.445	104.50%	107.25%	111.25%	3.95%	5.78%	11.11%				
	0.434	0.403	0.398	108.50%	100.75%	99.50%	7.95%	-0.72%	-0.64%				
	0.398	0.378	0.432	99.50%	94.50%	108.00%	-1.05%	-6.97%	7.86%				
0.20	0.218	0.207	0.19	109.00%	103.50%	95.00%	8.45%	2.03%	-5.14%	5.65%	7.38%	6.11%	6.38%
	0.195	0.209	0.177	97.50%	104.50%	88.50%	-3.05%	3.03%	-11.64%				
	0.216	0.184	0.175	108.00%	92.00%	87.50%	7.45%	-9.47%	-12.64%				
	0.199	0.22	0.199	99.50%	110.00%	99.50%	-1.05%	8.53%	-0.64%				
0.08	0.082	0.078	0.087	102.50%	97.50%	108.75%	1.95%	-3.97%	8.61%	6.81%	4.14%	5.09%	5.35%
	0.076	0.076	0.08	95.00%	95.00%	100.00%	-5.55%	-6.47%	-0.14%				
	0.073	0.083	0.085	91.25%	103.75%	106.25%	-9.30%	2.28%	6.11%				
	0.07	0.082	0.078	87.50%	102.50%	97.50%	-13.05%	1.03%	-2.64%				
Average (%)				100.55%	101.47%	100.14%	0.00%	0.00%	0.00%			RSD% ≤	5.02%
Standard Deviation (%)				5.79%	5.55%	6.31%	5.79%	5.55%	6.31%				

	Day 1	Day 2	Day 3
Variance of repetitions (%²)	0.34%^2	0.31%^2	0.40%^2
St-dev (%)	5.79%	5.55%	6.31%
Variance of repetability (%²)	1.04%^2		
Average recovery (%)	100.72%		
Average - Average of averages^2 (%^2)	0.00%^2	0.01%^2	0.00%^2

Homogeneity of variances inside groups
Cochran C test inter-days
C 0.38
C (0,05,2,19 0.7164

C < C (0,05,;Homoscedasticity conditions are met

Repetability error	
Average (%)	100.72%
Reproducibility error (%)	1.03%

Spleen **LOD/LLOQ**

Assay 4		St weight
		20
N	x (mg/L)	y (mA)
B	0.00	0
St 1	0.80	215
St 2	0.60	155
St 3	0.40	108
St 4	0.20	66
St 5	0.08	22

Slope b	261.565934
Intercept a	3.65714286
R^2	0.99531164

Assay 5		St weight
		20.2
N	x (mg/L)	y (mA)
B	0.00	5
St 1	0.81	204
St 2	0.61	161
St 3	0.40	111
St 4	0.20	62
St 5	0.08	28

Slope b	246.627135
Intercept a	8.81428571
R^2	0.99810741

Assay 6		St weight
		19.7
N	x (mg/L)	y (mA)
B	0.00	3
St 1	0.79	203
St 2	0.59	154
St 3	0.39	115
St 4	0.20	55
St 5	0.08	33

Slope b	249.484019
Intercept a	8.64285714
R^2	0.99538007

Slope b		
	Assay 1	250.338332
	Assay 2	270.183898
	Assay 3	254.597162
	Assay 4	261.565934
	Assay 5	246.627135
	Assay 6	249.484019
	Average slope	255.46608

Blank		
	Assay 1	0
	Assay 2	2
	Assay 3	-3
	Assay 4	0
	Assay 5	5
	Assay 6	3
	St-dev	2.786874

LLOQ (mg/L digestate)	0.109089786
LOD (mg/L digestate)	0.036363262

Mediastinum Linearity

Assay 1

	St weight
	20.3

N	x (mg/L)	y (mA)	x^2	y^2	xy
B	0.00	3	0.0	9.0	0.0
St 1	0.81	188	0.7	35344.0	152.7
St 2	0.61	144	0.4	20736.0	87.7
St 3	0.41	101	0.2	10201.0	41.0
St 4	0.20	55	0.0	3025.0	11.2
St 5	0.08	22	0.0	484.0	1.8

Sum	6	2.1	513.0	1.2	69799.0	294.3
Average		0.4	85.5	0.2		

Sxx	0.5	Slope b	227.6024	r		0.999307097
Syy	25937.5	Intercept a	5.414286	r^2		0.998614675
Sxy	113.8					
S^2xy	8.98296703			S^2r	8.982967	
SE b	4.23861334			S^2a	5.218676	
				S^2b	17.96584	

One-sided test on the slope

F	227.602				
dof num.		4	F(0,05;1;4) 7.71	*significant*	
dof denom.		4			
				→ Existence of a slope	

One-sided test on r

t	53.697			
ddl		4	t(0,05;4) 2.776	*significant*
			→ Existence of a correlation between x and y	

Two-sided comparison between intercept and 0

t	2.3701			
ddl		4	t(0,05;4) 2.776	*non-significant*
			→ Intercept different from 0	

Assay 2

	St weight
	19.6

N	x (mg/L)	y (mA)	x^2	y^2	xy
B	0.00	-3	0.0	9.0	0.0
St 1	0.78	201	0.6	40401.0	157.6
St 2	0.59	144	0.3	20736.0	84.7
St 3	0.39	105	0.2	11025.0	41.2
St 4	0.20	55	0.0	3025.0	10.8
St 5	0.08	26	0.0	676.0	2.0

Sum	6	2.0	528.0	1.2	75872.0	296.2
Average		0.3	88.0	0.2		

Sxx	0.5	Slope b	250.7008	r		0.998088754
Syy	29408.0	Intercept a	2.828571	r^2		0.996181162
Sxy	116.9					
S^2xy	28.0760989			S^2r	28.0761	
SE b	7.76108153			S^2a	16.31088	
				S^2b	60.23439	

One-sided test on the slope

F	250.701				
dof num.		4	F(0,05;1;4) 7.71	*significant*	
dof denom.		4			
				→ Existence of a slope	

One-sided test on r

t	32.302			
ddl		4	t(0,05;4) 2.776	*significant*
			→ Existence of a correlation between x and y	

Two-sided comparison between intercept and 0

t	0.7004			
ddl		4	t(0,05;4) 2.776	*non-significant*
			→ Intercept different from 0	

Assay 3 | St weight: 19.9

N	x (mg/L)	y (mA)	x^2	y^2	xy
B	0.00	-3	0.0	9.0	0.0
St 1	0.80	189	0.6	35721.0	150.4
St 2	0.60	151	0.4	22801.0	90.1
St 3	0.40	99	0.2	9801.0	39.4
St 4	0.20	54	0.0	2916.0	10.7
St 5	0.08	22	0.0	484.0	1.8

Sum	6	2.1	512.0	1.2	71732.0	292.5
Average		0.3	85.3	0.2		

Sxx	0.5	Slope b	241.1784	r	0.998348698
Syy	28041.3	Intercept a	2.142857	r^2	0.996700122
Sxy	115.9				
S^2xy	23.1332418		S^2r	23.13324	
SE b	6.93865201		S^2a	13.43931	
			S^2b	48.14489	

One-sided test on the slope

F	241.178			
dof num.		4	F(0,05;1;4) 7.71	significant
dof denom.		4		

→ Existence of a slope

One-sided test on r

t	34.759			
ddl		4	t(0,05;4) 2.776	significant

→ Existence of a correlation between x and y

Two-sided comparison between intercept and 0

t	0.5845			
ddl		4	t(0,05;4) 2.776	non-significant

→ Intercept different from 0

Symbols		r	Correlation coefficient
N	Number of observations	r^2	Coefficient of determination
k	Number of groups	S^2r	Variance of the correlation coefficient
Sxx	Standard-deviation of x	S^2a	Variance of the intercept
Syy	Standard-deviation of y	S^2b	Variance of the slope
Sxy	Covariance of x and y	F	Fisher F test
S^2xy	Regression variance, Residual variance	t	Student t test
SE b	Error on the slope	dof	Degrees of freedom
a	Intercept of the regression line		x = Cisplatin concentration (mg/L)
b	Slope of the regression line		y = Measured absorbance (mA)

Comparison between the slopes

J1/J2
t	2.61202641	non-significant
t (0,05;8)	2.306	

J1/J3
t	1.66968661	non-significant
t (0,05;8)	2.306	

J2/J3
t	0.91468964	non-significant
t (0,05;8)	2.306	

The three slopes are not significantly different

Comparison between the intercepts

J1/J2
t	0.557267	non-significant
t (0,05;8)	2.306	

J1/J3
t	0.757365	non-significant
t (0,05;8)	2.306	

J2/J3
t	0.125718	non-significant
t (0,05;8)	2.306	

The three intercepts are not significantly different

Mediastinum	Accuracy							
Real concentration of sampled assays				100	75	50	25	10
	Weight assay 1	20.2	mg	0.808	0.606	0.404	0.202	0.0808
	Weight assay 2	20	mg	0.8	0.6	0.4	0.2	0.08
	Weight assay 3	20.1	mg	0.804	0.603	0.402	0.201	0.0804

	x measured	x real (ppb)	Recovery (%)	Variances	Y	yi-Y/	(yi-Y/)²	yi-Y//	(yi-Y//)²
Assay 1-100	803	808	99.38%		99.08%	0.30%	0.0000	-2.23%	0.0005
Assay 2-100	778	800	97.25%		99.08%	-1.83%	0.0003	-4.36%	0.0019
Assay 3-100	809	804	100.62%	0.0003	99.08%	1.54%	0.0002	-0.99%	0.0001
Assay 1-75	571	606	94.22%		102.73%	-8.51%	0.0072	-7.39%	0.0055
Assay 2-75	644	600	107.33%		102.73%	4.60%	0.0021	5.72%	0.0033
Assay 3-75	643	603	106.63%	0.0054	102.73%	3.90%	0.0015	5.02%	0.0025
Assay 1-50	400	404	99.01%		94.68%	4.33%	0.0019	-2.60%	0.0007
Assay 2-50	363	400	90.75%		94.68%	-3.93%	0.0015	-10.86%	0.0118
Assay 3-50	379	402	94.28%	0.0017	94.68%	-0.40%	0.0000	-7.33%	0.0054
Assay 1-25	215	202	106.44%		98.83%	7.61%	0.0058	4.82%	0.0023
Assay 2-25	197	200	98.50%		98.83%	-0.33%	0.0000	-3.11%	0.0010
Assay 3-25	184	201	91.54%	0.0056	98.83%	-7.28%	0.0053	-10.07%	0.0101
Assay 1-10	95	80.8	117.57%		112.74%	4.83%	0.0023	15.96%	0.0255
Assay 2-10	82	80	102.50%		112.74%	-10.24%	0.0105	0.89%	0.0001
Assay 3-10	95	80.4	118.16%	0.0079	112.74%	5.41%	0.0029	16.55%	0.0274
		AVG (%)	101.61%						
N	15	SUM (%)	1524.19%	0.0209	15.2419	0.00%	0.0418	0.00%	0.0980
k	5	STDEV (%)	8.37%						

Cochran C test between groups (Homoscedasticity)

C	0.3774	C < C (0.05;5;2)
C (0.05;5;2)	0.6838	Homoscedasticity of variances between groups is met

Validity of means

Variation	dof	Sum of squares	Variance (%²)	St-dev (%)	CV (%)	F	
Total variation	15	0.0980					
Intra-group variation	10	0.0418	0.0042	0.0646	0.0636	F	3.37
Inter-group variation	4	0.0562	0.0141	0.1186	0.1167	p	0.05
						F (0,05;4;10)	3.48

F < F (0.05;4;10)
Variation of observations between groups are due to experimental errors

Estimation of the mean recovery

Mean recovery (%)	101.61%		
Stdev (%)	8.37%		
N	15		
t (0,05;14)	2.1448		
t*S/√(N) (%)	0.0463279		
CI 95 (%)	96.98%	to	106.25%

Mediastinum — Precision

Concentration (mg/L)	Results SpectrAA			Recovery (%)			(Recovery - Average)			RSD%			
	Day 1	Day 2	Day 3	Day 1	Day 2	Day 3	Day 1	Day 2	Day 3	Day 1	Day 2	Day 3	Average
0.80	0.846	0.819	0.763	105.75%	102.38%	95.38%	4.13%	1.19%	-4.86%				
	0.756	0.815	0.783	94.50%	101.88%	97.88%	-7.12%	0.69%	-2.36%				
	0.807	0.791	0.811	100.88%	98.88%	101.38%	-0.74%	-2.31%	1.14%				
	0.84	0.768	0.812	105.00%	96.00%	101.50%	3.38%	-5.19%	1.26%	5.08%	2.96%	2.99%	3.68%
0.60	0.635	0.591	0.646	105.83%	98.50%	107.67%	4.21%	-2.69%	7.43%				
	0.593	0.62	0.632	98.83%	103.33%	105.33%	-2.79%	2.15%	5.09%				
	0.552	0.587	0.56	92.00%	97.83%	93.33%	-9.62%	-3.35%	-6.91%				
	0.599	0.598	0.644	99.83%	99.67%	107.33%	-1.79%	-1.52%	7.09%	5.72%	2.46%	6.58%	4.92%
0.40	0.408	0.408	0.36	102.00%	102.00%	90.00%	0.38%	0.81%	-10.24%				
	0.408	0.414	0.366	102.00%	103.50%	91.50%	0.38%	2.31%	-8.74%				
	0.407	0.443	0.359	101.75%	110.75%	89.75%	0.13%	9.56%	-10.49%				
	0.413	0.38	0.407	103.25%	95.00%	101.75%	1.63%	-6.19%	1.51%	0.66%	6.28%	6.13%	4.36%
0.20	0.207	0.188	0.175	103.50%	94.00%	87.50%	1.88%	-7.19%	-12.74%				
	0.197	0.197	0.204	98.50%	98.50%	102.00%	-3.12%	-2.69%	1.76%				
	0.194	0.178	0.203	97.00%	89.00%	101.50%	-4.62%	-12.19%	1.26%				
	0.191	0.205	0.192	95.50%	102.50%	96.00%	-6.12%	1.31%	-4.24%	3.52%	6.06%	6.97%	5.52%
0.08	0.091	0.093	0.09	113.75%	116.25%	112.50%	12.13%	15.06%	12.26%				
	0.081	0.081	0.085	101.25%	101.25%	106.25%	-0.37%	0.06%	6.01%				
	0.081	0.089	0.092	101.25%	111.25%	115.00%	-0.37%	10.06%	14.76%				
	0.088	0.081	0.081	110.00%	101.25%	101.25%	8.38%	0.06%	1.01%	5.93%	6.98%	5.71%	6.21%
			Average (%)	101.62%	101.19%	100.24%	0.00%	0.00%	0.00%			RSD% ≤	4.93%
			Standard Deviation (%)	5.10%	6.21%	7.59%	5.10%	6.21%	7.59%				

Variance of repetitions (%²)	0.26%^2	0.39%^2	0.58%^2
St-dev (%)	5.10%	6.21%	7.59%
Variance of repeatability (%²)		1.22%^2	
Average recovery (%)		101.01%	
Average - Average of averages^2 (%^2)	0.00%^2	0.00%^2	0.01%^2

Homogeneity of variances inside groups
Cochran C test inter-days
C 0.47
C (0,05,2,19 0.7164
C < C (0,05,: Homoscedasticity conditions are met

Repeatability error

Average (%)	101.01%
Reproducibility error (%)	1.21%

Mediastinum	LOD/LLOQ	

Assay 4		St weight
		20
N	x (mg/L)	y (mA)
B	0.00	1
St 1	0.80	204
St 2	0.60	159
St 3	0.40	93
St 4	0.20	52
St 5	0.08	24

Slope b	254.148352
Intercept a	0.72857143
R^2	0.99585495

Assay 5		St weight
		20.2
N	x (mg/L)	y (mA)
B	0.00	0
St 1	0.81	191
St 2	0.61	133
St 3	0.40	95
St 4	0.20	49
St 5	0.08	19

Slope b	230.71483
Intercept a	0.38571429
R^2	0.99713945

Assay 6		St weight
		19.7
N	x (mg/L)	y (mA)
B	0.00	0
St 1	0.79	202
St 2	0.59	144
St 3	0.39	104
St 4	0.20	52
St 5	0.08	26

Slope b	249.009873
Intercept a	2.97142857
R^2	0.99745502

Slope b		
	Assay 1	227.602447
	Assay 2	250.70083
	Assay 3	241.17842
	Assay 4	254.148352
	Assay 5	230.71483
	Assay 6	249.009873
	Average slope	242.225792

Blank		
	Assay 1	3
	Assay 2	-3
	Assay 3	-3
	Assay 4	1
	Assay 5	0
	Assay 6	0
	St-dev	2.33809039

LLOQ (mg/L digestate)	0.096525245
LOD (mg/L digestate)	0.032175082

Total Blood (1) Linearity

Assay 1

						St weight
						20.3

N	x (mg/L)	y (mA)	x^2	y^2	xy
B	0.00	0	0.0	0.0	0.0
St 1	0.81	276	0.7	76176.0	224.1
St 2	0.61	205	0.4	42025.0	124.8
St 3	0.41	144	0.2	20736.0	58.5
St 4	0.20	81	0.0	6561.0	16.4
St 5	0.08	33	0.0	1089.0	2.7

Sum	6	2.1	739.0	1.2	146587.0	426.5
Average		0.4	123.2	0.2		

Sxx	0.5	Slope b	333.0266	r	0.998980878
Syy	55566.8	Intercept a	5.985714	r^2	0.997962794
Sxy	166.5				
S^2xy	28.3002747		S^2r	28.30027	
SE b	7.52331461		S^2a	16.44111	
			S^2b	56.60026	

One-sided test on the slope

F	333.027				
dof num.		4	F(0,05;1;4) 7.71	*significant*	
dof denom.		4			
				→ Existence of a slope	

One-sided test on r

t	44.266				
ddl		4	t(0,05;4) 2.776	*significant*	
			→ Existence of a correlation between x and y		

Two-sided comparison between intercept and 0

t	1.4762				
ddl		4	t(0,05;4) 2.776	*non-significant*	
				→ Intercept different from 0	

Assay 2

						St weight
						19.6

N	x (mg/L)	y (mA)	x^2	y^2	xy
B	0.00	2	0.0	4.0	0.0
St 1	0.78	271	0.6	73441.0	212.5
St 2	0.59	211	0.3	44521.0	124.1
St 3	0.39	140	0.2	19600.0	54.9
St 4	0.20	80	0.0	6400.0	15.7
St 5	0.08	35	0.0	1225.0	2.7

Sum	6	2.0	739.0	1.2	145191.0	409.8
Average		0.3	123.2	0.2		

Sxx	0.5	Slope b	340.6313	r	0.999189678
Syy	54170.8	Intercept a	7.442857	r^2	0.998380013
Sxy	158.8				
S^2xy	21.939011		S^2r	21.93901	
SE b	6.86060455		S^2a	12.74552	
			S^2b	47.06789	

One-sided test on the slope

F	340.631				
dof num.		4	F(0,05;1;4) 7.71	*significant*	
dof denom.		4			
				→ Existence of a slope	

One-sided test on r

t	49.650				
ddl		4	t(0,05;4) 2.776	*significant*	
			→ Existence of a correlation between x and y		

Two-sided comparison between intercept and 0

t	2.0848				
ddl		4	t(0,05;4) 2.776	*non-significant*	
				→ Intercept different from 0	

				St weight
				19.9

	N	x (mg/L)	y (mA)	x^2	y^2	xy
	B	0.00	-3	0.0	9.0	0.0
	St 1	0.80	285	0.6	81225.0	226.9
	St 2	0.60	221	0.4	48841.0	131.9
	St 3	0.40	152	0.2	23104.0	60.5
	St 4	0.20	83	0.0	6889.0	16.5
	St 5	0.08	30	0.0	900.0	2.4

Sum	6	2.1	768.0	1.2	160968.0	438.2
Average		0.3	128.0	0.2		
Sxx	0.5		Slope b	360.6494	r	0.99866378
Syy	62664.0		Intercept a	3.6	r^2	0.997329346
Sxy	173.3					
S^2xy	41.8384615			S^2r	41.83846	
SE b	9.33135501			S^2a	24.30615	
				S^2b	87.07419	

One-sided test on the slope

F	360.649				
dof num.	4	F(0,05;1;4)	7.71	significant	
dof denom.	4				
			→ Existence of a slope		

One-sided test on r

t	38.649				
ddl	4	t(0,05;4)	2.776	significant	
		→ Existence of a correlation between x and y			

Two-sided comparison between intercept and 0

t	0.7302				
ddl	4	t(0,05;4)	2.776	non-significant	
		→ Intercept different from 0			

Symbols

N	Number of observations		r	Correlation coefficient
k	Number of groups		r^2	Coefficient of determination
Sxx	Standard-deviation of x		S^2r	Variance of the correlation coefficient
Syy	Standard-deviation of y		S^2a	Variance of the intercept
Sxy	Covariance of x and y		S^2b	Variance of the slope
S^2xy	Regression variance, Residual variance		F	Fisher F test
SE b	Error on the slope		t	Student t test
a	Intercept of the regression line		dof	Degrees of freedom
b	Slope of the regression line			x = Cisplatin concentration (mg/L)
				y = Measured absorbance (mA)

Comparison between the slopes

J1/J2		
t	0.7468975	non-significant
t (0,05;8)	2.306	

J1/J3		
t	2.30450825	non-significant
t (0,05;8)	2.306	

J2/J3		
t	1.72838382	non-significant
t (0,05;8)	2.306	

The three slopes are not significantly different

Comparison between the intercepts

J1/J2		
t	0.269718	non-significant
t (0,05;8)	2.306	

J1/J3		
t	0.37374	non-significant
t (0,05;8)	2.306	

J2/J3		
t	0.631321	non-significant
t (0,05;8)	2.306	

The three intercepts are not significantly different

Total Blood (1) Accuracy

Real concentration of sampled assays				100	75	50	25	10
	Weight assay 1	20.2	mg	0.808	0.606	0.404	0.202	0.0808
	Weight assay 2	20	mg	0.8	0.6	0.4	0.2	0.08
	Weight assay 3	20.1	mg	0.804	0.603	0.402	0.201	0.0804

	x measured	x real (ug/L)	Recovery (%)	Variances	Y	y_i-Y/	$(y_i$-Y/$)^2$	y_i-Y//	$(y_i$-Y//$)^2$
Assay 1-100	799	808	98.89%		97.38%	1.50%	0.0002	2.25%	0.0005
Assay 2-100	772	800	96.50%		97.38%	-0.88%	0.0001	-0.14%	0.0000
Assay 3-100	778	804	96.77%	0.0002	97.38%	-0.62%	0.0000	0.13%	0.0000
Assay 1-75	568	606	93.73%		99.13%	-5.40%	0.0029	-2.91%	0.0008
Assay 2-75	597	600	99.50%		99.13%	0.37%	0.0000	2.86%	0.0008
Assay 3-75	628	603	104.15%	0.0027	99.13%	5.02%	0.0025	7.51%	0.0056
Assay 1-50	441	404	109.16%		97.48%	11.68%	0.0136	12.52%	0.0157
Assay 2-50	366	400	91.50%		97.48%	-5.98%	0.0036	-5.14%	0.0026
Assay 3-50	369	402	91.79%	0.0102	97.48%	-5.69%	0.0032	-4.85%	0.0023
Assay 1-25	184	202	91.09%		101.68%	-10.60%	0.0112	-5.55%	0.0031
Assay 2-25	214	200	107.00%		101.68%	5.32%	0.0028	10.36%	0.0107
Assay 3-25	215	201	106.97%	0.0084	101.68%	5.28%	0.0028	10.33%	0.0107
Assay 1-10	60	80.8	74.26%		87.51%	-13.25%	0.0176	-22.38%	0.0501
Assay 2-10	72	80	90.00%		87.51%	2.49%	0.0006	-6.64%	0.0044
Assay 3-10	79	80.4	98.26%	0.0149	87.51%	10.75%	0.0116	1.62%	0.0003
		AVG (%)	96.64%						
N	15	SUM (%)	1449.55%	0.0364	14.4955	0.00%	0.0728	0.00%	0.1077
k	5	STDEV (%)	8.77%						

Cochran C test between groups (Homoscedasticity)

C	0.4084
C (0.05;5;2)	0.6838

C < C (0.05;5;2)
Homoscedasticity of variances between groups is met

Validity of means

Variation	dof	Sum of square	Variance (%^{2})	St-dev (%)	CV (%)	F	
Total variation	15	0.1077					
Intra-group variation	10	0.0728	0.0073	0.0853	0.0883	F	1.20
Inter-group variation	4	0.0349	0.0087	0.0934	0.0967	p	0.37
						F (0,05;4;10)	3.48

F < F (0.05;4;10)
Variation of observations between groups are due to experimental errors

Estimation of the mean recovery

Mean recovery (%)	96.64%		
Stdev (%)	8.77%		
N	15		
t (0,05;14)	2.1448		
t*S/√(N) (%)	0.04857537		
CI 95 (%)	91.78%	to	101.49%

Total Blood (1) Precision

Concentration (mg/L)	Results SpectrAA			Recovery (%)			(Recovery - Average)			RSD%			
	Day 1	Day 2	Day 3	Day 1	Day 2	Day 3	Day 1	Day 2	Day 3	Day 1	Day 2	Day 3	Average
0.80	0.771	0.831	0.816	96.38%	103.88%	102.00%	-3.35%	1.41%	4.10%				
	0.756	0.788	0.782	94.50%	98.50%	97.75%	-5.23%	-3.97%	-0.15%				
	0.763	0.752	0.844	95.38%	94.00%	105.50%	-4.35%	-8.47%	7.60%				
	0.828	0.84	0.791	103.50%	105.00%	98.88%	3.77%	2.53%	0.97%	4.22%	5.07%	3.44%	4.25%
0.60	0.57	0.605	0.61	95.00%	100.83%	101.67%	-4.73%	-1.64%	3.76%				
	0.627	0.63	0.584	104.50%	105.00%	97.33%	4.77%	2.53%	-0.57%				
	0.591	0.554	0.65	98.50%	92.33%	108.33%	-1.23%	-10.14%	10.43%				
	0.572	0.602	0.623	95.33%	100.33%	103.83%	-4.40%	-2.14%	5.93%	4.48%	5.31%	4.45%	4.75%
0.40	0.361	0.448	0.404	90.25%	112.00%	101.00%	-9.48%	9.53%	3.10%				
	0.361	0.413	0.422	90.25%	103.25%	105.50%	-9.48%	0.78%	7.60%				
	0.398	0.406	0.426	99.50%	101.50%	106.50%	-0.23%	-0.97%	8.60%				
	0.354	0.421	0.407	88.50%	105.25%	101.75%	-11.23%	2.78%	3.85%	5.41%	4.36%	2.62%	4.13%
0.20	0.192	0.217	0.21	96.00%	108.50%	105.00%	-3.73%	6.03%	7.10%				
	0.214	0.202	0.21	107.00%	101.00%	105.00%	7.27%	-1.47%	7.10%				
	0.2	0.211	0.193	100.00%	105.50%	96.50%	0.27%	3.03%	-1.40%				
	0.2	0.2	0.183	100.00%	100.00%	91.50%	0.27%	-2.47%	-6.40%	4.54%	3.83%	6.70%	5.02%
0.08	0.094	0.084	0.07	117.50%	105.00%	87.50%	17.77%	2.53%	-10.40%				
	0.09	0.09	0.065	112.50%	112.50%	81.25%	12.77%	10.03%	-16.65%				
	0.082	0.078	0.063	102.50%	97.50%	78.75%	2.77%	-4.97%	-19.15%				
	0.086	0.078	0.066	107.50%	97.50%	82.50%	7.77%	-4.97%	-15.40%	5.87%	6.96%	4.46%	5.76%
	Average (%)			99.73%	102.47%	97.90%	0.00%	0.00%	0.00%			RSD% ≤	4.78%
	Standard Deviation (%)			7.46%	5.24%	8.95%	7.46%	5.24%	8.95%				

Variance of repetitions ($\%^2$)	0.56%^2	0.28%^2	0.80%^2
St-dev (%)	7.46%	5.24%	8.95%
Variance of repetability ($\%^2$)	1.63%^2		
Average recovery (%)	100.03%		
Average - Average of averages^2 ($\%^2$)	0.00%^2	0.06%^2	0.05%^2

Homogeneity of variances inside groups
Cochran C test inter-days
C 0.49
C (0,05,2,19 0.7164

C < C (0,05,;Homoscedasticity conditions are met

Repetability error	
Average (%)	100.03%
Reproducibility error (%)	1.63%

Total Blood (1) | LOD/LLOQ

Assay 4

		St weight
		20

N	x (mg/L)	y (mA)
B	0.00	0
St 1	0.80	276
St 2	0.60	215
St 3	0.40	147
St 4	0.20	80
St 5	0.08	30

Slope b	345.521978
Intercept a	4.88571429
R^2	0.99797447

Assay 5

		St weight
		20.2

N	x (mg/L)	y (mA)
B	0.00	3
St 1	0.81	271
St 2	0.61	209
St 3	0.40	140
St 4	0.20	82
St 5	0.08	34

Slope b	328.718311
Intercept a	8.07142857
R^2	0.99825192

Assay 6

		St weight
		19.7

N	x (mg/L)	y (mA)
B	0.00	5
St 1	0.79	285
St 2	0.59	208
St 3	0.39	144
St 4	0.20	84
St 5	0.08	36

Slope b	347.074246
Intercept a	8.48571429
R^2	0.9981481

Slope b		
	Assay 1	333.026579
	Assay 2	340.631307
	Assay 3	360.649401
	Assay 4	345.521978
	Assay 5	328.718311
	Assay 6	347.074246
	Average slope	342.603637

Blank		
	Assay 1	0
	Assay 2	2
	Assay 3	-3
	Assay 4	0
	Assay 5	3
	Assay 6	5
	St-dev	2.786874

LLOQ (mg/L digestate)	0.08134397
LOD (mg/L digestate)	0.027114657

Total Blood (B') Linearity

Assay 1

					St weight
					20

N	x (mg/L)	y (mA)	x^2	y^2	xy
B	0.00	9	0.0	81.0	0.0
St 1	0.25	180	0.1	32400.0	45.0
St 2	0.19	133	0.0	17689.0	24.9
St 3	0.13	88	0.0	7744.0	11.0
St 4	0.06	50	0.0	2500.0	3.1
St 5	0.03	30	0.0	900.0	0.8

Sum	6	0.7	490.0	0.1	61314.0	84.8
Average		0.1	81.7	0.0		

Sxx	0.0	Slope b	669.4505	r	0.99867912
Syy	21297.3	Intercept a	9.142857	r^2	0.997359985
Sxy	31.7				
S^2xy	14.0563187		S^2r	14.05632	
SE b	17.2212914		S^2a	8.166052	
			S^2b	296.5729	

One-sided test on the slope

F	669.451				
dof num.		4	$F(0,05;1;4)$ 7.71		significant
dof denom.		4			
			→ Existence of a slope		

One-sided test on r

t	38.873				
ddl		4	$t(0,05;4)$ 2.776		significant
		→ Existence of a correlation between x and y			

Two-sided comparison between intercept and 0

t	3.1995				
ddl		4	$t(0,05;4)$ 2.776		significant
		→ Intercept not different from 0			

Assay 2

					St weight
					20

N	x (mg/L)	y (mA)	x^2	y^2	xy
B	0.00	10	0.0	100.0	0.0
St 1	0.25	179	0.1	32041.0	44.8
St 2	0.19	141	0.0	19881.0	26.4
St 3	0.13	91	0.0	8281.0	11.4
St 4	0.06	61	0.0	3721.0	3.8
St 5	0.03	27	0.0	729.0	0.7

Sum	6	0.7	509.0	0.1	64753.0	87.1
Average		0.1	84.8	0.0		

Sxx	0.0	Slope b	673.2308	r	0.997884885
Syy	21572.8	Intercept a	11.9	r^2	0.995774244
Sxy	31.9				
S^2xy	22.7903846		S^2r	22.79038	
SE b	21.9283394		S^2a	13.24013	
			S^2b	480.8521	

One-sided test on the slope

F	673.231				
dof num.		4	$F(0,05;1;4)$ 7.71		significant
dof denom.		4			
			→ Existence of a slope		

One-sided test on r

t	30.701				
ddl		4	$t(0,05;4)$ 2.776		significant
		→ Existence of a correlation between x and y			

Two-sided comparison between intercept and 0

t	3.2704				
ddl		4	$t(0,05;4)$ 2.776		significant
		→ Intercept not different from 0			

Assay 3

	St weight
	20

	N	x (mg/L)	y (mA)	x^2	y^2	xy
B		0.00	10	0.0	100.0	0.0
St 1		0.25	177	0.1	31329.0	44.3
St 2		0.19	126	0.0	15876.0	23.6
St 3		0.13	91	0.0	8281.0	11.4
St 4		0.06	43	0.0	1849.0	2.7
St 5		0.03	22	0.0	484.0	0.6

Sum	6	0.7	469.0	0.1	57919.0	82.5
Average		0.1	78.2	0.0		

Sxx	0.0	Slope b	668.3956	r	0.998007841
Syy	21258.8	Intercept a	5.757143	r^2	0.996019651
Sxy	31.7				
S^2xy	21.1543956		S^2r	21.1544	
SE b	21.1266301		S^2a	12.2897	
			S^2b	446.3345	

One-sided test on the slope

F	668.396				
dof num.		4	F(0,05;1;4)	7.71	*significant*
dof denom.		4			

→ Existence of a slope

One-sided test on r

t	31.638				
ddl		4	t(0,05;4)	2.776	*significant*

→ Existence of a correlation between x and y

Two-sided comparison between intercept and 0

t	1.6422				
ddl		4	t(0,05;4)	2.776	*non-significant*

→ Intercept different from 0

Symbols				
N	Number of observations	r	Correlation coefficient	
k	Number of groups	r^2	Coefficient of determination	
Sxx	Standard-deviation of x	S^2r	Variance of the correlation coefficient	
Syy	Standard-deviation of y	S^2a	Variance of the intercept	
Sxy	Covariance of x and y	S^2b	Variance of the slope	
S^2xy	Regression variance, Residual variance	F	Fisher F test	
SE b	Error on the slope	t	Student t test	
a	Intercept of the regression line	dof	Degrees of freedom	
b	Slope of the regression line		x = Cisplatin concentration (mg/L)	
			y = Measured absorbance (mA)	

Comparison between the slopes

J1/J2			
t	0.13557756	*non-significant*	
t (0,05;8)	2.306		

J1/J3			
t	0.03870459	*non-significant*	
t (0,05;8)	2.306		

J2/J3			
t	0.15879167	*non-significant*	
t (0,05;8)	2.306		

The three slopes are not significantly different

Comparison between the intercepts

J1/J2			
t	0.595922	*non-significant*	
t (0,05;8)	2.306		

J1/J3			
t	0.748588	*non-significant*	
t (0,05;8)	2.306		

J2/J3			
t	1.215756	*non-significant*	
t (0,05;8)	2.306		

The three intercepts are not significantly different

Total Blood (B') — Accuracy

Real concentration of sampled assays			100	75	50	25	10
	Weight assay 1	20 mg	0.25	0.1875	0.125	0.0625	0.025
	Weight assay 2	20 mg	0.25	0.1875	0.125	0.0625	0.025
	Weight assay 3	20 mg	0.25	0.1875	0.125	0.0625	0.025

	x measured	x real (ppb)	Recovery (%)	Variances	Y	yi-Y/	$(yi-Y/)^2$	yi-Y//	$(yi-Y//)^2$
Assay 1-100	280	250	112.00%		96.13%	15.87%	0.0252	9.59%	0.0092
Assay 2-100	216	250	86.40%		96.13%	-9.73%	0.0095	-16.01%	0.0256
Assay 3-100	225	250	90.00%	0.0192	96.13%	-6.13%	0.0038	-12.41%	0.0154
Assay 1-75	201	187.5	107.20%		109.51%	-2.31%	0.0005	4.79%	0.0023
Assay 2-75	215	187.5	114.67%		109.51%	5.16%	0.0027	12.26%	0.0150
Assay 3-75	200	187.5	106.67%	0.0020	109.51%	-2.84%	0.0008	4.26%	0.0018
Assay 1-50	141	125	112.80%		100.53%	12.27%	0.0150	10.39%	0.0108
Assay 2-50	106	125	84.80%		100.53%	-15.73%	0.0248	-17.61%	0.0310
Assay 3-50	130	125	104.00%	0.0205	100.53%	3.47%	0.0012	1.59%	0.0003
Assay 1-25	70	62.5	112.00%		107.20%	4.80%	0.0023	9.59%	0.0092
Assay 2-25	71	62.5	113.60%		107.20%	6.40%	0.0041	11.19%	0.0125
Assay 3-25	60	62.5	96.00%	0.0095	107.20%	-11.20%	0.0125	-6.41%	0.0041
Assay 1-10	30	25	120.00%		98.67%	21.33%	0.0455	17.59%	0.0309
Assay 2-10	21	25	84.00%		98.67%	-14.67%	0.0215	-18.41%	0.0339
Assay 3-10	23	25	92.00%	0.0357	98.67%	-6.67%	0.0044	-10.41%	0.0108
		AVG (%)	102.41%						
N	15	SUM (%)	1536.13%	0.0869	15.3613	0.00%	0.1738	0.00%	0.2129
k	5	STDEV (%)	12.33%						

Cochran C test between groups (Homoscedasticity)

C	0.4111
C (0.05;5;2)	0.6838

C < C (0.05;5;2)
Homoscedasticity of variances between groups is met

Validity of means

Variation	dof	Sum of squares	Variance ($\%^2$)	St-dev (%)	CV (%)	F	
Total variation	15	0.2129					
Intra-group variation	10	0.1738	0.0174	0.1318	0.1287	F	0.56
Inter-group variation	4	0.0391	0.0098	0.0989	0.0965	p	0.70
						F (0,05;4;10)	3.48

F < F (0.05;4;10)
Variation of observations between groups are due to experimental errors

Estimation of the mean recovery

Mean recovery (%)	102.41%		
Stdev (%)	12.33%		
N	15		
t (0,05;14)	2.1448		
t*S/√(N) (%)	0.06829371		
CI 95 (%)	95.58%	to	109.24%

Total Blood (B') Precision

Concentration (mg/L)	Results SpectrAA Day 1		Recovery (%) Day 1		(Recovery - Average) Day 1		RSD% Day 1	RSD% Average
0.250	0.275		110.00%		7.40%		5.55%	5.55%
	0.281		112.40%		9.80%			
	0.255		102.00%		-0.60%			
	0.251		100.40%		-2.20%			
0.188	0.2		106.67%		4.07%		10.82%	10.82%
	0.215		114.67%		12.07%			
	0.205		109.33%		6.73%			
	0.166		88.53%		-14.07%			
0.125	0.114		91.20%		-11.40%		10.25%	10.25%
	0.143		114.40%		11.80%			
	0.14		112.00%		9.40%			
	0.126		100.80%		-1.80%			
0.063	0.06		96.00%		-6.60%		6.83%	6.83%
	0.065		104.00%		1.40%			
	0.055		88.00%		-14.60%			
	0.061		97.60%		-5.00%			
0.025	0.03		120.00%		17.40%		19.77%	19.77%
	0.029		116.00%		13.40%			
	0.022		88.00%		-14.60%			
	0.02		80.00%		-22.60%			
	Average (%)		102.60%		0.00%		RSD% ≤	10.64%
	Standard Deviation (%)		11.27%		11.27%			

Variance of repetitions (%²)	1.27%^2
St-dev (%)	11.27%
Variance of repetability (%²)	1.27%^2
Average recovery (%)	102.60%
Average - Average of averages^2 (%^2)	0.00%^2

Homogeneity of variances inside groups
Cochran C test inter-days
C =
C (0,05,2,19 0.7164

C < C (0,05,;Homoscedasticity conditions are met

Repetability error

Average (%)	102.60%
Reproducibility error (%)	1.24%

Total Blood (B')   LOD/LLOQ

Assay 4

		St weight
		20

N	x (mg/L)	y (mA)
B	0.000	7
St 1	0.250	181
St 2	0.188	133
St 3	0.125	88
St 4	0.063	50
St 5	0.025	30

Slope b	677.010989
Intercept a	8.15714286
R^2	0.99697515

Assay 5

		St weight
		20

N	x (mg/L)	y (mA)
B	0.000	7
St 1	0.250	201
St 2	0.188	141
St 3	0.125	99
St 4	0.063	55
St 5	0.025	33

Slope b	743.912088
Intercept a	8.74285714
R^2	0.99490835

Assay 6

		St weight
		20

N	x (mg/L)	y (mA)
B	0.000	6
St 1	0.250	177
St 2	0.188	131
St 3	0.125	84
St 4	0.063	51
St 5	0.025	31

Slope b	659.868132
Intercept a	8.51428571
R^2	0.99486

Slope b		
	Assay 1	669.450549
	Assay 2	673.230769
	Assay 3	668.395604
	Assay 4	677.010989
	Assay 5	743.912088
	Assay 6	659.868132
	Average slope	681.978022

Blank		
	Assay 1	9
	Assay 2	10
	Assay 3	10
	Assay 4	7
	Assay 5	7
	Assay 6	6
	St-dev	1.72240142

LLOQ (mg/L digestate)	0.025255967
LOD (mg/L digestate)	0.008418656

2. Abstract and Poster at Respiratory Drug Delivery (RDD) Conference 2016, Phoenix AZ, USA. April 17-21 2016.
"Development of Cisplatin-based Dry Powder for Inhalation with Controlled Release Properties for the Lung Cancer Therapy"

Levet V., Amighi K., Wauthoz N.

This abstract was peer-reviewed and published in RDD Online and in the Conference book. It is a shortened version of the work presented in Article 1.

Development of Cisplatin-based Dry Powder for Inhalation with Controlled Release Properties for the Lung Cancer Therapy

Vincent Levet, Karim Amighi,
and Nathalie Wauthoz

*Laboratory of Pharmaceutics and Biopharmaceutics,
Université Libre de Bruxelles (ULB),
Brussels, Belgium*

KEYWORDS: dry powder for inhalation (DPI), lipid microparticles,
spray drying, high-pressure homogenization, controlled-release,
chemotherapy

INTRODUCTION

Lung cancer was the attributed cause of 1.6 million deaths worldwide in 2012, making it the leading cause of death by cancer – 19.4% of the cancer morbidity – and a very prominent research matter [1]. Cisplatin is a key drug in the chemotherapy regimen for lung cancer patients. It is currently administered intravenously (IV) by slow diffusion (30 to 100 mg/m^2) with high hydration to prevent cumulative renal adverse effects. The delivery of cisplatin directly to the lung as an adjuvant treatment could increase the drug concentrations at the site of action and reduce acute and chronic systemic exposure. Because it is slightly soluble in water (<1 g/L), highly reactive, and hydrolyzes without high chloride concentrations [2], dry powder for inhalation (DPI) seem to be the best formulation strategy for the administration of cisplatin to the lungs. A controlled-release formulation for pulmonary delivery could also limit peak concentrations and acute exposure while maintaining high efficacy through long-acting release at the site of action. Therefore, DPI formulations of cisplatin microparticles embedded in lipids were investigated to modulate dissolution properties.

MATERIALS AND METHODS

The compositions of the DPI formulations are presented in Table 1.

Table 1.

Theoretical composition of produced DPIs.

DPI	Cisplatin / Lipid ratio	Lipid composition (%)		
		Tristearin	TPGS[1]	DSPE-PEG[2]
F0	100:0	-	-	-
F1	95:5	-	5.0	-
F2	75:25	100.0	-	-
F3	50:50	100.0	-	-
F4	50:50	99.0	1.0	-
F5	50:50	99.5	-	0.5

[1]D-alpha-tocopheryl PEG-1000, [2]distearoylphosphoethanolamine-PEG-2000

An isopropanol (IPA) suspension of 5% w/v cisplatin was first subjected to high-shear and high-pressure homogenization (HPH) using a lab-scale Emulsiflex C5 (Avestin, Canada) during pre-milling cycles (10 cycles at 5 000 psi and 10 000 psi) and 20 high-pressure milling cycles at 20 000 psi. The lipid excipients dissolved in heated IPA (65°C) were then added to the cisplatin suspension, to obtain 2% w/v in total of material in IPA. The suspension was then spray-dried with a Mini-spray Dryer® B-290 (Büchi Labortechnik AG, Switzerland) at 70°C inlet temperature (resulting in 40 ± 2°C of outlet temperature), 800 L/min spraying airflow, 35 m³/h drying gas flow, 3.0 g/min feed rate, with a 0.7 mm binary nozzle.

Geometric particle size distribution (PSD) of cisplatin suspension and DPIs were characterized by laser diffraction using a Mastersizer® 3000. (Malvern Instruments, UK) Aerodynamic properties of DPIs were evaluated by impaction with a Axahaler® (SMB S.A., Belgium) connected to a Multi-Stage Liquid Impinger ((MsLI) Copley, UK) at 100 L/min for 2.4 seconds, with a loaded mass of 20 mg in a size 3 HPMC capsule (Qualicaps, USA). Dissolution profiles of cisplatin were assessed in sink conditions in 400 mL of modified simulated lung fluid (mSLF) [3] from the respirable fraction ($d_{aer} \leq 5$ µm) obtained through impaction on a 0.45 µm hydrophobic PTFE Fluoropore filter (Merck-Millipore, Germany) using the fast screening impactor ((FSI) Copley, UK) at 100 L/min during 2.4 seconds. The Fluoropore filter was then covered with a 0.4 µm hydrophilic polycarbonate filter (Merck-Milipore, Germany) and fixed onto a watchglass/ PTFE assembly (Copley, UK). The formed sealed disk assembly was then submerged in mSLF contained in a dissolution vessel (paddle apparatus) for dissolution testing at 37°C at 50 rpm. An equivalent-mass of 3 mg cisplatin was deposited by impaction on the hydrophobic filter for each dissolution test. Cisplatin was quantified throughout experiments with a validated electrothermic atomic absorption spectrometry method.

RESULTS AND DISCUSSION

Bulk cisplatin was reduced from a d(0.5) of 17 µm to 0.89 µm and a d(0.9) of 37 µm to 1.8 µm during size-reduction by HPH (Table 2). All the formulated powders (Table 2) had a d(0.5) under 6 µm. Compared to F0, PSD was increased for F1, probably because of some aggregation in the sample due to the presence of TPGS. For all the cisplatin lipid microparticle formulations (F2-F6), d(0.5) ranged from 3 µm to 6 µm (Table 2).

<div align="center">Table 2.</div>

PSD of cisplatin particles during size-reduction and DPIs after redispersion, aerodynamic performances characterized by fine particle fraction (FPF) which is expressed as a percentage of recovered dose and mass median aerodynamic diameter (MMAD) of DPIs (mean ± SD, n=3).

	d(0.5) (µm)	d(0.9) (µm)	FPF (%)	MMAD (µm)
Raw powder	**16.5 ± 3.6**	**36.6 ± 8.3**	**4.2 ± 2.1**	**6.6 ± 1.4**
After HPH	**0.89 ± 0.01**	**1.8 ± 0.1**	**N.A.**	**N.A.**
F0	**1.6 ± 0.0**	**2.9 ± 0.0**	24.2 ± 6.3	2.0 ± 0.2
F1	**2.1 ± 0.0**	**4.7 ± 0.0**	51.5 ± 2.9	2.5 ± 0.3
F2	**4.8 ± 1.4**	**17.4 ± 7.8**	51.9 ± 4.0	2.3 ± 0.2
F3	**5.7 ± 0.2**	**44.4 ± 9.2**	50.1 ± 5.1	2.2 ± 0.3
F4	**4.2 ± 0.2**	**7.5 ± 0.4**	37.3 ± 2.0	2.4 ± 0.2
F5	**3.1 ± 0.0**	**5.2 ± 0.0**	50.3 ± 5.8	2.3 ± 0.7

N.A.: not applicable

A two-fold deposition increase was observed for F1 in comparison to F0 (FPF of 52% vs. 24%) because of its 5% TPGS content, which helped to reduce particle interaction with the capsule and the device. Cisplatin lipid microparticle-based DPIs (F2-F5) showed high FPFs ranging from 37-52% with a high drug-to-lipid ratio (≥ 50%), which enables delivery of high doses with controlled release properties.

Considering the dissolution properties of DPIs (Figure 1), F0 and F1 were rapidly dissolved (85% in less than five minutes). Dissolution of DPIs comprised of a tristearin-only matrix (F2, F3) was slowed with a limited burst-effect, which was lower with a higher lipid loading (F3), as only 52% and 39% were dissolved after one hour to reach 81% and 79% after 24 hours, respectively. The addition of TPGS or DPSE-PEG at 1% and 0.5% decreased the burst-effect – 29% and 24% were dissolved after one hour – and the dissolution was slowed with 55% and 56% dissolved after 24 hours, respectively. This could be explained by a better encapsulation around microcrystals during atomization thanks to the surface active effect of both excipients.
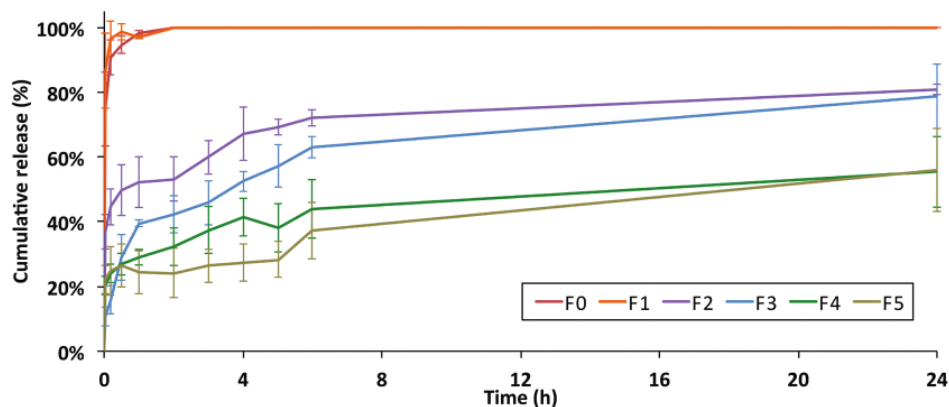

Figure 1. *In vitro* release profiles of cisplatin from DPIs.

CONCLUSION

Immediate-release and controlled-released cisplatin DPIs were successfully produced and characterized *in vitro* for deposition and dissolution. Lipid microparticles comprising tristearin proved to be a good approach to slow the dissolution of cisplatin for more than 24 hours while maintaining good aerodynamic performance for inhalation purposes. The addition of PEGylated excipients further prolonged *in vitro* release while maintaining aerosol properties.

REFERENCES

1. IARC CancerBase. [http://globocan.iarc.fr]. Accessed November 11, 2015.

2. Berners-Price SJ, Appleton TG: The chemistry of cisplatin in aqueous solution. In *Platinum-Based Drugs in Cancer Therapy*. Humana Press; Totowa, NJ: 2000: 3-35.

3. Son YJ, Horng M, Copley M, McConville JT: Optimization of an *in vitro* dissolution test method for inhalation formulation. *Dissolution Technologies* 2010, 17(2): 6-14.

Development of Cisplatin-based Dry Powder for Inhalation with Controlled Release properties for the Lung Cancer Therapy

Vincent Levet*, Karim Amighi, Nathalie Wauthoz

Laboratory of Pharmaceutics and Biopharmaceutics, Faculty of Pharmacy, Université libre de Bruxelles (ULB), Brussels, Belgium. *vlevet@ulb.ac.be.

INTRODUCTION

Cisplatin, the main component of the platinum doublet chemotherapy against lung cancer, is currently administered by **slow I.V. infusion** and **high hydration** due to its **acute** and **cumulative dose-limiting nephrotoxicity**. Pulmonary administration could overcome these issues by lowering **systemic toxicity** while **increasing exposure** at the site of action and in local lymph node to **enhance efficacy** and **limit cancer recurrence**.

Usual IV doses: 30-100 mg/m²
- Stage-dependent
- Once a week & 3 weeks / cycle
- High toxicity
- Long administration time

→

Lung target doses: 5-20 mg
- Lowered systemic toxicity
- Higher local dose
- More frequent administration
- Faster administration time

Cisplatin-based **Dry Powder for inhalation (DPI)** with **high lung deposition** and **controlled-release** using well-tolerated lipids such as **Tristearin (TS)** and **PEGylated excipients** such as D-alpha-tocopheryl PEG-1000 (**TPGS**) or disteroyl-phosphoethanolamine-PEG-2000 (**DSPE-PEG**) could help lower peak concentration, inflammatory reactions and drug clearance by macrophages.

DPI PRODUCTION

Bulk cisplatin was reduced to a low micrometer range in isopropanol dispersion by **High Pressure** and **High Speed Homogenizing** (HPH) for 10 cycles at 5 000 psi and 10 000 psi and 20 cycles at 20 000 psi.

DPI were obtained by **spray-drying** of cisplatin alone or with a matrix based on **TS, TPGS** or **DSPE-PEG**, previously solubilized in heated isopropanol (Table 1). Drug-content in DPI was established with a SpectrAA 300® Atomic Absorption Spectrometer (Varian, Australia).

Table 1. Theoretical composition of cisplatin-based DPI formulations after spray-drying and established drug content.

DPI	Cisplatin / Lipid ratio	Matrix composition (%) TS	TPGS	DSPE-PEG	Drug content (% w/w)
F0	100:0	-	-	-	101.0 ± 2.0
F1	95:5	-	5.0	-	95.6 ± 2.6
F2	75:25	100.0	-	-	77.7 ± 3.1
F3	50:50	100.0	-	-	48.5 ± 2.2
F4	50:50	99.0	1.0	-	48.9 ± 2.3
F5	50:50	99.5	-	0.5	49.9 ± 2.7

THERMAL PROPERTIES

Differential Scanning Calorimetry (DSC) showed that TS-comprising DPI (**F2, F3, F4, F5**) were spray-dried directly in **the most stable ß form**. TPGS and DSPE-PEG (**F4, F5**) did not alter the ß polymorph of TS in the lipid matrix (Figure 1).
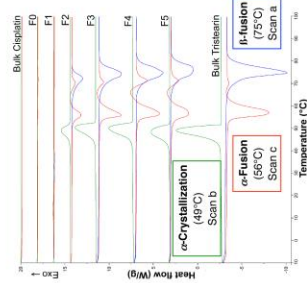

Figure 1. DSC heating and cooling curves of bulk products and DPI formulations obtained with a DSC 2000® (TA Instruments, USA) at 10°C/min: scan a (-10 → 180°C), scan b (180 → -10°C), scan c (-10 → 180°C).

RESULTS

GEOMETRIC SIZE & AERODYNAMIC PERFORMANCES

Size-reduction was able to produce small cisplatin microcrystals in a low micrometer range below 1 µm (Table 2).

Spray-drying provided small particles with a d(0.5) under 5.7 µm (Table 2). Overall yield was 47%.

Highly enhanced Fine Particle Fraction (FPF) (Figure 2) compared to solely reduced cisplatin (**F0**) were obtained with the addition of:
- A limited 5% w/w TPGS addition (**F1**)
- A lipid matrix based on TS only (**F2, F3**)
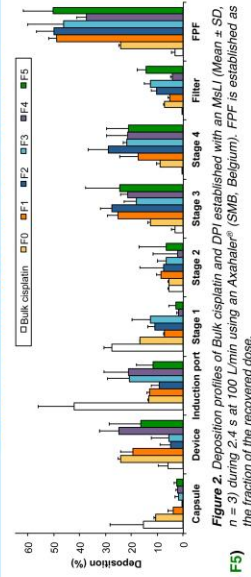- Or associated with PEGylated excipients (**F4, F5**)

Figure 2. Deposition profiles of Bulk cisplatin and DPI established with an MsLI (Mean ± SD, n = 3) during 2.4 s at 100 L/min using an Axahaler® (SMB, Belgium). FPF is established as the fraction of the recovered dose.

Table 2. Geometric (d(0.5)) and Aerodynamic (MMAD) median mass diameters of Bulk cisplatin, reduced cisplatin and of DPI. d(0.5) was established with a Mastersizer 3000® (Malvern, UK). Aerodynamic features were established as described for Figure 2. Fine Particle Dose (FPD) is the cisplatin dose related to a 20 mg DPI-filled capsule (Mean ± SD, n = 3).

Formulation	d(0.5) (µm)	MMAD (µm)	FPD (mg)
Bulk cisplatin	16.5 ± 3.6	6.6 ± 1.4	0.8 ± 0.4
After HPH	0.89 ± 0.01	-	-
F0	1.6 ± 0.0	2.0 ± 0.2	4.9 ± 1.3
F1	2.1 ± 0.0	2.5 ± 0.3	9.8 ± 0.5
F2	4.8 ± 1.4	2.3 ± 0.2	7.8 ± 0.8
F3	5.7 ± 0.2	2.2 ± 0.3	4.5 ± 0.7
F4	4.2 ± 0.2	2.4 ± 0.2	3.6 ± 0.2
F5	3.1 ± 0.0	2.3 ± 0.7	5.0 ± 0.6

DISSOLUTION PROFILES

Dissolution method: USP Apparatus 2 *"Paddle over disk"* adapted method (Figure 3), using a Fast Screening Impactor (FSI™, Copley, UK) during 2.4 s at 100 L/min, in modified Simulated Lung Fluid (mSLF) at 37°C, 50 rpm, pH 7.35 [1].
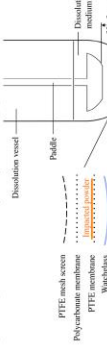

Figure 3. Watchglass disk-assembly (Copley, UK) dissolution apparatus adapted for DPI.

Immediate-release with 85% cisplatin released in **less than 5 min.** was observable with **F0** (100% w/w reduced cisplatin) and **F1** (5% w/w TPGS addition) as shown in Figure 4.

Controlled-release with 81% and 79% cisplatin released after **24 h** was obtained with a low 25 and 50% w/w TS matrix (**F2, F3**). It was reduced to 55 and 56% after 24h in presence of PEGylated excipients in the TS matrix (**F4, F5**) as shown in Figure 4.

Burst-effect was also lowered by the addition of small amounts of PEGylated excipients in the lipid matrix with 29 and 24% **dissolved after 1h** (**F4, F5**) vs. 52 and 39% (**F2, F3**) without (Figure 4), probably because they promoted a better organization of the lipid component around cisplatin microcrystals.
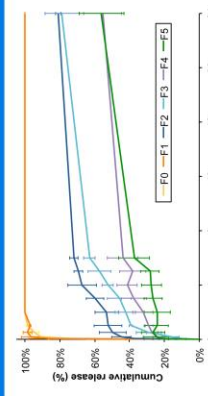

Figure 4. In vitro release profiles of cisplatin from DPI (Mean ± SD, n = 3) established with an USP apparatus 2 adapted method for DPI in mSLF.

CONCLUSION

Size-reduction and spray-drying of cisplatin were proven as being **effective methods** for the production of DPI with **good aerosolization properties** and high FPF values, altogether with FPD compatible with lung cancer therapy. The addition of about 50% TS and PEGylated excipients as a lipid matrix promoted cisplatin **controlled-release over more than 24 h** and limited **burst-effect** with good potential stability. The "stealth" properties of DPI will now have to be assessed *in vitro*, along with their tolerance and efficacy *in vivo*.

[1] Son YJ, et al. Dissolut Technol 2010, 17(2): 6-14.

3. Abstract and Poster at Drug Delivery to the Lungs (DDL 27) Conference 2016, Edinburgh, Scotland, UK. December 7-9, 2016.
"Development of Cisplatin-based Dry Powder for Inhalation with Controlled Release Properties for the Lung Cancer Therapy"

This abstract was peer-reviewed and is to be published in the Journal of Aerosol Medicine and Pulmonary Drug Delivery. The poster was peer-reviewed and presented at the DDL27 conference. It contains a shortened version of the work presented in Article 2.

Local and systemic pharmacokinetic evaluation of immediate-release and controlled-release cisplatin dry powders for inhalation against lung cancer

Vincent Levet, Rémi Rosière, Karim Amighi & Nathalie Wauthoz

Laboratory of Pharmaceutics and Biopharmaceutics, Faculty of Pharmacy, Université libre de Bruxelles (ULB), CP 207, Boulevard du Triomphe, 1050 Brussels, Belgium

Summary

Immediate-release and controlled-release cisplatin dry powder formulations based on solid-lipid microparticles (SLMs) with high drug-content (≥ 50%) and exhibiting high deposition abilities *in vitro* (fine particle fractions (FPF) between 37% and 52%), were produced by high-pressure homogenization and spray-drying using tristearin and polyethylene glycol (1000) tocopheryl-vitamin E succinate[1]. Dry powder blends (DPB) were realized using a spray-dried Mannitol:L-Leucine (10:1) diluent and mixed with the formulations for accurate and reliable administration to mice. DPB were characterized by their drug-content, uniformity of content, recovered mass, recovered cisplatin and particle size distribution by laser diffraction with a Malvern Spraytec® through the actuation of a Penn-Century Dry Powder Insufflator™ model DP-4M for mouse. All but one of the DPB were able to be reliably delivered *in vitro*. The local and systemic pharmacokinetic distributions of cisplatin from formulations were then evaluated *in vivo* in CD-1 mice *vs*. IV and *vs*. a nebulized cisplatin aqueous solution. Quantification of platinum (Pt) content in organs was realized using validated methods by electrothermal atomic absorption spectrometry (ETAAS) in lungs, kidneys, liver, spleen, mediastinum and total blood of mice after a single 1.25 mg/kg administration and dosed over 48 hours. It showed (1) that the inhaled route could effectively lower systemic exposure while increasing lung exposure when compared to IV, (2) that immediate-release formulations were very quickly absorbed in the lungs and (3) that controlled-release formulations promoted higher total exposure in the lungs, but that the presence of PEGylated excipient was needed to avoid active and fast elimination of particles from the lungs.

Introduction

Non-small cell lung cancer (NSCLC) accounts for 1.6 million deaths per year and has a very poor prognosis at advanced stages, with one of the lowest 5-year survival rates of all cancers[2]. Treatment includes combinations of surgery, radiotherapy and chemotherapy, depending on the stage of the disease. Cisplatin is one of the most potent and the most employed anti-cancer drug against various cancers and is the principal constituent of doublet chemotherapy against NSCLC[3]. It is currently only administered by IV infusion with concomitant hydration with nephroprotective agents because of its acute and chronic dose-limiting renal toxicity[4]. Local administration of cytotoxic agents against lung cancer has been investigated in the past using various agents, mostly by aerosol therapy, but lacked the ability to reach efficacious doses within a suitable timeframe compatible with clinical practice[5]. Dry powder formulations for inhalation are able to deliver large doses of active agent to the deeper lung in a few minutes and are patient actuated, which could help limit environmental and healthcare personnel exposure. They could also help lower systemic exposure while increasing exposure in the lungs. Controlled-release (CR) formulations could also help lower acute exposure locally in order to limit lung toxicity and diminish the strain of repeated administrations. However, inhaled particles undergo many challenges as they are confronted by elimination processes such as mucocilliary clearance and uptake by alveolar macrophages in the lungs, which could hinder their CR properties. Potential stealth properties of inhaled particles, provided by the addition of PEGylated excipients to formulations, are very much needed in order to promote their local residence[6]. These aspects have to be fully evaluated through preclinical studies using animal models such as rodents, along with adapted endotracheal administration devices[7]. Formulation behavior using those devices has to be fully characterized *in vitro* in order to ensure the reliability of *in vivo* results. This study focuses on the development and *in vitro* characterization of suitable dry powder blends (DPB) for the administration of cisplatin to mice and on the comparative pharmacokinetic (PK) results obtained *in vivo* with different immediate-release (IR) and CR formulation strategies for pulmonary nebulization and the IV route.

Previous work

Cisplatin formulations for human use have been previously produced and characterized[1]. Briefly, cisplatin at 5% w/v was micronized in an isopropanol suspension through high-pressure-homogenization for 40 cycles up to 20 000 psi. The resulting microcrystals, with a d(0.5) of 0.89 ± 0.01 ㎜, were then spray-dried with polyethylene glycol (1000) tocopheryl-vitamin E succinate (TPGS, F1) or with solubilized tristearin (TS) only (F2) or with TS and a PEGylated excipient using TPGS (F3) or distearoyl phosphoethanolamine polyethylene glycol 2000 (DSPE-mPEG-2000, F4), all at 2% w/v in solids content (Table 1). These formulations exhibited a high fine particle fractions (FPF) based on the nominal dose and a high fine particle dose (FPD). The inhalable fraction of these formulations also displayed IR for the carrier-free formulation F1, CR over more than 24 h for the 50% TS-comprising formulations (F2, F3) and a low burst-effect *in vitro* in modified simulated lung fluid (mSLF)[8].

Drug Delivery to the Lungs 27, 2016 - Local and systemic pharmacokinetic evaluation of immediate-release and controlled-release cisplatin dry powders for inhalation against lung cancer

Table 1. Theoretical compositions, FPFs and FPDs related to a 20 mg-filled capsule of cisplatin formulations obtained using a multistage liquid impinger operated at 100 L/min for 2.4s (n = 3) using an Axahaler® dry powder inhaler (SMB S.A., Belgium), and the *in vitro* drug released fractions after 10 min and 24 h from the inhalable fraction (particles below 5 mm) of formulations.

Formulation	Theoretical composition (% w/w)		FPF (% w/w)	FPD (mg)	Released fractions (%w/w)	
					10 min	24 h
F1	Cisplatin	95%	**52 ± 3**	**9.8 ± 0.6**	**97 ± 5**	**100 ± 0**
	TPGS	5%				
F2	Cisplatin	50%	**46 ± 7**	**4.5 ± 0.7**	**16 ± 4**	**79 ± 10**
	TS	50%				
F3	Cisplatin	50.0%	**37 ± 2**	**3.6 ± 0.2**	**24 ± 3**	**55 ± 11**
	TS	49.5%				
	TPGS	0.5%				
F4	Cisplatin	50.00%	**50 ± 6**	**5.0 ± 0.6**	**25 ± 7**	**56 ± 13**
	TS	49.75%				
	DSPE-mPEG-2000	0.25%				

Materials and methods

1. Production and characterization of dry blends

In order to administer dry powder formulations to mice *in vivo* at a 1.25 mg/kg dose, DPB of formulations had to be realized using a suitable diluent for a repeatable and accurate administration with an inhalation device, a Dry Powder Insufflator™ model DP-4M for mouse (Penn-Century Inc., USA). The diluent was obtained by spray drying an aqueous solution of 1.0% w/v Pearlitol 25C mannitol (Roquette Frères, France) and 0.1% w/v L-Leucine (Merck-Millipore, Germany) with a Mini Spray Dryer B-290 (Büchi, Switzerland). The spray-drying parameters were as follows: solution feed rate 3 g/min, inlet temperature 130°C, 0.7 mm nozzle, 1.5 mm nozzle-cap, spraying air flow 800 L/min, drying air flow 35 m^3/h and the use of a B-296 dehumidifier (Büchi, Switzerland). The actual outlet temperature was 54°C and the process yield was around 71%. DPB were then prepared by mixing the formulations with diluent using a Turbula 2C three-dimensional motion mixer (Bachofen AG, Switerzland) for 4 hours in a 2-mL glass vial, aiming at a target concentration of 2.0% w/w cisplatin in DPB. F1 was therefore diluted 50-fold, while F2, F3 and F4 were diluted 25-fold. DPB were then characterized by their drug content (mean and uniformity of content) by ETAAS[1] with a 2.0 mg mass for each DPB (n = 10). They were then characterized for their ability to be administered with the DP-4M. The *in vitro* delivery from the DP-4M was assessed by its efficiency and repeatability of deliverance for each DPB by weighing the device before and after activating the device 5 times (mean ± SD, n = 15). The *in vitro* accuracy of delivery was established between the theoretical dose calculated from the delivered mass of DPB and the actual emitted dose of DPB, which was measured by activating the device 5 times into an empty 5-mL glass vial, and quantifying the deposited Pt content with ETAAS (mean ± SD, n = 10). Particle size distributions (PSD) of DPB were measured in the plume from the DP-4M (n = 5) using a Spraytec laser diffractometer[7] (Malvern Instruments Ltd., UK) and expressed as d(0.5), d(0.9) and percentage particle volume undersize (particles below 5 mm).

2. Administration protocol

200 CD-1 (ICR) female mice aged between 5 and 15 weeks were administered cisplatin at a 1.25 mg/kg dose either in solution via the intravenous route (IV) or by nebulization or with a DPB via inhalation. Inhaled formulations were administered to mice via the endotracheal route using a MicroSprayer© Aerosolizer - Model 1A-1C-M for mouse (Penn-Century Inc., USA) or the DP-4M (i.e. for solution or for DPB, respectively), using the protocols described elsewhere[9]. Briefly, the MicroSprayer and the DP-4M are comprised of a reservoir (syringe or sample chamber, respectively) that connected to a hollow stainless-steel tip. They can deliver nebulized solutions or powders into a plume directly into the lungs of anesthetized mice through endotracheal insufflation using the syringe or a pump, respectively. Mice were then euthanized with sodium pentobarbital (Nembutal®, Ceva Animal Health, Belgium) at 10 min, 30 min, 1 h, 2 h, 4 h, 8 h, 24 h and 48 h (n = 5). Blood was sampled by retro-orbital bleeding in a lithium-heparin tube (Sarstedt, Germany) and organs (i.e. lungs, kidneys, liver, spleen and mediastinum) were removed, washed in saline and weighed and frozen until analysis using ETAAS. All animal experiments were approved by the ethical committee of the Faculty of Medicine, ULB (CEBEA) under the agreement number 585N.

3. Quantification of the platinum content in organs and in total blood

Organs were thawed and digested in 69% v/v Suprapur© nitric acid (Merck-Millipore, Germany) under ultrasonication at 65°C for 3 hours to obtain completely clear yellow solutions. Pt content in total blood was established by digesting 50 mL of heparinized blood using 50 mL Suprapur nitric acid and 100 mL 0.5% w/v Triton X-100 (Merck-Millipore, Germany). Measurements were then realized with a SpectrAA 300 atomic absorption spectrometer using adapted[1] and validated methods consistent with the requirements of the FDA[10]. Calibration was realized by the autosampler from freshly prepared matrix-matched 800 ng/mL cisplatin standards and blank matrix for each organ. Results were all adjusted to the same drug dose based on the emitted mass and drug content of DPB. AUC was calculated using the trapezoidal rule between measured data points.

Results and discussion

The IR formulation F1 and CR formulations F2, F3 and F4 were diluted to obtain the DPBs (Table 2), showing a smaller PSD for DPB1 and a uniformity of drug content comprised between 7.3 and 8.9% for all formulations except for DPB4, for which a higher variability of 13.4% w/w was observed. *In vitro* results showed that delivery from the DP-4M endotracheal device was more efficient and more repeatable with DPB1. This is probably attributable to the greater quantity of excipients present in this blend (50-fold dilution *vs.* 25-fold dilution for all the others formulations). Moreover, DPB1 was the only formulation without lipids, which could have impaired delivery. This is because it could have increased interparticle interactions with the diluent during mixing and within the device, causing more particle aggregates, especially as the initial formulation exhibit larger PSD[1]. Finally, the accuracy of delivery showed that emitted cisplatin levels were in accordance with the expected values calculated from the weighed device before and after actuations for DPB1, DPB2 and DPB3. These values were later on used *in vivo*. In contrast, a great variability in accuracy was observed for DPB4, probably due to its lesser uniform content and by particle demixing during actuation of the device. DPB4 was therefore discarded for the *in vivo* part of the study. *In vivo,* the DPB were administered to mice with lower delivery efficiency and a greater variability than *in vitro*. This could be caused by a blockage of the device tip or by powder sticking caused by the damper environment in mouse trachea.

Table 2. Measured parameters for the DPBs (PSD, drug-content, delivery with the DP-4M device).

	Laser diffraction		Drug content		*In vitro* delivery		*In vivo* delivery to the lung
Dry powder blend	d(0.5) (mm, mean ± SD, n = 5)	Undersize (% below 5 mm, mean ± SD, n = 5)	Cisplatin content (% w/w, mean ± SD, n = 10)	Unifor-mity of content (% w/w, n = 10)	Efficiency and repeatability (% w/w, mean ± SD, n = 15)	Accuracy (% w/w, mean ± SD, n = 10)	Efficiency and repeatability (% w/w, mean ± SD, n = 40)
DPB1	**2.4** ± 0.8	**86.5** ± 6.7	**2.37** ± 0.21	**8.9**	**96.3** ± 7.6	**97.2** ± 4.3	**72.9** ± 33.7
DPB2	**3.7** ± 0.8	**69.1** ± 14.0	**1.67** ± 0.17	**9.9**	**85.8** ± 17.4	**98.0** ± 16.2	**67.3** ± 26.1
DPB3	**3.6** ± 0.5	**69.2** ± 10.3	**1.64** ± 0.12	**7.3**	**87.3** ± 16.7	**104.8** ± 19.3	**82.9** ± 25.5
DPB4	**3.4** ± 0.5	**73.8** ± 9.0	**1.60** ± 0.21	**13.4**	**85.8** ± 19.3	**198.3** ± 78.5	-

PK results (Figure 1) showed that lung exposure was relatively higher with all inhaled experiments compared to IV. It also showed that nebulization and IR DPB1 had similar PK profiles, and that Pt levels fell very rapidly, already before the first dosing time (10 min). PK profiles of CR formulations *in vitro* (DPB2 and DPB3) showed that DPB2, despite being preserved in larger amounts at the first dosing times, was rapidly eliminated within the first hour. This suggests an active elimination process, probably by alveolar macrophages uptake. However, the PEGylated excipient-comprising formulation F3, showed high and sustained levels of platinum for up to 24 hours, confirming the well-described abilities of PEG chains to delay macrophage recognition and capture of particles[6]. Blood platinum levels, were higher with IV than with the pulmonary route and showed absorption profiles compatible with the slow distribution from the lungs to the systemic compartment for all inhaled experiments.
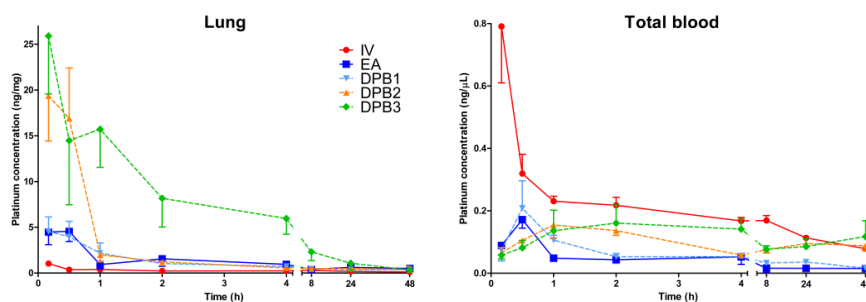

Figure 1. Local and systemic pharmacokinetic profiles showing Pt content in lungs and in total blood after a single 1.25 mg/kg administration (Mean ± SEM, n = 5 for each dosing time).

Pt C_{max} which is more representative of the acute toxicity linked to cisplatin exposure, was also reduced in total blood (Figure 2a) for all the inhaled experiments as compared to IV. This was especially the case for CR formulation DPB3 (161 ± 57 ng/mL vs. 791 ± 181 ng/mL for IV). The reduced exposure was also particularly observable in kidneys (Figure 2b) for IR formulation DPB1 and nebulization (0.6 ± 0.2 ng/mg and 1.1 ± 0.5 ng/mg vs. 3.0 ± 0.7 ng/mg for IV). Observed C_{max} at 10 min was, however, significantly increased in lungs for DPB2 and DPB3 (Figure 2c), which does not reflect CR properties of these formulations as ETAAS does not differentiate between available Pt, dissolved Pt and undissolved Pt from particles in the lung parenchyma (Kruskall-Wallis test with Dunn's multiple comparison test, $p < 0.01$). It also showed that IR formulations were quickly absorbed (less than 10 min). Analysis of the area under the curve (AUC) for all PK profiles (Figure 2d) showed that the global exposure of lungs to Pt was increased for inhaled formulations compared to IV injection (very significantly with

Drug Delivery to the Lungs 27, 2016 - Local and systemic pharmacokinetic evaluation of immediate-release and controlled-release cisplatin dry powders for inhalation against lung cancer

DPB3 with a more than 10-fold increase, $p < 0.001$). Interestingly, AUC in kidneys was lowered for all inhaled formulations, as compared with IV (for instance, AUC in kidneys of 475 ± 187 ng.min.mL^{-1} vs. 2168 ± 149 ng.min.mL^{-1} for DPB2 and IV, respectively). An exception was observed for DPB3, for which AUC in kidneys was closer to IV with 1625 ± 806 ng.min.mL^{-1} (mean ± SEM, n = 5 per group per dosing time, 8 times). Further experiments are needed to explain this phenomenon. Exposure was also lowered in liver for all inhaled formulations, as compared with IV.
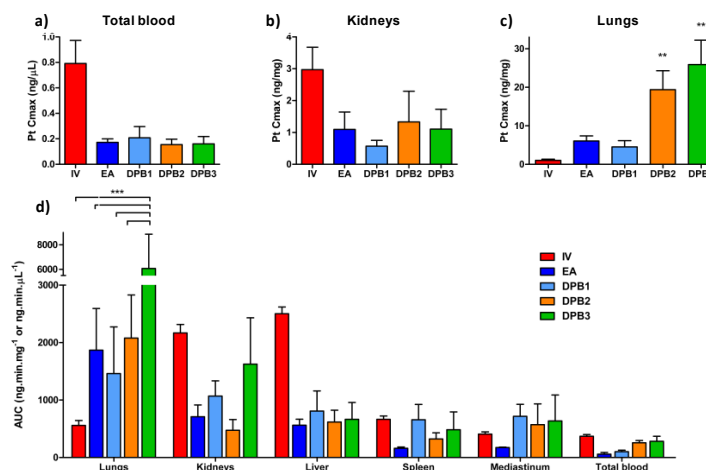
Figure 2. C_{max} in total blood (**a**), kidneys (**b**) and lungs (**c**) (mean ± SEM, n = 5 per group) and total exposure of organs (**d**) expressed as the AUC in organs for all considered routes and formulations (mean ± SEM, n = 5 per group per dosing time, 8 times). Significance of the difference with the IV control group or the mentioned group was calculated using a Kruskall-Walis test with Dunn's multiple comparison test (**c**) or a two-way ANOVA with Bonferroni's multiple comparison test (**d**) and is expressed as follow: ** = $p < 0.01$, *** = $p < 0.001$.

Conclusion

The PK of cisplatin is of tremendous interest in order to assess the outcome of cisplatin or its reactive species after lung administration. We showed that a formulation comprised of TS and PEGylated excipients greatly improves Pt exposure in the lungs for more than 8 hours compared with (i) an IV-delivered cisplatin solution, (ii) a nebulized cisplatin solution or (iii) IR formulations. The use of PEGylated excipients seems crucial in order to prolong residency of inhaled SLMs in the respiratory tract. The increased Pt exposure observed with the CR formulation in the kidneys will have to be further assessed using more specific renal parameters for renal toxicity such as blood urea nitrogen or creatinine levels. Lung toxicity will also have to be assessed using broncho-alveolar lavage fluid analysis[9].

References

[1]Levet V, Amighi K, Wauthoz N: Development of cisplatin-based dry powder for inhalation with controlled release properties for the lung cancer therapy. *Respiratory Drug Delivery* (2016) 3(549-552).
[2]Howlader N, Noone A, Krapcho M, Garshell J, Miller D, Altekruse S, Kosary C, Yu M, Ruhl J, Tatalovich Z, Mariotto A *et al*: Seer cancer statistics review, 1975-2012. In: National Cancer Institute. Bethesda, MD (2015).
[3]Clinical practice guidelines in oncology non-small cell lung cancer. V 3.2014 (2014).
http://www.nccn.org/professionals/physician_gls/pdf/nscl.pdf.
[4]NHS: Guidelines for intravenous hydration for chemotherapy regimes in adults. In: network sc (Ed) (2012).
[5]Phase 2 study of inhaled lipid cisplatin in pulmonary recurrent osteosarcoma (2012).
http://clinicaltrials.gov/ct2/show/NCT01650090.
[6]Muralidharan P, Mallory E, Malapit M, Hayes D, Jr., Mansour HM: Inhalable pegylated phospholipid nanocarriers and pegylated therapeutics for respiratory delivery as aerosolized colloidal dispersions and dry powder inhalers. *Pharmaceutics* (2014) 6(2):333-353.
[7]Duret C, Wauthoz N, Merlos R, Goole J, Maris C, Roland I, Sebti T, Vanderbist F, Amighi K: In vitro and in vivo evaluation of a dry powder endotracheal insufflator device for use in dose-dependent preclinical studies in mice. *European journal of pharmaceutics and biopharmaceutics : official journal of Arbeitsgemeinschaft fur Pharmazeutische Verfahrenstechnik eV* (2012) 81(3):627-634.
[8]Son YJ, McConville JT: Development of a standardized dissolution test method for inhaled pharmaceutical formulations. *International Journal of Pharmaceutics* (2009) 382(1-2):15-22.
[9]Rosiere R, Van Woensel M, Mathieu V, Langer I, Mathivet T, Vermeersch M, Amighi K, Wauthoz N: Development and evaluation of well-tolerated and tumor-penetrating polymeric micelle-based dry powders for inhaled anti-cancer chemotherapy. *International Journal of Pharmaceutics* (2016) 501(1-2):148-159.
[10]Food and Drug Administration: Bioanalytical method validation guidelines for industry (2013).

218

Local and systemic pharmacokinetic evaluation of immediate-release and controlled-release cisplatin dry powders for inhalation against lung cancer

Vincent Levet, Rémi Rosière, Karim Amighi, Nathalie Wauthoz*

Laboratory of Pharmaceutics and Biopharmaceutics, Faculty of Pharmacy, Université libre de Bruxelles.   *nawautho@ulb.ac.be

Introduction

Cisplatin is the major component of the IV doublet chemotherapy regimen to combat lung cancer. However it exerts very high toxicities (i.e. nephrotoxicity, ototoxicity, myelosupression). Inhaled cisplatin chemotherapy could lower them by increasing local concentration in the lungs near the tumor site while decreasing the acute and chronic exposure in non-targeted organs. To limit local toxicity and optimize the tumor exposure, drug release after deposition of high cisplatin doses in the lungs should be controlled. Therefore, we developed dry powders for inhalation including solid lipid microparticles (SLMs) with controlled release properties with or without PEGylated excipients (F3, F4 and F2, respectively) [1] to modulate their clearance by alveolar macrophages. Therefore the aim of the study was to evaluate the platinum pharmacokinetic of these controlled-release formulations in comparison to a dry powder for inhalation with immediate-release (F1) and cisplatin solution by endotracheal nebulization (EN) and intravenous (IV) route.
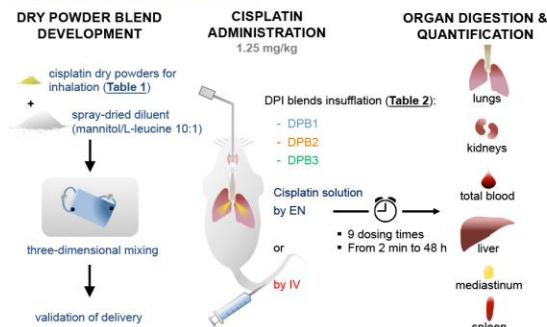
Results and Discussion

Figure 1. Overview of the study's methodology.

1. Validation of delivery (Table 2)

→ *In vitro* delivery: reliable emission efficiency (CV < 25%) and recovery (~100 %) except for DPB4 which was excluded from *in vivo* delivery.

→ *In vivo* delivery: lower emission but acceptable efficiency because of powder sticking in the device caused by a damper environment in mouse trachea [2]. Lung recoveries were reproducible and around 30%.

2. Platinum Pharmacokinetics

in lungs (Figure 2a)

→ Higher lung exposure with inhalation than IV and very fast absorption of EN ($t_{1/2}$ 5.0 min) and immediate-release DPB1 ($t_{1/2}$ 2.6 min).

→ Fast elimination of DPB2 (without PEG) after ~1 h ($t_{1/2}$ 9 min).

→ Longer retention in the lungs of DPB3 (with PEG) after ~7 h ($t_{1/2}$ 60 min).

in total blood (Figure 2b)

→ Confirmation of controlled-release from the blood profiles *vs.* IV and EN: smoother distribution from the lungs for DPB2 and even more so for DPB3.

3. Chronic Exposure (Figure 3)

→ AUC in lungs increased 3 to 4-fold for EN, DPB1 and DPB2 and up to 11 fold for DPB3 *vs.* IV.

→ AUC in all non-targeted organs decreased *vs.* IV but to a lower extent for DPB3 in kidneys because of saturable platinum clearance mechanisms of kidneys combined with controlled-release properties of DPB3.
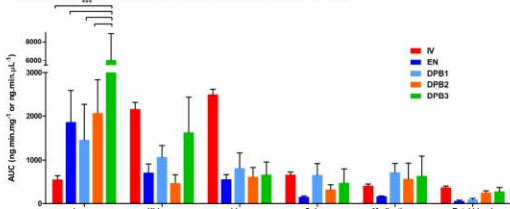

Figure 3. $AUC_{10min-48h}$ in all organs (mean ± SE, n = 5).

Table 1. Dry powder formulations compositions, FPF and *in vitro* release fractions of cisplatin (mean ± SD, n = 3).

	Theoretical composition (% w/w)		FPF (% w/w)	Released fractions (% w/w)	
				10 min	24 h
F1	Cisplatin	95	52 ± 3	97 ± 5	100 ± 0
	TPGS (PEG₁₀₀₀)	5			
F2	Cisplatin	50	46 ± 7	16 ± 4	79 ± 10
	Tristearin	50			
F3	Cisplatin	50.0	37 ± 2	24 ± 3	55 ± 11
	Tristearin	49.5			
	TPGS (PEG₁₀₀₀)	0.5			
F4	Cisplatin	50.0	50 ± 6	25 ± 7	56 ± 13
	Tristearin	49.75			
	DSPE-PEG₂₀₀₀	0.25			

Table 2. *In vitro* and *in vivo* delivery efficiencies and recoveries. Recovery in mouse lungs was assessed at the first dosing time (t ~2 min). Results are expressed as mean ± SD.

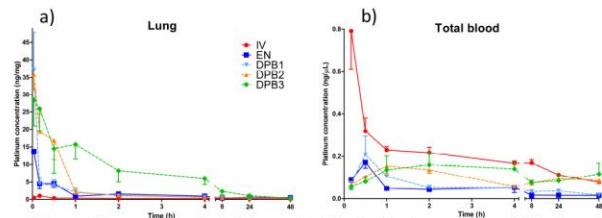| Powder Blends	Dilution factor	In vitro		In vivo	
		Delivery efficiency (% w/w, n = 15)	Recovery (% dose, n =10)	Delivery efficiency (% w/w, n = 45)	Recovery (% dose, n = 5)
DPB1	1:50	96 ± 8	97 ± 4	73 ± 34	27 ± 14
DPB2	1:25	86 ± 17	98 ± 16	67 ± 26	29 ± 7
DPB3	1:25	87 ± 17	105 ± 19	83 ± 26	35 ± 21
DPB4	1:25	86 ± 20	198 ± 78	N.A.	N.A.

N.A.: not administered

Figure 2. Platinum pharmacokinetic in lung and total blood profiles (mean ± SEM, n = 5 / time in total blood (8 times) and in lung (9 times). t ~2 min was added in lung PK profiles to establish the recovery of the emitted dose *in vivo*).

4. Acute Exposure (Figure 4)

→ Pt C_{max} in blood and kidneys were reduced up to 5-fold *vs.* IV.

→ Pt C_{max} in lungs were comparable for all inhaled formulations (30 to 35-fold higher than IV), slightly lower for EN (15-fold) because cisplatin was very quickly absorbed through the lung epithelium.
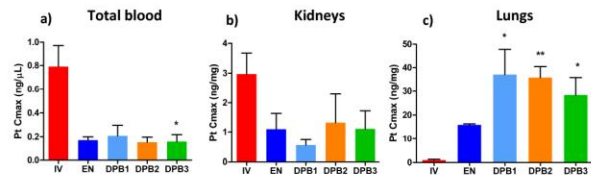

Figure 4. C_{max} of total blood (a), kidneys (b) and lungs (c) (mean ± SD, n = 5)

Conclusions

Delivery using the DP-4M endotracheal device was reliable using DPB made of a spray-dried diluent but needs to be assessed for each formulation. PEGylated excipients embedded into cisplatin SLM are essential to provide prolonged lung retention and maintain controlled-release properties of the formulations after their deposition. Local and systemic toxicity and efficacy of these formulations must now be assessed on mice models.

References
[1] Levet *et al*. Int J Pharm, 2016, [2] Duret *et al*. Eur J Pharm Biopharm, 2012.

DDL27 drug delivery to the lungs 27

4. Poster Abstract for Respiratory Drug Delivery Europe conference 2017, Nice (Antibes), France. April 25-28, 2017.
"Tolerance of Cisplatin Dry Powders for Inhalation and Efficacy on a Orthotopic Grafted Lung Tumor Preclinical Model"

Levet V., Rosière R., Langer I., Amighi K., Wauthoz N.

Respiratory Drug Delivery

Editors: Dalby RN, Byron PR, Peart J, Suman JD, Farr SJ, Young PM, Traini D.

This abstract was peer-reviewed and will be published in RDD Online and in the Conference book. It is a shortened version of the Article presented in part III.

Tolerance of Cisplatin Dry Powders for Inhalation and Efficacy on an Orthotopic Grafted Lung Tumor Preclinical Model

Vincent Levet,[1] Rémi Rosière,[1] Julien Hecq,[1] Ingrid Langer,[2]
Karim Amighi,[1] and Nathalie Wauthoz[1]

[1]*Laboratory of Pharmaceutics and Biopharmaceutics,
Université libre de Bruxelles (ULB), Brussels, Belgium*

[2]*Institut de Recherche Interdisciplinaire en
Biologie Humaine et Moléculaire (IRIBHM),
ULB, Brussels, Belgium*

KEYWORDS: lung cancer, inflammation, cytotoxicity,
maximum tolerated dose, anticancer drug,
dry powder inhaler formulations

INTRODUCTION

Lung cancer remains the primary cause of cancer-related death worldwide and conventional chemotherapy seems to have reached a therapeutic plateau [1, 2]. Cisplatin remains the most potent chemotherapeutic agent used by the classic IV route, but is associated with high cumulative nephrotoxicity, limiting the administrable dose and requiring large hydration phases before and after administration [3-5]. Inhaled delivery of cisplatin to combat lung tumors could be a promising concept. Some nebulizer formulations have already reached the clinical stage with acceptable grade 2 local toxicities but exhibited heavy limitations regarding the deliverable dose and excessive treatment duration [6, 7]. To overcome these issues, we have previously developed CR_PEG, a cisplatin-based dry powder for inhalation (DPI) with high drug-loading and high fine-particle fraction [8] with controlled-release and lung retention abilities (Table 1) [9]. The aim of this work was to evaluate the CR_PEG DPI in relation to an immediate-release DPI (IR DPI) and an endotracheal nebulized solution (EN) but also to solutions administered by intravenous route (IV) in terms of 1) maximum tolerated dose (MTD), 2) local tolerance, and 3) efficacy in terms of survival curves on a preclinical model of lung tumor. The effect of the excipient composition was also evaluated with CR_PEGv, the corresponding DPI formulation without cisplatin.

MATERIALS AND METHODS

Determination of the MTD of Repeated Administrations

The cisplatin-based formulations described in Table 1 were administered to six-week old BALB/cAnNRj mice (Janvier Labs, France) under a three days/week for two weeks scheme (n = 3). The cisplatin doses were escalated from 0.5 mg/kg up to the MTD, defined as the last dose for which body weight (bw) loss did not exceed 5% at any time over the 40 days following first dosing. EN solution and IR DPI and CR_PEG DPI were administered by endotracheal administration under anesthesia using the Microsprayer IA-1C© and the DP-4M© devices (Penn-Century Inc., USA), respectively, as well as IV, following the procedures, powder blending, and solution preparation described previously [3].

Table 1.

Formulation composition and their respective lung and systemic pharmacokinetic parameters reflecting the cisplatin lung clearance (Lung $t_{1/2}$) and maximum concentration available for pharmacological action and therefore blood absorption (systemic C_{max}) after a 1.25 mg/kg administration, as reported from Levet *et al.* [9].

Formulations	Cisplatin/ Lipid ratio	Composition	Relative concentration (w/w and w/w/w)	Lung $t_{1/2}$ (min)	Total blood platinum C_{max} (mean ± SD, n = 5)
IV	100:0	Cisplatin in NaCl 0.9%	-	13.1	0.79 ± 0.40
EN	100:0	Cisplatin in NaCl 0.9%	-	5.0	0.17 ± 0.06
IR DPI	95:50	Cisplatin:TPGS[1]	95:5	2.6	0.21 ± 0.20
CR_PEG	50:5	Cisplatin:TS[2]:TPGS[1]	50:49.5:0.5	59.9	0.16 ± 0.13
CR_PEGv	0:1	TS[2]:TPGS[1]	99:1	N.D.	N.D.

[1]D-alpha-tocopheryl polyethylene (1000) succinate, [2]Tristearin, N.D. not determined

Evaluation of the Local Tolerance

IR and CR_PEG DPIs (Table 1) were administered once in mouse lung (n = 7) at their MTD. CR_PEGv (Table 1) was administered at the same concentration than at the MTD of CR_PEG DPI (i.e., 50% w/w of 1.0 mg/kg, n = 4). Negative and positive controls were non-treated mice (Ctrl-, n = 4) and 1 µg lipopolysaccharide (LPS, n = 5) from *E. coli*-treated mice, respectively. A broncho-alveolar lavage (BAL) was performed 24 hours after administration except for LPS (8 hours), as described previously in Rosière *et al.* [10]. The cell-count of BAL was performed with a Coulter® counter (Beckman Coulter, Belgium) and the differential cell composition was determined using optical microscopy after May-Grünwald Giemsa cell staining. On the BAL fluid supernatants, the total protein-content was determined using a bicinchoninic acid (BCA) assay (Thermo Scientific, USA), the cytotoxic activity was evaluated using a lactate dehydrogenase (LDH) assay (Thermo Scientific) and pro-inflammatory cytokines (IL-1ß, IL-6, TNF-α) concentration was determined using an ELISA DuoSet® assay (R&D Systems, UK).

Efficacy on an Orthotopic M109 Tumor Model

The Madison 109 (M109) lung carcinoma cell line was cultured and grafted in six-week old BALB/cAnNRj mice as described in Rosière *et al.* [10], by injecting orthotopically 1.4×10^6 cells suspended in 20 µL of a Matrigel® (Corning, Belgium) and cell-culture medium mix (1:1). Five days after the tumor graft, mice were either left untreated (Ctrl group, n = 11) or treated with IR DPI (n = 15), or

CR_PEG DPI (n = 15) at their respective MTD by endotracheal administrations, or treated by IV (n = 11) at a dose of 0.5 mg/kg or 1.0 mg/kg, following the MTD dosing scheme. Survival was evaluated starting from the last administered dose.

RESULTS AND DISCUSSION

A chronic MTD of 0.5 mg/kg was determined for EN and IR DPI, but was doubled at 1.0 mg/kg for CR_PEG DPI. Knowing that inhalation concentrated the delivered dose in the lung about 15-40 times [9], the chronic MTD in the lung from DPI is relatively high in comparison to a chronic MTD of 1.5 mg/kg by IV. This revealed a higher toxicity by the inhalation route than for the general route for all formulations, but to a lower extent for the CR_PEG approach.

In terms of local toxicity, administration of cisplatin formulations in the lungs lowered the cell-count in the BAL (Table 2) for more than 50% with the highest decrease for EN at 0.5 mg/kg. This seems to be linked to cytotoxic cisplatin as the cell-count for the vehicle (CR-PEGv) related to the Ctrl- in percentage was superior or equal to 100%. In addition, this decrease was also observed for IV in relation to the adminis-tered dose. In terms of cell-type proportions (Table 2), cisplatin formulations delivered by inhalation increased polymorphonuclear neutrophil proportion, whereas very few polymorphonuclear neutrophil were observed in untreated mice (< 1%), which primarily exhibited alveolar macrophages (> 99%). The highest proportion of polymorphonuclear neutrophils was observed with CR_PEG DPI and seems to be linked to the higher and sustained cisplatin dose and not to the PEGylated lipidic microparticles (CR_PEGv). In terms of pro-inflammatory cytokine (IL-1ß, IL-6, or TNF-α) concentrations, cytotoxicity (via LDH) and protein-content (Table 2), no significant increases were observed for cisplatin formulations administered in the lungs or IV when compared to Ctrl-, except for a non-significant increase of IL-6 with CR_PEG.

Table 2.

Evaluation in BAL: Total cells related to the negative control ; alveolar macrophages and polymorphonuclear neutrophils determined on 200 counted cells ; IL-1ß, Il-6, and TNF-α cytokine concentrations (negative control in brackets); LDH activity as a proportion of cytotoxicity vs. the manufacturer's internal standard (100% cytotoxicity) and the Ctrl- in brackets ; and protein-content related to the negative control. All results are presented as mean ± SD.

	Total cells (% vs. Ctrl-)	Alveolar macrophages (% cells)	Polymorpho-nuclear neutrophils (% cells)	IL-1β (pg/mL)	IL-6 (pg/mL)	TNF-α (pg/mL)	LDH activity (% vs. internal standard)	Protein content (% vs. Ctrl-)
IV 0.5 mg/kg	75 ± 91	99 ± 1	0 ± 1	91 ± 31 (89 ± 42)	< LOQ (< LOQ)	< LOQ (< LOQ)	17 ± 16 (12 ± 8)	121 ± 41
EN 0.5 mg/kg	21 ± 38	69 ± 18	29 ± 18	93 ± 19 (89 ± 42)	< LOQ (< LOQ)	< LOQ (< LOQ)	13 ± 11 (12 ± 8)	110 ± 54
IR DPI 0.5 mg/kg	32 ± 127	91 ± 11	9 ± 11	70 ±11 (89 ± 42)	< LOQ (< LOQ)	< LOQ (< LOQ)	10 ± 3 (12 ± 8)	151 ± 54
IV 1.0 mg/kg	54 ± 85	97 ± 2	0 ± 0	45 ± 19 (50 ± 16)	51 ± 16 (55 ± 36)	< LOQ (< LOQ)	20 ± 1 (29 ± 3)	82 ± 17
CR_PEG 1.0 mg/kg	45 ± 57	58 ± 37	40 ± 38	52 ± 20 (50 ± 16)	92 ± 41 (55 ± 36)	< LOQ (< LOQ)	24 ± 1 (29 ± 3)	97 ± 16
CR_PEGv 0.5 mg/kg	117 ± 25	93 ± 4	0 ± 0	< LOQ (< LOQ)	< LOQ (< LOQ)	< LOQ (< LOQ)	9 ± 1 (13 ± 3)	71 ± 40

Limit of quantification for IL-1β: 15.6 pg/mL, IL-6: 15.6 pg/mL, TNF-α: 31.3 pg/mL, from the manufacturer's kit.

Following the tolerance studies, cisplatin was administered to M109-grafted mice (Figure 1). During administration of the IR DPI formulation, a high number of mice died immediately following administration (9/15), which was less but still observed for the CR_PEG DPI (4/15). This was not observed for both IR DPI and CR_PEG during the previous MTD study, probably because it was done on healthy mice, whereas grafted mice were weakened by the prior surgery and tumor involvement. While control mice were all dead after 42 days with a median survival (MS) of 29 days, the CR_PEG at 1.0 mg/kg group showed a significantly increased survival ($p < 0.01$, Kaplan-Meier, log-rank test) with a MS of 40 days. This survival was comparable to the IV group at 0.5 mg/kg group ($p \geq 0.05$ Kaplan-Meier, test log-rank) with a MS of 44 days. Again, the CR_PEG 1.0 mg/kg group showed its superiority in comparison to IR DPI at 0.5 mg/kg where no significant difference was observed with the control ($p \geq 0.05$ Kaplan-Meier, log-rank test). However, survival of CR_PEG (1.0 mg/kg) was significantly lower than IV (1.0 mg/kg), presenting a MS of 69 days ($p < 0.01$, Kaplan-Meier, log rank test). This could be attributed to the high number of metastases in the thoracic cavity observed on dead mice in the inhalation groups, while IV mice showed pulmonary involvement as the primary cause of death.
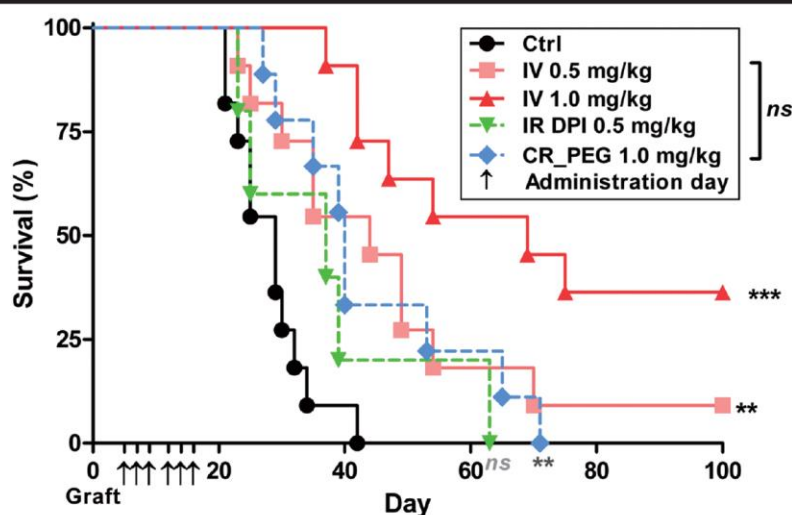

Figure 1. Kaplan-Meier survival curves and log-rank test following cisplatin administration, *** ($p < 0.001$), ** ($p < 0.01$), ns ($p > 0.05$).

CONCLUSION

Despite an increase in polynuclear neutrophil proportion in BAL, local and systemic tolerance of inhaled cisplatin was the highest with the CR_PEG DPI formulation, probably because of lower acute local concentrations. This approach led to a comparable tumor response *in vivo* than the IV regimen at half the dose, but the latter treated metastases while inhaled cisplatin seemed more active against primary tumors. Future studies will assess the local and systemic toxicity of chronic administrations of inhaled cisplatin and the efficacy of the combination of IV and inhalation therapy.

REFERENCES

1. Ferlay J, Soerjomataram I, Dikshit R, Eser S, Mathers C, Rebelo M, Parkin DM, Forman D, Bray F: Cancer incidence and mortality worldwide: Sources, methods and major patterns in GLOBOCAN 2012. *Int J Cancer* 2015, 136: E359-86.

2. Gridelli C, Rossi A, Maione P: Treatment of non-small-cell lung cancer: state of the art and development of new biologic agents. *Oncogene* 2003, 22: 6629-38.

3. NHS: Guidelines for intravenous hydration for chemotherapy regimes in adults. (Network SC Ed): Cancer Chemotherapy Group: 2012.

4. NCCN Clinical Practice Guidelines in Oncology Small Cell Lung Cancer. v2.2014. https://www.tri-kobe.org/nccn/guideline/lung/english/small.pdf. Accessed January 1, 2017.

5. NCCN Clinical Practice Guidelines in Oncology Non-Small Cell Lung Cancer. v 7.2015 http://www.nccn.org/professionals/physician_gls/pdf/nscl.pdf. Accessed January 1, 2017.

6. Chou AJ, Gupta R, Bell MD, Riewe KO, Meyers PA, Gorlick R: Inhaled lipid cisplatin (ILC) in the treatment of patients with relapsed/progressive osteosarcoma metastatic to the lung. *Pediatr Blood Cancer* 2013, 60: 580-86.

7. Wittgen BP, Kunst PW, van der Born K, van Wijk AW, Perkins W, Pilkiewicz FG, Perez-Soler R, Nicholson S, Peters GJ, Postmus PE: Phase I study of aerosolized SLIT cisplatin in the treatment of patients with carcinoma of the lung. *Clin Cancer Res* 2007, 13: 2414-21.

8. Levet V, Rosière R, Merlos R, Fusaro L, Berger G, Amighi K, Wauthoz N: Development of controlled-release cisplatin dry powders for inhalation against lung cancers. *Int J Pharm* 2016, 515: 209-20.

9. Levet V, Merlos R, Rosière R, Amighi K, Wauthoz N: Platinum pharmacokinetics in mice following inhalation of cisplatin dry powders with different release and lung retention properties. *Int J Pharm* 2017, 517: 359-72.

10. Rosiere R, Van Woensel M, Mathieu V, Langer I, Mathivet T, Vermeersch M, Amighi K, Wauthoz N: Development and evaluation of well-tolerated and tumor-penetrating polymeric micelle-based dry powders for inhaled anti-cancer chemotherapy. *Int J Pharm* 2016, 501: 148-59.